2807 West County Road 75
Monticello, MN 55362

800.895.4999
xcelenergy.com

Xcel Energy®
RESPONSIBLE BY NATURE®

October 18, 2017

L-MT-17-053
10 CFR 72.7

U.S. Nuclear Regulatory Commission
ATTN: Document Control Desk
Director, Division of Spent Fuel Storage and Transportation
Office of Nuclear Material Safety and Safeguards
Washington, DC 20555-0001

Monticello Nuclear Generating Plant
Docket No. 50-263
Renewed Facility Operating License No. DPR-22
Independent Spent Fuel Storage Installation Docket No. 72-58

<u>Exemption Request for Nonconforming Dye Penetrant Examinations of Dry Shielded Canisters (DSCs) 11 through 15</u>

References:
1) NRC Letter to NSPM, "Confirmatory Order Related to NRC Reports No. 05000263/2015008; 07200058/2014001 and [Office of Investigation] OI Report 3-2014-004; Monticello Nuclear Generating Plant", dated December 21, 2015 (ADAMS Accession No. ML15355A459)
2) NSPM letter to NRC, "Exemption Request for Dry Shielded Canisters 11-16 Due to Nonconforming Dye Penetrant Examinations", dated July 16, 2014 (ADAMS Accession No. ML14199A370)
3) NSPM letter to NRC, "Withdrawal of Exemption Request for Dry Shielded Canisters 11-16 Due to Nonconforming Dye Penetrant Examinations, Supplemental Information (TAC No. L24939)", dated December 16, 2014 (ADAMS Accession No. ML14351A155)
4) NRC Letter to NSPM, "Exemption from Certain Provisions of 10 CFR 72.212 and 72.214 – Storage of Standardized NUHOMS® Dry Shielded Canister 16 at Monticello Nuclear Generating Plant Independent Spent Fuel Storage Installation (CAC No. L25058)", dated June 15, 2016 (ADAMS Accession No. ML16167A036)
5) NSPM letter to NRC, "Thirty (30) Day Notification Pursuant to 10 CFR 72.212, Conditions of General License Issued Under 10 CFR 72.210, for the Storage of Spent Fuel", dated October 7, 2013 (ADAMS Accession No. ML13283A101)
6) NSPM letter to NRC, "Thirty (30) Day Notification for the Fourth and Fifth Dry Shielded Canisters Pursuant to 10 CFR 72.212, Conditions of General

License Issued under 10 CFR 72.210, for the Storage of Spent Fuel", dated November 4, 2013 (ADAMS Accession No. ML13310A568)

7) NSPM letter to NRC, "Project Plan Progress Toward Restoring 10 CFR 72 Compliance to Dry Shielded Canisters Designated 11 through 16", dated June 6, 2017

Pursuant to 10 CFR 72.7, "Specific Exemptions", the Northern States Power Company, a Minnesota corporation (NSPM), doing business as Xcel Energy, requests an exemption from the requirements of 10 CFR 72.212(a)(2), 10 CFR 72.212(b)(3), 10 CFR 72.212(b)(5)(i), 10 CFR 72.212(b)(11), and 10 CFR 72.214 for five NUHOMS® Dry Shielded Canisters (DSCs) designated DSCs 11-15 due to nonconforming dye penetrant (PT) examinations performed during the loading campaign that started in September 2013. These nonconforming PT examinations are the subject of a Confirmatory Order (Reference 1).

Please note that an earlier submittal (Reference 2) was made to request an exemption for all six canisters (designated DSCs 11-16) that were originally found to be nonconforming. However, that request was withdrawn (Reference 3) in 2014.

Pursuant to the NSPM corrective action program and the Confirmatory Order, DSC 16 was restored to compliance with the regulations by an exemption granted in June 2016 (Reference 4). Currently, the subject five DSCs are loaded into Horizontal Storage Modules (HSMs), as reported in References 5 and 6. The enclosed exemption request is structured as discussed in NSPM's most recent project plan update (Reference 7).

In summary, the exemption request has determined that the integrity of the field closure welds for DSCs 11-15 can be reasonably assured even though the Technical Specification required dye penetrant examinations were nonconforming. The fuel cladding integrity, weld design, materials, welding process, tests performed, adequate stress margin in the welds to accommodate maximized representative flaws, and demonstration of additional stress margins to address any remaining uncertainties demonstrates the closure weld integrity of DSCs 11-15 is sufficient to ensure that the affected closure welds will continue to perform their design basis functions over the service lifetime of these canisters. In addition, the exemption request demonstrates that the consequences of non-mechanistic weld failures are very low and that the overall risk to the public is also very low. Enclosure 1 provides the exemption request including a description of the basis and technical justification for granting an exemption. The exemption request provides the basis and technical justification to permit continued storage of DSCs 11-15 in their respective HSMs.

Enclosure 2 provides Structural Integrity Associates, Inc. (SIA) Report 1301415.301, "Development of an Analysis Based Stress Allowable Reduction Factor (SARF) – Dry Shielded Canister (DSC) Top Closure Weldments", which provides an analysis-based Stress Allowable Reduction Factor, which supports the values used in the analysis of record for the NUHOMS® 61BTH model canister, the canister design used at the Monticello Nuclear Generating Plant.

Enclosure 3 provides SIA Report 700388.401, “Evaluation of the Welds on DSCs 11-15”, which evaluates the available weld head video, general area video, documentation, and DSC 16 Phased Array Ultrasonic Testing (PAUT) results determining that the types of flaws and extent of flaw distributions found in DSC 16 are considered representative of the comparable closure welds of DSCs 11-15.

Enclosure 4 provides AREVA Calculation 11042-0204, “Allowable Flaw Size Evaluation in the Inner Top Cover Plate Closure Weld for DSC #16”, which calculates a maximum allowable flaw size in the Inner Top Cover Plate (ITCP) weld for DSC 16 assuming a weld depth of 0.25 inches.

Enclosure 5 provides AREVA Calculation 11042-0205, “61BTH ITCP and [Outer Top Cover Plate] OTCP Closure Weld Flaw Evaluation”, which evaluates the DSC 16 closure weld flaw indications discovered by PAUT examination. This calculation uses the limit load analysis methodology of the American Society of Mechanical Engineers (ASME) Operation and Maintenance Code, Section III. Additionally, elastic-plastic analyses were performed to document the actual predicted strains in the welds and to demonstrate adequate margin against plastic collapse.

Enclosure 6 provides AREVA Calculation 11042-0207, “NUHOMS® 61BTH Type 1 DSC ITCP and OTCP Maximum Weld Flaw Evaluation”, which evaluates the DSCs 11-15 closure welds per ASME Section III criteria using design bases loads with flaws located based on DSC 16 PAUT results and maximized such that the weld flaws are close to acceptable design limits.

Enclosure 7 provides AREVA Calculation 11042-0208, “Site Specific NUHOMS® 61BTH Type 1 DSC ITCP and OTCP Margin Evaluation for Maximum Weld Flaw”, which evaluates the stress margins for DSCs 11-15 with the maximized flaws in the ITCP and OTCP closure welds based on as-loaded temperature and pressure conditions.

Enclosure 8 provides AREVA Calculation 11042-0209, “Site Specific NUHOMS® 61BTH Type 1 DSC ITCP and OTCP Margin Evaluation for Maximum Weld Flaw with Side Drop Loads”, which evaluates the stress margins for DSCs 11-15 with the maximized flaws in the ITCP and OTCP closure welds based on the as-loaded temperature and pressure conditions and site-specific side-drop loads.

Enclosure 9 provides AREVA Calculation 11042-0400, “Site-Specific Thermal Evaluation of 61BTH Type 1 DSCs Stored in HSM-H at Monticello Nuclear Generating Plant”, which evaluates the bounding DSC shell temperature and internal pressure during storage based on as-loaded conditions. This calculation provides an input to the calculations submitted as Enclosures 7 and 8, which are used to establish the actual safety margins based on the as-loaded conditions of DSCs 11-15. This calculation provided in Enclosure 9 contains proprietary information and is sought to be withheld from public disclosure in accordance with 10 CFR 2.390. As the entirety of the calculation is considered to be the intellectual property of AREVA, a redacted version of the calculation has not been included. The affidavit for the enclosure is provided in Enclosure 12.

Enclosure 10 provides Applied Analysis Corp. Calculation MNGP-018, "Accident Dose Assessment for MNGP DSCs 11-15". This calculation determines the offsite dose assuming a non-mechanistic release from the DSC closure welds.

Enclosure 11 provides Jensen Hughes Report 016045-RPT-01, "Risk Assessment of MNGP DSCs 11-15 Welds Using NUREG-1864[1] Methodology". This report compares the calculated risk of the alternative of leaving these casks, as-is, in their current stored location versus the alternative of transferring these casks back into the reactor building for inspection and then returning them to their storage locations.

Enclosure 12 contains an affidavit executed by AREVA. As the owner of the proprietary information submitted in Enclosure 9, AREVA certifies that the enclosed proprietary information has been handled and classified as proprietary, is customarily held in confidence, and has previously been withheld from public disclosure. AREVA requests that the enclosed proprietary information be withheld from public disclosure in accordance with 10 CFR 2.390.

NSPM requests the NRC grant the requested exemption by October 31, 2018, to support restoration of compliance with 10 CFR 72 and also to meet the requirements of the Confirmatory Order issued in Reference 1.

If there are any questions or if additional information is required, please contact Mr. Shane Jurek at (612) 330-5788.

Summary of Commitments

This letter makes no new commitments and no revisions to existing commitments.

Timothy J. O'Connor
Senior Vice President and Chief Nuclear Officer
Northern States Power Company – Minnesota

Enclosures (12)

cc: Administrator, Region III, USNRC
Rob Kuntz, Project Manager, Monticello Nuclear Generating Plant, USNRC
Christian Jacobs, Project Manager, Spent Fuel Storage and Transportation, USNRC
Resident Inspector, Monticello Nuclear Generating Plant, USNRC

[1] NUREG-1864, "A Pilot Probabilistic Risk Assessment of a Dry Cask Storage System At a Nuclear Power Plant"

Exemption Request for
Nonconforming Dry Shielded Canister
Dye Penetrant Examinations

Table of Contents Page

Exemption Request for Nonconforming Dry Shielded Canister Dye Penetrant Examinations

Table of Contents   Page

Appendices

List of Tables

List of Figures

Exemption Request for Nonconforming Dry Shielded Canister Dye Penetrant Examinations

Executive Summary

During the 2013 Independent Spent Fuel Storage Installation (ISFSI) cask loading campaign at the Monticello Nuclear Generating Plant (MNGP), owned and operated by Northern States Power Company, a Minnesota corporation (NSPM), doing business as Xcel Energy, six Type 1 NUHOMS®-61BTH Dry Shielded Canisters (DSCs) were loaded under Certificate of Compliance (CoC) 1004, Amendment 10. Condition 1 of the CoC allows use of the Standardized NUHOMS® System subject to the conditions of 10 CFR 72.212 and the CoC 1004 Technical Specifications (TS). TS 1.2.5 of CoC 1004 requires that all DSC closure welds not subjected to full volumetric inspection be dye penetrant tested (PT) in accordance with the American Society of Mechanical Engineers (ASME) Boiler and Pressure Vessel (B&PV) Code. The NRC questioned and NSPM subsequently determined that certain elements of the PT examinations performed on these six DSCs (called DSCs 11-16) did not comply with the examination procedures for compliance with TS 1.2.5. The NRC granted an exemption for DSC 16 from 10 CFR 72.212(a)(2), 10 CFR 72.212(b)(3), 10 CFR 72.212(b)(5)(i), 10 CFR 72.212(b)(11), and 10 CFR 72.214 in 2016 (Reference 6.1). NSPM is requesting an exemption from 10 CFR 72.212(a)(2), 10 CFR 72.212(b)(3), 10 CFR 72.212(b)(5)(i), 10 CFR 72.212(b)(11), and 10 CFR 72.214 to continue the storage of DSCs 11-15 in their respective Horizontal Storage Modules (HSMs).

This exemption request concludes that there is a reasonable assurance of safety to grant the requested exemption to continue the storage of DSCs in their safest possible configuration – in the storage condition in their respective HSMs. This reasonable assurance of safety is based on the following factors:

1. Reasonable Assurance of Weld Integrity: Based on the existing Quality Assurance (QA) documentation, engineering analysis, and expert evaluations presented herein, the following conclusions demonstrate that the subject welds possess sufficient quality to perform their design functions:

    a. Fuel Cladding Integrity: Cask loading reports and supporting radiochemistry records indicate that all fuel assemblies loaded into DSCs 11-15 met the TS requirements (TS Table 1-1t) for cladding integrity. No damaged fuel was loaded. The integrity of the fuel was further demonstrated by the fact that no unexpected dose rate readings were observed during the vacuum drying processes of DSCs 11-15. Therefore, the integrity of the first barrier against fission product release was confirmed by QA records.

    b. Weld Design: Multiple-layer welds effectively eliminate a pinhole leak since the chance of pinholes being in alignment on successive weld passes is not credible. There is no source for fatigue flaw extension; therefore, cycle fatigue growth of flaws

is not a credible phenomenon. Service-induced flaws under normal and off-normal conditions of storage are not credible.

c. Material and Welding Process: Shell, lid, and weld filler quality requirements were met. Austenitic stainless steels do not have a nil ductility transition temperature and thus the weld can sustain “large” flaws without a concern for flaw growth. Weld process qualification, welder qualification, and the automated welding processes designed for the specific application all ensure a quality weld.

d. Tests Performed: In-process visual inspections of welds performed by the welders, Quality Control (QC) visual examination (VT) inspections of fit-ups and welds and the vacuum hold, helium pressure and helium leak test all ensured confinement and quality of the welds.

e. Adequate Stress Margin in Welds to Accommodate Flaws: Stress margins were demonstrated by structural analysis using an analysis-based stress allowance reduction factor, theoretically bounding full-circumferential flaws, and a structural analysis assuming flaw distributions conservatively derived from Phased Array Ultrasonic Testing (PAUT) examination of DSC 16. A review of the weld head video, general area video, welding records, and DSC 16 was performed and determined that the indications found on DSC 16 are representative of those that might be found on DSCs 11-15. Additionally, it was determined that the same bounding analyses performed for DSC 16 should provide similar conservative results for the closure welds on DSCs 11-15. Regardless, further analyses have been performed to maximize the flaws located based on DSC 16 PAUT to demonstrate substantial margin to account for potential flaw uncertainties. These analyses are provided in Enclosures 2 through 5.

f. Additional Stress Margins in Welds: DSCs 11-15 heat loads and site-specific side drop conditions were applied to demonstrate additional margin exists and is available to account for any remaining flaw uncertainty that may exist. These analyses are provided in Enclosures 6 through 9.

2. Low Dose Consequences for a DSC in Storage: Notwithstanding the weld integrity demonstrated for DSCs 11-15, a reasonable assurance of safety is further supported by a radiological dose analysis. The dose analysis concludes that a non-mechanistic failure of the weld and a postulated release would result in no danger to the public as the dose consequences would be far below the regulatory limit of 5 rem Total Effective Dose Equivalent (TEDE) (Note: unless otherwise specified, all dose quantities identified in this Enclosure are TEDE). The dose analysis is provided in Enclosure 10.

3. Low Risk to the Public: Notwithstanding the weld integrity demonstrated for DSCs 11-15, a reasonable assurance of safety is further supported by a probabilistic risk assessment (PRA). This assessment concludes the risk of a potential Latent Cancer Fatality (LCF) for all five DSCs with noncompliant PT exams over a 20 year storage period is extremely unlikely (1.39E-12 LCF) and the risk associated with the

alternative of transferring all five DSCs into the MNGP reactor building to perform PAUT inspections, and then returning the DSCs to their respective HSMs for 20 years of storage is 1.66 times greater. The PRA analysis is provided in Enclosure 11.

Furthermore, the regulatory review provides an evaluation that satisfies the three basic criteria of 10 CFR 72.7 (authorized by law, will not endanger life or property or the common defense and security, and be in the public interest), including an assessment of alternatives. That assessment concludes that the continued storage of these five DSCs in their respective HSMs will not endanger life or property, will not endanger the common defense and security, and is in the public's best interest because the radiological risks of moving them for re-inspection are greater than the radiological risks associated with leaving them in their designed storage location.

Figure 1 provides a graphical representation of the defense-in-depth associated with the DSC design and NSPM's conclusion that the health and safety of the public and the common defense and security are preserved, and the public interest is best served, if the NRC grants the requested exemption.

Figure 1 – Preservation of Defense-in-Depth with Requested Exemption

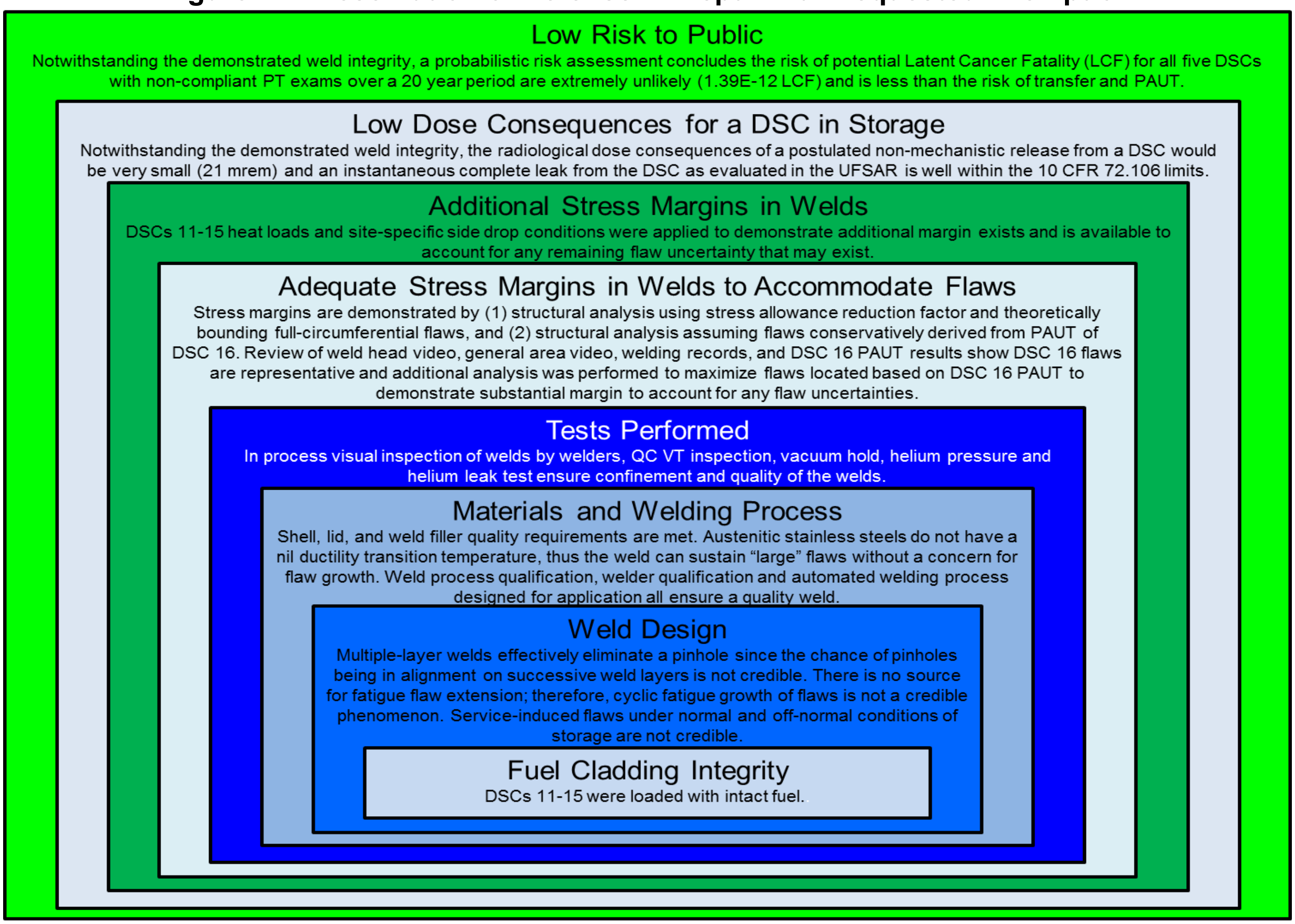

1.0 Background

During the 2013 ISFSI cask loading campaign at the MNGP, six Type 1 NUHOMS® 61BTH DSCs were loaded under CoC 1004, Amendment 10. Condition 1 of the CoC allows use of the Standardized NUHOMS® System subject to the conditions of 10 CFR 72.212 and the CoC 1004 TS. TS 1.2.5 of CoC 1004 requires that all DSC closure welds not subjected to full volumetric inspection be PT tested in accordance with the ASME B&PV Code. The NRC questioned and NSPM subsequently determined that certain elements of the PT examinations performed on these six DSCs did not comply with the examination procedures that support compliance with TS 1.2.5. As a result of this nonconforming condition, the NRC issued Confirmatory Order EA-14-193 on December 21, 2015. Action 1 from the order requires:

1. The licensee shall restore compliance to 10 CFR Part 72 to DSCs 11 through 16 within 5 years of the date the NRC takes final action upon the September 29, 2015, exemption request pending for DSC 16 (ML15275A023) or the exemption request is withdrawn, whichever is earlier.

The NRC took final action on the September 29, 2015, exemption request on June 15, 2016 (Reference 6.1), granting NSPM an exemption from the requirements of 10 CFR 72.212(a)(2), 72.212(b)(3), 72.212(b)(5)(i), 72.212(b)(11), and 72.214 only with regard to meeting TS 1.2.5 of Attachment A of CoC No. 1004, Amendment No. 10, for DSC 16. This exemption restored DSC 16 to compliance with 10 CFR 72 and allowed NSPM to transfer DSC 16 into an HSM for continued storage at the MNGP ISFSI for the service life of the canister.

Therefore, with DSC 16 restored to compliance, the purpose of this submittal is to request an exemption from 10 CFR 72.212(a)(2), 72.212(b)(3), 72.212(b)(5)(i), 72.212(b)(11), and 72.214 to allow the continued storage of DSCs 11-15 in their respective HSMs. In the interim, the condition of these DSCs has been evaluated in accordance with the NSPM Corrective Action Program (CAP). The CAP assessments concluded that there is reasonable assurance that DSCs 11-15 are safe in their current configuration and that they will continue to be safe for their service lifetime.

1.1 NUHOMS® System Design, Transfer and Storage

The Standardized NUHOMS® System is used for storage of spent fuel at the MNGP ISFSI. As listed in 10 CFR 72.214, the Standardized NUHOMS® System is approved for storage of spent fuel under the conditions specified in CoC No. 1004, Amendment 10, Revision 1. The system used at MNGP is under the general license provisions of 10 CFR 72.210.

The Standardized NUHOMS® System consists of:

- A DSC that provides criticality safety, confinement boundary, shielding, structural support and heat transfer (removal) for fuel assemblies.

- An HSM that provides structural support, heat transfer (heat removal), and shielding during storage on the ISFSI pad.

- A Transfer Cask (TC) that provides structural support and shielding during loading and DSC transfer to the HSM.

The NUHOMS® 61BTH DSC is a redundant weld-sealed containment pressure vessel with no penetrations in the storage configuration. For all practical purposes, the helium used to backfill the DSCs does not diffuse through stainless steel, so the design keeps leakage rates negligible. The multi-layer closure welds of the DSC effectively eliminate any pinhole leaks that might occur in a single-layer weld as the chance of pinholes aligning on successive weld layers is not credible.

The primary confinement boundary of the NUHOMS® 61BTH DSC consists of the Shell, Inner Top Cover Plate (ITCP), Inner Bottom Cover Plate, siphon/vent block, siphon/vent port covers, and the associated welds for these components. The redundant sealing of the DSC consists of the Outer Top Cover Plate (OTCP) and its associated welds. Refer to Figures 2, 3, and 4 for an illustration of the NUHOMS® 61BTH design.

While the ASME Code is not strictly applicable to the DSC, pursuant to TS 1.1.12.2, the DSC is designed, fabricated, inspected, and tested to the maximum extent practical to the ASME B&PV Code 1998 Edition through 2000 Addenda, Section III, Subsection NB. The confinement welds of the DSC are inspected in accordance with the Code, including alternatives to the ASME Code documented within TS 1.1.12.4.

After the canister is loaded, the remainder of the confinement boundary and seal welds[2] is welded to comply with the guidance of Interim Staff Guidance 15 (ISG-15) (Reference 6.2), ISG-18 (Reference 6.3), and the ASME Code alternatives. These are all multi-layer welds that receive root and final weld PT examinations with the exception of the weld for the OTCP, which receives root, mid-layer, and final PT examinations. Numerous tests are performed throughout the loading operations that directly or indirectly confirm DSC confinement integrity.

ISG-18 provides guidance for the design and testing of a redundant closure system. The NUHOMS® 61BTH System satisfies ISG-18 via the dual lid design option (refer to Sketch B of ISG-18) where the ITCP weld is a small partial penetration weld subject to PT examination and helium leak testing to the leak tight criterion of American National Standards Institute (ANSI) ANSI N14.5-1997, “American National Standard for Radioactive Materials – Leakage Tests on Packages for Shipment” (Reference 6.4). Although not credited as a confinement boundary in the ISFSI Updated Final Safety Analysis Report (UFSAR), the OTCP weld satisfies the large weld exception criteria for helium leak testing by incorporating a three layer minimum weld requirement where

[2] The confinement boundary and seal welds performed in the field are composed of the Inner Top Cover Plate weld, the Siphon Port Cover Plate weld, and the Vent Port Cover Plate weld. The redundant seal welds are the Test Port Plug weld and Outer Top Cover Plate weld.

each of the layers is subject to PT. The layer depth is limited by a flaw evaluation performed in accordance with ISG-15.

After loading the DSC with spent fuel and completion of the welding and welding inspection activities described above, the DSCs are transferred from the refuel floor to the ISFSI and inserted into an HSM. The HSM is the design location for interim storage of a DSC.

Transfer of the DSC is performed by lifting the DSC in a TC from the refuel floor and lowering it to the reactor building loading bay. In the reactor building loading bay, the DSC/TC is loaded onto a Transfer Trailer (TT). The DSC/TC on the TT is then moved via tugger (prime mover) out of the reactor building bay airlock to the ISFSI pad along an approved heavy haul path.

During the transfer, precautions for weather conditions and temperature conditions enhance the safety of the transfer of the DSC/TC to the HSM. Transfer of the DSC/TC is not permitted during severe weather, including ice and snow, lightning, tornadoes and high wind conditions. Other precautions such as verifying fire hydrants are operable, not permitting delivery trucks with flammable liquids or gases to pass the security checkpoint during transfer and insertion operations, and prohibiting the use of vehicles not associated with the transfer operations to be within 12 feet of the DSC/TC during transfer and insertion operations, are taken to enhance the safety of the move.

Each DSC is assigned a designated HSM location. After arriving at the ISFSI, the DSC/TC is moved in front of the designated HSM, the HSM door is removed and the DSC is prepared for transfer into the HSM. The TC is prepared for release of the DSC and the DSC/TC is aligned for insertion of the DSC into the HSM. Once aligned, a hydraulic ram system is used to insert the DSC into the HSM. The DSC slides into the HSM on rails located on the bottom of the HSM. After the HSM is closed, dose rates are verified to be within TS requirements.

1.2 Scope of Welds Included in the Exemption Request

The closure welds for a DSC are all multiple layer welds (also called multi-layer welds). That is, the welds are built up through successive layering of weld material. This technique is used to eliminate the effects of pinhole leaks that might occur on a single layer, taking advantage of the likelihood that pinholes in successive weld layers will not align. The following welds were subject to PT examinations:

- ITCP Weld – two weld layers – root and cover
- Siphon Port Cover Plate (SPCP) Weld – two weld layers – root and cover
- Vent Port Cover Plate (VPCP) Weld – two weld layers – root and cover
- Test Port Plug (TPP) Weld – two weld layers – root and cover

- OTCP Weld – three weld layers – root, intermediate, and cover

See Figures 2, 3, and 4 for illustrations of the welds.

1.3 Scope of Nonconforming PT Examinations

In the Fall of 2013, NSPM started a dry cask loading campaign at MNGP. By October 17, 2013, six canisters had been loaded in sequence with intact spent nuclear fuel[3] and welded closed. Five canisters (designated DSCs 11-15) had been placed into service in their respective HSMs. One canister (designated DSC 16) was located on the reactor building refuel floor in a TC and had been welded closed in preparation for transfer to the HSM.

During the loading campaign, two sets of videos were made of the loading activities. First, videos were made from cameras located onboard the automated weld machine. This video provides a close-up view of the weld development. The second video recorded general area activities performed on the refuel floor during canister loading. This video shows a wider range of the loading activities and was used to verify the PT/developer dwell times, hold time for certain TS activities, and other data. None of these videos are considered QA records.

On October 17, 2013, the NRC Senior Resident Inspector at MNGP observed part of the PT examination on the final weld of the OTCP for DSC 16. The inspector questioned if the dwell and development times of the examination were sufficient to meet the requirements of the PT examination procedure. Video recordings of the examination were reviewed by the loading services vendor (TriVis, Inc.), NSPM supervision, and the inspector. Procedural noncompliances were discovered and the loading campaign activities were stopped.

As part of an extent-of-condition review performed under the Root Cause Evaluation, video recordings of every PT examination performed during the 2013 campaign were reviewed to determine the extent of the noncompliance. Noncompliance with the PT examination procedure was noted for all of the examinations performed on DSCs 11-16. TriVis reviewed these noncompliant services pursuant to 10 CFR 21 and issued two reports (References 6.5 and 6.6).

[3] The 2013 ISFSI campaign loaded only intact fuel assemblies in accordance with TS 1.2.1 and Table 1-1c. The cladding of these assemblies is an additional confinement barrier for radioactive material.

Figure 2 – Typical Cross-Section View of DSC to Illustrate Confinement Boundaries

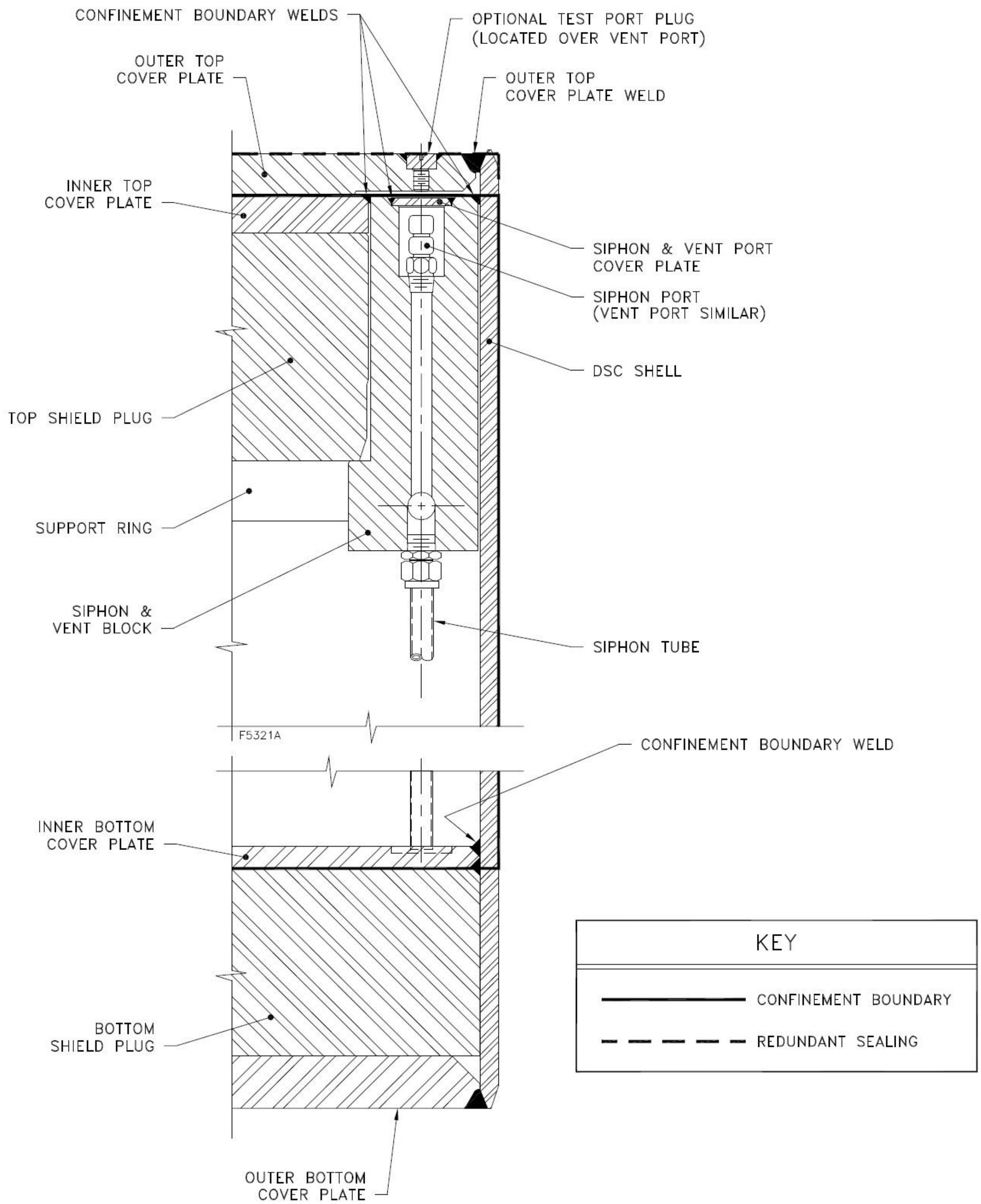

Figure 3 – ITCP, SPCP, and VPCP Field Closure Welds

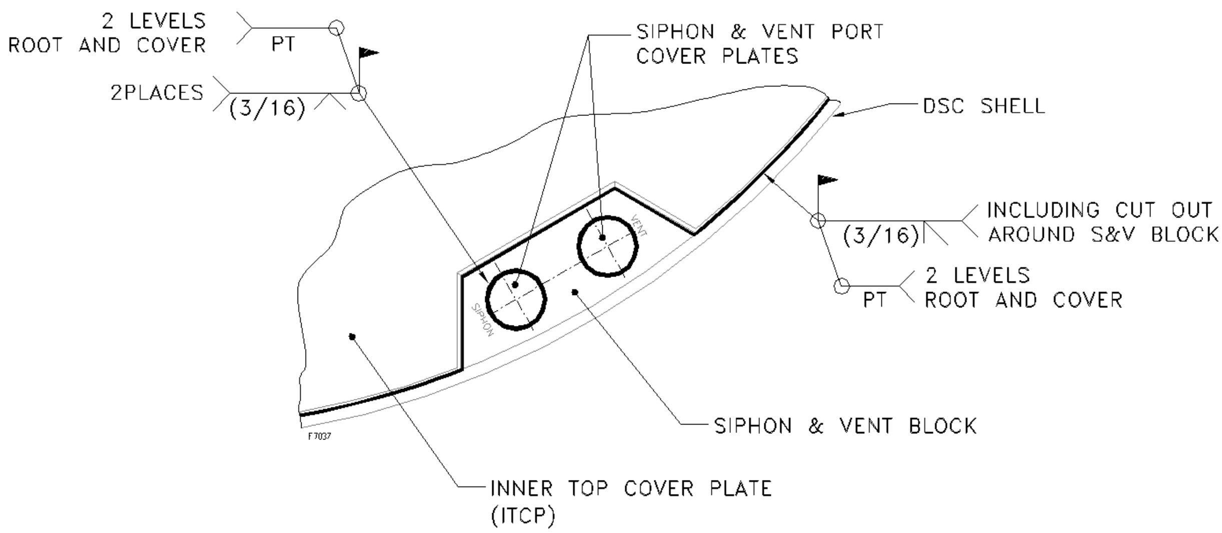

Figure 4 – OTCP and TPP Field Closure Welds

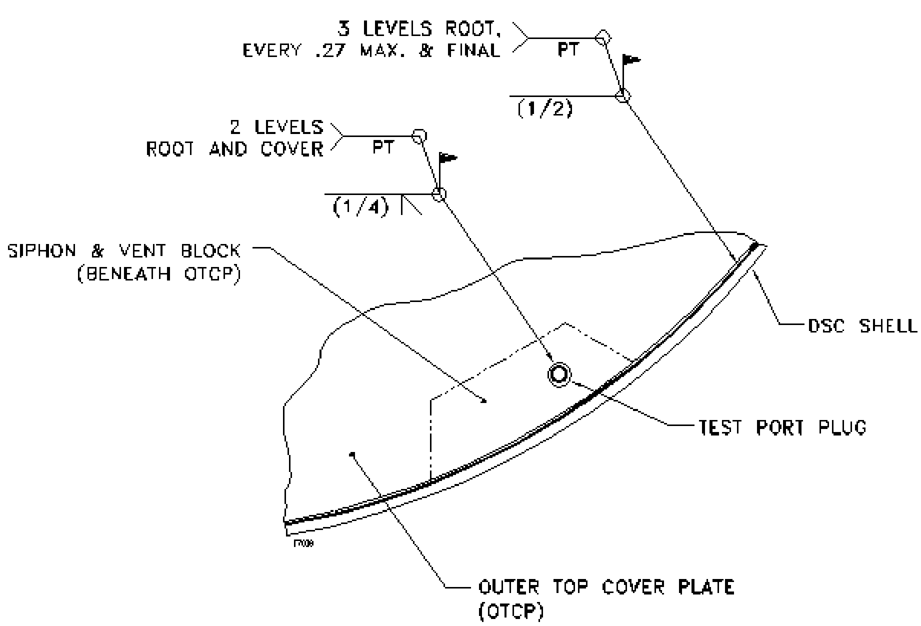

1.4 General Efficacy of Dye Penetrant (PT) Examinations

NUREG-1536, Revision 1, “Standard Review Plan for Spent Fuel Dry Storage Systems at a General License Facility”, Section 10.5.1.3 specifies that nondestructive examination (NDE) of weldments, including use of PT, should be established and documented. A written weld inspection plan prepared in accordance with an approved QA program that complies with 10 CFR Part 72, Subpart G must include this NDE plan. The inspection plan should identify welds to be examined, the examination sequence, type of examination, and the appropriate acceptance criteria as defined by either the ASME B&PV Code or an alternative approach proposed and justified by the applicant. NUREG-1536 specifically states that the NRC has accepted multiple surface examinations of welds, combined with helium leak tests for inspecting the final redundant seal welded closures.

In accordance with NUREG-1536, Revision 1, the procedures used for loading of DSCs 11-16 contained instructions for performance of PT examinations on every weld, including separate PT examinations for multiple layer welds.

The PT examinations required for the 61BTH DSC are specified in TS 1.2.5. TS 1.2.5 requires that PT examinations be performed in accordance with ASME B&PV code, 1998 Edition through 2000 Addenda, Section III, Division 1, Article NB-5000. The liquid penetrant test acceptance standards are described in Subsection NB-5350 of the Code.

For the field closure welds, the multi-layer weld technique with multi-layer PT examination specified in TS 1.2.5 was developed as an alternative to the ASME Code, Subsection NB requirement for volumetric examination.

In accordance with NB-5350, the PT procedure contains acceptance criteria that establish a minimum dimension of 1/16 inch for relevancy; specifically, “*only imperfections producing indications with major dimensions greater than 1/16 inch shall be considered relevant imperfections*.” Imperfections producing the following indications are considered unacceptable:

- cracks or linear indications
- rounded indications with dimensions greater than 3/16 inch
- four or more indications in line separated by 1/16 inch or less edge-to-edge
- ten or more rounded indications in any 6 square inches of surface

Thus, the PT examinations allow weld acceptance with some degree of imperfection.

PT examination performance is described in the ASME code, 1998 Edition through 2000 Addenda, Section V, Article 6. Section T-621.1 of Article 6 states that the procedure shall consider at least the following information:

a. The materials, shapes, or sizes to be examined and the extent of the examination;

b. Type (number or letter designation if available) of each penetrant, penetrant remover, emulsifier, and developer;

c. Processing details for pre-examination cleaning and drying, including the cleaning materials used and minimum time allowed for drying;

d. Processing details for applying the penetrant; the length of time that the penetrant will remain on the surface (dwell time), and the temperature of the surface and penetrant during the examination if outside the 50°F to 125°F range;

e. Processing details for removing excess penetrant from the surface and for drying the surface before applying the developer;

f. Processing details for applying the developer and length of developing time before interpretation; and

g. Processing details for post-examination cleaning.

The PT examination procedure used by TriVis incorporated these parameters. The PT examination materials specified in the procedure were Sherwin Hi-Temp® Penetrant Inspection System.

Appendix A of this enclosure includes Tables A-1 and A-2, which provide the overall weld temperatures, penetrant dwell times, cleaning method, cleaning dry time, and developer dwell time for the welds under the scope of this exemption request for DSCs 11-15.

Appendix B of this enclosure summarizes a report prepared by TriVis (Reference 6.6), which details testing performed by TriVis and Sherwin regarding noncompliant PT examinations. The intent of the testing by TriVis and Sherwin was to reproduce the penetrant and developer dwell times to demonstrate that they could have been effective examinations.

Although the TriVis assessment concluded that the majority of PT examinations could have produced interpretable results, NSPM determined from video records that the examiners did not follow the procedural and ASME code requirements, thus not meeting the TS requirements. See Appendix B for details.

1.5 Extent of Condition

Subsequent to the discovery of the noncompliant PT exams, the Nuclear Oversight (NOS) organization performed an extent of condition review to ensure the PT examinations were the only portion of the DSC loading campaign that was determined to be noncompliant. This extent of condition review included review of documentation (e.g., work packages, loading reports, welder qualifications, equipment calibration records), available video records and interviews with involved personnel. In accordance with 10 CFR 50 Appendix B, NOS is an independent organization within NSPM responsible for performing QA-related activities. This independence ensures the ability to prioritize safety over cost and schedule. As a result of the NOS extent of condition review, the following actions were taken:

- Non-destructive examination (NDE) personnel qualifications were reviewed and found to not meet the TriVis written practice and the ASME code. Specifically, the Level III NDE (who qualified the Level II personnel) did not complete a written examination as part of the qualification process. The vendor modified their qualification process to comply with the more rigorous requirements for Level III NDE qualification. The review also determined that the NDE personnel did not perform any welding inspection (VT or PT activities) on MNGP components other than DSCs 11-16.

- Since the QC individuals involved in the nonconforming PT examination process also performed the VT inspections for DSCs 11-16 and in order to determine extent of condition, NSPM also evaluated the process utilized for the VT inspection to determine if it might be suspect or in any manner noncompliant. NSPM reviewed remote video recordings of the VT inspections performed on the closure welds and the documentation of the VT examinations for DSCs 11-16. The review concluded that there is a reasonable level of confidence that the VT inspections were properly performed. The VT inspection process for these DSCs appeared to be diligent: flashlights were used at the proper distance from the weld surface, viewing angles were proper, and proper weld conditioning was evident.

- Additional verification activities were performed for DSCs 11-16, as described in Reference 6.7, including review of welding procedures, leak testing, weld depth measurement, etc. Physical verifications were performed on DSC 16 as this was the only DSC readily available when the nonconforming PT examinations were discovered. Additional details regarding the physical verifications performed on DSC 16 are contained in Reference 6.7.

- Subsequent to the final 10 CFR 21 report, TriVis issued an assessment of simulated PT conditions, using the actual dwell times and development times determined from video recordings of refuel floor activities, to determine if the PT examinations performed on DSCs 11-16 field closure welds would have been capable of producing interpretable results for detection of critical weld flaws (Reference 6.8). Although the TriVis assessment concluded that the majority of PT examinations could have produced interpretable results, NSPM determined from video records that the examiners did not follow the procedural and ASME code requirements, thus not meeting the TS requirements.

- Based on the results of the initial extent-of-condition review, NSPM determined that additional reviews were necessary. NSPM used an independent vendor to assess the quality of the welding performed during the performance of field closure welds on DSCs 11-16. This review indicated that there were good welding practices present in all of the welds examined and, in general, visible evidence of tie-in between the weld layers and the sidewall was present. However, the video also showed infrequent indications of areas where the potential for small weld flaws could exist. Regardless, the results did provide confidence that, for the vast majority of the time, welding was performed with automated welding processes in a manner consistent with well-done field welding practices. See Enclosure 2 for more details.

Through these additional reviews, NSPM has determined that there are no additional identified process deficiencies in the welding, TS testing, or examinations associated with the loading activities for DSCs 11-15.

1.6 <u>DSC 16 Exemption Request</u>

At the time of discovery of the noncompliant PT examinations, DSC 16 was in the TC on the reactor building refuel floor. In addition to performing compliant PT examinations, NSPM enlisted the cask vendor to develop and qualify a PAUT technique to examine the OTCP and ITCP welds of DSC 16. These examinations were performed in February 2015.

The PAUT of DSC 16 involved inspections from the DSC outside diameter (OD) using ultrasonic transducers. Special transducers were designed, manufactured, and tested to fit within the annular space between the TC inside diameter and the shell outside diameter. The OTCP and ITCP welds are contained within the top four inches of the TC cavity where the annular region is larger to accommodate the inflatable seal. In this region of the TC, the annular space (i.e., radial gap) is a minimum of 1/2 inch with an average of about 7/8 inch, which is large enough to accommodate a custom ultrasonic testing (UT) transducer. Performing a UT from the surface on the canister OD eliminates the concerns for weld surface conditions and partially filled weld preparation on the OTCP weld. This option achieves extensive coverage of the closure welds with better results, while eliminating the need to remove the OTCP to access the ITCP weld. Appendix E provides more description of the PAUT process that was employed on DSC 16.

NSPM subsequently submitted an exemption request for DSC 16 (Reference 6.7), asserting a reasonable assurance of safety based on integrity of the fuel, quality of the welding process employed, advantages of the multi-layer weld technique, visual inspections performed on the welds, helium leak and DSC backfill testing, lack of failure mechanisms and stress margins. The margins of safety were demonstrated by (1) structural analysis using an analysis-based stress allowance reduction factor and theoretically-bounding full-circumferential flaws and (2) structural analysis assuming flaw distributions conservatively derived from the PAUT examination.

In reviewing the PAUT approach, the NRC staff determined that the approach taken by NSPM was acceptable, because: (1) the PAUT system was capable of identifying and sizing the flaws in the ITCP and OTCP welds with the exception of small sections of the OTCP closure weld as a result of longitudinal welds in the canister shell and the portion of the ITCP closure weld around the siphon and vent block; (2) the size of the flaws used in the analysis conservatively bounds the size and distributions of flaws identified by PAUT; and (3) the applicant applied a reduction factor of 0.8 on the ASME B&PV Code specified minimum elongations to the weld material to account for flaws that may not have been detected by the PAUT examination. The NRC granted the exemption on June 15, 2016 (Reference 6.1). This exemption restored DSC 16 to compliance with 10 CFR 72 and allowed transfer of DSC 16 into an HSM for continued storage at the MNGP ISFSI for the service life of the canister.

1.7 Nature of Spent Nuclear Fuel in DSCs 11-15

DSCs 11-15 were loaded with spent fuel and all required welding was completed prior to them being placed into service. At the time of loading (in 2013), calculations showed that the combined decay heat load in the limiting DSC did not exceed 10.96 kilowatts (kW) and only one of the 305 loaded fuel assemblies had a burnup exceeding 45 gigawatt days per metric ton uranium (GWD/MTU). The maximum recorded burnup was 45.12 GWD/MTU (in DSC 15). Cask loading reports and supporting radiochemistry records indicate that all of the fuel assemblies loaded into DSCs 11-15 met the TS requirements (TS Table 1-1t) for cladding integrity. No damaged fuel was loaded. The integrity of the fuel was further demonstrated by the fact that no unexpected dose rate readings were observed during the vacuum drying processes of DSCs 11-15.

1.8 Summary of the Current Condition – DSCs 11-15

DSCs 11-15 were previously transferred to their respective HSMs. The condition of these DSCs has been evaluated in accordance with the NSPM CAP. The CAP Action Request 500001402246 assessments concluded that there is reasonable assurance that DSCs 11-15 are safe in their current configuration and that they will continue to be safe based on the closure weld design, welding process, and tests performed.

ISFSI in-service surveillances and monitoring includes daily temperature monitoring and annual HSM roof inspections. At this time, no adverse trends have been noted with respect to DSC leakage. Further, the NSPM Radiological Environmental Monitoring Program (REMP), among other things, requires weekly air sampling and analysis (although the air sample locations are not near the ISFSI). Additionally, the REMP requires monitoring of Thermoluminescent Dosimeters (TLDs) at the ISFSI. At this time, no adverse trends have been noted.

1.9 Regulatory Criteria

The regulatory criteria for this exemption request are those stated in 10 CFR 72.7, "Specific Exemptions":

> *The Commission may, upon application by any interested person or upon its own initiative, grant such exemptions from the requirements of the regulations in this part as it determines are authorized by law and will not endanger life or property or the common defense and security and are otherwise in the public interest.*

Each of the three criteria (Authorized by Law; Will Not Endanger Life, Property or Common Defense and Security; and is Otherwise in the Public Interest) is fully addressed in Section 4 of this exemption request.

The design criteria that are applicable to spent fuel handling, packaging, transfer, and storage systems are contained in 10 CFR 72.124, "Criteria for nuclear criticality safety". Specifically, 10 CFR 72.124(b) provides requirements for nuclear criticality safety of spent fuel handling, packaging, transfer, and storage systems. This regulation specifies that:

> *When practicable, the design of an ISFSI …must be based on favorable geometry, permanently fixed neutron absorbing materials (poisons), or both. Where solid neutron absorbing materials are used, the design must provide for positive means of verifying their continued efficacy. For dry spent fuel storage systems, the continued efficacy may be confirmed by a demonstration or analysis before use, showing that significant degradation of the neutron absorbing materials cannot occur over the life of the facility.*

10 CFR 72.104, "Criteria for radioactive materials in effluents and direct radiation from an ISFSI", specifies radiological protection requirements for ISFSIs. Specifically, 10 CFR 72.104(b) states:

> *(b) Operational restrictions must be established to meet as low as is reasonably achievable objectives for radioactive materials in effluents and direct radiation levels associated with ISFSI … operations.*

10 CFR 72.106(a) and (b) require that a controlled area be established for each ISFSI such that any individual located on or beyond the nearest boundary of the controlled area may not receive from any design basis accident the more limiting of a TEDE of 0.05 Sv (5 rem), or the sum of the deep-dose equivalent and the committed dose equivalent to any individual organ or tissue (other than the lens of the eye) of 0.5 Sv (50 rem). The lens dose equivalent may not exceed 0.15 Sv (15 rem) and the shallow dose equivalent to skin or any extremity may not exceed 0.5 Sv (50 rem).

10 CFR 72.122(b) requires that structures, systems, and components (SSCs) important to safety must be designed to accommodate expected site characteristics and environmental conditions associated with normal operations, maintenance, and testing, and to withstand postulated accidents.

10 CFR 72.128(a)(2) requires that the ISFSI be designed to ensure suitable radiological shielding under normal and accident conditions.

10 CFR 72.212(a)(2) provides the general license limitation to store spent fuel in casks approved under the provisions of this part.

10 CFR 72.212(b)(3) requires that each cask used by the general licensee conforms to the terms, conditions, and specifications of a CoC or an amended CoC listed in 10 CFR 72.214.

10 CFR 72.212(b)(5)(i) requires written evaluations, before use and before applying the changes authorized by an amended CoC to a cask loaded under the initial CoC or an earlier amended CoC, which establish that: (i) The cask, once loaded with spent fuel or once the changes authorized by an amended CoC have been applied, will conform to the terms, conditions, and specifications of a CoC or an amended CoC listed in 10 CFR 72.214.

10 CFR 72.212(b)(11) requires maintenance of a copy of the CoC and, for those casks to which the licensee has applied the changes of an amended CoC, the amended CoC, and the documents referenced in such Certificates, for each cask model used for storage of spent fuel, until use of the cask model is discontinued. The licensee shall comply with the terms, conditions, and specifications of the CoC and, for those casks to which the licensee has applied the changes of an amended CoC, the terms, conditions, and specifications of the amended CoC, including but not limited to, the requirements of any Aging Management Program put into effect as a condition of the NRC approval of a CoC renewal application in accordance with 10 CFR 72.240.

10 CFR 72.214 lists the approved designs for spent fuel storage casks, to include Certificate Number 1004 Amendment 10, Revision 1, representing model number NUHOMS® 61BTH.

10 CFR 72.236(f) requires the cask design to have adequate heat removal capacity without active cooling systems. 10 CFR 72.122(h) provides that the fuel cladding should be protected against degradation that leads to gross rupture. 10 CFR 72.126(a) provides that radioactive waste storage and handling systems must be designed and tested to control external and internal radiation exposures and control radiation exposure to personnel. 10 CFR 72.236(e) requires that the cask must be designed to provide redundant sealing of confinement systems. 10 CFR 72.236(j) requires that the cask must be inspected to ascertain that there are no cracks, pinholes, uncontrolled voids, or other defects that could significantly reduce its confinement effectiveness. 10 CFR 72.236(l) requires that the spent fuel storage cask and its systems important to

safety must be evaluated, by appropriate tests or by other means acceptable to the NRC, to demonstrate that they will reasonably maintain confinement of radioactive material under normal, off-normal, and credible accident conditions. This would require the structural fidelity of the DSC to be maintained during cask load drops, seismic and thermal events.

From these regulatory criteria, five design functions are derived for the DSCs:

- Criticality Safety
- Shielding (Radiological Safety)
- Heat Removal
- Confinement
- Structural Support

Each of the five design functions are assessed in this exemption request to demonstrate that they are not affected by the requested exemption and that the integrity of the field closure welds for DSCs 11-15 can be assured notwithstanding the nonconforming TS required PT examinations.

2.0 Requested Exemption

In accordance with 10 CFR 72.7, “Specific Exemptions”, NSPM requests the NRC grant an exemption for the MNGP ISFSI from the following requirements of 10 CFR 72.212 and 72.214, due to noncompliance with TS 1.2.5 of CoC No. 1004, Amendment 10, Revision 1:

- 10 CFR 72.212(a)(2), which states that this general license is limited to storage of spent fuel in casks approved under the provisions of this part.
- 10 CFR 72.212(b)(3), which states the general licensee must *"[e]nsure that each cask used by the general licensee conforms to the terms, conditions, and specifications of a CoC or an amended CoC listed in § 72.214”*
- 10 CFR 72.212(b)(5)(i), which requires that the general licensee perform written evaluations, before use and before applying the changes authorized by an amended CoC to a cask loaded under the initial CoC or an earlier amended CoC, which establish that the cask, once loaded with spent fuel or once the changes authorized by an amended CoC have been applied, will conform to the terms, conditions, and specifications of a CoC or an amended CoC listed in § 72.214.
- The portion of 10 CFR 72.212(b)(11), which states that *"[t]he licensee shall comply with the terms, conditions, and specifications of the CoC . . .”.*

- 10 CFR 72.214, which lists the approved spent fuel storage casks.

The proposed exemption is limited in scope in that it only relates to restoring compliance with consideration of the PT examinations that were improperly performed on certain field weld layers as described above. The proposed exemption involves no physical change to the canister design, and no change to the canister materials or the loading operation. The proposed exemption would allow DSCs 11-15 to be maintained in their safest possible configuration – in the storage condition in their respective HSMs.

Specifically, the PT examinations of DSCs 11-15 identified below in Table 2-1 were not performed in accordance with the approved procedures such that compliance with the TS 1.2.5 requirements cannot be assured.

For the DSCs, PT examinations are required for each weld layer listed below. Therefore, this exemption request is applicable to each of these weld layers. The weld layers affected by the nonconforming PT examinations are:

- ITCP Weld – two weld layers – root and cover
- SPCP Weld – two weld layers – root and cover
- VPCP Weld – two weld layers – root and cover
- TPP Weld – two weld layers – root and cover
- OTCP Weld – three weld layers – root, intermediate, and cover.

Table 2-1 – DSCs 11-15 Information

DSC Information		HSM Information		
Serial Number	**Model**	**Serial No.**	**Model**	**Placed into Service**
MNP-61BTH-1-B-2-011	61BTH	HSM-6A	HSM-H	9/9/2013
MNP-61BTH-1-B-2-012	61BTH	HSM-6B	HSM-H	9/17/2013
MNP-61BTH-1-B-2-013	61BTH	HSM-7A	HSM-H	9/26/2013
MNP-61BTH-1-B-2-014	61BTH	HSM-8A	HSM-H	10/7/2013
MNP-61BTH-1-B-2-015	61BTH	HSM-9A	HSM-H	10/14/2013

Upon receipt of the requested exemption, DSCs 11-15 will be treated as fully compliant with 10 CFR 72 in every respect. This exemption request does not apply to 10 CFR 71 transport designs, and transport applications.

NSPM requests the NRC grant this exemption request no later than October 31, 2018 to support restoration of compliance with 10 CFR 72 and meet the requirements of Confirmatory Order EA-14-193.

The exemption request demonstrates that DSCs 11-15 are safe to store for the duration of the license period and should be exempt from meeting the requirements of TS 1.2.5 for the subject welds. Therefore, upon receipt of the requested exemption, DSCs 11-15 will be treated as fully compliant with 10 CFR 72 in every respect.

3.0 Technical Assessment

The purpose of the technical assessment is to provide a justification for the current weld integrity in the DSCs necessary for the NRC to grant the exemption request. In addition to the PRA and dose assessment described in Section 4, this technical assessment directly supports the 10 CFR 72.7 criteria that the exemption will not endanger life, property or the common defense and security, and is otherwise in the public interest. This assessment is structured so as to address each of the DSC safety functions determined in Section 1.9 for the subject closure welds, noting that each of the welds has a different set of functions.

Table 3-1 – Weld Design Functions

Weld	Weld Effect on DSC Design Functions				
	Criticality Safety	Shielding	Heat Removal*	Confinement	Structural Support
Inner Top Cover Plate	NA	NA	NA	X	X
Siphon Port Cover Plate	NA	NA	NA	X	NA
Vent Port Cover Plate	NA	NA	NA	X	NA
Outer Top Cover Plate	NA	NA	NA	NA**	X
Test Port Plug	NA	NA	NA	NA**	NA

* Direct effects only
** Redundant barrier function for Confinement Design Function if the ITCP weld leaks.

Each of the five design functions is assessed in this exemption request to demonstrate none is affected by the requested exemption and that the integrity of the field closure welds for DSCs 11-15 can be assured notwithstanding the nonconforming TS-required PT examinations. Table 3-1 compares the welds covered in the exemption request to the functions that they are credited with performing.

3.1 General Weld Integrity

a. Fuel Cladding Integrity: As the first fission product barrier for nuclear fuel, it is important to note that the cladding of fuel loaded into DSCs 11-15 is known to be intact. In accordance with TS, BWR fuel is considered intact if it can be characterized with no cladding damage in excess of pinhole leaks or hairline cracks. Prior to loading each of the subject DSCs, NSPM confirmed, through cask loading reports and supporting radiochemistry reports, that the loaded fuel had no such through-cladding defects. Starting with the assurance that fuel cladding is intact helps ensure that any postulated leak through an undetected flaw would yield an insignificant release of fission products to the environment. NSPM verified the fuel loaded into DSCs 11-15 met the requirements of Table 1-1c of the TS. This was further demonstrated by the fact that no unexpected radiological dose readings were documented during the vacuum drying process required by TS 1.2.2.

b. Weld Design: The UFSAR only describes weld failure in terms of a possible pinhole leak in individual weld layers; otherwise the UFSAR does not describe weld failure as a malfunction of an SSC important to safety. Whereas this weld malfunction (pinhole leak in one weld layer) is described in the UFSAR, the likelihood (probability) is not credible. The UFSAR makes no explicit mention about how a pinhole leak in a weld layer is formed, whether it occurs during the weld formation or by subsequent canister loading operations, fatigue cycles during storage, or accidents. Rather, the UFSAR assumes/stipulates that pinholes may exist in individual layers. Thus, the existence of pinhole leaks is a non-mechanistic assumption of the UFSAR; and there is no underlying malfunction that causes its formation. The UFSAR discusses further assurance of safety by recognizing that the function of the multiple-layer welds is to reduce the chance that any pinhole leak through one layer will align with a pinhole in a successive weld layer (Section 3.3.2.1).

   Once in storage, there is no credible failure mechanism of the DSC top cover plate closure welds that would adversely affect DSC confinement. This fact is supported by the UFSAR, which identifies no long-term degradation mechanism that could cause the confinement welds to fail during the life of the DSC. Nevertheless, potential mechanisms were assessed in the NRC Safety Evaluation Report for NUHOMS® (Reference 6.9) and are summarized below:

   - Top cover plate and weld material are stainless steel with an established corrosion resistance described in UFSAR Section T.3.4.1. Further, the only welds subject to the outside environment are the outer layer of the OTCP weld and the TPP weld. The root layers of the ITCP and vent/siphon port covers are subject to the inert gas environment of the DSC cavity, which will preclude corrosion.

   - A reduction in cross section from plastic strain is not applicable to the top cover plate welds because the differential pressure across the top cover plates (between the cavity pressure and the environment) during storage conditions is minimal (less than one atmosphere).

- The mechanism of cyclic loading is not applicable to the top cover plate and closure welds because the extent of fatigue cycling experienced by the canister is below the threshold which the ASME B&PV Code Section III has established.

c. Materials: Procurement records (such as Certified Material Test Reports) demonstrate that the canister, lid, and weld filler materials met design standards and quality requirements, thereby assuring compatibility between materials and satisfactory material performance characteristics (e.g., material strength).

d. Welding Process: Notwithstanding the nonconforming PT examinations, the weld closures of DSCs 11-15 were performed under a 10 CFR 50 Appendix B QA program, such that the canister integrity is otherwise assured. Accordingly, welding materials were procured to quality requirements, welding processes were developed and qualified for the given configuration, and welders were appropriately qualified to the Code requirements. Welding parameters were specified in associated procedures and monitored as required. Any anomalies in welding processes would have been subject to identification and disposition in accordance with the CAP. See Appendix D for details concerning weld performance criteria.

The original weld head video review by an independent expert indicated that there were good welding practices present in all of the welds examined, and in general, visible evidence of tie-in between the weld layers and the sidewall was present. However, the video also shows infrequent indications of areas where the potential for small weld flaws could exist; a result commensurate with the extent of indications found by PAUT examination of DSC 16. See Appendix C for more details on this report.

A further examination of weld head video in conjunction with general area video (and the PAUT results from DSC 16) provided correlation between weld techniques and typical weld flaw characteristics for the given cask loading campaign of 2013.

The significance of any latent surface defect left undetected because of the noncompliant PT is minor. The design basis does not take any credit for detecting any particular flaw size, and any undetected flaw in one layer is not postulated to propagate into any other weld layer. Structural Integrity Associates, Inc. (SIA) concluded that defects would be limited in the through thickness dimension to the thickness of a single bead.

Even considering the possibility that any given layer of weld may have a leak through that layer, the licensing basis criterion stated in UFSAR Section 3.3.2.1 assures that the chance of pinholes being in alignment on successive independently-deposited weld layers is not credible.

It is also important to note that the presence of weld flaws is accounted for in the structural analysis of welds. The method of calculation of weld stresses includes a stress allowable reduction factor of 0.80 (per ISG-15) to account for flaws in the weld since the weld was never expected to receive a volumetric examination.

e. Tests Performed: The welding procedures used for this campaign required welder in-process inspections prior to each QC NDE examination to ensure a weld surface free of coarse ripples, arc strikes, coarse grooves, overlap, abrupt ridges and valleys, cracks, porosity or fish-eyes, lack of fusion, lack of penetration, undercut in excess of 1/32 inch or root concavity that results in less than minimum wall. QC VTs were required for fit-up and tack welds of the ITCP, siphon cover, vent cover, and OTCP joints. QC VTs were also required prior to the PT exams on the ITCP, siphon cover, vent cover, TPP and OTCP root and cover weld layers, and the OTCP intermediate weld layer.

NSPM evaluated the process utilized for the VT inspection to determine if it might also be suspect or in any manner noncompliant. NSPM reviewed remote videotape of the available VT inspections performed on the closure welds and the documentation of the VT examinations for DSCs 11-15. The review concluded that there is a reasonable level of confidence that the VT inspections were properly performed. The VT inspection process appeared to be diligent based on observation of proper lighting, proper distance from the weld surface, proper viewing angle, and proper weld conditioning. Therefore, the VT inspections for the field closure welds on DSCs 11-15 provide a reasonable basis that satisfactory welds were constructed with an acceptable level of quality and safety.

Satisfactory completion of two required vacuum pump-downs conducted on the DSCs demonstrated weld integrity of the ITCP confinement boundary. These pump-downs (conducted per TS 1.2.2) establish a differential pressure across the ITCP and siphon/vent block welds of approximately one atmosphere, which exceeds the magnitude of the 10 psig design pressure used in stress analyses for normal conditions. Although the vacuum pump-down imparts a pressure differential in a reverse direction from the confinement function, the pump-down demonstrates the basic function of the confinement barrier and the lack of a through-weld flaw in the ITCP and siphon/vent block welds sufficient to cause a loss of cavity helium (when in service).

Satisfactory completion of a required helium backfill pressure hold conducted on the DSCs also demonstrated weld integrity of the ITCP and siphon/vent block welds confinement boundary. These backfills (conducted per TS 1.2.3a) established and held a differential pressure of approximately 2.5 psig across the ITCP weld. This backfill pressure hold is performed above the required helium fill pressure for placing the canister in service. Further, this backfill imparts a differential pressure in the same direction as the confinement function and uses a test medium of helium, which is an appropriately small molecule that is very effective in revealing any through-weld flaws. In this respect, the backfill pressure hold further demonstrated the basic integrity of the confinement barrier and the lack of a through-weld flaw that would lead to a loss of cavity helium in the DSCs.

Satisfactory completion of the required helium leak test conducted on the DSCs specifically demonstrates the integrity of the primary confinement boundary (ITCP and siphon/vent cover plate) welds. Leak testing is performed after the root layer of the OTCP weld is completed such that the OTCP acts as a test lid. A vacuum is drawn through the test port plug to evacuate the space between the ITCP and OTCP to check for leakage across the confinement boundary. These tests (conducted per TS 1.2.4a) specifically demonstrate that the primary confinement barrier field welds are leak tight as defined in ANSI N14.5-1997. In this respect, the helium leak test demonstrates the basic integrity of the confinement barrier and the lack of a through-weld flaw in the field closure welds that would lead to a loss of cavity helium in the DSCs. To some extent, this test also demonstrates the integrity of the OTCP root layer welding because through-weld flaws of sufficient size would have prevented the necessary vacuum from being drawn in the space between the ITCP and OTCP. Following the helium leak test, the remainder of the OTCP weld was performed.

For the confinement boundary welds of the ITCP and siphon and vent port cover plates, helium leak testing is performed to satisfy 10 CFR 72 requirements, which is not required nor recognized by the ASME Code as a method of interrogating these welds. However, the helium leak test performed to the leak tight acceptance criterion of ANSI N14.5-1997 provides assurance that no through-weld flaws exist, and is a more direct indication than multi-layer PT of the integrity of the confinement boundary. Therefore, for the confinement boundary welds, the application of VT inspection for each weld layer and helium leak testing of the completed confinement boundary provides a basis that the welds were constructed with an acceptable level of quality and safety.

Therefore, a number of independent tests are available to verify adequate welds were performed on DSCs 11-15. In-process visual examination and QC VT examinations demonstrate that weld processes were followed and a weld meeting VT inspection criteria was developed. Vacuum pump-downs, helium backfill, and helium leakage tests verify the confinement integrity function and, to some extent, the structural integrity function of the DSC welds. As stated in Section 1.5, NOS independently reviewed these test activities and determined that they were performed in accordance with the appropriate procedures. Therefore, NSPM believes that it is reasonable to conclude the nonconforming PT examinations do not result in a lack of overall weld quality.

3.2 <u>Assessment of Criticality Safety Function</u>

10 CFR 72.124 requires that the ISFSI system should be designed to be maintained subcritical and to ensure that, before a nuclear criticality accident is possible, at least

two unlikely, independent, and concurrent or sequential changes have occurred in the conditions essential to nuclear criticality safety. The design of the system must include margins of safety for the nuclear criticality parameters that are commensurate with the uncertainties in the data and methods used in calculations and demonstrate safety for the handling, packaging, transfer and storage conditions and in the nature of the immediate environment under accident conditions. The design must also be based on favorable geometry, permanently fixed neutron absorbing materials, or both.
10 CFR 72.236(c) requires that the cask must be designed and fabricated so that the spent fuel is maintained in a subcritical condition under credible conditions.

To meet these requirements, the Standardized NUHOMS® System employs both fixed neutron absorbers and favorable geometry. The fixed neutron absorber is present in the form of metallic aluminum plates that include boron-containing particles. This material is ideal for long-term use in the radiation and thermal environment of a DSC. The favorable geometry is ensured by the basket assembly, which ensures fuel compartment pitch is maintained.

NSPM has determined that the elements of the criticality safety analysis are not impacted by the requested exemption. Criticality control of the spent fuel assemblies is assured through the use of fixed neutron absorber material installed in the basket assembly. The geometry of the basket must be maintained for all design loading conditions in order to support the assumptions for fuel compartment pitch and neutron absorber plate configuration. The field closure welds do not directly support the criticality design function, but do provide indirect support via the structural design function, which assures the geometry of the DSC and basket is maintained within the assumptions of the criticality analyses for all loading conditions.

3.3 Assessment of Shielding – Radiological Safety Function

10 CFR 72.104(b) requires that ISFSI systems must establish operational restrictions to meet the as low as is reasonably achievable (ALARA) objective for radioactive materials in effluents and direct radiation levels. 10 CFR 72.106(b) requires that any individual located on or beyond the nearest boundary of the controlled area may not receive from any design basis accident the more limiting of a TEDE of 0.05 Sv (5 rem), or the sum of the deep-dose equivalent and the committed dose equivalent to any individual organ or tissue (other than the lens of the eye) of 0.5 Sv (50 rem). The lens dose equivalent may not exceed 0.15 Sv (15 rem) and the shallow dose equivalent to skin or any extremity may not exceed 0.5 Sv (50 rem). 10 CFR 72.126(a) provides that radioactive waste storage and handling systems should be designed and tested to control external and internal radiation exposures and reliably minimize radiation exposure to personnel.

To meet these requirements, the Standardized NUHOMS® System provides multiple, independent layers of shielding to ensure doses remain as low as reasonably achievable. The DSC is constructed from stainless steel with carbon steel internals. A thick steel plug and two stainless steel cover plates provide axial shielding at each end of the DSC. The penetrations in the plug are located at the perimeter, away from the fuel assemblies. The DSC is loaded into an HSM, which provides substantial shielding during storage. The thick reinforced concrete walls and roof slab provide neutron and gamma shielding. The HSM's access opening is covered with a concrete door.

NSPM has determined that the elements of the radiological safety assessment are not impacted by the requested exemption. Such elements include: (1) the fuel selection process, and (2) the availability of canister metal for shielding. For the former, the existence of nonconforming PT has no bearing on the fuel selection process. For the latter, the top closure welds are not explicitly modeled in the shielding analyses such that a flaw or missed indication in the field closure welds has no influence on shielding effectiveness of the DSC, and hence, has no impact on the shielding design function.

3.4 Assessment of Thermal Performance (Heat Removal) Function

10 CFR 72.236(f) requires the cask design to have adequate heat removal capacity without active cooling systems. 10 CFR 72.122(h) provides that the fuel cladding should be protected against degradation and gross rupture. 10 CFR 72.122(b) states that SSCs important to safety should be designed to accommodate the effects of, and be compatible with, site characteristics and environmental conditions associated with normal operation, maintenance, and testing; and to withstand postulated accidents. 10 CFR 72.122(f) states that systems and components that are important to safety should be designed to permit inspection, maintenance, and testing.

To meet these requirements, the Standardized NUHOMS® System is designed to passively reject decay heat during storage and transfer for normal, off-normal and accident conditions while maintaining temperatures and pressures within specified regulatory limits. Within the HSM, the DSC is cooled by buoyancy-driven air flow through openings at the base of the HSM, which allows ambient air to be drawn into the HSM. Heated air exits through vents in the top of the shield block in the HSM ceiling, creating a chimney or "stack" effect. Metal heat shields are placed above and to either side of the DSC to protect the concrete surfaces of the HSM from thermal radiation effects.

NSPM has determined that the elements of the heat removal assessment are not impacted by the requested exemption. Such elements include: (1) the fuel selection process, and (2) the thermal character of the weld material on heat removal capacity. For the former, the existence of nonconforming welds has no bearing on the fuel selection process. For the latter, the field closure welds are not explicitly modeled in the thermal analyses such that a flaw or missed indication in the field closure welds has no influence on thermal performance of the DSC, and hence, has no impact on the thermal design function. However, the field closure welds indirectly support the thermal design function by virtue of their confinement function which assures the helium atmosphere in the DSC cavity is maintained in order to support heat transfer. The confinement integrity function is further evaluated below.

3.5 Assessment of Confinement Integrity Function

10 CFR 72.236(e) requires that the cask be designed to provide redundant sealing of confinement systems. 10 CFR 72.236(j) requires that the cask be inspected to ascertain that there are no cracks, pinholes, uncontrolled voids, or other defects that could significantly reduce its confinement effectiveness. 10 CFR 72.236(l), requires the design analysis and submitted bases for evaluation acceptably demonstrate that the cask and other systems important to safety will reasonably maintain confinement of radioactive material under normal, off-normal, and credible accident conditions.

10 CFR 72.122(h)(1) requires that the spent fuel cladding be protected during storage against degradation that leads to gross ruptures or the fuel must be otherwise confined such that degradation of the fuel during storage will not pose operational safety problems with respect to its removal from storage.

To meet these requirements, the Standardized NUHOMS® System employs redundant sealing. The confinement boundary for the system is comprised of the DSC shell, inner bottom cover plate, ITCP, siphon and vent block, siphon and vent port cover plate, and the welds that join them together. The confinement boundary is designed and tested to meet the leak tight criteria of ANSI N14.5-1997. The operating procedures require leak tight testing (i.e., less than or equal to 1.0E-7 cc/sec) in accordance with TS 1.2.4a, for the ITCP weld and the vent/siphon port plate weld.

Although the OTCP, TPP, and associated welds are not defined as confinement boundary components, they provide a redundant barrier to the release of radioactive material. However, since these welds are not subject to helium leak testing, they are not credited as part of the confinement boundary. For the redundant closure weld of the OTCP, multiple weld layers are specified (minimum of root, intermediate and cover). The thickness of each weld layer is less than the flaw size determined by a fracture mechanics evaluation performed per ISG-15 requirements. This design ensures there is low probability for flaws to align through successive weld layers, such that the existence of a critical flaw in the OTCP weld is not credible based simply on the multi-layer weld technique. This is similar to the basis used in UFSAR Section 3.3.2.1 for pinhole leaks. The redundant closure weld of the TPP is not subject to significant design loading, such that a two layer weld application is sufficient to ensure the integrity of the weld. Therefore, for the redundant closure welds, the application of the weld design contributes to the basis for an acceptable level of quality and safety in the welds.

NSPM has determined that the confinement integrity function is not impacted by the requested exemption. Satisfactory completion of the required helium leak test conducted on the DSCs has specifically demonstrated the integrity of the primary confinement boundary (ITCP and siphon/vent cover plate) welds. These tests (conducted per TS 1.2.4a) specifically demonstrate that the primary confinement barrier field welds are leak tight as defined in ANSI N14.5-1997. In this respect, the helium leak test demonstrates the basic integrity of the confinement barrier and the lack of a through-weld flaw in the field closure welds that would lead to a loss of cavity helium in the DSCs.

3.6 Assessment of DSC Closure Weld Structural Function

10 CFR 72.236(l) requires that the spent fuel storage cask and its systems important to safety must be evaluated, by appropriate tests or by other means acceptable to the NRC, to demonstrate that they will reasonably maintain confinement of radioactive material under normal, off-normal, and credible accident conditions. This would require the structural fidelity of the DSC to be maintained during cask load drops, seismic, and thermal events.

To meet these requirements, the Standardized NUHOMS® System partial penetration welds of the OTCP and ITCP are evaluated in accordance with the ASME B&PV Code Section III, Subsection NB code limits including applicable alternatives to the Code requirements.

NSPM has determined that the structural integrity function, including DSC retrievability, is not impacted by the requested exemption. An evaluation of weld design, materials, welding process, examinations and structural analysis has determined that no weld failure is expected under the design loading conditions and that additional margin exists and is available to account for any remaining uncertainty in the closure weld.

a. Current Licensing Basis Structural Functions of Closure Welds

As shown in Table 3-1, welds for the VPCP, SPCP, and vent port plug serve no structural function, so they are not assessed further in this section. The condition of the ITCP and OTCP welds has no bearing on the DSC retrievability.

As shown in Table 3-1, the ITCP, OTCP and associated welds perform structural design functions for the top closure on the DSC. These welds are explicitly modeled in the design bases analyses at their minimum effective throat thickness and are designed to accommodate loads due to normal, off-normal and accident conditions, and are required to satisfy ASME Code design criteria with the stress reduction factor applied per ISG-15.

In a broad sense, ISG-15 recognizes the multi-layer PT examination technique as an acceptable NDE method for partial penetration closure welds. This document acknowledges that imperfections or flaws may not be identified when using a progressive PT surface examination (i.e., performing PT examinations between individual weld passes) in lieu of volumetric examination, and therefore requires that a stress reduction factor of 0.80 (i.e., 20% penalty) be applied to the closure weld design. The stress reduction factor is analogous to weld quality factors which are applied for progressive PT examination in ASME B&PV Code Section III, Subsection NG-3000. Therefore, the stress reduction factor accounts for a potential reduction in weld quality due to the partial penetration vs. full penetration weld, the surface examination (i.e., PT) vs. volumetric examination technique (i.e., PAUT), and the potential for subsurface flaws to exist when only surface examinations are performed. Additionally, the maximum weld deposit depth for intermediate layers is kept smaller than the critical flaw depth in accordance with ISG-15.

b. <u>Methodology for Assessing DSC 11-15 Closure Weld Structural Functions</u>

Previous analyses that demonstrated stress margins for the DSC 16 closure welds were provided to the NRC in Reference 6.7, and again in Enclosures 2, 4 and 5 to this letter. These evaluations included (1) structural analysis using an analysis-based stress allowance reduction factor and theoretically-bounding full-circumferential flaws, and (2) a structural analysis assuming flaw distributions conservatively derived from the DSC 16 PAUT examination.

To further evaluate the structural integrity of DSCs 11-15, evaluations were performed to determine if it was reasonable to expect that the types and extent of flaw distributions found in DSC 16 could be used to represent the comparable closure welds of DSCs 11-15 (Enclosure 3) and additional analysis was performed using design basis loads with flaws located based on DSC 16 PAUT and maximized such that the weld flaws reached close to acceptable design limits (Enclosure 6). Following these evaluations, additional analysis was performed using site-specific heat load and side drop conditions to demonstrate additional margin exists and is available to account for any remaining uncertainty related to the welds (Enclosures 7 and 8). A description of each of these evaluations follows:

i. DSC 16 Closure Weld Flaw Evaluation

a. Analysis-Based Structural Analysis with Theoretical Flaws

For the OTCP, the original design basis calculations determined critical flaw sizes. Per ISG-15, the stress reduction factor of partial penetration welds with PT examination is 0.80. Since these welds are noncompliant with the PT requirements, the weld reduction factor is reduced beyond 0.80 based on a set of theoretical flaw distributions that might conceivably have gone undetected during DSC closure weld examinations. Thus, an analysis-based stress allowable reduction factor of 0.7 was calculated. The analysis is included in its entirety in Enclosure 2. Since the original design basis critical flaw calculations already uses a reduction factor of 0.7, the original analysis remains applicable. These design basis analyses determined for a 360^{o} circumferential flaw, an allowable flaw depth of 0.19 inch and 0.29 inch could exist for surface connected and sub-surface flaws respectively. The flaw sizes determined by these calculations bound any of the indications found on DSC 16 by PAUT.

For the ITCP weld, the calculation provided in Enclosure 4 documents the critical flaw size based on the maximum radial stresses in the welds due to design loads. The analysis calculates the critical flaw size for a weld size of 0.25 inch per the PAUT results for DSC 16 (which indicated a distance between the root and crown at the canister wall from 0.25 to 0.40 inches) in lieu of the design thickness of 3/16 inch. This increased weld size is considered equally applicable to DSCs 11-15 based on the joint configuration and same welding process application. The calculation assumes both a buried (sub-surface) and a surface flaw. A 360^{o} circumferential flaw was modeled and the critical flaw depth was calculated using ASME Section XI criteria. The critical flaw depth determined, 0.15 inches, is larger than the half of the weld which would exceed the typical weld layer. The original design basis calculation already considered a 0.7 stress reduction factor; therefore, no further analyses were performed to show that all component stresses remain below the stress allowable limits.

The flaw sizes determined by these calculations bound any of the indications found on DSC 16 by PAUT. Therefore, these calculations demonstrate that sufficient margin is included in the welds and indicates a reasonable expectation of satisfactory performance of each DSC for the design service lifetime of the DSC.

b. Structural Analysis Using PAUT Flaw Distribution:

A structural analysis was performed assuming flaw distributions conservatively derived from DSC 16 PAUT examination by applying bounding flaw heights and modeling the intermittent flaws as full circumferential. This structural analysis is fully described in Enclosure 6 and concludes that DSC 16 will continue to perform its function due to the adequate margins for the accident pressure and drop loads with the presence of the ITCP and OTCP weld flaw indications documented in the PAUT exam.

ii. Applicability of DSC 16 PAUT to DSCs 11-15

As part of the original extent of condition review, weld head videos were reviewed by SIA in 2014. This review determined that good welding practices were used. However, the video also shows infrequent indications of areas where the potential for small weld flaws could exist. Both inner and outer cover plate closure welds were recorded in some cases, but the video coverage was incomplete for all weld beads. Specifically, the video review covered the ITCP root and cover weld layers; the OTCP tack, root, intermediate and cover weld layers for DSCs 13 and 16; and the OTCP tack, root, intermediate and cover weld layers for DSCs 12, 14 and 15. No weld head video was available for DSC 11. The DSC 16 outer closure weld was concluded to be the most vulnerable to potential defects, because a greater frequency of irregular surface conditions was generated during welding.

Subsequent to this initial review, NSPM again contracted SIA to perform further reviews of available weld head videos along with general area videos, welding records, and PAUT results for DSC 16 to identify any correlations between the welding processes used during the 2013 loading campaign and the flaws identified by the PAUT. By correlating indications to the particular welding methods used on all six canisters (including DSCs 11-15), a reasonable case has been made that the types of indications found on DSC 16 are representative of those that may be found on DSCs 11-15. The results of the SIA analysis are provided in their entirety in Enclosure 3.

Regarding the ITCP, SIA concluded the flaws were related to sidewall lack of fusion (LOF) because of the flaw locations and also noted the weld joint geometry, the welding system used for the ITCP and the welding setup had potential for forming defects on the sidewall like the ones identified in DSC 16. From the review, SIA concluded the other five canister ITCP closure welds were welded in a similar manner, using similar welding procedures, equipment, welding process, filler material, and welding operators. Thus, it is reasonable to assume the other canister ITCP welds will have intermittent defects similar to those characterized in DSC 16. Therefore, the conditions of the ITCP welds are judged as similar for all canisters. In particular, the vertical weld wall of the weld groove is inherent to a single bevel design, and because there is limited room to tilt the tungsten electrode towards the side wall, any LOF defects that might form would likely be located on the vertical sidewall. LOF defects of similar sizes and locations seen in DSC 16 are reasonable assumptions for the other ITCP closure welds. The assumptions made for the ITCP closure weld bounding analysis in DSC 16 are considered reasonable for all ITCP canister closure welds.

Regarding the OTCP, SIA concluded that the defects located within the weld deposit are believed to be inter-bead LOF formed specifically at the interface between adjacent weld bead surfaces when conditions are favorable. The schematic model suggests that when the defects are present they would be found at the interfaces between weld beads 2 and 3 for bounding Flaw No.2, and between weld beads 3 and 4 for the representative flaw grouping. Such defects are displayed in Figures 5 and 6, respectively. The model would place the defects intermittently along two approximately vertical planes and distributed around the circumference. These vertical representations are characterized as parallel and offset. Defects would be limited in the through thickness dimension to the thickness of a single bead, because the mechanism develops the interbead LOF between the sides of adjacent weld beads where complete fusion is not achieved. This necessarily limits the height of defects developed in this way to something less than the heights of adjoining surfaces of the adjacent beads being deposited. Noting the DSC 16 flaw distributions were conservatively modeled as full circumference in the structural analyses by AREVA, and structural analysis results are clearly bounding for the DSC 16 OTCP closure weld, then the same bounding analyses should provide for similar conservative results for the other DSC OTCP closure welds.

Figure 5 – LOF between Bead 2 and Bead 3

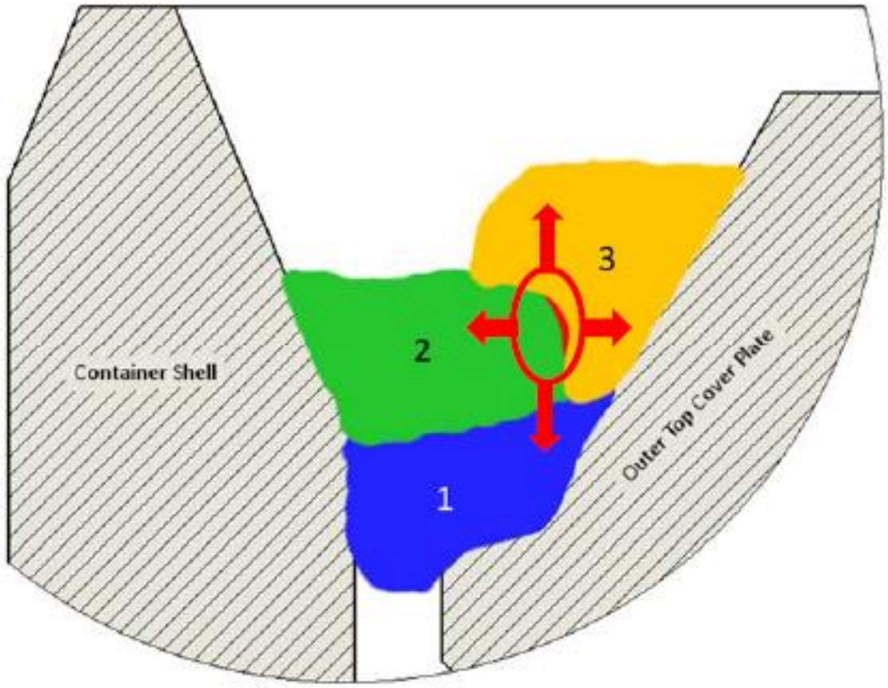

Although there were no welding videos available for DSC 11, general area videos were available to view the overall activities of fit-up, welding, and inspection for all or portions of those activities for all canisters, including DSC 11. It was seen that the operations for DSC 11 were like DSC 12 and DSC 13 in terms of types of activities, starts and stops for individual beads, and how often the activities were undertaken. The implication is that those welds should be similar in terms of potential defect size and frequency distributions. No significant differences were observed when welding the DSC 11 closure welds. These observations suggest that defect distributions in DSC 11 would be represented by the distributions in DSCs 12-15 based on similar welding procedures, similar welders, similar filler metals, similar equipment, similar welding technique, similar deposit thickness levels at inspection, and similar in-process corrective measures. Although more in process corrections were observed with all the canister closure welds prior to DSC 16; it does not necessarily follow that there will be more defects present simply because more corrective measures were observed. In fact, it is likely that the in-process corrections taken during welding likely are characterized by fewer conditions potentially leading to the types of defects described, suggesting that those welds have fewer defects and would be less prone to any longer continuous defects.

Figure 6 – LOF Between Bead 3 and Bead 4

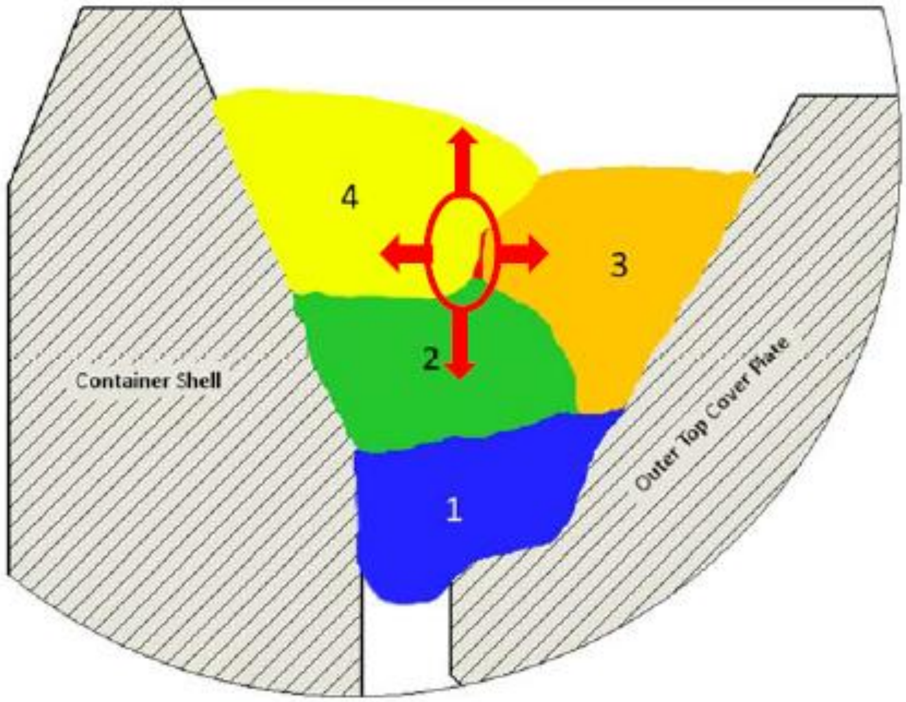

iii. Structural Analyses of DSCs 11-15 for Maximum Weld Flaw and Stress Margin Evaluation

a. Maximized Representative Flaw Evaluation

Notwithstanding the conclusions reached by SIA that the bounding flaws used to model the DSC 16 PAUT results would be reasonable to assume for all canisters (DSCs 11-15), NSPM contracted with AREVA to evaluate DSCs 11-15 closure welds per ASME Section III criteria. The analysis used design basis loads with flaws located based on DSC 16 PAUT results and maximized such that the weld flaws reach close to acceptable design limits. The purpose of this analysis was to address uncertainties related to the potential flaws that may be present in DSCs 11-15 by demonstrating the maximum flaws that could be shown to still meet the code limits. The analysis is provided in its entirety in Enclosure 6.

All of the applicable design bases loading conditions are considered in accordance with the requirements of ASME Section III Subsection NB. Similar to previous analysis, the uncertainties in the PAUT examination were accounted for by using a 0.8 reduction factor on the limit load and elastic plastic analyses.

The DSC design used in the calculation was typical of MNGP DSCs 11-16, and the modeled baseline flaws were representative of those indications identified by PAUT of DSC 16. Initial ANSYS finite element iterations were performed by increasing all the four flaws by a very small length resulting in a negligible increase in plastic strain. In the second step very large flaws were considered (leaving only one element of the model connected at each flaw) resulting in excessive strain for the elastic plastic side drop analysis. Similarly, additional iterations were performed such that the weld flaw reaches close to acceptable strain limit for the elastic-plastic side drop analysis. The final flaw configuration is presented in Figure 7.

Figure 7 – Maximum Weld Flaws based on the Allowed Design Limits

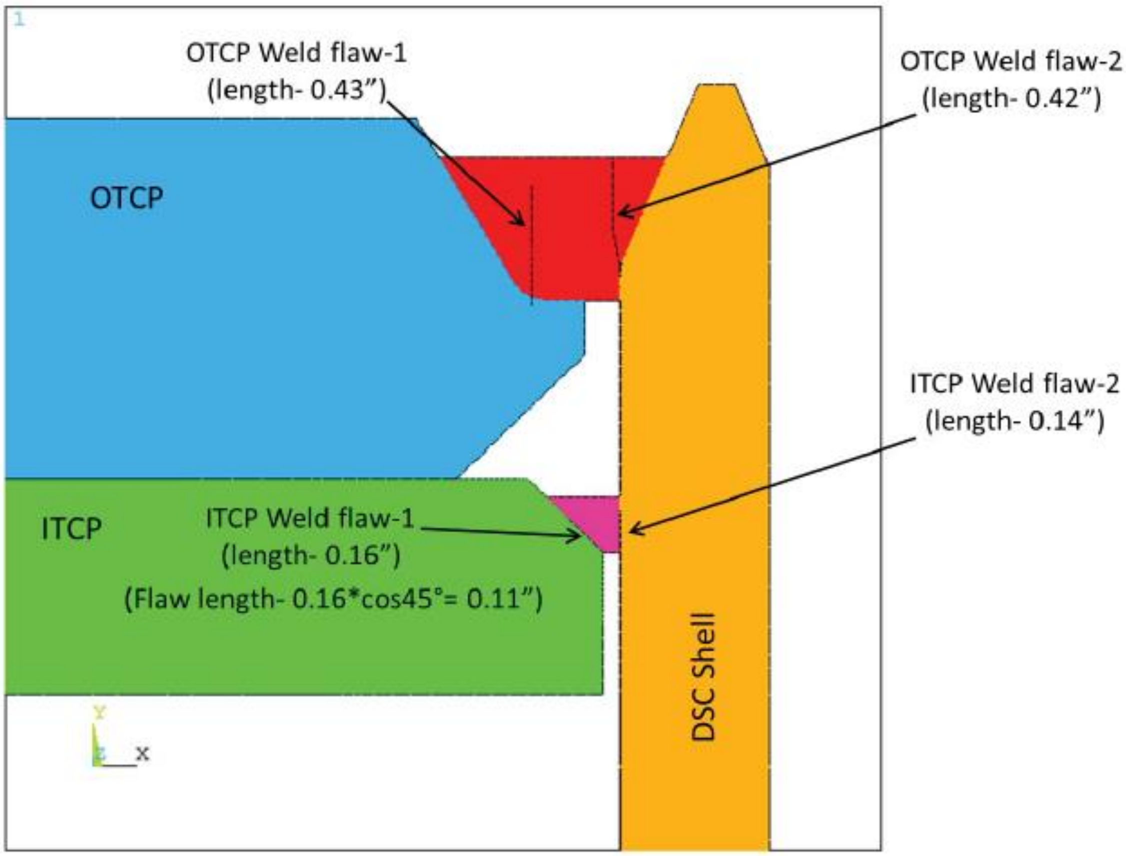

For both OTCP and ITCP, all weld flaws were maximized such that the weld flaw reaches close to acceptable design limits. The maximum modeled weld flaws for OTCP to DSC shell weld are 0.43 inch and 0.42 inch in height, which represents about 85% through-wall of the 0.5-inch minimum weld throat. The maximum modeled full-circumferential weld flaws for ITCP to DSC shell weld are 0.16 * cos(45°) = 0.11 inch and 0.14 inch in height, which represents respectively 58% and 74% through-wall of the 0.19-inch minimum weld throat as shown in Figure 7 (note that in Figure 7, weld heights are labeled as weld lengths). All four assumed flaws represent defects spreading over more than one weld bead. These flaws were located based on DSC 16 PAUT results and are considered representative locations for DSCs 11-15.

b. Additional Stress Margins in Welds

Notwithstanding the conclusions reached by SIA that the bounding flaws used to model the DSC 16 PAUT results would be reasonable to assume for DSCs 11-15, and the analysis by AREVA showing large flaws that could still be shown to meet the code limits, additional analyses were performed by AREVA to demonstrate additional stress margin exists using site-specific heat loads and side drop conditions. The purpose of these analyses was to address any remaining uncertainties related to potential flaws that may be present in DSCs 11-15 by demonstrating additional stress margins. These analyses are provided in their entirety in Enclosures 7 and 8.

Enclosure 7 evaluates the margins for DSCs 11-15 with the maximum flaws in the ITCP and OTCP closure welds based on the as–loaded temperature and pressure conditions.

Load Limit Analysis: The lower bound collapse pressure for Service Level A/B criteria was found to be 98.4 psi which is greater than the limiting pressure of 60 psi. Therefore the Service Level A/B criterion is satisfied. The lower bound collapse pressure for Service Level D criteria was found to be 144.1 psi which is greater than the limiting pressure of 90.2 psi. The lower bound collapse G-Load for Service Level D side drop criteria was found to be 204 g which is greater than the limiting G-Load of 104 g. Therefore the Service Level D criterion is satisfied.

Elastic-Plastic Analyses: The peak strains predicted by the elastic-plastic analyses for the bounding Service Level D event are shown to remain below the material ductility limits (28%) at the specified loading conditions, and also at one and a half times the specified loads, with a minimum margin of safety of 1.86. Therefore the elastic plastic analyses criteria are satisfied.

Enclosure 8 evaluates margins for the DSCs with the maximum flaws in the ITCP and OTCP closure welds based on the as-loaded temperature and pressure conditions, and the site specific side drop loads (i.e., actual approach slab parameters).

Limit Load Analysis: The lower bound collapse G-Load for Service Level D side drop criteria was found to be 204 g which is greater than the limiting G-Load of 104 g. Therefore the Service Level D criterion is satisfied.

Elastic-Plastic Analysis: The peak strain values remain below the material ductility limits at the specified loading conditions with a minimum margin of safety of 3.83. Therefore the elastic plastic analyses criteria are satisfied. It should be noted that with the as-loaded temperature and pressure conditions, and site specific side drop loads the margin of safety is higher than the margin of safety in similar analyses for DSC 16 (3.83 vs. 3.60).

Additionally, the analysis used to determine the bounding DSC shell temperature and internal pressure during storage operations based on the as-loaded configuration of DSCs 11-15 is included as Enclosure 9.

3.7 Conclusion

Based on the technical assessment presented previously, the proposed activity does not adversely affect the criticality safety, shielding/radiological safety, heat removal, confinement integrity or structural support functions of DSCs 11-15 as described in the UFSAR. In summary, the requested exemption results in continued safe operation of the MNGP ISFSI.

The integrity of the field closure welds for DSCs 11-15 can be assured with confidence even though the TS-required PT examinations were nonconforming. The fuel cladding integrity, weld design, materials, welding process, tests performed, adequate stress margins in the welds to accommodate the maximized representative flaws, and demonstration of additional stress margins to address any remaining uncertainties demonstrates the closure weld integrity of DSCs 11-15 is sufficient to ensure that the affected closure welds will continue to perform their design basis functions over the service lifetime of these canisters.

Application of the alternatives described in Section 4.3 would increase the radiological dose to workers, generate additional radiological waste, potentially create foreign material concerns and increase other operational risks to the station without a commensurate increase in safety as compared to receipt of the exemption request.

4.0 Basis for Approval

The proposed exemption is limited in scope in that it only relates to compliance with the inspection of certain field closure welds. The proposed exemption involves a change in compliance, but no physical change to the canister design, and no change to the canister materials or the loading operation. In this regard, the proposed activity cannot affect the frequency of any accident caused by the loading process (e.g., dropped TC or jammed DSC). It has no bearing on the frequency of natural events (flood, earthquake, tornado) that are natural phenomena. Therefore, the proposed activity does not result in an increase in the frequency of any previously evaluated accident. Furthermore, since the exemption does not affect the canister design and procedures this ensures that no new type of malfunction would be created.

The Technical Assessment herein provides the basis for the conclusion that a reasonable assurance of safety exists for the service lifetime of DSCs 11-15. Even though regulations

10 CFR 72.212(a)(2), 10 CFR 72.212(b)(3), 10 CFR 72.212(b)(5)(i), 10 CFR 72.212(b)(11) and 10 CFR 72.214 are not explicitly met, the nonconforming condition does meet the applicable criteria in 10 CFR 72.104, 10 CFR 72.124 and 10 CFR 72.236, and does meet the five necessary design functions of a DSC. Thus, the requested exemption is authorized by law; will not endanger life, property, or the common defense and security; and is otherwise in the public interest as described herein.

4.1 Authorized by Law

NSPM is requesting an exemption from requirements of 10 CFR 72.212(a)(2), 10 CFR 72.212(b)(3), 10 CFR 72.212(b)(5)(i), 10 CFR 72.212(b)(11) and 10 CFR 72.214. 10 CFR 72.7 provides the NRC with the authority to grant exemptions from the requirements of 10 CFR Part 72 provided they will not endanger life or property, or the common defense and security, and are otherwise in the public interest. This exemption request documents that these criteria are met. The exemption is thereby authorized by law.

4.2 Will Not Endanger Life, Property or Common Defense and Security

To demonstrate that the proposed exemption will not endanger life, property, or the common defense and security, NSPM presented three different analytical approaches that independently support the common conclusion of a reasonable assurance of safety. These three analyses demonstrated: (1) a reasonable assurance of weld integrity, (2) low consequences in the event of a non-mechanistic weld failure, and (3) low risk to the public. Each of these analyses is summarized below.

1. Reasonable Assurance of Weld Integrity: Based on the existing QA documentation, engineering analysis, and expert evaluations presented herein, the following conclusions demonstrate that the subject welds possess sufficient quality to perform their design functions:

   a. Fuel Cladding Integrity: Cask loading reports and supporting radiochemistry records indicate that all of the fuel assemblies loaded into DSCs 11-15 met the TS requirement (TS Table 1-1t) for cladding integrity. No damaged fuel was loaded. The integrity of the fuel was further demonstrated by the fact that no unexpected dose rate readings were observed during the vacuum drying processes of DSCs 11-15. Therefore, the integrity of the first barrier against fission product release was confirmed by QA records.

   b. Weld Design: Multiple-layer welds effectively eliminate a pinhole leak since the chance of pinholes being in alignment on successive welds is not credible. There is no source for fatigue flaw extension; therefore cycle fatigue growth of flaws is not a credible phenomenon. Service-induced flaws under normal and off-normal conditions of storage are not credible.

c. Material and Welding Process: The shell, lid, and weld filler quality requirements were met. Austenitic stainless steels do not have a nil ductility transition temperature and thus the weld can sustain “large” flaws without a concern for flaw growth. Weld process qualification, welder qualification, and automated welding processes designed for the specific application all ensure a quality weld.

d. Tests Performed: The welding procedures used for this campaign required welder in-process inspections prior to each QC NDE examination to ensure a weld surface free of coarse ripples, arc strikes, coarse grooves, overlap, abrupt ridges and valleys, cracks, porosity or fish-eyes, lack of fusion, lack of penetration, undercut in excess of 1/32 inch or root concavity that results in less than minimum wall. QC VTs were required for fit-up and tack welds of the ITCP, siphon cover, vent cover, and OTCP joints. QC VTs were also required prior to the PT exams on the ITCP, siphon cover, vent cover, TPP and OTCP root and cover weld layers, and the OTCP intermediate weld layer.

e. Adequate Stress Margin in Welds to Accommodate Flaws: Stress margins were demonstrated by structural analysis using an analysis-based stress allowance reduction factor and theoretically-bounding full-circumferential flaws and a structural analysis assuming flaw distributions conservatively derived from PAUT examination. A review of weld head video, general area video, welding records and DSC 16 PAUT was performed that has determined that the indications found on DSC 16 are representative of those that may be found on DSCs 11-15 and that the same bounding analyses performed for DSC 16 should provide for similar conservative results for the other DSC closure welds. Regardless, additional analysis has been performed to maximize the flaws located based on DSC 16 PAUT to demonstrate substantial margin to account for potential flaw uncertainties.

f. Additional Stress Margins in Welds: DSCs 11-15 heat loads and site-specific side drop conditions were applied to demonstrate additional weld margin exists and is available to account for any remaining flaw uncertainty that may exist.

2. Low Dose Consequences for a DSC in Storage: Notwithstanding the weld integrity that is demonstrated for DSCs 11-15, a reasonable assurance of safety is further supported by a radiological dose analysis which concludes that a non-mechanistic failure of the weld and a postulated release would result in dose consequences that would be far below the regulatory limit (5 rem). The dose analysis is provided as Enclosure 10.

   In general, the analysis used the guidance contained within NUREG-1567 (and other relevant guidance documents as described in Enclosure 10) to develop the dose acceptance criteria, source term isotopes of concern, isotopic fuel rod activity released from the rods to the DSC, DSC deposition rates, and calculated atmospheric dispersion factors (X/Q). Additionally, the dose analysis takes into account DSCs 11-15 specific fuel parameters to conservatively determine the radiological dose consequences from a postulated release from a single DSC at the MNGP ISFSI pad location to the site boundary. Source terms were generated using the ORIGEN-ARP computer code and organ dose calculations were performed using the RADTRAD computer code. Based on a licensing basis that postulates no confinement failure and a satisfactory leak tight helium leak test (i.e., less than or equal to 1.0E-07 cc/sec) for each canister (DSC 11-15), there is no basis and no method for theorizing a potential leak flow rate based on leak testing requirements. To arrive at a hypothetical accident release for the DSCs 11-15 with noncompliant dye penetrant examinations, the following methodology was utilized:

- The hypothetical accident release is not triggered by a cask drop event, fire or any known material stress/corrosion failure process.

- As such, a reasonable upper limit realistic leak diameter (hole size) is postulated to be no larger than the maximum allowable leak diameter associated with the packaging and transport of radioactive materials.

- Review of the DSC activity identifies isotopes of interest and is used to determine the specific activity within the DSCs. 10 CFR 71 is then utilized to determine the maximum allowable “package” activity limit. As shown in the calculation, Kr-85 is the limiting isotope remaining within the subject DSCs.

- ANSI N14.5-1997 may then be used to calculate an allowable release rate (consistent with 10 CFR 71) and applying Table B.2 to back-calculate an associated leak diameter (hole size).

- The leak diameter calculated above can then be used to calculate a hypothetical accident release based upon the critical mass flux release rate resulting from the limiting pressure/temperature conditions within the DSCs from other postulated events. For this assessment, the limiting event is considered to be the Blocked Vent event with elevated internal pressure and temperature conditions within the subject DSCs.

The assumed hole size of 0.011 cm diameter determined using this method is among the largest hole sizes considered in Table B.2 of ANSI N14.5-1997. Thus this hole size, based on the allowable leak rate, is deemed conservative for a postulated accident event not involving a cask drop or fire. The described approach results in a leakage rate of 1.573 cc/sec, which is conservative when compared to the DSC accident leak rate postulated in SMSAB-00-03, “Best-Estimate Offsite Dose from Dry Storage Cask Leakage” (Reference 6.10), of 1.3E-05 cc/sec. In addition to the DSC leakage rate calculated above, three additional, progressively larger leaks, are assumed based on holes sizes of 4.0E-03 cm^2, 2.4E-02 cm^2 and 1.0E-01 cm^2.

The computed accident dose results are considered to be conservative for several reasons. Conservatisms that are directly scalable include the Regulatory Guide (RG) 1.109, "Calculation of Annual Doses to Man from Routine Releases of Reactor Effluents for the Purpose of Evaluating Compliance with 10 CFR Part 50, Appendix I", X/Q and use of a 100% occupancy factor assumed for the public at the nearest plant boundary. Conservatisms that are not directly scalable include the impact from the failed fuel percentage, the calculated natural deposition coefficient, and the consideration of DSC leakage at the maximum critical flux rate for the entire 30-day postulated accident duration.

The calculation determines that in the storage condition, the controlled area boundary radiological dose consequences of a postulated non-mechanistic release from a DSC would be very small (21 millirem), and when applying more realistic dispersion factors would be even lower (5 millirem). The results when applying the more realistic dispersion factors are summarized in Table 4-1.

Achieving the conservatively-calculated dose result of 21 millirem supports a reasonable assurance of safety because of its considerable margin to the 10 CFR 72.106 regulatory limit of 5 rem.

Table 4-1 – Organ Dose with Realistic Dispersion Factor Data for Four Different Hole Sizes

Organ Dose with Realistic Dispersion Factor Data		
Area (cm^2)	Leakage Rate (CFM)	Effective Dose (mrem TEDE)
9.5033E-05	3.333E-03	5
4.0000E-03	1.403E-01	156
2.5000E-02	8.768E-01	953
1.0000E-01	3.507E+00	3,674

3. Low Risk to the Public: Notwithstanding the weld integrity that is demonstrated for DSCs 11-15, a reasonable assurance of safety is further supported by a PRA which concludes the risk of a potential LCF for all five DSC with noncompliant PT exams over a 20 year storage period is extremely unlikely (1.39E-12 LCF). The risk associated with the alternative of transferring all five DSCs back into the MNGP reactor building, performing PAUT inspections and returning the DSCs to their HSMs for 20 years of storage is 1.66 times higher. The risk analysis is provided in Enclosure 11.

   The approach and methodologies in NUREG-1864 were used as the basis for this risk assessment. NUREG-1864 documents the NRC risk assessment of a spent fuel dry cask storage system at a BWR site. The NUREG-1864 study is for the Holtec International HI-STORM 100 cask system and covers the onsite handling, transfer, and storage phases of the cask life cycle. The analysis covers a broad spectrum of postulated initiating events and hazards (e.g., drop scenarios, external hazards) and calculates the risk associated with the postulated initiating events.

Jensen Hughes, Inc. developed a methodology to apply NUREG-1864 and extrapolate the methodologies and results by utilizing the configuration similarities between the MNGP model and the NUREG-1864 model, and applying MNGP site specific considerations (the fuel loaded, flood hazard, seismic risk, etc.) and the technology specific configuration (horizontal storage versus vertical) inputs where applicable. The overall goal was to compare the calculated risk of the alternative of leaving these casks as-is in their current storage location versus the alternative of transferring DSCs 11-15 back into the reactor building for inspection and then returning them to their respective HSM storage location on the ISFSI pad.

The assessments determined the absolute value of LCF risk for DSCs 11-15 and the relative risk of the alternative considering the potential presence of flaws in the DSC lid welds. The major assumptions used in this quantitative evaluation are:

a. Consistent with NUREG-1864, time based initiating events (seismic events, high winds, floods) are assumed not to occur during transfer of the DSC to and from the reactor building and during inspection of the welds, based on the short amount of time that occurs during transport and inspection.

b. Tipping of the HSM due to a seismic or high wind event is assumed incredible, based on the horizontal configuration of the HSMs.

c. Sliding of the HSM is assumed to have no impact on the DSC. The likelihood of sliding is low based on the size and weight of the HSMs and the low likelihood that a wind or seismic event occurs. If sliding occurred, no damage would occur to the DSC unless the HSM was slid into another object or off of the ISFSI pad.

d. The failure probabilities for the DSC shell given a drop are based on similarity to the Multipurpose Canister (MPC) shell evaluated in NUREG-1864. DSC lid welds with flaws, are assumed to be the same capacity as the shell, which gives an overall DSC failure probability of twice the MPC shell failure probability from NUREG-1864 for the applicable drops. This is based on the evaluation in NUREG-1864 that lid welds are robust compared to the MPC shell, based on weld type and weld redundancy, so the presence of weld flaws degrades the capacity from robust to be equal to the shell capacity.

e. Thermal scenarios were considered incredible based on the evaluation of the MPC in NUREG-1864, which included weld flaws for shell welds, which indicate robust design capacity against thermal events, and the assumed equivalence of the DSC shell and lid welds to the MPC, and the short time duration of blocked vent and aircraft fire events.

f. Consistent with NUREG-1864, the conditional probability of failure of the fuel cladding and the DSC is assumed to be 1.0 for large aircraft overflight strikes, and meteorite strikes. The presence of potential weld flaws does not impact the resulting risk calculations. If detailed evaluations showed the potential for DSC survival given a large aircraft or meteorite strike, the potential for weld flaws may impact the resulting probability of release, but given the uncertainty and the potential magnitude of these two events, it is assumed that the DSC will fail regardless of the presence of potential weld flaws.

In conclusion the risk of both alternatives is very small and the difference in risk between the alternatives is not significant. With regards to the effects of the welds having noncompliant PT examinations, the risk of transferring these casks back into the reactor building for inspection includes higher failure probabilities given a cask drop for drops that occur prior to the inspection. For the alternative of the continued storage in the HSMs, risk as estimated in this evaluation is not affected by the potential presence of weld flaws because the included initiating events that could fail the DSC are assumed to fail the DSC with probability of 1.0, consistent with NUREG-1864, for aircraft strikes and meteorite strikes, based on the uncertainty of, and the potential magnitude of such events.

The magnitude of risk of either alternative is similar to the magnitude of risk of the reference site in NUREG-1864, with the differences attributable to the number of stages applied to the risk model for MNGP and the different frequency of the initiating events at each site. Overall, the differences are small, in the context of the total quantified risk.

In considering the acceptance criteria, NRC document “Risk-Informed Decision-Making for Nuclear Material and Waste Applications”, (Reference 6.11) was reviewed. This document indicates that, for exemptions and changes to the licensing basis of a facility that would tend to increase risk, very general guidance can be adapted from the RG 1.174, “An Approach for Using Probabilistic Risk Assessment in Risk-Informed Decisions on Plant-Specific Changes to the Licensing Basis”, using quantitative health guidelines (QHGs). NUREG-1864 indicates that the risk metrics associated with QHG-1 (public individual risk of acute fatality) and QHG-2 (public individual risk of LCF) were quantified for the reference site, and also indicates that the contribution for QHG-1 was negligible for the reference site. Therefore, it is reasonable to assume that the MNGP results for QHG-1 would be similar and consequently, the primary focus of the risk analysis was with respect to QHG-2. For QHG-2, Reference 6.11 proposes that a public individual risk of LCF is negligible if it is less than or equal to 2.0E-06 LCF/year.

As seen above, the overall risk of continued storage of DSCs 11-15 in their respective HSMs on the ISFSI pad is very low and is several orders of magnitude lower than the criteria for considering the risk negligible as proposed in Reference 6.11. In addition, the continued storage risk, as estimated in this evaluation, is not affected by the potential presence of weld flaws because the included initiating events that can fail the DSC are assumed to fail the DSC with a probability of 1.0. Therefore, the proposed exemption does not reduce the risk from its present value, whereas the proposed alternative of transferring these casks back into the reactor building for inspection and then returning them to their storage location, would increase the risk.

Receipt of this exemption for DSCs 11-15 will allow them to be maintained in their safest possible configuration – in the storage condition in their respective HSMs. By restoring DSCs 11-15 to fully compliant status with respect to 10 CFR 72, the proposed exemption restores a licensed configuration that will not endanger life, property, or the common defense and security.

4.3 Otherwise In the Public Interest - Alternatives

NSPM has evaluated and discussed with NRC staff many alternatives to the proposed exemption request (References 6.7, 6.12 and 6.13). To facilitate the evaluation of those alternatives, the credible alternatives are grouped as follows:

- Unload DSCs, discard, and replace
- Repair DSC welds (remove and re-perform with compliant PT exams)
- DSC lid augmentation
- PAUT In-Situ (at the ISFSI)
- PAUT in the reactor building

It is noted that in all cases the proposed alternatives result in an occupational radiological dose significantly greater than the projected dose in the event of receipt of this exemption. In accordance with 10 CFR 20, NSPM is required to maintain radiological exposure ALARA. Performance of any of the alternatives would expose workers to additional radiological dose with no discernible safety benefit as discussed previously. Therefore, use of any of the alternatives in lieu of receipt of this exemption would result in NSPM failing to maintain doses ALARA.

4.3.1 Methodology for Evaluating Alternatives

Each group of alternatives is evaluated for technological and licensing challenges (i.e., feasibility), and the potential to increase safety confidence and the criteria of:

- Operational safety and risk
- Occupational dose
- Contaminated material and radioactive waste
- Cost

4.3.2 Unload DSCs, Discard, and Replace

Consideration was given to cut open and unload DSCs to the spent fuel pool (SFP) in accordance with approved procedures, then process and dispose of the DSC, and reload the same quantity of spent fuel into a new DSC, sealing and transferring the DSC to its respective HSM. The activity of returning a DSC from the HSM, cutting open and unloading is described in the UFSAR and approved plant procedures are available to perform this activity. Therefore, this alternative is both technologically feasible and accounted for under the license. However, there remains an open question associated with transfer of a noncompliant DSC from the HSM to the reactor building[5]. Resolving this open question would require addressing many of the same elements as those in the proposed alternative, while also taking into account the increased operational risks associated with performance of the transfer operations. Regardless, this alternative provides no discernible safety benefit over the proposed alternative for which it has been demonstrated that the DSCs will continue to meet their design functions.

Operational and Safety Risk:

This alternative involves extracting the DSCs from their HSMs and transferring them to the reactor building for lid removal, unloading, and disposal. This alternative also includes the evolution of re-flooding the cavity. The fuel would then be loaded into a new canister, decontaminated, sealed, and transferred to the HSM. Therefore, this alternative increases the risk of fuel handling accidents, heavy load handling accidents, and risks damaging the DSCs (e.g., scratching). Additionally, this alternative carries the risk associated with re-flooding the DSCs

[5] NSPM has identified in prior interactions with the NRC that there remains an open question regarding the ability to move the DSCs with noncompliant PT exams. NSPM has reviewed the current licensing basis and believes it may require a licensing action to perform any evolution that involves moving the DSCs out of their HSMs because the DSCs are not in compliance with the TS. The NRC has requested that NSPM identify what available actions are within the current licensing basis and provide a request for NRC review, if necessary.

and the potential for SFP foreign material entry and SFP contamination due to the necessary SFP operations.

Occupational Dose:

To perform this alternative on a single DSC, the transfer and unloading activities on the reactor building refuel floor would expose workers to an occupational radiological dose of approximately 0.5 rem per canister. Furthermore, the dose of 0.5 rem per canister is an estimated dose involving the loading of a new canister, based on the dose for a typical canister loading operation. This estimate does not include the radiation dose associated with the decontamination, shipping, processing, and disposal of a discarded canister associated with this alternative.

Contaminated Material and Radioactive Waste:

This alternative would generate potentially-contaminated metal shavings and a contaminated DSC that would have to be decontaminated and packaged for shipment, then processed for disposal and shipped to a disposal site.

Cost:

Based on computations using previous cost history and simplified assumptions, it is estimated that applying this alternative would cost approximately $19 million to unload the DSCs, procure, and load new canisters into their respective HSMs. This estimate does not include the cost of radioactive waste processing and disposal.

4.3.3 <u>Repair DSC Welds (Remove and Re-Perform with Compliant PT Exams)</u>

Consideration was given to a specially-planned evolution to cut off the OTCP of the DSCs without re-flooding the cavity. The operation would gain access to the ITCP welds, and then cut the ITCP welds down to the vicinity of the original root layer. The vent port cover and siphon port cover welds would be removed as well. A new OTCP would then be installed during re-sealing. Weld inspection would then be re-performed with compliant PT exams. Some of the necessary activities (e.g., returning a DSC from the HSM, and cutting it open) are described in the UFSAR and controlled under approved plant procedures. However, the evolution of a partial cutting of the welds is not a described or proven activity, and therefore this alternative has technological and regulatory risks. There also remains the open question associated with the transfer of a noncompliant DSC from the HSM to the reactor building. Resolving this open question would require addressing many of the same elements as those in the proposed alternative, while also taking into account the increased operational risks associated with the transfer operation. Regardless, this alternative provides no discernible safety benefit over the proposed alternative for which it has been demonstrated that the DSCs will continue to meet their design functions.

Operational and Safety Risk:

This alternative would involve extracting the DSCs from their HSMs, and transferring them to the reactor building for removal of the OTCP and partial cutting of the ITCP, followed by the sealing and return of the re-welded DSCs to the HSM. Therefore, this alternative increases the risk of releases during cutting operations, heavy load handling accidents, and risks damaging the DSCs (e.g., scratching). Additionally, this alternative risks damaging the DSC shell during the cutting process.

Occupational Dose:

To perform this alternative on a single DSC, the transfer, lid removal, and repair would expose workers to an occupational radiological dose of approximately 0.5 rem. Furthermore an additional dose of 0.14 rem per DSC is estimated for returning the DSC to its HSM.

Radiological Waste Generation of this Alternative:

This alternative would generate potentially-contaminated metal shavings and a potentially-contaminated OTCP from each DSC that would have to be decontaminated or discarded as radioactive waste.

Cost:

Based on computations using previous cost history, vendor input and simplified assumptions, it is estimated that applying this alternative would cost approximately $14 million to repair the DSCs and return them to their respective HSMs. This estimate does not include the cost of radioactive waste processing and disposal.

4.3.4 DSC Lid Augmentation

Consideration was given to two lid augmentation alternatives:

- Additional ITCP Weld Layer: This alternative would proceed similar to the weld repair described previously, but once the ITCP was exposed, rather than partially cutting and re-performing the ITCP weld, a compliant PT would be performed on the existing ITCP weld, and then an additional weld layer would be applied to arrive at two weld layers with compliant PT exams. A new OTCP would then be placed and welding performed with compliant PT exams. The inclusion of this additional weld may cause an interference with the OTCP.

- <u>Additional OTCP Lid</u>: This alternative would involve placing a secondary lid over the top of the DSC and welding.

Neither evolution is described in the current licensing basis for the DSCs nor have they been designed or proven. For the additional OTCP lid, changes would be required to both the TC and the HSM to accommodate the additional height. Therefore, both lid augmentation alternatives have technological and regulatory risks. There also remains the open question associated with the transfer of a noncompliant DSC from the HSM to the reactor building. Resolving this open question would require addressing many of the same elements as those in the proposed alternative, while also taking into account the increased operational risks associated with the transfer operation. Regardless, this alternative provides no discernible safety benefit over the proposed alternative for which it has been demonstrated that the DSCs will continue to meet their design functions.

Operational and Safety Risk:

This alternative would involve extracting the DSCs from their HSMs, and transferring them to the reactor building for lid augmentation followed by return to the HSMs. Therefore, this alternative increases the risk of releases during the cutting operations, heavy load handling accidents, and risks damaging the DSCs during the moving and cutting processes.

Occupational Dose:

The alternative to perform additional welds on the ITCP so as to have two weld layers with compliant PTs would result in similar occupational dose to the weld alternative discussed previously. To perform this alternative on a single DSC, the transfer, lid removal, and lid augmentation would expose workers to an occupational radiological dose of approximately 0.5 rem per DSC. Furthermore, an additional dose of 0.14 rem per DSC is estimated for returning the DSC to its HSM. The alternative of placing an additional OTCP over the top of the existing canister, the transfer of the DSC between the HSM and the reactor building would expose workers to an occupational radiological dose of approximately 0.28 rem per DSC. Further dose of 0.18 rem per DSC is estimated for fit-up and welding activities.

Contaminated Material and Radioactive Waste:

This alternative would generate potentially-contaminated metal shavings and a potentially-contaminated OTCP from each DSC that would have to be decontaminated or discarded as radioactive waste.

Cost:

Based on computations using previous cost history, vendor input and simplified assumptions, it is estimated that either of these alternatives would cost approximately $14 million to repair the DSCs. This estimate does not include the cost of radioactive waste processing and disposal.

4.3.5 PAUT In Situ (at the ISFSI)

Consideration was given to alternatives that would involve PAUT of one or more DSCs at the ISFSI.

- PAUT in the TC at ISFSI: This alternative would extract the DSC from the HSM to gain access to the lid area and then perform PAUT with the DSC in the TC in the horizontal position. This alternative limits the heavy load movements.

- PAUT in the HSM: This alternative would remove the HSM door and then using the annular space and a long tool, deliver PAUT transducers to the back of the HSM. Due to the HSM rail configuration, this alternative would be limited to less than 360° of the weld circumference.

The activity of extracting a DSC from the HSM is described in the UFSAR and approved plant procedures are available for this activity. However the remainder of these activities is not described in the licensing basis and relies upon undeveloped and unproven technology. Therefore, these alternatives both have technological and regulatory risks. For the alternative of performing the PAUT within the TC, there also remains the open question associated with transfer of a noncompliant DSC from the HSM to the TC and returning it back to the HSM following data collection, but prior to data analysis or processing of an exemption request. Resolving this open question would require addressing many of the same elements as those in the proposed alternative, while also taking into account the increased operational risks associated with the transfer operation. Regardless, this alternative provides no discernible safety benefit over the proposed alternative for which it has been demonstrated that the DSCs will continue to meet their design functions.

Operational and Safety Risk:

Generally these alternatives minimize the risk to the DSC by reducing the amount of required handling and transfer. The most significant risks would be involved with the extraction of the DSC to the TC and the potential for DSC exposure to external events during the period the HSM door is removed or the DSC is in the TC with the lid removed for PAUT.

Occupational Dose:

The alternative to perform PAUT in the TC would result in an occupational radiological dose to workers of approximately 0.35 rem per DSC during the PAUT inspection. Furthermore an additional dose of approximately 0.07 rem per DSC is estimated during the transfer between the TC and HSM. The alternative to perform PAUT in the HSM would result in an occupational radiological dose to workers of approximately 0.25 rem per DSC.

Contaminated Material and Radioactive Waste:

This alternative would generate minimal contaminated material that would need to be discarded as radioactive waste.

Cost:

Based on computations using previous cost history, vendor input and simplified assumptions, PAUT in the TC or in the HSM would cost approximately $5 million for PAUT of a single DSC, and $9 million to examine all five. For the alternative to perform the PAUT in the TC, the estimates assume that the open question described above can be resolved to permit transfer of the DSC to/from the TC, followed by analysis and development of an exemption request based on the PAUT data.

4.3.6 PAUT in the Reactor Building

Consideration was given to alternatives that would involve moving one or more DSCs to the controlled environment of the reactor building for examination by PAUT in the vertical configuration. The activity of returning a DSC from the HSM is described in the UFSAR and approved plant procedures are available to perform this activity. PAUT in this configuration has been previously performed. Therefore, this alternative is both technologically feasible and accounted for under the license. However, there remains the open question associated with transfer of a noncompliant DSC from the HSM to the reactor building and returning it back to the HSM following data collection but prior to analysis or processing of an exemption request. Resolving this open question would require addressing many of the same elements as those in the proposed alternative, while also taking into account the increased operational risks associated with the transfer operation. Regardless, this alternative provides no discernible safety benefit over the proposed alternative for which it has been demonstrated that the DSCs will continue to meet their design functions.

Operational and Safety Risk:

This alternative would involve extracting one or more DSCs from their HSMs and transferring them to the reactor building for PAUT followed by a return to the

HSM. Therefore this alternative increases the risk of heavy load handling accidents and risks damaging the DSCs (e.g., scratches).

Occupational Dose:

To perform this alternative on a single DSC, it is estimated that the transfer and PAUT would expose workers to an occupational radiological dose of approximately 0.63 rem per DSC based on experience with DSC 16 PAUT and transfer to the HSM.

Contaminated Material and Radioactive Waste:

This alternative would generate minimal contaminated material that would need to be discarded as radioactive waste.

Cost:

Based on computations using previous cost history, vendor input and simplified assumptions, this alternative is estimated to cost approximately $5M for PAUT of a single DSC and $9M to examine all five. For these alternatives, the estimates assume that the open question described above can be resolved to permit transfer of the DSC to/from the TC followed by analysis and development of an exemption request based on the PAUT data.

4.4 Conclusion

Based on the previous discussion, the requested exemption is authorized by law and will not endanger life or property or the common defense and security and is otherwise in the public interest; the granting of an exemption results in the least risk, the least dose, the least radioactive waste, and is the least cost option. Any campaign to perform any of the identified alternatives would create operational safety challenges, occupational doses, and generation of quantities of radioactive wastes as well as significant additional economic costs that would not be offset by any discernible safety benefits.

5.0 Environmental Considerations

5.1 Background

The potential environmental impact of using the Standardized NUHOMS® System was initially analyzed in the environmental assessment for the final rule to add the system to the list of approved spent fuel storage casks in 10 CFR 72.214 (59 FR 65898). The environmental assessment for the December 22, 1994, final rule concluded that there would be no significant environmental impact to adding the Standardized NUHOMS® System, and therefore, the NRC issued a finding of no significant impact, which was validated through issuance of Amendment 10 to the Certificate of Compliance (see Reference 6.14).

Standardized NUHOMS® casks are designed to mitigate the effects of design basis accidents that could occur during storage. Design basis accidents account for human-induced events and the most severe natural phenomena reported for the site and surrounding area. Postulated accidents analyzed for an ISFSI include tornado winds and tornado-generated missiles, a design basis earthquake, a design basis flood, a postulated accidental cask drop, lightning effects, fire, explosions, and other incidents.

Considering the specific design requirements for each accident condition, the design of the cask would continue to prevent the loss of confinement, shielding, and criticality control. Without the loss of confinement, shielding, or criticality control functions, the risk to public health and safety is not compromised. The NRC staff performed a detailed safety evaluation of the CoC amendment under which the subject canisters (DSCs 11-15) were loaded, i.e., Amendment 10, and found that an acceptable safety margin was maintained, that the proposed changes provide reasonable assurance that the spent fuel could be stored safely, met the acceptance criteria specified in 10 CFR Part 72, and that there continued to be reasonable assurance that public health and safety and the common defense and security will be adequately protected. The actual conditions of the MNGP and the spent fuel stored in DSCs 11-15 provide additional safety margin and further assurance that the public health and safety and the common defense and security will be maintained.

5.2 Environmental Impact of the Proposed Action

Based on the technical review provided in Section 3, the integrity of the closure welds on the subject DSCs is assured by means other than performance of the nonconforming PT. Thus, the canister's confinement function and accident mitigating design function are not compromised by granting of the proposed exemption. As a result, there is no environmental impact of the proposed action. Thus, the conclusions with respect to the DSC performance in the original environmental assessment and the applicable Amendment 10 environmental assessment are maintained and assured.

The proposed exemption restores DSCs 11-15 to a compliant status, allowing them to continue to store spent fuel assemblies for their licensed lifetime. No changes in operations would be necessary if the exemption is granted. The proposed exemption would not create a new unforeseen risk of environmental impact. Therefore, the conclusions made within the original environmental assessment and Amendment 10 remain valid.

The exemption request provides the bases for the acceptability of DSCs 11-15 notwithstanding the nonconforming PT examinations. The requested exemption meets the categorical exclusion criterion of 10 CFR 51.22(c)(25) as a regulatory action eligible for exclusion not requiring an environmental review. This provision applies because the requested regulatory action is for the "Granting of an exemption from the requirements of any regulation of this chapter, provided that:

(i) There is no significant hazards consideration;

(ii) There is no significant change in the types or a significant increase in the amounts of any effluents that may be released offsite;

(iii) There is no significant increase in individual or cumulative public or occupational radiation exposure;

(iv) There is no significant construction impact;

(v) There is no significant increase in the potential for or the consequences from radiological accidents; and

(vi) The requirements from which an exemption is sought involve:…(C) Inspection or surveillance requirements;…"

The "no significant hazard consideration" analysis is set forth in Section 5.3. The other criteria (with the exception of construction impacts) have been previously discussed, demonstrating that granting the exemption will not increase effluents, will not increase public or occupational radiation exposure, and will not increase the potential for or consequences of radiological accidents. In fact, not granting the exemption request will result in the necessity of implementing one of the alternatives discussed above and will increase effluents, radiation exposures, and the potential and consequences of radiological accidents. As for construction impacts, since granting the exemption request will not result in any construction, that criterion is met.

Further, the proposed exemption does not require any changes to the MNGP ISFSI Environmental Report and applicable UFSAR analyses remain bounding.

5.3 <u>No Significant Hazards Consideration</u>

In order to support the assertion in Section 5.3 that this exemption request meets the definition under 10 CFR 51 of a regulatory action eligible for categorical exclusion or otherwise does not require an environmental review, NSPM is providing a No Significant Hazards Consideration (NSHC). The NSHC was performed in accordance with the criteria of 10 CFR 50.92, insofar as 10 CFR Part 72 does not establish separate significant hazards consideration criteria. NSPM has evaluated the proposed exemption request in accordance with the standards in 10 CFR 50.92 and has determined that the requested exemption presents no significant hazards. NSPM's evaluation against each of the criteria in 10 CFR 50.92 follows.

1. **Does the proposed change involve a significant increase in the probability or consequences of an accident previously evaluated?**

   Response: No.

   The probability (frequency of occurrence) of any UFSAR evaluated accident occurring is not affected by the requested exemption because MNGP continues to comply with the regulatory and design basis criteria established for the DSCs. DSCs 11-15 currently reside and will continue to remain in their respective HSMs upon the granting of the requested exemption.

   There is no change in consequences of postulated accidents, because the analysis indicates that there is margin to the most limiting accident (cask drop) assuming flaws in the welds to account for the nonconforming PT examination. The results of accident evaluations remain within the NRC approved acceptance limits.

   Therefore, the proposed exemption does not involve a significant increase in the probability or consequences of an accident previously evaluated.

2. **Does the proposed change create the possibility of a new or different kind of accident from any accident previously evaluated?**

   Response: No.

   The exemption request does not create the possibility of a new operating mode or accident scenario, nor does the exemption request rely on new equipment or postulate a new equipment failure mode. In order for an activity to create the possibility for an accident of a different type, the activity would have to introduce a new material, a new man-machine interface, a new operational process, or other significant change that would initiate a new type of failure or cause a previously-described accident to propagate differently. The proposed activity is technical in nature in that it recognizes and reconciles the nonconforming NDE but it does not involve a physical change to the canister design and no changes are involved with the canister materials or the loading operations.

   Therefore, the proposed exemption does not create the possibility for an accident of a different type nor does it result in more than a minimal increase in the likelihood of occurrence of a malfunction of an SSC important to safety previously evaluated in the UFSAR.

3. **Does the proposed change involve a significant reduction in a margin of safety?**

   Response: No.

The five design criteria (design functions) of the DSCs have been evaluated. The design criteria of criticality safety, radiological safety, and heat removal are not affected by the performance of nonconforming PT examinations. The confinement and structural support design criteria, while marginally affected, are not significantly impacted and there is margin to safety in these design criteria as determined by analysis and evaluation.

Therefore, the proposed exemption does not involve a significant reduction in a margin of safety.

Based on the considerations above, NSPM has determined that storage of spent fuel in DSCs 11-15 in accordance with the proposed exemption does not involve a significant hazards consideration as defined in 10 CFR 50.92(c), in that it does not: (1) involve a significant increase in the probability or consequences of an accident previously evaluated; or (2) create the possibility of a new or different kind of accident from any accident previously evaluated; or (3) involve a significant reduction in a margin of safety.

5.4 Environmental Impact of Alternatives to the Proposed Action

As discussed in Section 4.3, NSPM has considered several alternatives to the proposed exemption.

a. Unload DSCs, Discard, and Replace

b. Repair DSC Welds (Remove and Re-Perform with Compliant PT Exam)

c. DSC Lid Augmentation

d. PAUT In Situ (at ISFSI)

e. PAUT in Reactor Building

These alternatives would result in both real and potential environmental impacts. NSPM has estimated that implementation of some of these alternatives would result in a significant amount of occupational dose and low-level radioactive waste (LLRW) that would have to be processed and disposed, as detailed below.

a. Unload DSCs, Discard, and Replace: This alternative would involve the unloading and replacement of the canisters. Occupational doses would be significant as grinding and welding activities would be performed in the vicinity of spent nuclear fuel. Each discarded DSC would become radioactive waste. Radioactive wastes would be generated from the grinding operations performed to remove the welds from the existing canister. Other radioactive wastes would be generated from radioactively contaminated consumables and anti-contamination clothing used during the unloading and reloading process.

This radioactive waste would be transported and ultimately disposed of at a qualified LLRW disposal facility, potentially exposing it to the environment.

b. Repair DSC Welds (Remove and Re-Perform with Compliant PT Exam): This alternative would involve cutting the DSC to access the ITCP, and then cutting the ITCP welds down to the vicinity of the original root layer. From that point, the DSC would be re-welded and inspected in conformance to TS 1.2.5 and other TS. Occupational doses would be significant as grinding and welding activities would be performed in the vicinity of spent nuclear fuel. Radioactive wastes would be generated from the grinding operations performed to remove the welds. Other radioactive wastes would be generated from radioactively contaminated consumables and anti-contamination clothing used during the transferring and re-inspecting of the DSC from the HSM to the reactor building and back again. This radioactive waste would be transported and ultimately disposed of at a qualified LLRW disposal facility, potentially exposing it to the environment.

c. DSC Lid Augmentation: This alternative may also involve cutting the DSC to access the ITCP and adding additional weld layers with compliant PT examinations to the ITCP or welding an additional OTCP to the DSC. Occupational doses would be significant as grinding and welding activities would be performed in the vicinity of spent nuclear fuel. Radioactive wastes would be generated from the grinding operations performed to remove the welds. Other radioactive wastes would be generated from radioactively contaminated consumables and anti-contamination clothing used during the transferring and re-inspecting of the DSC from the HSM to the reactor building and back again. This radioactive waste would be transported and ultimately disposed of at a qualified LLRW disposal facility, potentially exposing it to the environment.

d. PAUT In Situ (at ISFSI): This alternative would involve opening the HSMs, and either performing PAUT with the DSCs unmoved or withdrawing the DSCs into the TC and performing PAUT in the transfer cask. Occupational doses would be significant as set up and performance of PAUT in the vicinity of spent nuclear fuel would occur. Radioactive wastes would be generated from radioactively contaminated consumables and anti-contamination clothing used during the examination. Also, radioactive waste would be generated from the cleanup of any coupling fluid (of the PAUT) that it picks up and then transports resulting in contamination from the surface of the DSC. This radioactive waste would be transported and ultimately disposed of at a qualified LLRW disposal facility, potentially exposing it to the environment.

e. PAUT in Reactor Building: This alternative would involve transferring a DSC (back and forth to the ISFSI) and performing the PAUT. Occupational doses would be significant as set up and performance of PAUT in the vicinity of spent nuclear fuel would occur. Radioactive wastes would be generated from radioactively contaminated consumables and anti-contamination clothing used during the transferring and re-inspecting of the DSC from the HSM to the reactor building and back again. This radioactive waste would be transported and ultimately disposed of at a qualified LLRW disposal facility, potentially exposing it to the environment.

In addition, each of the alternatives would result in additional risks of both off-normal events and design basis accidents, such as a fuel handling or cask drop event, both of which could involve a radiological release to the environment.

5.5 Conclusion

As a result of this environmental assessment, NSPM concludes that the proposed exemption, which will allow NSPM to maintain DSCs 11-15 in their current state at their storage locations with noncompliant PT examinations, is in the public interest in that it avoids adverse environmental effects associated with the alternatives to the proposed action.

6.0 References

6.1 NRC Letter to NSPM, "Exemption from Certain Provisions of 10 CFR 72.212 and 72.214 – Storage of Standardized NUHOMS® Dry Shielded Canister 16 at Monticello Nuclear Generating Plant Independent Spent Fuel Storage Installation (CAC No. L25058)", dated June 15, 2016 (Agencywide Document Access and Management System (ADAMS) Accession No. ML16167A036)

6.2 NRC Spent Fuel Project Office Interim Staff Guidance (ISG)-15, "Materials Evaluation", dated January 10, 2001 (ADAMS Accession No. ML010100170)

6.3 NRC Spent Fuel Storage and Transportation ISG-18, "The Design and Testing of Lid Welds on Austenitic Stainless Steel Canisters as the Confinement Boundary for Spent Fuel Storage", Revision 1, dated October 3, 2008 (ADAMS Accession No. ML082750469)

6.4 American National Standards Institute ANSI N14.5-1997, "American National Standard for Radioactive Materials – Leakage Tests on Packages for Shipment", dated February 5, 1998

6.5 TriVis Letter to NRC, "Report of Potential Substantial Safety Hazard in accordance with Title 10 Code of Federal Regulation, Part 21", dated December 13, 2013 (ADAMS Accession No. ML14006A004)

6.6 TriVis Letter to NRC, "Final Report of Potential Substantial Safety Hazard in accordance with Title 10 Code of Federal Regulation, Part 21, Event Number 49628", dated January 29, 2014 (ADAMS Accession No. ML14042A201)

6.7 NSPM Letter to NRC, "Exemption Request for Nonconforming Dry Shielded Canister Dye Penetrant Examinations", dated September 29, 2015 (ADAMS Accession No. ML15275A023)

6.8 TriVis Report, "Assessment of Field Closure Weld Liquid Penetrant Examinations Performed on Dry Shielded Canisters 11 through 16 during the 2013 MNGP ISFSI Loading Campaign", Revision 1, dated February 5, 2014

6.9 NRC Document, "Safety Evaluation Report of Vectra Technologies, Inc. a.k.a. Pacific Nuclear Fuel Services Inc. Safety Analysis Report for the Standardized NUHOMS Horizontal Modular Storage System for Irradiated Nuclear Fuel", dated December 1994

6.10 NRC Document SMSAB-00-03, "Best-Estimate Offsite Dose from Dry Storage Cask Leakage", dated June 2000 (ADAMS Accession No. ML031540409)

6.11 NRC Document, "Risk-Informed Decisionmaking for Nuclear Material and Waste Applications", Revision 1, dated February 2008 (ADAMS Accession No. ML080720238)

6.12 NRC Memorandum, “Summary of March 2, 2017, Meeting with Xcel Energy to Discuss Xcel Energy’s Proposed Exemption Request for Dry Storage NUHOMS® Canisters, Numbers 11-15, at the Monticello Nuclear Generating Plant”, dated March 30, 2017 (ADAMS Accession No. ML17089A146)

6.13 NRC Memorandum, “Summary of November 9, 2016, Meeting with Xcel Energy to Discuss Xcel Energy’s Draft Project Plan for the Remaining Dry Storage NUHOMS Canisters, Numbers 11-15, at the Monticello Nuclear Generating Plant”, dated November 30, 2016 (ADAMS Accession No. ML16336A028)

6.14 NRC Document “Environmental Assessment and Finding of No Significant Impact on Proposed Amendment to 10 CFR PART 72, List of Approved Spent Fuel Storage Casks: Standardized NUHOMS® System Revision 10”, Office of Federal and State Materials and Environmental Management Programs, U.S. Nuclear Regulatory Commission (NRC), dated March 2009 (ADAMS Accession No. ML091320168)

Appendix A

Dye Penetrant Examination (PT) Data

Note: The information in this Appendix is provided only to quantify the magnitude of the procedural noncompliances associated with the PT examination of DSCs 11-16. This information is not used in this exemption request to justify the nonconforming condition. The time data is a best-estimate, using approximate start and end times that can be ascertained from video imagery.

This appendix documents the results of the PT examinations performed during the 2013 ISFSI loading campaign at MNGP. During the performance of PT examination on DSCs 11-16, penetrant and developer dwell times varied by quite large margins depending on the weld being tested and which DSC was being examined. The PT examinations for DSCs 11-16 were signed off, indicating that acceptable results were obtained.

This appendix includes Tables A-1 and A-2 which provide the overall weld temperatures, penetrant dwell times, cleaning method, cleaning dry time and developer dwell time for the welds under the scope of this exemption request for each DSC. Each of the PT examinations indicates a deficiency in performance of the PT examination penetrant and/or developer dwell time.

The data used in these tables comes from videos of refueling floor activities as documented in the TriVis report (Reference 6.8) that show the workers performing DSC loading and closure activities, and TS compliance and welding/inspection activities. These videos provide detailed indication of worker performance and are time stamped to permit the duration of timed activities to be determined. These videos are not considered quality records.

The conclusion of these data indicates that longer penetrant dwell times and developer dwell times occurred during the PT examination of the ITCP and OTCP welds (Table A-1) as compared to the PT examination of the SPCP, VPCP and TPP welds (Table A-2).

Table A-1 – PT Performance Parameters for ITCP and OTCP Welds

DSC	Weld*	Weld Temp (^oF)	Penetrant Dwell Time (min:sec)	Cleaning Method (Wet or Dry)	Cleaning Dry Time (min:sec)	Developer Dwell Time (min:sec)
11	ITCP-R	106	13:00	Wet	1:59	1:31
11	ITCP-F	110	15:32	Wet	2:59	2:39
11	OTCP-R	97	17:56	Wet	3:54	2:00
11	OTCP-I	168	5:50	Wet	6:30	1:37
11	OTCP-F	207	3:03	Wet	1:08	4:13
12	ITCP-R	151	9:50	Wet	2:12	5:11
12	ITCP-F	158	6:36	Wet	3:56	3:51
12	OTCP-R	157	6:28	Wet	2:18	3:38
12	OTCP-I	156	3:23	Wet	1:16	8:38
12	OTCP-F	190	2:07	Dry	0:00	4:58
13	ITCP-R	174	7:34	Wet	2:12	2:51
13	ITCP-F	179	5:22	Wet	1:53	2:13
13	OTCP-R	194	5:47	Wet	0:38	2:31
13	OTCP-I	190	2:09	Dry	0:00	6:15
13	OTCP-F	188	2:48	Dry	0:00	5:09
14	ITCP-R	131	9:26	Wet	1:46	3:40
14	ITCP-F	145	7:54	Wet	1:51	2:33
14	OTCP-R	161	10:30	Wet	3:08	2:18
14	OTCP-I	158	6:45	Wet	2:09	2:52
14	OTCP-F	149	2:05	Dry	0:00	4:17
15	ITCP-R	151	10:21	Wet	1:58	3:22
15	ITCP-F	144	9:16	Wet	1:50	2:58
15	OTCP-R	148	2:13	Dry	0:00	1:55
15	OTCP-I	146	2:20	Dry	0:00	3:32
15	OTCP-F	175	6:13	Wet	1:50	3:09
16	ITCP-R	128	3:23	Wet	1:38	4:14
16	ITCP-F	138	2:39	Dry	0:00	6:07
16	OTCP-R	144	3:31	Dry	0:00	5:13
16	OTCP-I	149	2:00	Dry	0:00	5:21
16	OTCP-F	PT on this weld layer was not completed once inadequate PT exams were discovered				

*R= root layer, I= intermediate layer, F= final layer

Table A-2 – PT Performance Parameters for SPCP, VPCP and TPP Welds

DSC	Weld*	Weld Temp (^oF)	Penetrant Dwell Time (min:sec)	Cleaning Method (Wet or Dry)	Cleaning Dry Time (min:sec)	Developer Dwell Time (min:sec)
11	SPCP-R	146	1:00	Wet	0:18	0:32
11	SPCP-F	146	2:56	Wet	0:16	0:22
11	VPCP-R	146	1:00	Wet	0:18	0:32
11	VPCP-F	146	2:56	Wet	0:16	0:22
11	TPP-R	207	3:03	Wet	1:08	4:13
11	TPP-F	235	video recording obstructed, no data available			
12	SPCP-R	152	4:20	Wet	0:34	0:57
12	SPCP-F	160	4:14	Wet	0:36	1:33
12	VPCP-R	152	4:20	Wet	0:34	0:57
12	VPCP-F	160	4:14	Wet	0:36	1:33
12	TPP-R	193	3:23	Wet	1:16	8:38
12	TPP-F	190	2:07	Dry	0:00	4:58
13	SPCP-R	169	3:44	Wet	0:43	0:49
13	SPCP-F	176	3:46	Wet	0:24	0:48
13	VPCP-R	169	3:44	Wet	0:43	0:49
13	VPCP-F	176	3:46	Wet	0:24	0:48
13	TPP-R	158	2:09	Dry	0:00	6:15
13	TPP-F	162	2:48	Dry	0:00	5:09
14	SPCP-R	130	2:00	Dry	0:00	3:13
14	SPCP-F	190	1:30	Dry	0:00	1:14
14	VPCP-R	130	2:00	Dry	0:00	3:13
14	VPCP-F	190	1:30	Dry	0:00	1:14
14	TPP-R	160	6:45	Wet	2:09	2:52
14	TPP-F	145	2:05	Dry	0:00	4:17
15	SPCP-R	128	3:54	Wet	0:28	0:36
15	SPCP-F	130	1:20	Dry	0:00	2:29
15	VPCP-R	128	3:54	Wet	0:28	0:36
15	VPCP-F	130	1:20	Dry	0:00	2:29
15	TPP-R	184	1:04	Wet	0:31	0:26
15	TPP-F	244	Penetrant not applied			3:09
16	SPCP-R	131	1:14	Dry	0:00	1:36
16	SPCP-F	136	1:29	Dry	0:00	3:05
16	VPCP-R	131	1:14	Dry	0:00	1:36
16	VPCP-F	136	1:29	Dry	0:00	3:05
16	TPP-R	189	2:00	Dry	0:00	1:23
16	TPP-F	PT on this weld layer was not completed when inadequate PT exams discovered				

*R= root layer, F= final layer

Appendix B

TriVis/Sherwin PT Performance and Testing Report

TriVis issued an assessment of simulated PT conditions using the actual dwell times and development times determined from video recordings of refuel floor activities. This assessment was performed to determine if the PT examinations performed on DSC 11-16 field closure welds would have been capable of producing interpretable results for detection of critical weld flaws (Reference 6.8).

The PT examination procedure used by TriVis incorporated ASME Code Section T-621.1 of Article 6. The PT examination materials specified in the procedure were Sherwin Hi-Temp® Penetrant Inspection System. This system is comprised of K-019 Solvent, K-017 Penetrant and D-350 Developer. This system is designed to work at temperatures above which ordinary penetrants are ineffective. D-350 Developer is recommended for temperatures between 175°F and 350°F. The PT procedure required D-350 use for surfaces in the range of 72°F to 325°F. Surface temperatures experienced during DSC field closure PT examinations are typically higher than standard temperatures for PT examinations.

The PT examination procedure specifies the following general procedural steps for performing a PT examination:

- Verify surface temperature - The surface temperatures ranged from 97°F to 244°F as identified in the PT reports.

- Pre-clean the weld area - The pre-clean method required by the procedure calls for the use of the K-019 Solvent, followed by a dry wipe and then a final wipe using a rag moistened with demineralized water.

- Allow the Pre-clean to dry - The procedural requirement is to allow two minutes for drying after the pre-cleaning step is completed.

- Apply the Penetrant – Apply K-017 Penetrant to the weld area.

- Allow Penetrant to dry – The actual dwell time required is based on the surface temperature, see Table B-1 below.

- Remove Penetrant - The penetrant removal method required by procedure calls for the technician to perform a dry wipe followed by a wipe with a clean rag moistened with K-019 Solvent, and a final wipe with a dry rag or cloth. Per video review, either a wet rag or a dry rag was used, but not both.

- Penetrant dry time - The procedural requirement is to allow two to fifteen minutes for drying after the excess penetrant has been removed, for surface temperatures in the range of 50°F to 125°F. For examinations above 125°F, the drying time is one to fifteen minutes.

- Apply the Developer– Apply D-350 Developer to the weld area.

- Allow Developer to dry - The actual dwell time has a minimum and maximum time limit and a specified surface temperature range, see Table B-2 below.

The PT examination procedure specified the following minimum dwell times for the K-017 penetrant based on the surface temperature:

Table B-1 – Penetrant Dwell Time

Surface Temperature Range	Minimum Dwell Time Required by PT Procedure
50°F to 75°F	30 minutes
76°F to 125°F	10 minutes
126°F to 200°F	3 minutes
201°F to 325°F	1 minute

And the procedurally-specified following dwell times for the D-350 developer based on the surface temperature:

Table B-2 – Developer Dwell Time

Surface Temperature Range	Minimum Dwell Time	Maximum Dwell Time
72°F to 325°F	10 minutes	15 minutes

During the performance of PT examination on DSCs 11-16, penetrant and developer dwell times varied by quite large margins depending on the examiner, the weld being tested, and which DSC was being examined. Appendix A includes Tables A-1 and A-2 which provide the overall weld temperatures, penetrant dwell times, cleaning method, cleaning dry time, and developer dwell time for the welds for each DSC. Review of each of the PT examinations indicates a deficiency in performance of the PT examination penetrant, cleaning and/or developer dwell time. See Appendix A for further details.

Upon discovery of the nonconforming PT examinations, NSPM requested TriVis to perform analysis of the consequences resulting from the issue. TriVis performed testing using the most limiting surface temperatures, drying times and dwell times for each particular weld, and sometimes multiple testing depending on the documented circumstances. TriVis used video and documentation to determine the limiting conditions for each weld performed on

DSCs 11-16[6] and thus the testing parameters applied. Test specimens were used to duplicate the testing conditions. (Reference 6.8)

The results of the testing demonstrated that hairline cracks in the test specimen and samples could be detected using the nonconforming PT examination methods.

Finally, Sherwin performed an independent PT test in their laboratory using the following parameters:

- a 130°F surface temperature,
- a one minute penetrant dwell time, and
- a one minute developer dwell time.

Sherwin performed the test with these parameters as well as with 10 minute penetrant and developer dwell times. The test was performed with the K-017 Penetrant, K-019 Solvent and D-100 Developer (as opposed to the D-350 used during the actual PT examinations). (Reference 6.8)

Sherwin concluded that the test results indicated that, while the indications were "slightly more visible" with the 10 minute penetrant dwell time, "all the indications seemed visible" after the one minute dwell time. While this is only one sample out of many possible data points, a temperature of 130°F, with a one minute penetrant dwell time and a one minute developer dwell time, was selected as one of the lowest temperature, least time combinations experienced in the PT exams, thus providing a reasonably conservative approach to the test.

Based on this testing and review of the PT examinations, while not conforming to procedural and ASME code requirements, the Sherwin and TriVis testing do provide some insight into the acceptability of the welds. The PT examinations performed in the tests indicate that flaws and hairline cracks could be detected using the nonconforming PT examination methods. The vast majority of the welds were represented in the testing.

The intent of the testing by TriVis and Sherwin was to reproduce the penetrant and developer dwell times to demonstrate that they could have been effective examinations.

Although the TriVis assessment concluded that the majority of PT examinations could have produced interpretable results, NSPM determined from video records that the examiners did not follow the procedural and ASME code requirements, thus not meeting the TS requirements.

---

[6] The following welds were not included as part of the PT parameters testing:

a. DSC 11, TPP Weld Final: The crane obstructed the video recording, preventing any data to be provided for verification.
b. DSC 15, TPP Weld Final: The NDE technician never applied penetrant to TPP Weld Final layer. As such, the TPP Final weld layer could not be effectively demonstrated.
c. DSC 16, OTCP Weld Final and TPP Weld Final: These are the outermost welds on DSC 16, which were accessible on the Refueling Floor and, therefore, testing was not necessary.

Appendix C

Structural Integrity Associates Weld Quality Reviews

Summary from <u>2014 Report</u>

Report No. 1301415.403, “Assessment of Monticello Spent Fuel Canister Closure Plate Welds based on Welding Video Records”, Revision 2, Structural Integrity Associates, May 22, 2014.

NSPM contracted the support of an independent vendor to review the weld quality for the welds performed on DSCs 11-16. This review was provided by SIA, who performed a review of weld quality and provided a report of their findings. The review was conducted by using video from the weld head of the automated welding process performed on DSCs 12-16 (DSC 11 was not included). The weld head videos are not considered a quality record. The results of this report were also reviewed by AREVA (the current license holder for the 61BTH DSC) and the report was reissued with their comments incorporated.

This review determined that the quality of the welding was for the most part satisfactory, but did contain some anomalous practices. Both inner and outer cover plate closure welds were recorded in some cases, but the video coverage was incomplete for all weld beads. The video review covered a sampling of the welding performed on DSCs 12-16. DSC 11 had no video available. Specifically, the video review covered the ITCP root and cover weld layers and the OTCP tack, root, intermediate and cover weld layers for DSCs 13 and 16; and the OTCP tack, root, intermediate and cover weld layers for DSCs 12, 14, and 15.

It was noted that good welding practices were present in all of the welds examined, and in general, visible evidence of tie-in between the weld layers and the sidewall was present. Conversely, small undesirable weld surface conditions (anomalies, e.g., contamination on weld surface, electrode tip oxidation, uneven weld deposit, etc.) were also observed, to some extent, in all of the welds examined. The presence of such undesirable weld surface conditions do not necessarily result in weld defects. When encountered, it is required for the welding operator to stop and assess the condition and then act to mitigate the condition as necessary.

The weld designs, the materials used, and the welding processes applied are designed for quality welds. The ER308 (or ER308/308L) dual certified filler materials are correct for the Type 304 stainless steel components. These material combinations tend to be quite forgiving in terms of achieving quality welds, especially with the machine Gas Tungsten Arc Welding (GTAW) welding process. The GTAW welding process was primarily used to weld these structures. These types of weld designs are generally considered to be readily weldable.

The results of this assessment were inconclusive regarding the overall acceptability of the welds, as some good welding practices and some undesirable welding practices were observed in the weld head videos for each DSC. The weld videos were not complete for each weld and the videos did not show the entire weld process, but consisted of fragments in some cases. The videos showed the presence of occasional irregular surface features on the welds and are considered applicable to each DSC. This suggests that there is a potential for welding discontinuities to exist in DSCs 11-16. The DSC 16 outer closure weld was concluded to be the most vulnerable to potential defects, because a greater frequency of irregular surface conditions was generated during welding.

All of the welds produced similar irregular weld surface conditions (anomalies) to some extent, based strictly on the weld head video clips for each canister closure weld. This does not imply that any of the welds are defective and in fact, clear evidence of sidewall and interbead tie-in is consistently observed around the entire circumference of the welds. It is entirely possible that all of the DSC welds are acceptable.

The probability for achieving quality welds is enhanced when good welding practices are followed. Good practices include proper and consistent fit-up, clean joint surfaces, minimizing weld surface irregularities, pure welding grade inert gas (argon), properly dressed and maintained tungsten electrode, proper electrode positioning, proven combinations of heat input (amps times volts divided by arc travel speed), and rates of filler wire additions. The written welding program controls, welding procedure specifications, welding procedure qualification records were all in order to produce sound welds. The component designs and manufacturing sequences are capable of producing quality welds. The final step is for the welding operators and their supervision to ensure that good welding practice is followed.

NSPM has concluded that this report provides a sampling of typical welding practices across the industry. Evidence of good welds being applied is ample and dominates the video. But the video also shows infrequent indications for areas where the potential for small weld flaws also exists. As stated, the results do not indicate an absolutely perfect weld was created; however, it does provide confidence that for the vast majority of the time, welding was performed with the automated welding process in a manner consistent with well-done field welding practices. It is also important to note that review of the automated weld video may identify an anomaly on the weld surface, but it does not show what was done about it and what remediation activities were performed. So from that standpoint, the review is incomplete.

<u>Summary from 2017 SIA Report</u>

Report No. 700388.401, "Evaluation of the Welds on DSC 11-15", Revision 1, Structural Integrity Associates, August 22, 2017.

In 2017, NSPM again contracted SIA to perform a more rigorous review of available weld head video, general area video, welding records, and PAUT results (for DSC 16) to identify any correlations between the welding processes used during the 2013 loading campaign and the flaws identified by the PAUT. By correlating indications to the particular welding methods used on all six canisters (including DSCs 11-15), a reasonable case can be made that the types of indications found on DSC 16 are representative of those that may be found on DSCs 11-15.

The PAUT results for DSC 16 were reviewed for both the ITCP and the OTCP closure welds. These results showed sidewall and groove bottom indications for the ITCP that are believed to be lack of fusion (LOF) based on location of the indications. The indications reported for the OTCP are primarily mid-wall weld deposit defects. It is believed that they are due to interbead

LOF. The mid-wall indications were further characterized as two separate flaw groupings represented as being roughly parallel and offset from each other, both near mid-wall. They are not aligned and cannot reinforce one another through-wall by some flaw growth mechanism such as fatigue.

It was observed that a learning curve resulted in welding activities with fewer interruptions in the later canister closure welds. No significant observations were seen in the welding videos for DSCs 12-15 nor in the general area video records that would suggest a different welding behavior from DSC 16, because the conditions causing the defects were generally observed in all the OTCP closure welds and for the two ITCP welds for which videos were available to review. According to the proposed flaw mechanism model, the observed conditions produced “sidewall LOF” in the ITCP and the OTCP closure welds, and “interbead LOF” in the OTCP closure welds.

There were no welding videos available for DSC 11; however, area videos for the welding and inspections of that canister were reviewed and no significant differences were observed when welding the DSC 11 closure welds. These observations suggest that defect distributions in DSC 11 would be represented by the distributions in DSCs 12-15 based on similar welding procedures, similar welders, similar filler metals, similar equipment, similar welding technique, similar deposit thickness levels at inspection, and similar in-process corrective measures. More corrections were observed with all the canister closure welds prior to DSC 16; however, it does not necessarily follow that there will be more defects present simply because more corrective measures were observed. In fact, it is likely that the in-process corrections taken during welding likely are characterized by fewer conditions potentially leading to the types of defects described, suggest that those welds have fewer defects and would be less prone to any longer continuous defects.

The Bounding Flaw Sets used conservatively modeled as completely around the closure weld for the structural analyses are clearly bounding for the DSC 16 OTCP closure weld. Those analyses concluded a satisfactory level of safety. The same bounding analyses should provide for similar conservative bounding analyses with the other DSC OTCP closure welds. Discussion was provided to suggest that the conservative assumption of similar flaw distributions in the other dry shielded canisters would be even more conservative, and the assumptions made for the DSC 16 OTCP closure weld are recommended for the same weld in all the other canisters reviewed, including DSC 11.

The VT inspection results obtained at the prescribed testing intervals were reported satisfactory for all the canister closure welds. It is suggested that any defects developed would be restricted in size to the deposit thickness developed for each interval, because the source of the defects in the OTCP closure weld is a defect described as ‘interbead LOF’. Since this defect is formed between two adjacent weld beads within the same intermediate interval for both flaw distributions, it cannot exceed the weld bead height because that is the only weld deposited material in that interval.

It is concluded that it is reasonable to assume that the conditions determined for the closure welds in DSC 16 reasonably represent the similar closure welds in DSCs 12-15. This conclusion is based on comparisons of evidence developed by reviewing each welding video available and the rest of the body of evidence pertaining to all of the welds. In addition, it is concluded that the conditions of the closure weld in DSC 11 are reasonably represented by those observed in DSC 16 based on how the welds were made, the continuity of welding operators that made the welds, the common welding consumables, and the valid visual inspections that were performed with satisfactory results. It is reasonable to assume that an experienced visual inspector would have detected the presence of any large defect penetrating the surface during the interval surface inspections. The most likely defects present would be bound by the interval layer thicknesses, because of the mechanism required to form the “interbead LOF”. This assumption supports the reasoning that the DSC 11 closure welds should have defect distributions no different from DSCs 12-15. DSC 16 was seen to have more conditions known to lead to welding discontinuities (such as LOF) than any of the other dry shielded canisters. It was noted that DSC 16 did not have the potentially beneficial in-process remedial actions applied to the others.

The analytical approach and results used to conservatively determine satisfactory performance for DSC 16 bounding flaws for the OTCP closure welds should be applicable to all the other canister OTCP closure welds. The conservative assumptions for full 360° defects coupled with conservative growth assessments are deemed representative of all the reviewed canister closure welds including DSC 11.

Appendix D

Extent of Condition Assessment

I. Introduction

NSPM performed an extent of condition review of weld information and overall DSC condition for DSCs 11-15, and the inaccessible welds on DSC 16. Since DSCs 11-15 are inserted into their horizontal storage modules (HSMs) no direct measurements could be taken. In addition, when the PT examination nonconformance was discovered, initial welding of DSC 16 had been completed, so only the OTCP weld was accessible. Therefore, record reviews were performed to ascertain the as-left weld conditions. This appendix provides the results to the extent of condition review for DSCs.

II. Scope of Review

The extent of condition review looked at DSCs 11-16 documentation including information and data related to overall condition of the DSCs. Specifically of interest was information associated with the welds covered in this exemption request. Items covered in this review are as follows:

- Welding procedures available at the job site
- Weld surface preparations completed – weld surface is dry, free of oil, grease, weld spatter, rust, slag, sand, discontinuities, or other extraneous material.
- Verification of weld crown height – ITCP, vent/siphon port
- VT examination of Welds - ITCP, OTCP, vent/siphon port
- Hydrogen Monitoring performed while welding
- Pressure testing of DSC shell to ITCP weld
- Vacuum drying and verification
- Helium backfilling, pressure verification and leak testing
- Weld depth measurements – OTCP

Other items, such as verification of other TS requirements, were also performed but are not discussed herein as they are not applicable to welding PT examinations.

III. Review Results

In summary, the review indicated that compliance with procedural and TS requirements were completed satisfactorily. Some details of the extent of condition findings are provided below in the following series of tables.

- *Table D-1 – Welding Administrative Requirements Compliance* – This table demonstrates that administrative requirements for welding were met for each DSC.
- *Table D-2 – Technical Specification Required Testing of Welds* – This table lists the following Technical Specifications and the resulting data used to demonstrate compliance with the TS.
    - *TS 1.1.11 – Hydrogen Gas Monitoring*
    - *TS 1.1.12.4 – Pressure Test of the DSC Cavity to ITCP Weld*
    - *TS 1.2.2 – DSC Vacuum Drying Test*
    - *TS 1.2.3a – DSC Backfill Pressure Test*
    - *TS 1.2.4a – DSC Helium Leak Test*
- *Table D-3 - Weld Depth Measurements for Outer Top Cover Plate Welds* – This table provides weld depth measurements for four locations on each OTCP (0^o, 90^o, 180^o, and 270^o). These four locations are specified by procedure. The DSC design requires a minimum of 0.500 inch weld depth to meet acceptance criteria.

Table D-1 – Welding Administrative Requirements Compliance

Procedural Requirement	DSC					
	11	12	13	14	15	16
Welding procedures available at the job site	X	X	X	X	X	X
Weld surface preparations completed (all welds)	X	X	X	X	X	X
Verification of weld crown height (all welds)	X	X	X	X	X	X
VT examination of welds (all welds)	X	X	X	X	X	X

Table D-2 – Technical Specification Required Testing of Welds

Procedural Requirement	DSC					
	11	12	13	14	15	16
TS 1.1.11 - Hydrogen Monitoring performed while welding.	X	X	X	X	X	X
TS 1.1.12.4 – Pressure test DSC cavity to ITCP weld. Pressurize to between 29.2 psia and 30.7 psia and hold for minimum of 10 minutes.	X	X	X	X	X	X
Hold time (minutes)	10	10	10	11	11	11
TS 1.2.2 (Initial pump down) - DSC kept at or below 2.8 torr for at least 30 minutes.	X	X	X	X	X	X
Initial vacuum reading (torr)	1.40	1.13	1.807	1.199	1.49	1.191
Final vacuum reading (torr)	2.044	1.90	2.53	2.02	2.08	2.011
Hold time (minutes)	30	31	31	31	31	30
TS 1.2.2 (Final pump down) - DSC kept at or below 2.8 torr for at least 30 minutes.	X	X	X	X	X	X
Initial vacuum reading (torr)	1.23	1.373	1.872	1.33	1.90	1.330
Final vacuum reading (torr)	1.77	1.859	2.50	1.84	2.34	1.770
Hold time (minutes)	30	33	32	30	31	34
Gauge Error	.011	.0042	.016	.005	.017	.011
TS 1.2.3a - DSC backfilled to pressure of 17.2 psia ± 1.0 psi for at least 30 minutes.	X	X	X	X	X	X
Initial pressure reading (psia)	17.283	17.203	17.234	17.20	17.12	17.031
Final pressure reading (psia)	17.272	17.207	17.210	17.22	17.141	17.04
Pressure Gauge error	0.00	.000174	.00029	.0006	.00012	0.00
Hold time (minutes)	30	30	31	31	31	34
TS 1.2.4a - Verified that DSC leakage rate is limited to ≤ 1.0 x 10^{-7} cubic centimeters/sec.	X	X	X	X	X	X
Leakage rate (cc/s)	9.5E-10	1.0E-9	1.4E-9	6.6E-10	5.4E-9	1.5E-9

Table D-3 – Weld Depth Measurements for Outer Top Cover Plate Welds

DSC	Measurement Location (Degrees)	Initial Depth (in.)	Final Crown depth (in.)	Weld Depth (initial depth - post-grind depth) (in.)
11	0	0.622	0.045	0.577
	90	0.640	0.022	0.618
	180	0.660	0.031	0.629
	270	0.628	0.044	0.584
12	0	0.624	0.091	0.533
	90	0.635	0.101	0.534
	180	0.642	0.075	0.567
	270	0.685	0.048	0.637
13	0	0.611	0.064	0.547
	90	0.622	0.090	0.532
	180	0.608	0.086	0.522
	270	0.614	0.054	0.560
14	0	0.642	0.111	0.531
	90	0.636	0.092	0.544
	180	0.633	0.121	0.512
	270	0.636	0.081	0.555
15	0	0.674	0.133	0.541
	90	0.637	0.075	0.562
	180	0.653	0.123	0.530
	270	0.632	0.058	0.574
16	0*	0.639	0.080	0.559
	90*	0.635	0.047	0.588
	180*	0.652	0.126	0.526
	270*	0.622	0.025	0.597

* DSC 16 weld depth measurements were re-verified at each of these cardinal locations. The 0° location was originally measured as 0.507 inch and re-verified as 0.488 inch. The 90° location was originally measured as 0.514 inch and re-verified as 0.503 inch. The 180° location was originally measure as 0.524 inch and re-verified as 0.525 inch. The 270° location was originally measure as 0.548 inch and re-verified as 0.543 inch. Weld repair brought the weld depth measurement at each location to values greater than 0.500 inch as indicated in Table D-3. The shortest as-found measured weld depth (after repair) on DSC 16 was 0.526 inch”.

Appendix E

Summary of Phased Array Ultrasonic Test (PAUT) Examination of Dry Shielded Canister DSC 16

NSPM contracted AREVA to develop equipment, qualify process and personnel, and perform UT examination of DSC 16. Although the PAUT technique is not approved for use in the NUHOMS® 61BTH licensing basis, ISG-15 accepts UT examination of closure welds in combination with root and final PT, with no stress reduction factor. PAUT is especially suitable due to the complex geometry and the limited space available for the transducer between the canister and the cask.

The Zetec/ONDT PA instrument (Model No. Z-Scan PA 64/128-R-O) and associated data acquisition system were used to develop a test procedure for PAUT examination that could examine the welds of the inner and outer top cover plates from the annular space in the TC where the inflatable seal is installed during loading operations as shown in Figure E-1. The equipment scanned both ITCP and OTCP welds, but not the weld of the ITCP to the siphon/vent block, nor the welds of the vent and siphon port covers. The mechanism for transporting the transducers provided the capability to record scanning data correlated to the location on the circumference.

Figure E-1 – PAUT Scanner

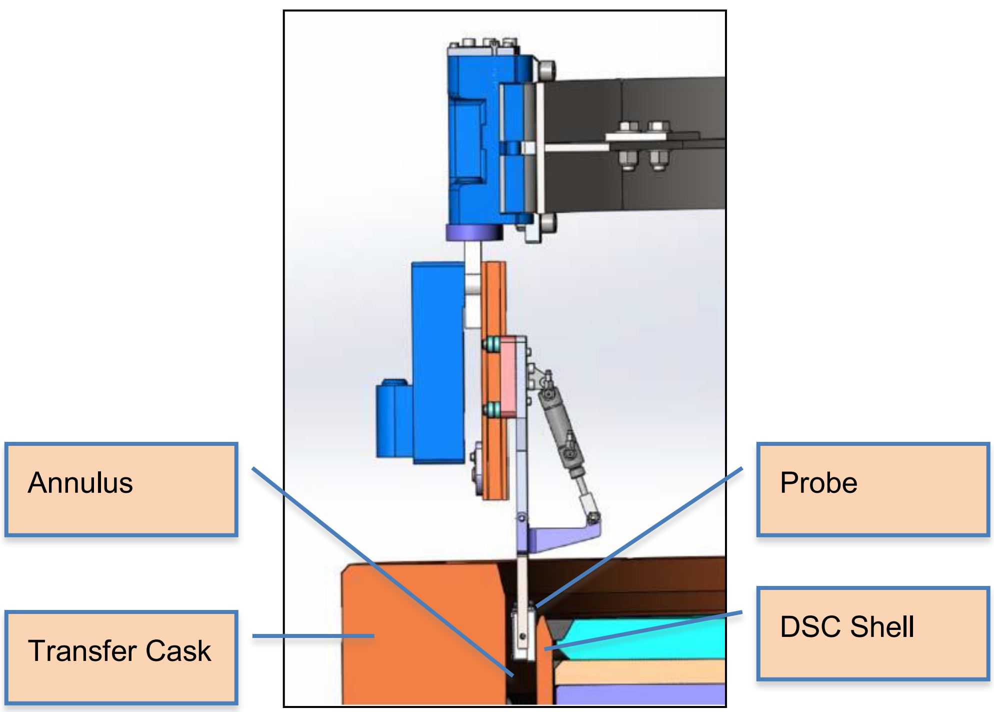

A protocol was developed for assessing the capability of the PAUT examination process. ASME Section V, Article 14, was used as a guide in the development of this process. The demonstration was performed to T-1424(b) (Intermediate Rigor) requirements, and the detection test used the method described in T-1471(a). That is, the mockup accurately represented the geometry of the two closure welds, with at least 10 flaws or grading units, and a probability of detection (POD) of 80% with a false call rate less than 20% was required for acceptable performance.

Two mockups were prepared. The development mockup is an open mockup that contains typical weld manufacturing flaws and was used to develop the examination procedure and to document basic flaw detection, location, and dimensioning capabilities. This mockup also provided geometric indicators for aligning the PAUT scans with the weld as shown in Figure E-2. A blind demonstration mockup was used to provide objective evidence of the examination procedure and personnel performance capability. The geometric configuration was similar to the development mockup, but the flaw location, number, and characteristics were unknown to the personnel to be qualified. Data analysis personnel were certified to Level II or Level III and qualified for flaw detection and flaw sizing.

Figure E-2 – Geometric Indications for Aligning Scans with the Welds

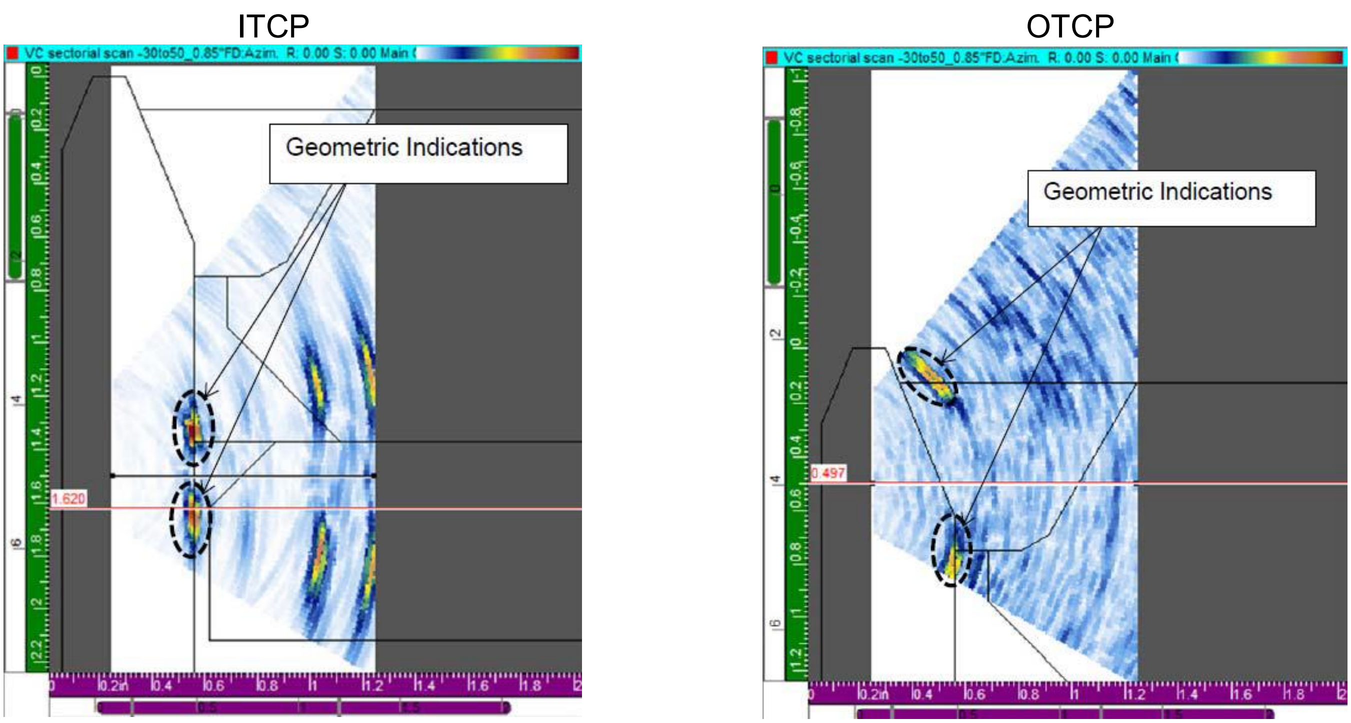

Both NSPM and the Electric Power Research Institute (EPRI) provided oversight to the demonstration. EPRI documented the sizes and locations of the intended flaws in the blind mockup, reviewed the open demonstration and blind personnel qualification protocols, independently evaluated the UT data collected by AREVA from the mock-ups, reviewed the results of the “blind” personnel tests and examination data, and verified in person that scans on the blind specimen were performed in accordance with the procedure.

This performance-based procedure qualification demonstrated the ability to detect and size welding fabrication flaws, but did not include evaluation of defects with respect to ASME Code criteria such as those of NB-5331.

The demonstration was performed in January 2015 at the AREVA facility on Mill Ridge Road in Lynchburg, VA, with NRC representatives present. Two data analysts were qualified with a POD of 97%, no missed detections, and one false call. These two analysts performed the actual PAUT examination of DSC 16.

<u>PAUT Examination Results of DSC 16</u>

The PAUT examination of DSC 16 was performed in February, 2015. Thirty-three flaws were identified in the OTCP weld, of which nine were intermittent over a length up to 14 inches, one was intermittent over 32 inches, one was intermittent over the full circumference, one was an isolated defect at the root, and the remaining 21 were separate embedded flaws. The largest single flaw size was 0.14 inch, well below the full circumference OTCP critical flaw height of 0.29 inch. The average underfill on the OTCP weld was 0.10 inch; this does not indicate undersized welds, but is rather due to placing the 0.50 inch weld into the 0.62 inch groove machined into the OTCP.

Thirty-four flaws were detected in the ITCP weld, of which one was intermittent over 10 inches. Individual flaw heights ranged from 0.04 to 0.11 inch. All of the defects were recorded at or near the fusion line; (most defects at the fusion line with the shell, some at the fusion line with the cover plate). The ITCP weld size is measured at 0.25 to 0.4 inches from root to crown at the canister wall, compared to the design minimum of 3/16 inch.

The ITCP critical flaw height was calculated to be 0.15 inch for the measured 0.25 inch minimum weld thickness, using the same method as for the OTCP weld. The largest ITCP weld flaw found in both length and height was designated Flaw No. 7 (shown in Figure E-3). At 0.11 inches height, it is smaller than the ITCP critical flaw. The flaw location is reported as “in the ITCP base metal, near the weld toe,” intermittent along 10.55 inches.

Due to dimensional variations (the ITCP is not perfectly centered in the shell, for example), the overlay of the ideal weld location on the UT plots is approximate. Because the defect tracks the circumference, and the plate has been examined by UT as required by ASME NB-2531, it is more likely the defect is at the fusion line rather than in the plate. In any case, this defect is not within the minimum throat region of the weld, but is either in the 3/4 inch thick plate or along the fusion line, which is at least 0.265 inch wide along the 45° bevel. The flaw is not a full circumferential flaw as assumed in the critical flaw size calculation.

The height of the individual flaws detected by PAUT in DSC 16 (no greater than 0.14 inch in the inner and outer covers) is consistent with the expectation in ISG-15 that flaws would be limited in height to the thickness of one weld bead.

Figure E-3 – Inner Top Cover Plate Flaw Number 7

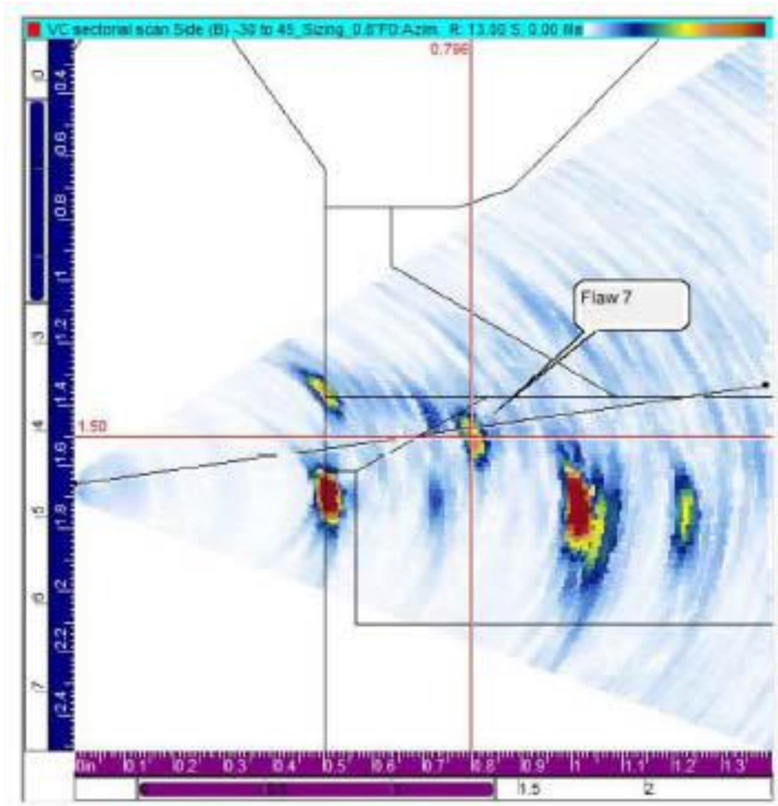

ENCLOSURE 2

STRUCTURAL INTEGRITY ASSOCIATES, INC. REPORT 1301415.301, REVISION 0

DEVELOPMENT OF AN ANALYSIS BASED STRESS ALLOWABLE REDUCTION FACTOR (SARF) – DRY SHIELDED CANISTER (DSC) TOP CLOSURE WELDMENTS

39 pages follow

Structural Integrity Associates, Inc.®

CALCULATION PACKAGE

File No.: 1301415.301

Project No.: 1301415

Quality Program Type: ☒ Nuclear ☐ Commercial

PROJECT NAME:
Monticello ISFSI – DSC 11 through 16 Exemption Request

CONTRACT NO.:
1005, Release 48, Amendment 6

CLIENT:
Xcel Energy

PLANT:
Monticello Nuclear Generating Station

CALCULATION TITLE:
Development of an Analysis Based Stress Allowable Reduction Factor (SARF) – Dry Shielded Canister (DSC) Top Closure Weldments

Document Revision	Affected Pages	Revision Description	Project Manager Approval Signature & Date	Preparer(s) & Checker(s) Signatures & Date
0	1 – 30 A-1 – A-2 B-1 – B-7	Initial Issue	Richard Bax 10/23/14 James W. Axline 10/23/14	Preparer: Wilson Wong 10/23/14 Checkers: J. Wu 10/23/14 C. Fourcade 10/23/14

Table of Contents

List of Tables

List of Figures

1.0 OBJECTIVE

The objective of this calculation is to develop a quantitative basis for a stress allowable reduction factor (SARF) to address weld quality in the inner top cover plate (ITCP) and outer top cover plate (OTCP) weldments of the NUHOMS dry shielded canister (DSC) system. This workscope is in support of the USNRC CofC Exemption submittal for DSC's 11 through 16, currently at the Monticello Nuclear Generating Plant (MNGP).

Weld quality is described as a global effect, for which a factor is used to reduce the stress allowables to account for potentially less than sound weldments. The SARF has historically been tied to the level of non-destructive examination (NDE) performed on the weldment. That is to say, the greater the degree of NDE performed (such as volumetric) the greater the SARF (less reduction in stress allowable).

The ASME Code [5, NG-3352] contains values for SARF for a range of NDE. Specifically, a VT only scope of NDE would state an SARF of 0.35 for a partial penetration weldment. However, it should be clearly noted that the ASME Code table for SARF's has no limitations/definitions/requirements on the weld size, the weld/base metal materials, the welding configuration, the welding position, and most importantly, the welding process. In addition, as this table is from NG, the level and comprehensiveness of the design analysis is less than that for an NB-type component, such as the DSC. The 0.35 SARF is a conservative factor that addresses all types of welding. In the case of the DSC weldments, these are specific joint geometries, with high quality materials, favorable welding positions, and again, most importantly, a high purity welding processes (GTAW), and therefore, strict adherence to the 0.35 SARF number for a VT only NDE examination weldment is not warranted.

The intent of this calculation, for this exemption request only, is to evaluate a series of postulated weld flaws and determine, for each configuration, the effect on the unflawed stress results. The effect of the stress results will be comparative, performed by comparing the analysis results of the flawed configuration to those from the same geometry, but in an unflawed configuration.

The determination of the impact on stress results will be performed by finite element analysis (FEA) in which selected elements of the ITCP and OTCP weldments will be "removed" to represent "flawed/suspect" weld quality.

Various distributions of flaw size (length and depth) and frequency (spacing), will be examined.

The intent of this calculation is to analytically determine the type of flaw distribution that would justify a specific SARF. A separate work scope has been performed to evaluate, for the specific DSC weldments (DSC's 11 through 16), what are the expected type and density of flaw distributions. It is the overall intent for this project workscope that it can be shown that the type of flaw distribution, which would support an acceptable SARF, will be of significantly greater magnitude than those populations that would be expected for the type of welding used for the DSC weldments.

2.0 TECHNICAL APPROACH

The determination of the impact of weld quality on stress results (SARF) will be performed by the finite element methods. Both the flawed and unflawed geometry of the top end of the DSC will be modeled. To represent the presence of postulated flaws, selected elements within the model will be removed and analyses performed using representative load cases. By comparing the results from the unflawed and flawed FE models for these loads cases, a ratio, or stress allowable reduction factor can be determined. A range of flaws will be analyzed to develop a range of SARF values corresponding to the range of flaw populations.

Typical types of flaws will be considered, and a range of distributions of flaw size (length and depth) and frequency (spacing), will be examined.

Three types of flaws will be addressed.

- Radial: a postulated flaw oriented in a plane radial to the DSC longitudinal axis and spanning the weldment from cover plate to shell.
- Circumferential: a planar flaw oriented in a plane parallel to the DSC axis and oriented circumferentially around the DSC.
- Laminar: a planar flaw in a plane perpendicular to the longitudinal axis of the DSC and spanning the weldment from cover plate to shell.

In the determination of what flaw types to analyze in the OTCP and the ITCP, the size/volume of the weldment was considered. The OTCP weldment is both large in size and volume absolutely, and also relative, to the weldment volume of the ITCP. Therefore, all three types of flaws are evaluated for the OTCP. The ITCP weldment, due to its reduced weldment size, is evaluated using a single flaw of significant cross-section, which represents elements of all three types. Figures showing these flaw types, location, and orientation are shown in Figures 2 through 9.

2.1 Finite Element Model and Flaw Simulation

A single finite element model (FEM) is developed using the ANSYS finite element analysis software [2]. The model represents a 180° sector of the upper end of the DSC. The model includes the outer top cover plate and weldment, the inner top cover plate and weldment, and a portion of the DSC shell.

The FEM utilizes the ANSYS 3-D structural element (SOLID45). The unflawed model contains all portions of the two weldments.

The modeling of the postulated flaw is done by “killing” the selected elements that represent the flaw size and location, using the EKILL command in ANSYS. This command deactivates the element such that it contributes near zero stiffness to the overall stiffness matrix. The result is a redistribution of loading and stresses around “killed” elements.

The ANSYS model of the top end geometry is shown in Figure 1 which illustrates the full model and then localized sections through the OTCP and ITCP.

3.0 ASSUMPTIONS / DESIGN INPUTS

The top end geometry of the DSC is defined in Reference 3. The OTCP, ITCP, and DSC shell dimensions, as well as the materials, are provided in Reference 3. A number of assumptions were made during development of the finite element model, which are listed as follows:

- The model consists of a half-symmetric portion of the inner top cover plate (ITCP), outer top cover plate (OTCP), and the top 20 inches of the outer DSC cylinder. The 20 inches equates to greater than $4.0\sqrt{Rt}$, thus avoiding any end affects at the free end constraint. The model is constructed of approximately 840,000 SOLID45 elements to ensure adequate mesh refinement for the ITCP and OTCP welds in the circumferential direction.
- The OTCP is modeled with the top surface set 1/8 of an inch below the end of the DSC. The J-groove weld preparation is as shown in Reference 3. The weldment is shown flush with the surface of the OTCP and not set below, as is allowed by the Reference 3 field assembly drawing. The modeled set back weldment is considered acceptable as this is a comparative analysis and the same geometries are used in both the flawed and unflawed condition.
- The ITCP is modeled as a flat plate and the closure weldment is modeled flush with the top surface of the ITCP.
- The DSC shell, the OTCP, the ITCP, and the OTCP and ITCP weldments are modeled as SA-240, Type 304 stainless steel. Material properties are taken from Reference 4. Standard room temperature material properties for Type 304 stainless steel are used: Young's Modulus = 28.30E6, Density = 0.283 lbs/in^3, and Poisson's Ratio of 0.3.
- The analysis is performed at 70°F. This temperature is selected as this is a comparative analysis and both the unflawed and flawed runs utilize the same temperature.
- The bottom edge of the outer cylinder is fixed in the axial and circumferential directions, and symmetry boundary constraints are placed on the symmetry plane. For the side drop runs, the outer cylinder is released in the circumferential direction and is supported at the point of "impact" via radial displacement couples to a support block with reduced stiffness properties.
- The analyses are all treated as elastic.
- The localized effects of the vent and siphon block and the ITCP weldment are not modeled. This is acceptable as the weldment connection to the V/S block (1/4" groove) is similar to the majority portions of the ITCP weldment, and the intent is to determine the effects of global weld quality, not localized stress concentrations. The effect of stress discontinuity at the V/S block will be addressed by the design analysis which models this explicitly, and then uses the SARF to further modify the stress allowables.
- The siphon/vent port cover plates are not modeled as the nominal stresses (primarily due to pressure) are sufficiently low to accommodate extremely low SARF's. Assuming a 3/16" closure groove weld [3] on a nominal 2 inch diameter cover plate results in a weld shear stress of

less than 500 psi. Thus even a worst case SARF of 0.10, would be acceptable given the nominal weld filler metal shear stress allowable of 0.6 Sm [5, NB-3227.2] = 0.6 * ~16 ksi = ~9.6 ksi.

- Dimensions for the components are taken as the nominal. This is acceptable as this is a comparative analysis.
- The evaluated paths for which the stress results are extracted and used for comparison (flawed vs unflawed) are shown in Figure 13.

4.0 CALCULATIONS

The determination of the SARF, as a function of weld quality (number and density of postulated flaws), is performed using two load cases. The pressure load is the primary normal and off normal load for these weldments and consists of internal pressure applied to the inner top cover and outer top cover. The specific definition and modeling details are described below for the pressure load case.

The drop load cases consist of a canister end drop, a canister corner drop, and a canister side drop. For this comparative analysis the canister side drop load case is utilized as it best represents the behavior of the drop event (an event that is germane to the MNGP ISFSI DSC hardware configuration) and is a more easily evaluated/modeled condition. The side drop load case develops localized stresses along a line of contact similar to the corner drop. The specific details for the side drop load case are described below.

4.1 Pressure Loading

The pressure loading consists of a nominal 100 psig internal pressure applied to the top cover plates. For evaluation of the ITCP (the nominal pressure boundary) weldment quality, the pressure is applied to the inside surface of the ITCP and the DSC shell, and the contacting surfaces between the ITCP and OTCP are bonded with sliding capability using ANSYS contact elements to allow for load transfer from the ITCP to the OTCP. For the ITCP pressure analysis, CONTA174 and TARGE170 contact elements were used to prevent the ITCP from penetrating the OTCP. In these cases the OTCP acts as a non-pressure retaining structural support for the ITCP. Figure 11 shows the displaced shape for the ITCP pressure load case.

For evaluation of the OTCP weldment quality, the pressure is applied only to the inside surface of the OTCP and the inside surface of the DSC. The ITCP and the weldment to the shell are both contained within this model and are not modeled as containing flaws, nor are they loaded by pressure. The intent of applying the pressure loading to the OTCP alone is to maximize the response of the OTCP-to-DSC shell weldment, as a result of postulated flaws within the weld. Applying the pressure to the ITCP, which in turn will load the OTCP, will diminish the response of the OTCP, as there exists supplemental stiffness from the ITCP. Figure 10 shows the displaced shape for the OTCP pressure load case.

4.2 Side Drop Loading

The side drop loading case is evaluated as a static 75G load case in which the FEM of the DSC shell is oriented with the symmetry plane in the direction of the drop. For the side drop analysis, the same contact element types (CONTA174 and TARGE170) were used to prevent the ITCP from penetrating the DSC outer cylinder. These are not used for the OTCP weld prep-to-DSC shell potential contact region, as the area of potential contact is small relative to the OTCP weld size.

To simulate the support of the transfer cask, the lower 20° of the DSC model is supported by a material which represents the stiffness of the transfer cask given that there is a difference in diameter between the DSC and the transfer cask. In the transfer condition, the DSC is supported within the Transfer Cask on thin guide rails, and the use of a lessor stiffness support in the lower 20° degree region is representative. Again this is a comparative analysis and the intent is to show the effect of weld quality in the weldments in the most highly stressed area of contact, which is at bottom dead center. Radial displacement couples between the DSC and support block are used. Figure 12 shows the geometry of this load case.

5.0 RESULTS OF ANALYSIS

The determination of the SARF for a given postulated flaw population is performed by extracting the stress results from the unflawed geometry, and the flawed geometry for the specific load case. These stresses are extracted and linearized along identical paths to capture the change in stresses due to the missing/flawed elements.

The comparison to determine the change in stress results, as a result of the postulated flaw population, typically compares the linearized membrane (P_m) and membrane plus bending ($P_m + P_b$) stress intensities for a path adjacent to the postulated flaw and at other regular spacings between the postulated flaws. These discrete ratios are then combined to produce a weighted SARF for the weld flaw pattern. Figure 13 shows the path locations and orientations for the three types of flaws for which stresses are extracted.

In general the comparison of stress results is done by comparing linearized membrane (P_m) and membrane plus bending ($P_m + P_b$) stress intensities. However, in the case of the side drop event for the radial and laminar flaws, the high compressive stresses in all three principal stresses make the use of stress intensity not representative. In these cases, where all three principal stresses are compressive, and the resultant stress intensity is of lesser magnitude than the principal stresses, the resulting SARF's are unrealistic. In these cases the greater stress values of the three principal stresses are combined by SRSS and compared for the flawed and unflawed configuration.

An initial set of postulated flaw populations for the radial, circumferential and laminar flaw were developed and analyzed. Subsequent to initial runs, additional flaw populations for the radial and circumferential flaw cases were run. The specific geometry of the flaw populations are shown in Tables 1 through 4, along with the resulting SARF's.

It should be noted that the intent of the calculation is to show a flaw population that is severe and thus demonstrate that large flaw populations (size, length, and density) can be tolerated, as the calculated SARF is acceptable. In the selection of the flaw population parameters, the depth of the flaws is typically set as a through-wall flaw. Obviously, such a flaw would have been unacceptable, and would have been identified by leak test examination. However, the intent of this calculation is to address structural capacity of the weldment, not confinement.[1] Thus the use of the through-wall flaw allows for a conservative determination of the SARF.

Table 1 documents the calculated SARF's for the OTCP weldment subjected to pressure loading. Table 2 documents the calculated SARF's for the OTCP weldment subjected to the side drop loading.

Table 3 documents the calculated SARF's for the ITCP weldment subjected to pressure loading. Table 4 documents the calculated SARF's for the ITCP weldment subjected to the side drop loading.

Table 5 presents the axial deflection at the centerline of the OTCP for the various flaw configurations analyzed for the pressure load case. The intent is to show that, as expected, the stiffness of the combined OTCP and ITCP is greater (less deflection) than the OTCP alone. This is the reason that the pressure loading was applied to the OTCP alone, so as to maximize the deflection of the OTCP, and therefore challenge to the OTCP weldment. A review of the table shows that the change in deflection of the OTCP as a result of the introduction of postulated flaws, in either the OTCP or ITCP weldment, is relatively low (< 15% in the worst case). Thus the evaluation of flaws does not require the explicit evaluation of concurrent flaws in the OTCP and ITCP, as their responses (unflawed/flawed) are basically similar, and this is a comparative evaluation.

In addition, a comparisons of the deflections of the OTCP in the unflawed and postulated flawed cases shows that for the less severe, but still significant flaw populations (Radial 2, Laminar, Circ 3, and Circ 4), the change in response (OTCP deflection) is small, typically 1% or less. It can therefore be presumed that a mix of flaw types would produce similar results as that for a single flaw type, e.g. a mix of radial, laminar, and circumferential flaws would have similar results as that for the bounding single flaw type. The worst case SARF for the selected flaw types will be utilized, thus any substitution of lesser SARF flaws (e.g. laminar) for greater SARF flaws (Circ) would be bounded.

Finally, the postulated 50% circumferential flaw for Circ 4 is positioned in the upper half of the weldment. The change in SARF values (Tables 3 and 4) between the Circ 3 and Circ 4 cases is an increase of ~4% for the pressure case, and ~14% for the side drop case. A 50% through-wall flaw, located in the lower portion of the weldment, would have an SARF no worse than the Circ 3 case, and the Circ 3 case SARF, for both pressure and side drop, is greater than 0.80. The placement of the 50% through-wall flaw in the lower half of the weldment would thus not change the results to a point where the Circ 3 case would not be bounding.

[1] The results demonstrate that the remaining ligaments of the DSC weldments have sufficient structural capacity, even with very severe and conservative penalties (postulated flaws) for nonconforming PT examinations, to perform their design function of restraining the OTCP and ITCP's, and additionally maintaining the confinement function during all service level load cases.

6.0 CONCLUSIONS AND DISCUSSION

The OTCP and ITCP weldments are made using both materials and processes, and in conditions which would result in high quality (very small flaw distribution). Specifically it is a stainless steel weldment made with argon cover gas in a flat position using a machine GTAW process. As such, concerns over weld porosity are minimized and the machine welding process will produce a very uniform and consistent weldment. Report 1301415.405 [1, See Appendix B] details the expected flaw distribution for this type of weldment.

A review of Tables 1 through 4 documents the calculated SARF for the selected flaw populations. The question of which flaw population to consider representative or typical, or bounding is based not on these analytical results but on the separate Reference 1 report. This report is based on the actual elements of the OTCP and ITCP welding, and considers industry experience and ISFSI Vendor experience [1, See Appendix B].

Reference 1 states in the conclusion that:

> *It is suggested a bounding subsurface defect condition is conservatively represented as an intermittent lack of fusion (LOF) defect evenly distributed along the canister weld. Further, the total length for LOF is conservatively estimated at 25% of the canister cover plate weld circumference. The estimated through thickness dimension is 1/8 inch, because this dimension represents a maximum weld bead thickness. One eighth inch is considered to be a conservative assumption, because it is recognized that most weld beads will be thinner especially as the weld cavity begins to fill. No credit is being taken for remelting even though remelting is normally associated with multipass welding."*

Comparing this to the analyzed flaw populations:

> OTCP: Both the radial and laminar flaws are not representative of the circumferentially oriented flaw described above. However, in both cases, the postulated flaws for these types are full thickness and full width, and thus would be considered more severe than a 1/8" thick, 25% total weld length flaw, with a width of one weld bead. As an example, the laminar flaw is the full width of the weld, and covers 72% of the circumferential arc. The radial Configuration 2 flaw (more limiting), shown in Figure 3, is a full height (through-wall) flaw, spanning the full weldment width, and occurring less than 2" apart.
>
> The circumferential flaw, Configuration 3, shown in Figure 7, is a full height (through-wall) flaw, 1" long and occurring every 5". The 1" in 5" spacing is a 20% occurrence of postulated flaws, which although less than 25%, is tempered by the fact that the analyzed flaw is full height, not the expected one bead thickness dimension (~ 1/8") described above. With this consideration, the Configuration 3 circumferential flaw bounds the "conservatively assumed" flaw stated in Reference 1.

ITCP: The 360 degree embedded flaw postulated and evaluated (Figure 9), is much more adverse than the expected flaw of Reference 1 described above.

In both the OTCP and the ITCP weldments, the weld is a multi-layer weldment, and both received multi-level VT and PT examinations. Although the PT cannot be credited, the VT can be assumed to have seen large surface breaking flaws. As a further argument that the postulated and analyzed flaws are bounding for flaws that would have not have been identified by the VT exams, the likelihood that multiple through–layer thickness flaws of the postulated percentage of arc length (e.g. the Circ 3 case flaw covers 20% of the total arc length) would occur in every layer, and would also line up with flaws below and above to create a through-wall combined flaw, and not be detected by the multiple VT's, is highly unlikely and not realistic.

Again the use of through-wall flaws is done to evaluate the structural integrity of the weldments. The validation of confinement of the weldments was separately confirmed by successful leak testing.

7.0 REFERENCES

1. SI Report No. 1301415.405, Revision 0, "Expectations for Field Closure Welds on the AREVA-TN NUHOMS 61BTH Type1 & 2 Transportable Canister for BWR Dry Fuel Storage," October 2014, SI File No. 1301415.405. [Appendix B]

2. ANSYS Mechanical APDL and PrepPost, Release 14.5 (w/ Service Pack 1), ANSYS, Inc., September 2012.

3. AREVA Design Drawings for the 61BTH, Type 1 and 2, NUH61BTH-3000, Rev 1, "NUHOMS 61BTH Type 1 DSC Main Assembly," and NUH61BTH-4008, Rev 1, NUHOMS 61BTH Type 1 & 2 Transportable Canister for BWR Fuel Field Welding, PROPRIETARY SI File No. 1301415.201P.

4. ASME Boiler and Pressure Vessel Code, Section II, Part D, Material Properties, 2004 Edition.

5. ASME Boiler and Pressure Code, Section III, Division 1, Rules for Construction of Nuclear Facility Components, 2004 Edition.

Table 1: OTCP Stress Reduction Factor Results – Pressure Loading

	PRESSURE LOADING																				
	Radial			Radial #2			Laminar			Circ #1			Circ #2			Circ #3			Circ #4		
	Pm	Pm+Pb(I)	Pm+Pb(O)	Pm	Pm+Pb(I)	Pm+Pb(O)	Pm	Pm+Pb(I)	Pm+Pb(O)	Pm	Pm+Pb(I)	Pm+Pb(O)	Pm	Pm+Pb(I)	Pm+Pb(O)	Pm	Pm+Pb(I)	Pm+Pb(O)	Pm	Pm+Pb(I)	Pm+Pb(O)
Average	0.908	0.762	0.900	0.955	0.879	0.973	0.911	0.911	0.950	0.515	0.534	0.436	0.759	0.771	0.703	0.924	0.920	0.888	0.940	0.956	0.919
MIN	**0.762**			**0.879**			**0.911**			**0.436**			**0.703**			**0.888**			**0.919**		
	Through Wall Flaw			Through Wall Flaw			Through Wall Flaw			Through Wall Flaw			Through Wall Flaw			Through Wall Flaw			50% Part Through Wall Flaw		
	Pattern Arc Spacing (in)		0.864	Pattern Arc Spacing (in)		1.734	Pattern Arc Spacing (in)		5.760	Pattern Arc Spacing (in)		5.184	Pattern Arc Spacing (in)		5.184	Pattern Arc Spacing (in)		5.184	Pattern Arc Spacing (in)		5.184
	Flaw Width (in)		0.144	Flaw Width (in)		0.144	Flaw Arc Length (in)		4.176	Flaw Arc Length (in)		3.600	Flaw Arc Length (in)		2.016	Flaw Arc Length (in)		1.012	Flaw Arc Length (in)		1.012
	Un-Flawed Arc Spacing (in)		0.720	Un-Flawed Arc Spacing (in)		1.590	Un-Flawed Arc Spacing (in)		1.584	Un-Flawed Arc Spacing (in)		1.584	Un-Flawed Arc Spacing (in)		3.168	Un-Flawed Arc Spacing (in)		4.172	Un-Flawed Arc Spacing (in)		4.172

Table 2: OTCP Stress Reduction Factor Results – Side Drop Loading

	SIDE DROP																	
	Radial			**Laminar**			**Circ #1**			**Circ #2**			**Circ #3**			**Circ #4**		
	Pm	Pm+Pb(I)	Pm+Pb(O)	Pm	Pm+Pb(I)	Pm+Pb(O)	Pm	Pm+Pb(I)	Pm+Pb(O)	Pm	Pm+Pb(I)	Pm+Pb(O)	Pm	Pm+Pb(I)	Pm+Pb(O)	Pm	Pm+Pb(I)	Pm+Pb(O)
Average	0.976	0.921	0.912	0.882	0.957	1.000	0.542	0.606	0.762	0.720	0.756	0.903	0.846	0.861	0.972	0.979	0.974	0.974
MIN	**0.912**			**0.882**			**0.542**			**0.720**			**0.846**			**0.974**		
	Through Wall Flaw			Through Wall Flaw			Through Wall Flaw			Through Wall Flaw			Through Wall Flaw			50% Part Through Wall Flaw		
	Pattern Arc Spacing (in)		0.864	Pattern Arc Spacing (in)		5.760	Pattern Arc Spacing (in)		5.184	Pattern Arc Spacing (in)		5.184	Pattern Arc Spacing (in)		5.184	Pattern Arc Spacing (in)		5.184
	Flaw Width (in)		0.144	Flaw Arc Length (in)		4.176	Flaw Arc Length (in)		3.600	Flaw Arc Length (in)		2.016	Flaw Arc Length (in)		1.012	Flaw Arc Length (in)		1.012
	Un-Flawed Arc Spacing (in)		0.720	Un-Flawed Arc Spacing (in)		1.584	Un-Flawed Arc Spacing (in)		1.584	Un-Flawed Arc Spacing (in)		3.168	Un-Flawed Arc Spacing (in)		4.172	Un-Flawed Arc Spacing (in)		4.172

Table 3: ITCP Stress Reduction Factor Results – Pressure Loading

ITCP		
Pressure		
Pm	Pm+Pb(I)	Pm+Pb(O)
0.964	1.000	0.954
0.954		
Flaw Cross Section Area		0.006 in^2
Pattern Arc Spacing (in)		5.184
Flaw Arc Length (in)		2.590
Flaw Arc Spacing (in)		2.590

Table 4: ITCP Stress Reduction Factor Results – Side Drop Loading

ITCP		
Side Drop		
Pm	Pm+Pb(I)	Pm+Pb(O)
1.000	0.931	1.000
0.931		
Flaw Cross Section Area		0.006 in^2
Pattern Arc Spacing (in)		5.184
Flaw Arc Length (in)		2.590
Flaw Arc Spacing (in)		2.590

Table 5: OTCP and ITCP Deflection Load Cases – Pressure Load Case

Component	Flaw Type	Axial Deflection - Unflawed Configuration (inches)(1)	Axial Deflection - Flawed Configuration (inches)(1)	Ratio of Increase (Percent change) Flawed/Unflawed
OTCP	Radial 1	0.9089	0.921	1.3%
	Radial 2	0.9089	0.9149	0.7%
	Laminar	0.9089	0.918	1.0%
	Circ 1	0.9089	1.0391	14.3%
	Circ 2	0.9089	0.9507	4.6%
	Circ 3	0.9089	0.9208	1.3%
	Circ 4	0.9089	0.9169	0.9%
ITCP	Circ	0.629	0.6314	0.4%

Note:

1) The deflection value was taken at the center top of each plate.

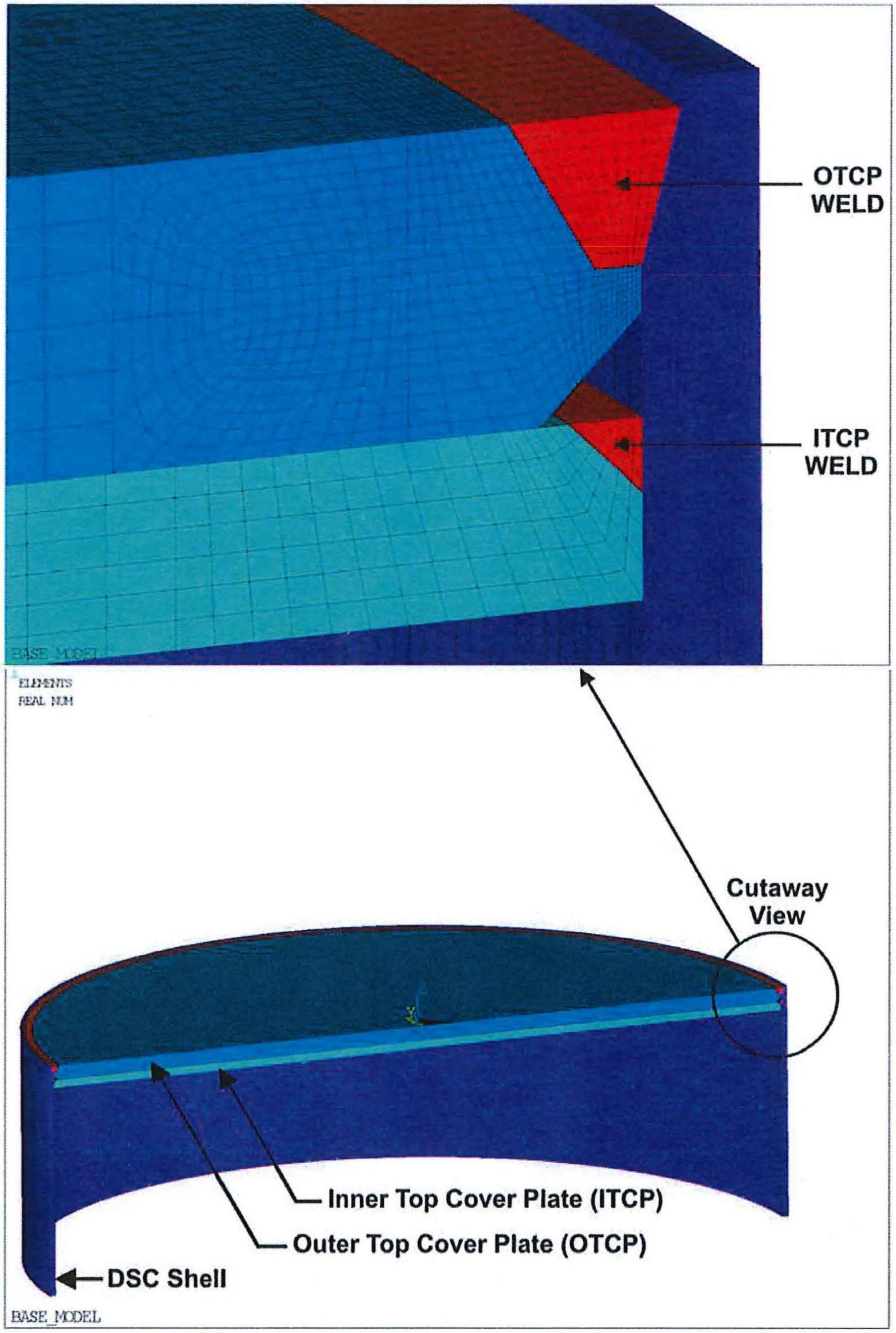

Figure 1. Finite Element Model and OTCP and ITCP Details

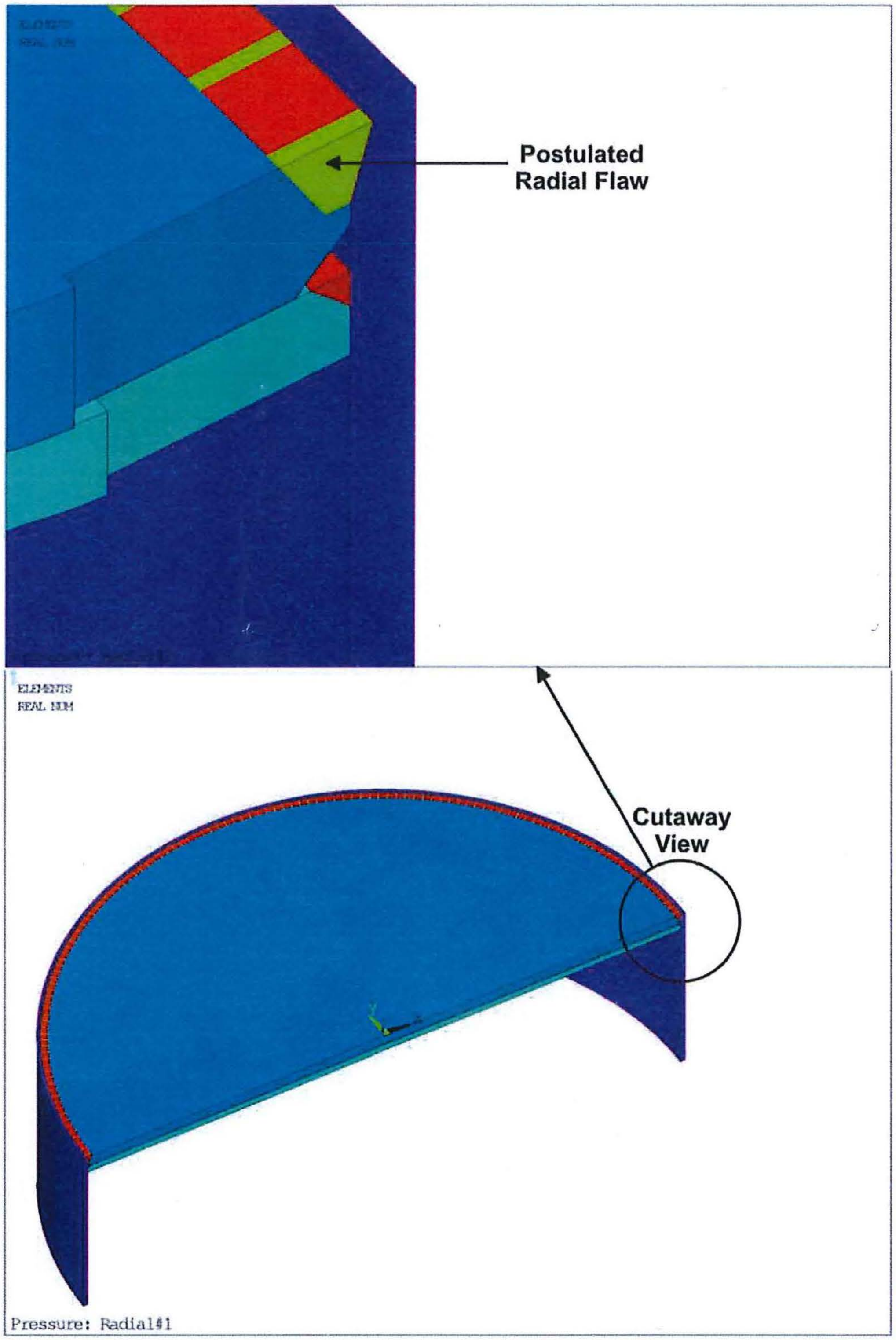

Figure 2. OTCP Postulated Flaw Configuration – Radial #1

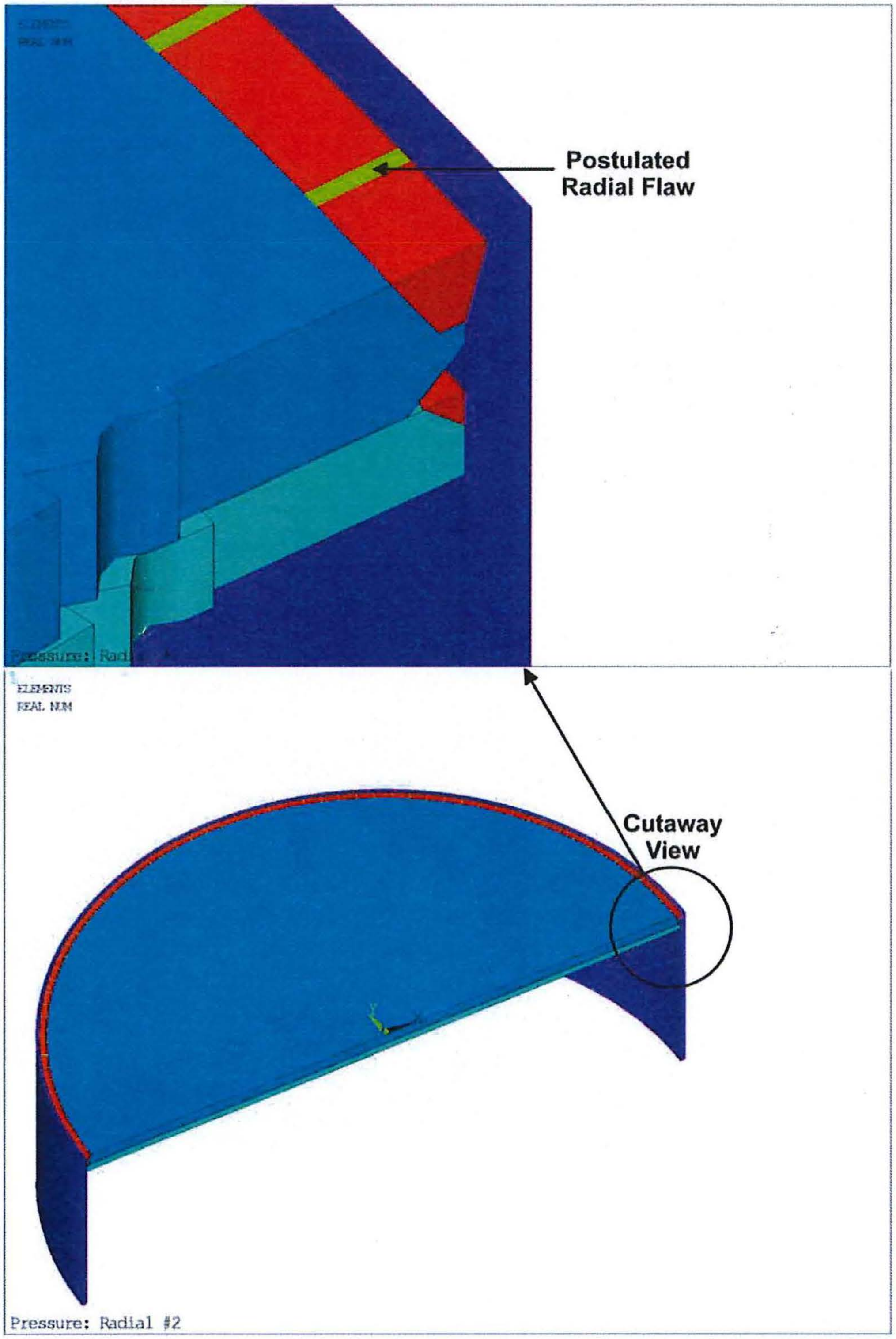

Figure 3. OTCP Postulated Flaw Configuration – Radial #2

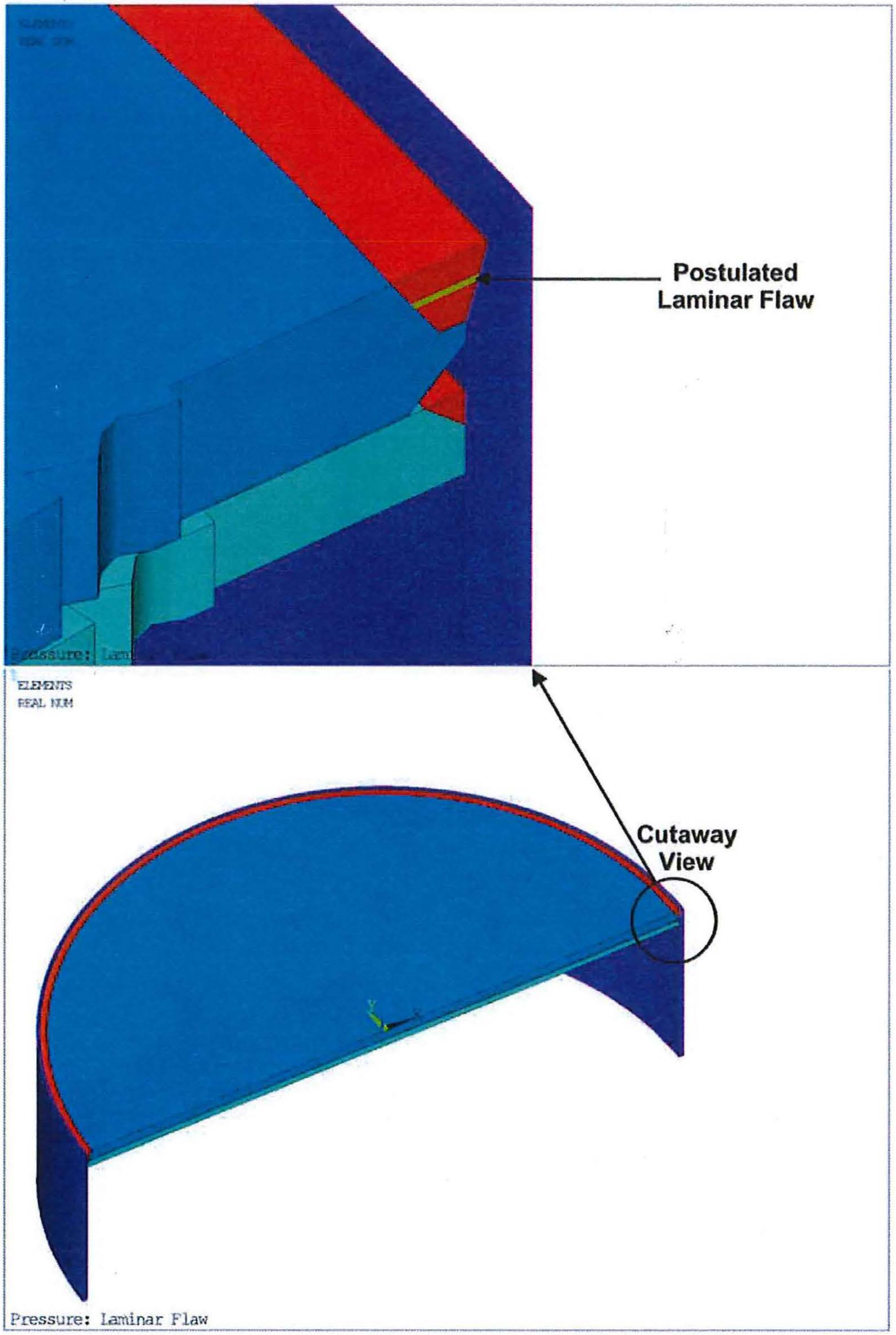

Figure 4. OTCP Postulated Flaw Configuration – Laminar

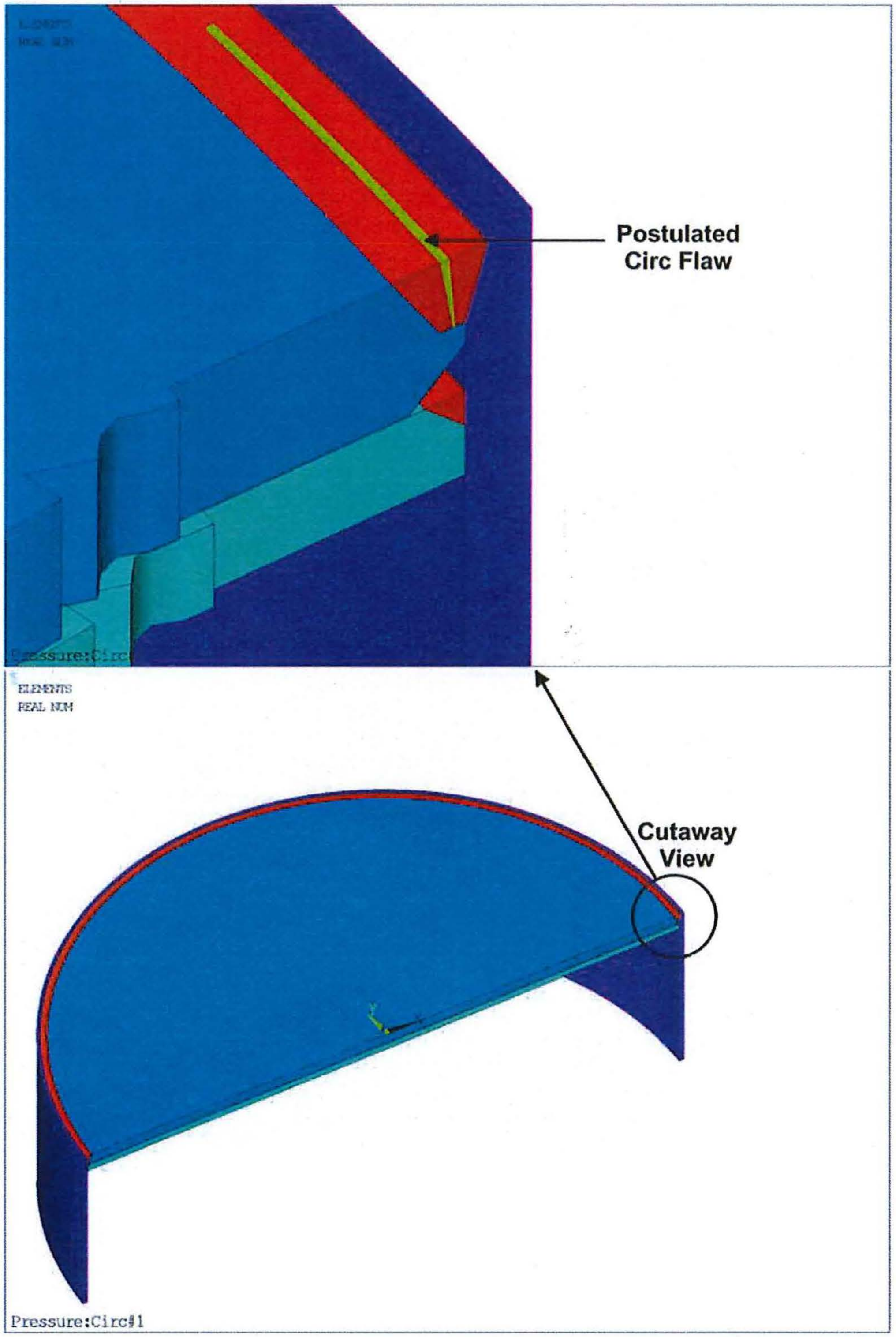

Figure 5. OTCP Postulated Flaw Configuration – Circumferential #1

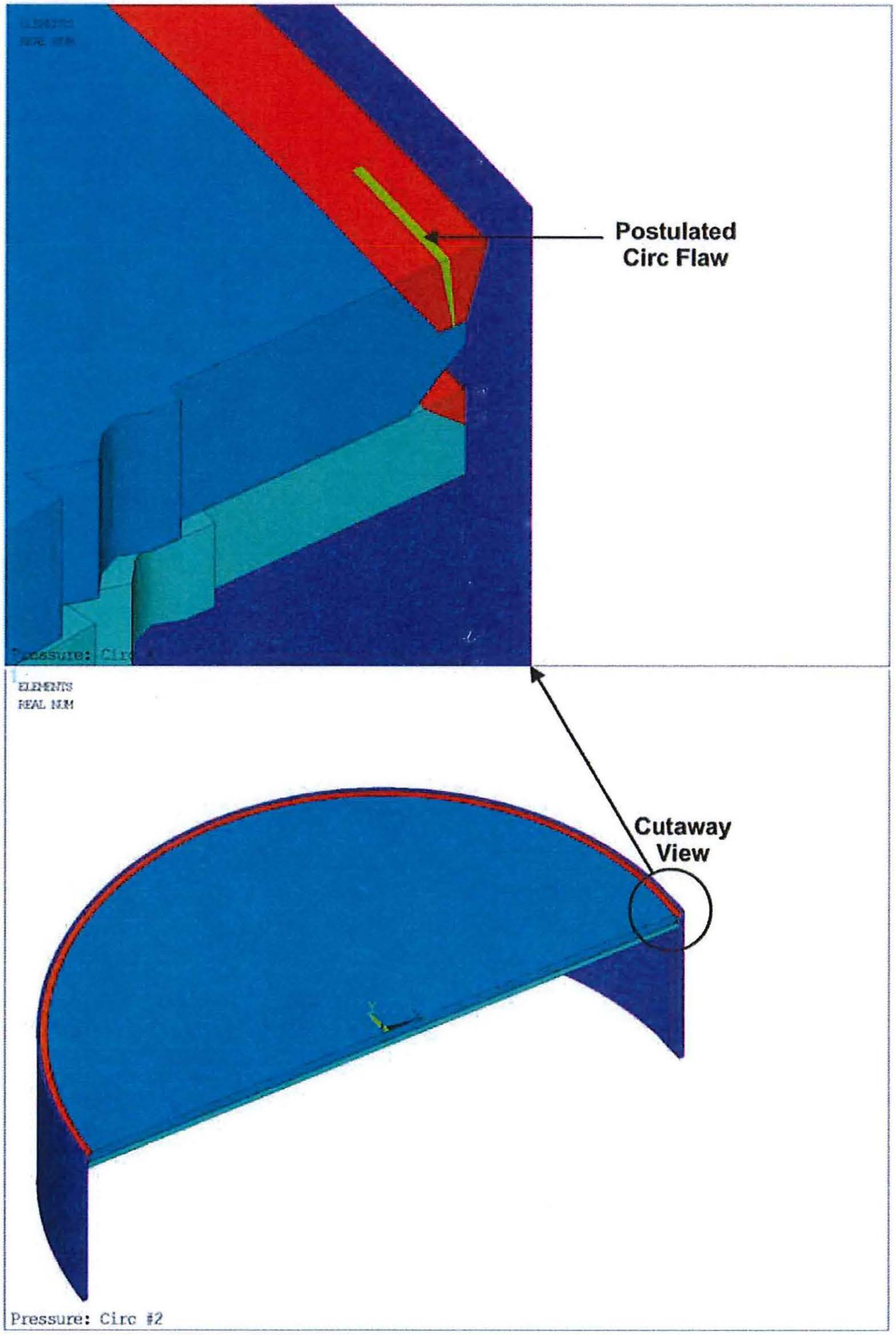

Figure 6. OTCP Postulated Flaw Configuration – Circumferential #2

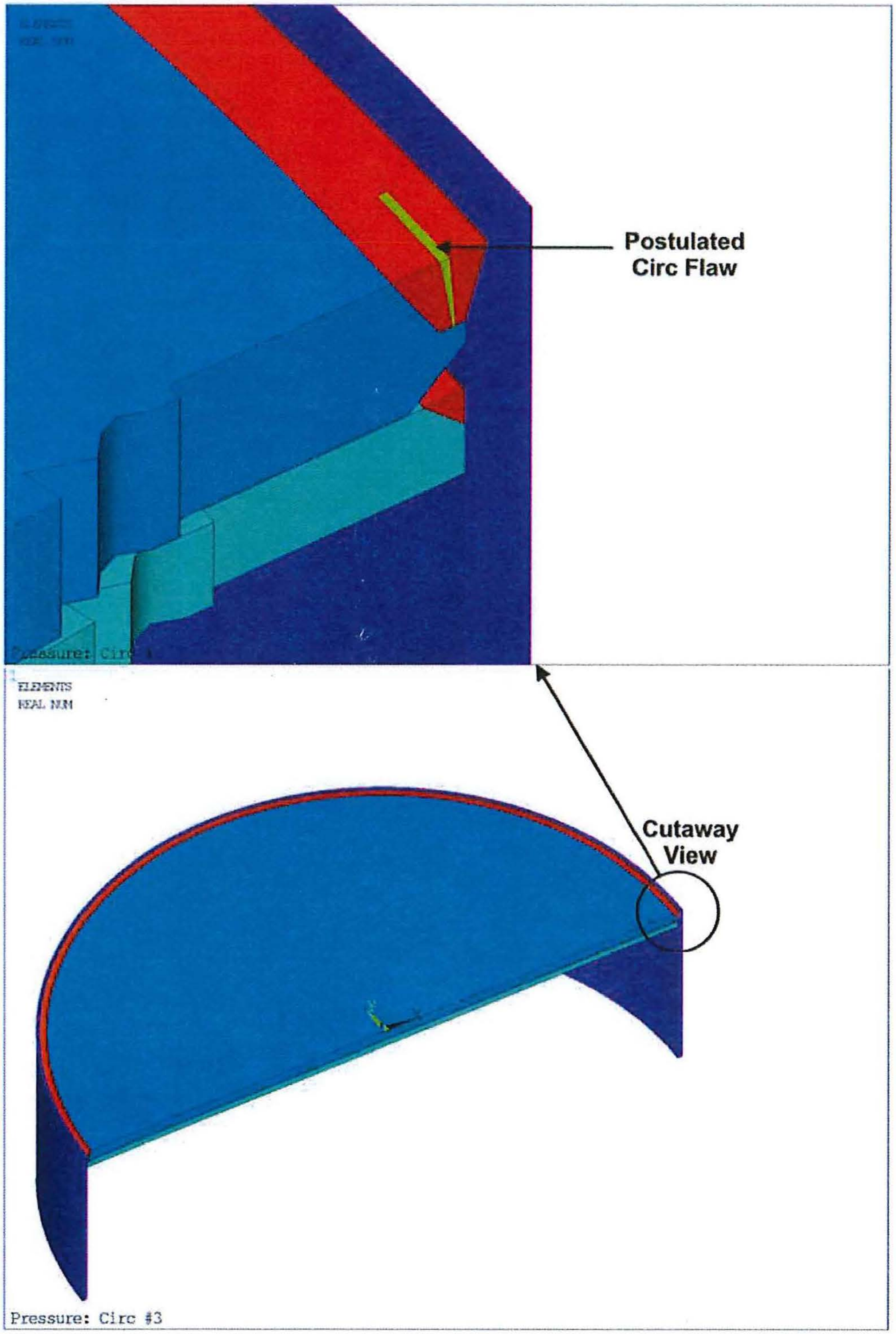

Figure 7. OTCP Postulated Flaw Configuration – Circumferential #3

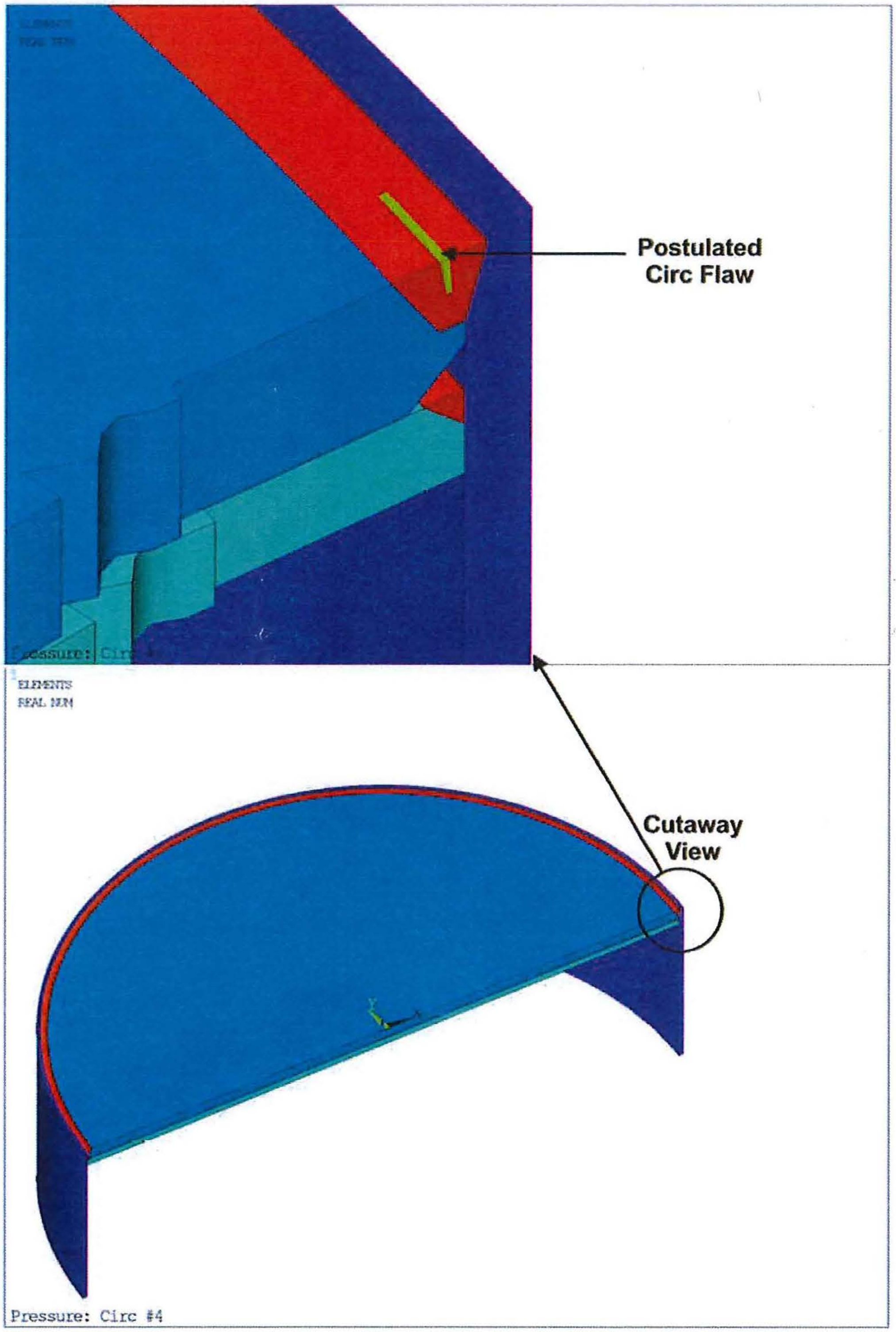

Figure 8. OTCP Postulated Flaw Configuration – Circumferential #4

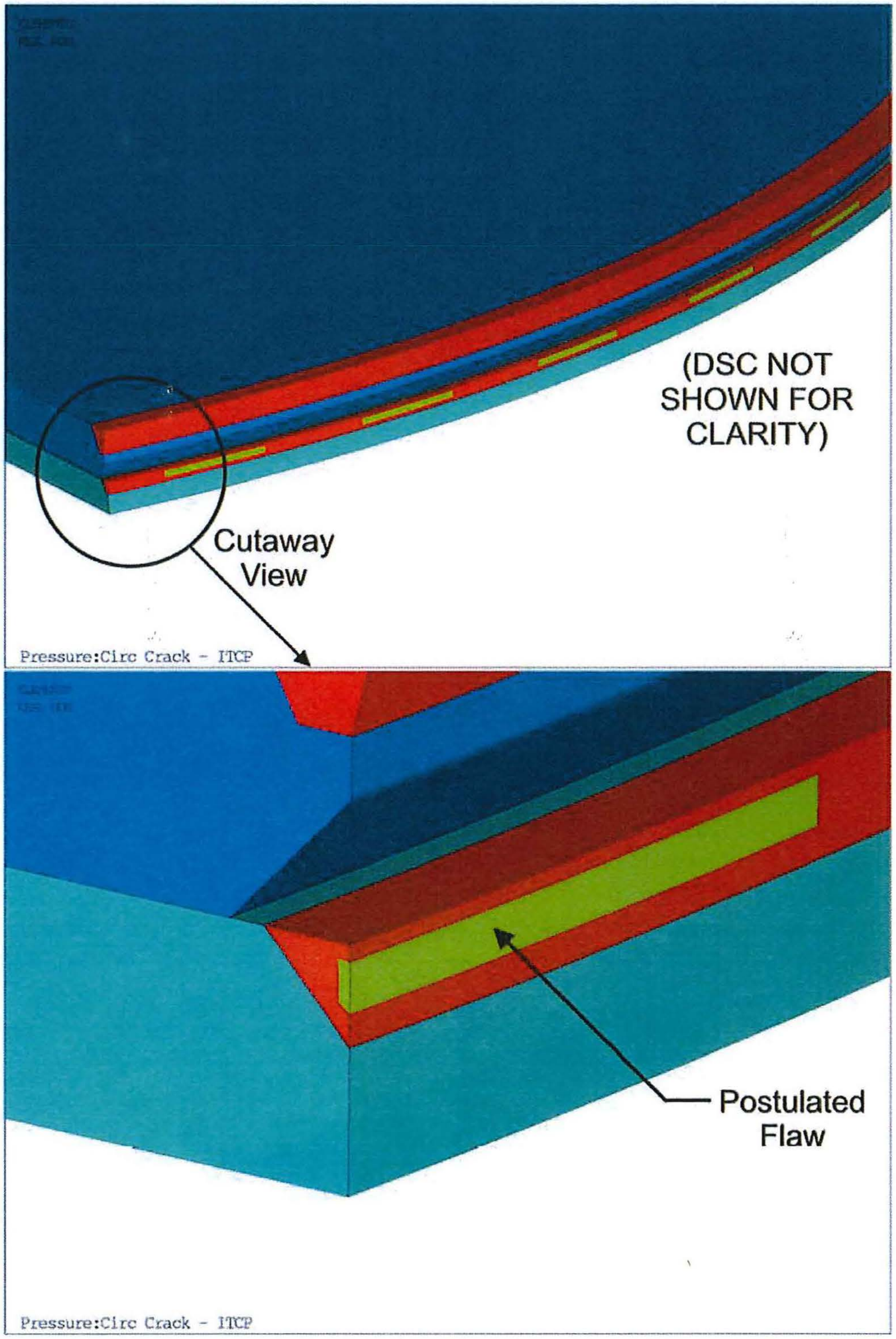

Figure 9. ITCP Postulated Flaw Configuration – Circumferential

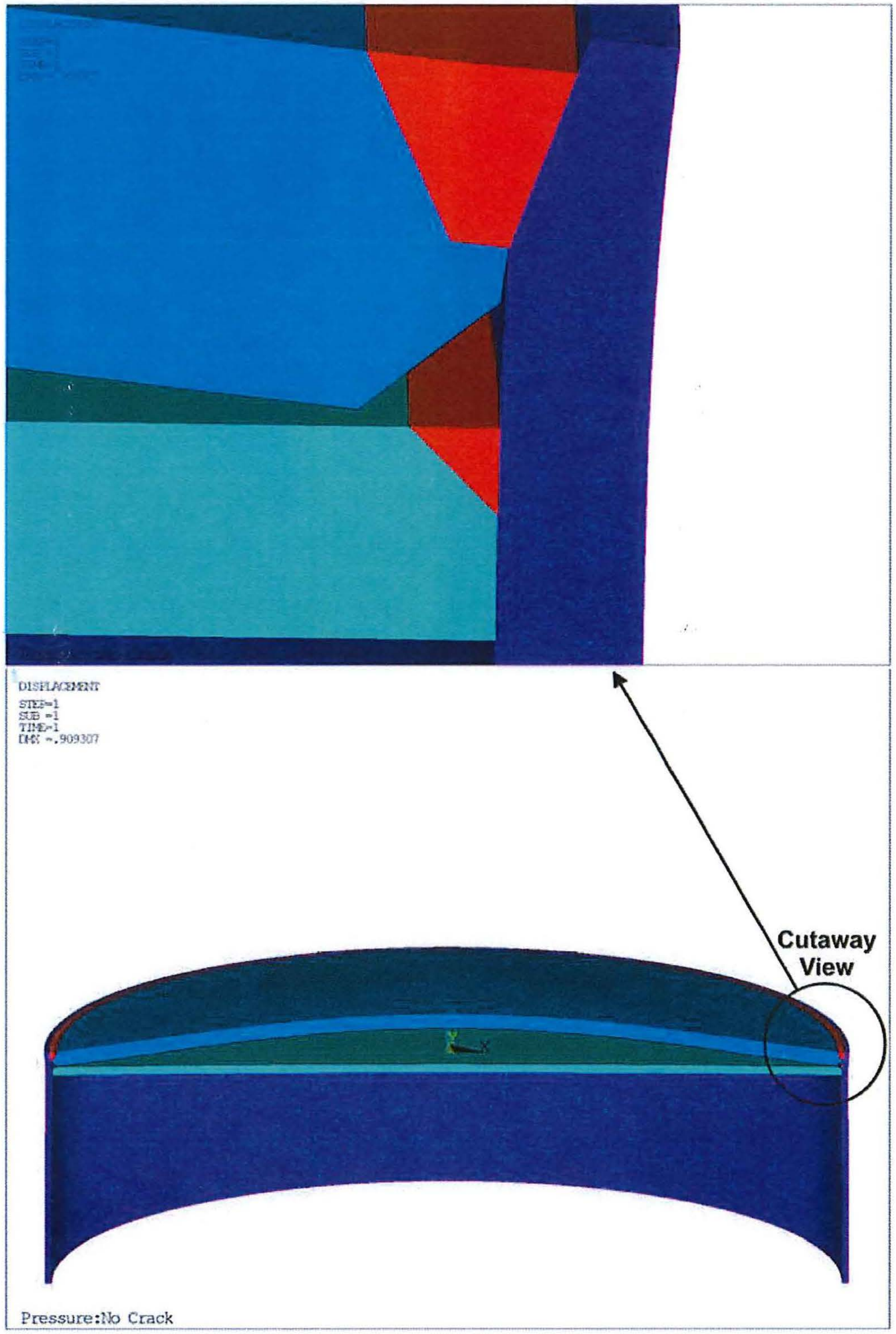

Figure 10. OTCP Pressure Load Case – Displaced Shape (Exaggerated)

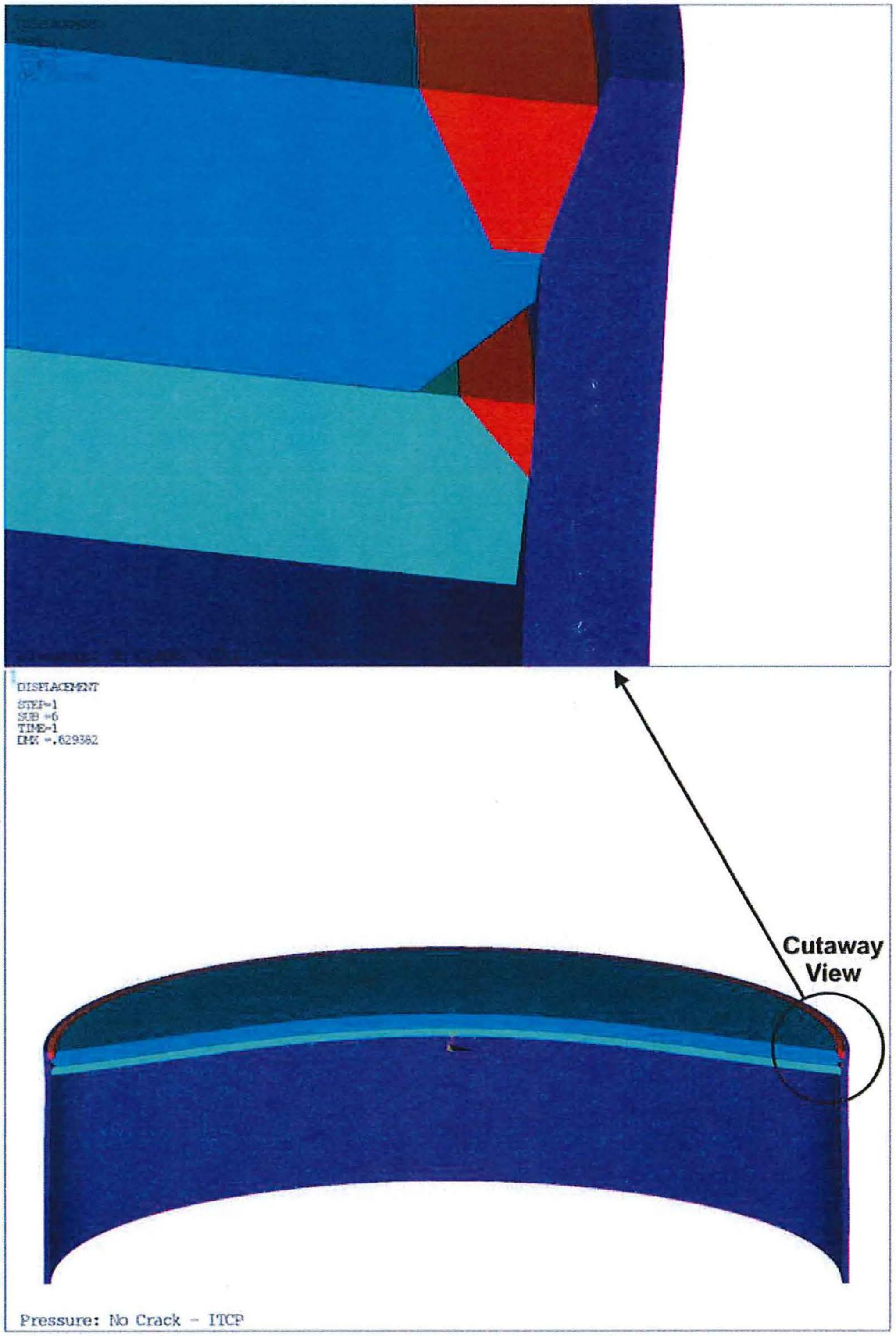

Figure 11. ITCP Pressure Load Case – Displaced Shape (Exaggerated)

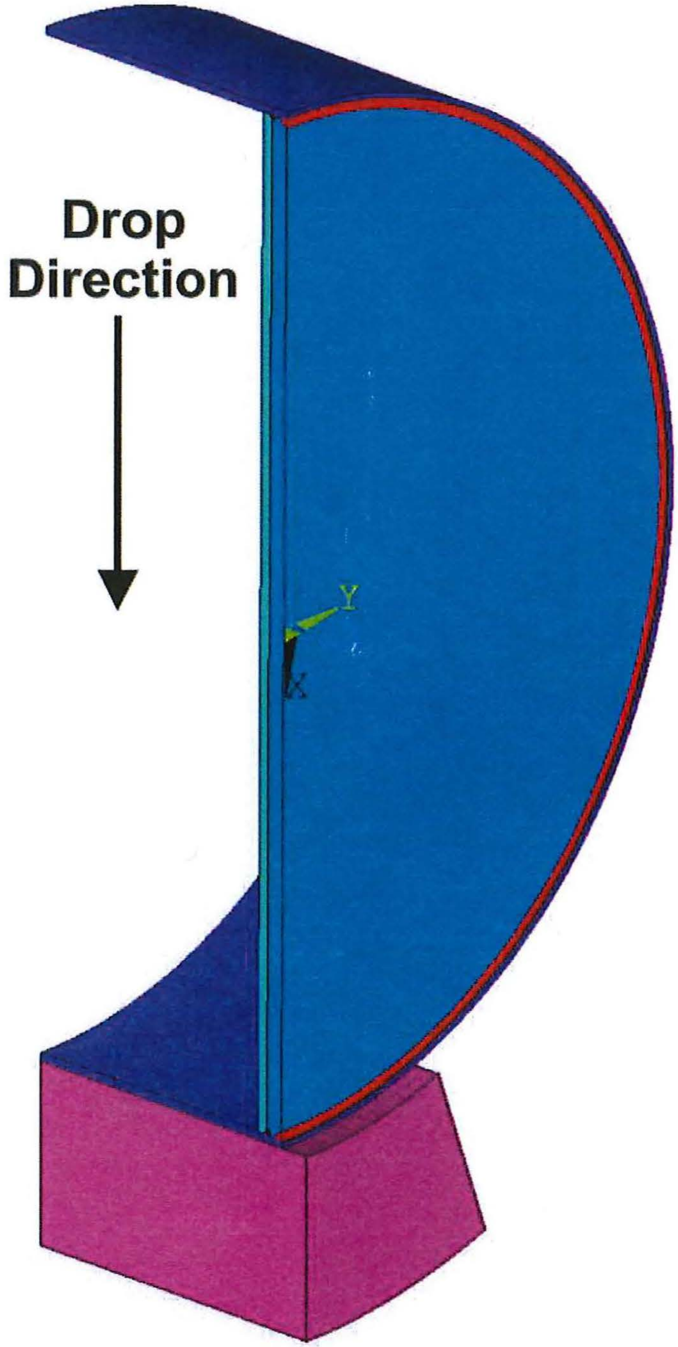

Figure 12. Side Drop Model

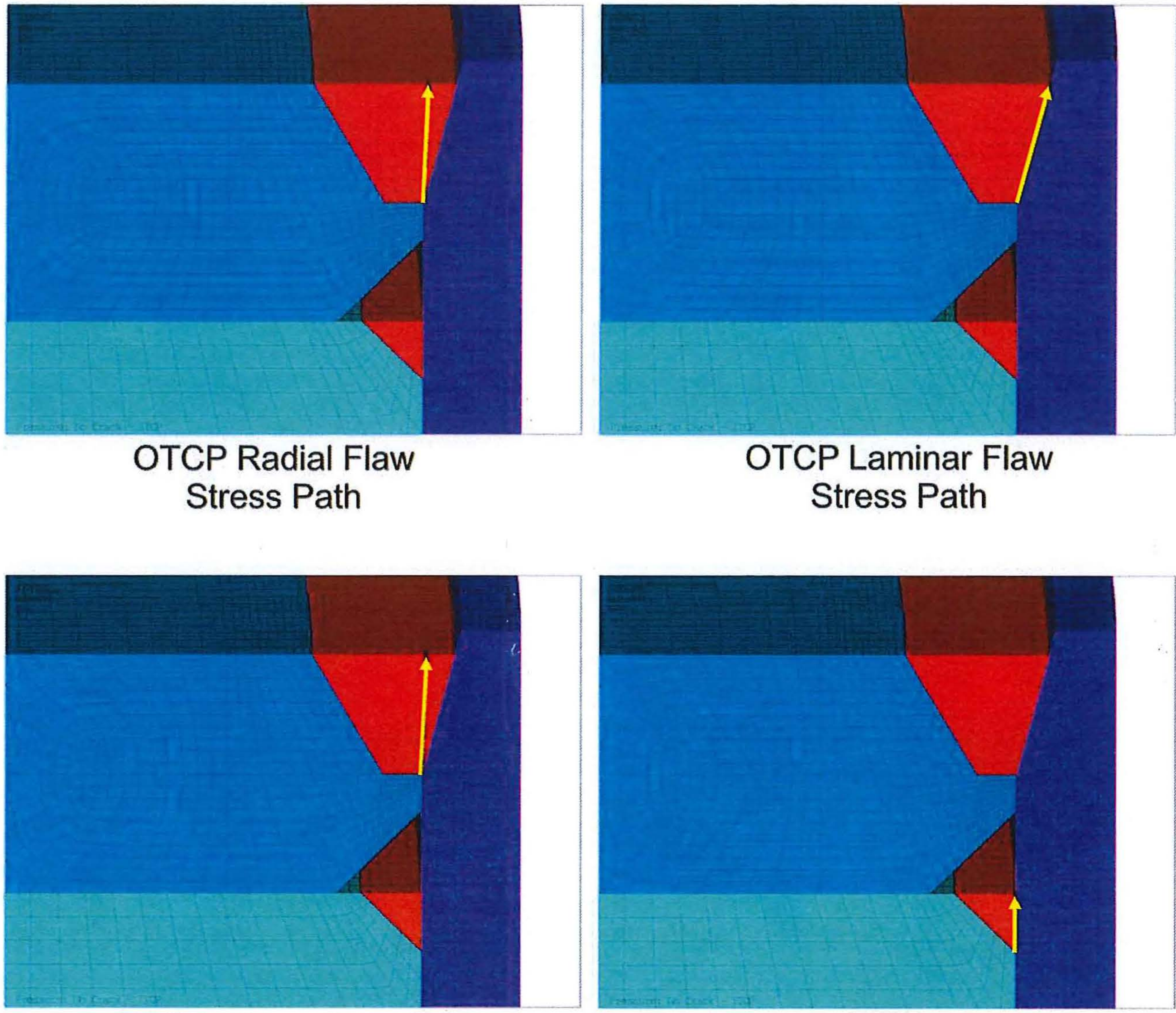

OTCP Radial Flaw Stress Path

OTCP Laminar Flaw Stress Path

OTCP Circumferential Flaw Stress Path

ITCP Stress Path

Figure 13. OTCP and ITCP Stress Path Definitions

APPENDIX A

ANSYS INPUT FILES

File Name	Description
Base_Model.INP	ANSYS input file to construct the 3-dimensional model.
C*_$_%.INP	ANSYS input file to perform OTCP flawed stress analyses * = 1-4 (Case Number) $ = Side, Pressure (Loading) % = Radial, Circ, Lam (Flaw Direction)
I1_$_CIRC.INP	ANSYS input file to perform ITCP flawed stress analyses $ = Side, Pressure (Loading)
Pressure.INP	ANSYS input file to perform OTCP non-flawed pressure stress analyses.
Side.INP	ANSYS input file to perform OTCP non-flawed side drop stress analyses.
I1_Pressure.INP	ANSYS input file to perform ITCP non-flawed pressure stress analyses.
I1_Side.INP	ANSYS input file to perform ITCP non-flawed side drop stress analyses.
Genstress.mac	Macro to perform linearized path stress extraction.
Lin_out.mac	Macro to perform linearized path stress extraction using the native ANSYS PRSECT command.
GETPATH.TXT	Path listing for stress extraction.
Data.xlsm	Excel file to compile stresses and compute ratios.

APPENDIX B

SI REPORT 1301415.405, REVISION 0,
"EXPECTATIONS FOR FIELD CLOSURE WELDS ON THE
AREVA-TN NUHOMS 61BTH TYPE 1 & 2 TRANSPORTABLE CANISTER
FOR BWR DRY FUEL STORAGE,"

Structural Integrity Associates, Inc.®

11515 Vanstory Drive
Suite 125
Huntersville, NC 28078
Phone: 704-597-5554
Fax: 704-597-0335
www.structint.com
rsmith@structint.com

October 23, 2014
Report No. 1301415.405.R0
Quality Program: ☒ Nuclear ☐ Commercial

Mr. James F. Becka
Xcel Energy
Project Supervisor – 2013 DFS Loading Campaign
Monticello Nuclear Generating Plant
2807 W. Country Road 75
Monticello, MN 55362

Subject: Expectations for Field Closure Welds on the AREVA-TN NUHOMS 61BTH Type 1 & 2 Transportable Canister for BWR Dry Fuel Storage

References:
1. Xcel Energy Contract No. 1005, Release 48, Amendment 6.
2. SI Report 1301415.402 R0, "Review of TRIVIS INC Welding Procedures used for Field Welds on the Transnuclear NUHOMS 61BTH Type 1 & 2 Transportable Canister for BWR Fuel", January 30, 2014
3. SI Report 1301415.403 R2, "Assessment of Monticello Spent Fuel Canister Closure Plate Welds based on Welding Video Records", May 2014
4. "E-mail train on Questions Regarding Postulated DCS Welding Flaw Distrubutions.pdf, from Peter Quinlan to Dick Smith, October 10, 2014, SI File No. 1301415.205.
5. Repair Rates in Welded Construction – An Analysis of Industry Trends, TWI, Cambridge/UK, Welding and Cutting, November 2012, SI File No. 1301415.204.

Dear Mr. Becka:

Details of the machine gas tungsten arc welding (GTAW) field closure welds used on the NUHOMS 61BTH transportable dry shielded canisters (DSC) located at Xcel Energy's Monticello Nuclear Generating Plant (MNGP) have been reviewed in an attempt to perform a qualitative assessment of the likelihood that the welds might contain unacceptable defects. It is known that the required NDE acceptance testing was not performed according to approved procedures. Sequential dye penetrant (PT) examinations were required on the inner top cover plate weld – first after the weld root and hot pass(es) were completed and again, after the final weld layer was completed. This is a relatively small weld (3/16 inch partial penetration weld) and it was not required to perform an intermediate inspection. The second weld is a 1/2 inch partial penetration weld that requires a root, intermediate, and final PT inspection due to the larger size. The problem identified was that the dwell times used for both dye penetrant and developer were less than required by procedure. The PT tests were performed, but procedures were not followed. This point is being emphasized because large open defects are seen very quickly with PT testing and likely would have been identified even though the dwell times were too short to meet procedure. Smaller tight defects might have been missed as the dye requires sufficient dwell time to wick and then be pulled out via the developer. This statement is in no way intended to justify the failure to follow approved PT procedures, but rather to apply perspective from a qualitative sense.

There are a number of reasons to believe that the field closure welds in their current condition do not contain large discontinuities that could challenge the effectiveness of the closure welds to meet their intended design function. It is the purpose of this review, performed in accordance with Reference 1, to identify valid reasons to support this conclusion. A <u>qualitative justification</u> is provided that is outlined in the listing below:

Reasons to expect the subject spent fuel canister welds are free from large discontinuities:

1. Use of qualified and proven welding procedures and techniques. [Reference 2]
2. Use of a machine GTAW process. [Reference 2]
3. Application of a proven and robust welding system designed specifically to support these types of field welds in these specific types of canisters. [Reference 5]
4. Use of ductile and easily weldable base materials (SA-240 Type 304 stainless steel). [Reference 2]
5. Use of solid wire filler metal designed for welding these base materials and formulated to eliminate hot cracking and other types of microfissures (SFA 5.9 ER308 austenitic stainless steel filler metal and welding grade gases for shielding the weld puddle. [Reference 2]
6. Canisters are oriented in the vertical position during welding such that the weld is performed in the flat welding position (the most forgiving welding orientation). [References 2,3 and 4]
7. Weld roots are typically about 1/8 inch or slightly thicker which is good practice for GTAW machine welds. [Reference 4]
8. Weld layers are thin (between 1/16 inch and 1/8 inch) requiring multiple layers (and multiple weld passes) to assist with developing weld deposit consistency via remelting. Layers become thinner as the groove is filled because the width is greater. [Reference 4]
9. AREVA-TN's historical record with these welds is excellent having a significant history of welds made with this system and these welding procedures that shows 1% repairs rates. [Reference 4]

The welding procedures and welder control documentation were reviewed in detail and specifics of that review are reported in Reference 2. The review concluded that

"...the procedures the GTAW welds in the subject spent fuel canisters can reasonably be expected to be of good quality and free of injurious defects. The expectation was based on the characteristics of the GTAW weld, the excellent controls outlined for the welding program, and the fact that the welds and base materials are austenitic stainless steel. Also the welding consumables are compatible with the structural materials used in the design...." [Reference 2]

The welding application itself is performed entirely in the flat position – a welding position that eliminates any complications related to welding out of position or having to negotiate restricted access. The reason for this viewpoint is that out of position welds have to compete against the forces of gravity and the joint design provides adequate access for arc manipulation. The result of a welding in the flat position is that defects are less likely to be introduced than might be expected with other weld orientations or restrictions.

The spent fuel canister welding system is robust and is proven. The welding head is mounted on a non-metallic shielding material weighing over 1500 lbs and is shown in Figure 1 below.

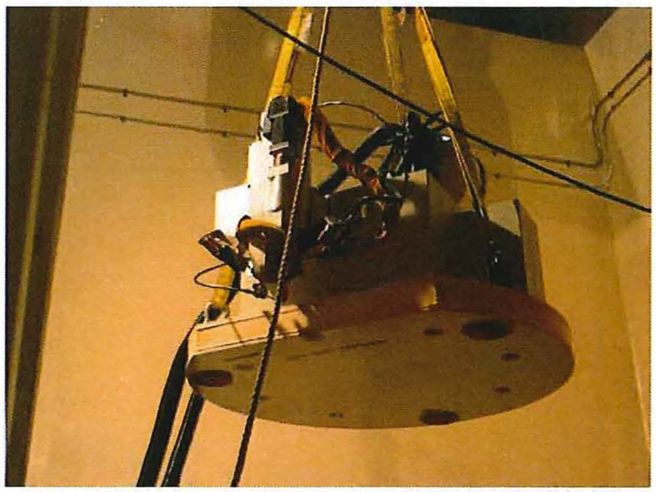

Figure 1 Photo of the robust welding head that is positioned on the dry storage cask as shown in Figure 2. The welding torch is visible in the photo just behind the rope. (Photo provided by AREVA-TN)

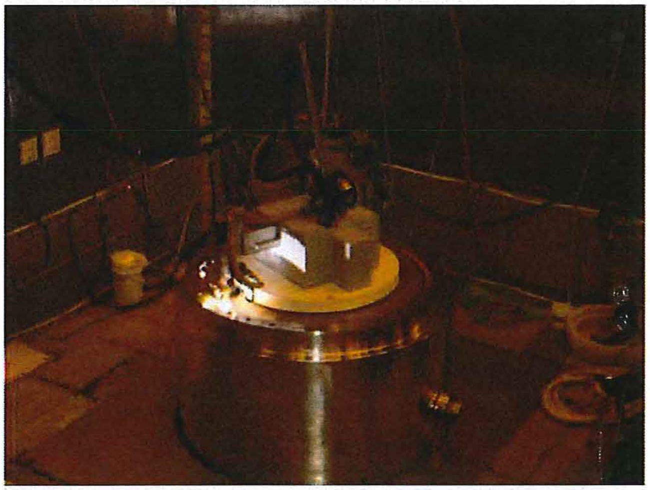

Figure 2 Welding system positioned on the storage canister for welding (Photo provided by AREVA-TN)

The entire welding system rotates similar to a "lazy-susan" and the welding torch is manipulated in and out as required for proper positioning. There are other torch adjustments such as tilt, lead, height, etc. Leading and trailing cameras are mounted to provide video of the front and rear of the torch and weld puddle. Welding videos have been reviewed [Reference 3] in an attempt to assess whether or not weld quality could be assessed. One objective of the video review was to look for key discontinuities such as porosity and evidence for any lack of fusion. The conclusions from the video review were that circumstances were observed at various times during welding that might support the generation of defects such as oxide buildup, weld root burn-thru, localized contamination on the surface, weld deposit surface irregularities, and tungsten drift requiring realignment. However, nothing could confirm either the generation of defects or the lack of defects. Since each weld is a unique entity one must rely on tendencies or trends if post weld inspections are not available. There were also observations of good welding practices as well as those events stated above. These included root repair, periodic adjustment of tungsten positioning, tungsten electrode replacement, electrode steering as needed, etc. Most of the videos were very similar (all having the same types of observations at about the same frequency). Canister No. 16 also had the same types of observations but the frequency appeared to be about twice any of the others. This was a judgment call by the reviewers and not quantitative. It was carefully pointed out that even so, there was no evidence to indicate that any specific discontinuities were generated – only that welding conditions were observed that sometimes lead to the various types of discontinuities. In addition, since these welds use multiple weld beads to complete the weld, there is the opportunity to "heal" conditions created by welding over them.

Historical Perspective

AREVA-TN was asked to describe their historical perspective on the welding of the canisters with this system. It is recognized that all of the canisters were not welded by AREVA-TN but might include a contractor or the utility themselves. However the same welding system likely would have been used (often rented from AREVATN). AREVA-TN noted that typical discontinuities might include local porosity (rare), occasional tungsten inclusions, usually resulting from torch tip contact with the solidifying weld puddle, lack of fusion or overlap. Regarding the potential for any linear indications (holidays or breaks), cracking typically does not occur with austenitic stainless welds. Maximum size of indications typically would be less than 1" to 2". Irregularities at starts and stops can occur, and rollover has been seen in some cases.

AREVA-TN also was asked for their historical experience regarding canister closure weld acceptance rates (i.e. first time PT rate). The response indicated that a best estimate would be less than 1 UNSAT PT per 10 canisters, with an average of 10 PT examinations per canister (includes root and final layer on inner top cover, vent port cover, siphon port cover and test port, with root, mid and final layer on outer top cover for certain DSC models). Therefore, the historical experience suggests a rate of about 1% UNSAT PTs for field closure welds. Further, the recent field experience as the welding process matured produced no weld repairs at all – on 50+ canisters the findings were 1 PT indication from starts and stops was found to hold developer, but light grinding was performed to smooth the surface and eliminated the indication. Thus, these minor indications required no weld repairs.

AREVA-TN was also asked regarding how many stainless steel canisters have been loaded and closed by welding to date. The estimate was for approximately 750 loaded/closed NUHOMS canisters, with closure performed by AREVA-TN, end user or other contractor. This represents an extensive sampling that indicated an indication rate of less than 1% and that rate appeared to significantly improve over the last 50 that have been welded.

There were no applicable mockups that had been used to examine for discontinuities or defects, so that information was unavailable. The historical evidence seems to paint a favorable picture lending a degree of comfort that the canisters in question at MNGP are not likely to have indications of a significant size.

Finally, literature was examined to find information regarding generation of defects in stainless steel weldments. The best paper found is indicated in Reference 5. This paper written by The Welding Institute in Cambridge, UK was published in Welding and Cutting, November 2012. The paper titled "Repair Rates in Welded Construction – An Analysis of Industry Trends" provided good insight. More than 800 professionals were contacted with about 10% responding. There were different kinds of responses such as % of welds requiring repair or % weld lengths requiring repair being the most prevalent. The following applicable conclusions were noted. GTAW stainless steel welds returned under 2% repair rates. The impact of different welding factors were parsed and suggested the following impacts: root repairs at 22.5%, fill layers 7.5%, joint type 15%, access limitations 26%, and other welding factors 11% . Most of these are not present in the canister welds as pointed out previously. It appears that the AREVA-TN canister weld repair experiences are slightly lower, but nevertheless are considered consistent with industrial expectations for a variety of manufactured and installed components. Since all welding is in the flat position using a proven welding system, the 1% defect rate appears to be reasonable. In addition it was pointed out that experience with the past 50 canisters has been even better.

Conclusions

Based on the sum of the information reviewed, it can be said that the likelihood for the occurrence of large defects is not supported by historical evidence. While there remains the potential for long lack of fusion defects either interbead or sidewall, the thin multilayer design and potential for subsequent bead healing by remelting would significantly limit the through-thickness dimension of any long defect. In fact, the most likely lack of fusion indication(s) would be intermittent in nature and not expected to have a through-thickness dimension greater than one weld bead. While a quantitative estimate of a limiting flaw size cannot be produced, the qualitative likelihood that large defects would not be present is assuring.

It is suggested a bounding subsurface defect condition is conservatively represented as an intermittent lack of fusion (LOF) defect evenly distributed along the canister weld. Further, the total length for LOF is conservatively estimated at 25% of the canister cover plate weld circumference. The estimated through thickness dimension is 1/8 inch, because this dimension represents a maximum weld bead thickness. One eighth inch is considered to be a conservative assumption, because it is recognized that most weld beads will be thinner especially as the weld cavity begins to fill. No credit is being taken for remelting even though remelting is normally associated with multipass welding."

Very truly yours,

Richard E. Smith

Richard E. Smith, PhD. FAWS
Senior Associate
res

ENCLOSURE 3

STRUCTURAL INTEGRITY ASSOCIATES, INC. REPORT 700388.401, REVISION 1

EVALUATION OF THE WELDS ON DSC 11-15

62 pages follow

Report No.: 700388.401
Revision: 1
Project No.: 1700388.00
August 2017
Purchase Order: 67027

Structural Integrity Associates, Inc.®

Evaluation of the Welds on DSC 11-15

Prepared for:

Scott R. Marty, Prairie Island Nuclear Station
Xcel Energy Services Inc.
414 Nicollet Mall, 8th floor
Minneapolis, MN 55401

Prepared by: Richard E. Smith — Richard E. Smith, Sr. Associate — Date: August 22, 2017

Reviewed by: David Segletes — David Segletes, Senior Consultant — Date: August 22, 2017

Approved by: Richard E. Smith — Richard E. Smith, Sr. Associate — Date: August 22, 2017

Prepared By: Richard E. Smith, Sr. Associate
11515 Vanstory Drive
Huntersville, NC 28078
(704) 799-1345

REVISION CONTROL SHEET

Document Number: **1700388.401.R1**

Title: Evaluation of the Welds on DSC 11-15

Client: Xcel Energy Services Inc.

SI Project Number: **1700388.00**

Quality Program: ☒ Nuclear ☐ Commercial

Section	Pages	Revision	Date	Comments
1 2 3 4 5 App. A App. B App. C App. D	1-1 – 1-2 2-1 – 2-3 3-1 – 3-23 4-1 – 4-3 5-1 – 5-1 A1 – A4 B1 – B5 C1 – C8 D1 – D7	0	08/14/17	Initial Issue
3 4	3-14 4-1	1	08/22/17	Reworded paragraph for clarification Reworded paragraph for clarification

Table of Contents

List of Tables

List of Figures

1.0 INTRODUCTION

Structural Integrity Associates (SI) has been working with Xcel Energy in their efforts to qualify the dry shielded canisters (DSCs) located at the Monticello Nuclear Station identified as DSC-11, 12, 13, 14, 15 and 16 over the past few years [1, 2]. SI has provided support for independent review of inspection, root cause assistance, review of fabrication records (procedures and video records), vendor analyses, and DSC-16 exemption request development to be used for regulatory licensing reviews. The DSCs listed above have been transported to the dry storage facility at the Monticello Nuclear Station and currently reside in concrete storage modules (HSM) at the facility.

Recent meetings among Xcel Energy, the Nuclear Regulatory Commission (NRC), and others have discussed the potential value of volumetric inspections of the lid closure welds for those DSCs that had not been inspected volumetrically versus the risks associated with the personnel dose attendant to those inspections.

DSC-16 is the only cask among the six cited that received the additional volumetric inspection using phased array ultrasonic inspection (PAUT) and subsequent supporting analyses performed in support of licensing. The effort produced a favorable licensing result for DSC-16. It is noted that DSC-11 through DSC-15 had already been placed in concrete HSMs when the liquid dye penetrant inspection (PT) compliance issues were discovered while welding the cover plates during loading of DSC-16. The visual inspection (VT) results performed at the same intervals as the PT were reported to be satisfactory and there was a reasonable level of confidence they were properly performed.

Xcel Energy contracted with SI to determine characteristics and features that could be applied for reevaluation of the closure welds on the other canisters and determine if an acceptable path could be reached without need for volumetric inspections. Video welding records (VIDs) were available for the inner top cover plate (ITCP) welding of DSC-13 and DSC-16, and the outer top cover plate (OTCP) welds for DSC-12 through DSC- 16 [1, 2]. VIDs were not available for DSC-11 welds; however, general area video records were available to view the overall activities of fit-up, welding, and inspection for all or portions of those activities for all canisters including DSC-11. These activities, in addition to the welding data sheets and inspection records, have been reviewed and evaluated. In addition, the PAUT inspection results for DSC-16 were reviewed. Thus the flaw distributions used to develop the bounding flaw models were included in this evaluation. It was noted that these bounding flaw models had been used to describe the capacity of DSC-16 to conservatively accommodate all design and accident loading conditions.

1.1 Objective

The objective of the project was to determine if it were reasonable to expect that the types and extents of flaw distributions found in the DSC-16 circumferential closure welds joining the ITCP and the OTCP to the canister shell could be used to represent the comparable closure welds of DSC-11, DSC-12, DSC-13, DSC-14 and DSC-15. The results of these reviews are summarized and evaluated to develop a foundation for this expectation based on welding and materials behavior observed in the available records for these welds. The flaw development mechanisms described to support the expected behavior is based on interpretations of the review results from subject matter experts.

2.0 TECHNICAL APPROACH

2.1 Strategy

In general, the objective will be accomplished by evaluating the details of DSC-16 closure welds for which the most complete data sets are available. This information will be used to better assess how the defects were created so that the behavior of DSC-16 can be compared to the welding records of the ITCP and the OTCP closure welds performed on DSC-11 through DSC-15. Thus, it can be determined if the condition of the subject welds in DSC-16 may be used to characterize them as "representative" of the similar welds in the other dry shielded canisters. Alternatively, it may be possible to develop a flaw set, based on the holistic review, that would support a reasonable "bounding flaw set" for DSC-11 through DSC-15.

The only path, given current state-of-art, to provide volumetric inspection information on the five DSCs that have not received a volumetric inspection is to remove each canister from its concrete storage module and perform a phased array ultrasonic inspection of the closure welds. The ability to do this exists, but significant worker radiation exposure (dose) would result making the cask welds accessible for inspection and then performing the PAUT inspections. The question posed is "What more could be done to support safety evaluations of DSC-11 through DSC-15?"

Previously, detailed reviews had been performed on available welding videos (VID) for all subject canisters except for DSC-11 (there were no welding VIDs available for DSC-11). In addition, welding procedure qualification specifications and test records, welding sequences, and available welding and inspection records were collected and reviewed as summarized in reports developed for Xcel Energy [1, 2]. Subsequently a PAUT procedure was developed by AREVA and performed on DSC-16 since it had yet to be placed in the HSM and the closure welds were still accessible. Those results were used in combination with the welding reviews to support detailed analyses to justify the DSC-16 licensing request for exemption from the unacceptable progressive dye penetrant examination. In addition, general area monitoring videos were recorded during the same fit-up, welding, and inspection time frames were made available for review. These reviews provided additional insight regarding the ITCP and OTCP welding activities of DSC-16 and to facilitate comparison of these results with similar information on all dry shielded canister closure welds including DSC-11.

2.2 Scope

The work was conducted in three phases as described below.

Phase 1

Evaluation of DSC-16 to determine if the characteristics and features correlated among the three information sets that can be applied – general area videos, welding videos and inspection results (depth measurements of weld layers, visual testing results, and volumetric PAUT results) can be applied for re-evaluation of the closure welds on the other canisters. Phase 1 activities focus on a better understanding the welding behavior of DSC-16 to sharpen the reviews of available information for the other canisters not inspected volumetrically, and to suggest viable mechanisms that would produce the defect distributions found in DSC-16.

Phase 2

Evaluate available results on canisters DSC-12 through DSC-15 based on the characterization results from DSC-16 to determine if an acceptability path can be reached without need for volumetric inspections. Phase 2 will make use of these correlations and will use them to interpret the welding video reviews for the other canister closure welds having welding video records.

Phase 3

Evaluate the potential for an acceptability path on DSC-11 based on the conditions of the other five canisters, the welding processes used, and information that could be gleaned from the general area video documentation during installation of the OTCP and ITCP.

2.2.1 Phase Descriptions

Phase 1 activities focused on identifying specific welding conditions in the video records for DSC-16 that potentially could produce defects in the ITCP and OTCP closure welds that either were observed in the previous evaluation [1] or during the rereviews of this evaluation. Next the defect distribution identified by the PAUT inspection results summary for DSC-16 [3] were compared to these welding conditions to attempt a correlation with the location of the flaws. Plausible mechanisms are determined that are consistent with the VID observations, the welding process and the flaw distributions. Finally, the overall area video records collected during welding and inspection activities during the time frame of the DSC-16 work were reviewed and documented. Measurements of deposited layer thicknesses for required inspections (VT in this case) were summarized. These information sources (including the welding assessment previously performed) [1,2] are used to better understand what happened during the welding process with respect to developing defect distributions found in DSC-16 using PAUT examinations. In addition, the treatment of defect distributions using conservative bounding analysis is reviewed [3].

Phase 2 compares similar information provided for DSC-12, DSC-13, DSC-14, and DSC-15 [1,2], plus the information developed in the current review to the understanding developed on DSC-16. The current study for these canisters includes reviews of available VIDs of the ITCP and OTCP welds, general area video review, inspection deposit thickness measurements, visual inspection results, and the controlling welding records. This information is used to determine if canister closure welds can be reasonably expected to develop similar defect distributions to those recorded on the DSC-16 canister. New information collected for the reviews includes welding techniques and procedures, craft personnel and materials used, in-process repairs, etc. This permitted a determination of the conservative nature of flaw modeling and analysis used for the bounding exemption request for DSC-16. It was noted in the prior assessment [1] that similar undesirable welding conditions (often associated with flaws) were observed in the welding VIDs of all canister closure welds, but were more prevalent in DSC-16. The correlation the undesirable welding conditions in DSC-16 with the locations of flaws will give insight into how the defects are formed. Assuming the flaw mechanisms are correct then the conditions seen in the other canister welds can be reviewed for comparability to those observed with DSC-16. The bounding flaw distributions would then be representative the others reviewed. The intent is to show that the conservative bounding flaw sets developed and analyzed for DSC-16 can reasonably be expected to represent the similar top closure welds in the other DSCs.

Phase 3 deals with the assessment of DSC-11 for which no welding VIDs are available for either ITCP or OTCP. What is available is all the other information used for the correlations among DSC-12, DSC-13, DSC-14, and DSC-15: specifically, the general area video documentation, weld deposit thickness measurements, visual inspection results, and written welding records including identification of craft personnel making the welds. It will be shown that that there is a consistent loading and closure welding methodology applied to all six of the canisters, and because of that, it is reasonable to expect that the flaw distribution and analysis used for DSC-16 is representative of the others, including DSC-11.

3.0 RESULTS AND DISCUSSION

3.1 General Observations

The gas tungsten arc welding (GTAW) procedures were well documented and qualified as discussed in previous reports [1, 2] for both manual and machine applications. The machine GTAW equipment is designed specifically to produce these welds. It is a single mast configuration mounted in the center of the canister cover plate being welded. The welding head is positioned in the weld groove and rotates clockwise around the circumference beginning and ending at the siphon/vent block. The ITCP weld starts on one end of the block and ends on the other end of the block. Manual GTAW is used for all the welds associated with the siphon/vent block and to tie the circumferential closure welds to the vent block where appropriate. The OTCP proceeds around the entire circumference just above the elevation of the siphon/vent block and accordingly is increased in length by approximately 11 inches. The following overall observations refer specifically to conditions of machine welding.

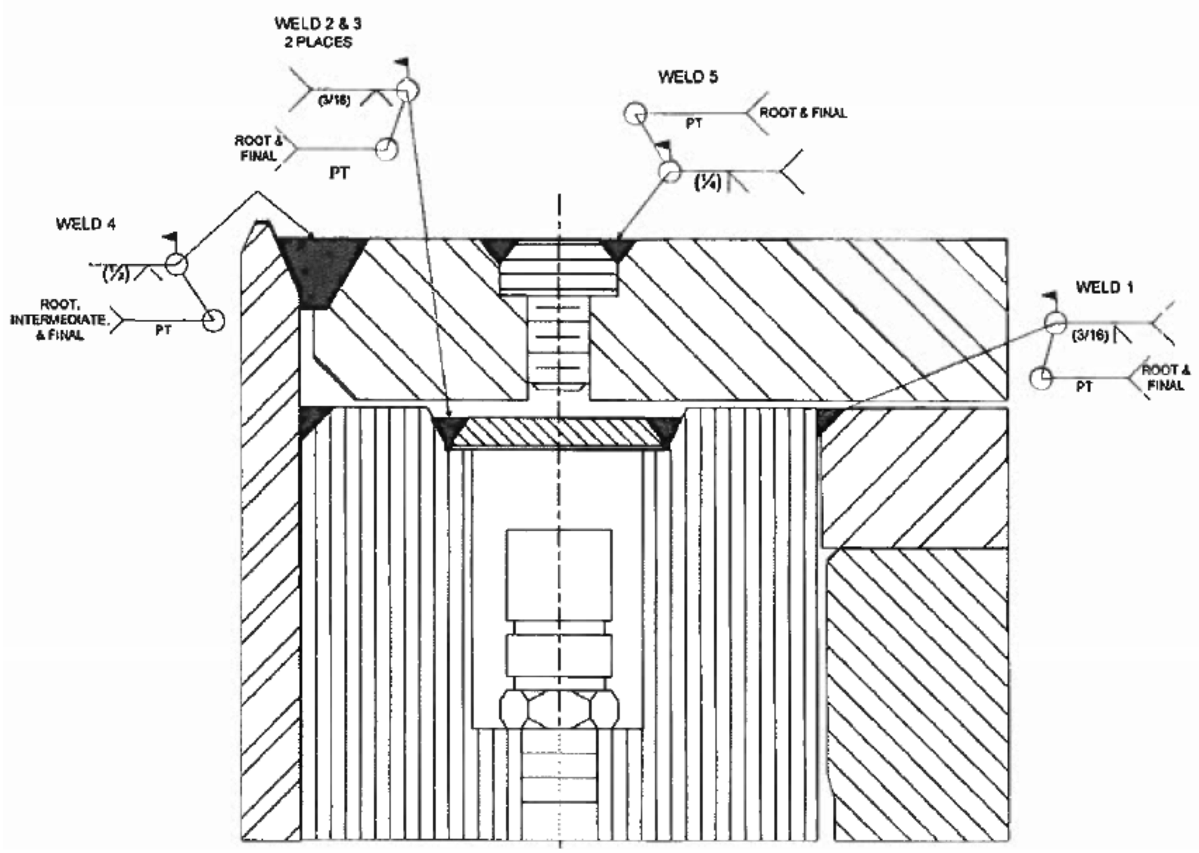

Figure 3-1. Schematic of the field welds at the siphon/vent block

Weld 1 in this cross-section attaches the ITCP to the siphon/vent block and is a manual GTAW weld. Beyond the siphon/vent block the same weld is made in two passes using the machine GTAW procedure and equipment. Weld 4 is a machine GTAW attaching the OTCP to the canister shell around the complete periphery.

All welds used ER308 solid filler wire using WPS SS-8-M-TN Rev 10 (machine GTAW) or SS-8-A-TN Rev 8 (manual GTAW) depending on the location [2]. All welds are either fillet welds or partial penetration welds having minimum deposit thicknesses. As noted below two heat/lot combinations of filler wire were used for cover plate closure welds (machine GTAW field welds). DSC-11, DSC-12, DSC-13 and DSC-14 use weld filler heat #736908 and DSC-15 and DSC-16 use weld filler heat #527221. DSC-12, DSC-13 and DSC-15 also made use of weld filler heat #737880. Weld geometries are shown in Figure 3-1.

Weld #1 shown in Figure 3-1 above is the shell to ITCP weld around the perimeter of the cover plate and this weld beyond the siphon/vent is applied using the machine GTAW process. The ITCP contains a keyway machined to fit around the periphery of the siphon/vent block. This portion of the ITCP perimeter weld is performed using the manual GTAW process. [Note that the tie-in between the machine and manual welds also are applied using the manual GTAW process.] A single 45° bevel prep is chamfered along the top edge of the cover plate including the cutout for the keyway for a 3/16-inch partial penetration weld. The gap to the shell wall is 1/16-inch.
Welds #2 and #3 are the siphon/vent port cover plate seal welds and these are manual GTAW field welds.

Weld #4 joins the outer top cover plate (OTCP) to the canister shell completely around the periphery of the OTCP. This weld joint geometry for this ½ inch partial penetration weld is makes use of a 22.5° chamfer on the top inner corner of the canister shell mated to a 30° J-bevel with an 1/8-inch land. A 1/8-inch root gap completes the joint design. This joint design is considered a modification of a double-bevel weld geometry. Machine GTAW procedures are used for this weld.

Weld #5 is the seal weld around the test plug that provides access to the top of the ITCP via a penetration in the OTCP. A manual GTAW procedure is used for these welds.

3.1.1 General Configuration

As identified above, there are two weld geometries used for the cover plate to shell closure welds – one for the ITCP and one for the OTCP as shown in Figure 3-2 below. Both weld geometries are partial penetration designs. The ITCP weld joint geometry is a single bevel groove (3/16 -inch depth) The OTCP weld joint geometry is a double bevel weld 5/8-inch depth [Note: ½ inch minimum deposit depth]. The land is machined along the top edge of the OTCP perimeter to mate to the inner chamfer of the shell to form a double bevel joint. An angled relief is machined on the bottom edge of the OTCP to provide clearance over the ITCP weld crown. The gaps shown between the inner surface of the shell and the root of the machined weld preparation on the perimeters of the cover plates will vary within specification limits for the plates and the canister shell wall. The VID reviews clearly showed changes in the gaps during the weld root pass as the weld progresses around the perimeter of the plate. The plates are tack welded in 8 locations equally spaced around the circumference (using approximately 2-inch long welds). The sequence used is to tack opposite quadrants and then weld the remaining four tacks equally spaced between previous tacks of the four quadrants. A prescribed tack welding sequence is used to maintain proper gap alignment and uniform concentricity. As was noted above, the welding VID reviews of the canisters showed that a uniform concentricity was not achieved resulting in the need for frequent adjustment of the welding head radial position to achieve proper tungsten position and thus bead location.

Security-Related Information
Figure Withheld Under 10 CFR 2.390.

Figure 3-2. Schematic of Cover Plate to Shell Welds

3.1.2 General Welding Observations

All top plate closure welding initiated at the end of the siphon/vent block location and proceeded clockwise fashion around the shell circumference. It was noted that the ITCP weld was deposited using 2 beads – a root bead and a cover bead. The deposit thicknesses were measured only for the root and the final inspections due to the limited weld size for this design.

All the OTCP welds were measured. The wire feed rate setting was unknown to the reviewer, but the travel speed was estimated based on peripheral weld length divided by the time to make the weld at approximately 3.0 inches per minute. The deposited bead thicknesses were estimated between 0.10 inch to 0.20 inch depending upon the individual bead width (see Figure 3-3). The plot shows average thickness measured at every quadrant around the circumference for all six dry shielded canisters. The results suggest that the deposit thicknesses are relatively consistent for all the canisters evaluated. Note that the deposited material between the root layer and the intermediate layer is relatively consistent and is believed to incudes deposit from weld beads 3 and 4 and possibly contribution from bead 2. The weld bead placement sketch shown in Figure 3-7 depicts how individual beads contribute to the layer thicknesses. The deposit consistency suggests that the procedures were being followed and the welding parameters were maintained consistently. The data also demonstrate that all the final weld deposit thicknesses met and exceeded the minimum joint deposit fill requirement (0.50 inch) when measured in the hot condition as shown in Figure 3-3 below. Later it was determined that DSC-16 had variations up to 0.020 inch below the minimum fill requirement at several locations around the circumference. Therefore additional weld metal was added to approximately ¾ of the circumference after all surface indications had been removed by grinding.

The variations in deposited depth seen for DSC-15 suggests that the root interval contained less deposit than the others or it may have been the result of the use of stripping beads (i.e. partial circumference bead deposits applied to adjust/correct low spots in the deposit or where in-process surface metal removal repairs may have been performed). Stripping beads are a common welding technique used in welding to fill locations where the weld deposit is less than optimum. This does not imply defective welding, but can influence the inspection interval deposit depth. Figure 3-4 below shows the individual deposit inspection intervals for all canisters in this study showing relative consistency around the circumference of each canister.

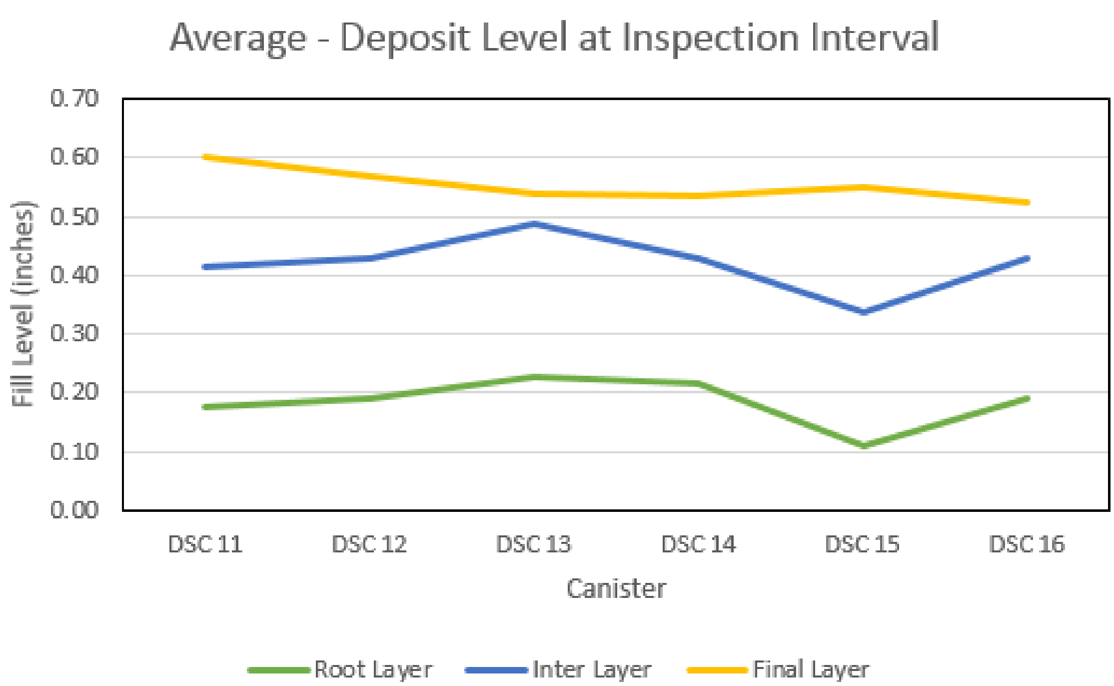

Figure 3-3. Average deposit thicknesses for each inspection interval are plotted for all Dry Shielded Canisters evaluated

[Information computed from Work Order Data Sheets provided in References 4, 5, 6, 7, 8 and 9]

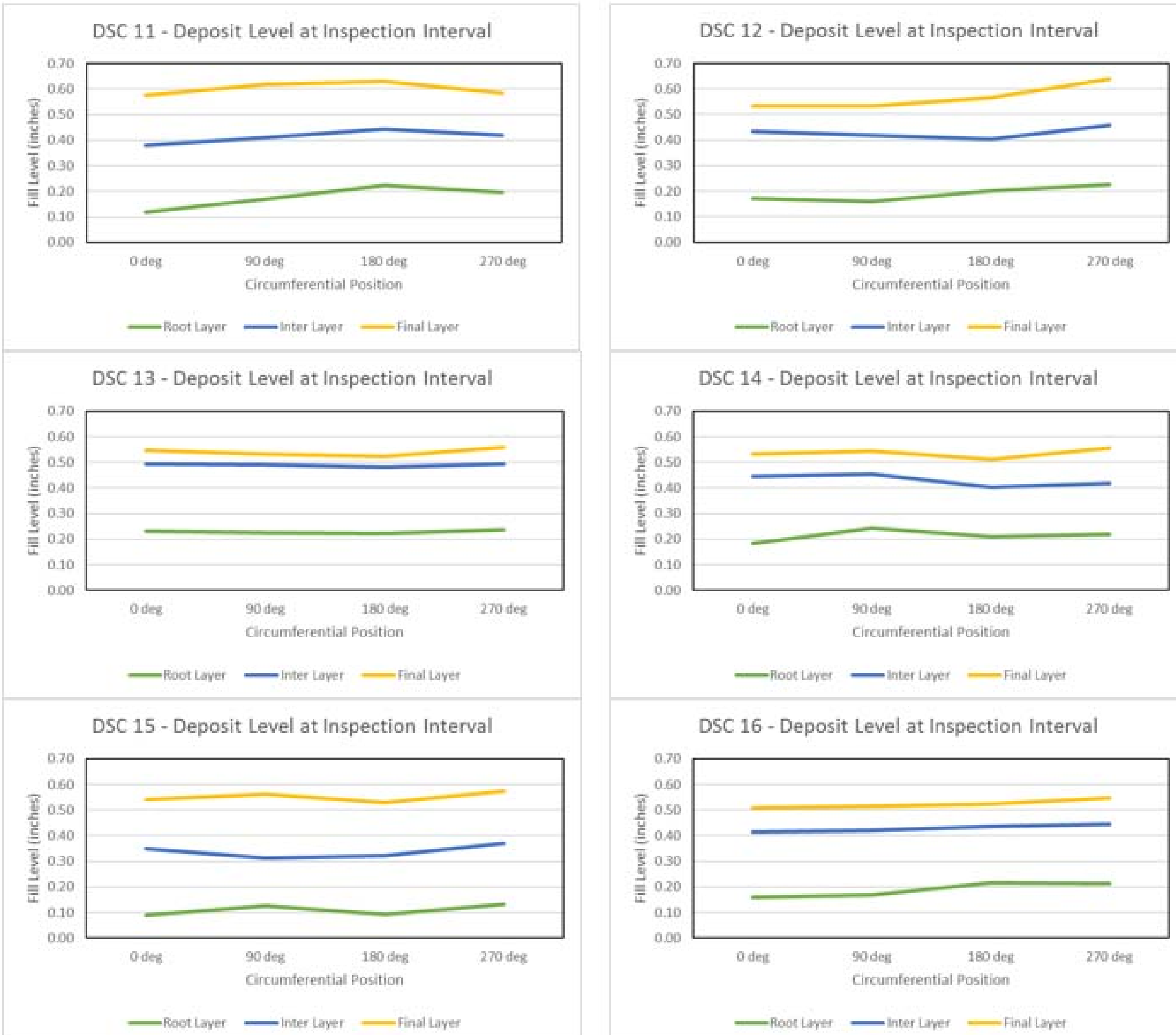

Figure 3-4. Deposit depth levels at each inspection interval are plotted for all six Dry Shielded Canisters reviewed

[Information computed from Work Order Data Sheets provided in References 4, 5, 6, 7, 8 and 9]

The filler wire entry location is guided via a flexible wire guide tube and directed towards the molten weld puddle near the center of the arc. The welding procedure and process was designed for filler material to be added to the front of the molten weld puddle. When the location of the wire entry changes, the heat pattern of the molten weld bead also changes, since the weld pool is chilled by the addition of cold filler wire. It was noted that the wire entry location frequently wandered and require adjustment to relocate the wire entry to the desired location. This was an ongoing issue requiring frequent attention by the welding operators. Typically, a wandering wire entry involves the "cast" of the filler metal wire being used. Cast is a welding term related to the residual set or "spring" in the wire. It is influenced by the final anneal of the solid weld wire during manufacturing. If the wire is annealed for too long or at too high a temperature, it will be too soft and will not feed properly. If the wire receives inadequate annealing, the cast can cause wire feed difficulties. The annealing response of each heat of material can differ resulting in curvature of the wire as it exits the wire guide and enters the molten weld puddle. When the curvature changes, the wire entry location also changes. If the cast turns downward, it can drag along the underlying material resulting in non-uniform feeding. Occasional adjustments were observed in the VIDs to correct this condition with all the canister welds (see Figures 3-5 and 3-6 for examples).

A dominant feature of the welding process used for all the welds is a viscous flow characteristic of the weld metal. The flow condition is described as "lavalike" or "lava flow" of the molten weld metal. The welding procedure makes use of straight current as evidenced by a lack of pulsing in the VID reviews. Pulsing is sometimes used to shape weld bead contours but was not used for this procedure. The welding parameters (i.e. welding energy, wire feed rate and travel speed) determine how much molten material is carried along at any point in time. The welding energy may be acceptable for the process, but may be marginal for the volume of molten material being applied to the joint. The molten puddle flow, in this case, had the appearance of flowing lava and was considered sluggish by the reviewer.

A sluggish weld bead dynamic is not ideal, because it is more difficult for a viscous liquid to fill cavities developed during welding and it is more difficult to wet the sidewalls and produce fusion. In some cases, the molten flow was seen to roll ahead of the tungsten arc beyond the wire entry location and divide the weld puddle into two molten paths at the same time (see Figure 3-5 for an example). This is an undesirable condition making it difficult for the weld pool to stir and likely hinders fusion with the solid side walls. This condition was observed periodically in all the available VIDs reviewed. It was noted that when these viscous flow conditions were absent, welding was calm, weld pool stirring was present and deposits were more uniform.

Figure 3-5. Example of molten "Lava Flow" proceeding ahead of tungsten resulting in a potential cold lap near the sidewall

Figure 3-6. Example of dragging filler metal wire resulting in irregular wire entry and weld puddle cooling changes

3.1.3 Welding Patterns

A cross-sectional sketch of the ideal weld bead sequence is shown in Figure 3-7. This sketch has been developed based on observations during review of the welding VIDs for both the ITCP and the OTCP of DSC-16. The bead sequences shown were generally consistent with the tungsten positioning in the grooves of all DSCs evaluated. The sketch presents an idealized view of the individual weld bead placements and depicts the remelted portions of each bead by the succeeding bead or beads. The weld arc progression for all machine GTAW welds was clockwise beginning at the siphon/vent block and continuing around the periphery of the cover plate until the weld bead was finished. Welding proceeded along a path perpendicular to the plane of the sketch. The beads shown in Figure 3-7 are numbered to show the sequence in which they were applied.

It should be noted in the sketch that each weld bead penetrates the surface of the material on which it is placed regardless of whether the material is a wrought substrate or a previously deposited weld bead. This intentional weld penetration is important to the weld quality. If the desired penetration is present, then the weld bead interface will be fused and not subject to fusion defects. Conversely, if penetration is absent or partial, then fusion defects will form at the interfaces between adjacent weld beads or between a weld bead and substrate material such as a sidewall. Fusion issues are believed to be the principal types of defects in these machine GTAW closure welds.

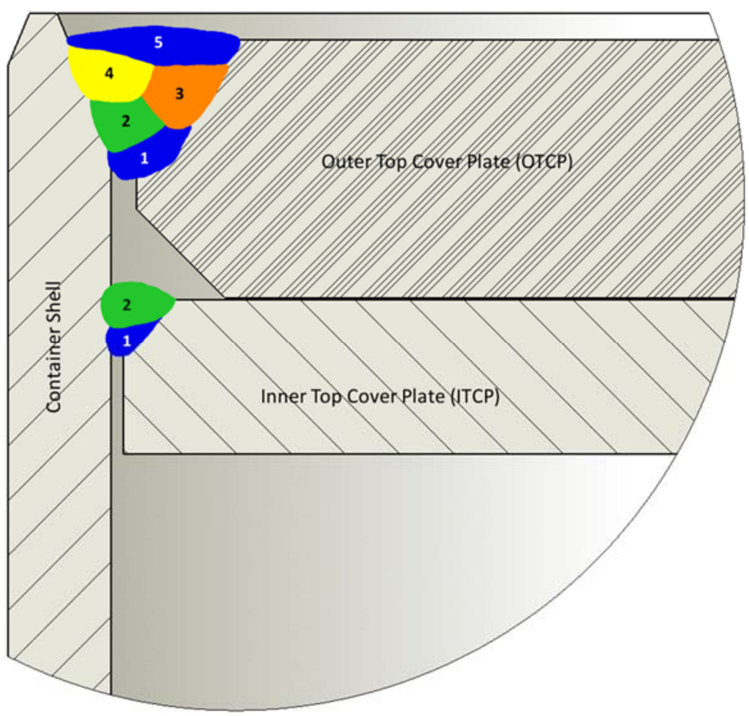

Figure 3-7. Idealized weld bead sequence used for the Dry Shielded Canisters

3.1.4 Defect Patterns

The ITCP and OTCP cover plate closure welds of DSC-16 were volumetrically inspected by AREVA using their phased array ultrasonic technique (PAUT). The defect indications were reported to be intermittently spaced around the circumference but limited in depth and length [3]. It is noted that the sketches provided below describe the defect condition. Each of the cover plate welds are discussed separately, and even though they were welded under the same conditions with the same equipment, they are different weld joint geometries and sizes (numbers of weld beads).

3.1.4.1 Inner Top Cover Plate Closure Weld

The DSC-16 ITCP closure weld is completed with two (2) circumferential weld beads – a root bead and a crown bead. The single bevel joint geometry is formed by a machining a 45° taper around the periphery of the top edge of the ITCP (abutted to the adjacent vertical canister shell wall). See the sketch shown in Figure 3-2 above. A 1/16-inch gap separates the plate from the shell to aid root penetration. The tungsten electrode is positioned on the cover plate side for the root pass so that the molten puddle flow provides the welding heat for tie-in to the vertical side.

The VIDs reviewed for this weld did not show evidence of electrode tilt (working angle) towards the vertical sidewall to facilitate optimum tie-in to the vertical wall of the weld joint. The reason for a lack of tilt could be due to a couple of reasons including restricted access limiting tilting in this small 3/16-inch high weld (i.e. interference between the gas cup and the side of the cover plate) or the weld head may have limited angles for tilt and/or lead. Regardless, the VIDs suggested a nearly vertical tungsten orientation that required the molten weld metal to flow to the side wall with sufficient heat to fuse the bottom of the machined groove to the shell sidewall. The sluggish nature of weld metal flow (lava flow) and the issues encountered with maintaining the proper wire entry location due to the filler wire cast created variability in fusion conditions on the sidewall. The PAUT examination of the ITCP of DSC-16 identified 34 intermittent indications associated with this weld. Most of these flaws (32 of 34) were distributed around the circumference at or near the canister wall fusion line between the root and the crown weld beads. These were flaws ranging in height from 0.04 to 0.09 inches and 0.12 to 2.09 inches long. One small flaw (#11) was identified at the fusion surface on the plate side of the groove having a length of 7.17 inches and a height of 0.09 inch. This flaw is remote from all the other flaws (in the circumferential direction) and was therefore considered bounded by the representative group of flaws. The longest flaw reported, #7, was 10.34 inches long and 0.11 inches high and appeared to be located just outside of the weld volume in the ITCP. However, it was conservatively treated as a continuous flaw completely around the full circumference.

All the flaws are treated as sidewall lack of fusion (LOF) because the flaw location places them along the edge of the root bead. The second (crown) bead did not penetrate sufficiently to consume the LOF defects. Appendix A provides a schematic pictorial of the LOF potential locations in Figures A-1, A-2 and A-3. Figure A-4 is a screenshot of a single location along the ITCP closure weld of DSC-16 showing visual evidence of conditions favorable for a LOF defect along the vertical shell sidewall. These screenshots taken during the deposit of weld bead #2. Figure 3-9 depicts the conservative bounding flaw assumptions used for the structural analysis of ITCP of DCP-16. Each flaw type is assumed to run the full length of the weld (full circumference) having assumed heights of 0.09 inch and 0.11 inch which bound the measured heights.

This weld joint geometry and the welding system used for the ITCP and the welding setup has potential for forming defects on the sidewall like the ones identified in DSC-16. The single defect formed along the tapered sidewall is less likely but should be assumed to be present for conservatism. Analysis for this weld demonstrated the required safety factors even with these conservative assumptions of the bounding model flaws, and the weld was considered satisfactory.

The other 5 canister ITCP closure welds were welded the same way, using the same welding procedures, equipment, welding process, and welding operators. Thus, it is reasonable to assume the other canister ITCP welds will have intermittent defects similar to those characterized in DSC-16. In addition, the same conservative bounding defect assumed for the DSC-16 analysis provides a conservative modeling for all the canister closure welds.

Security-Related Information
Figure Withheld Under 10 CFR 2.390.

Figure 3-8. Representation of the defects identified in the ITCP closure weld of DSC-16 (collapsed to a single cross-sectional plane) [3]

Security-Related Information Figure Withheld Under 10 CFR 2.390.

Figure 3-9. Assumed bounding flaw set used to analyze the ITCP closure weld of DSC-16 [3]

3.1.4.2 Outer Top Cover Plate Closure Weld

The following listing of general observations was identified during the VID reviews for DSC-16 and are pertinent to conceptualizing weld bead changes as it progresses along the weld length. They are observed as reoccurring characteristics that fluctuate along each weld bead. When undesirable characteristics align and result in conditions that exceed some critical condition, an interbead LOF will form and continue until the critical conditions are no longer met.

- Welding conditions, in general, produce a viscous weld puddle described herein as having the appearance of "lava flow" (see Figure 3-12)
- Weld metal added and travel speed applied produce large weld bead cross-sections
- Weld wire has significant and variable "cast" or "set" that moves the wire entry point and causes dragging and chatter as it drags against the solid material (see Figure 3-6)
- Weld wire guide tube requires periodic adjustment to maintain desired wire entry location
- Weld bead contours are observed having steep sides that were seen to develop into sharp valleys between adjacent beads
- Weld beads positions tend to drift from side to side for a variety of reasons, then require physical adjustment to maintain intended tungsten electrode position

- Weld joint gap varies around the circumference (see example in Figure 3-12 (root weld issue)

Security-Related Information
Figure Withheld Under 10 CFR 2.390.

Figure 3-10. Plot of the PAUT indications found in the OTCP of DSC-16 (All indications around the circumference have been compressed to a single cross-section) [3]

Security-Related Information
Figure Withheld Under 10 CFR 2.390.

Figure 3-11. Assumed Full Circumference Flaws in the OTCP closure weld of DSC-16 that conservatively bound the flaw population [3]

It is emphasized that the interbead LOF defects (as evidenced by the volumetric inspection results of the DSC-16 OTCP closure weld) are intermittent with limited height (i.e. less than one bead in height through thickness). For most of the weld circumference interbead lack of fusion does not occur and the weld deposit will be satisfactory as shown in Figure 3-7. However, in a few locations, variations in bead deposition alters the interface between adjacent weld beads such that a flaw trap is created and segments do not fuse properly. The result is a defect condition described as "interbead LOF". As the weld bead progresses, it continues to vary (profile and location) until interbead LOF ceases. This process repeats itself and results in intermittent defects distributed along the weld length. This mechanism will produce defects limited in height to the height of the interface between adjacent weld beads.

This mechanism implies that the material thicknesses deposited between inspection intervals will necessarily bound the heights of any defects generated during that interval. Layer thicknesses were calculated from depth measurements at each inspection interval. Figure 3-3 plots the average thickness height at each inspection interval. Because the interbead LOF would be located primarily in the material deposited between the root interval and the intermediate interval, the heights of defects would be less than 0.2 inch. The PAUT defect height measurements provided on DSC-16 [3] are consistent with this reasoning.

The defect patterns observed with PAUT volumetric examination of the DSC-16 OTCP closure weld are shown in Figure 3-10 [3], and are different from those identified in the ITCP closure weld discussed in 3.1.4.1 above. These differences are to be expected, because this weld geometry is different and the weld is larger requiring the stacking of additional weld beads to complete. The OTCP closure weld is a double bevel joint geometry instead of the single bevel used on the ITCP closure weld. This change is beneficial because the sidewall taper helps to minimize potential for sidewall LOF defects – the dominant defect seen in the ITCP closure weld. Also, the OTCP closure weld is larger and requires a minimum of five (5) weld beads to complete the weld. The consistent placement of these beads in a manner that promotes full fusion of the weld bead interfaces is a key requirement. The sketch displayed in Figure 3-7 describes complete fusion of sidewalls and weld bead interfaces, and should be viewed as optimum weld bead placement plan. If this plan is carried out, then a defect free weld will result. However, when the bead shape contours change and the bead placements deviate from the required path (drift), a risk is developed for incomplete interbead fusion. This is what is believed to have happened with the OTCP closure weld for DCP-16.

The volumetric inspection results describe intermittent defects having a height dimension between 0.05 inch to 0.14 inch that is on the order of the thickness of a single weld bead or less. The indications are variable lengths ranging up to 206.28 inches. In other words, individual defects are characterized as having a limited height and distributed in intermittent segments along the circumference of the OTCP closure weld.

For the purposes of structural modeling, the defects have been collapsed into three planar flaw sets as shown in Figure 3-11 – all assumed to be continuous around the full circumference. This set of three flaws was labeled as Bounding Set #2 in the structural analysis. The individual defects are summarized in the plot shown in Figure 3-10. Individual defects are numbered for identification as taken from Reference 3. Viewed this way, there is a Group Flaw (on the shell side), Flaw #2 on the lid side), and Flaw #14 (at the root) all approximately parallel. Flaw #2 is closely aligned with interbead LOF. Flaw #14 is located near the bottom of the groove, based on the PAUT scan images, and may be LOF based on its location. Flaw #20 is a small sidewall LOF and is not considered explicitly in the finite element structural analyses. Flaw #3 is a small flaw (estimated at 0.18 inch long and 0.09 inch tall) near Flaw #2 which also is not explicitly considered in the analysis, but is much smaller than the analyzed critical subsurface flaw size of 0.29 inch which is bounding.

There were several observations typical of the OTCP weld that were identified in the welding reviews. First, root gap is inconsistent around the circumference. The welding procedures are designed to tolerate some changes in the root gap; however, excessive root gaps can be related to LOF type defects associated with the substrate material separated by the gap. A changing root gap also can result in changes in weld deposit thickness along the sidewalls. Figure 3-12 shows a typical example of variation seen in the width of the root gap that was observed in all the OTCP closure welds reviewed. The width of the gap is likely due to geometrical and fit-up tolerances associated with centering the top cover plate in the canister shell. The sluggish weld metal flow characteristic with these materials and this procedure, the changing root gap and the frequent repositioning of the tungsten electrode likely resulted in the short sidewall defect seen at the break-point of the shell side taper. It is also interesting to note in Figure 3-12 that the viscous molten puddle is being pushed ahead of the tungsten electrode arc due to the arc force. This characteristic suggests that the weld puddle is improperly wetting the substrate and causes the weld metal to ball on the leading edge of the puddle. This can lead to weld metal roll-over where steep vertical contours can develop on open sides of the weld bead cross-section. This condition suggests that the welding heat is too low and too much metal is being added for the available heat supplied. It is noted that some weld metals are naturally sluggish such as nickel base materials, but stainless steel should not have that characteristic. Also visible in Figure 3-12 is the chilling effect on the weld puddle where the filler wire enters the weld puddle. Note how the molten metal flow divides at the entry. The molten material will always be chilled by filler wire entry, but the welding heat should be sufficient to maintain the full stirring of the puddle. When the welding heat is marginal, then the puddle will ball up and divide as seen in the VID screen shot. It is noted that these are characteristic observations for all the VID records that were available for review and is believed to be a characteristic of the welding procedure used.

Figure 3-12. Photo sequence captured from VIDs showing differences in root gap width as the weld bead progressed clockwise around the circumference. The shell wall is on the right side of the photo and the cover plate is on the left. The VID camera is mounted to view the front of the arc.

The defects located within the weld deposit are believed to be interbead LOF formed specifically at the interface between adjacent weld bead surfaces when conditions are favorable. The interface locations can be at triple point intersections among three bead surfaces, or more likely, along the vertical interface between adjacent beads. The formation of defects is strongly related to the presence of a steep contour along the sides of adjoining beads and to the relative positioning of those beads relative to each other. This condition is periodic and the defects produced will be intermittent along the length of the closure weld.

Visualizing the development of these types of defects can be difficult in that several necessary conditions for the defects are developing concurrently. Accordingly, Appendix B has been developed to show sequential development of the interbead defects in the OTCP closure welds. Figures B-1 and B-2 show potential locations for LOF defects associated with the root area. The weld groove sidewall and root LOF defects are typically observed at locations where weld penetration is insufficient to achieve fusion with the sidewall or root base material. LOF issues of this type were covered earlier in the discussion of the ITCP closure weld defects, and a similar reasoning is appropriate for OTCP closure weld. However, conditions leading to the intermittent mid-wall defects are more complicated to visualize. Conceptual sketches related to forming these defects are shown in the sketches depicted in Figures B-3 and B-4 and their formation will be discussed below.

Individual defect heights are small in magnitude (less than one bead thickness approximately 0.10 inch), but have been modeled conservatively as a continuous crack completely around the circumference. Thus, any analytical crack extension would necessarily grow thru thickness. This is another conservative assumption, and even with these assumptions, the bounding defect analyses found a satisfactory margin for safe performance.

The main questions to be addressed are 1) "How do these types of defects form?", and 2) "Why are they small and intermittent?". The answers are believed to be related to weld bead deposition characteristics observed to vary along the weld length in terms of placement and bead shape or contour. The VIDs provide evidence that bead placements drift horizontally across the weld width requiring periodic repositioning to correct the deposit buildup, and bead shape changes develop according to the molten "lavalike" viscous metal flow. The variations observed with the 2nd, 3rd, and 4th beads deposited sequentially along the length of the weld are the keys to the defect formation. The ideal plan would be for each bead to be precisely placed per a prescribed pattern as described in Figure 3-7. If this were done for the full length of the weld then there would be no conditions present to support interbead LOF, because the measurable fusion would be developed both along sidewalls of the groove and bead to bead. The weldability of the Type 304 stainless steel base material using ER308 filler metal is excellent, and there is significant margin for deviations from ideal welding parameters. However, the welding VIDs show that weld beads are not consistently positioned in the weld groove. Second, the cross-sectional bead shape is constantly changing along the bead length due to the sluggishness of the molten material and the placement of the preceding weld bead due to drifting placement. These two factors continue to change concurrently without creating defects until conditions are superimposed that are favorable for developing an interbead LOF defect. Since the concurrent conditions are constantly changing, the circumstances favoring interbead LOF will cease, the interface will fuse, and the defect will end. This behavior is viewed as the reason for the intermittent pattern of cracking as described in Appendix B Figures B-3 and B-4.

The defect distributions identified by PAUT in DSC-16 were shown in Figure 3-10. Figure B-3 depicts the conditions forming defects identified to the right of center involving the interface between adjacent surfaces of bead 2 and bead 3 that developed when bead 3 was deposited to fill the valley created with the plate sidewall. Bead 2 had been deposited previously with the tungsten electrode positioned favoring the shell side of the weld groove. Recalling that the bead placement is subject to some degree of drifting, the fill from bead 2 will have portions of the bead length that buildup along the shell sidewall. The deposit at this point will fill towards the plate side wall, but will assume a contour across the bead cross-section that is dictated by the volume and viscous nature of the molten weld metal. As noted previously, the weld puddle is characterized by a lava-like flow that can develop a steep contour on the side of the bead adjacent to the groove sidewall. This creates a steep walled cavity that must be filled by the next weld bead. Subsequently, weld bead 3 is deposited over this cavity purposed to consume all the material under it and to both sides. However, the drifting of the beads side-to-side coupled with the sluggish nature of the molten material results conditions at the interface between beads 2 and 3 that do not fuse as intended and LOF results (area colored red in Figure B-3). As the bead continues to drift, conditions change and fusion is reestablished. Thus, the defect ceases and the intermittent defect characterization develops.

Weld bead 4 is positioned over weld bead 2 to fill the cavity created between the upper portion weld bead 3 and the shell sidewall. A similar interaction to that described above between weld beads 2 and 3 will be developed between weld beads 3 and 4. The defect creation is depicted in Figure B-4 (defect shown in red). Figures B-5 and B-6 are screenshots of the welding VIDs for the OTCP closure weld in DSC-16 showing examples of the welding conditions that promote interbead LOF according to the described model. This depiction provides a viable mechanism for the formation of defects described by the representative Group Flaw shown in Figure 3-11.

Bead 5 is intended as the cover, or crown bead, and is deposited to crown the weld cavity. A second function is to fill the groove and complete the weld thickness or height requirement of 0.50 inch.

It was noted in the VID reviews that in-process weld repairs were recorded where partial circumferential weld beads (strips) were added to fill low spots and/or to improve the weld deposit contours in DSC-12, -13, -14 and -15. In-process weld repairs were not observed in the VID reviews of OTCP closure weld of DSC-16. In-process weld repairs were confirmed during the general area video reviews and also were observed during the welding of DSC-11. Additional weld material was added to DSC-16 to correct a fill height condition below design requirements (as described in Section 3.1.2), but this correction was performed after the closure welding sequences had been completed.

3.1.5 Welding Learning Curve

The ITCP and OTCP closure welds completed sequentially beginning with DSC-11 and continuing through DSC-16. Weld head video records (front and trailing VIDs) were available for review for OTCP closure welds on DSC-12 through DSC-16. VID records for the ITCP closure welds were only available for DSC-13 and DSC-16. No welding VIDs were available for DSC-11 – the first canister loaded and sealed.

A tabulation of the welding details, sequences, and durations plus observations were prepared based on reviews of the available VIDs for DSC-12 through DSC-16, and are provided in Appendix C. The tabulations offer a sequential history of the closure welds for each canister reviewed including welding stops and starts, issues encountered with root welding, use of partial length welds beads (stripping beads) to fill in low areas around the circumference, to contour weld beads or to complete other in-process repairs. It was not always possible to identify what was being done except for the timing and personnel present. These same weld head video records had been reviewed previously by the author and the results of those reviews were factored into the evaluation [1, 2]. It was concluded in the earlier evaluations that specific deposit characteristics, known to increase the potential for welding defects, were common to all the closure welds reviewed. However, DSC-16 appeared to exhibit more of the undesirable conditions than those observed in DSC-12 through DSC-15.

The general work area video records were examined during an on-site visit to determine, to the extent possible, if the canister welding VIDs could be confirmed and to compare available information for all the canisters welding activities including DSC-11. All work area videos were not reviewed; however, the reviews focused on those times where welding and inspection activities were taking place. The SI review information was captured in a Structural Integrity internal letter trip report that is replicated in Appendix D. The observer noted local grinding repairs were performed but were limited, and in-process adjustments were made as-necessary.

One additional observation of the area review suggested that welding experienced less frequent interruptions with each succeeding canister weld. Whether this observation was due to additional care in alignment (concentricity of the shell to the cover plate during fit-up or centering the welding equipment) could not be determined, but the welding encountered fewer interruptions in the later canister welds as evidenced by longer weld lengths without stopping for adjustments. It is possible that the welding operators became more comfortable with the welding and may have been less attentive. These general area video review results are consistent with similar observations obtained from the fore and aft weld head camera VIDs.

The least frequent interruptions during weld deposition were seen for the OTCP closure weld of DSC-16 (the last to be welded). Each of the five weld beads making up this weld appeared to be deposited without interruption. The previous canister closure welds experienced multiple stops and starts to address various welding conditions observed with the fore and aft mounted cameras on the welding head and as viewed by the welding operators on the welding console. Most interruptions seemed to be related to correcting the tungsten arc position, adjusting the wire feed entry position, correcting weld deposit surface profile, or cleaning. The root weld experienced burn-through or an undesirable deposit condition necessitating repair and/or adjustment of the welding technique in response to a wide root gap condition (introduction of tungsten oscillation to prevent burn-through).

It should be noted that continuous weld beads (without stops and starts for any given bead) should not be construed to imply that the weld will have fewer defects. In fact, the opposite may be inferred. The reason is that specific placement and profiles of weld beads associated with welding defects may have been corrected by in-process adjustments before developing defects.

The previous review [1] of these same VID records concluded that more of the physical conditions historically associated with weld deposit defects, were seen in DSC-16 than in any of the other canisters for which VIDs were available. It was noted that all canister closure welds prior to DSC-16 paused multiple times to implement corrective measures such as, adjustments to the welding equipment setup, minor grinding, surface cleaning, and application of limited length partial weld beads (strip beads) to properly fill and contour weld deposits. This remedial action likely eliminated some of the bead deposit conditions associated with defects like those identified in the volumetric (PAUT) inspections of the DSC-16 closure welds. Since none of the in-process corrective measures were performed in DSC-16 (other than electronic steering of the weld head while the welding arc was active), it is plausible that there may be more defects in the DSC-16 closure welds than any of the other canister closure welds.

It was noted that DSC-12 and DSC-13 experienced one or more burn-throughs during root welding. This condition was corrected by changes to operating parameters (lower heat and/or use of oscillation) accompanied by removal of the defective material by grinding. The burn-throughs appeared to be related to arc heat management (tungsten position and wire feed entry location) especially at locations having wide root gap openings. Figure 3-12 displays a root gap that gradually changes as the weld progresses around the circumference. It was noted that the root gap widens followed by narrowing two times around the circumference. This implies a certain degree of ovality most likely in the canister shell. This feature was observed with all canisters having VID records available for review. The cover plates (both ITCP and OTCP) are securely tacked in place during fit-up using eight short, but substantial weld segments. These tacks align and secure the gap prior to welding the root bead. Tack welds are sequenced to minimize gap distortion produced by shrinkage of the tack welds; however, the effectiveness of sequencing will be less than perfect and some asymmetrical weld shrinkage will occur. The inner shell diameter is a little over five feet and small differences in concentricity, even within specification tolerances, may result in root gap dimensions significant to depositing the weld root.

It was noted in the review of the welding VIDs that a large volume of molten material is developed with the applied welding schedule. This feature was seen with all weld beads including the root pass for all canister closure welds. Welding parameters appear to be the fixed (at least similar) for all weld passes based on the molten puddle size and apparent viscosity as seen in all welds reviewed. This includes wire feed speed and tungsten electrode travel speed (both have acceptable ranges in the detailed welding procedures). Changes to these combinations alter both weld bead size and shape.

All the welds around the vent/siphon block were manual GTAW welds using straight current and the same composition solid wire/rod welding consumables according to the welding procedures [2]. No welding VIDs were recorded during manual welding and these could only be viewed in the general area video records. Therefore, available welding information included welding procedures, welding sequences, welders ID, filler metal heats, etc. and the overall camera views. These are not discussed in this report.

The area cameras views did confirm the interrupted weld progression of the early canister closure welds that were not present for DSC-16. The general area videos did provide some information on DSC-11 for which no weld head VIDs were available. It was observed in the area camera views that the same type and frequency of in-process remedial measures for DSC-11 was similar to the other canisters except for DSC-16. This provides some confidence that the DSC-11 welds would be expected to have defect conditions like those developed in DSC-12 through DSC-15.

3.1.6 Progressive Weld Inspections

The weld acceptance inspections were progressive surface inspections performed on the root and final passes for the ITCP closure weld, and after the root, intermediate and final layers on the OTCP closure welds. Visual testing (VT), performed at the same intervals as the PT, were reported to be satisfactory and there was a reasonable level of confidence they were properly performed. These results suggest that any defect would be contained within the successful inspection boundaries, and if so, the thickness of the interval would bound any defect height. That indicates that any defect developed within the interval thickness should be no deeper than the thickness of the deposited material for the interval inspected. The fact that all VT results were satisfactory, suggests that the heights of any defects present would be bounded by the thicknesses of the weld deposited material between inspection intervals as discussed previously and was seen consistent with the PAUT volumetric results performed on both ITCP and OTCP closure welds of DSC-16 – the characteristic heights of all defects identified were smaller than the thickness of weld deposited material between the root and intermediate inspection intervals.

As described previously, Figure 3-3 displayed the average fill thickness for all six of the canister OTCP closure welds showing the fill depths where each of the three inspection intervals were conducted. Figure 3-4 shows the fill thickness for each of the six canisters where inspections were performed as a function of the quadrant where the measurements took place. The measurements recorded were the depths from the top of the plate to the top of the layers inspected, and from these measurements, the deposited material thickness was computed for each inspection interval, and finally the total deposited thickness for each layer was computed showing that all canisters met the minimum 0.50 inch fill thickness design requirement. An independent vendor PT inspection of the OTCP closure weld was performed about 3 months after the weld had been completed. A surface sidewall indication about 1 inch long was identified along the weld crown edge. This indication was surface conditioned by cleaning and light grinding. Twenty-one (21) additional surface indications were identified, considered non-relevant, and eligible for removal by surface conditioning [10]. The conditioning process removed the 21 indications on the crown surface, but did not eliminate the indication on the edge. Instead, the indication length increased to 1.6 inches during surface conditioning. Three months later the flaw was removed by grinding.

The OTCP closure weld bead thicknesses were estimated from the interval depth measurements and the numbers of beads deposited for each layer. The root layer thickness suggests a root and hot pass (beads 1 and 2), the intermediate layer (beads 3 and 4), and the final layer (bead 5). It was noted previously that strip beads (partial circumference weld beads) were used to correct undesirable conditions and/or to adjust deposited heights in the first five canisters. Based on these considerations, the most likely location for the interbead LOF indications is the deposited material between the root and intermediate intervals containing weld beads 3 and 4. No VT indications were reported for the inspections of either interval suggesting that any defects present were contained within the intermediate inspection layer boundaries (previously described). Thus depths would be limited to less than approximately 0.2 inch. The ITCP only required two beads and VT examinations would have been performed after the root and final. Any defects would have been sidewall LOF because each bead traversed the weld groove width, and no side-to-side bead interfaces were present to develop interbead LOF. The vertical sidewall was the primary vulnerability for LOF – a condition confirmed by the DSC-16 PAUT results.

3.1.7 Assessment of DSC-11 Closure Welds

The lack of welding VIDs required a different approach to assess the use of the DSC-16 analysis as representative for DSC-11. In this case the review of the general area video records was used to assess if there were notable differences among the canister welds and especially for DSC-11. It was observed in the review that the visible activities in kind and frequency for DSC-11 were similar to DSC-12 and 13, but DSC-14 and DSC-15 displayed a few less stops and starts. Each of the DSC-16 weld beads were deposited without interruption for the full circumference (see subsection 3.1.5).

It is unknown if the reduction of in-process corrections was due to improved welding performance or to an improved level of confidence with the welding operators. However, the welding VID observations reported previously [1] identified more of the undesirable conditions (known by the welding community as potential precursors to defects) in DSC-16 than with any of the other canister welds for which the information was available. This analogy applies directly to DSC canisters 12 through 15, but excludes DSC-11 due to lack of available VID evidence for DSC-11.

The general area videos during welding activities were reviewed comparing DSC-11 with all the others. It was seen that DSC-11 was like DSC-12 and DSC-13 in terms of the types of activities, starts and stops for individual beads, and how often the activities were undertaken. The implication is that those welds should be similar in terms of potential defect size and frequency distributions. DSC-14 and DSC-15 were seen to have the same types of activities, but less frequent. DSC-16 did not have any of the stops during a bead run, but some conditioning of the surface between beads was performed as evidenced in the general area video review. It was also noted that inspections were performed to the same testing intervals and VT inspection results were reported to be satisfactory for all of the canister welds. The inspection interval layer depths were measured and found to be relatively consistent among all the OTCP closure welds including DSC-11.

The same welding procedures were used for all the lid closure welds, welding sequences were the same, weld filler metal was the same, and a mix of the same welding operators were used for all the canister closure welds. The welder ID numbers and filler metal heats used are summarized in Table 3-1. Only the machine welds (#1 and #4 from Figure 3-1) are provided in Table 3-1 as those are the welds in question. Therefore, it is reasonable to expect a degree of consistency among the welds.

Table 3-1. Welder ID numbers and filler metal heat numbers used [4, 5, 6, 7, 8, 9]

		Welder ID							Filler Heat		
DSC No.	Weld No.	1	11	18	21	31	43	55	737880	736908 Spool	527221 Spool
11	1	x		x		x				x	
11	4	x	x	x	x	x	x	x		x	
12	1		x			x			x	x	
12	4			x		x				x	
13	1		x				x			x	
13	4	x	x	x		x	x	x	x	x	
14	1		x				x			x	
14	4	x	x				x	x		x	
15	1		x				x		x		x
15	4	x	x	x		x	x	x			x
16	1		x	x			x				x
16	4		x				x				x

4.0 SUMMARY AND CONCLUSIONS

A detailed review of the available welding VIDs, the area surveillance videos, and the PAUT inspection information developed for DSC-16 has been completed. The reviews initially focused on the closure welds of DSC-16 for which the most complete information set was available to relate to the PAUT results.

The PAUT results for DSC-16 were presented by AREVA [3] for both the ITCP and the OTCP closure welds. These results showed sidewall and groove bottom indications for the ITCP that SIA believes are LOF based on location of the indications. The indications reported for the OTCP were modeled as three separate bounding flaws, two associated with mid-wall indications (described as the representative flaw grouping and Flaw #2), and the third (Flaw #14) that appears to be LOF based on its location at the bottom of the weld groove. All three bounding flaws were conservatively assumed full circumference. The two mid-wall bounding flaw representations are approximately parallel, and because they are not aligned, would not be favorably oriented to reinforce flaw growth by fatigue.

A schematic model describing physical conditions that lead to the "interbead LOF" flaws has been proposed based on observations during reviews of the welding VID records of 1) weld bead location, 2) weld bead profiles, and 3) weld bead drift. The model considers the interaction of these features and the sluggish nature of the molten weld metal fluidity (described as lava flow), and the sequence of weld bead deposits as-applied to DSC-16. The bounding flaw distributions and sizes reported by AREVA are consistent with the proposed model and appear to faithfully represent the development of intermittent defects (small in height) as defined by the PAUT test results. The model suggests that when the defects are present they would be found at the interfaces between weld beads 2 and 3 for bounding Flaw #2, and between weld beads 3 and 4 for the representative flaw grouping. The model would place the defects intermittently along two approximately vertical planes and distributed around the circumference. These vertical representations are characterized as parallel and offset. Defects would be limited in the through thickness dimension to the thickness of a single bead, because the mechanism develops the interbead LOF between the sides of adjacent weld beads where complete fusion is not achieved. This necessarily limits the height of defects developed in this way to something less than the heights of adjoining surfaces of the adjacent beads being deposited. Since weld bead height is estimated at approximately 0.10 inch, any defects formed according to this mechanism would be limited to this dimension.

The sidewall indications reported by AREVA for the ITCP closure weld in DSC-16 are described in this report as "sidewall LOF" caused by incomplete sidewall penetration. In addition, the small sidewall indications identified in the OTCP are also the result of incomplete sidewall penetration resulting in LOF at the edge of the base metal.

It was observed that a learning curve resulted in welding activities with fewer interruptions in the later canister closure welds. No significant observations were seen in the welding VIDs for DSC-12 through 15 nor the general area video records that would suggest a different welding behavior from DSC-16, because the conditions causing the defects were generally observed in all the OTCP closure welds and for the two ITCP welds for which VIDs were available to review. According to the proposed flaw mechanism model, the observed conditions produced "sidewall LOF" in the ITCP and the OTCP closure welds, and "interbead LOF" in the OTCP closure welds.

There were no welding VIDs available for DSC-11; however, area videos for the welding and inspections of that canister were reviewed and no significant differences were observed when welding the DSC-11 closure welds. These observations suggest that defect distributions in DSC-11 would be represented by the distributions in DSC-12 through DSC-15 based on similar welding procedures, similar welders, similar filler metals, similar equipment, similar welding technique, similar deposit thickness levels at inspection, and similar in-process corrective measures. More corrections were observed with all the canister closure welds prior to DSC-16; however, it does not necessarily follow that there will be more defects present simply because more corrective measures were observed. In fact, it is likely that the in-process corrections taken during welding likely are characterized by fewer conditions potentially leading to the types of defects described, suggesting that those welds have fewer defects and would be less prone to any longer continuous defects.

The flaw distributions are conservatively modeled as full circumference for the structural analyses by AREVA. Structural analysis results are clearly bounding for the DSC-16 OTCP closure weld and concluded that a satisfactory level of safety is supported. The same bounding analyses should provide for similar conservative results for the other DSC OTCP closure welds. Discussion was provided to suggest that the assumption of similar flaw distributions, as seen in DSC-16, would be appropriate assumptions for the other dry shielded canisters, and would represent a reasonable conservative approach. Therefore, the assumptions made for the DSC-16 OTCP closure weld are recommended for the similar welds in all the other canisters reviewed, including DSC-11.

The VT inspection performed at the prescribed testing intervals were reported to be satisfactory for all the canister closure welds, and it had been determined that there was a reasonable level of confidence they were properly performed. It is suggested in this review that any defects developed would be restricted in depth to the deposit thickness developed for each interval, because the source of the defects in the OTCP closure weld is a defect described as 'interbead LOF'. Since this defect is formed between two adjacent weld beads within the same intermediate interval for both flaw distributions, it cannot exceed the weld bead height because that height is necessarily bounded by the thickness of an interval.

It is concluded that it is reasonable to assume that the conditions determined for the closure welds in DSC-16 reasonably represent the similar closure welds in DSC-12, DSC-13, DSC-14 and DSC-15. This conclusion is based on comparisons of evidence developed by reviewing each welding VID available and the rest of the body of evidence pertaining to all of the welds. In addition, it is concluded that the conditions of the closure welds in DSC-11 are reasonably represented by those observed in DSC-16 based on how the welds were made, the continuity of welding operators that made the welds, the common welding consumables and the visual inspections that were performed with satisfactory results. It is reasonable to assume that an experienced visual inspector would have detected the presence of any large defect penetrating the surface during the interval surface inspections. The most likely defects present would be bound by the interval layer thicknesses, because of the mechanism required to form the "interbead LOF". This assumption supports reasoning that the DSC-11 closure welds should have defect distributions no different from DSC-12 through DSC-15. DSC-16 was seen to have more conditions known to lead to welding discontinuities (such as LOF) than any of the other dry shielded canisters. It was noted that DSC-16 did not have the potentially beneficial in-process remedial actions applied to the others.

The analytical approach and results used to conservatively determine satisfactory performance for DSC-16 bounding flaws for the OTCP closure welds should be applicable to all the other canister OTCP closure welds. The assumption for full 360° bounding defects are considered very conservative for all the reviewed canister closure welds including DSC-11.

The conditions of the ITCP welds are judged as similar for all canisters. The vertical weld wall of the weld groove is inherent to a single bevel design, and because there is limited room to tilt the tungsten electrode towards the side wall, any LOF defects that might form would likely be located on the vertical sidewall. LOF defects of similar sizes and locations seen in DSC-16 are reasonable assumptions for the other ITCP closure welds. The assumptions made for the ITCP closure weld bounding analysis in DSC-16 are considered reasonable for all ITCP canisters closure welds.

5.0 REFERENCES

1. "Assessment of Monticello Spent Fuel Canister Closure Plate Welds based on Welding Video Records", R. Smith and N. Mohr, SI Report 1301415.403.R2, dated May 22, 2014.
2. Letter report from R. Smith (SI) to J. Becka (Xcel) on "Review of TRIVIS INC Welding Procedures used for Field Welds on the Transnuclear NUHOMS 61BTH Type 1 & 2 Transportable Canister for BWR Fuel", SI Report 1301415.402.R0, dated January 30, 2014.
3. Nuclear Regulatory Commission Adams Report Accession Number "ML16097A460 (AREVA Calculation 11042-0205 Rev. 03, "61BTH ITCP and OTCP Closure Weld Flaw Evaluation", pages 49-51 of 87), as sent to SIA via e-mail on 6/28/2017.
4. Work Order 00464956 Task 20 for DSC-11, SI File No. 1700388.201
5. Work Order 00464956 Task 21 for DSC-12, SI File No. 1700388.201
6. Work Order 00464956 Task 22 for DSC-13, SI File No. 1700388.201
7. Work Order 00464956 Task 24 for DSC-14, SI File No. 1700388.201
8. Work Order 00464956 Task 26 for DSC-15, SI File No. 1700388.201
9. Work Order 00464956 Task 28 for DSC-16, SI File No. 1700388.201
10. AR Number 01419279 "Apparent Cause Evaluation", SI File No. 1700388.202
11. Work Order 00464956 Task 76 for DSC-16, SI File No. 1700388.201

APPENDIX A

INNER TOP COVER PLATE CLOSURE WELD BEAD SEQUENCE (BASED ON VID OBSERVATIONS)

Flaw references are taken from the AREVA calculation package 11042-0205 Rev. 03 [3].

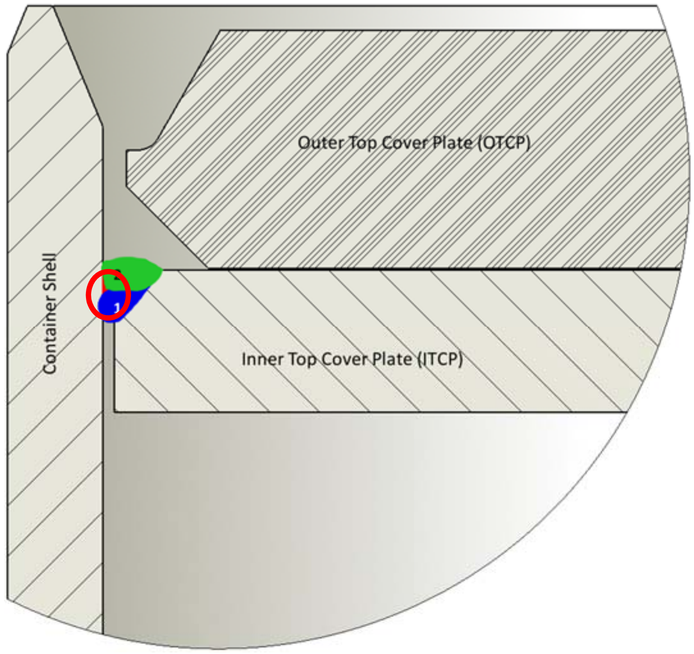

Figure A-1. Pass 2 LOF (Group flaw)

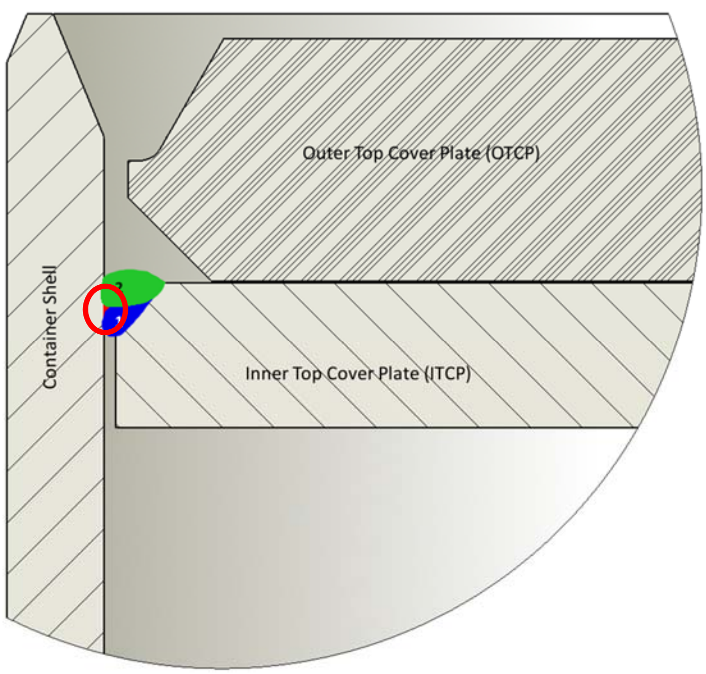

Figure A-2. Pass 1 / 2 Lack of Fill (Group Flaw)

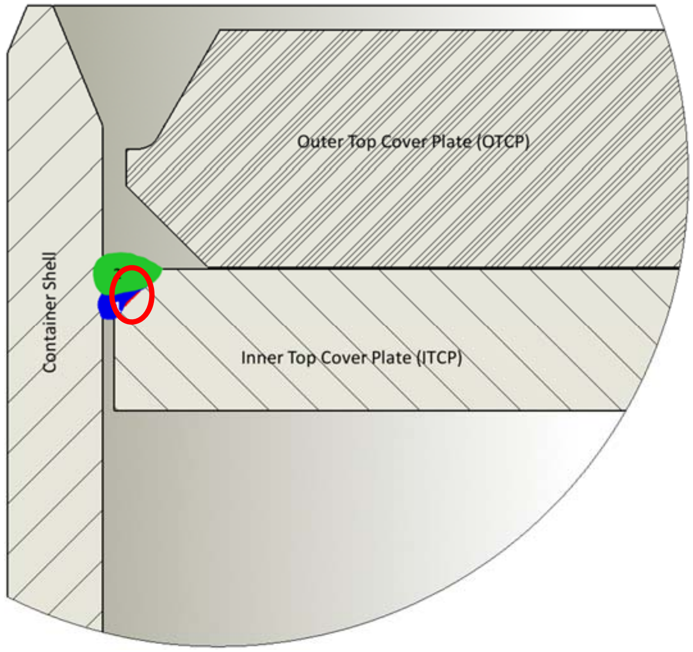

Figure A-3. Pass 1 LOF (Flaw 11)

ITCP Shell Sidewall Lack-of-Fusion Potential

(DSC-16 Weld Bead #2)

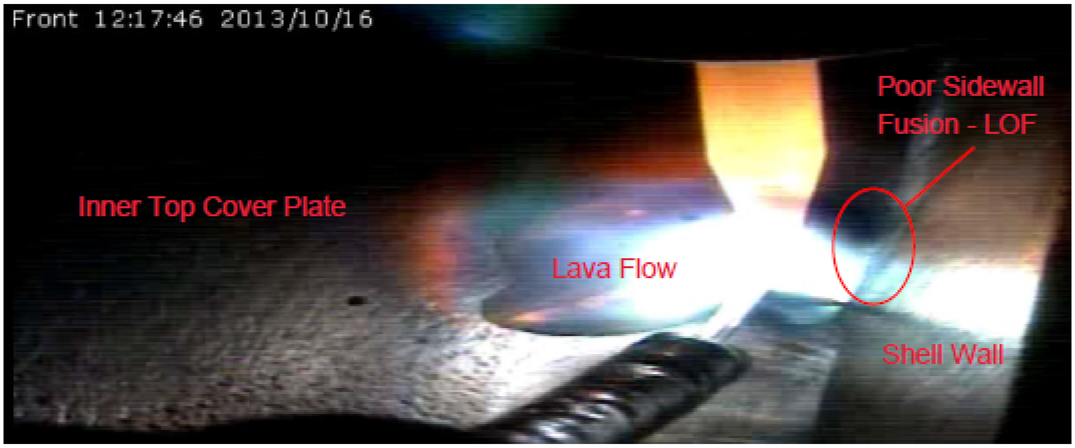

Weld bead #2 for DSC-16 showing poor sidewall penetration is poor with high probability for LOF. Next photo shows position adjustment to correct but too late to prevent short defect.

Electrode position adjustment 16 seconds later:

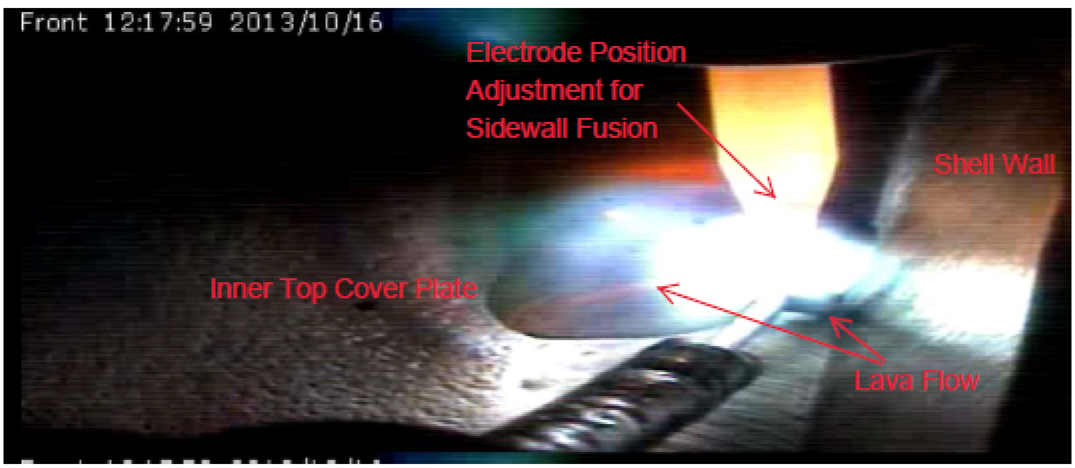

Repositioning corrected the sidewall penetration issue. Viscous lava-like flow and chilling of the weld pool at the filler wire entry location also are apparent. There is very little stirring of the weld puddle.

Figure A-4. Example of Weld Bead #2 deposit displaying poor sidewall fusion in the upper screenshot corrected shortly afterwards as shown in the lower screenshot.

APPENDIX B

OUTER TOP COVER PLATE CLOSURE WELD BEAD SEQUENCE BASED ON VID OBSERVATIONS)

Flaw references are taken from the AREVA calculation package 11042-0205 Rev. 03 [3].

Outer Top Cover Plate – Hypothetical Bead Shapes Producing Flaws

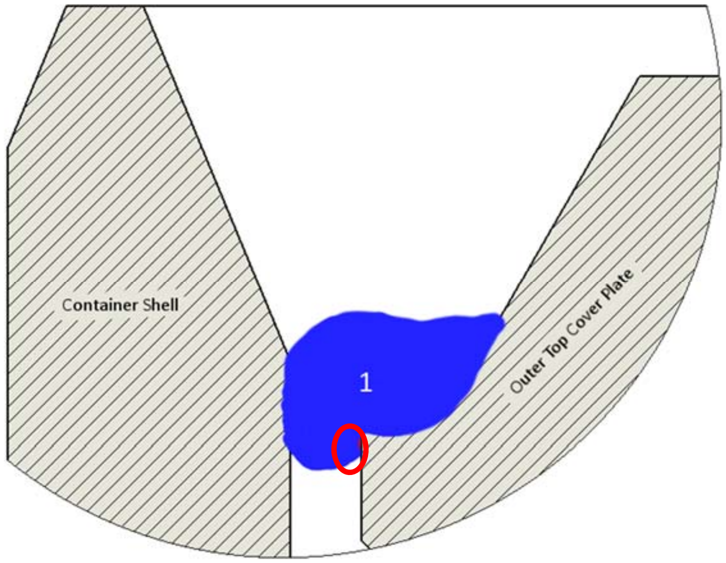

Figure B-1. Root Bead 1 LOF at bottom (Flaw 14)

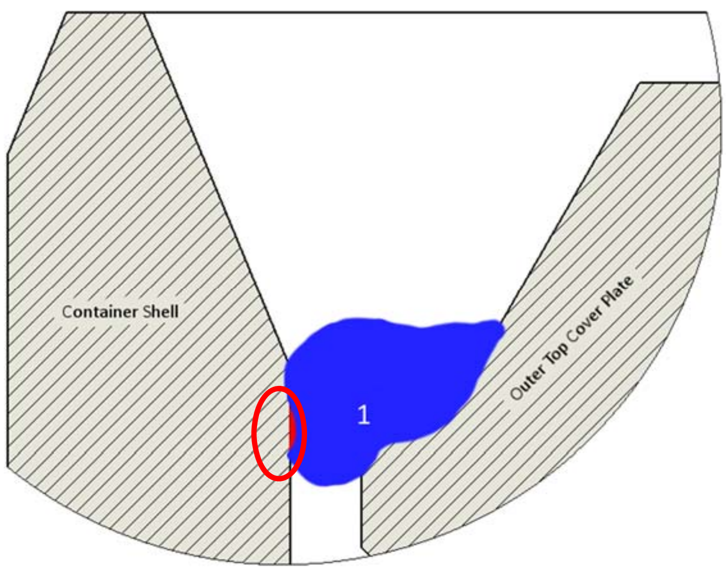

Figure B-2. LOF between Root Bead 1 and Container Shell (Flaw 20)

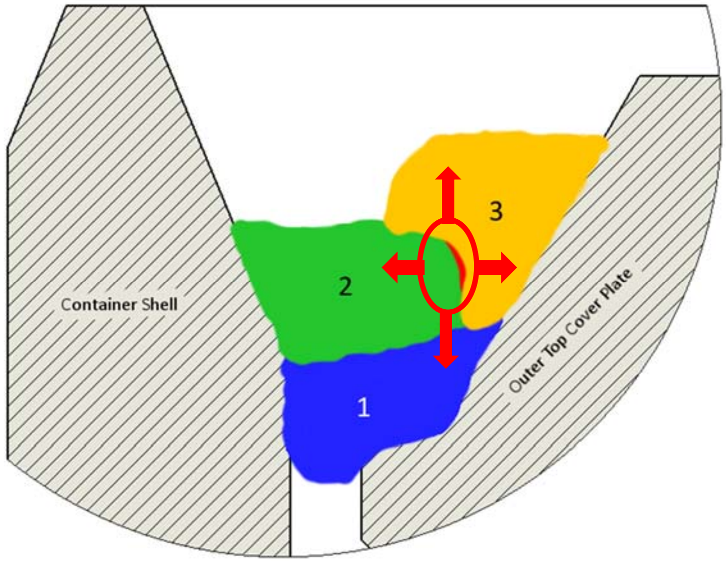

Figure B-3. LOF between Bead 2 and Bead 3 (Flaws 2 & 3)

[Note: flaw position can shift up / down / left / right. See report text for details]

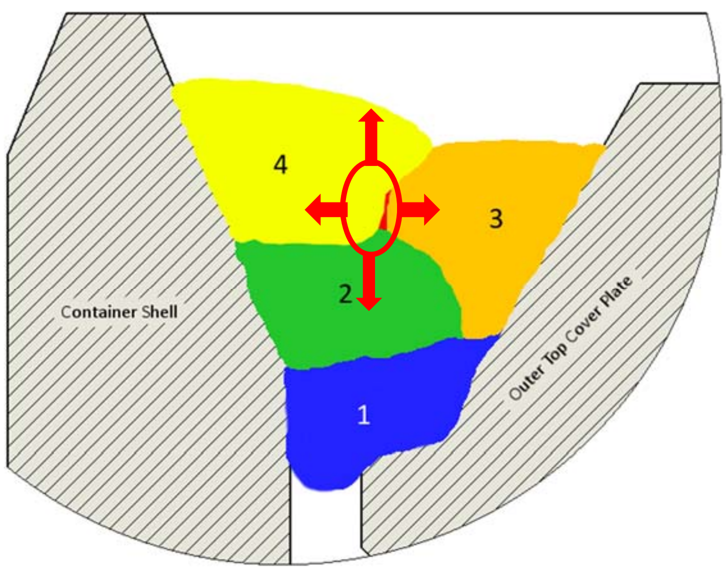

Figure B-4. LOF between Bead 3 and Bead 4 (Group Flaw)

[Note: Flaw position can shift up / down / left / right depending on specific bead position. See report text for details]

OTCP Interbead Lack-of-Fusion Potential between Weld Beads 3 and 4

(DSC-16 Weld Bead #4)

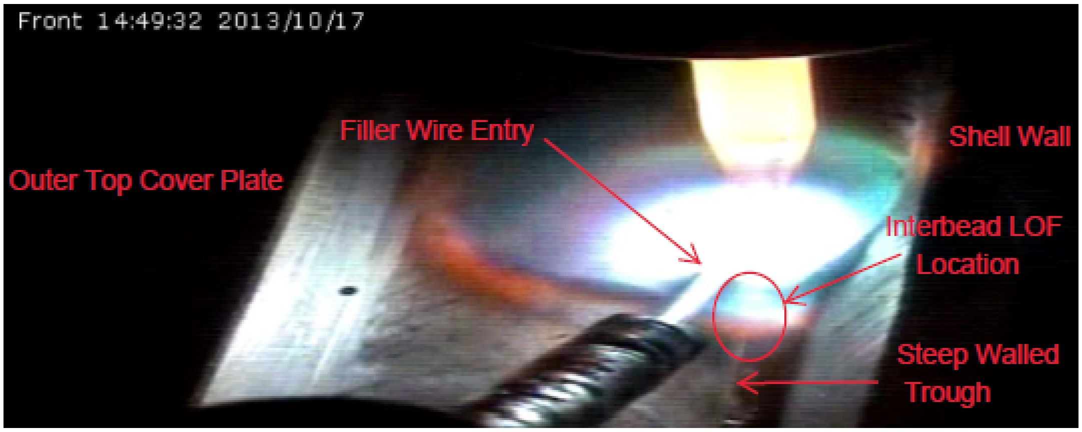

Note steep edge of weld metal buildup from weld bead #3 leaving steep trough for weld bead #4 to fill. Bead #4 is positioned near the shell wall, developing good fusion with the shell wall, and resulting in weld deposit build-up along the shell wall. The molten material over weld bead #3 side of the trough is being chilled by the wire entry location. This makes fusion with the side of weld bead #3 more difficult and leaves potential for an "interbead LOF" type defect as described in Figure B-4.

The electrode position was shifted away from the shell sidewall towards the cover plate immediately after this photo when the welding operator recognized excessive buildup along the shell wall and a need to reposition. It was just before this shift that the interbead location was vulnerable to interbead LOF. It was also noticed at this location that the cast on the filler wire was dragging resulting in nonuniform wire feed and thus another factor requiring correction.

Figure B-5. Screenshot of welding condition noted in OTCP closure weld of DSC-16 leading to "interbead LOF" as weld bead #4 is deposited adjacent to weld bead #3. See description below screenshot.

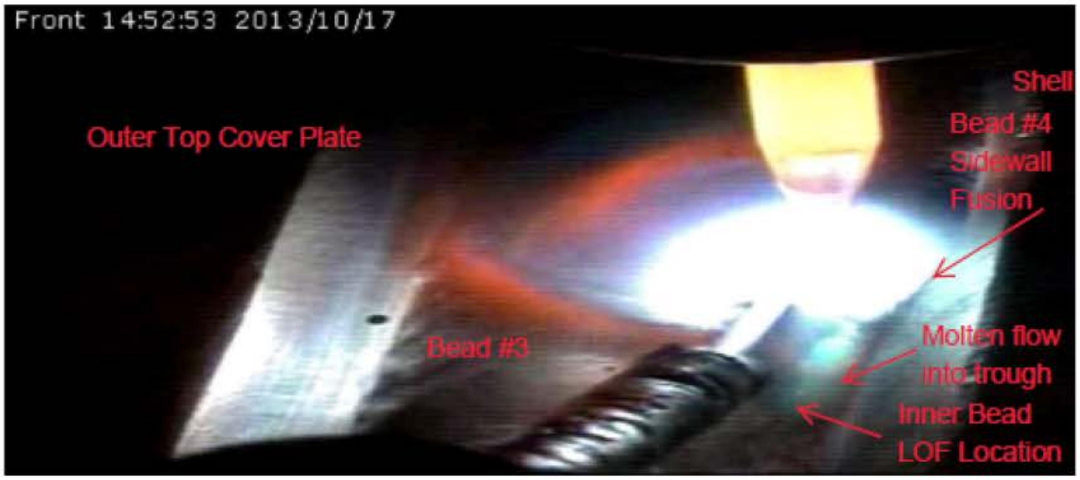

Photo of welding arc about 10 inches further along the weld length displaying non-uniform filling of the trough under the electrode arc. Notice the molten filler metal dropped into the trough without fusion. Fusion of bead #4 with the shell sidewall is seen along the top of the bead, but less so with the previously deposited bead #3 and in the bottom of the trough where a drop of molten metal is seen in the trough but not fused. This condition can insulate the sidewall of weld bead #3 and make it difficult to fuse the trough interbead sidewall. This condition promotes "interbead LOF". Distance stated above is based on the timestamp with an assumed travel speed of 3-inch/min.

Immediately following the photo above shows a surface condition where the electrode position for the bead #3 deposit was adjusted abruptly towards the shell wall. This action changed surface topography on which bead #4 was deposited (see bottom of photo). This welding feature is seen as contributing to the intermittent distribution of interbead LOF defects along the closure weld.

Figure B-6. Additional Screenshots of the DSC-16 OTCP closure weld showing undesirable deposit conditions between weld beads #3 and #4 caused by a previous repositioning of weld bead #3. The deposit conditions shown are consistent with the proposed model for 'interbead LOF"

APPENDIX C

TABULATED REVIEW OF AVAILABLE VIDS FOR MONTICELLO DSC-12 THRU DSC-16

1700388 - Monticello Spent Fuel Dry Storage Cask (DSC) VID Records

ITCP is Inner Top Cover Plate - 0.75" Thick	Weld 3/16"high X 0.31"wide	Weld Length (OTCP 66.25 x PI = 208") & (ITCP = 197")
OTCP - Outer Top Cover Plate - 1.25" Thick	Weld 5/8"high X 1.0"wide	Siphon Vent Block 80.5" to 91.5" location of Weld starts)

Weld Location	VID File Name	Date	Time Start	Time End	Duration (min)	Length (in)	TS (in/min) comp	Layer No.	Tungsten Bias	Comments
DSC-16 (VIDs Inner and Outer 16)										
ITCP to Shell	01	10/16/2013	9:24:19	10:29:42	65.5	197	3.0	1 (Root)	Lid	
ITCP to Shell	02 and 03	10/16/2013	11:14:48	12:32:08	72	197	2.7	2	Shell	6 min lost to adjustments of wire feed on 02 series.
OTCP to Shell	03	10/17/2013	9:39:40	10:50:18	70	208	3.0	1 (Root)	Lid	
OTCP to Shell	05	10/17/2013	11:50:32	12:56:10	66	208	3.2	2	Shell	
OTCP to Shell	06	10/17/2013	13:01:57	14:10:25	68	208	3.1	3	Lid	
OTCP to Shell	09	10/17/2013	14:47:30	15:46:40	59	208	3.5	4	Shell	
OTCP to Shell	11	10/17/2013	15:52:11	16:49:41	57.5	208	3.6	5	Lid	

Weld Location	VID File Name	Date	Time Start	Time End	Duration (min)	Length (in)	TS (in/min) comp	Layer No.	Tungsten Bias	Comments
DSC-12 (VIDs 12 - 12 and 464956_12)										
OTCP to Shell	03	9/14/2013	16:28:31	17:36:46	69	208	3.0	1 (Root)	Lid bias at root	Top of Root Surface was ground smooth at least in places.
OTCP to Shell	06	9/14/2013	18:56:09	19:03:28	7	21	3.0	2 strip	Lid	Blow through of root 06_00009
OTCP to Shell	07	9/14/2013	19:07:21	19:34:53	27.5	82.5	3.0	2 strip	Lid to Shell	Weld apparently welded at lower power and started weaving across groove
OTCP to Shell	08	9/14/2013	20:11:31	20:12:37	1	3	3.0	2a	Lid	Grinding then moved arc to lid side for short repair of deposit.
OTCP to Shell	09	9/14/2013	20:17:14	20:17:41	0.5	1.5	3.0	2b	Lid	Wire entry at wrong place and had to shut down quickly.
OTCP to Shell	10	9/14/2013	20:19:38	20:41:30	22	66	3.0	2c	Lid	Oscillating at plate wall (0.15 or 0.20) blow hole at end on root see pic
OTCP to Shell	11	9/14/2013	20:44:03	21:00:18	44	132	3.0	2d	Lid	Completed bead.
OTCP to Shell	15	9/14/2013	22:30:00	23:07:57	38	114	3.0	3	Shell	Stopped weld for possible wire guide or weld head adjustment
OTCP to Shell	16	9/14/2013	23:12:07	23:32:37	20.5	61.5	3.0	3	Lid	Stopped weld for possible wire guide or weld head adjustment
OTCP to Shell	17	9/14/2013	23:37:42	23:45:22	7	21	3.0	3	Lid	Tape stopped for unknown reason
OTCP to Shell	00	9/16/2013	2:02:39	2:21:44	19	57	3.0	3 strip	Shell	Weld deposition appeared to improve
OTCP to Shell	02	9/16/2013	2:31:33	3:05:04	33.5	100.5	3.0	3 strip	Lid	Weld deposition appeared to improve
OTCP to Shell	03	9/16/2013	4:16:54	5:25:07	68	204	3.0	4	Shell	Wire feed dragging and arc adjustment
OTCP to Shell	04	9/16/2013	5:46:18	6:52:07	66	198	3.0	5	Lid	Weld deposition appeared to improve

Weld Location	VID File Name	Date	Time Start	Time End	Duration (min)	Length (in)	TS (in/min) comp	Layer No.	Tungsten Bias	Comments
DSC-13 (VID 464956_13)										
OTCP to Shell	01	09/24/2013	14:37:49	14:46:29	8.5	25.5		1	Lid	Small oscillation in root pass at start, soon stopped osc. Gap widened 8 min into root (picture captured for record. Blow out at 14:46:29 and stopped to repair.
OTCP to Shell	03	09/24/2013	14:53:01	15:13:50	21	63		1	Lid	Second try to repair. Manually adjusted TS to add more wire and proceeded using oscillation to push filler metal from lid to gap. Photo record in file. Oscillation stopped as groove tightened about the 15 :00:37 mark. Lava flow can be seen from mirror reflection position on molten material.
OTCP to Shell	04	09/24/2013	15:15:21	15:31:51	16.5	49.5		1	Lid	Restarted to repair blowout. Oscillation continued with bias on lid side. Another blowout at 15:31:51. Appears to be burning through weld land on the lid side.
OTCP to Shell	05	09/24/2013	15:37:08	15:37:43	0.5	1.5		1	Lid	Restarted to repair blowout but burned through at the same location being repaired.
OTCP to Shell	07	09/24/2013	15:59:18	16:02:38	3	9		1	Lid	Restarted to repair blowout. Oscillation continued with bias on lid side. Another blowout occurred at 16:02:38
OTCP to Shell	09	09/24/2013	16:23:49	16:46:43	23	69		1	Lid	Restarted to repair blowout. Oscillation continued with bias on lid side. Stepped back about 12 inches and reinitiated arc with the same technique.
OTCP to Shell	11	09/24/2013	16:52:50	17:16:45	23	69		1 strip	Shell	Applied a wider oscillation but shifted to center on the shell side.
OTCP to Shell	13	09/24/2013	17:36:25	18:05:14	28.5	85.5		2	Shell	No oscillation
OTCP to Shell	14	09/24/2013	18:09:41	18:38:39	29	87		2 strip	Lid	Covering the 2-3 overlap. Appears to be clean. Having intermittent camera issues.
OTCP to Shell	16	09/24/2013	19:48:18	20:33:33	45	135		2	Shell	Surface grinding prior to welding.
OTCP to Shell	18	09/24/2013	20:49:39	21:35:53	50.5	151.5		3	Lid	Begin new layer. No oscillation

Weld Location	VID File Name	Date	Time Start	Time End	Duration (min)	Length (in)	TS (in/min) comp	Layer No.	Tungsten Bias	Comments
DSC-13 (VID 464956_13) cont.										
OTCP to Shell	20	09/24/2013	21:58:11	22:42:08	44	132		4	Shell	Begin new layer. No oscillation
OTCP to Shell	21	09/24/2013	22:53:12	22:53:35	N/A				Strip fill	Begin new layer. No oscillation
OTCP to Shell	22	09/24/2013	22:58:44	23:46:54	47	141		4	Shell	Weld ran smoothly
OTCP to Shell	25	09/25/2013	0:31:19	1:22:48	51	153		4	Shell	Weld appeared to have been ground, weld stepped back to correct fill in patter, then the weld appeared to run smoothly
OTCP to Shell	28	09/25/2013	1:34:23	2:38:40	64	192		5	Lid	Weld ran smoothly
ITCP to Shell	01	09/23/2013	12:08:30	13:18:38	70	197	2.8	1	Lid	Ran smoothly
ITCP to Shell	02	09/23/2013	14:36:13	15:42:09	66	197	2.9	2	Shell	Initially centered on crown of root pass but weld metal flow was seen to lap over the top on the lid. Initially the flow was minimal on shell side and tungsten repositioned to shell side. Lava flow covers side to side. Photo captured shows lava flow well ahead of tungsten on lid side. Good bit of drifting of the tungsten

Weld Location	VID File Name	Date	Time Start	Time End	Duration (min)	Length (in)	TS (in/min) comp	Layer No.	Tungsten Bias	Comments
DSC-14 (VID 464956_14)										
OTCP to Shell	02	10/2/2013	12:49:49	14:00:32	71	208	2.9	1	Lid	Centered on Tack then bias to lid. Wire appears to have a good bit of cast causing it to wanderfrom side to side. No stops for entire run.
OTCP to Shell	05	10/02/2013	15:43:36	16:37:19	54			2a	Center	Begin oscillating from center towards shell. Wire entry adjustements required. May be leaving intermittent defects on the shell sidewall at layer 2 level. Will be difficult to melt in on the fourth bead. Oscillation dug into the shell sidewall at frame O5_00119. Photo record made.
OTCP to Shell	06	10/02/2013	16:39:10	16:54:29	15	208	3	2b	Center	Repositioned tungsten and completed bead.
OTCP to Shell	09	10/02/2013	17:11:18	17:54:14	43	129 est.		3	Shell	Smooth run on layer 3. Weld pass filled in the arc gouge on the shell sidewall from the previous pass. (likely partial circumference to address an incompletely filled location)
OTCP to Shell	11	10/02/2013	18:06:50	19:09:51	63	208	3.3	4a	Lid	There are intermittent deep pockets (limited lengths) that may result in intermittent short defects between beads 3 and 4 shortly after start of the 4th bead. Similar to the DSC-16 conditions.
OTCP to Shell	13	10/02/2013	20:11:25	20:54:13	43	129 est.		5a	Shell	Surface ground in some places to begin
OTCP to Shell	15	10/02/2013	21:01:06	21:48:39	47.5	142.5 est.		5b	Lid	Stepped over to the Lid side to fill in incompleted 4th bead. The entire DSC-14 seemed to strip beads to attempt to correct incomplete filling of the groove welding sequence.

Weld Location	VID File Name	Date	Time Start	Time End	Duration (min)	Length (in)	TS (in/min) comp	Layer No.	Tungsten Bias	Comments
DSC-15 (VID 15-15)										
OTCP to Shell	00	10/11/2013	03:04:48	3:48:37	44	132	3	1	Center to Lid	Wire feed oscillating back and forth. Tungsten moved further from the center to the Lid side after the tack is passed. Appears to be a good bit of lava flow down into the gap but the root is flowing smoothly at 03:09:2013. Adjusted arc position towards Lid in process after it had drifted more to center at 03:12:00 am. Running very smoothly. Gap widening about 03:33:20 am. Continues to run smoothly at VID 55. There is a large amount of lava flow seen in the gap area. Large and deep separation being welded over to make uniform tie-in with molten material used for remelting. Wirefeed entry point moved way off to the shell sidewall and may have chilled the puddle such that it created fusion defects at 3:48 and arc was stopped. Photo is provided showing this issue.
OTCP to Shell	01	10/11/2013	04:10:09	04:35:54	26	208	3.0	1	Center to Lid	Continuation of root pass after repairing blow through. Wire feed entry point was corrected and apparently the lack of cooling derived from the wire entry caused the blow through. Arc extinguished normally according to the downslope programmed.
OTCP to Shell	02	10/11/2013	06:04:09	07:13:27	69	208	3.0	2	Shell	Welding smoothly with wire feed initially well centered on the tungsten tip. Moved to the Lid side at the very end.
OTCP to Shell	03	10/11/2013		No Welding						Manipulating the Tungsten to begin welding. Saw no evidence of surface grinding or cleaning.
OTCP to Shell	04	10/11/2013	07:30:39	08:37:26	67	208	3.1	3	Lid	Tungsten appears to be well centered on the trough formed from bead w and the lid sidewall. Wire feed is at the torch tip as it should be. Appears to be breaking down the material properly. Some wandering of the tungsten but not severe. Appeared to be related to the ovality of the shell relative to the lid position.
OTCP to Shell	05	10/11/2013		No Welding						
OTCP to Shell	06	10/11/2013		No Welding						
OTCP to Shell	07	10/11/2013		No Welding						

Weld Location	VID File Name	Date	Time Start	Time End	Duration (min)	Length (in)	TS (in/min) comp	Layer No.	Tungsten Bias	Comments
DSC-15 (VID 15-15) cont.										
OTCP to Shell	08	10/11/2013	09:42:28	09:57:26	15			4	Shell	Buildup to shell wall but flowing all the way across to the lid in some instances. Bead running well but wire feed appeared to stop and may have required changing wire.
OTCP to Shell	09	10/11/2013	10:13:31	11:07:34	54	208	3.0	4	Shell	Starts in center of bead then moves to the side as the weld passes the prior stopping point. Beads ran pretty much steadily without apparent incidents. Tie in to the shell sidewall appeared to be uniform and successful.
OTCP to Shell	10	10/11/2013		No Welding						
OTCP to Shell	11	10/11/2013	11:12:29	12:21:09	69	208	3.0	5	Lid	Tungsten positioned at lid sidewall where prior bead truncated. Lava flow is well ahead of tungsten making a U-shape around the wire entry. Not sure what that is doing. Flowing over top of lid starting at 11:20 and finishing at 12:21. Completed without incident.
OTCP to Shell	12	10/11/2013	12:30:52	13:19:50	49	208	4.2	6	Shell	Filling in from shell side and flowing to approximately the crown of the weld. May have increased the travel speed since the weld pool seemed smaller and flow only went to the apex of the weld crown.

APPENDIX D

MONTICELLO DSC VIDEO INSPECTION

(Letter to Richard Smith from Gerry Davina, Structural Integrity dated 6/8/2017)

Richard Smith
Senior Associate
Chief Welding Engineer
Structural Integrity Associates
11515 Vanstory Drive, Suite 125
Huntersville, NC 28078

June 6, 2017

Dick:

As part of Structural Integrity's efforts to support Monticello's efforts to qualify the long-term integrity of the DCS (dry cask storage) welds (SI Job No. 1700388), I visited the Monticello site (May 31 - June 1, 2017) to perform a detailed review of the available historical video records from the DSC welding evolutions during the 2013 cask loading campaign. The focus was to complete area observations of the welding activities, including any corrective actions, for both the ITCP (inner top cover plate) and OTCP (outer top cover plate) for each cask.

A summary of my findings after reviewing the associated video files during my recent site visit are included below.

DSC Welding Location & Orientation

Welding of the dry storage casks was performed on Reactor Building 1027' elevation along the south wall adjacent to the spent fuel pool. Figure 1 below illustrates the installation orientation for both the inner top cover plate (ITCP) and outer top cover plate (OTCP) for each cask. Note that the assigned orientation is based on the Reactor Building's cardinal points (i.e. north, south etc.). However, my assigned reference angles (0°, 90°, etc.) may need to be rectified with those assigned for the NDE review. It appears the NDE review assigns a reference angle of approximately 225° at the vent/siphon location. I did not rectify my assigned orientations to those assigned for the NDE review.

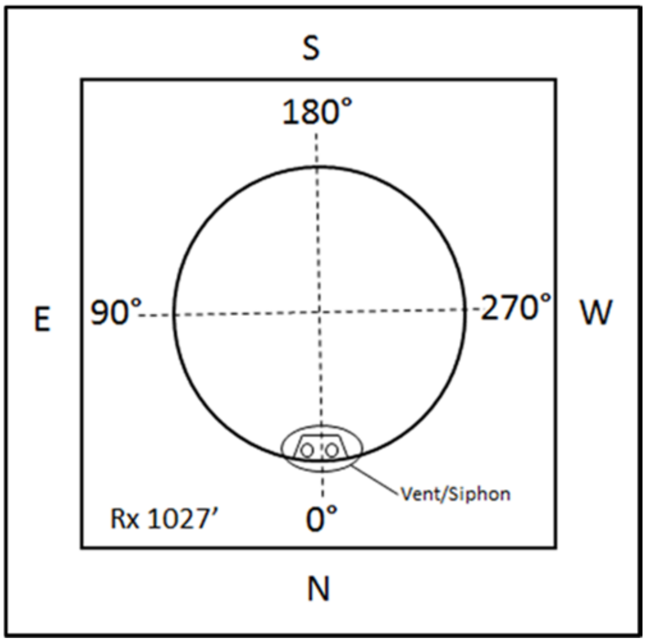

Figure 5-1: DSC Cover Plate Installation Orientation

Reactor Building Cameras

During the 2013 spent fuel transfer and associated DSC welding evolutions, several cameras on the RB 1027' elevation were oriented to remotely monitor and record the welding work and corresponding inspections/tests. The cameras associated with the 2013 DCS welding work are provided in Table 1 below.

Table 5-1: RB 1027' Elevation Cameras

Camera Name (Location)	IP Address
West Wall	172.27.52.18
North Wall	172.27.52.16
South Wall	172.27.52.65
Service Platform East	172.27.52.75
Service Platform West	172.27.52.36

DSC Welding Evolution Schedule

The six dry storage casks (DSC 11 through DSC 16) were loaded with spent fuel and sealed for dry storage in the fall of 2013. The dates for each of the associated cask's welding evolution are provided in Table 2 below:

Table 5-2: 2013 Dry Storage Cask Welding Schedule Dates

DSC	Start Date	End Date
11	09/05/2013	09/08/2013
12	09/13/2013	09/16/2013
13	09/23/2013	09/24/2013
14	10/01/2013	10/02/2013
15	10/09/2013	10/10/2013
16	10/16/2013	10/17/2013

Area Observations During DSC Welding

Area observations during the DSC welding were focused on operation of the TIG welder as well as any follow-up corrective actions (e.g. grinding, weld buildup, etc.). Note that the stitch (tack) welding operations during ITCP/OTCP installation/alignment were not included in the focused observations. Note that the time in-between each of the identified weld passes was typically dedicated to weld inspection as well as any corrective actions (if necessary). The details of the area observations for each DSC ITCP/OTCP welding evolution are outlined in the tables below.

Table 5-3: DSC-11 Welding Area Observations

Cask Plate	Date	Activity	Time Start	Time End	Notes
ITCP	09/05/2013	1st Pass	04:01:38	06:38:00	TIG was stopped and started approx. 7x for adjustment. Minimal spot grinding.
		2nd Pass	09:01:21	10:51:43	TIG was stopped and started approx. 4x for adjustment. Minimal spot grinding.
OTCP	09/07/2013	1st Pass	09:09:28? (Note 1)	09:27:43	TIG was stopped and started approx. 4x for adjustment. Minimal spot grinding.
		2nd Pass	09:39:02 (Note 1)	11:35:32	TIG was stopped and started approx. 4x for adjustment. Minimal spot grinding.
		3rd Pass	13:47:00	15:33:17	TIG was stopped and started 1x for adjustment. Minimal spot grinding.
		4th Pass	16:20:03	17:57:13	TIG was stopped and started approx. 1x for adjustment. Minimal spot grinding.
		5th Pass	20:16:10	00:54:15 (09/08/2013)	TIG was stopped and started approx. 2x for adjustment. Minimal spot grinding.

Table 5-4: DSC-12 Welding Area Observations

Cask Plate	Date	Activity	Time Start	Time End	Notes
ITCP	09/13/2013	-no information collected- (trouble operating historical video files on 09/13/2013)			
OTCP	09/14/2013	1st Pass	15:14:00	16:21	TIG ran uninterrupted. Minimal spot grinding.
		2nd Pass	17:40:24	19:44:25	TIG was stopped and started approx. 4x for adjustment. No grinding.
		3rd Pass	21:14:16	22:29:37	TIG was stopped and started approx. 2x for adjustment. No grinding.
	09/16/2013	4th Pass	00:48:05	01:50:28	TIG ran uninterrupted. No grinding.
		5th Pass	04:30:38	05:36:14	TIG ran uninterrupted. No grinding.

Table 5-5: DSC-13 Welding Area Observations

Cask Plate	Date	Activity	Time Start	Time End	Notes
ITCP	09/23/2013	1st Pass	10:53:25	12:07:25	TIG ran uninterrupted. No grinding. Manual weld buildup.
		2nd Pass	13:19:41	14:30:45	TIG ran uninterrupted. No grinding.
OTCP	09/24/2013	1st Pass	13:22:36	17:21:58	TIG was stopped and started approx. 5x for adjustment. No grinding. Manual weld buildup.
		2nd Pass	18:31:38	19:16:55	TIG ran uninterrupted. No grinding.
		3rd Pass	19:32:55	20:19:21	TIG ran uninterrupted. No grinding.
		4th Pass	20:41:46	21:25:35	TIG ran uninterrupted. No grinding.
		5th Pass	21:42:03	22:30:12	TIG ran uninterrupted. No grinding.
		6th Pass	23:14:42	00:06:07	TIG ran uninterrupted. No grinding.
	09/25/2013	7th Pass	00:17:46	01:22:04	TIG ran uninterrupted. No grinding.

Table 5-6: DSC-14 Welding Area Observations

Cask Plate	Date	Activity	Time Start	Time End	Notes
ITCP	10/01/2013	1st Pass	10:39:51	11:50:51	TIG ran uninterrupted. No grinding.
		2nd Pass	12:58:25	14:09:01	TIG ran uninterrupted. No grinding.
OTCP	10/02/2013	1st Pass	11:33:37	12:43:19	TIG ran uninterrupted. No grinding.
		2nd Pass	14:26:16	15:37:07	TIG ran uninterrupted. No grinding.
		3rd Pass	15:54:05	16:36:51	TIG ran uninterrupted. No grinding.
		4th Pass	16:49:37	17:52:35	TIG ran uninterrupted. No grinding.
		5th Pass	18:54:10	19:36:57	TIG ran uninterrupted. No grinding.
		6th Pass	19:43:50	20:31:23	TIG ran uninterrupted. No grinding.

Table 5-7: DSC-15 Welding Area Observations

Cask Plate	Date	Activity	Time Start	Time End	Notes
ITCP	10/09/2013	1st Pass	10:32:48	11:51:20	TIG was stopped and started approx. 3x for adjustment. No grinding.
		2nd Pass	12:47:25	13:52:56	TIG was stopped and started approx. 2x for adjustment. No grinding.
OTCP	10/10/2013	1st Pass	01:47:51	03:19:00	TIG was stopped and started approx. 1x for adjustment. No grinding.
		2nd Pass	04:47:13	05:56:27	TIG ran uninterrupted. No grinding.
		3rd Pass	06:13:37	07:20:30	TIG ran uninterrupted. No grinding.
		4th Pass	08:25:28	09:50:37	TIG was stopped and started approx. 1x for adjustment. No grinding.
		5th Pass	09:55:31	11:04:13	TIG ran uninterrupted. No grinding.
		6th Pass	11:13:10	12:02:50	TIG ran uninterrupted. No grinding.

Table 5-8: DSC-16 Welding Area Observations

Cask Plate	Date	Activity	Time Start	Time End	Notes
ITCP	10/16/2013	1st Pass	08:06:50	09:26:28	TIG ran uninterrupted. No grinding.
		2nd Pass	10:09:19	11:22:37	TIG ran uninterrupted. No grinding.
OTCP	10/17/2013	1st Pass	08:23:29	09:32:51	TIG ran uninterrupted. No grinding.
		2nd Pass	10:32:58	11:38:41	TIG ran uninterrupted. No grinding.
		3rd Pass	11:44:21	12:52:51	TIG ran uninterrupted. No grinding.
		4th Pass	13:29:51	14:29:09	TIG ran uninterrupted. No grinding.
		5th Pass	14:34:36	15:32:10	TIG ran uninterrupted. No grinding.

Summary of Observations

The available historical video files for the 2013 spent fuel cask loading campaign were reviewed. The review focused on area observations (i.e. activities taking place associated with the automated TIG welding of the cover plates) on the 1027' elevation of the Reactor Building during the DCS welding evolutions. Where available, welding of both the ITCP (inner top cover plate) and OTCP (outer top cover plate) for each cask were included in the review. As illustrated in the Tables 3 through 8 above, DSC-11 and DSC-12 required significantly more effort to complete the cask cover plate welds than the subsequent casks.

The multiple start and stops of the TIG welder during the DSC-11 evolutions are most likely indicative of difficulty in aligning the TIG welding head with the inconsistent gap between cover plate and cask wall or, possibly, inexperience with operation of the TIG welder. In either case, there was a marked evolution of refinement in regards to the operation of the TIG welder between DSC-11 and DSC-12. Area observations indicate that a large percentage of the TIG interruptions were associated with adjustment to the weld head and wire guide while there were minimal interruptions that involved corrective actions to the welds (e.g. grinding, weld buildup, etc.). The minimal amount of corrective action between each weld pass suggested that both welders and inspectors were satisfied that the TIG welds produced fulfilled requisite quality.

Sincerely,

Gerald F. Davina

Gerry Davina
Senior Mechanical/I&C Engineer
Structural Integrity Associates, Inc.®
Experts in the prevention and control of structural and mechanical failures

ENCLOSURE 4

AREVA CALCULATION 11042-0204, REVISION 3

ALLOWABLE FLAW SIZE EVALUATION IN THE INNER TOP COVER PLATE CLOSURE WELD FOR DSC #16

10 pages follow

AREVA	Form 3.2-1 Calculation Cover Sheet Revision 10	Calculation No.:	11042-0204
		Revision No.:	3
		Page 1 of 10	

DCR NO (if applicable) : 11042-022 Rev.0	**PROJECT NAME:** NUHOMS® 61BTH Type 1 DSCs for Monticello Nuclear Generating Plan
PROJECT NO: 11042	**CLIENT:** Xcel Energy

CALCULATION TITLE:
Allowable Flaw Size Evaluation in the Inner Top Cover Plate Closure Weld for DSC #16

SUMMARY DESCRIPTION:

1) Calculation Summary

An allowable flaw size of 0.15 inch is calculated for a 0.25 inch Inner Top Cover Plate (ITCP) weld in DSC # 16. Limit load analysis per ASME Code, Section XI, Appendix C is used to determine the allowable flaw size.

2) Storage Media Location

Rev.0: Secure network drive initially, then redundant tape backup.
Rev.1, 2 and 3 – No additional software files.

If original issue, is licensing review per TIP 3.5 required?
Yes ☐ **No** ☐ **(explain below)** **Licensing Review No.:** N/A

Software Utilized (subject to test requirements of TIP 3.3): ANSYS	**Software Version:** 14.0.3	**Software Log Revision:** Not applicable when Rev.0 was issued.

Calculation is complete: Originator Name and Signature: Veeresh Sayagavi Veeresh Sayagavi 2015.09.10 13:52:13 -04'00'	Date: 09/10/2015
Calculation has been checked for consistency, completeness and correctness: Checker Name and Signature: Raheel Haroon HAROON Raheel 2015.09.10 15:07:27 -04'00'	Date: 9/10/2015
Calculation is approved for use: Project Engineer Name and Signature: SHIH Yueh-Kan Digitally signed by SHIH Yueh-Kan DN: o=AREVA GROUP, 2.5.4.45=5A3923106548495977FE3, cn=SHIH Yueh-Kan Date: 2015.09.10 16:20:11 -04'00'	9/10/2015 Date:

REVISION SUMMARY

Rev.	Description	Affected Pages	Affected Disks
0	Initial issue	All	All
1	Excel Energy comments incorporated.	1-11, 13 and 14	None
2	Correct editorial error on Table 4 and Table 6. The nodal force reported should be "lbs" instead of "kips". Add clarification about nodal force and force/in in Table 4 through Table 7 per DCR 11042-020, Rev. 0.	1,2, 13 and 14	None
3	Revised such that this calculation only evaluates the critical flaw size in the Inner Top Cover Plate (ITCP) and increased the weld size to 0.25 inch from 3/16 inch evaluated earlier.	As indicated by the revision bars.	Files related to Outer Top Cover Plate Weld (OTCP) are removed.

TABLE OF CONTENTS

LIST OF TABLES

LIST OF FIGURES

1.0 PURPOSE

The calculation calculates the NUHOMS® 61BTH Type 1 DSC allowable flaw size for increased Inner Top Cover Plate (ITCP) closure weld size of 0.25 inch.

2.0 CONSERVATISM / ASSUMPTIONS

1. The weld allowable flaw size is based on radial tensile membrane force acting on the weld; however it is conservatively evaluated based on SRSS method excluding the compressive stresses in the weld.

2. ASME Code, Section XI, Appendix C Limit Load evaluation uses only primary stresses. Residual stress being a secondary stress are not considered.

3.0 DESIGN INPUT/DATA

Per Ref. [5.9], the distance between the weld root and crown at the canister wall ranges from 0.25 inches to 0.4 inches for ITCP lid weld. Thus, the ITCP weld size is modified to 0.25 inch in lieu of 3/16 inches per design.

3.1 Bounding Load Combinations

All bounding normal, off-normal and accident load combinations are taken from Ref. [5.2].

4.0 METHODOLOGY

4.1 Allowable Flaw Evaluation

The allowable flaw evaluation is based on flaw evaluation methodology per ASME Code, Section XI, Appendix C Ref. [5.1]. Although the affected component is not subject to in-service inspection activities, the methodology of Section XI is deemed appropriate for this application. Determination of the allowable surface and sub-surface flaw depth is accomplished by means of the methodology, outlined below. Figure 1 shows the possible circumferential flaw for ITCP Welds. It is stipulated that the allowable flaw configuration is a circumferential weld flaw exposed to the tensile component radial stress. Conservatively the weld flaw is evaluated for all the component stresses except the compressive stresses onto the weld.

Safety factors used to determine the allowable flaw size are taken from Appendix C, Section C-2621 of Ref. [5.1]. All bounding normal, off-normal and accident load combinations are taken from Ref ([5.2], Table 52).

The following are basic steps that are performed in order to determine the allowable flaw depth:

1) Identification of bounding load and load combinations analyzed in Ref. [5.2].

2) Calculate the resultant force acting on the weld ignoring the compressive load. Evaluate membrane stresses occurring at the ITCP weld.

3) Determine limiting membrane stresses in the ITCP weld for all load combinations.

4) Multiply limiting stresses with safety factors SF_m for the corresponding Service Levels (Ref. [5.1]) as presented in Table 1.

5) Since ITCP weld is GTAW (Non-Flux weld), thus according to ASME Code Sec XI, Division 1, Fig C-4210-1, Ref. [5.1] maximum allowable flaw depth is estimated using Limit Load criteria.

4.2 Limit Load Analysis

The relation between the allowable membrane stress and flaw depth at incipient stress is taken from Ref. [5.7], Table 12.28, which is given as

$$\sigma'_m = \frac{3\sigma_f(1-\alpha)^2}{\lambda + \sqrt{\lambda^2 + 9(1-\alpha)^2}} \quad \text{.......... (1)}$$

where:

σ'_m = The allowable membrane stress, which is the applied membrane stress times the different service factors, SF_m determined from Appendix C, Section C-2621 of Ref. [5.1].

σ_f = the flow stress, defined as $\sigma_f = (S_y + S_u)/2$, where S_y and S_u are yield and ultimate strengths, respectively.

$\alpha = \frac{ac}{tW}$ and $\lambda = \frac{\sigma_b}{\sigma_m} = 0$, for no bending stress on the weld.

a = half crack length for center cracked plate,
= crack depth for single edge cracked plate

t = half plate thickness for center cracked plate,
= plate thickness for single edge cracked plate

for a 360° circumferential flaw, $c = w$, hence equation (1) reduces to

$$\sigma'_m = \sigma_f\left(1 - \frac{a}{t}\right) \quad \text{.......... (2)}$$

Using equation (2) the allowable flaw depth (a) is obtained as

$$a = \left(\sigma_f - \sigma'_m \cdot SF_m\right)\frac{t}{\sigma_f} \quad \text{.......... (3)}$$

Equation (3) can be applied for both surface and subsurface crack (center-cracked plate and single edge crack plate model), respectively.

5.0 REFERENCES

5.1 ASME Boiler and Pressure Vessel Code, Section XI, Division 1, Appendix C, 2004 edition through 2006 Addenda.
5.2 TN Calculation NUH61BTH-0200, Rev.0, "NUHOMS®-61BTH Type 1 Dry Shielded Canister Shell Assembly Structural Analysis".
5.3 ANSYS Computer Code and User's Manual, Release 14 (used only for post processing results).
5.4 ISG-15, Rev. 0, "Materials Evaluation".
5.5 ASME Boiler and Pressure Vessel Code, Division 1, Subsection NG, 1998 edition through 2000 Addenda.
5.6 TN Calculation No. NUH61BTH-0403, Rev. 2, "NUHOMS®-61BTH DSC Thermal Evaluation for Storage and Transfer Conditions".
5.7 T.L. Anderson, "Fracture Mechanics, Fundamentals and Applications", Second Edition.
5.8 TN Engineering Evaluation No. 11042-EE-001, "Monticello Nuclear Generating Plant: Engineering Evaluation of Spent Fuel Storage Canisters with Nonconforming Closure Welds".
5.9 Design Input Document DI-11042-02 Rev.0, AREVA Document Number 180-9236022-000, NDE Services Final Report, Monticello, DSC-16, Phased Array UT Examination Results of the Inner and Outer Top Cover Lid Welds.

6.0 NOMENCLATURE

ITCP: Inner Top Cover Plate
DSC: Dry Shielded Canister
DW_H: Horizontal Dead Weight
PI : Internal Pressure
F_{weld} : Resultant weld load (excluding compressive load)
R : Radius of the ITCP weld
T_{weld} : Weld size
Weld Stress: The weld stress for the ITCP.
σ'_m : Weld membrane stress at limit load for ITCP.
SRSS: Square root of sum of squares.

7.0 COMPUTATIONS

7.1 Allowable Flaw Size Evaluation

7.1.1 Weld Post-Processing and Stress Calculation

All the controlling load combinations for ITCP weld are listed in Ref. [5.2, Table 54]. It is evident from these results that the critical cases are 75g side drop and 25g corner drop load cases.

Weld nodal forces for ITCP weld nodes are post-processed using ANSYS. The compressive radial forces on the welds would have no impact on the allowable weld flaw evaulation. Thus, these forces are excluded from the weld flaw evaluation.

The weld membrane stress (σ'_m) at limit load for ITCP is calculated using SRSS method, for a 0.25 inch ITCP weld, while excluding the compressive loads onto the weld. Weld membrane stress for individual load cases and the bounding load combinations are listed in Table 2 and Table 3 respectively for ITCP.

The top cover plate welds are evaluated assuming the shear load on the top cover plate welds due to a 25g corner drop. The outer top cover plate of the DSC is assumed to be unsupported by the cask in the axial direction. ITCP welds resist the load such that the stress can be calculated based on the total weld area of both ITPC and OTCP welds. The allowable is based on a maximum temperature of not more than 300°F for any transfer condition (Ref. [5.6]).

For the corner drop the total shear load on the welds is 9,437 lb/in (Ref. [5.2], Section 10.2). The load shared by the ITCP weld (1/4") and OTCP weld (0.50") are calculated below.

$$P_{ITCP} = \left(\frac{1/4}{(1/4+0.50)}\right)\times 9{,}437 = 3{,}146\ lb/in$$

These shear loads are used in calculating the load combinations for the 25g corner drop. Weld membrane stress (σ'_m) for individual load cases are calculated for ITCP.

7.1.2 Determination of Allowable Weld Flaw Size

Table 3 lists the bounding load combinations to specify limiting depth of weld flaw for ITCP weld. The yield strength (σ_y) and ultimate tensile strength (σ_u) for SA-240 Type 304 at 300 °F are 22.4 ksi and 66.2 ksi (Ref. [5.2]). So flow stress (σ_f) as per Section 4.3 is

$$\sigma_f = (22.4+66.2)/2 = 44.3 \text{ ksi}$$

The allowable flaw depths, calculated by means of the methodology described in Section 4.0.

Note that in the case of subsurface flaws, the 't' and 'a' in equation (1) are half-width and half-crack depth, respectively, whereas for surface flaws 't' and 'a' respectively represent the weld thickness and the crack depth.

ITCP Allowable Weld Flaw

The weld membrane stress (σ'_m) are listed in Table 3. The bounding weld membrane stress is 17.08 ksi. The allowable flaw size for a 360° weld flaw is calculated below.

$$a = \left(\sigma_f - \sigma'_m \cdot SF_m\right)\frac{t}{\sigma_f}$$

= (44.3 – 17.08) 0.25 / 44.3 = 0.15" (Using a single edge cracked plate model)

For center crack plate model (used for a subsurface flaw), the half-crack length a, is 0.15/2 =0.075". The total allowable crack length is 2*a = 0.15".

8.0 RESULTS

The ITPC closure welds for individual and combination load cases are listed in Table 2 and Table 3 respectively. The allowable flaw for surface (crack depth =a) and subsurface (half-crack length =a, total crack length =2a) flaws for ITCP is 0.15 inch and 360° along the circumference.

9.0 CONCLUSIONS

The evaluations performed in this calculation indicate that the minimum allowable flaw size for the ITCP is 0.15" for a full 360° weld flaw.

10.0 LISTING OF FILES

Below is the listing of all files used in the ANSYS for Finite Element Analysis. All the nodal forces have been extracted using ANSYS Release 14.0.3 Ref. [5.3].

Load Case No.	File Name	Date Time	Description
4	QT61BIP.db and .rst	12/09/1999 12:40a	20 psi internal pressure evaluation, Ref. [5.2, Table 22]. These files are not part of the archived files.
4	T61BSD.db and .rst	05/27/2000 2:40a	75g side drop acceleration, Ref. [5.2, Table 22]. These files are not part of the archived files.
1	Weld_forces_QT61BIP, inp and .out, W9PFQK~L.err, QT61BIP_weld_20psi_ITCP.txt	05/22/2014 14:14:34	Post processing files for 20psi internal pressure.
1	Weld_forces_T61BSD, inp and .out, WT35B3~E.err, T61BSD_weld_ITCP.txt	05/22/2014 14:09:35	Post processing files for 75g side drop.

Note: For the above listed files, date is reported by the OS on the report issue date and time, these values may be changed by windows depending on time of the year (e.g., daylight savings time) and time zones

Table 1 Safety Factors for Circumferential Flaw (Ref. [5.1])

Service Level	Circumferential Flaws Membrane Stress SF_m
A	2.7
B	2.4
C	1.8
D	1.3

Table 2 Weld Stress Results of Inner Top Cover Plate Welds for Individual Loads

Load Step	Description	Load Case	F'_m Nodal Force (lbs)[1]	F'_m Force [2] (lbs/in)	σ'_m [3] (ksi)
4	20 psi internal pressure on inner pressure boundary	PI(20)	277	139	0.56
4	75g side drop acceleration	Side Drop	5495	2761	11.05

Notes

(1) The .db and .rst files are taken from Ref. [5.2] and are listed in Section 9.0.
(2) The element size of ANSYS elements is 1.99 inch Ref. [5.2]. Hence, the F'_m Force = F'_m Nodal force /1.99
(3) The weld throat size is ¼ in., hence the σ'_m = F'_m Force /(1/4)

Table 3 Load Combination Weld Membrane Stress (σ'_m) Result for Inner Top Cover Plate Weld

Load Case	Service Level	Stress Category	Loads	σ'_m (ksi)	Safety Factor SFm	σ'_m (ksi) x SFm
TR-9	D	P	PI(20) + 25g Corner Drop [1]	13.14	1.3	17.08
TR-10	D	P	PI(20) + 75g Side Drop	11.61	1.3	15.09

Notes

(1) The corner drop load combination is calculated by adding 3,146 lbs/in of shear load to the individual loads for PI(20) load case obtained from Ref. [5.2].

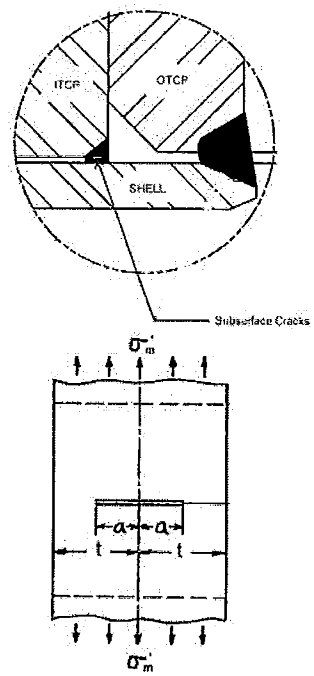

Figure 1 Subsurface Crack Model for ITCP Welds

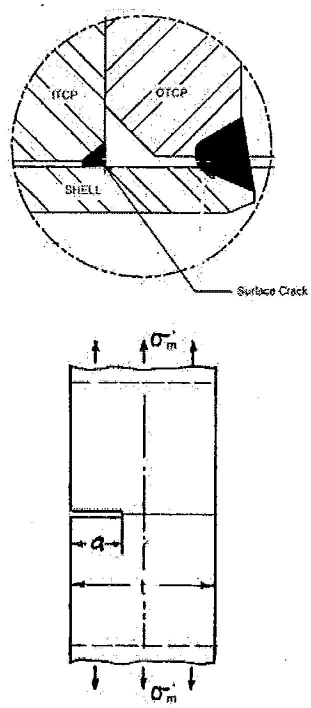

Figure 2 Surface Crack Model for ITCP Welds

ENCLOSURE 5

AREVA CALCULATION 11042-0205, REVISION 3

61BTH ITCP AND OTCP CLOSURE WELD FLAW EVALUATION

90 pages follow

CONTROLLED COPY E-203

AREVA	Form 3.2-1 Calculation Cover Sheet TIP 3.2 (Revision 10)	**Calculation No.**	11042-0205
		Revision No.	3
		Page 1 of 90	
DCR NO (if applicable): 11042-025 Revision 0	**PROJECT NAME:**	NUHOMS® 61BTH Type 1 DSCs for Monticello Nuclear Generating Plant	
PROJECT NO: 11042	**CLIENT:**	Xcel Energy	

CALCULATION TITLE:
61BTH ITCP and OTCP Closure Weld Flaw Evaluation

SUMMARY DESCRIPTION:

1) Calculation Summary

This calculation qualifies Monticello DSC-16, a 61BTH Type 1 DSC, for all design basis loads in consideration of observed flaws in the Inner Top Cover Plate (ITCP) and Outer Top Cover Plate (OTCP) closure welds.

2) Storage Media Location

- Coldstor - /areva_tn/11042/11042-0205-000
- Coldstor - /areva_tn/11042/11042-0205-002

If original issue, is licensing review per TIP 3.5 required? N/A
Yes ☐ **No** ☐ **(explain below)** **Licensing Review No.:**

Software utilized (subject to test requirements of TIP 3.3): ANSYS	Software Version: 14.0	**Software Log Revision** R-31

Calculation is complete Originator Name and Signature: Jeff Pieper	**Date:** 3/10/16
Calculation has been checked for consistency, completeness, and correctness Checker Name and Signature: Gabriel Lomas	**Date:** 3/10/16
Calculation is approved for use Project Engineer Name and Signature: HAROON Raheel 2016.03.21 17:41:22 -04'00'	**Date:** 3/21/16

REVISION SUMMARY

Rev.	Description	Affected Pages	Affected Data
0	Initial Issue	All	All
1	Revised per DCR 11042-022 Revision 0. Made editorial clarifications, updated information from revised Reference calculations, removed extraneous sensitivity analyses.	1-10, 13, 14, 17, 18, 21, 22, 24-34, 36, 45, 46, 48-50, 59-77	Removed extraneous data.
2	Revised per DCR 11042-023 Revision 0. Added elastic-plastic analyses in Appendix A. Additional discussion and clarifications added throughout.	1-4, 6-10, 13-17, 19-22, 24, 27-29, 31, 33-35, 44, 60, 62-63, 68-78, Appendix A (79-87)	Added files in Appendix A
3	Revised per DCR 11042-025 Revision 0 to address RAI-2-1. Clarified limit load vs elastic plastic results. Added Table 7. Added additional results plots in Appendix A.	1-7, 13, 15, 21, 22, 29, 35, 36, 45, 46, 81, 82, 90	None

TABLE OF CONTENTS

LIST OF TABLES

Page

LIST OF FIGURES

1.0 PURPOSE

The purpose of this calculation is to evaluate DSC-16 at the Monticello Nuclear Generating Plant (MNGP) per ASME Section III criteria in consideration of flaws observed in the Inner and Outer Top Cover Plate (ITCP and OTCP) closure welds. The flaws are documented in the Reference 5.1 Phased Array Ultrasonic Testing (PAUT) inspection report. The canister is a 61BTH Type 1 design. The ASME Section III Subsection NB Code limits on primary stress are evaluated using the limit load analysis criteria prescribed in the Code [Ref. 5.7]. Additional elastic-plastic analyses are performed to document the actual predicted strains in the welds and to demonstrate adequate margin against plastic collapse.

The body of this calculation is predominately concerned with the limit load analyses, including several finite element model mesh sensitivity analyses. The limit load analyses demonstrate satisfaction of the ASME NB limits on primary stress.

The elastic-plastic analyses are performed in Appendix A and the results are summarized in Section 7.0 and Table 7. The elastic plastic analyses demonstrate adequate margin against the material ductility limits and against plastic collapse.

2.0 ASSUMPTIONS

1. The ITCP weld to the siphon and vent block and the welds of the siphon and vent port cover plates are inaccessible for PAUT inspection. Approximately 11" are obscured due to the location of the siphon and vent block. Whereas the main circumferential lid-to-shell welds are made with an automated welding machine, some manual welding was performed around the siphon/vent block and ports. As discussed in Section 3.4, a strength reduction factor of 0.8 is considered for both the ITCP and OTCP welds. This factor accounts for the siphon and vent block welds and uncertainties in the UT technique.

   Note that the bounding flaws evaluated in this analysis are treated as full circumferential flaws. In other words, it is not assumed that the siphon and vent block is free of flaws, but rather contains the same bounding flaws as the examined welds. The geometry of the siphon and vent block is not assumed in this analysis. It is assumed that the stresses in the circular configuration bound the stresses that would be computed for a configuration that explicitly includes the siphon and vent block.

2. The longitudinal seams in the canister shell caused attenuation in the PAUT energy beam at locations 24.3" to 24.8" and 129.5" to 130" [Ref. 5.1] that can potentially diminish the effectiveness of the examination in these half inch areas. These regions are considered limited examination zones. It is assumed that the flaws observed outside of these regions are representative, and that no larger or more bounding flaws exist in the regions behind the canister seam welds. The use of the 0.8 weld strength reduction factor discussed above in Assumption 1 accounts for any uncertainty in this region.

3. [Not used]

4. The flaws are considered to be planar cracks lying on circumferential planes, parallel with the longitudinal axis of the cask. (I.e. the crack tips are pointed in the axial directions of the cask). This is a conservative flaw orientation since the welds primarily resist normal stresses in the plane of the lids due to plate bending caused by DSC internal pressure. Also, during the side drop loading, normal stresses in the plane of the lids resist the ovalizing mode of shell deformation.

   This flaw orientation is also conservative for through-thickness shear stresses in the lid welds since it maximizes the reduction in available shear area. (A flaw of equal length, but placed at an angle, would result in less reduction of the weld throat thickness).

5. Many of the flaws identified in the Reference 5.1 PAUT examination report lie in very similar locations within the weld cross section. As discussed in detail in Section 3.2, flaws that lie in similar radial and axial positions within the weld are considered bounded by a representative "group flaw." The locations and sizes of the "group flaws" are chosen conservatively to ensure they are bounding of the individual flaws.

6. The analysis is based on the nominal dimensions of the components as shown in the design drawings [References 5.3 and 5.4] including the as-fabricated radial gap between the outer diameter of the lids and the inner diameter of the DSC shell. Although weld shrinkage will close this gap during closure operations, the resulting compressive load path between the lids and shell is conservatively ignored. Further discussion is provided in Section 4.3.

3.0 DESIGN INPUT/DATA

3.1 DSC Geometry

The 61BTH Type 1 DSC geometry is detailed in the Reference 5.3 and 5.4 drawings. The Reference 5.5 drawing shows the details for the final ITCP and OTCP closure field welds. Sketches from Reference 5.1 and details from References 5.3 and 5.4 are shown in Figure 1 through Figure 4.

The material for all structural components (DSC Shell, OTCP, and ITCP) is SA-240 Type 304 stainless steel.

The shield plug material is SA-36 carbon steel.

The DSC shell is 0.5" nominal thickness.

The ITCP is 0.75" nominal thickness. Per the Reference 5.5 drawing, it is welded to the DSC shell and vent/siphon block with a 3/16" groove weld. However, the ITCP lid groove (weld prep) is 0.25" minimum, and it was confirmed that the weld is also 0.25" [Ref. 5.1].

The OTCP is 1.25" nominal thickness. It is welded to the DSC shell with a 1/2" groove weld.

The ITCP and OTCP closure welds (with the exception of the ITCP welds around the vent/siphon block and the welds of the vent and siphon port cover plates) are made using the GTAW process with an automated welder. This is a non-flux type of weld. The vent/siphon block and the vent and siphon port cover plate welds are performed manually, also using a non-flux process.

3.2 Flaw Details and Geometry

Various sets of bounding flaws are chosen for the detailed analyses based on the flaw dimensions in Reference 5.1 and the discussion below. Note that flaws are identified in this calculation using the numerical flaw listings in the Reference 5.1 inspection report.

3.2.1 Outer Top Cover Plate

3.2.1.1 Case 1

Figure 5 shows all of the OTCP weld flaws from Reference 5.1 plotted on an outline of the DSC geometry. Figure 6 shows a similar plot but with the main cluster of flaws bounded by a box, and showing a representative “group flaw” for this region. The longest flaw within the group region is 31.7” long and the tallest flaw is 0.14” high. Therefore, the bounding flaw for this region is taken as a full circumferential flaw, 0.14” in height.

Note that all flaws in the group region were reviewed to ensure that no two flaws in close circumferential proximity, considered as being joined, would produce a taller flaw. For example, OTCP Flaw #9 and OTCP Flaw #10 are within 0.17” of each other in the circumferential direction, but their combined height is only 0.47-0.38=0.09”. Therefore these flaws, considered combined, are bounded by the 0.14” high group flaw.

The radial and axial positions of the bounding flaw were chosen to be at the center of the group region. This radial position is within the critical failure plane of the weld (i.e. a plane containing the minimum weld throat thickness of 0.5”).

Figure 6 also shows additional information about the flaws outside of the group region. OTCP Flaw #2 is intermittent around the entire circumference of the DSC. Therefore this flaw, at 0.12” in height, is considered a full circumferential flaw. Since OTCP Flaw #14 is in close proximity to Flaw #2, it is conservatively considered joined to OTCP Flaw #2, and the combined flaw height is considered to be present around the entire circumference. The combined flaw height is determined based on the geometry to be 0.195”.

As seen in Figure 6, OTCP Flaw #20 is remote from the group region and from OTCP Flaw #s 2 and 14. OTCP Flaw #20 is only 0.32” in length, and only 0.07” in height. This flaw is separated from OTCP Flaw #19 by 0.36” in the circumferential direction and by 0.19” in the axial direction. It is separated from OTCP Flaw #21 by 1.66” in the circumferential direction and by 0.23” in the axial direction. Since extension of the flaws under the postulated loading is negligible (since only one cycle of the critical loads is applied) this flaw will not join with the adjacent flaws. Additionally, since OTCP Flaw #20 is much smaller than the critical surface flaw size of 0.29” from Reference 5.17, it is not considered explicitly in the FEA analyses and is considered bounded by the other modeled flaws which are very conservative.

Similarly, OTCP Flaw #3 is remote from all flaws with the exception of OTCP Flaw #2. However, OTCP Flaw #3 is very small, only 0.18” long and 0.09” tall. Inspection of the PAUT plots (see Page 22 of Reference 5.1) also shows that OTCP Flaw #2, which is considered as fully continuous in this analysis, is actually very intermittent at the circumferential position of OTCP Flaw #3. Furthermore, OTCP Flaw #3 is much smaller than the critical subsurface flaw size of 0.29” from Reference 5.17. Therefore, it is not considered explicitly in the FEA analyses and is considered bounded by the other modeled flaws which are very conservative.

Figure 7 shows the first bounding flaw set considered for the OTCP in the ANSYS collapse analyses.

3.2.1.2 Case 2

The discussion above and the flaw locations shown in Figure 5 through Figure 7 are based primarily on the tabulated flaw data from Reference 5.1. Since OTCP Flaw #2 is intermittent around the circumference of the weld, a closer inspection of the PAUT scan images is performed, and an additional flaw set for the OTCP is created. In this additional case, the location of OTCP Flaw #2 is based on the PAUT scan image of the flaw at the circumferential position of OTCP Flaw #14, which is the only additional flaw that could be considered to interact with OTCP Flaw #2. Based on the PAUT scan images, the flaws are located as seen in Figure 8. In this case the height of both Flaw #2 and Flaw #7 are estimated based on the PAUT scan images and are conservatively larger than the flaw heights tabulated in Reference 5.1.

3.2.2 Inner Top Cover Plate

Figure 9 shows all of the ITCP weld flaws from Reference 5.1 plotted on an outline of the DSC geometry. All but two of the flaws are clustered in the region of the weld root at the inner surface of the DSC shell. Figure 10 shows the bounding flaw set considered for the ITCP in the ANSYS collapse analyses. Both the representative group flaw and ITCP Flaw #7 are considered to be full circumferential flaws. ITCP Flaw #11 is remote from all other flaws (in the circumferential direction) and is therefore considered bounded by the representative group flaw. The representative group flaw for the ITCP is conservatively placed at the tension side of the weld when resisting internal pressure.

All of the ITCP flaws documented in Reference 5.1 were reviewed to ensure that no two (or more) flaws, which are in close proximity to each other, could be considered as combined and therefore creating a more critical flaw. The following cases are considered in particular:

- ITCP Flaw #2 and Flaw #3 are within 0.12” from each other in the circumferential position, but their maximum combined height (1.58-1.49 = 0.09”) is bounded by the group flaw height of 0.09”.
- ITCP Flaw #5 and Flaw #8 partially overlaps with Flaw #6 in the circumferential direction and would have a combined height of 0.15”. However, Flaw #5 (0.15” in length) and Flaw #8 (0.14” in length) are extremely small. Due to their overlap in the circumferential direction, their combined length would be only 0.16”, and therefore would not affect the global or local stability of the weld. This very short region with a potential 0.15” high flaw is bounded by the full-circumferential representation of the modeled flaws.
- ITCP Flaw #10 is within 0.04” of Flaw #12 in the circumferential direction. The individual flaws are 0.05” tall and 0.04” tall, respectively, and 0.49” long and 0.18” long, respectively. They are also separated in the axial direction by 0.09”. Postulating a flaw from the bottom of Flaw #12 to the top of Flaw #10 would imply a height of 0.18”. However, the combined-height region would be over a very short length and would not affect the global or local stability of the weld. Therefore this postulated combined flaw is considered bounded by the full-circumferential representation of the modeled flaws.

It is noted that based on Figure 9 and Figure 10, ITCP Flaw #7 appears to be in the base metal of the inner top cover plate. It is likely that the flaw is actually at the fusion / heat affected region between the weld metal and the base metal. The ANSYS models used in this calculation place the flaw at 0.81” inward from the outer surface of the DSC shell whereas the tabulated data in Reference 5.1 places the flaw at 0.80” from the outer surface. The 0.01” discrepancy is considered negligible. The exact location of the flaw is not considered critical in light of the significant margin that is available (See Section 7.0) and the generally very conservative idealization of the flaws (i.e. full circumferential).

3.3 Material Properties

The material properties for the DSC structure are taken from Reference 5.11. The properties of the two materials of construction, SA-240 Type 304 stainless steel and SA-36 carbon steel, are provided in Table 4 and Table 5, respectively. The weld metal is considered to be composed of the same properties as the base metal, as the welds are made with the non-flux GTAW method [Reference 5.14] using bare metal ER308 (stainless) filler material. The tensile strength of the ER308 electrode (80 ksi at room temperature [Ref. 5.15]) is slightly greater than the type 304 base metal (75 ksi at room temperature [Ref. 5.16]). The yield stress value of the weld metal is assumed to be equal to or greater than the base metal. Therefore, the treatment of the weld metal as being identical to the base metal is appropriate for the Section III limit load analyses and the elastic-plastic analyses performed in this calculation.

Temperatures used for material properties are discussed in Section 4.2 and are shown in Table 3.

Poisson's ratio for all modeled parts is taken as 0.29.

Weight density for SA-240 Type 304 is taken as 0.285 lb/in^3.

Weight density for SA-36 is taken as 0.284 lb/in^3.

3.4 Design Criteria

All of the applicable design basis loading conditions are considered in accordance with the requirements of ASME Section III Subsection NB [Ref. 5.7]. Section 4.1 details the methods used to perform the code [Ref. 5.7] qualifications. Section 4.2 details the selection of the bounding load cases.

The mockup used in the PAUT process development contained weld manufacturing flaws intentionally distributed in locations that would be expected with the weld process used for the DSC lid closure welds. Approximately 30% of those flaws were placed at the weld root and 27% were placed near the weld toe to demonstrate that they could be reliably detected in the presence of typical geometric responses from those regions. The flaws include incomplete root penetration, lack of fusion, and tungsten inclusions. AREVA document 54-PQ-114-001 [Ref. 5.19], Section 8.0, provides images of the UT responses for these flaws and demonstrates that the PAUT process can effectively detect these flaws. Furthermore, the qualification performed on the blind mockup provides objective evidence that detection of flaws in these regions of the weld is not a problem. The blind mockup used for qualification contained a similar percentage/number and distribution of flaws as the development mockup. Although the flaw information for the blind mockup cannot be disclosed in order to preserve the security of the mockup for future qualifications, EPRI and NRC personnel present at the demonstration have reviewed that information. In addition, uncertainties in the PAUT examination are accounted for by using a 0.8 reduction factor on the limit load and a 0.8 reduction factor on the material ductility for the elastic-plastic analyses. This factor, which is in agreement with ISG-15 [Ref. 5.20], conservatively accounts for any additional limitations in the efficacy of the PAUT examinations and also accounts for the inaccessible area around the vent and siphon block as well as the geometric reflectors at the root and near the toe of the weld.

4.0 METHODOLOGY

4.1 Analysis Method and Acceptance Criteria

The 61BTH DSC including the ITCP and OTCP welds are designed and analyzed per ASME Section III Subsection NB (the Code) [Ref. 5.7] in the Reference 5.2 calculation. The presence of the ITCP and OTCP weld flaws will cause high local stresses and complex stress fields that will render an elastic analysis (such as those performed in Reference 5.2) very difficult. Therefore, the flaws are explicitly included in the finite element models as "design features", and the applicable ASME code [Ref. 5.7] stress limits are evaluated as described below.

Primary Stress Limits

In order to satisfy the primary stress limits of Reference 5.7 paragraphs NB-3221.1, NB-3221.2, and NB-3221.3, a Limit Analysis will be performed per Paragraph NB-3228.1. The acceptance criterion is that the specified loadings not exceed two-thirds of the lower bound collapse load, as determined using an ideally plastic (non-strain hardening) material model, with the yield stress set at a value of 1.5*S_m. This criterion is used for evaluation of the Service Level A and B load cases discussed in Section 4.2.

Note that Service Level C acceptance criteria are generally 20% greater than Service Level A criteria, per Paragraph NB-3224 of Reference 5.7. This information is used in the discussion in Section 4.2 to eliminate some non-critical load cases.

For the Service Level D loadings (accident level internal pressure and side drop), the rules of ASME Section III Appendix F Paragraph F-1341.3 [Ref. 5.9] are used, which indicate that the loads "shall not exceed 90% of the limit analysis collapse load using a yield stress which is the lesser of 2.3S_m and 0.7S_u." This criterion is used for evaluation of the Service Level D load cases discussed in Section 4.2.

An additional increase factor of 1/0.8=1.25 is applied to the required limit load collapse pressure in order to account for the weld strength reduction factor of 0.8 to account for UT sensitivity and inaccessible weld regions discussed in Section 3.4. Typically, the weld strength reduction factor is applied to the weld allowable stress during qualification. In the case of limit-load analysis, reduction of the material yield stress is applicable. The reduction in yield stress would have a direct, 1:1 correlation to the calculated lower bound collapse pressure due to the perfectly-plastic (i.e. non-strain hardening) material model. In this analysis, rather than decrease the material yield stress the required calculated collapse pressure is increased by the factor of 1.25.

Note that the Service Level D criterion is essentially 2.1 times greater than the Service Level A/B criterion, as calculated below. This information is used in the discussion in Section 4.2 to eliminate some non-critical load cases.

> At a temperature of 500 ºF, the limit load yield stress for SA-240 Type 304 for Service Levels A/B and D are 26.3 ksi and 40.3 ksi, respectively.
>
> The code [Ref. 5.7] required factors against the lower bound collapse load as determined by the limit load analyses for Service Levels A/B and D are 1.5 and 1.11, respectively.
>
> The ratio of the acceptance criteria is therefore: $\frac{(40.3\times1.5)}{(26.3*1.1)} = 2.1$.
> (i.e. the Service level A/B criteria are 2.1 times as severe)

Limit Load Analysis Background

ASME Section III Subsection NB provides only a basic description of the Limit Load analysis technique. A more thorough description is provided in ASME Section VIII Division 2 Paragraph 5.2.3 [Ref. 5.18]:

> *Limit-load analysis addresses the failure modes of ductile rupture and the onset of gross plastic deformation (plastic collapse)…*
>
> *Limit-Load analysis provides an alternative to elastic analysis and stress linearization and the satisfaction of primary stress limits...*
>
> *Displacements and strains indicated by a limit analysis have no physical meaning.*
>
> *Limit load analysis is based on the theory of limit analysis that defines a lower bound to the limit load of a structure as the solution of a numerical model with the following properties:*
>
> 1. *The material model is elastic-perfectly plastic with a specified yield strength.*
>
> 2. *The strain-displacement relations are those of small displacement theory.*
>
> *The limit load is the load that causes overall structural instability. This point is indicated by the inability to achieve an equilibrium solution for a small increase in load (i.e. the solution will not converge).*

Separately, in order to address questions on the potential for material rupture due to potentially high plastic strains, supplemental elastic-plastic analyses are performed in Section 10.0 (Appendix A).

Material Ductility Limits

In order to show adequate margin against material failure at regions of high localized plastic strain, elastic-plastic analyses are performed in Appendix A. The peak strain values are compared against the material minimum specified elongation limit reduced by the weld uncertainty factor of 0.8 discussed in Section 3.4.

Primary Plus Secondary Stress Limits

The Code [Ref. 5.7] also prescribes limits on primary plus secondary stresses for Service Levels A and B [Ref. 5.7 Paragraph NB-3222.2]. Secondary stresses may be developed in the DSC due to differential thermal expansion of the interconnected parts and thermal gradients within the structure. The code stress limit for primary plus secondary stress (calculated on an elastic basis) is $3S_m$. However, as shown in Ref. 5.7 Figure NB-3222-1, rules for exceeding the $3S_m$ limit are provided in Paragraph NB-3228.5, which states that "the $3S_m$ limit … may be exceeded provided that the requirements of (a) through (f) below are met."

Requirement (a) states that "the range of primary plus secondary membrane plus bending stress intensity, excluding thermal bending stresses, shall be ≤ $3S_m$." This provision is related to the potential for "plastic strain concentrations" occurring in "localized areas of the structure", and the potential for these concentrations to affect the "fatigue behavior, ratcheting behavior, or buckling behavior of the structure" [Ref. 5.7 Paragraph NB-3228.1]. Requirements (b) through (d) are also limitations related to fatigue and thermal stress ratchet. As detailed in Section 10.5 of Reference 5.2, the DSC is exempt from fatigue analysis requirements since all of the criteria in NB-3222.4 of Reference 5.7 are satisfied. Similarly, since the DSC thermal loads are not cyclic in nature (other than small daily and seasonal fluctuations), thermal stress ratchet is not a concern. Therefore, the $3S_m$ limit as it relates to fatigue is not applicable.

Requirement (e) requires that the component temperature be less than 800 ºF for austenitic stainless steel. The maximum DSC shell temperature (entire shell including the lid region) is 611 ºF (See Table 3). Therefore this requirement is satisfied.

Requirement (f) states that the material must have a specified yield stress to ultimate stress ratio of less than 0.8. For the 61BTH DSC which used SA-240 Type 304 steel, the ratio is 30/75 = 0.4. Therefore this requirement is satisfied.

Based on the discussion above (primarily the fact that cyclic conditions are not a design factor for the DSC), there is no need to consider limits on primary plus secondary stresses. Therefore, thermal stresses are not included in this analysis.

Special Stress Limits

In addition to the primary and primary plus secondary stress limits the Code [Ref. 5.7] also imposes Special Stress Limits as detailed in paragraph NB-3227. The applicable special stress limits are discussed below in relation to the DSC top end cover plate welds.

Bearing Loads: There are no significant bearing loads affecting the ITCP and OTCP closure welds during Service Level A, B, or C loading. During the Service Level D side drop event, bearing stress exists at the contact surface between the DSC and Transfer Cask. However, as noted in ASME Section III Appendix F [Ref. 5.9] paragraph F-1331.3, bearing stress need only be evaluated for pinned and/or bolted joints. Therefore this special stress limit is not applicable to this evaluation.

Pure Shear: Although the ITCP and OTCP closure welds are loaded in shear by internal pressure loading, the stress state is not pure shear due to the additional bending stresses. Paragraph NB-3227.2 of Reference 5.7 clarifies that this stress limit is applicable to “for example, keys, shear rings, screw threads.” Therefore this special stress limit is not applicable to this evaluation.

Progressive Distortion of Nonintegral Connections: The ITCP and OTCP closure welds are integral and therefore not nonintegral connections. Furthermore, there are no sources of significant cyclic loading that would cause progressive distortion of the DSC. Therefore this special stress limit is not applicable to this evaluation.

Triaxial Stress: The purpose of the code [Ref. 5.7] limit on triaxial stress is to provide protection against failure due to uniform triaxial tension [Ref. 5.13 Chapter 4.5]. Internal pressure in the DSC and bending of the cover plates may cause tension in the weld in the radial and circumferential directions, but there is no source for tension in the axial direction. Therefore failure due to hydrostatic tension in the weld metal is not credible. Therefore this special stress limit is not applicable to this evaluation.

Fracture and Flaw Extension

Although linear-type flaws have been identified in the structure, the critical failure mode of the welds is plastic collapse. Under one-time loading, elastic and plastic crack extension are not a concern for the very tough type 304 stainless steel materials of the DSC shell, OTCP, and ITCP. This conclusion is supported by ASME Section XI Article C-4000 “Determination of Failure Model” [Ref. 5.10] which states that for austenitic wrought material and non-flux welds, “plastic collapse is the controlling failure mode.” Note that the 61BTH Type 1 DSC OTCP and ITCP closure welds are made with the GTAW method [Reference 5.14] which is a non-flux type of weld.

Additionally, there is no source for fatigue flaw extension. The only cyclic loads on the DSC are minor daily and seasonal temperature fluctuations. Therefore, cyclic fatigue growth of the flaws in not a credible phenomenon.

Combined with the discussions above, the limit load analysis of the DSC top cover plates and closure welds is sufficient to satisfy all of the applicable stress criteria of the Code [Ref. 5.7].

Residual Stress

Residual stress due to welding is a secondary stress and therefore is not considered in the limit load analyses performed in this calculation, as the Section III Code [Ref. 5.7] does not require it in the limit load analysis.

4.2 Load Cases

Table 1 lists the design basis load combinations for the 61BTH DSC. This calculation is concerned with all load cases beginning with the inner top cover plate weld, identified as Load FL-6 in Table 1.

The loading conditions of interest in this evaluation are internal and external pressure and inertial loads due to handling, transfer, seismic, and accidental drop conditions.

As discussed in Section 4.1, secondary (thermal) loading is not considered.

Note that the discussions below, and the analyses performed in this calculation, are based on the conservative design values for internal pressure loading, rather than the actual calculated values of internal pressure. Table 2 summarizes the conservative design values as well as the actual calculated values.

Temperatures used for the material properties for each Service Level condition are listed in Table 3 and discussed further in the paragraphs below.

Service Level A

The bounding Service Level A load combination for the DSC top end cover plates and welds is load case TR-5 which combines the hot ambient condition with internal pressure and 1g axial inertial loading. The other directions of inertial loading are not considered critical since their effects are not directly additive to the internal pressure loading, and furthermore they are bounded by the 75g side drop load discussed further below.

The 1g axial load will cause the DSC payload weight (fuel, basket, holddown ring, shield plug) to bear against the ITCP. The total maximum payload weight is 75,811 lbs conservatively including the weights of the ITCP and OTCP [Ref. 5.2 Section 10.2]. The equivalent uniform pressure applied to the top-end components is therefore:

$$P_{fuel,1g} = \frac{75{,}811}{\frac{\pi}{4} \times (66.25in)^2} = 22.0\,psi$$

Where the inner diameter of the DSC shell is 66.25 inches.

Therefore, the bounding Service Level A case is a uniform 10 psi internal pressure (for a Type 1 DSC) plus an additional 22.0 psi acting on the shield plug in the outward axial direction of the DSC Shell. Conservatively, this analysis considers the combined 10+22=32 psi load as a uniform internal pressure in the DSC Shell. This is very conservative since the fuel pressure load which is applied to the inner surface of the shield plug would in reality be distributed to the perimeter of the ITCP as a line load by the significant stiffness of the 7-inch thick shield plug. In other words, the approach used in this calculation maximizes the bending loads on the cover plates and therefore maximizes the loading on the closure welds.

Note that the cases with external pressure loading are discussed below.

Service Level B

The bounding Service Level B load combination for the DSC top end cover plates and welds is the combination of the hot ambient condition with the off-normal internal pressure of 20 psi (LD-6). All of the other Service Level B conditions, such as ram push/pull loads, do not affect the top end components. Therefore, the bounding Service Level B case is a uniform 20 psi internal pressure. Since the pressure loading is smaller (20 psi for SL B versus 32 psi for SL A as described above), the temperature used for SL A (500 ^oF) bounds the maximum SL B temperatures (416 ^oF), and since the same limit load acceptance criterion is used for Service Levels A and B, this case is bounded by Service Level A.

Service Level C

The bounding Service Level C load combination for the DSC top end cover plates and welds is one that bounds HSM-4 and HSM-8 which combines the hot ambient condition, normal internal pressure (20 psi), and seismic loading. However, the seismic loads are bounded by the handling loads [Ref. 5.2 Section 7.8] discussed above for Service Level A. In addition, the acceptance criteria for Level C limit load analysis is greater than Service Levels A and B. Therefore, all Service Level C conditions are bounded by the Service Level A case described above.

Note that the other Service Level C cases (such as LD-7 and UL-7) are for accident condition DSC ram push/pull loads. These loads do not affect the DSC top end components. Therefore they are not applicable to this analysis.

Note that cases with external pressure loading are discussed below.

Service Level D

Three load combinations are found to be critical for Service Level D loading of the DSC top end components, namely:

- accident level internal pressure
- corner drop
- side drop

The first load combination is bounded by HSM-5 or HSM-6 which consist of 65 psi internal pressure due to HSM blocked vent thermal conditions. This load is not combined with any other load that affects the top-end components. Therefore, the first bounding Service Level D load case considered in this analysis is 65 psi internal pressure. Note that in this condition the maximum DSC shell temperature is 611 ^{o}F and 625 ^{o}F is conservatively used in this analysis (See Table 3).

The other Service Level D conditions consist of the drop events and accident-level seismic loading. The accident seismic loads are bounded by the handling loads [Ref. 5.2 Section 7.8] discussed above for Service Level A. The end-drop load is not a credible event [see footnote 12 to Table 1] but was used in the original calculation [Ref. 5.2] to bound the corner drop event. However, that analysis produced negligible load in the top cover plate welds due to the idealized boundary conditions. As a result of an RAI by the NRC, the corner drop is considered using an alternate idealization that maximizes the load in the top cover plate welds. In this case, the 25-g corner drop load has an axial component that may be considered to load the top end cover plates with the inertia of the fuel, shield plug, hold-down ring, ITCP and OTCP. This case is evaluated in Section 6.4.

The 75g side drop load TR-10 is considered a critical load case and is evaluated in detail. Note that this load case represents 75x more load than the Service Level A 1g inertial loads. As discussed in Section 4.1, the Service Level D acceptance criterion is only 2.1 times less stringent than the Service Level A/B criterion. Therefore, evaluation of the 75g side drop case using the Service Level D criterion is bounding of the Service Level A transverse inertial loading. (Also, as discussed in Section 4.3, the boundary conditions used for the 75g side drop analysis are conservative and representative of the boundary conditions encountered for the Service Level A inertial loads and seismic loading.) The 75g side drop case also includes the off-normal internal pressure of 20 psi, as shown in Table 1.

Note that the side drop event TR-10 occurs during transfer operations which result in a maximum DSC shell temperature of 500 ^{o}F as shown in Table 3. The higher Service Level D temperature of 625 ^{o}F discussed above occurs only during DSC storage in the HSM, and therefore is not combined with the side drop loading.

External Pressure Loading

External pressure is present on the DSC in load cases DD-2 (vacuum drying, Service Level A) and HSM-9/10 (flood load, Service Level C). (The load cases with hydrostatic external pressure are due to the cask annulus being filled with water while the cask and DSC are in the vertical position. In this case the pressure load varies from zero at the top of the DSC to a maximum value at the bottom of the cask. Since the external pressure near the cover plates is essentially zero, these cases are not critical and are not considered further in this calculation.)

In load case DD-2, the external pressure is 14.7 psi (full vacuum). This pressure is bounded by the Service Level B off-normal pressure (20 psi) and therefore primary stresses in the cover plates and welds are bounded by the internal pressure load cases. Stability concerns of the DSC shell are not affected by the presence of weld flaws since they are at the end of the cask, remote from the locations at which buckling would occur. Additionally, the external pressure is resisted directly by the shield plug and the shield plug support ring, rather than by the OTCP and ITCP welds. Therefore external pressure load case DD-2 is not critical and is not considered further in this analysis.

In load case HSM-9/10, the flood load is due to a 50-foot static head of water, which is equivalent to 22 psi external pressure [Ref. 5.2 Section 7.9]. This pressure is bounded by the 32 psi internal pressure considered for Service Level A discussed above. Therefore the flood load case HSM-9/10 is bounded by the other internal pressure load cases.

Summary

The bounding load cases considered for the limit load collapse analyses are therefore:

(See Table 3 for temperature references)

(See Section 4.1 for explanation of the 1.5 and 1.11 factors for Service levels A/B and D, respectively, and also for the 0.8 factor which accounts for limitations in the weld examination and inaccessible weld regions, as discussed in Section 2.0, Assumption No. 1.

Service Level A/B: 32 psi Uniform Internal Pressure, Properties at 500 ºF
(Accounts for internal pressure + inertial load of DSC contents onto Lid)
Limit load collapse pressure required to satisfy criteria: 1.5*32/0.8 = 60 psi

Service Level D-1: 65 psi Uniform Internal Pressure, Properties at 625 ºF
Limit load collapse pressure required to satisfy criteria: 1.11*65/0.8 = 90.2 psi

Service Level D-2: 75g Side Drop Acceleration plus 20 psi Uniform Internal Pressure, Properties at 500ºF.
Limit load collapse acceleration required to satisfy criteria: 1.11*75/0.8 = 104 g

For the elastic-plastic analyses performed in Appendix A, the same bounding load cases described above are performed in order to predict plastic strains for comparison to the material strain limits and to demonstrate adequate margin against collapse.

4.3 FEA Model Details

Several finite element models of the top half of the 61BTH DSC are constructed in ANSYS based on the Reference 5.3, 5.4, 5.5 drawings. The models fall into two basic categories: axisymmetric (2D) and half-symmetric (3D).

The axisymmetric models use ANSYS plane element type PLANE182, a 4-node axisymmetric plane element with non-linear capabilities. Each node has 2 degrees of freedom (translation in the X (radial) and Y (axial) directions). The default element options are used in the analysis. Sensitivity studies were performed to ensure that there were no adverse effects on the results due to the potential shear locking of the elements. (Sensitivity runs used KEYOPTION 1=3 to invoke the simplified enhanced strain formulation to relieve shear locking.) Additional discussion of the sensitivity analyses is provided in Section 6.0.

Contact between the ITCP and OTCP is simulated using nodal coupling in the Y (axial) direction. (See Section 6.1.2 for a sensitivity study using contact elements at this interface.)

No contact is defined between the opposing faces of the weld flaws. In other words, whereas compressive loading normal to the plane of the flaw may in reality be transmitted via compression through the crack face surfaces, this load path is ignored. This is conservative, and considered necessary since it is difficult (or impossible) to deduce from the PAUT data what separation may exist between the two faces of the flaws.

Also, no contact is considered between the DSC shell inner diameter and the ITCP and OTCP outer diameters. As seen in Figure 4, the fabricated dimensions of the lids and shell result in small radial gaps between the outer diameter of the lids and the inner surface of the shell. During the welding process, these gaps close, but since a small remaining gap cannot be ruled out, this analysis conservatively assumes that the as-fabricated gap exists, as shown in Figure 4. Even if the lids deflect in the analysis such that the gaps would close, the resulting contact/compressive load path is conservatively neglected. This is conservative since it forces all loads in the lid to travel through the weld, rather than through compression between the lids and shell.

Figure 11 and Figure 12 show images of the axisymmetric model. Loading and boundary conditions are discussed in the following sections. These sections are focused on the limit load analyses. See Appendix A for discussion of the elastic-plastic analyses.

The 3D, half-symmetric model uses ANSYS solid element type SOLID185, an 8-node brick (or 6-node prism) element with non-linear capabilities. Each node has 3 degrees of freedom (translation in the X, Y, and Z directions). The default element options are used in the analysis. Sensitivity studies were performed to ensure that the mesh was adequate. Additional discussion of the sensitivity analyses is provided in Section 6.0.

Contact in the half-symmetry model is defined using ANSYS element types CONT173 and TARGE170. Contact is defined between the following interfaces:

- OTCP to ITCP
- ITCP to Shield Plug
- Shield Plug outer diameter to DSC Shell
- Shield Plug bottom surface to Support Ring
- Support Ring to DSC Shell

The default contact parameters are used, although the contact stiffness is reduced in some cases to aid in convergence. Due to the large contact areas and since the contact areas are generally remote from the critical stress regions, the contact stiffness is not considered a critical parameter. The default contact parameters include: [Reference 5.6]

- Penetration tolerance factor: Default value = 0.1. This parameter controls the acceptable level of penetration of the contact node into the target surface, based on the depth of the element underlying the target element.
- Pinball region scale factor: Default Value = 1.0. This parameter controls the extents of the region around each contact node that is checked for contact with target segments. The default volume is a sphere of radius 4*depth of the underlying element.
- KeyOption 2: Contact algorithm: Default = Augmented Lagrangian. The contact method is an iterative penalty method where the contact pressure is augmented during the equilibrium iterations so that the final penetration is within the acceptable tolerance.
- KeyOption 4: Location of contact detection point: Default = On Gauss Point. Other options include using the nodal points, normal to either the contact surface or the target surface. The default option is suggested for general cases.

Other features and controls of the CONTA173 elements are related to advanced features (bonded contact, cohesion, etc.) and initial penetration and gap controls which are not utilized in this analysis.

Figure 19 through Figure 21 show images of the half-symmetry model. Loading and boundary conditions are discussed in the following sections.

Table 6 shows a summary of the ANSYS models and analyses which are performed. Further details on the various ANSYS models are provided below.

4.3.1 Axisymmetric Case #1

The first case considered is a combination of OTCP Flaw Set #1 and the ITCP bounding flaw set discussed in Sections 3.2.1.1 and 3.2.2, respectively. The mesh and flaw details for this case, called Axisymmetric Case #1, are shown in Figure 13 and Figure 14.

The mesh shown in these figures was created based on a basic goal of having at least 4 elements across the thickness of the net sections of the weld, as reduced by the flaws. In order to investigate the effects of mesh density, a refined mesh was created for this case, as shown in Figure 15. Since the sensitivity model shown in Figure 15 only refined the weld region an additional model was created as shown in Figure 16 to ensure a sufficient mesh in the lid interior region.

This model, and all of the other axisymmetric models discussed below, are used for analysis of uniform internal pressure loading. The model is constrained in the radial direction at the axis of symmetry and in the axial direction at the bottom cut of the DSC shell near the mid-length of the cask (remote from the top end components of interest.) The pressure loading is applied to the internal pressure boundary (bottom surface of ITCP, surface of ITCP weld to Shell, and Shell inner surface). (See Section 6.1.2 for a sensitivity analysis where internal pressure is included on the ITCP weld root flaw internal surfaces.)

4.3.2 Axisymmetric Case #2

The second case considered is a combination of OTCP Flaw Set #2 and the ITCP bounding flaw set discussed in Sections 3.2.1.2 and 3.2.2, respectively. The mesh and flaw details for this case, called Axisymmetric Case #2, are shown in Figure 17 and Figure 18 for the refined mesh. Based on the results of the Axisymmetric Case #1 (See Section 6.1.2), the initial mesh level described above for Case #1 would be sufficient. However, since the run times remained reasonable, a refined mesh model (weld and lid interior regions) was generated and is used for Case #2.

4.3.3 Axisymmetric Case #0

In order to study the effect of the flaws, a 3rd case is considered in which the flaws are removed and the as-designed collapse load is determined. Only the refined mesh model (weld and lid interior regions) is considered. The mesh is identical to Figure 16 but the coincident nodes along the crack faces are merged.

4.3.4 Half-Symmetry (3D) Case #1

The 3D model is based on the Axisymmetric Case #1. (Analysis results showed that there was negligible difference in the results from Axisymmetric Case #1 and Case #2. The total projected cross-sectional area of the flaws in Case #1 is greater than Case #2. Therefore, Case #1 is considered critical for the side drop loading).

The same flaw pattern is modeled, but the initial mesh is slightly less refined in order to obtain reasonable run times. Mesh sensitivity studies are described below. The half-symmetry model is used for internal pressure loading (as a benchmark case to study the effects of mesh refinement) and also for side-drop loading.

The shield plug support ring is connected to the DSC shell at the two corners using nodal DOF couples to represent the fillet welds used to join the two parts.

In order to improve the numerical stability of the ANSYS model, soft springs (COMBIN14) elements are used to connect the shield plug to the support ring. The springs have a stiffness of 1 lb/in. The low stiffness combined with the very small relative deflections between these parts results in negligible internal force in the springs. The forces in the springs at the final converged solution are reviewed to confirm that the spring forces are small.

In all load cases, symmetry conditions are applied to the cut face of the model. Axial constraints are applied at the bottom cut of the DSC shell near the mid-length of the cask (remote from the top end components of interest.) For the internal pressure load case, the model was further reduced to a 90-degree model and symmetry constraints were placed on both cut faces of the model.

The purpose of this calculation is to evaluate the effects of the closure weld flaws and qualify the welds and any other components affected by the welds. All other aspects of the DSC (such as the shell remote from the welds) are not in the scope of this calculation. The modeling approach (loads and boundary conditions) for the side drop event are considered in light of this purpose and are described in the following paragraphs.

For the side drop cases, the OD of the canister shell is constrained in the vertical (drop) direction for a small sector (approximately 1.5" inches or 2.8 degrees) of assumed contact. In reality the DSC is supported inside the Transfer Cask (TC) during this event. Therefore the true boundary condition would either be a line of contact along a TC rail (which is 3" wide) or a line of contact at areas remote from the rails. As deformations increase, the area of contact would also increase. As discussed below in Section 4.4, deflections are over-estimated in a limit load analysis. Therefore, the area of contact with the TC rail or inner surface is assumed to be constant. This conservatively neglects the increase in contact area that would occur during the drop deformations. Additionally, this boundary condition is representative of the DSC storage condition inside the HSM, where the DSC rests on the 3-inch wide steel rails.

As discussed in the Reference 5.2 calculation, the DSC payload (basket and fuel) are located approximately 21.5 inches away from the ITCP and are therefore considered to have no effect on the DSC lid components. The effect of the basket and fuel loading on the DSC shell is considered in the basket design-basis calculation for side-drop loading. The basket hold-down ring is a grid-type structure that does not represent significant weight and is of sufficient strength and stiffness to be self-supporting during the side drop and not significantly affect the DSC shell and adjacent regions. Therefore, as in the Reference 5.2 calculation, the DSC payload is not considered as affecting the top-end components and the weight is applied as a pressure along a strip of elements at the impact region, beginning approximately 23" below the ITCP. Since the loads are essentially applied directly over the supported (impact) region of the DSC shell, they have no appreciable effect on the shell deformations.

Images of the Half-Symmetry model are shown in Figure 19 to Figure 21.

In order to study the adequacy of the mesh for the half-symmetry model, an internal pressure load case was performed and compared to the results of the axisymmetric case refined mesh. This study confirms the adequacy of the mesh in the cross-section of the 3D model. In order to evaluate the mesh in the circumferential direction, a model was created with a refined mesh in the regions of the model showing large plastic strains (the impact region) and locations where tensile stress is expected in the weld (at the 90-degree location where the lid resists ovalization of the DSC shell). This model is shown Figure 22.

4.3.5 Half-Symmetry (3D) Case #0

In order to study the effect of the flaws, an additional case is considered in which the flaws are removed from the model and the as-designed side drop limit load capacity is determined.

4.4 Limit Load Solution Details

As discussed in Section 4.1, this calculation is based on predicting the lower-bound collapse loads of the DSC based on limit load analysis. All materials are modeled as elastic-perfectly plastic[1], with yield stress values based on the limit load analysis requirements of the ASME code [Ref. 5.7]. Table 3 lists the temperatures used for each load case, and the values of the material properties are shown in Table 4 and Table 5.

The prescribed loads are applied to the model, and then are increased linearly until the solution fails to converge.

The analyses use small deflection theory (NLGEOM,OFF). This is conservative since deflections are unrealistically high in a limit load analysis due to the lower-bound non-strain-hardening material properties that are used. If large deflections were to be considered, the beneficial effects of OTCP and ITCP membrane action and of increased contact areas would be over-estimated, resulting in non-conservative effects. This was verified with a sensitivity study using NLGEOM,ON, which resulted in much higher collapse pressures. This confirmed that using NLGEOM,OFF is appropriate, and conservative.

In addition, Paragraph 5.2.3.1 of Reference 5.18 states that small displacement theory is to be used in a limit load analysis.

[1] "Elastic-perfectly plastic is standard mechanics of materials term that describes an idealized material that behaves in a linear-elastic manner up to the yield point, and thereafter is perfectly-plastic, i.e. non-strain hardening.

5.0 REFERENCES

5.1. AREVA Document No. 180-9236022-000. NDE Services Final Report. “Monticello, DSC-16, Phased Array UT Examination Results of the Inner and Outer Top Cover Lid Welds.” Revision 0.

5.2. AREVA (Transnuclear) Calculation No. NUH61BTH-0200 Revision 0. “NUHOMS-61BTH Type 1 Dry Shielded Canister Shell Assembly Structural Analysis.”

5.3. AREVA (Transnuclear) Drawing No. NUH61BTH-3000 Revision 8. “NUHOMS 61BTH Type 1 DSC Main Assembly.”

5.4. AREVA (Transnuclear) Drawing No. NUH61BTH-3001 Revision 4. “NUHOMS 61BTH Type 1 DSC Shell Assembly.”

5.5. AREVA (Transnuclear) Drawing No. NUH61BTH-4008 Revision 1. “NUHOMS 61BTH Type 1 & 2 Transportable Canister for BWR Fuel Field Welding.”

5.6. ANSYS Version 14.0. ANSYS Inc. (Including the ANSYS Mechanical APDL Documentation).

5.7. ASME Boiler and Pressure Vessel Code, Section III Subsection NB. 1998 Edition with Addenda through 2000.

5.8. AREVA (Transnuclear) Document Number NUH-003 Revision 14. “Updated Final Safety Analysis Report for the Standardized NUHOMS Horizontal Modular Storage System for Irradiated Nuclear Fuel.”

5.9. ASME Boiler and Pressure Vessel Code, Section III Appendices. 1998 Edition with Addenda through 2000.

5.10. ASME Boiler and Pressure Vessel Code, Section XI. Rules for Inservice Inspection of Nuclear Power Plant Components. 1998 Edition with Addenda through 2000.

5.11. AREVA (Transnuclear) Document No. NUH61BTH1-0101 Revision 2. “Design Criteria Specification for the NUHOMS-61BTH Transportable Storage Canister.”

5.12. AREVA Calculation No. 11042-0204 Revision 3. “Allowable Flaw Size Evaluation in the Inner Top Cover Plate Closure Weld for DSC #16”

5.13. Chattopadhyay, Somnath. “Pressure Vessels Design and Practice.” CRC Press. 2004.

5.14. TriVis Incorporated Welding Procedure Specification No. SS-8-M-TN Revision 10.

5.15. ASME Boiler and Pressure Vessel Code, Section II, Part C. “Specifications for Welding Rods, Electrodes, and Filler Metals.” 1998 Edition with Addenda through 2000.

5.16. ASME Boiler and Pressure Vessel Code, Section II, Part D. “Properties.” 1998 Edition with Addenda through 2000.

5.17. AREVA (Transnuclear) Calculation No. NUH61BTH-0253 Revision 0. “NUHOMS 61BTH Type 1 DSC Shell Assembly Outer Top Cover Plate Critical Flaw Size of Weld.”

5.18. ASME Boiler and Pressure Vessel Code, Section VIII Division 2. 2010.

5.19. AREVA Document No. 54-PQ-114-001 Revision 0. “Phased Array Ultrasonic Examination of Dry Storage Canister Lid Welds.”

5.20. NRC Spent Fuel Project Office Interim Staff Guidance -15. Materials Evaluation. (ISG-15). 1/10/2001.

6.0 ANALYSIS

Table 6 shows a summary of the results of all of the limit load analyses performed for this calculation and includes a comparison of the results with the acceptance criteria. Each limit load analysis case is discussed in more detail below.

6.1 Axisymmetric Analyses for Internal Pressure

6.1.1 Axisymmetric Case #1 – Initial Mesh Model

Two analyses are performed with the Axisymmetric Case #1 initial-mesh model described in Section 4.3.1: one case using the Service Level A/B material properties and one case using the Service Level D material properties. The collapse pressures were determined to be 95.9 psi for Service Level A/B and 136.6 psi for Service Level D. Figure 23 shows various plots of the plastic strain in the initial-mesh model for Service Level A/B at various locations and levels of loading. These strain plots are also representative of the behavior of the Service Level D analysis. Figure 24 shows the deflection history at the center of the lid, and indicates the expected plastic instability that occurs as the limit load is approached. Note that both the strains and displacements presented in these figures have no physical meaning and the displacement plots show only the loading (pressure) at which the solution fails to converge.

Since the initial mesh contains several element divisions at each critical cross-section, it is not expected that element shear locking (due to the default fully-integrated elements) will be significant. To confirm this, a test case was done using the Service Level A/B model but with the Simplified Enhanced Strain element formulation (KEYOP 1=3). The collapse pressure was found to be 96.1 psi, which is essentially identical to the initial results.

6.1.2 Axisymmetric Case #1 – Refined Mesh Models

Additional analyses are performed using the Service Level A/B material properties with the refined mesh models described in Section 4.3.1. Figure 25 and Figure 26 show the plastic strain results for the refined mesh at the weld region and the refined mesh at the weld and lid interior regions, respectively. The collapse pressures were found to be 94.8 psi and 93.8 psi, respectively, for these models. The OTCP deflection histories are shown in Figure 27. Note that both the strains and displacements presented in these figures have no physical meaning and the displacement plots show only the loading (pressure) at which the solution fails to converge.

Figure 28 shows a comparison of the maximum displacement history curves for the various Axisymmetric Case #1 models, done as part of the mesh sensitivity study. As seen in the figure, the results match very well. The results of the refined mesh models deviate at most (95.9-93.8)/93.8 = 2.2% from the initial mesh results. This is very close agreement particularly due to the non-linear nature of the analysis. Therefore, the initial mesh is considered sufficient. However since the analysis run times for the axisymmetric cases are reasonable even for the refined mesh model, the remaining axisymmetric cases use a refined mesh.

The Axisymmetric Case #1 with refined weld and lids for Service Level D criteria reported a collapse pressure of 132.6 psi.

Note that the nodal coupling in the axial direction between the ITCP and OTCP is a valid method to model the contact between the plates since the internal pressure loading ensures that the ITCP lid will bear against the OTCP, and since the nodes that are coupled remain coincident throughout the analysis, with only very minor differences in radial position occurring at the later load steps. In order to confirm the behavior of the nodal coupling, the Axisymmetric Case #1 model with refined welds and lids was modified to include contact between the ITCP and OTCP. The model replaces the nodal coupling with CONTA171 and TARGE169 elements, using the default element parameters. Figure 29 shows a comparison between the model using DOF couples and the model using contact elements. As seen in the figure, the results are very similar, with the DOF-couple-model showing slightly more conservative results. Therefore, the nodal coupling is acceptable and is used in all other axisymmetric models.

Note that in all of the FEA models, the internal pressure loading was not applied to the faces of the ITCP weld root flaw that is exposed to the internal region of the cask. Pressure loading on this crack face is negligible since the flaw is only 0.09” high, and in reality the ITCP flaws are generally very short (i.e. not full-circumferential flaws). In order to support this conclusion, a sensitivity analysis is performed where the pressure loading is applied to the ITCP weld root crack faces. The results, shown in Figure 30, confirm that pressure loading on the faces of this flaw are negligible.

6.1.3 Axisymmetric Case #2

Two analyses are performed with the Axisymmetric Case #2 refined-mesh model described in Section 4.3.2: one case using the Service Level A/B material properties and one case using the Service Level D material properties. The collapse pressures were determined to be 93.7 psi for Service Level A/B and 132.9 psi for Service Level D. Figure 31 shows various plots of the plastic strain for Service Level A/B at various locations and levels of loading. These strain plots are also representative of the behavior of the Service Level D analysis. Note that both the strains and displacements presented in these figures have no physical meaning and the displacement plots show only the loading (pressure) at which the solution fails to converge.

6.1.4 Axisymmetric Case #0

One analysis is performed with the Axisymmetric Case #0 refined-mesh model described in Section 4.3.3 using the Service Level A/B material properties. The collapse pressures were determined to be 94.5 psi for Service Level A/B. Figure 32 shows various plots of the plastic strain at various locations and levels of loading. Note that both the strains and displacements presented in these figures have no physical meaning and the displacement plots show only the loading (pressure) at which the solution fails to converge.

Figure 33 shows a comparison of the maximum center-of-lid displacement history for all three axisymmetric cases. As seen in the figure, there is essential no difference between Axisymmetric Case #0, Case #1 and Case #2. The Case #1 and Case #2 analyses show slightly larger deflections early in the analysis due to the slightly reduced rotational fixity of the welds. However, the final collapse pressure are within (94.5-93.7)/93.7=0.9% of each other. This supports a supposition that the observed flaws have negligible impact on the governing failure mode of the top end closure plates and welds. Again, displacements from the limit load analyses have no physical meaning, other than to show the onset of non-convergence of the FE model.

6.2 Half Symmetry Analyses for Internal Pressure (Benchmark Cases)

The model described in Section 4.3.4 is used for an internal pressure collapse analysis in order to benchmark the model against the axisymmetric cases. The collapse pressure was calculated to be approximately 97 psi. (The run was terminated at 95 psi and the final collapse pressure was estimated to avoid excessive computer run time). Figure 34 shows various plots of the plastic strain at various locations and levels of loading. A comparison of the half-symmetry case to the refined-mesh axisymmetric case is shown in Figure 35. As seen in the figure, the half-symmetry case closely matches the behavior of the refined mesh axisymmetric model although the results indicate a slightly greater collapse pressure. Therefore, the half-symmetry model is considered sufficiently accurate for this analysis. As shown by the results, and as discussed in Section 7.0, there is significant safety margin available such that further mesh refinement of the half-symmetry model is not warranted. However, the effects of circumferential mesh density for the half-symmetry model can be seen in Section 6.3.1.

6.3 Half Symmetry Analyses for Side Drop Loading

6.3.1 Half-Symmetry Case #1

The model described in Section 4.3.4 is used to perform two side-drop limit load analysis. One case includes side-drop acceleration loading only, while the second case includes the DSC off-normal internal pressure of 20 psi. For this later case, the 20 psi internal pressure is applied simultaneously with a 75g acceleration, and then both the pressure and the acceleration are increased linearly until the collapse g-load is obtained. (For example, for collapse occurring at 181g, the internal pressure at collapse is 20*181/75 = 48.3 psi.)

Note that the side drop loading is combined with the design-basis off-normal internal pressure of 20 psi, as opposed to the internal pressure value of 32 psi used for the SL A/B cases which was the sum of the 10 psi normal pressure and an additional 22 psi to account for inertial handling/seismic loads. See Section 4.2

The collapse g-load for side-drop-only loading was found to be approximately 181g. The collapse g-load when internal pressure loading was included was found to be greater than 181g. This later run terminated at 181g, but based on the collapse behavior (see Figure 41) it is expected that smaller time steps would allow the solution to continue to larger loads.

Various images of the stress and strain in the side drop analyses are shown in Figure 36 to Figure 38. Note that both the strains and displacements presented in these figures have no physical meaning and the displacement plots show only the loading (pressure) at which the solution fails to converge.

The Half-Symmetry Case #1 model with refined mesh in the circumferential direction was used to evaluate the side drop load case (without internal pressure). This analysis was performed up until a load of 185 g's, at which time the analysis was terminated manually to avoid large file sizes and excessive run time. As seen in Figure 41, this model showed a greater resistance to the side-drop loading, and would eventually result in collapse g-loads in excess of 185 g if smaller timesteps and longer run times were provided. Images of the stress and strain from this analysis are shown in Figure 39. Note that both the strains and displacements presented in these figures have no physical meaning and the displacement plots show only the loading (pressure) at which the solution fails to converge.

This analysis confirms that the mesh used in the other half-symmetry cases is adequate, and conservative.

6.3.2 Half-Symmetry Case #0

One side drop analysis is performed with the Half-Symmetry Case #0 model (no flaws) described in Section 4.3.5. Based on the results discussed above, only the case without internal pressure loading was considered. This analysis resulted in a collapse load of 189g. Stress and strain plots from this analysis are shown in Figure 40. As noted previously, these strain plots have no physical meaning. As shown in Figure 41, the collapse behavior was nearly identical to the case with weld flaws, indicating that the flaws had negligible effect on the results.

6.4 Evaluation of the 25g Corner Drop

Reference 5.2 Section 10.2 evaluated the OTCP weld to resist a 25g inertial load on the entire DSC contents and neglecting the strength of the ITCP weld. Furthermore, a conservative stress was assumed in the weld due to internal pressure. The Reference 5.2 calculation is revised below to account for the strength of both welds and include a reduction in the weld thickness due to the observed flaws. The total weld thickness is taken as the combined weld throats from the ITCP and OTCP minus the height of the flaws present in the welds. (See Reference 5.2 Section 10.2 for the basis of the following values and calculations.)

Note that the allowable weld stress noted below includes a joint efficiency factor of 0.7 as described in Reference 5.2 Section 6.2. This reduction factor conservatively bounds the reduction factor of 0.8 discussed in Section 3.4. Therefore, no further reduction factor is applied, and the calculation below is conservative.

$W_{TOT} = 75{,}811 lbs \qquad (total\ weight\ of\ fuel + basket + lids\ and\ shield\ plug)$

$W_P = 68{,}943\ lbs \qquad (load\ due\ to\ axial\ component\ of\ pressure)$

$W_{TOT25g} = 25 \times 75{,}811 + 68{,}943 = 1{,}964{,}218\ lbs$

$w_{25g} = \frac{W_{TOT25g}}{L_{weld}} = \frac{1{,}964{,}218}{208.131} = 9{,}437\,\frac{lb}{in} \qquad (length\ of\ weld\ is\ 208.131")$

$t_{weld} = \frac{3}{16} + \frac{1}{2} - (0.23 + 0.11) = 0.3475\ in\ (*\ See\ Note)$

$\tau_{25g} = \frac{w_{25g}}{t_{weld}} = \frac{9{,}437}{0.3475} = 27{,}157\ psi \qquad (weld\ shear\ stress\ due\ to\ 25g\ corner\ drop)$

$\tau_{20psi} = 4{,}120\ psi \qquad (weld\ stress\ radial\ component\ due\ to\ 20\ psi\ internal\ pressure)$

$\tau_{TOT} = \tau_{25g} + \tau_{20psi} = 27{,}157 + 4{,}120 = 31{,}277\ psi$

$\tau_{Allow} = 32{,}400\ psi$

$\frac{\tau_{TOT}}{\tau_{Allow}} = \frac{31{,}277}{32{,}400} = 0.97 \leq 1\ (OK)$

*Note: the reduction of the weld to account for the flaws is based on the maximum flaw heights in any one plane through each of the welds. This is taken as 0.23” for the OTCP weld and 0.11” for the ITCP weld.)

Therefore, the top end closure welds, with the observed flaws, are OK for the Service Level D corner drop event.

7.0 DISCUSSION AND CONCLUSIONS

This calculation qualifies the as-welded DSC-16 canister using a combination of limit load analyses and elastic-plastic analyses. The limit load analyses are used to show that the DSC satisfies the primary stress limits of ASME Section III Subsection NB. The elastic-plastic analyses are used to show that the actual predicted strain values are below the material ductility limits and that adequate design margin above and beyond the specified loading exists. Both the limit load and elastic-plastic analyses account for any remaining uncertainty in the weld (e.g. non-inspected weld regions and PAUT technique limitations) by including an uncertainty factor of 0.8 which is described in detail in Section 3.4.

Limit Load Analyses:

The lower bound collapse pressure for Service Level A/B criteria was found to be 93.7 psi which is greater than the required pressure of 1.5x32/0.8=60 psi (where 1.5 is the code-required [Ref. 5.7] factor on the 32 psi design pressure loading and 0.8 is the weld strength reduction factor- see Section 4.2). Therefore the Service Level A/B criteria is satisfied.

The lower bound collapse pressure for Service Level D criteria was found to be 132.6 psi which is greater than the required pressure of 1.11x65/0.8=90.2 psi (where 1.11 is the code-required [Ref. 5.7] factor on the 65 psi design pressure loading and 0.8 is the weld strength reduction factor - see Section 4.2). Therefore the Service Level D criteria for internal pressure is satisfied.

As noted in Section 6.1.4 and as shown in Figure 33, there is essentially no difference in the collapse pressure and extremely little difference in the overall collapse behavior of the DSC subjected to internal pressure loading with and without flaws in the weld.

The lower bound collapse acceleration for side drop (Service Level D) loading was found to be 181g which is greater than the required load of 1.11x75/0.8=104g. Therefore the Service Level D criteria for side drop loading is satisfied.

As noted in Section 6.3.2 and as shown in Figure 41, there is essentially no difference in the collapse load and behavior between the as-designed DSC and the DSC with closure weld flaws.

Elastic-Plastic Analyses:

Table 7 lists the peak strains predicted by the elastic-plastic analyses for the bounding Service Level D load cases performed in Appendix A. As shown in the table, the peak strain values remain below the material ductility limits at the specified loading conditions, and also at 1.5x the specified loads. The ductility limit conservatively includes a reduction factor of 0.8 to account for weld uncertainties as discussed in Section 3.4.

The Reference 5.12 and 5.17 calculations document the ITCP and OTCP closure weld critical flaw sizes, respectively, based on the maximum radial stresses in the welds. The guidance and safety factors of Reference 5.10 are used in the critical flaw size analysis. The critical flaw sizes are determined to be 0.19 and 0.29 inches for surface and subsurface flaws, respectively, in the OTCP weld and 0.15 inches for surface and subsurface flaws in the ITCP weld. The largest single OTCP flaw size documented in Reference 5.1 is 0.14 inches. As discussed in Section 3.2 a very conservative maximum combined flaw height of 0.195 inches is assumed in this analysis. The largest single ITCP flaw size documented in Reference 5.1 is 0.11 inches. Therefore, the observed flaws actually are smaller than the critical flaw size limits and therefore it is not surprising that the flaws are shown to have little effect on the capacity of the structure. This analysis shows that the quantity and close proximity of some of the flaws also has no significant adverse effects on the structural capacity of the DSC.

Even though all observed flaws in the ITCP and OTCP welds are included in the analysis models using conservative representations, an additional weld strength reduction factor of 0.8 is considered by increasing the limit load acceptance criteria by a factor of 1/0.8=1.25 times and by reducing the elastic-plastic strain limit by a factor of 0.8. The 0.8 factor, which is the same magnitude reduction factor as in ISG-15 [Ref. 5.20], conservatively accounts for any additional limitations in the efficacy of the PAUT examinations and also accounts for the inaccessible area around the vent and siphon block as well as the geometric reflectors at the root and near the toe of the weld.

Therefore it is concluded that Monticello DSC-16, remains in compliance with the ASME Section III Subsection NB [Ref. 5.7] stress limits and has adequate design margin above and beyond the specified loadings with the presence of the ITCP and OTCP closure weld flaws as documented in Reference 5.1.

8.0 LISTING OF COMPUTER FILES

Analyses performed on Computer HEA-0213A using ANSYS Version 14.0 [Ref. 5.6].

File Date & Time listing is as displayed by the Windows 7 Operating System – Differences may occur due local time zone and daylight savings settings.

Analysis Case	File Name	Date & Time
Axisymmetric 1 Initial Mesh Internal Pressure SL A/B	61BTH_WeldFlaw_1F_AX_2_DETACH.db	4/7/2015 10:45 AM
	61BTH_WeldFlaw_1F_AX_2_DETACH.rst	4/7/2015 10:45 AM
	61BTH_WeldFlaw_1F_AX_2_DETACH.mntr	4/7/2015 10:45 AM
	SOLUTION_AXISYMM_IP_LimitLoad.INP	4/7/2015 10:20 AM
Axisymmetric 1 Refined Weld Mesh Internal Pressure SL A/B	61BTH_WeldFlaw_1F_AX_2_DETACH.db	4/7/215 11:59 AM
	61BTH_WeldFlaw_1F_AX_2_DETACH.rst	4/7/215 11:58 AM
	61BTH_WeldFlaw_1F_AX_2_DETACH.mntr	4/7/215 11:59 AM
	SOLUTION_AXISYMM_IP_LimitLoad.INP	4/7/2015 11:55 AM
Axisymmetric 1 Refined Weld and Lid Mesh Internal Pressure SL A/B	61BTH_WeldFlaw_1F_AX_2_DETACH.db	4/21/2015 9:04 AM
	61BTH_WeldFlaw_1F_AX_2_DETACH.rst	4/21/2015 9:03 AM
	61BTH_WeldFlaw_1F_AX_2_DETACH.mntr	4/21/2015 9:04 AM
	SOLUTION_AXISYMM_IP_LimitLoad.INP	4/7/2015 11:55 AM
Axisymmetric 1 Initial Mesh Internal Pressure SL D	61BTH_WeldFlaw_1F_AX_2_DETACH.db	4/20/2015 10:43 AM
	61BTH_WeldFlaw_1F_AX_2_DETACH.rst	4/20/2015 11:09 AM
	61BTH_WeldFlaw_1F_AX_2_DETACH.mntr	4/20/2015 11:09 AM
	SOLUTION_AXISYMM_IP_LimitLoad_SLD.INP	4/7/2015 11:20 AM
Axisymmetric 1 Refined Weld and Lid Mesh Internal Pressure SL D	61BTH_WeldFlaw_1F_AX_2_DETACH.db	4/30/2015 8:12 AM
	61BTH_WeldFlaw_1F_AX_2_DETACH.rst	4/30/2015 8:12 AM
	61BTH_WeldFlaw_1F_AX_2_DETACH.mntr	4/30/2015 8:12 AM
	SOLUTION_AXISYMM_IP_LimitLoad_SLD.INP	4/7/2015 12:02 PM
Axisymmetric 2 Refined Weld and Lid Mesh Internal Pressure SL A/B	61BTH_WeldFlaw_2G_AX_2.db	4/21/2015 3:06 PM
	61BTH_WeldFlaw_2G_AX_2.rst	4/21/2015 2:58 PM
	61BTH_WeldFlaw_2G_AX_2.mntr	4/21/2015 3:06 PM
	SOLUTION_AXISYMM_IP_LimitLoad.INP	4/7/2015 11:55 AM
Axisymmetric 2 Refined Weld and Lid Mesh Internal Pressure SL D	61BTH_WeldFlaw_2G_AX_2.db	4/21/2015 3:10 PM
	61BTH_WeldFlaw_2G_AX_2.rst	4/21/2015 3:10 PM
	61BTH_WeldFlaw_2G_AX_2.mntr	4/21/2015 3:10 PM
	SOLUTION_AXISYMM_IP_LimitLoad_SLD.INP P	4/7/2015 12:02 PM
Axisymmetric 0 Refined Weld and Lid Mesh Internal Pressure SL A/B	61BTH_WeldFlaw_1F_AX_2_DETACH.db	4/21/2015 10:39 AM
	61BTH_WeldFlaw_1F_AX_2_DETACH.rst	4/21/2015 10:31 AM
	61BTH_WeldFlaw_1F_AX_2_DETACH.mntr	4/21/2015 10:39 AM
	SOLUTION_AXISYMM_IP_LimitLoad.INP	4/15/2015 11:07 AM
Axisymmetric 1 Initial Mesh with Keyoption 1=3 Internal Pressure SL A/B	61BTH_WeldFlaw_1F_AX_2_DETACH.db	4/17/2015 5:40 PM
	61BTH_WeldFlaw_1F_AX_2_DETACH.rst	4/17/2015 5:40 PM
	61BTH_WeldFlaw_1F_AX_2_DETACH.mntr	4/17/2015 5:40 PM
	SOLUTION_AXISYMM_IP_LimitLoad.INP	4/16/2015 12:27 PM

Analysis Case	File Name	Date & Time
Axisymmetric 1 Refined Weld and Lid Mesh Internal Pressure, SL A/B ITCP/OTCP couples replaced with Contact	61BTH_WeldFlaw_1F_AX_2_DETACH.db	5/19/2015 8:45 AM
	61BTH_WeldFlaw_1F_AX_2_DETACH.rst	5/19/2015 8:02 AM
	61BTH_WeldFlaw_1F_AX_2_DETACH.mntr	5/19/2015 8:45 AM
	SOLUTION_AXISYMM_IP_LimitLoad.INP	5/18/2015 5:03 PM
Axisymmetric 1 Refined Weld and Lid Mesh Internal Pressure, SL A/B With Pressure on ITCP Weld Root Flaw Surfaces	61BTH_WeldFlaw_1F_AX_2_DETACH.db	5/18/2015 2:42 PM
	61BTH_WeldFlaw_1F_AX_2_DETACH.rst	5/18/2015 1:37 PM
	61BTH_WeldFlaw_1F_AX_2_DETACH.mntr	5/18/2015 2:42 PM
	SOLUTION_AXISYMM_IP_LimitLoad.INP	5/18/2015 1:25 PM
Half Symmetry 1 Initial Mesh Internal Pressure SL A/B	61BTH_WeldFlaw_1GC.db	4/29/2015 2:10 PM
	61BTH_WeldFlaw_1GC.rst	4/29/2015 4:52 PM
	61BTH_WeldFlaw_1GC.mntr	4/29/2015 4:52 PM
	SOLUTION_HALFSYM_LimitLoad.INP	4/29/2015 2:10 PM
Half Symmetry 1 Initial Mesh Side Drop SL D	61BTH_WeldFlaw_1GC.db	4/30/2015 8:20 AM
	61BTH_WeldFlaw_1GC.rst	4/30/2015 3:35 PM
	61BTH_WeldFlaw_1GC.mntr	4/30/2015 3:35 PM
	SOLUTION_HALFSYM_SD.INP	4/30/2015 8:21 AM
Half Symmetry 1 Initial Mesh Side Drop + Internal Pressure SL D	61BTH_WeldFlaw_1GC.db	5/1/2015 6:58 PM
	61BTH_WeldFlaw_1GC.rst	5/1/2015 4:29 PM
	61BTH_WeldFlaw_1GC.mntr	5/1/2015 4:13 PM
	SOLUTION_HALFSYM_SD.INP	4/30/2015 10:26 PM
Half Symmetry 1 Refined Circumferential Mesh Side Drop SL D	61BTH_WeldFlaw_1GD_Refined.db	5/6/2015 1:54 PM
	61BTH_WeldFlaw_1GD_Refined.rst	5/6/2015 11:48 AM
	61BTH_WeldFlaw_1GD_Refined.mntr	5/6/2015 11:47 AM
	SOLUTION_HALFSYM_SD.INP	5/5/2015 9:01 PM
Half Symmetry 0 Initial Mesh Side Drop SL D	61BTH_WeldFlaw_1GC.db	5/2/2015 6:53 AM
	61BTH_WeldFlaw_1GC.rst	5/2/2015 6:53 AM
	61BTH_WeldFlaw_1GC.mntr	5/2/2015 3:37 AM
	SOLUTION_HALFSYM_SD.INP	4/30/2015 8:21 AM

9.0 TABLES AND FIGURES

Table 1 – Summary of Design Basis Load Combinations for the 61BTH DSC [Ref. 5.8]

Load Case	Horizontal DW		Vertical DW		Internal Pressure[9]	External Pressure	Thermal Condition	Lifting Loads	Other Loads	Service Level
	DSC	Fuel	DSC	Fuel						
Non-Operational Load Cases										
NO-1 Fab. Leak Testing	--	--	--	--	--	14.7 psig	70°F	--	155 kip axial	Test
NO-2 Fab. Leak Testing	--	--	--	--	15/23 psig [13]	--	70°F	--	155 kip axial	Test
NO-3 DSC Uprighting	x	--	--	--	--	--	70°F	x	--	A
NO-4 DSC Vertical Lift	--	--	x	--	--	--	70°F	x	--	A
Fuel Loading Load Cases										
FL-1 DSC/Cask Filling	--	--	Cask	--	--	Hydrostatic	120°F Cask	x	x	A
FL-2 DSC/Cask Filling	--	--	Cask	--	Hydrostatic	Hydrostatic	120°F Cask	x	x	A
FL-3 DSC/Cask Xfer	--	--	Cask	--	Hydrostatic	Hydrostatic	120°F Cask	--	--	A
FL-4 Fuel Loading	--	--	Cask	x	Hydrostatic	Hydrostatic	120°F Cask	--	--	A
FL-5 Xfer to Decon	--	--	Cask	x	Hydrostatic	Hydrostatic	120°F Cask	--	--	A
FL-6 Inner Cover plate Welding	--	--	Cask	x	Hydrostatic	Hydrostatic	120°F Cask	--	--	A
FL-7 Fuel Deck Seismic Loading	--	--	Cask	x	Hydrostatic	Hydrostatic	120°F Cask	--	Note 10	C
Draining/Drying Load Cases										
DD-1 DSC Blowdown	--	--	Cask	x	Hydrostatic + 10/15 psig	Hydrostatic	120°F Cask	--	--	A
DD-2 Vacuum Drying	--	--	Cask	x	0 psia	Hydrostatic + 14 psig	120°F Cask	--	--	A
DD-3 Helium Backfill	--	--	Cask	x	12 psig	Hydrostatic	120°F Cask	--	--	A
DD-4 Final Helium Backfill	--	--	Cask	x	3.5 psig	Hydrostatic	120°F Cask	--	--	A
DD-5 Outer Cover Plate Weld	--	--	Cask	x	3.5 psig	Hydrostatic	120°F Cask	--	--	A
Transfer Trailer Loading										
TL-1 Vertical Xfer to Trailer	--	--	Cask	x	10/15 psig	--	0°F Cask	--	--	A
TL-2 Vertical Xfer to Trailer	--	--	Cask	x	10/15 psig	--	120°F Cask	--	--	A
TL-3 Laydown	Cask	X	--	--	10/15 psig	--	0°F Cask	--	--	A
TL-4 Laydown	Cask	X	--	--	10/15 psig	--	120°F Cask	--	--	A
Transfer To/From ISFSI										
TR-1 Axial Load - Cold	Cask	X	--	--	10/15 psig	--	0°F	1g Axial	--	A
TR-2 Transverse Load - Cold	Cask	X	--	--	10/15 psig	--	0°F	1g Transverse	--	A
TR-3 Vertical Load - Cold	Cask	X	--	--	10/15 psig	--	0°F	1g Vertical	--	A
TR-4 Oblique Load - Cold	Cask	X	--	--	10/15 psig	--	0°F	½ g Axial + ½ g Trans + ½ g Vert.	--	A
TR-5 Axial Load – Hot	Cask	X	--	--	10/15 psig	--	100°F	1g Axial	--	A
TR-6 Transverse Load - Hot	Cask	X	--	--	10/15 psig	--	100°F	1g Trans.	--	A
TR-7 Vertical Load - Hot	Cask	X	--	--	10/15 psig	--	100°F	1g Vertical	--	A
TR-8 Oblique Load - Hot	Cask	X	--	--	10/15 psig	--	100°F	½ g Axial + ½ g Trans + ½ g Vert.	--	A
TR-9 25g Corner Drop[12]	Note 1, 14		Note 1, 14		20 psig	--	100°F[2]		25g Corner Drop	D
TR-10 75g Side Drop[12]	Note 1		--	--	20 psig	--	100°F[2]		75g Side Drop	D
TR-11 Top or Bottom End Drops[12]			Note 1, 12		20 psig	--	100°F[2]		60g End Drop	D

Table 1 (Continued) - Summary of Design Basis Load Combinations for the 61BTH DSC [Ref. 5.8]

HSM LOADING	Horizontal DW		Vertical DW		Internal Pressure[9]	External Pressure[9]	Thermal Condition	Handling Loads	Other Loads	Service Level
	DSC	Fuel	DSC	Fuel						
LD-1 Normal Loading - Cold	Cask	X	--	--	10/15 psig	--	0°F Cask	+80 Kip	--	A
LD-2 Normal Loading –Hot	Cask	X	--	--	10/15 psig	--	100° F Cask	+80 Kip	--	A
LD-3	Cask	X	--	--	10/15 psig	--	117° F w/shade[5]	+80 Kip	--	A
LD-4 Off-Normal Loading –Cold	Cask	X	--	--	20 psig	--	0° F Cask	+80 Kip	FF	B
LD-5 Off-Normal Loading - Hot	Cask	X	--	--	20 psig	--	100° F Cask[5]	+80 Kip	FF	B
LD-6	Cask	X	--	--	20 psig	--	117° F w/shade[5]	+80 Kip	FF	B
LD-7 Accident Loading	Cask	X	--	--	20 psig	--	117° F w/shade[5]	+80 Kip	FF	C/D

HSM STORAGE	Horizontal DW		Vertical DW		Internal Pressure[9]	External Pressure[9]	Thermal Condition	Handling Loads	Other Loads	Service Level
	DSC	Fuel	DSC	Fuel						
HSM-1 Off-Normal HSM-2 Normal Storage	HSM HSM	X X	-- --	-- --	15 psig 15 psig	-- --	-40° F HSM 0° F HSM	-- --	-- --	B A
HSM-3 Off-Normal HSM-4 Off-Normal Temp. + Failed Fuel	HSM HSM	X X	-- --	-- --	15 psig 20 psig	-- --	117° F HSM 117° F HSM	-- --	-- FF	B C
HSM-5 Blocked Vent Storage HSM-6 B.V. + Failed Fuel Storage	HSM HSM	X X	-- --	-- --	65/120 psig 65/120 psig	-- --	117° F HSM/BV[2][4] 117° F HSM/BV[2][4]	-- --	-- FF	D D
HSM-7 Earthquake Loading –Cold HSM-8 Earthquake Loading –Hot	HSM HSM	X X	-- --	-- --	10/15 psig 10/15 psig	-- --	0° F HSM 100°F HSM	-- --	EQ EQ	C/D[15] C/D[15]
HSM-9 Flood Load (50' H_2O) –Cold HSM-10 Flood Load (50' H_2O) - Hot	HSM HSM	X X	-- --	-- --	10/15 psig 10/15 psig	22 psig 22 psig	0° F HSM 100°F HSM	-- --	Flood[3] Flood[3]	C C

HSM UNLOADING	Horizontal DW		Vertical DW		Internal Pressure[9]	External Pressure[9]	Thermal Condition	Handling Loads	Other Loads	Service Level
	DSC	Fuel	DSC	Fuel						
UL-1 Normal Unloading – Cold	HSM	X	--	--	10/15 psig	--	0°F HSM	+60 Kip	--	A
UL-2 Normal Unloading –Hot	HSM	X	--	--	10/15 psig	--	100° F HSM	+60 Kip	--	A
UL-3	HSM	X	--	--	10/15 psig	--	117° F w/shade	+60 Kip	--	A
UL-4 Off-Normal Unloading –Cold UL-5 Off-Normal Unloading – Hot	HSM HSM	X X	-- --	-- --	20 psig 20 psig	-- --	0° F HSM 100° F HSM	+60 Kip +60 Kip	FF FF	B B
UL-6 UL-7 Off. Norm. Unloading-FF/Hot[6,11]	HSM HSM	X X	-- --	-- --	20 psig 20 psig	-- --	117° F w/shade 100° F HSM	+60 Kip +80 Kip	FF FF	B C
UL-8 Accident Unloading –FF/Hot[7,11]	HSM	X	--	--	65/120[7] psig	--	100° F HSM	+80 Kip	FF	D
RF-1 DSC Reflood	--	--	Cask	X	20 psig (max)	Hydrostatic	120° F Cask	--	--	D

Table 1 (Concluded) – Summary of Design Basis Load Combinations for the 61BTH DSC [Ref. 5.8]

(Notes for the preceding portions of Table 1)

1. 25g and 75g drop acceleration includes gravity effects. Therefore, it is not necessary to add an additional 1.0g load.
2. For Level D events, only maximum temperature case is considered. (Thermal stresses are not limited for level D events and maximum temperatures give minimum allowables).
3. Flood load is an external pressure equivalent to 50 feet of water.
4. BV = HSM vents are blocked.
5. At temperature over 100°F a sunshade is required over the Transfer Cask. Temperatures for these cases are enveloped by the 100°F (without sunshade) case.
6. As described in Section T.4, this pressure assumes release of the fuel cover gas and 30% of the fission gas. Since unloading requires the HSM door to be removed, the pressure and temperatures are based on the normal (unblocked vent) condition. Pressure is applied to the confinement boundary.
7. As described in Section T.4, this pressure assumes release of the fuel cover gas and 30% of the fission gas. Although unloading requires the HSM door to be removed, the pressure and temperatures are based on the blocked vent condition. Pressure is applied to the shell, inner bottom and inner and outer top cover plates.
8. Not used.
9. Unless noted otherwise, pressure is applied to the confinement boundary. 10 psig and 65 psig are applicable to Type 1 DSC, while 15 psig and 120 psig are applicable to Type 2 DSC.
10. Fuel deck seismic loads are assumed enveloped by handling loads.
11. Load Cases UL-7 and UL-8 envelop loading cases where the stresses due to insertion loading of 80 kips are added to stresses due to internal pressure (in reality, the insertion force is opposed by internal pressure).
12. The 60g top end drop and bottom end drop are not credible events, therefore these drop analyses are not required. However, consideration of 60g end drop and 75g side drop conservatively envelops the effect of 25g corner drop.
13. Conservatively based on normal operating pressure times 1.5 to cover future 10CFR Part 71 requirements.
14. A 25g corner drop analysis (30° from horizontal) of 61BTH DSC without support from the TC is to be documented.
15. *Service Level C is for the standard seismic event and Service Level D is for the high seismic event.*

Table 2 – Internal Pressure in the 61BTH Type 1 DSC

Design Condition	Maximum Calculated Pressure [psi]	Design Pressure used in Ref. 5.2 and This Calculation [psi]	Reference
Normal	7.3	10	Ref. 5.8 Table T.4-16
Off-Normal	10.9	20	Ref. 5.8 Table T.4-20
Accident	56.1	65	Ref. 5.8 Table T.4-24

Table 3 – Maximum Temperatures in the 61BTH Type 1 DSC Shell

Design Condition		Maximum Calculated Temperature [^oF]	Design Temperature used in This Calculation [^oF]	Reference
Normal	Storage	374	500	Ref. 5.8 Table T.4-13
	Transfer	439	500	
Off-Normal	Storage	399	500	Ref. 5.8 Table T.4-18
	Transfer	416	500	
Accident	Storage	611	625	Ref. 5.8 Table T.4-22
	Transfer	467	500	

Table 4 – Properties of SA-240 Type 304. [Ref. 5.11]

Temp [°F]	E Modulus of Elasticity [ksi]	S_m Allowable Stress Intensity [ksi]	S_y Yield Stress [ksi]	S_u Ultimate Tensile Strength [ksi]	Yield Stress for SL A/B Limit Load Analysis (Note 1) [ksi]	Yield Stress for SL D Limit Load Analysis (Note 2) [ksi]
70	28,300	20.0	30.0	75.0	30.0	46.0
100	28,138	20.0	30.0	75.0	30.0	46.0
200	27,600	20.0	25.0	71.0	30.0	46.0
300	27,000	20.0	22.4	66.2	30.0	46.0
400	26,500	18.7	20.7	64.0	28.1	43.0
500	25,800	17.5	19.4	63.4	26.3	40.3
600	25,300	16.4	18.4	63.4	24.6	37.7
625	25,175	16.3	18.2	63.4	24.5	37.5
700	24,800	16.0	17.6	63.4	24.0	36.8
(1) The yield strength to be used in a Limit Analysis for Service Level A and B Loading is 1.5*Sm, per Paragraph NB-3228.1 of Reference 5.7.						
(2) The yield strength to be used in a Limit Analysis for Service Level D Loading is the lesser of 2.3*Sm and 0.7*Su, per Paragraph F-1341.3 of Reference 5.9.						

Table 5 –Properties of SA-36. [Ref. 5.11]

Temp [°F]	E Modulus of Elasticity [ksi]	S_m Allowable Stress Intensity [ksi]	S_y Yield Stress [ksi]	S_u Ultimate Tensile Strength [ksi]	Yield Stress for SL A/B Limit Load Analysis (Note 1) [ksi]	Yield Stress for SL D Limit Load Analysis (Note 2) [ksi]
70	29,500	19.3	36.0	58.0	29.0	40.6
100	29,338	19.3	36.0	58.0	29.0	40.6
200	28,800	19.3	33.0	58.0	29.0	40.6
300	28,300	19.3	31.8	58.0	29.0	40.6
400	27,700	19.3	30.8	58.0	29.0	40.6
500	27,300	19.3	29.3	58.0	29.0	40.6
600	26,700	17.7	27.6	58.0	26.6	40.6
625(3)	26,400	17.6	27.2	58.0	26.4	40.4
700	25,500	17.3	25.8	58.0	26.0	39.8
(1) The yield strength to be used in a Limit Analysis for Service Level A and B Loading is 1.5*Sm, per Paragraph NB-3228.1 of Reference 5.7.						
(2) The yield strength to be used in a Limit Analysis for Service Level D Loading is the lesser of 2.3*Sm and 0.7*Su, per Paragraph F-1341.3 of Reference 5.9.						
(3) All values are interpolated from the 600 °F and 700 °F values.						

Table 6 –Summary of Load Cases, Mesh Refinement Results, and NB-3228.1 Limit Load Analysis Results

Name	Mesh Level	Loading	Temp. [ºF]	Analysis Criteria	Required/ Design Pressure (Note 4) [psi]	Required Pressure to Satisfy Limit Load Criteria (Note 5) [psi]	Limit Load Collapse Pressure [psi]	Code Limit Load Criteria Satisfied?
Axisymmetric 1	Initial	Internal Pressure	500	SL A/B	32	60.0	95.9	Yes
	Refined Welds	Internal Pressure	500	SL A/B	32	60.0	94.8	Yes
	Refined Welds and Lid	Internal Pressure	500	SL A/B	32	60.0	93.8	Yes
	Initial	Internal Pressure	625	SL D	65	90.2	136.6	Yes
	Refined Welds and Lid	Internal Pressure	625	SL D	65	90.2	132.6	Yes
Axisym. 2	Refined Welds and Lid	Internal Pressure	500	SL A/B	32	60.0	93.7	Yes
	Refined Welds and Lid	Internal Pressure	625	SL D	65	90.2	132.9	Yes
Axy-0 (No Flaws)	Refined Welds and Lid	Internal Pressure	500	SL A/B	32	60.0	94.5	Yes
Half-Symm 1 Benchark	Initial (Note 2)	Internal Pressure	500	SL A/B	32	60.0	97	Yes

Name	Mesh Level	Loading	Temp. [ºF]	Analysis Criteria	Required/ Design G-Load [g]	Required G-Load to Satisfy Limit Load Criteria (Note 5) [g]	Collapse G-Load [g]	Code Limit Load Criteria Satisfied?
Half Symmetry 1	Initial	Side Drop	500	SL D	75	104.0	181	Yes
	Refined Circumferential Mesh (Note 3)	Side Drop	500	SL D	75	104.0	185	Yes
	Initial (Note 3)	Side Drop with Off-Normal IP	500	SL D	75	104.0	181	Yes
Half-Symm-0 (No Flaws)	Initial	Side Drop	500	SL D	75	104.0	189	Yes

Notes:

1) [Not Used]

2) The 97 psi collpase load is estimated / extrapolated from the final obtained solution at 95 psi. Excessive run times make more precise results impractical.

3) The reported collapse load is conservative - based on the collapse behavior it is expected that smaller analysis time steps would yield larger collapse loads. This was deemed impractical due to the long run time and the large margin available.

4) The Service Level A/B required pressure of 32 psi is based on the design internal pressure of 10 psi plus an equivalent internal pressure of 22 psi which accounts for other Service Level A loads. See Section 4.2

5) Includes both the ASME code required factor and the 0.8 weld strength reduction factor to account for examination limitations.

Table 7 –Evaluation of Peak Strain Values at Specified Loads and at 1.5x Specified Loads from Elastic-Plastic Analyses.

Load Case	Specified Loading Internal Pressure [psi]	Peak Equivalent Plastic Strain [in/in]		Material Strain Limit (Note 1)	Margin of Safety at Specified Loading (Note 2)
		at 65 psi internal pressure	at 100 psi internal pressure		
Internal Pressure Service Level D	65	0.0597 (5.97%)	0.126 (12.6%)	0.28 (28%)	3.69
Load Case	Specified Loading Side Drop G-Load [g]	Peak Equivalent Plastic Strain [in/in]		Material Strain Limit (Note 1)	Margin of Safety at Specified Loading (Note 2)
		at 75g loading	at 112.5g loading		
Side Drop Service Level D	75	0.0609 (6.09%)	0.126 (12.6%)	0.28 (28%)	3.60

Notes:

1) The weld uncertainty factor of 0.8 (See Section 3.4) is applied to the minimum of the ASME specified minimum elongations of SA-240 Type 304 (40%) and E308-XX electrode (35%). Therefore the strain limit is taken as 0.8*0.35=0.28.

2) Margin of Safety is calculated as [(Strain Limit)/(Actual Strain)]-1

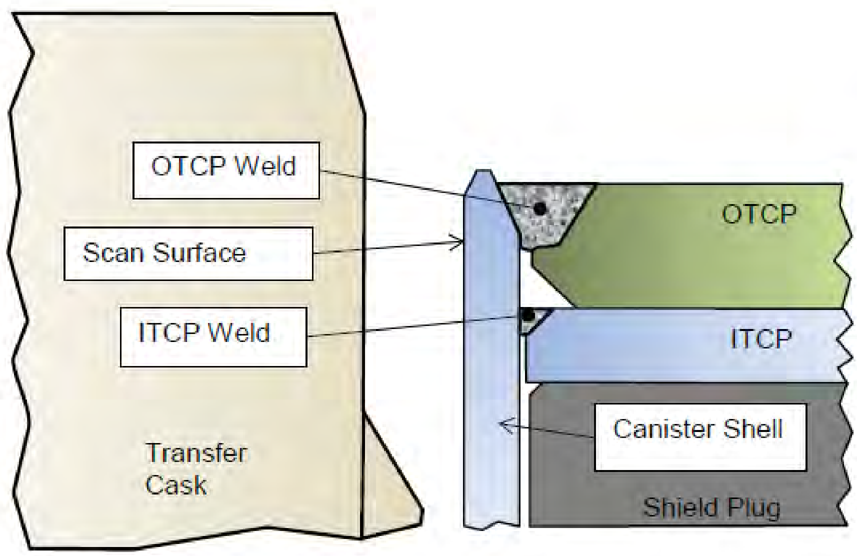

Figure 1 – Sketch of the 61BTH DSC Top End and Transfer Cask from Reference 5.1

Security-Related Information
Figure Withheld Under 10 CFR 2.390.

Figure 2 – Details of the 61BTH Top End Component Interfaces

Security-Related Information
Figure Withheld Under 10 CFR 2.390.

Figure 3 – ITCP and OTCP Closure Weld Details from Reference 5.5
(Note: Section B-B above is rotated 90 degrees clockwise from Figure 2.)

Security-Related Information
Figure Withheld Under 10 CFR 2.390.

Figure 4 – DSC Top End Detailed Dimensions

(Note: See Section 2.0 Assumption No. 6 and Section 4.3 for discussions and justifications regarding the modeled dimensions and lid-to-shell gaps.)

Security-Related Information
Figure Withheld Under 10 CFR 2.390.

Figure 5 – OTCP Flaws – Raw Data from Reference 5.1
(Numbers indicate the Flaw Number from Reference 5.1)

Security-Related Information
Figure Withheld Under 10 CFR 2.390.

Figure 6 – OTCP Flaws – Main Flaw Group Reduced and Bounded

Security-Related Information
Figure Withheld Under 10 CFR 2.390.

Figure 7 – OTCP Flaws – Bounding Set #1 for ANSYS Collapse Analysis

Security-Related Information
Figure Withheld Under 10 CFR 2.390.

Figure 8 – OTCP Flaws –Bounding Set #2 for ANSYS Collapse Analysis

Security-Related Information
Figure Withheld Under 10 CFR 2.390.

Figure 9 – ITCP Flaws – Raw Data from Reference 5.1

Security-Related Information
Figure Withheld Under 10 CFR 2.390.

Figure 10 – ITCP Flaws – Bounding Flaw Set for ANSYS Collapse Analysis

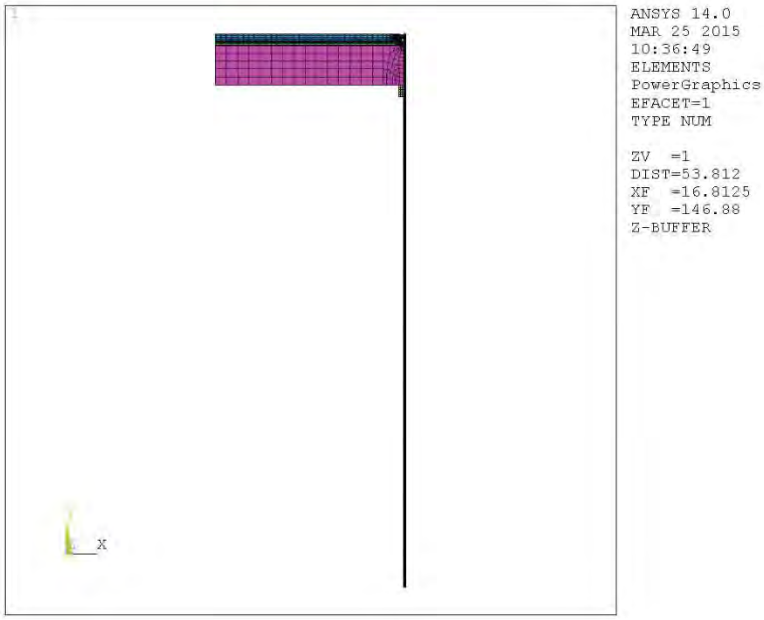

Figure 11 – Overview of the Axisymmetric Model

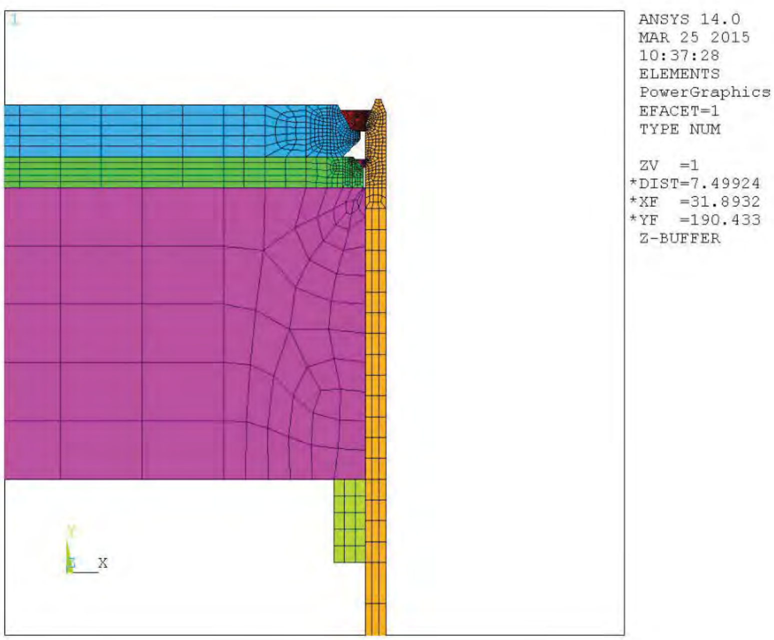

Figure 12 – Mesh Details Near the Lid Regions of the Axisymmetric Model
(Small differences in the mesh exist amongst the sub-models)

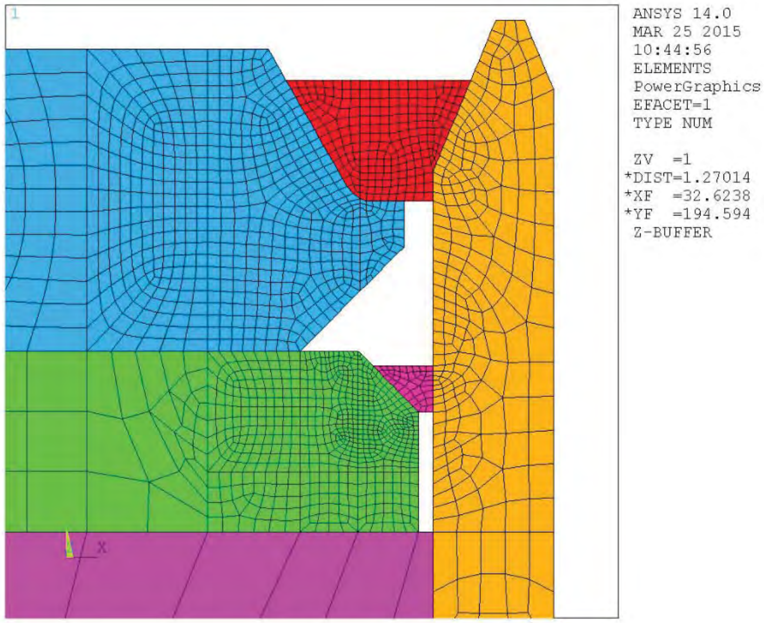

Figure 13 – Mesh Details at the Welds for Axisymmetric Case #1

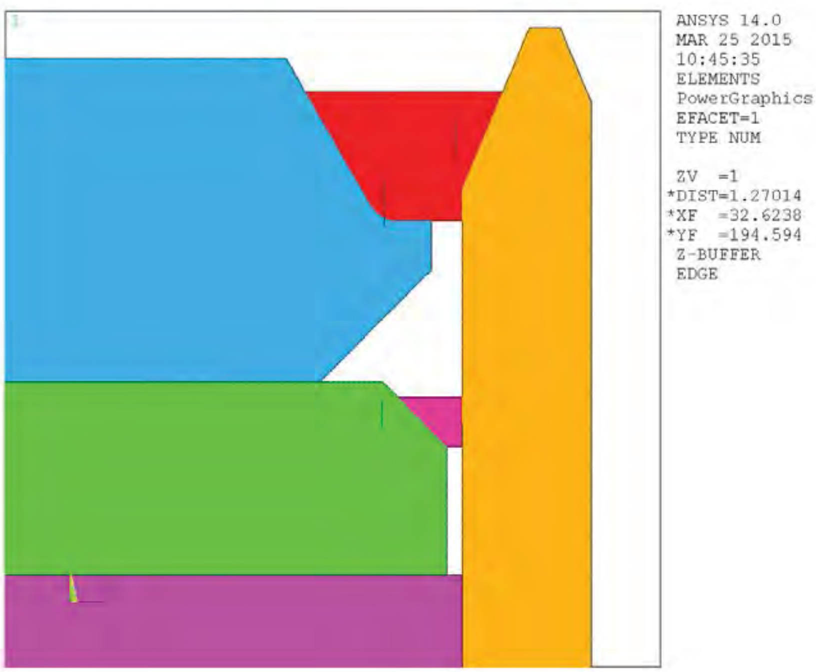

Figure 14 – Flaw Locations for Axisymmetric Case #1

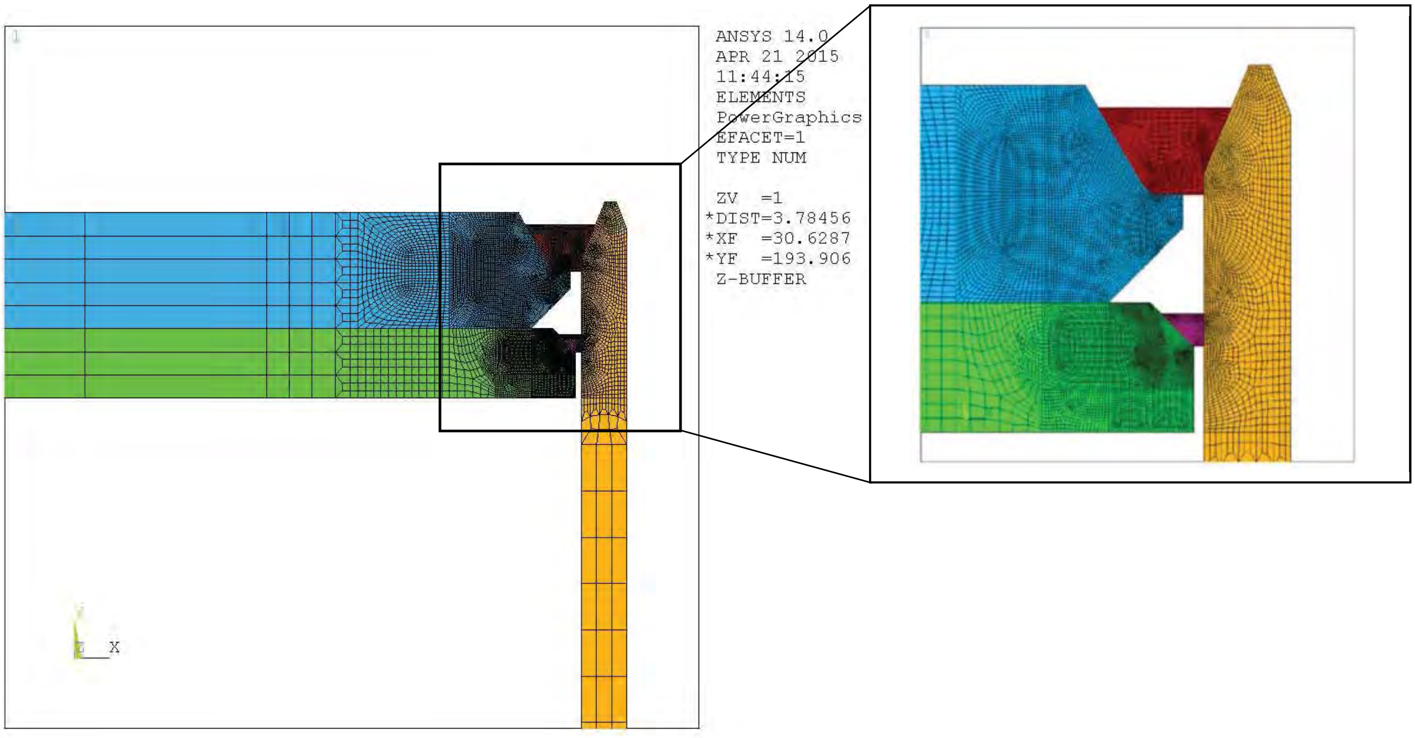

Figure 15 – Refined Mesh (Weld Region) for Axisymmetric Case #1

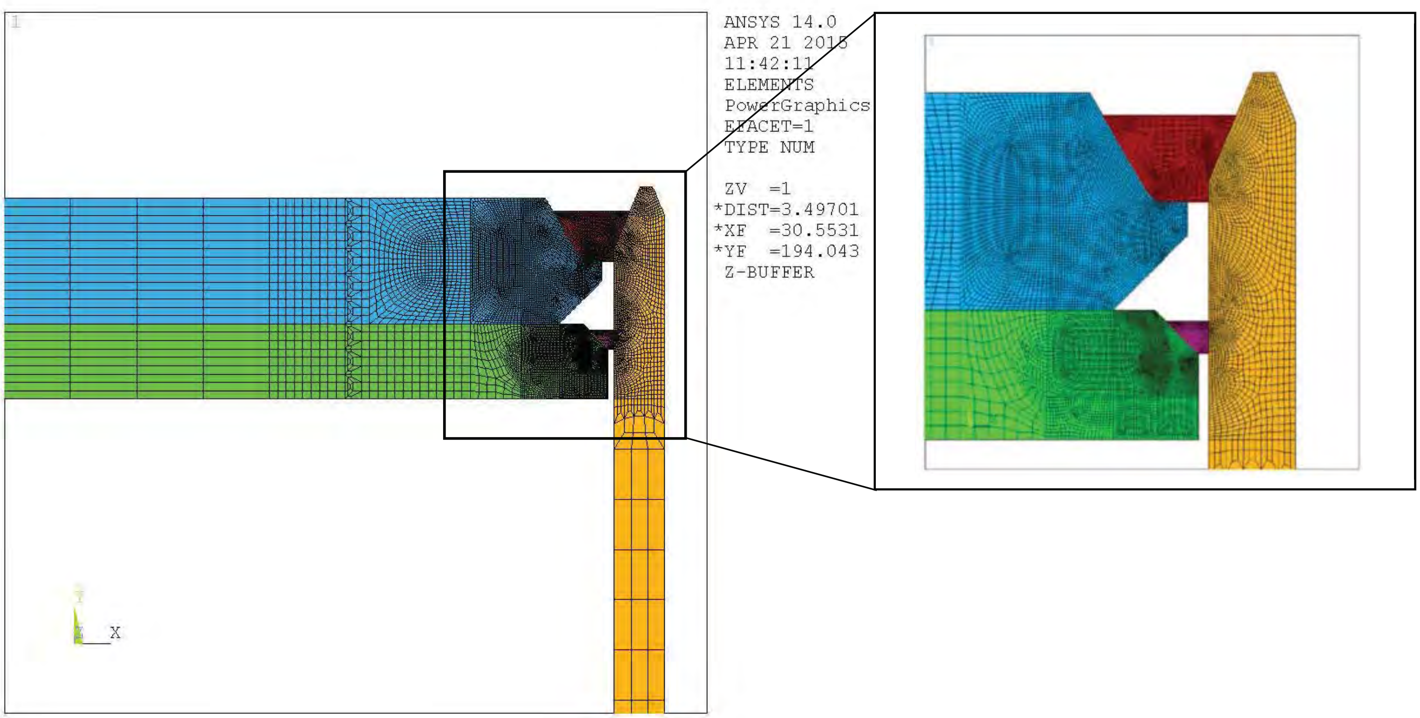

Figure 16 – Refined Mesh (Weld and Lid Interior Region) for Axisymmetric Case #1

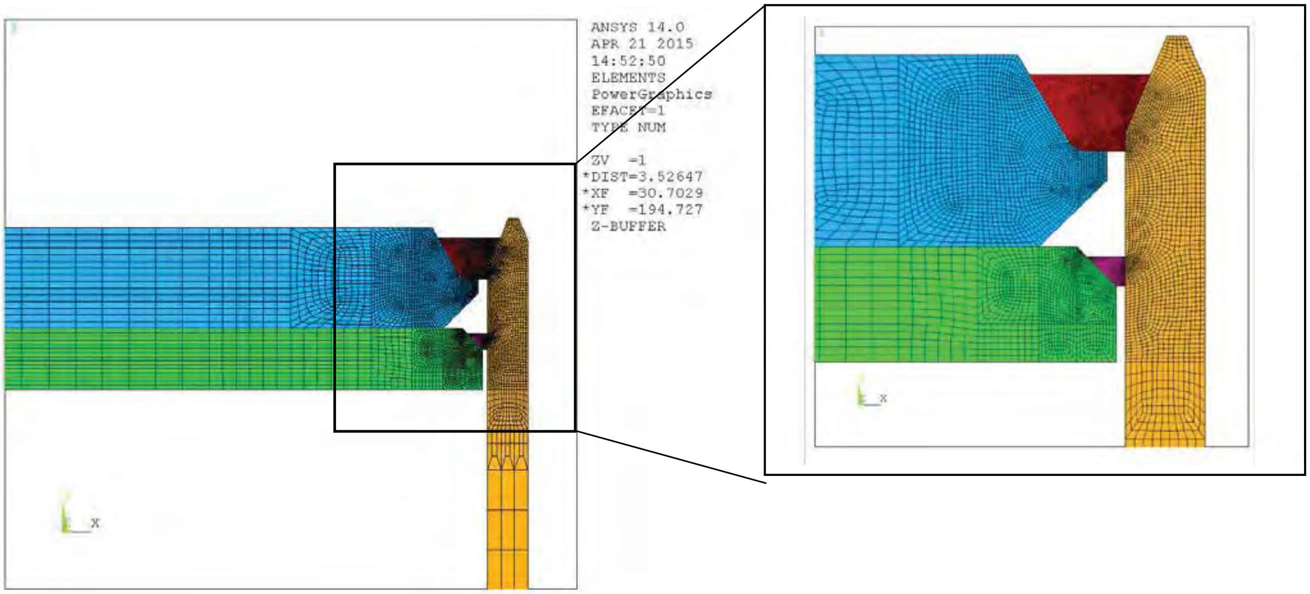

Figure 17 – Mesh Details at the Welds for Axisymmetric Case #2

Figure 18 – Flaw Locations for Axisymmetric Case #2

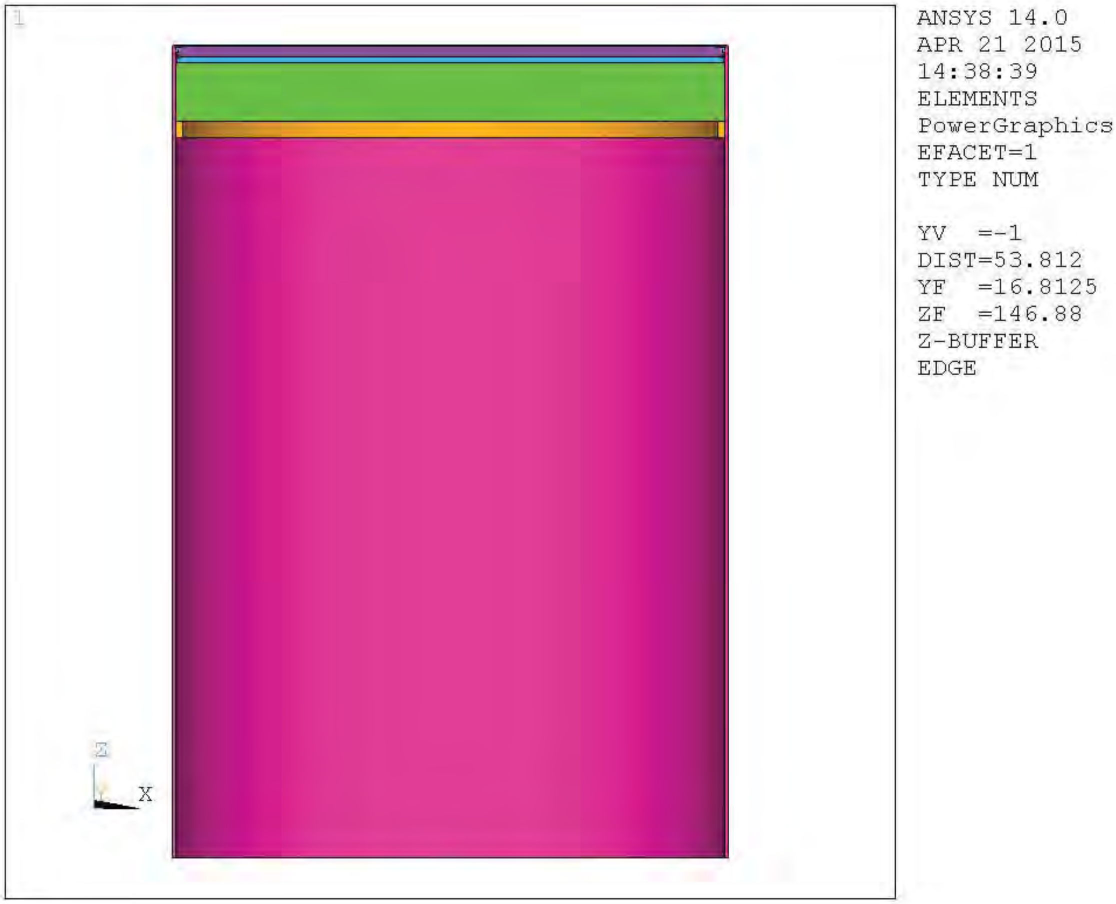

Figure 19 – Overview of the Half-Symmetry Model

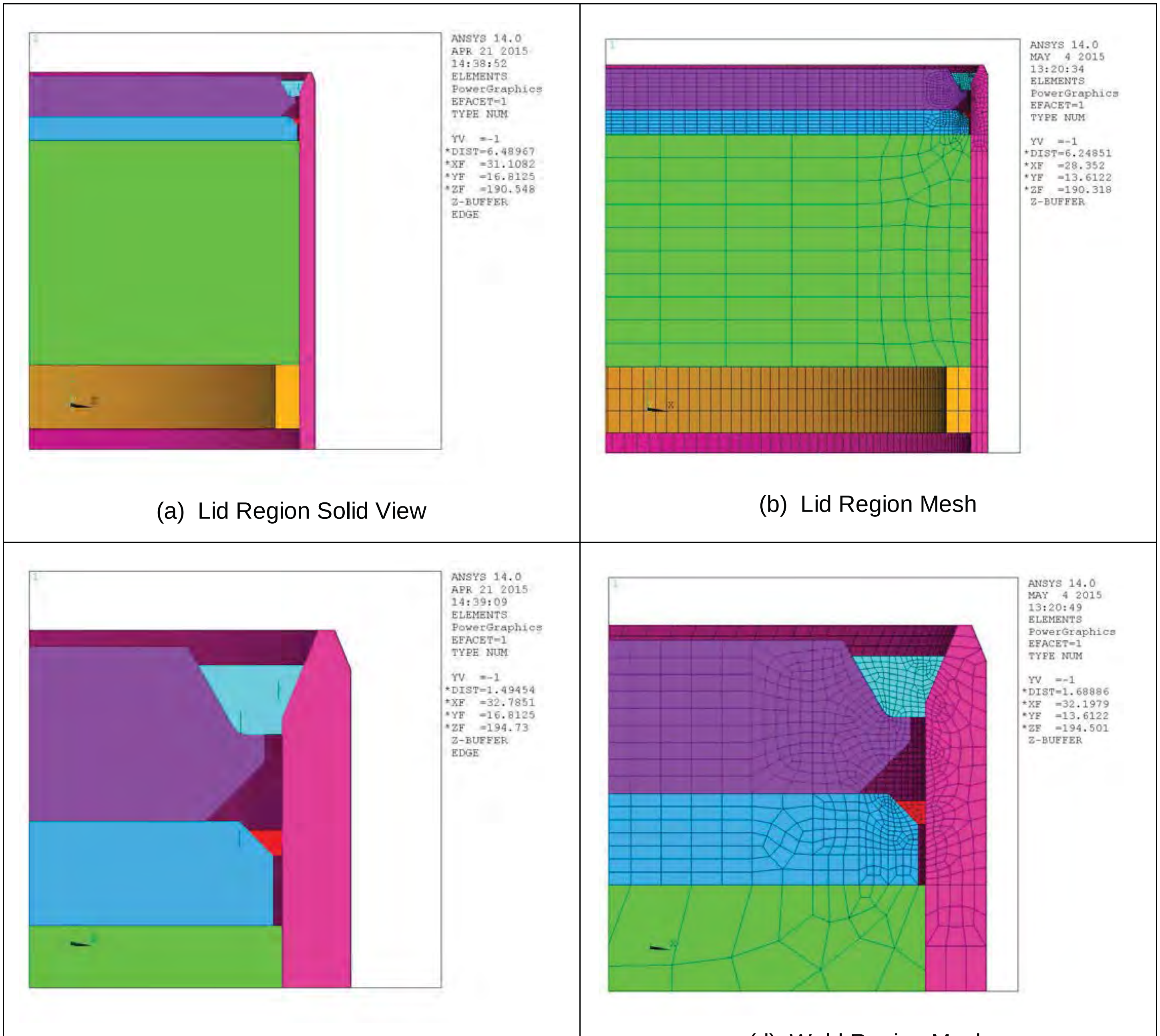

(a) Lid Region Solid View

(b) Lid Region Mesh

(c) Weld Region Solid View with Flaws Visible

(d) Weld Region Mesh

Figure 20 – Detail Views and Mesh Plots of the Half Symmetry Model

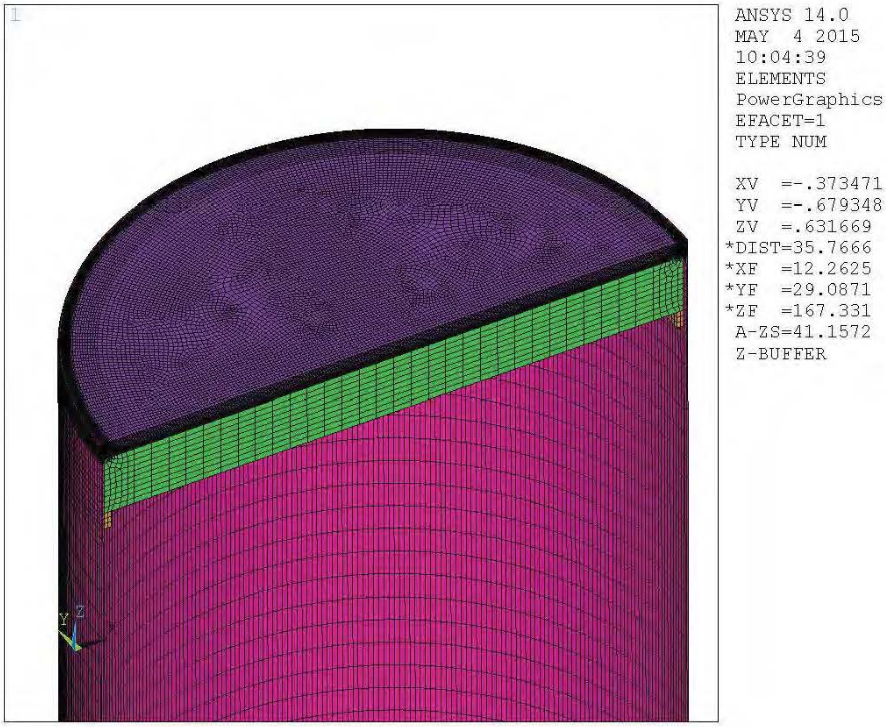

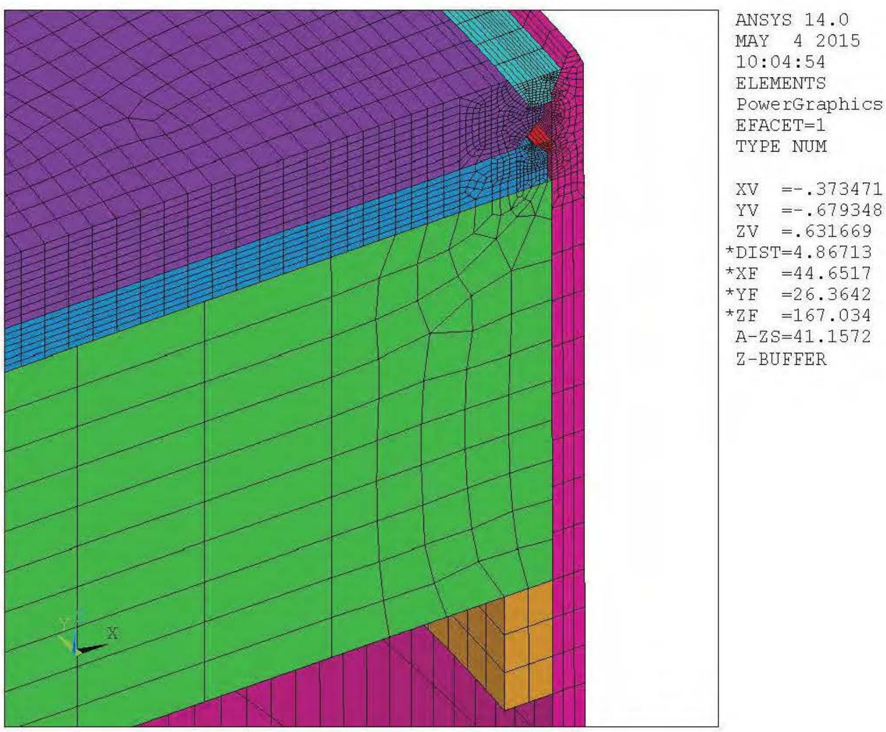

Figure 21 – Isometric Views of Half-Symmetry Model

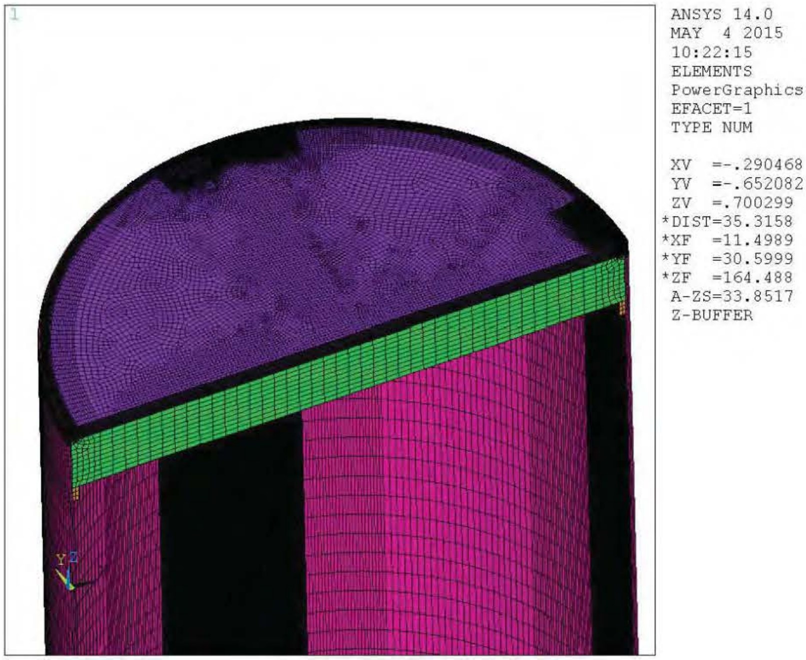

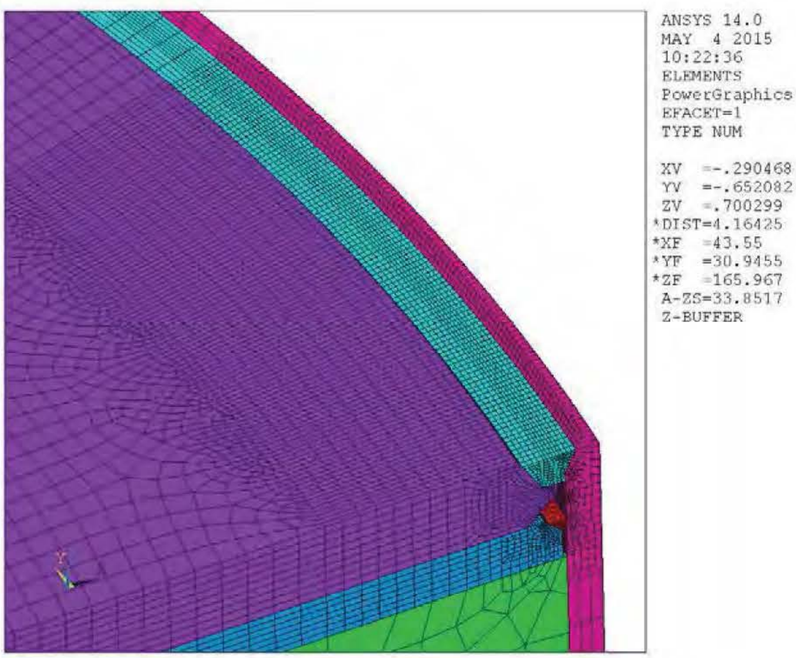

Figure 22 – Isometric Views of Half-Symmetry Model (Refined Circumferential Mesh)

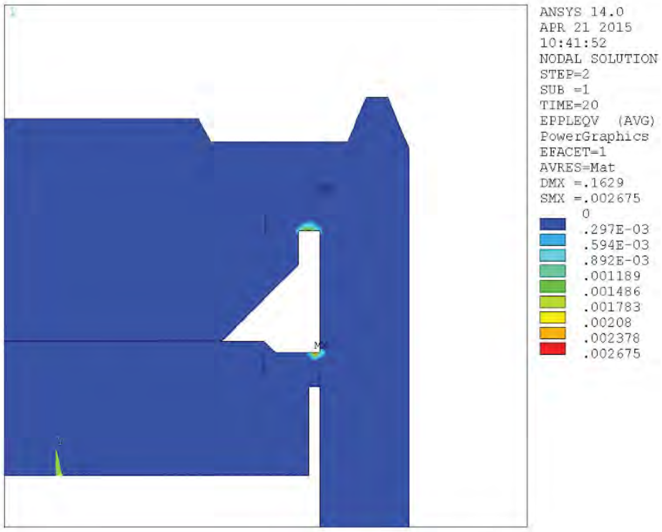

(a) Equivalent Plastic Strain in Weld Region [in/in] at 20 psi Internal Pressure

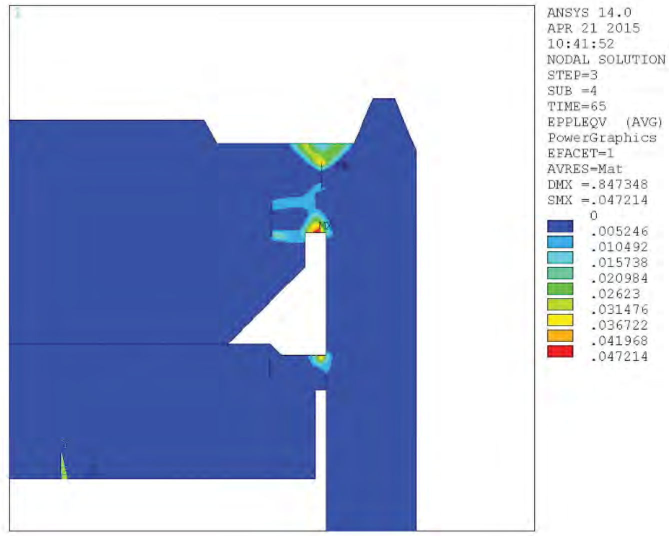

(b) Equivalent Plastic Strain in Weld Region [in/in] at 65 psi Internal Pressure

(c) Equivalent Plastic Strain in Weld Region [in/in] at 95.9 psi Internal Pressure

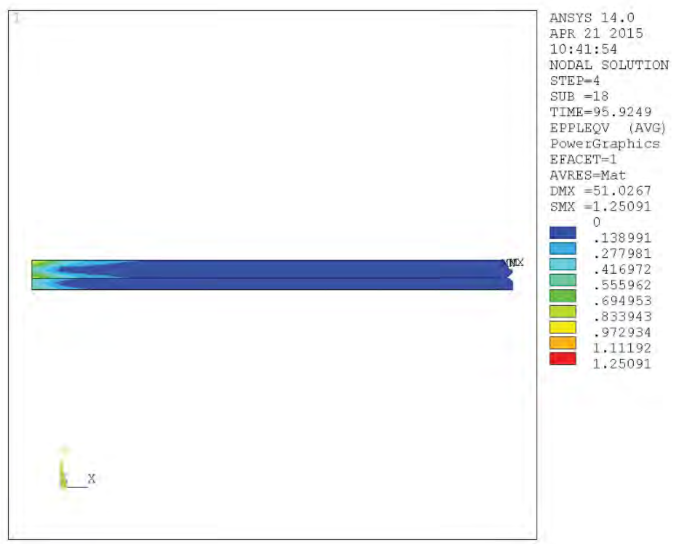

(d) EQV Plastic Strain in the Cover Plates at 95.9 psi

Figure 23 – Results for Axisymmetric Case #1 – Initial Mesh – Service Level A/B

(Note that the magnitude of the strains and deflections has no true physical meaning due to the nature of limit load analysis)

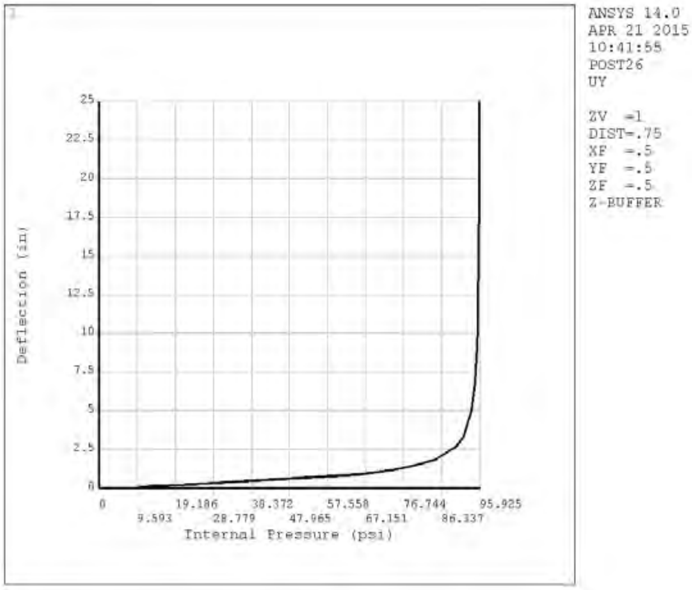

(a) Service Level A/B Material Properties

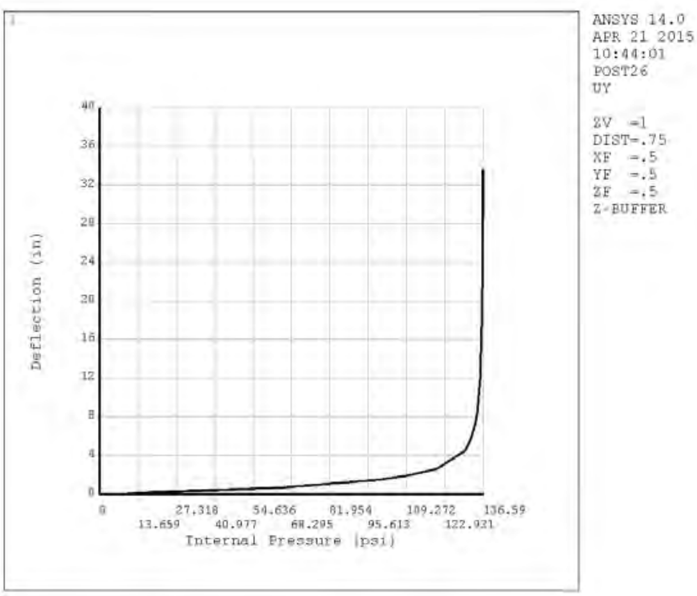

(b) Service Level D Material Properties

Figure 24 – Deflection History of the Center of the OTCP for the Axisymmetric Case #1 Initial Mesh

(Maximum deflection occurs at the center point of the lids, in the outward axial direction)

(Note that the magnitude of the deflections has no true physical meaning due to the nature of limit load analysis)

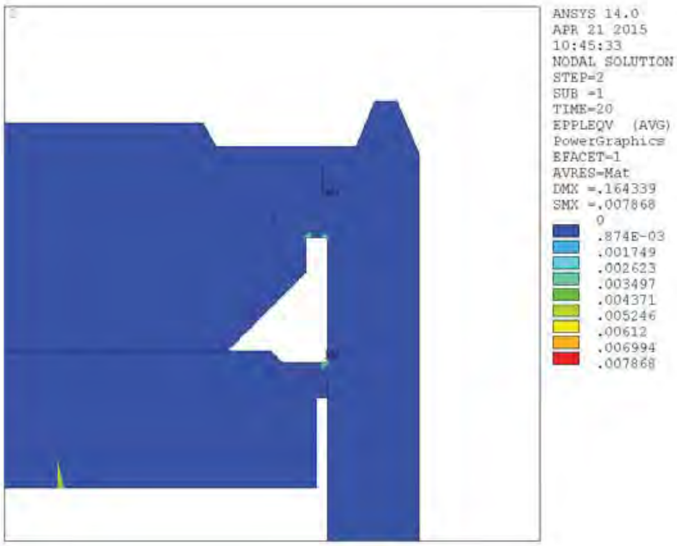

(a) Equivalent Plastic Strain in Weld Region [in/in] at 20 psi Internal Pressure

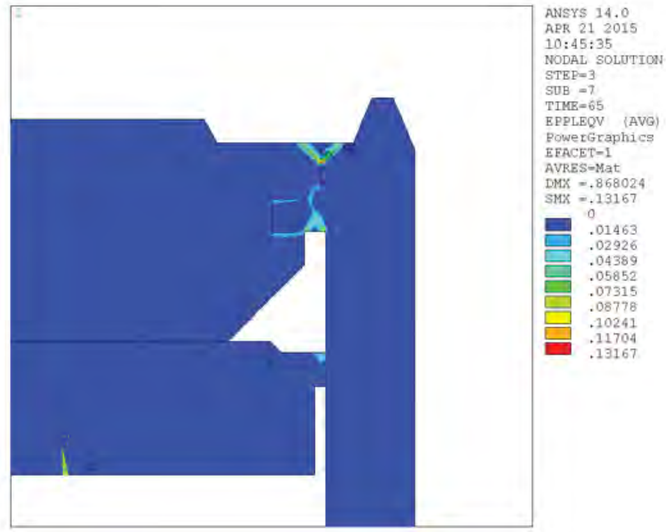

(b) Equivalent Plastic Strain in Weld Region [in/in] at 65 psi Internal Pressure

(c) Equivalent Plastic Strain in Weld Region [in/in] at 94.8 psi Internal Pressure

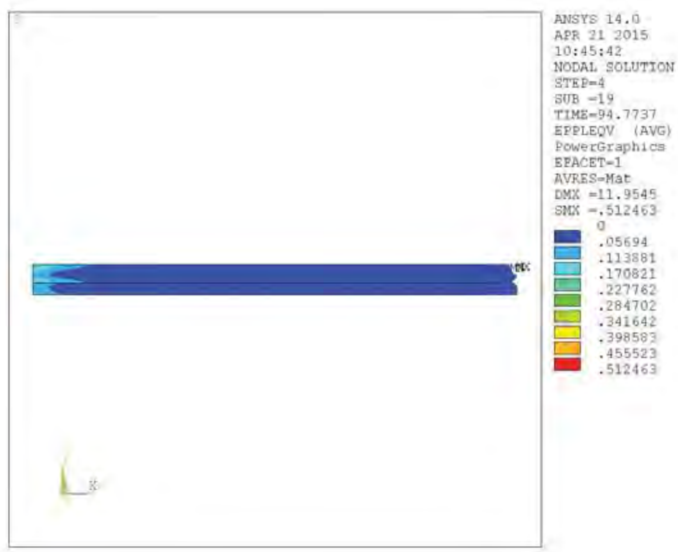

(d) EQV Plastic Strain in the Cover Plates at 94.8 psi

Figure 25 – Results for Axisymmetric Case #1 – Refined Mesh in Weld Region – Service Level A/B

(Note that the magnitude of the strains and deflections has no true physical meaning due to the nature of limit load analysis)

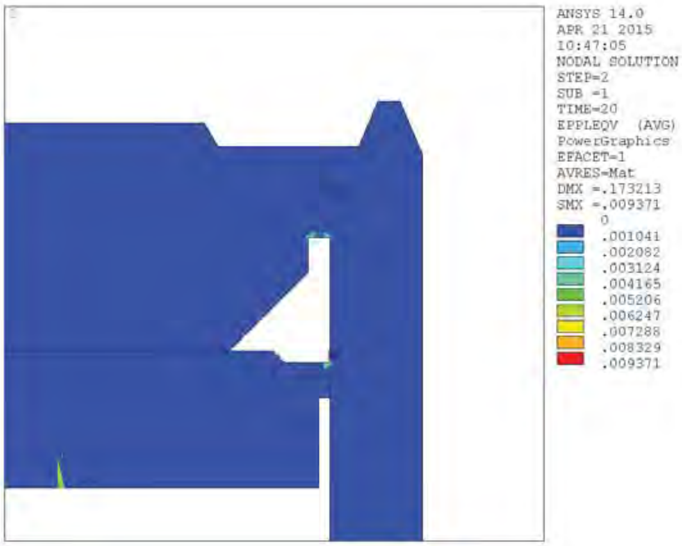

(a) Equivalent Plastic Strain in Weld Region [in/in] at 20 psi Internal Pressure

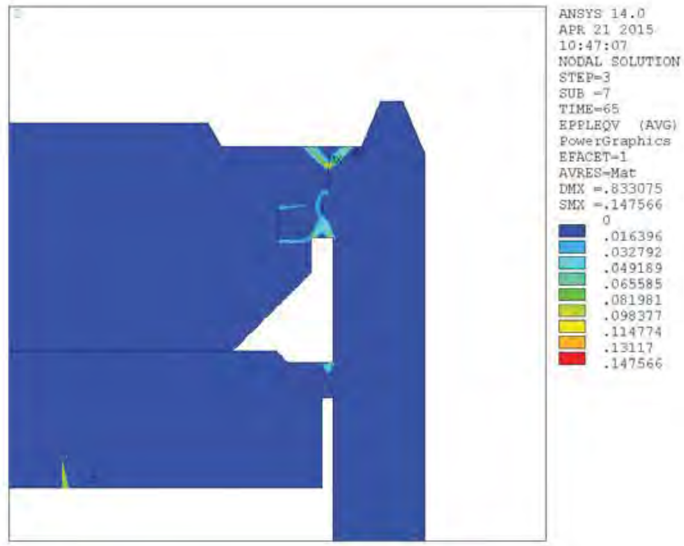

(b) Equivalent Plastic Strain in Weld Region [in/in] at 65 psi Internal Pressure

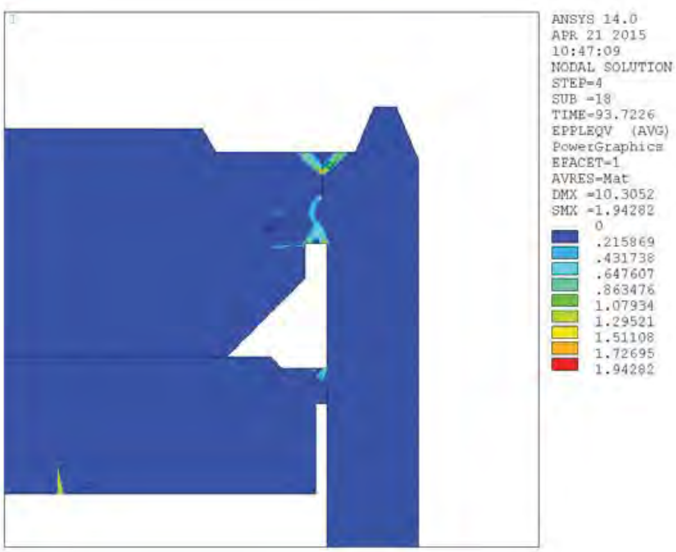

(c) Equivalent Plastic Strain in Weld Region [in/in] at 93.7 psi Internal Pressure

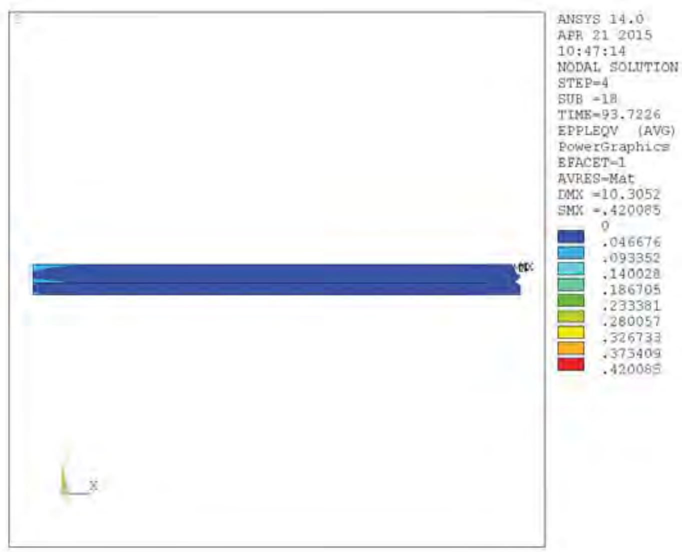

(d) EQV Plastic Strain in the Cover Plates at 93.7 psi

Figure 26 – Results for Axisymmetric Case #1 – Refined Mesh in Weld and Lid Interior Region – Service Level A/B

(Note (c) and (d) are plotted one timestep before the collapse pressure)

(Note that the magnitude of the strains and deflections has no true physical meaning due to the nature of limit load analysis)

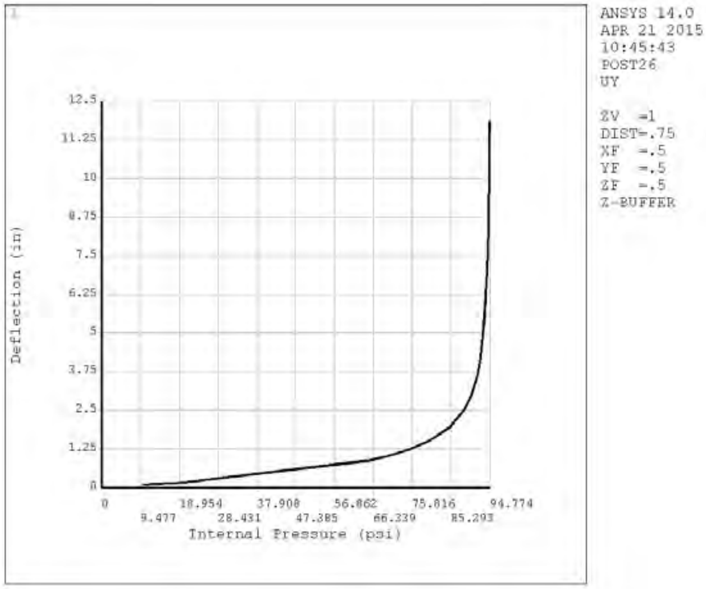

(a) Service Level A/B Material Properties

Refined Mesh at Weld Region Only

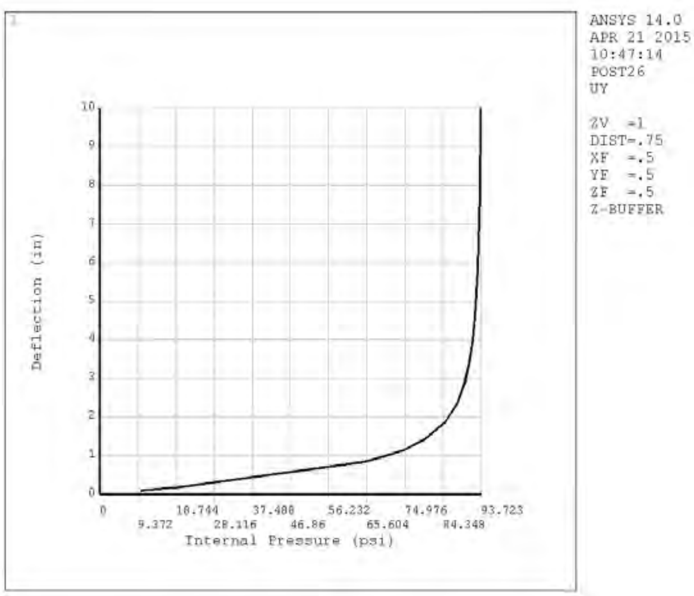

(b) Service Level A/B Material Properties

Refined Mesh at the Weld and Lid Interior Regions

Figure 27 – Deflection History of the Center of the OTCP for the Axisymmetric Case #1 Refined Mesh

(Maximum deflection occurs at the center point of the lids, in the outward axial direction)

(Note that the magnitude of the deflections has no true physical meaning due to the nature of limit load analysis)

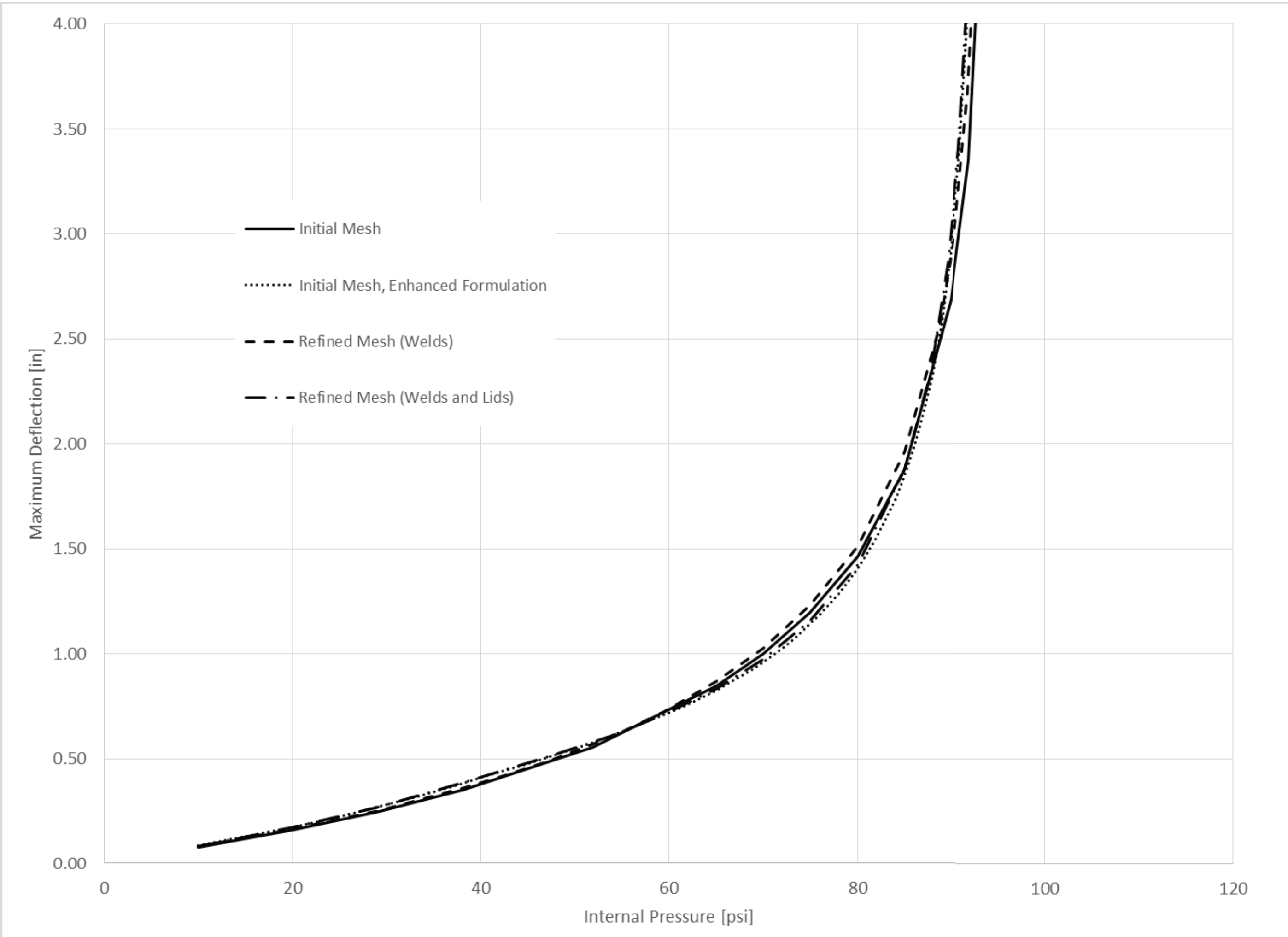

Figure 28 – Comparison of Maximum Displacement Histories for Axisymmetric Model Sensitivity Studies

(Maximum deflection occurs at the center point of the lids, in the outward axial direction)

(Note that the magnitude of the deflections has no true physical meaning due to the nature of limit load analysis)

(Service Level A/B material Properties)

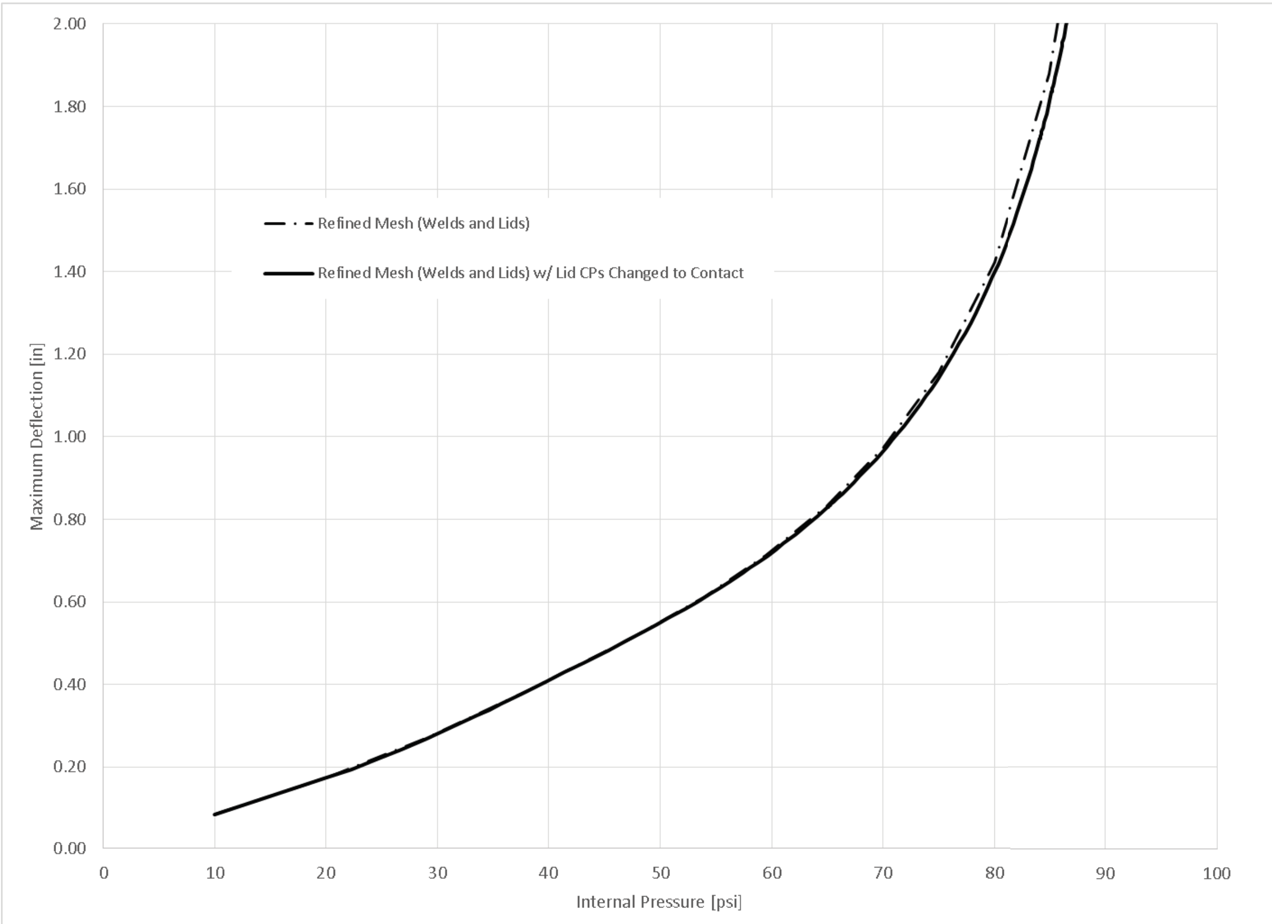

Figure 29 – Comparison of Maximum Displacement Histories for Axisymmetric Model with Lid Contact Defined using Nodal DOF Couples vs. Contact Elements

(Maximum deflection occurs at the center point of the lids, in the outward axial direction)

(Note that the magnitude of the deflections has no true physical meaning due to the nature of limit load analysis)

(Service Level A/B material properties)

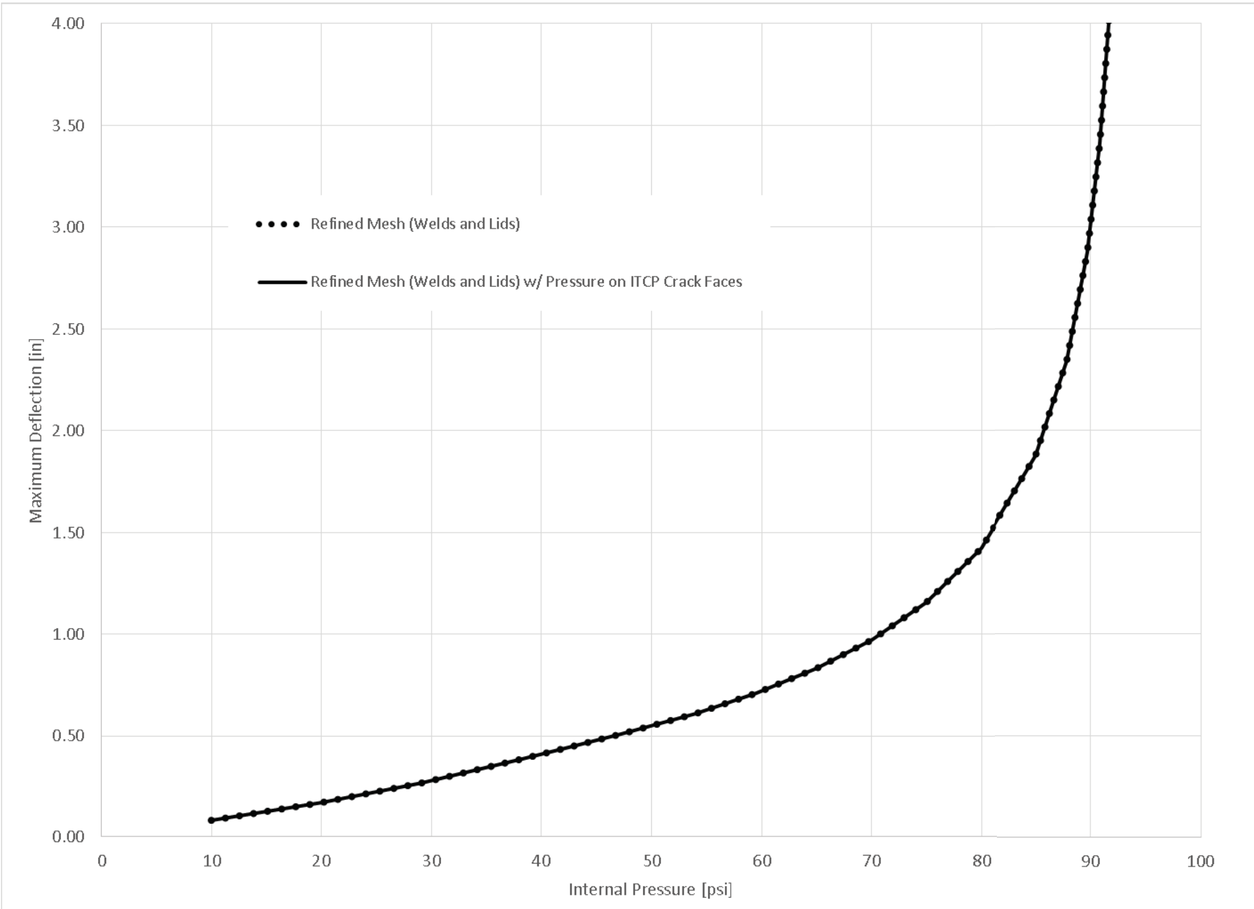

Figure 30 – Comparison of Maximum Displacement Histories for Axisymmetric Model With and Without Pressure Loading Applied to the ITCP Weld Root Flaw Faces

(Maximum deflection occurs at the center point of the lids, in the outward axial direction)

(Note that the magnitude of the deflections has no true physical meaning due to the nature of limit load analysis)

(Service Level A/B material properties)

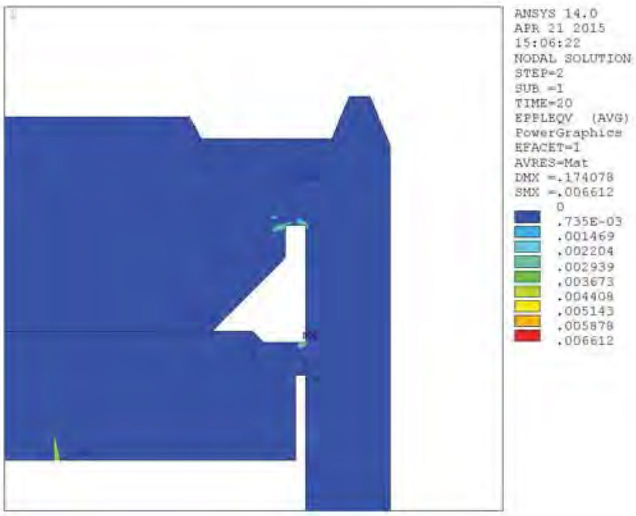

(a) Equivalent Plastic Strain in Weld Region [in/in] at 20 psi Internal Pressure

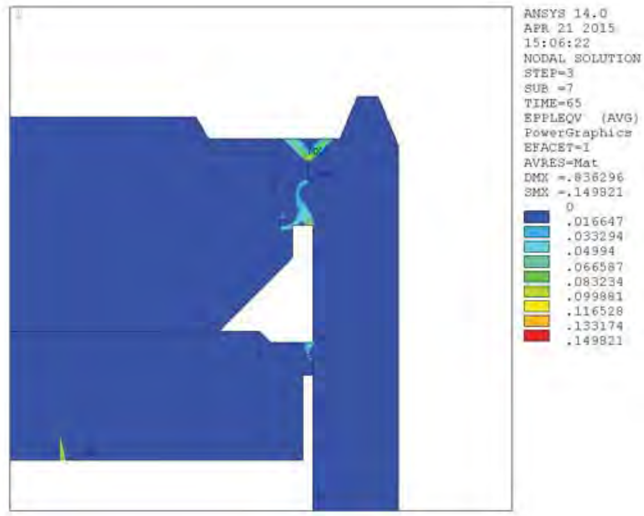

(b) Equivalent Plastic Strain in Weld Region [in/in] at 65 psi Internal Pressure

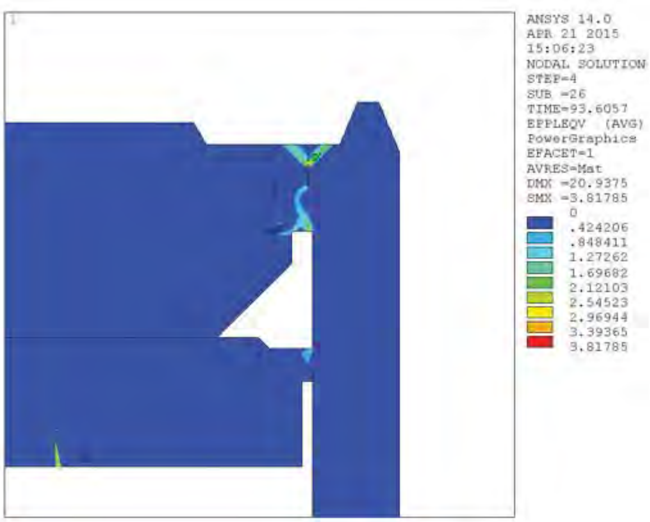

(c) Equivalent Plastic Strain in Weld Region [in/in] at 93.6 psi Internal Pressure

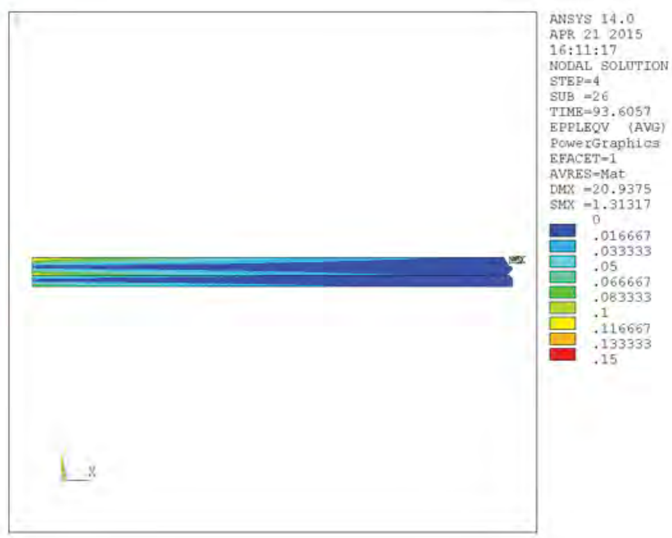

(d) EQV Plastic Strain in the Cover Plates at 93.6 psi

Figure 31 – Results for Axisymmetric Case #2 – Refined Mesh in Weld and Lid Interior Region – Service Level A/B

(Note (c) and (d) are plotted one timestep before the collapse pressure)

(Note that the magnitude of the strains and deflections has no true physical meaning due to the nature of limit load analysis)

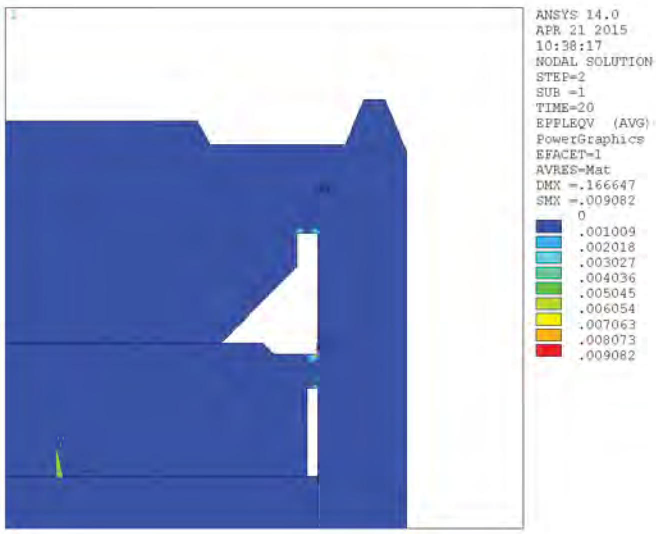

(a) Equivalent Plastic Strain in Weld Region [in/in] at 20 psi Internal Pressure

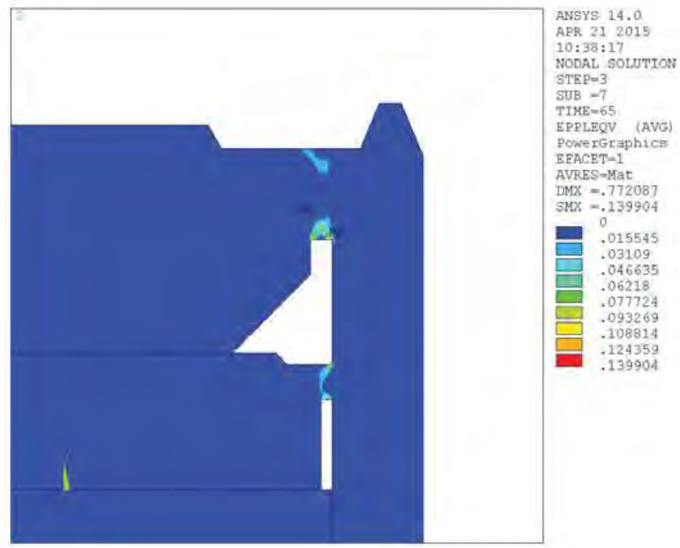

(b) Equivalent Plastic Strain in Weld Region [in/in] at 65 psi Internal Pressure

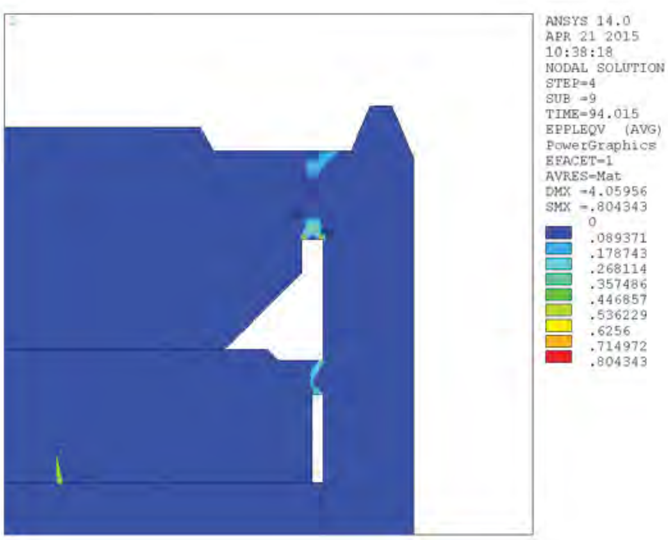

(c) Equivalent Plastic Strain in Weld Region [in/in] at 94.0 psi Internal Pressure

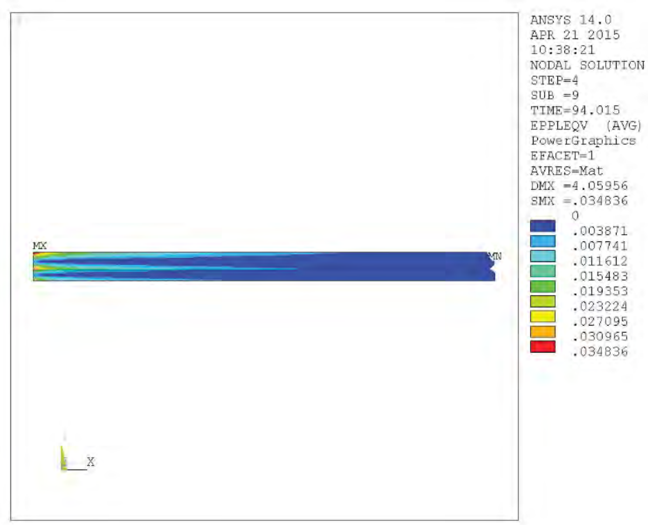

(d) EQV Plastic Strain in the Cover Plates at 94.0 psi

Figure 32 – Results for Axisymmetric Case #0 – Refined Mesh in Weld and Lid Interior Region – Service Level A/B

(Note (c) and (d) are plotted one timestep before the collapse pressure)

(Note that the magnitude of the strains and deflections has no true physical meaning due to the nature of limit load analysis)

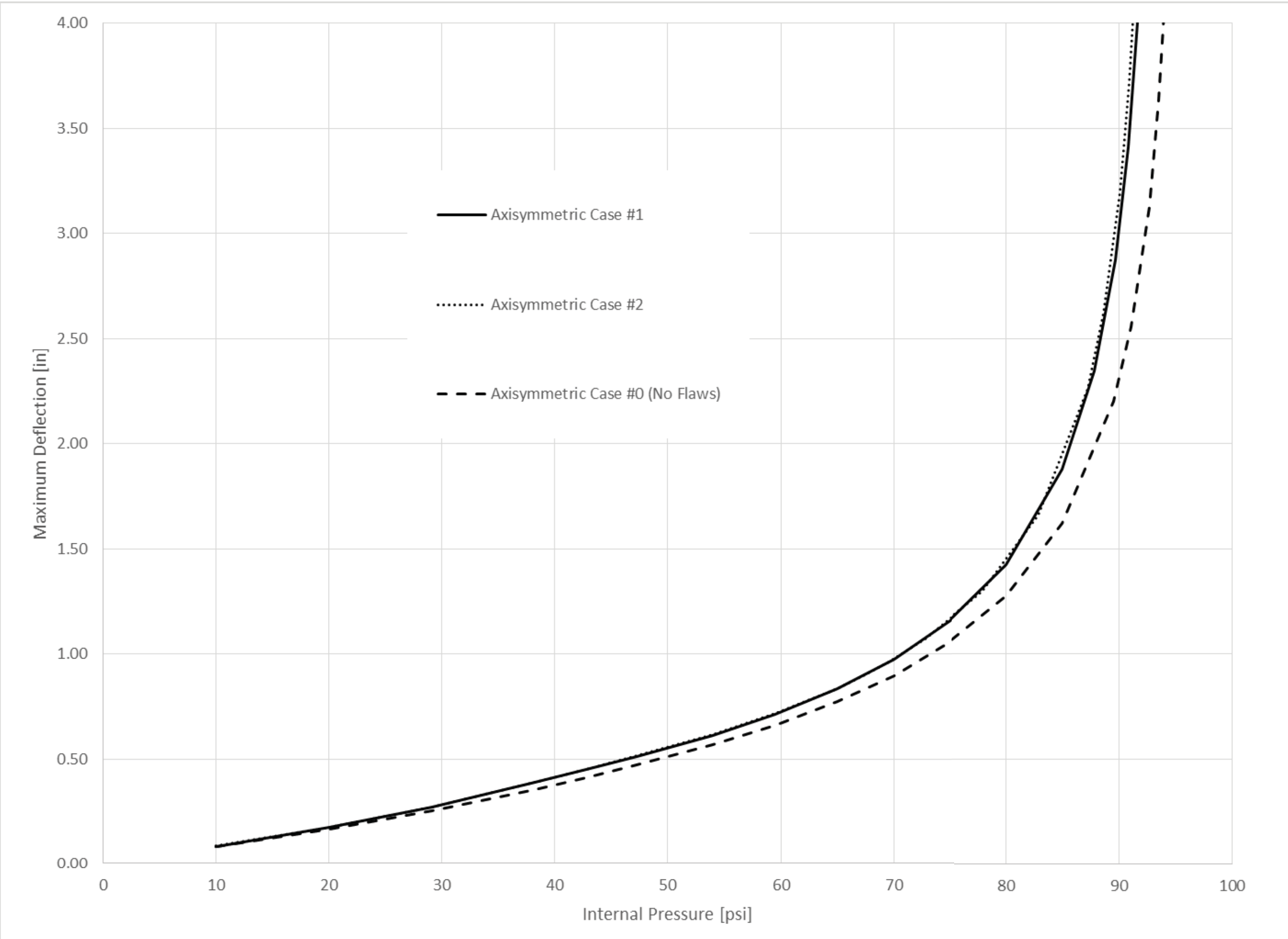

Figure 33 – Comparison of Maximum Center-of-Lid Displacement Histories for the Various Flaw Models

(Service Level A/B material properties)

(Note that the magnitude of the deflections has no true physical meaning due to the nature of limit load analysis)

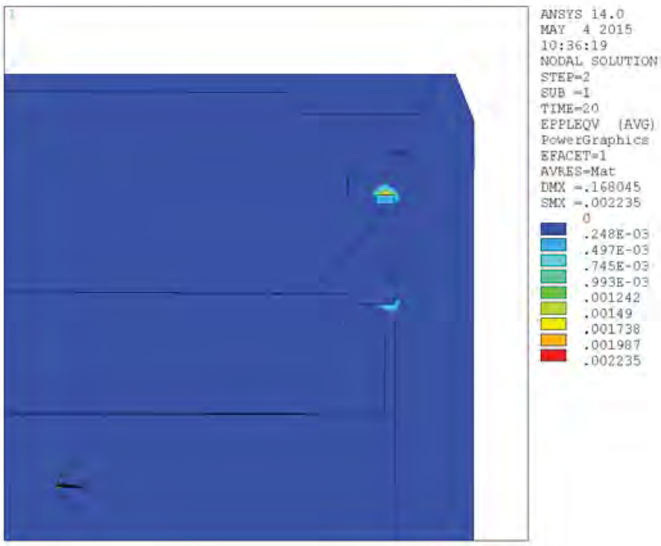

(a) Equivalent Plastic Strain in Weld Region [in/in] at 20 psi Internal Pressure

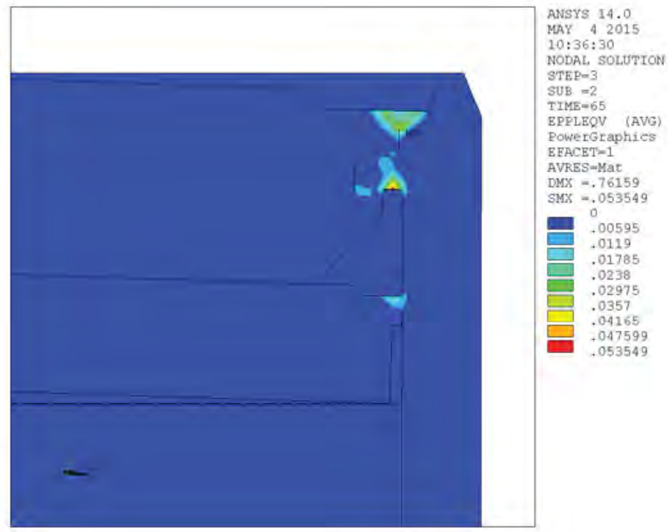

(b) Equivalent Plastic Strain in Weld Region [in/in] at 65 psi Internal Pressure

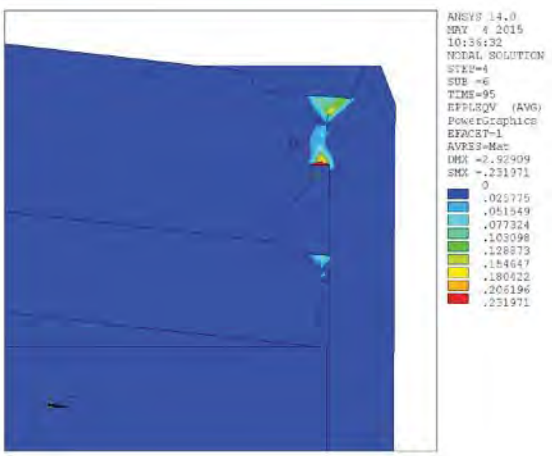

(c) Equivalent Plastic Strain in Weld Region [in/in] at 95 psi Internal Pressure

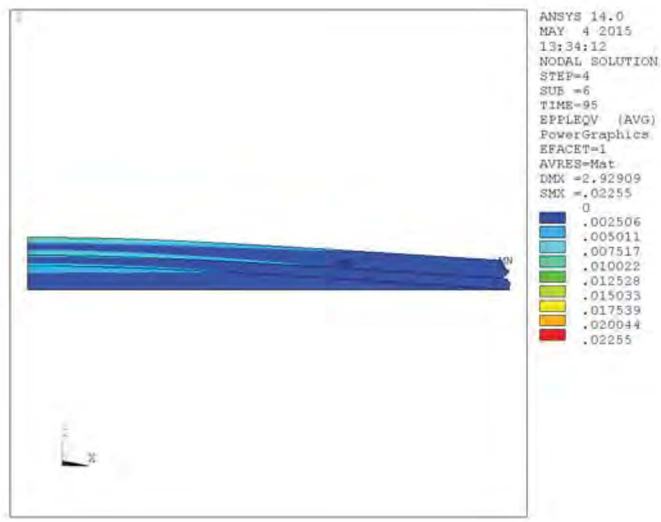

(d) EQV Plastic Strain in the Cover Plates at 95 psi

Figure 34 – Results for Half-Symmetry Case #1 Internal Pressure Loading Benchmark Analysis – Service Level A/B

(Note that the magnitude of the strains and deflections has no true physical meaning due to the nature of limit load analysis)

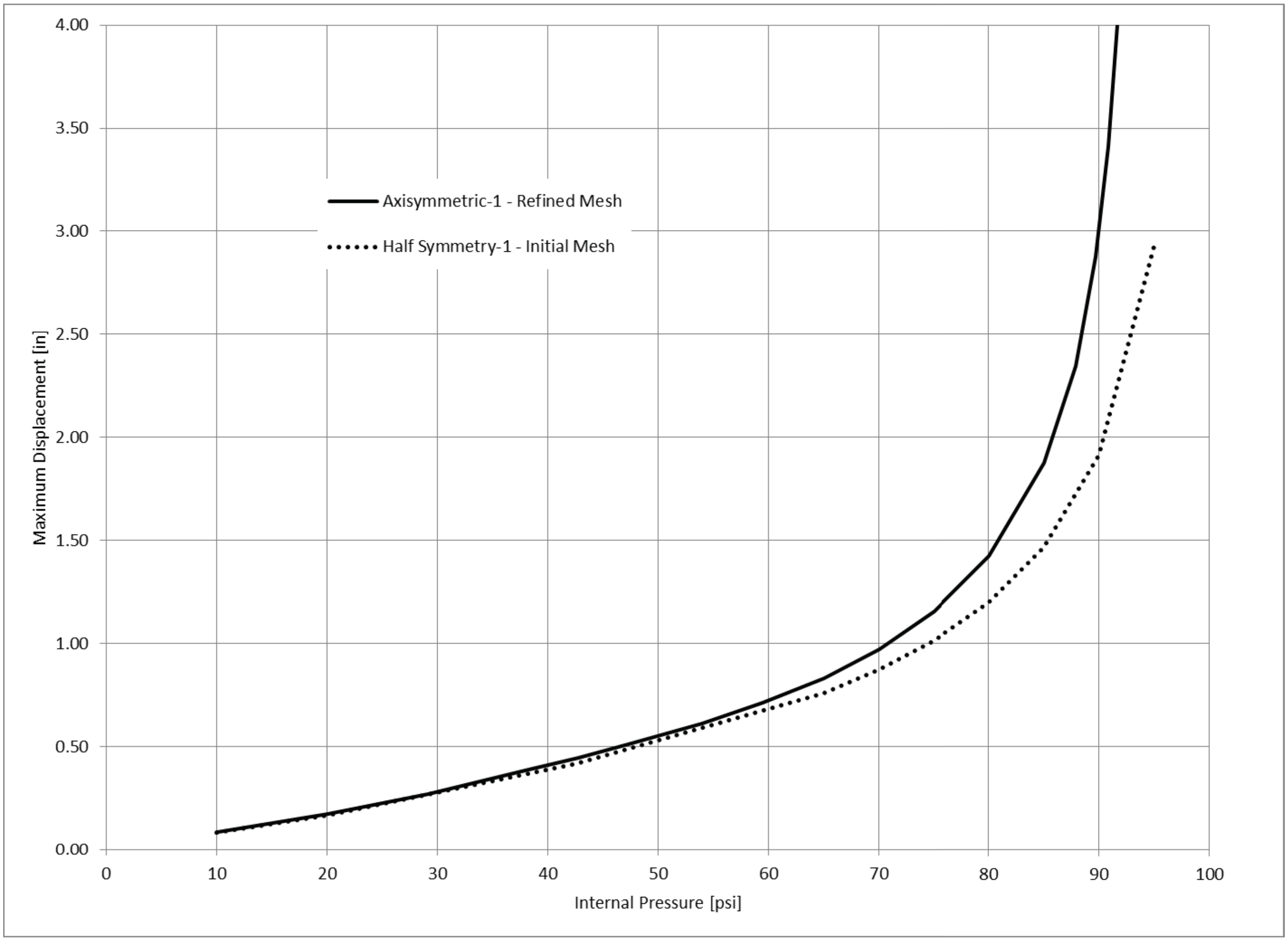

Figure 35 – Benchmark of the Half Symmetry model with the Axisymmetric Analysis

(Service Level A/B material properties)

(Note that the magnitude of the deflections has no true physical meaning due to the nature of limit load analysis)

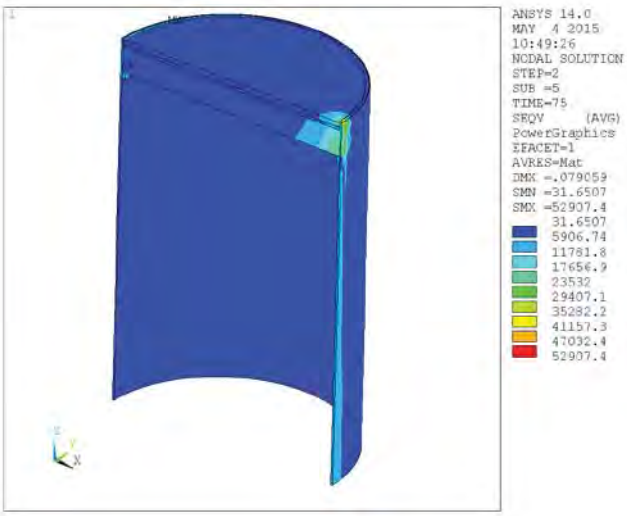

(a) Equivalent (von Mises) Stress [psi] at 75g

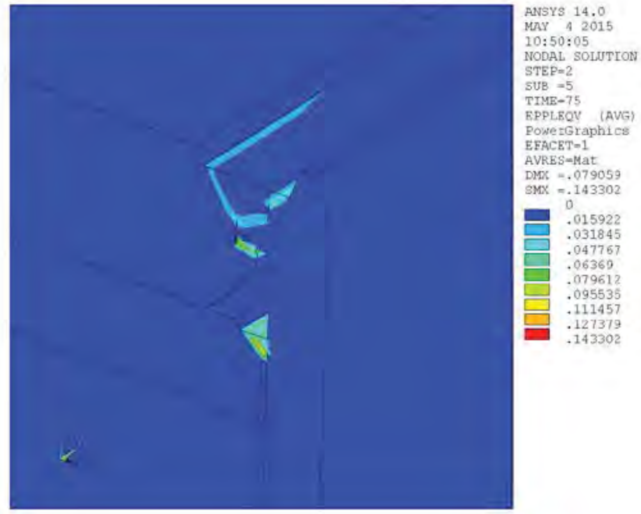

(b) Equivalent Plastic Strain in Weld Region [in/in] at 75g.

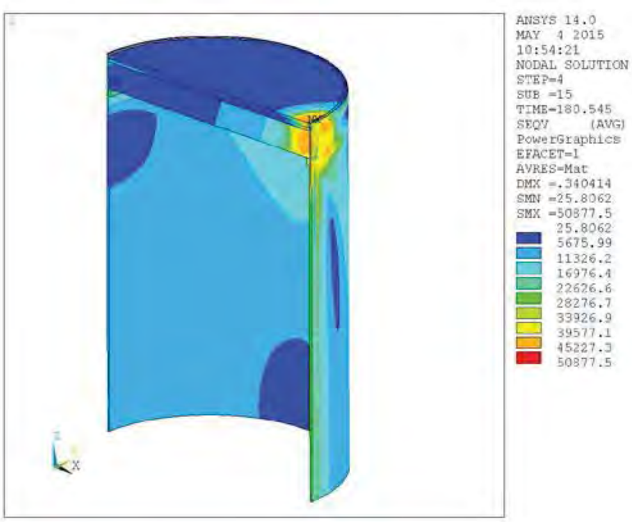

(c) Equivalent (von Mises) Stress [psi] at 181g

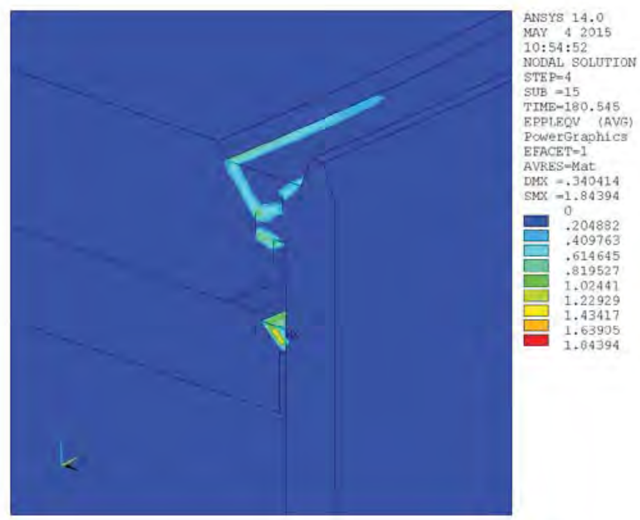

(d) Equivalent Plastic Strain in Weld Region [in/in] at 181g.

Figure 36 – Equivalent Stress and Plastic Strain Plots from the Half-Symmetry #1 Side Drop Analysis

(Note that the magnitude of the strains and deflections has no true physical meaning due to the nature of limit load analysis)

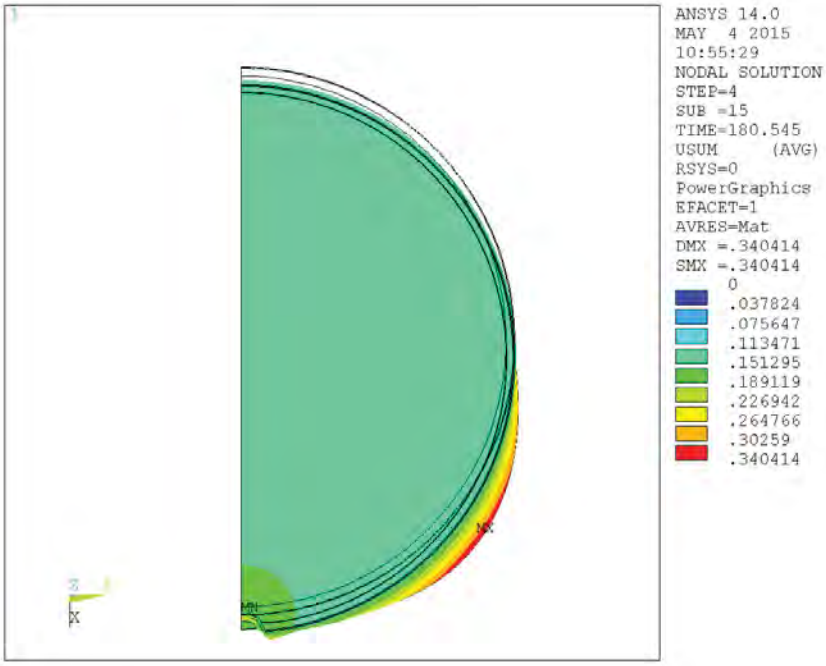

(a) Deformed Shape Plot – Axial View – Exaggerated Scale

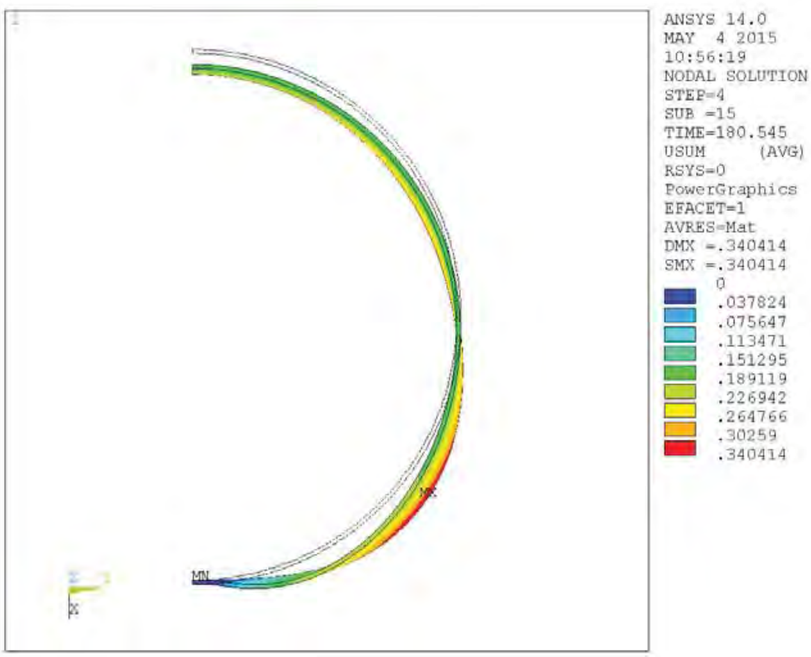

(b) Deformed Shape Plot of DSC Shell – Axial View – Exaggerated Scale

Figure 37 – Additional Results Plots from the Half-Symmetry #1 Side Drop Analysis

(Note that the magnitude of the deflections has no true physical meaning due to the nature of limit load analysis)

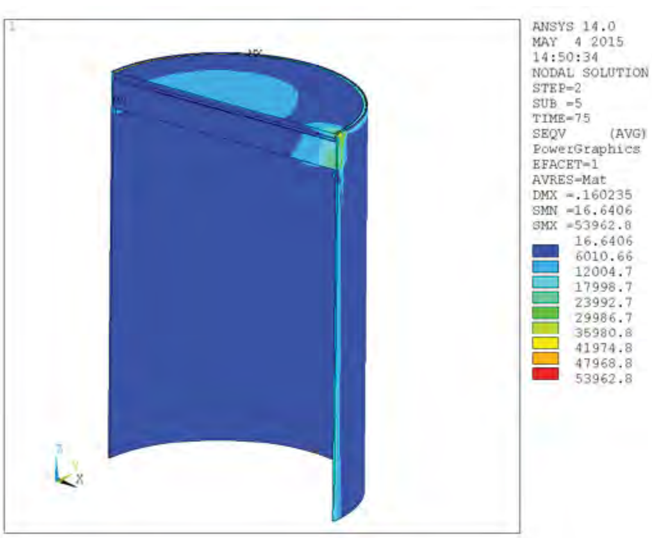

(a) Equivalent (von Mises) Stress [psi] at 75g

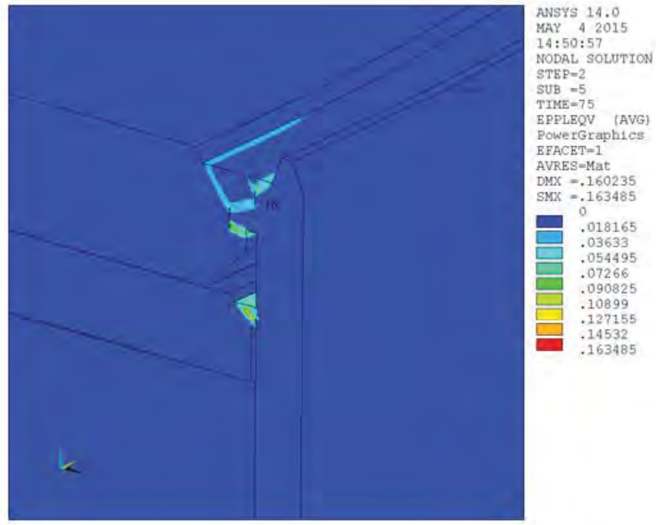

(b) Equivalent Plastic Strain in Weld Region [in/in] at 75g.

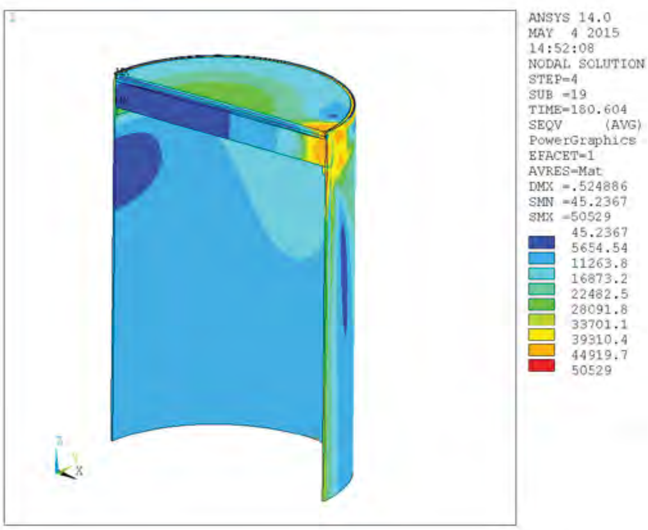

(c) Equivalent (von Mises) Stress [psi] at 181g

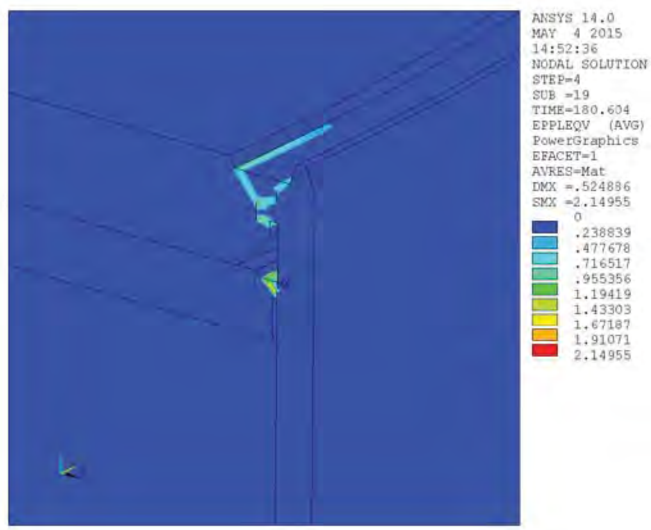

(d) Equivalent Plastic Strain in Weld Region [in/in] at 181g.

Figure 38 – Equivalent Stress and Plastic Strain Plots from the Half-Symmetry #1 Side Drop Analysis with Off-Normal Internal Pressure

(Note that the magnitude of the strains and deflections has no true physical meaning due to the nature of limit load analysis)

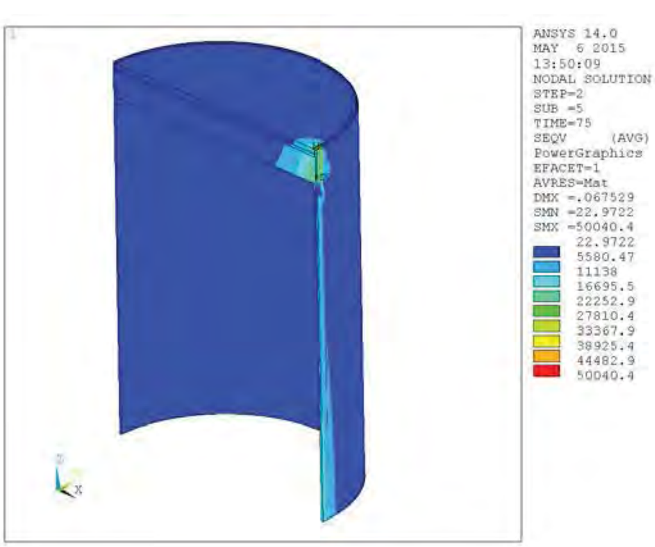

(a) Equivalent (von Mises) Stress [psi] at 75g

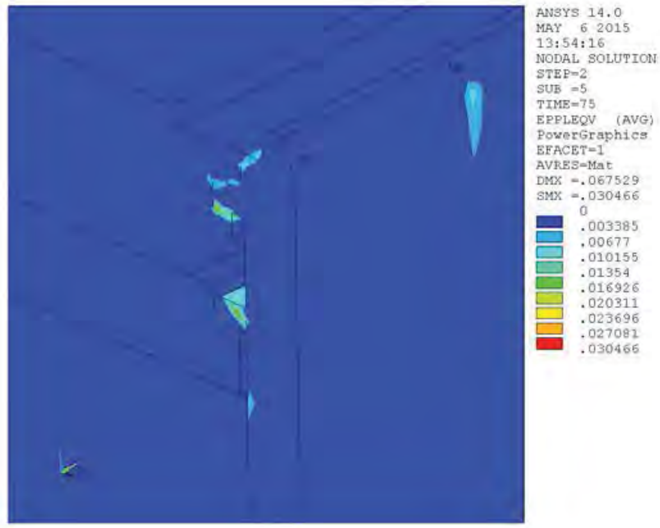

(b) Equivalent Plastic Strain in Weld Region [in/in] at 75g.

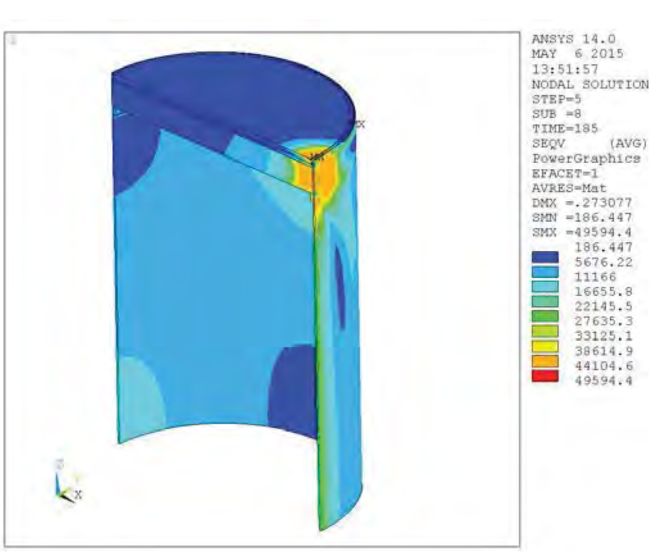

(c) Equivalent (von Mises) Stress [psi] at 185g

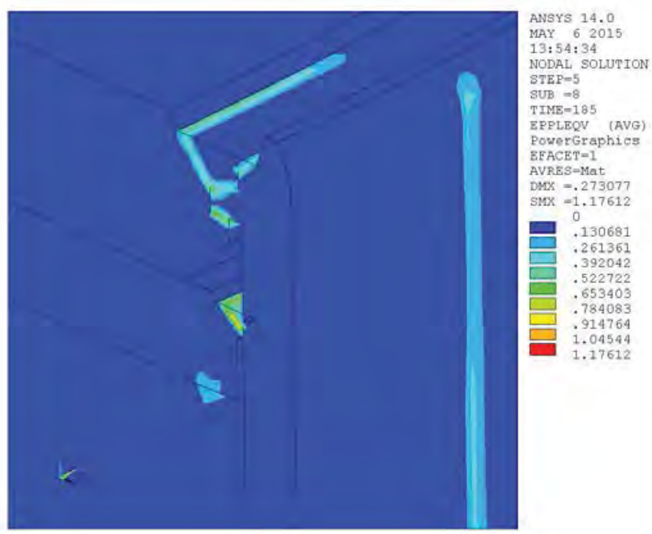

(d) Equivalent Plastic Strain in Weld Region [in/in] at 185g.

Figure 39 – Equivalent Stress and Plastic Strain Plots from the Half-Symmetry #1 Side Drop Analysis with Refined Circumferential Mesh

(Note that the magnitude of the strains and deflections has no true physical meaning due to the nature of limit load analysis)

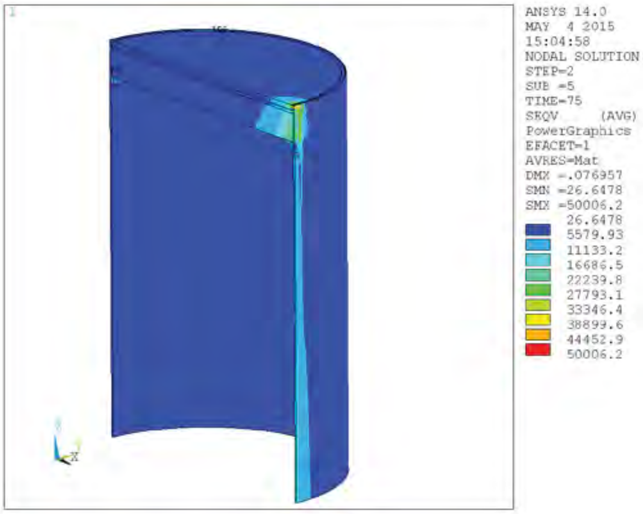

(a) Equivalent (von Mises) Stress [psi] at 75g

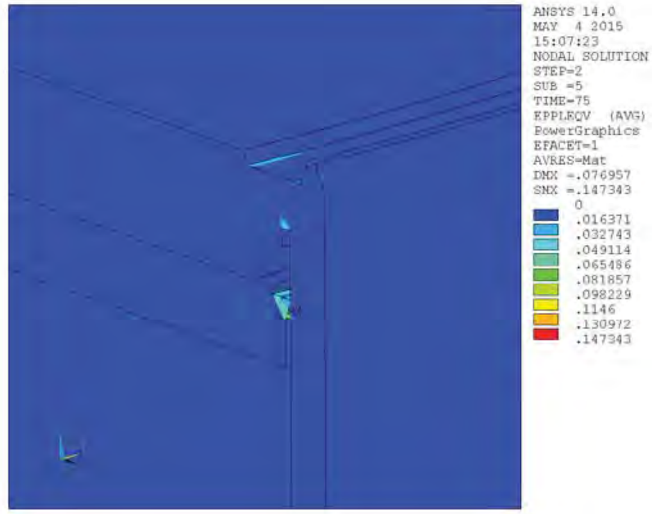

(b) Equivalent Plastic Strain in Weld Region [in/in] at 75g.

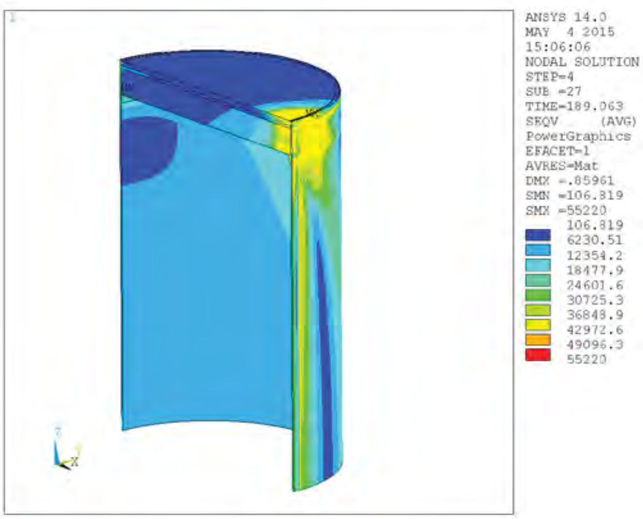

(c) Equivalent (von Mises) Stress [psi] at 189g

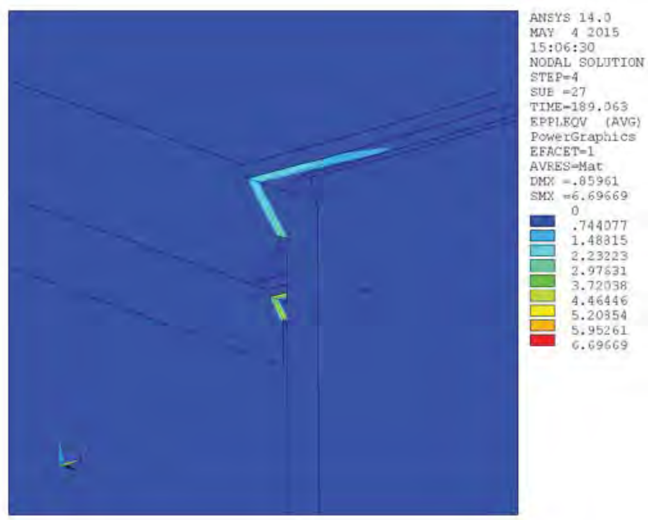

(d) Equivalent Plastic Strain in Weld Region [in/in] at 189g.

Figure 40 – Equivalent Stress and Plastic Strain Plots from the Half-Symmetry #0 (No Flaws) Side Drop Analysis

(Note that the magnitude of the strains and deflections has no true physical meaning due to the nature of limit load analysis)

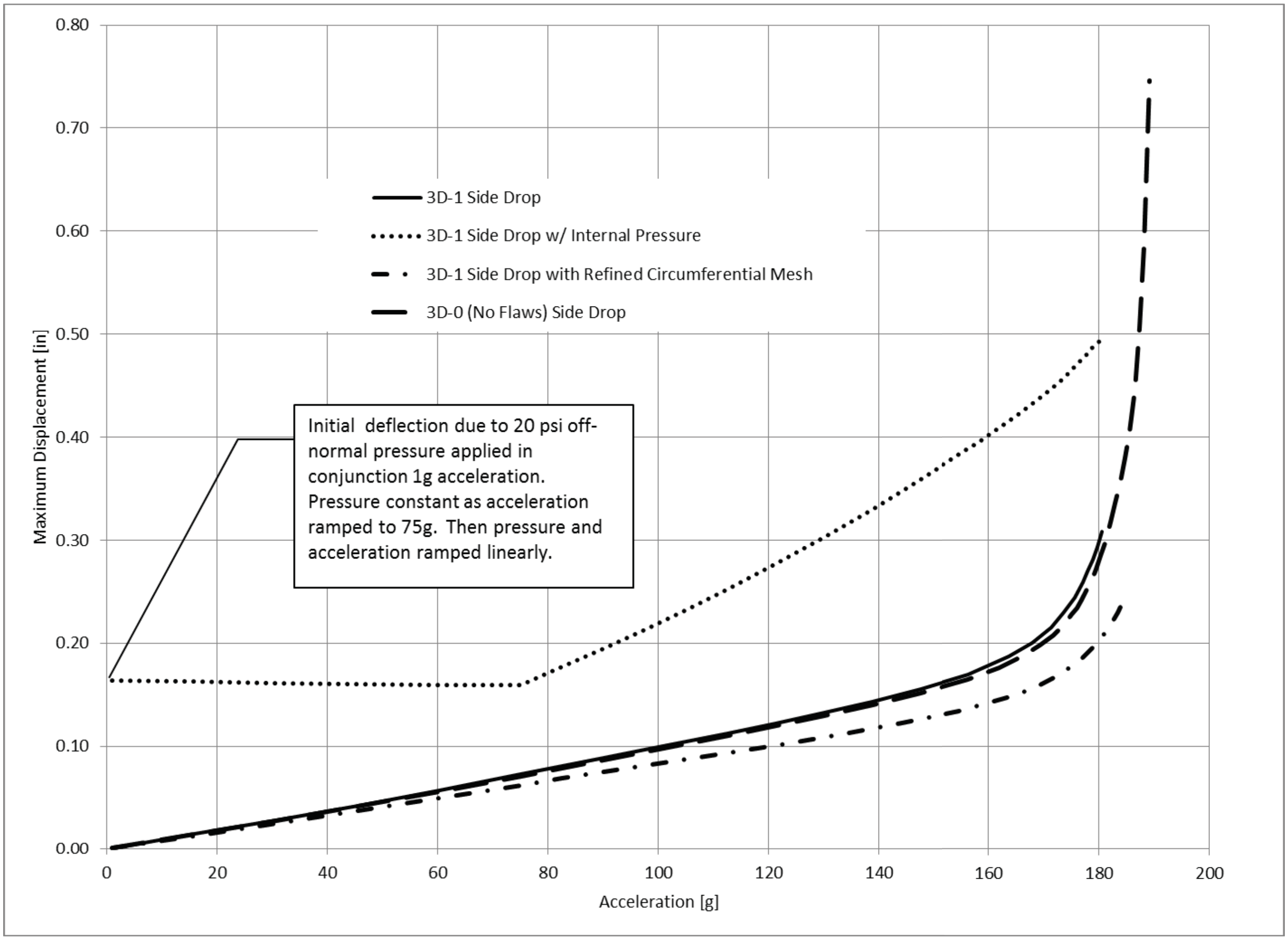

Figure 41 – Comparison of Maximum Displacement Histories for the Various Half-Symmetry Analyses

(Service Level D material properties)

(Note that the magnitude of the strains and deflections has no true physical meaning due to the nature of limit load analysis)

10.0 APPENDIX A –ELASTIC-PLASTIC ANALYSES

Purpose

The purpose of this appendix is to document elastic-plastic analyses of DSC-16. The models listed below are used as a basis for the analyses.

Axisymmetric 1 with Refined Welds and Lid Mesh

Half Symmetry 1 with Initial Mesh

These models produced the bounding results using the limit load methodology. The models are updated to include the elastic-plastic material properties described below. In addition, these new runs consider the effects of large-deformations (NLGEOM,ON). The intent of these analyses is to provide a more realistic prediction of the actual material strains that would occur under the design basis loading, as opposed to the over-estimated strains and deformations which result from the limit-load analysis methodology.

Material Properties

The elastic-plastic behavior of SA-240 Type 304 stainless steel is idealized using Ramberg-Osgood stress-strain curve constants calculated using the equations in Appendix B of Reference A1[2]. The constants are calculated using the ASME code [Ref.5.16] specified minimum yield and ultimate strength values at the applicable temperatures. In order to incorporate the curves into the ANSYS analysis, the initial slope of the curves must match the defined elastic modulus. Therefore the first data point in the curves is defined at the (strain,stress) data point (S_y/E,S_y). The material behavior is based on true stress and true strain, since the ANSYS analysis accounts for changes in geometry (e.g. necking). The following equations from Reference A1 were used to develop the curves:

$$\frac{\epsilon}{\epsilon_o} = \frac{\sigma}{\sigma_o} + \alpha\left(\frac{\sigma}{\sigma_o}\right)^n$$

$$\epsilon = true\ strain$$

$$\epsilon_o = true\ strain\ at\ yield$$

$$\sigma = true\ stress$$

$$\sigma_o = true\ stress\ at\ yield$$

$$n = \frac{1}{ln(1+e_u)}$$

$$\alpha = \left[\frac{ln(1+\mathrm{e_u})}{ln\left(1+\frac{\sigma_y}{\mathrm{E}}\right)} - \frac{\sigma_u(1+\mathrm{e_u})}{\sigma_y\left(1+\frac{\sigma_y}{\mathrm{E}}\right)}\right]\left[\frac{\sigma_u(1+\mathrm{e_u})}{\sigma_y\left(1+\frac{\sigma_y}{\mathrm{E}}\right)}\right]^{-\mathrm{n}}$$

$$e_u = engineering\ strain\ at\ the\ ultimate\ tensile\ strength$$

$$\sigma_y = engineering\ yield\ stress$$

[2] The equations in Reference A1 to develop the full-range true stress-strain curve are based on curve fits of tensile test data. The resulting curve is not indicative of a specific failure type or analysis approach. Rather, it is a method to develop a full-range stress-strain curve of a material using a limited set of data (i.e. minimum specified yield and ultimate strengths.)

$$\sigma_u = engineering\ ultimate\ strength$$

The value of e_u is taken as 0.35, which is assumed to be e_{tot}-0.05, where e_{tot} is taken as the minimum specified elongation of the material (40%), per Reference A2.

The relationship between true and engineering stress and strain is per the following equations:

$$\sigma_{true} = \sigma_{eng}(e_{eng} + 1)$$
$$\epsilon_{true} = ln(e_{eng} + 1)$$

Figure A-1 shows both the true and engineering stress strain curves based on the Ramberg-Osgood equations. The curves at various temperatures as coded into the ANSYS analysis are shown in Figure A-2.

The SA-36 shield plugs use a bi-linear stress strain curve with a tangent modulus of 1% of the initial elastic modulus. This results in a less stiff representation of the shield plug, which will result in conservatively greater strains in the DSC.

Load Cases

Analyses are performed for the following load cases:

1. Internal pressure loading (32 psi) for Service Level A/B.
2. Internal pressure loading (65 psi) for Service Level D.
3. Side drop Loading (75g) for Service Level D.

As discussed in Section 4.2, these three load cases bound all of the design loading conditions for the DSC OTCP and ITCP welds.

<u>Results and Conclusion</u>

Plots of the equivalent plastic strain for the three analyses are shown in Figure A-3 through A-5. The results are summarized in Table A-1. As shown by the results, the strain levels remain well below the minimum specified elongation limits of Type 304 steel and Type 308 weld electrodes [Ref. A2 and A3]. Therefore, material rupture will not occur at the design conditions.

The maximum strains at loads up to 1.5x the specified loading are also extracted. These results are shown in Table 7, which also includes a comparison of the peak strain values to the ductility limit of the material reduced by the weld uncertainty factor of 0.8 discussed in Section 3.4. See Section 7.0 for further discussion and conclusions.

References

A1. EPRI NP-5531. Evaluation of High-Energy Pipe Rupture Experiments. January 1988.

A2. ASME Section II Part A. Ferrous Material Specifications. 1998 Edition with Addenda through 2000.

A3. ASME Section II Part C. Specifications for Welding Rods, Electrodes, and Filler Metals. 1998 Edition with Addenda through 2000.

Computer Files

Analyses performed on Computer HEA-0213A using ANSYS Version 14.0 [Ref. 5.6]

File date & time listing is as displayed by the Windows 7 Operating System – Differences may occur due to local time zone and daylight savings settings.

Analysis Case	File Name	Date & Time
Elastic-Plastic Axisymmetric 1 Refined Lids and Welds Internal Pressure SL A/B	61BTH_WeldFlaw_1F_AX_2_DETACH.db	11/29/2015 8:41 AM
	61BTH_WeldFlaw_1F_AX_2_DETACH.rst	11/29/2015 8:18 AM
	SOLUTION_AXISYMM_IP_500F.INP	11/27/2015 4:03 PM
Elastic-Plastic Axisymmetric 1 Refined Lids and Welds Internal Pressure SL D	61BTH_WeldFlaw_1F_AX_2_DETACH.db	11/27/2015 3:36 PM
	61BTH_WeldFlaw_1F_AX_2_DETACH.rst	11/27/2015 3:33 PM
	SOLUTION_AXISYMM_IP_625F.INP	11/19/2015 11:46 AM
Elastic-Plastic Half-Symmetry 1 Initial Mesh Side Drop SL D	61BTH_WeldFlaw_1GC.db	11/29/2015 8:16 AM
	61BTH_WeldFlaw_1GC.rst	11/27/2015 6:26 PM
	SOLUTION_HALFSYM_SD.INP	11/20/2015 10:08 AM
Stress-Strain Curve Development	Stress-Strain.xls	11/30/2015 10:59 AM

Table A-1 – Summary of Elastic-Plastic Analysis Results.

Analysis Case	Result	Value [in/in]
Internal Pressure Service Level A Axisymmetric (Note 1)	Equivalent Plastic Strain at 32 psi Internal Pressure (Note 1)	0.0183 (1.83%)
Internal Pressure Service Level D Axisymmetric	Equivalent Plastic Strain at 65 psi Internal Pressure	0.0597 (5.97%)
Side Drop Service Level D Half-Symmetry	Equivalent Plastic Strain at 75g Acceleration	0.0609 (6.09%)

Note 1: The 32 psi internal pressure is bounding for Service Levels A and B and includes design internal pressure of 10 psi plus an additional 22 psi to account for inertial loading of the DSC contents onto the lid. See Section 4.2 for details.

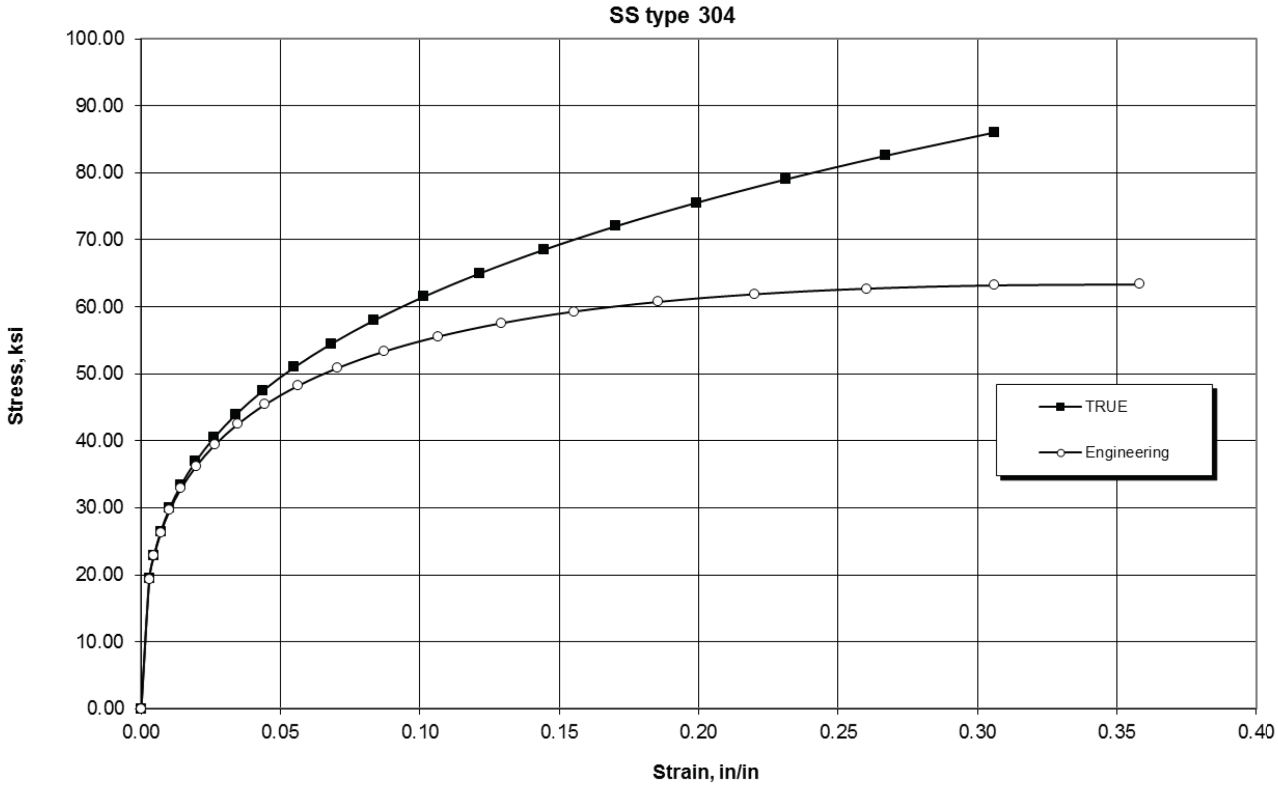

Figure A-1 – Ramberg-Osgood Derived Stress Strain Curve for SA-240 Type 304 at 500 ^{o}F.

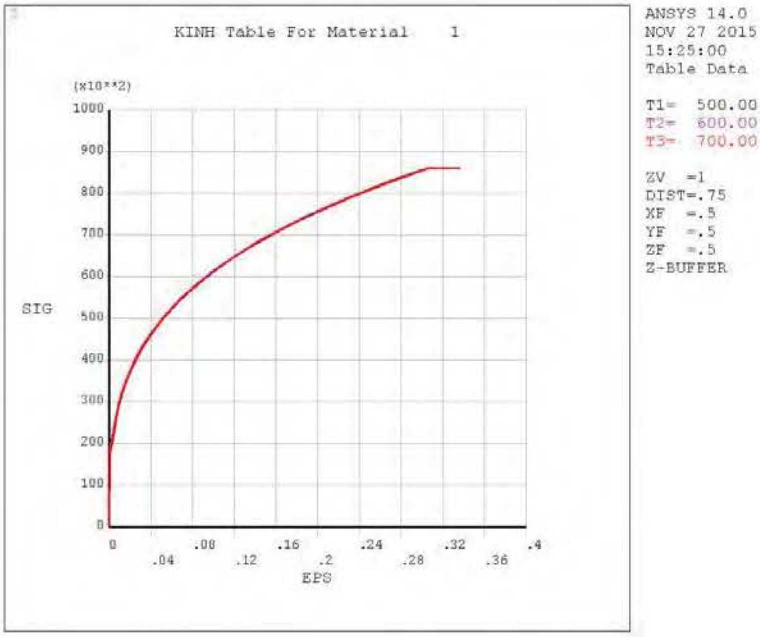

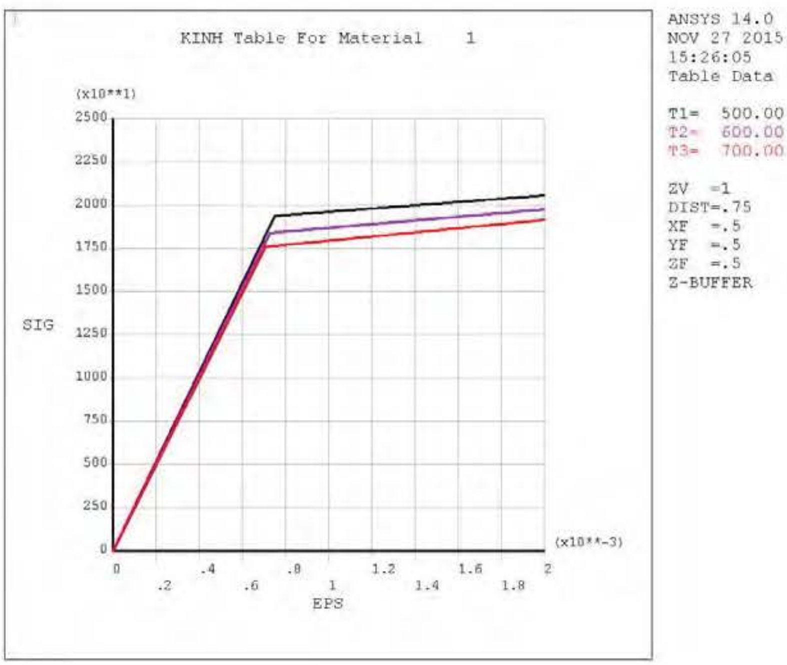

Figure A-2 – Ramberg-Osgood Stress Strain Curves for SA-240 Type 304 from ANSYS Model at Various Temperatures.
Upper image shows full range of curves (strain axis from 0 to 40%), lower image shows detail of the initial yield point (strain axis from 0 to 0.2%)

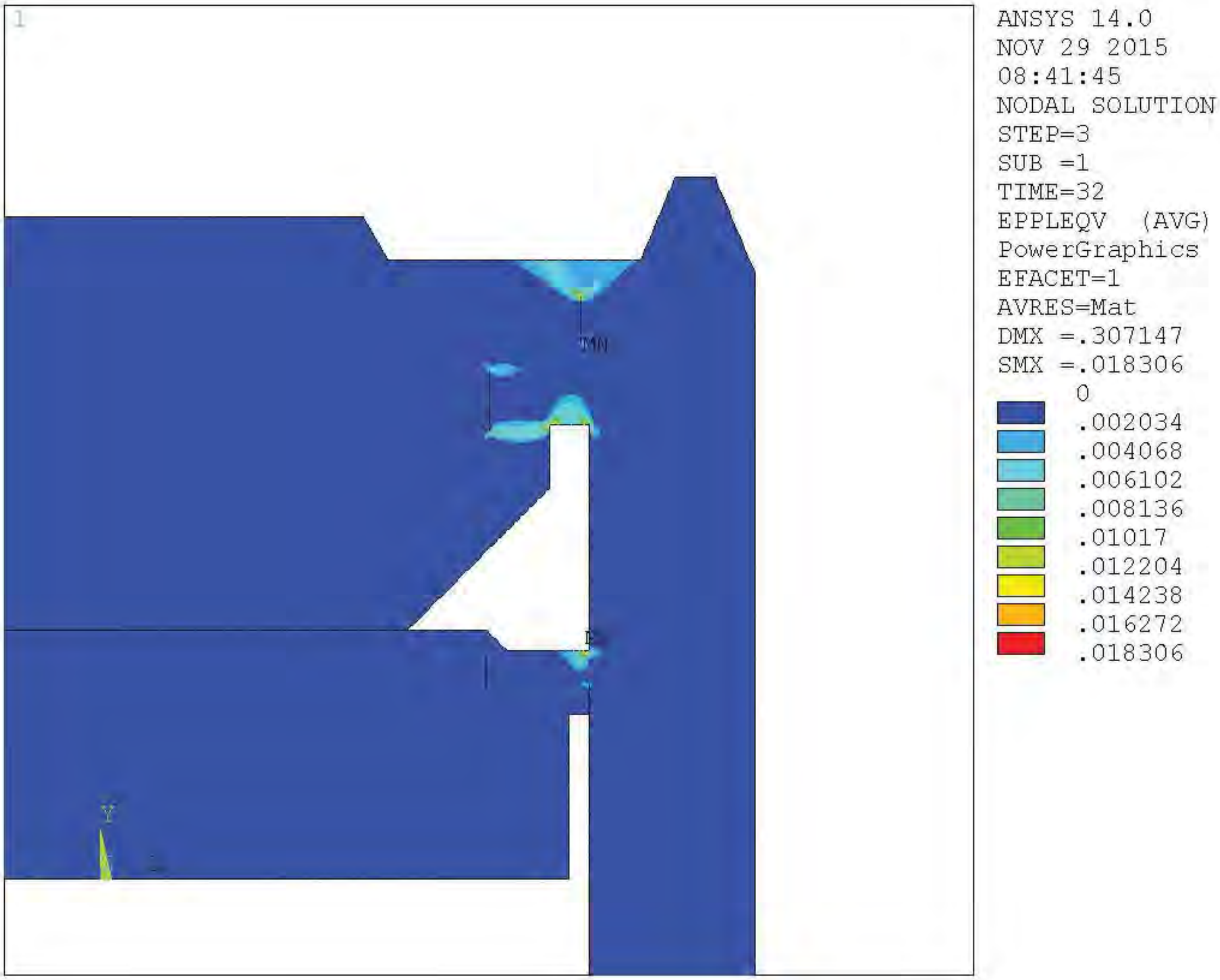

Figure A-3 – Service Level A Internal Pressure - Equivalent Plastic Strain at 32 psi *Note

*Note: The 32 psi internal pressure is bounding for Service Levels A and B and includes design internal pressure of 10 psi plus an additional 22 psi to account for inertial loading of the DSC contents onto the lid. See Section 4.2 for details.

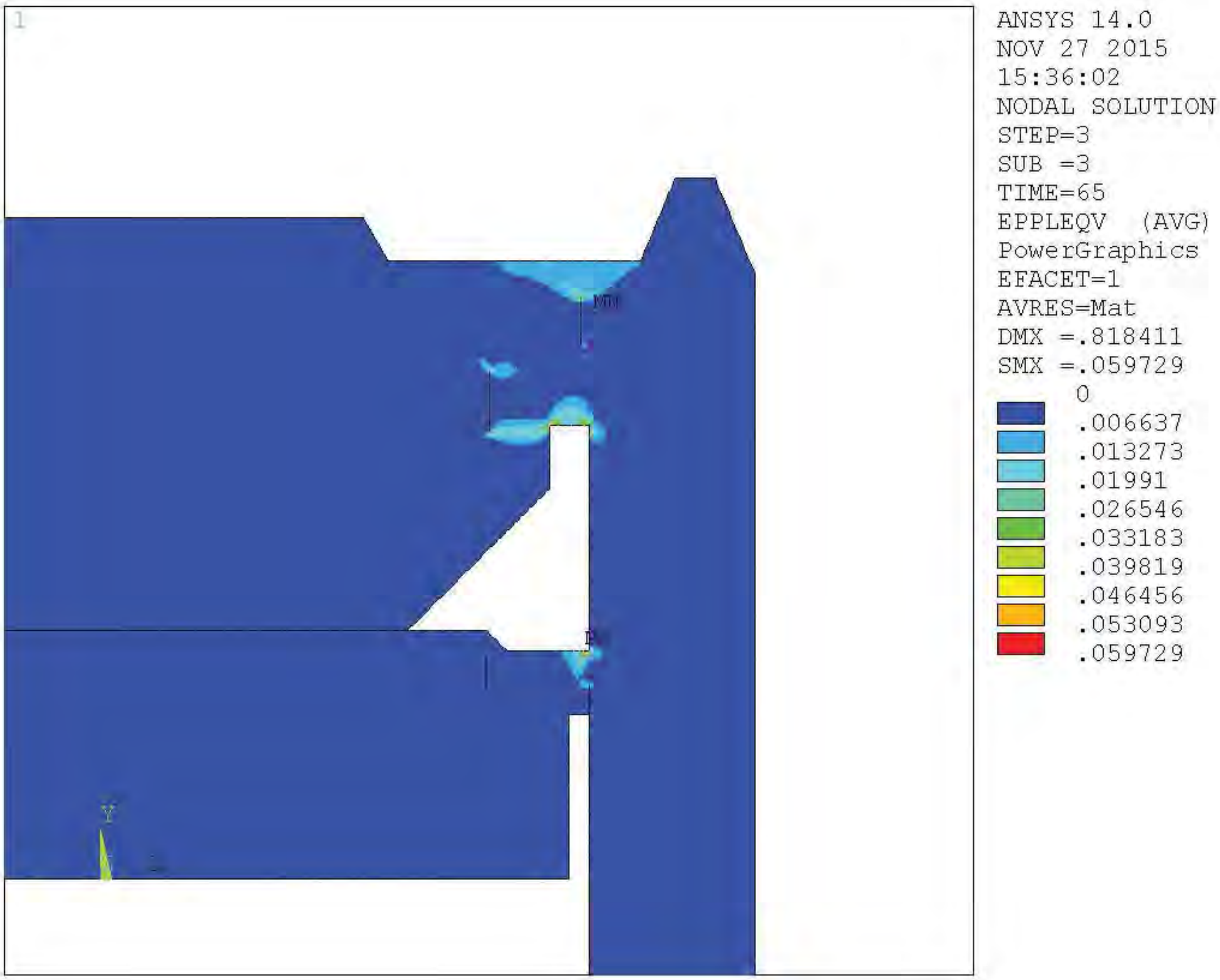

Figure A-4 – Service Level D Internal Pressure - Equivalent Plastic Strain at 65 psi

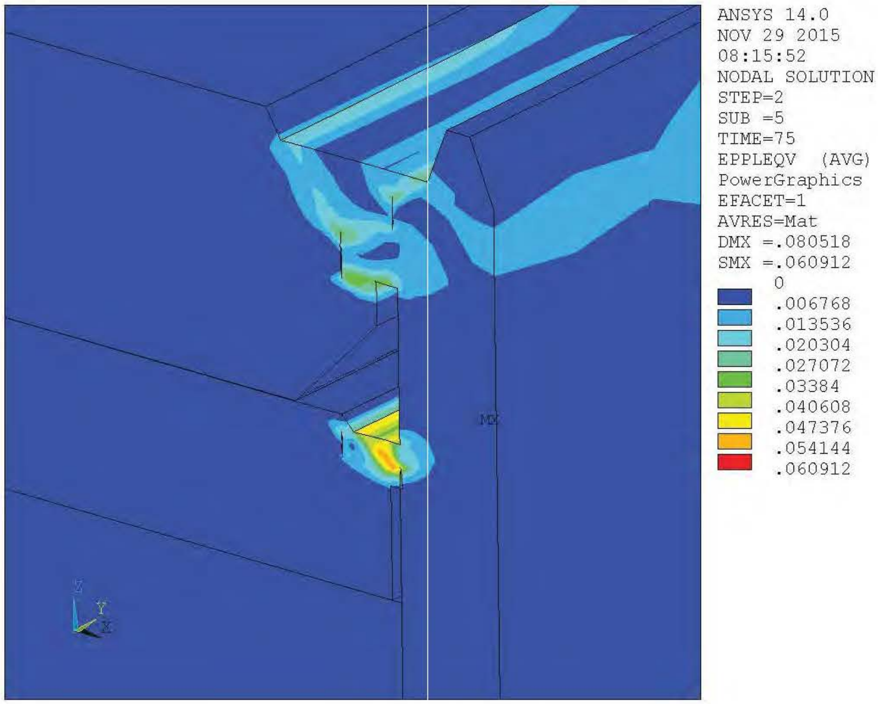

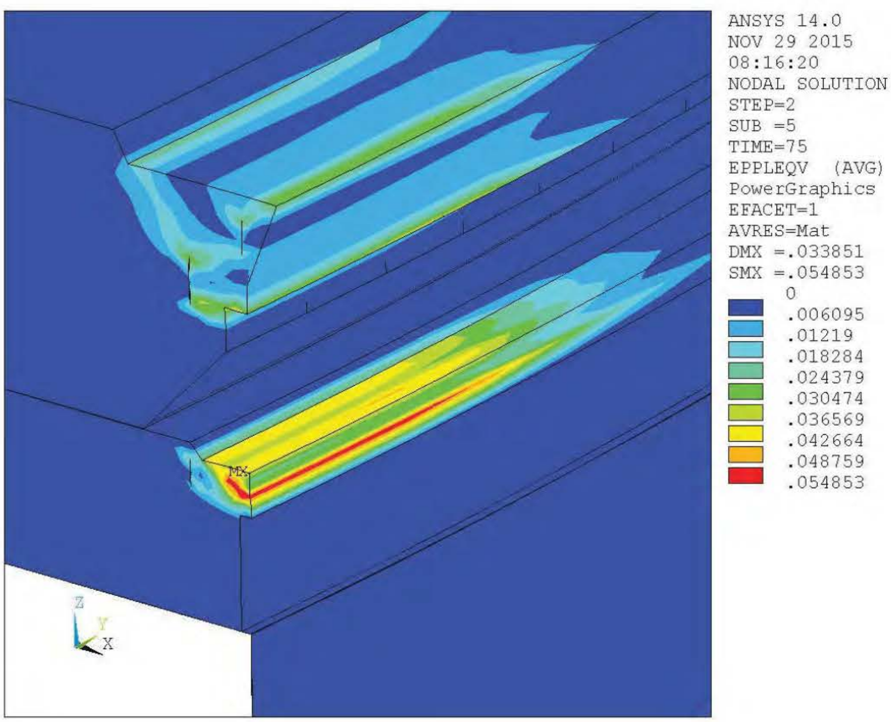

Figure A-5 – Service Level D Side Drop - Equivalent Plastic Strain at 75g.
Upper image shows all DSC components, lower image is without shell to allow view of the weld surface. The peak strain of 6.09% occurred on the surface of the shell. Therefore, when the shell was removed for the lower image, the peak strain reported reduced to 5.49%.

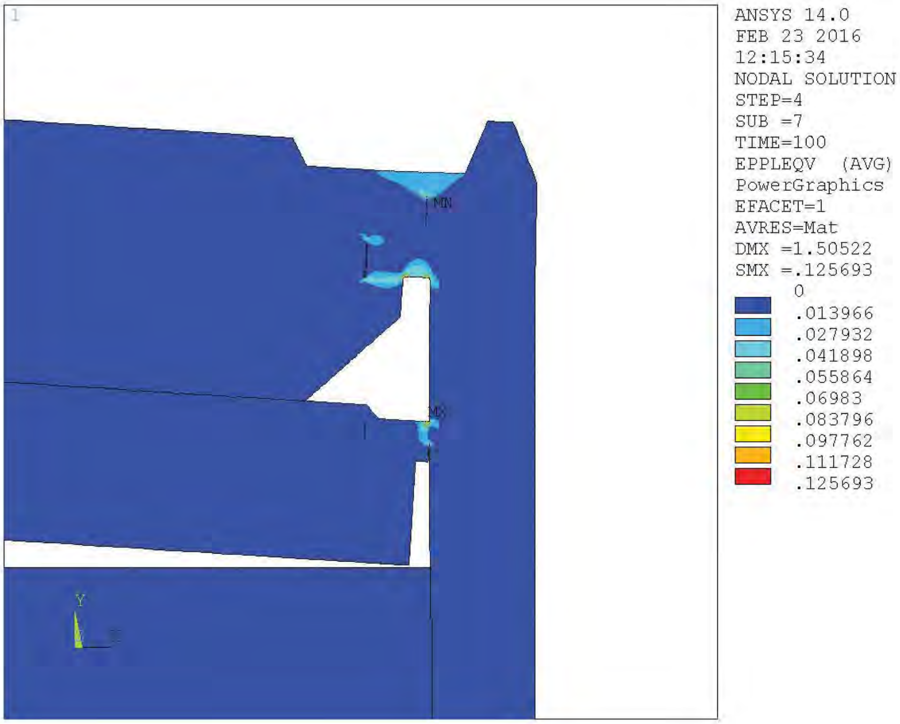

Figure A-6 – Service Level D Internal Pressure - Equivalent Plastic Strain at 100 psi.

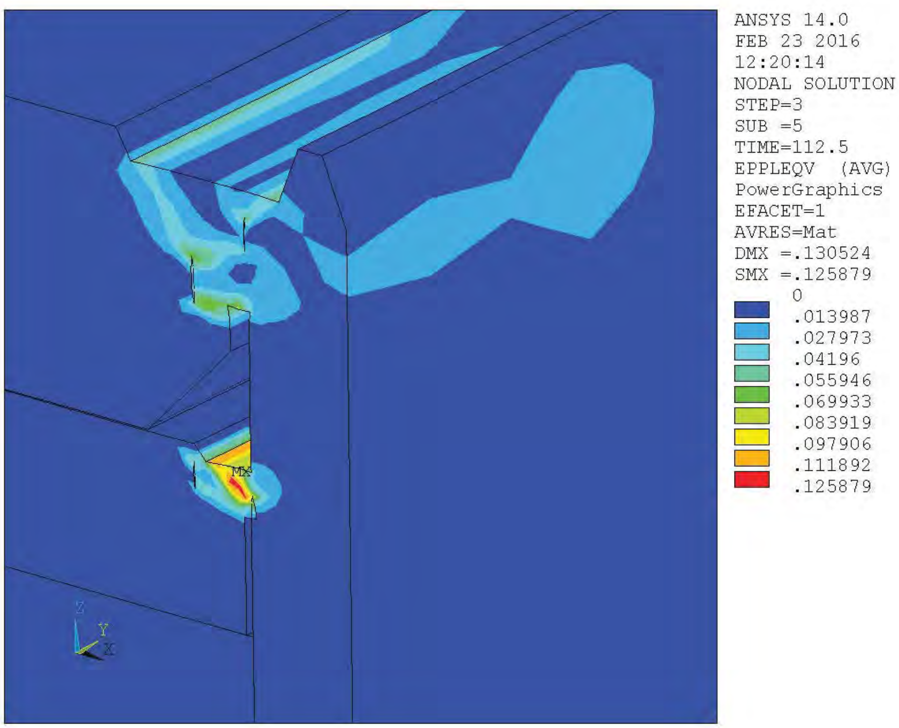

Figure A-7 – Service Level D Side Drop - Equivalent Plastic Strain at 112.5g.

ENCLOSURE 6

AREVA CALCULATION 11042-0207, REVISION 0

NUHOMS® 61BTH TYPE 1 DSC ITCP AND OTCP MAXIMUM WELD FLAW EVALUATION

34 pages follow

AREVA	Form 3.2-1 Calculation Cover Sheet Revision 12	Calculation No.:	11042-0207
		Revision No.:	0
		Page: 1 of 34	
DCR NO (if applicable): N/A	**PROJECT NAME:** NUHOMS® 61BTH Type 1 DSCs for Monticello Nuclear Generating Plant		
PROJECT NO: 11042	**CLIENT:** Xcel Energy		

CALCULATION TITLE:
NUHOMS® 61BTH Type 1 DSC ITCP and OTCP Maximum Weld Flaw Evaluation

SUMMARY DESCRIPTION:

1) Calculation Summary

This calculation qualifies Monticello 61BTH Type 1 DSCs 11-15 with the maximum flaws in the Inner Top Cover Plate (ITCP) and Outer Top Cover Plate (OTCP) closure welds.

2) Storage Media Description

Coldstor - \areva_tn\11042\11042-0207-000

If original issue, is licensing review per TIP 3.5 required?
Yes ☐ **No** ☒ **(explain below)** **Licensing Review No.:**

This calculation is prepared in support of license exemption request which will be reviewed and approved by the NRC. Therefore, a licensing review per TIP 3.5 is not required.

Software utilized (subject to test requirements of TIP 3.3): ANSYS	**Software Version:** 17.1	**Software Log Revision:** 35
Calculation is complete Originator Name and Signature: Naveen SINGH *2D-Axisymmetric (model + documentation)* Naveen Samuel TISSOT *Half-symmetric (model + documentation)*		**Date:** 08/09/17 08/08/2017
Calculation has been checked for consistency, completeness, and correctness Checker Name and Signature: Lakshmi Pendyala *2D-Axisymmetric FE model* Lakshmi Pendyala Vereesh Sayagavi *Half-symmetric FE model + documentation*		**Date:** 8.9.2017 08.09.17
Calculation is approved for use Project Engineer Name and Signature: Raheel Haroon		**Date:** 8/9/2017

REVISION SUMMARY

Rev.	Description	Affected Pages	Affected Files
0	Initial issue	All	All

TABLE OF CONTENTS

LIST OF TABLES

LIST OF FIGURES

Page

1.0 PURPOSE

The purpose of this calculation is to evaluate NUHOMS® 61BTH Type 1 (DSCs 11-15) at the Monticello Nuclear Generating Plant (MNGP) per ASME Section III criteria with the maximum flaws in the Inner and Outer Top Cover Plates (ITCP and OTCP) closure welds based on the evaluation performed in the reference calculation [5.3].

2.0 ASSUMPTIONS

1. Assumptions 1 through 6 of Ref. [5.3] are applicable to this calculation.
2. The flaws (at the same locations as Ref. [5.3]) are allowed to be increased until the design limits criteria are reached.
3. The DSC design in this calculation is typical of MNGP DSCs 11-16, and the modeled baseline flaws are representative of those indications identified by Phased Array Ultrasonic examination (PAUT) of DSC 16 (performed in 2015).

3.0 DESIGN INPUT/DATA

3.1 Flaw Details and Geometry

Two cases of flaws are described and analyzed in Ref. [5.3]. The ITCP weld flaw is the same for both cases, and OTCP increased weld flaw covers both sets (case #1 & case #2 weld flaws). The results of Limit load for both cases are very similar. Figure 1 shows OTCP & ITCP flaws in the reference model (Flaw case #1 and Flaw case #2) and Figure 2 shows maximized OTCP & ITCP flaws evaluated in this calculation.

3.2 Material Properties

The material properties for the DSC structure are identical to Ref. [5.3]. They are duplicated here in Table 3 and Table 4.

3.3 Design Criteria

All of the applicable design bases loading conditions are considered in accordance with the requirements of ASME Section III Subsection NB Ref. [5.2]. Section 4.1 details the methods used to perform the code Ref. [5.2] qualifications. The uncertainties in the PAUT examination are accounted for by using a 0.8 reduction factor on the limit load. This factor is in agreement with ISG-15, conservatively accounts for any additional limitations in the PAUT examinations. This weld uncertainty factor of 0.8 is applied to the minimum of the ASME specified minimum elongation of SA-240 304 (40%) and E308-XX (35%). Therefore strain limit is taken as 0.8*35=28% Ref. [5.3].

4.0 METHODOLOGY

4.1 Analysis Method and Acceptance Criteria

The analysis methods, finite element models details and acceptance criteria are the same as discussed tin Ref. [5.3]. The ITCP and OTCP weld flaws are maximized and analyzed per Limit load and Elastic Plastic analyses.

Initial ANSYS finite element iterations were performed by increasing all the four flaws by a very small length resulting in a negligible increase in plastic strain. In the second step very large flaws where considered (leaving only one element of the model connected at each flaw) resulting in excessive strain for the elastic-plastic side drop analysis (Section 4.4). Similarly, few more iterations were performed such that the weld flaw reaches close to acceptable strain limit for the elastic-plastic side drop analysis. Only the final flaw configuration (see Figure 2) is presented in the document.

4.2 FEA Model Details

Finite element models of the top half of the 61BTH DSC are used based on Ref. [5.3]. The models fall into two basic categories: axisymmetric (2D) and half-symmetric (3D). The original evaluation in Ref. [5.3] uses ANSYS 14.0. The evaluation in this calculation uses ANSYS 17.1 Ref. [5.1]. APPENDIX A performs the sensitivity analysis between the 2 ANSYS versions. As discussed in APPENDIX A, the default ANSYS 17.1 contacts stiffness's for the 3D-Half-Symmetric model were modified to match the default ANSYS 14.0 stiffness's.

The models were modified to increase the weld flaws as described in Section 4.1.

Axisymmetric Model (2D)

An axisymmetric model is used as described in Section 4.3.1 of Ref. [5.3]. Figure 3 to Figure 5 show images of the axisymmetric model with maximum flaws.

Half-Symmetric Model (3D)

A half-symmetric model is used as described in Section 4.3.4 of Ref. [5.3]. Figure 6 to Figure 8 show images of the half-symmetric model with maximum flaws.

4.3 Limit Load Solution Details

Limit load solution details are the same as detailed in Section 4.4 of Ref. [5.3].

4.4 Elastic Plastic Solution Details

Elastic Plastic solution details are the same as detailed in Appendix-A of Ref. [5.3].

4.5 Load Cases

The analyses performed in this calculation, are based on the conservative design values for internal pressure loading, rather than the actual calculated values of internal pressure. Table 1 summarizes the conservative design values as well as the actual calculated values which are taken from Ref. [5.3].

Temperatures used for the material properties for each Service Level condition are listed in Table 2.

Four 2D-Axisymmetric analyses for bounding Service Level (SL) A/B and D, and two 3D-Half-Symmetric analyses for bounding SL D are performed in this calculation.

5.0 REFERENCES

5.1. ANSYS Version 17.1. ANSYS Inc. (Including the ANSYS Mechanical APDL Documentation).

5.2. ASME Boiler and Pressure Vessel Code, Section III Subsection NB. 1998 Edition with Addenda through 2000.

5.3. AREVA Document No. 11042-0205 Revision 3. "61BTH ITCP and OTCP Closure Weld Flaw Evaluation"

5.4. ASME Section II Part A. Ferrous Material Specifications. 1998 Edition with Addenda through 2000.

5.5. ASME Section II Part C. Specifications for Welding Rods, Electrodes, and Filler Metals 1998 Edition with Addenda through 2000

6.0 ANALYSIS AND RESULTS

6.1 LIMIT LOAD ANALYSIS

6.1.1 2D-Axisymmetric Analyses for Internal Pressure

Two analyses are performed with the 2D-Axisymmetric model: one case for Service Level A/B and the other case for Service Level D. The collapse pressures were determined to be 86.3 psi for Service Level A/B and 122.2 psi for Service Level D. Figure 9 shows various plots of the plastic strain for Service Level A/B at various locations and levels of loading. Figure 10 shows various plots of the plastic strain for Service Level D. These strain plots are also representative of the behavior of the Service Level D analysis. Figure 11 shows the deflection history at the center of the lid, and indicates the expected plastic instability that occurs as the limit load is approached. Note that both the strains and displacements presented in these figures show only the load (pressure) at which the solution fails to converge.

6.1.2 3D-Half Symmetric Analyses for Side Drop Loading

The 3D-half-symmetric model described in Section 4.2 is used to perform the side-drop limit load analysis. The case includes the side-drop acceleration loading of 75g as well as the off-normal internal pressure of 20 psi. The collapse g-load for side-drop loading was found to be approximately 179.5g. Plots of the plastic strains in the side drop analyses are shown in Figure 15.

The results for Limit load analysis are summarized in Table 5.

6.2 ELASTIC-PLASTIC ANALYSIS

6.2.1 2D-Axisymmetric Analyses for Internal Pressure

Two analyses are performed with the 2D-Axisymmetric model: one case for Service Level A/B and the other case for Service Level D. The Equivalent Plastic Strain was determined to be 3.1% for Service Level A/B pressure and 7.4% for Service Level D pressure. Figure 12 shows plot of the plastic strain for Service Level A/B. Figure 13 shows plot of the plastic strain for Service Level D. The results for elastic-plastic analyses are summarized in Table 7. As shown by the results, the strain levels remain well below the minimum specified elongation limits of Type 304 steel and Type 308 weld electrodes Ref. [5.4] and Ref. [5.5]. Therefore, material rupture will not occur at the design conditions.

The maximum strains at loads up to 1.5x the specified loading are also extracted. These results are shown in Table 6, which also includes a comparison of the peak strain values to the ductility limit of the material reduced by the weld uncertainty factor of 0.8 discussed in Section 3.4 of Ref. [5.3].

6.2.2 3D-Half Symmetric Analyses for Side Drop Loading

The 3D-half-symmetric model described in Section 4.2 is used to perform the SL D side-drop limit load analysis. The case includes the 75g side-drop acceleration loading only. The maximum strains at loads up to 1.5x the specified loading (112.5g) are also extracted and compared with the material strain limit.

The equivalent plastic strain was determined to be 11.1% for 75g and 23.0% for 112.5g presented in Table 6. Figure 16 and Figure 17 show the corresponding plastic strain plots. The results for elastic-plastic analyses are summarized in Table 7.

7.0 DISCUSSION AND CONCLUSIONS

This calculation qualifies the NUHOMS® 61BTH Type 1 (DSCs 11-15) at the Monticello Nuclear Generating Plant with maximum weld flaw using a combination of limit load analyses and elastic-plastic analyses. The limit load analyses are used to show that the DSC satisfies the primary stress limits of ASME Section III Subsection NB. The elastic-plastic analyses are used to show that the actual predicted strain values are below the material ductility limits. Both the limit load and elastic-plastic analyses account for any remaining uncertainty in the weld (e.g. non-inspected weld regions and PAUT technique limitations) by including an uncertainty factor of 0.8 which is described in detail in Section 3.4 of Ref. [5.3].

For both OTCP and ITCP, all weld flaws were maximized such that the weld flaw reaches close to acceptable design limits. The maximum modeled weld flaws for OTCP to DSC shell weld are 0.43” and 0.42” in length, which represents about 85% through-wall of the 0.5-inch minimum weld throat. The maximum modeled full-circumferential weld flaws for ITCP to DSC shell weld are 0.16” * cos(45°)=0.11” and 0.14” in length, which represents respectively 58% and 74% through-wall of the 0.19-inch minimum weld throat as shown in Figure 2. All four assumed flaws represent defects spreading over more than one weld bead. These flaws were located based on DSC #16 PAUT results and are considered representative locations for DSC’s # 11 to 15.

8.0 LISTING OF COMPUTER FILES

Finite Element Analyses were performed using ANSYS Version 17.1 Ref. [5.1]. All analyses were performed on HPC v2 Linux platform.

Load Case	Analysis Type	File Name	Description	Date / Time[1]
Internal Pressure 2D-Axisymmetric model	Limit load analysis SL- A/B	61BTH_WeldFlaw_1F_AX_2_DETACH.db	Reference .db file for Axisymmetric SL- A/B Limit load analysis	Note [2]
		AXISYMM_IP_LimitLoad.ext .ext = .inp, .err, .mntr, .out, .db, .rst	Limit load analysis files for SL- A/B	06/20/2017 11:33:31
	Limit load analysis SL- D	61BTH_WeldFlaw_1F_AX_2_DETACH.db	Reference .db file for Axisymmetric SL- D Limit load analysis	Note [2]
		AXISYMM_IP_LimitLoad_SLD.ext .ext = .inp, .err, .mntr, .out, .db, .rst	Limit load analysis files for SL- D	06/20/2017 12:29:27
	Elastic-plastic analysis SL- A/B	61BTH_WeldFlaw_1F_AX_2_DETACH.db	Reference .db file for Axisymmetric SL- A/B Elastic-plastic analysis	Note [2]
		AXISYMM_IP_500F.ext .ext = .inp, .err, .mntr, .out, .db, .rst	Elastic-plastic analysis files for SL- A/B	06/20/2017 12:34:31
	Elastic-plastic analysis SL- D	61BTH_WeldFlaw_1F_AX_2_DETACH.db	Reference .db file for Axisymmetric SL- A/B Elastic-plastic analysis	Note [2]
		AXISYMM_IP_625F.ext .ext = .inp, .err, .mntr, .out, .db, .rst	Elastic-plastic analysis files for SL- D	06/20/2017 12:39:21
Side Drop 3D-Half-Symmetric model	Limit load analysis SL- D	61BTH_WeldFlaw_1GC.db	Reference .db file for half-symmetric limit load analysis	Note [2]
		LIMIT_HALFSYM.ext .ext = .inp, .err, .mntr, .out, .db, .rst unmerge.mac, unmerge2.mac	Limit load SL D analysis files.	06/20/2017 11:39:15
	Elastic-plastic analysis SL- D	61BTH_WeldFlaw_1GC.db	Reference .db file for half-symmetric elastic-plastic analysis	Note [2]
		STRAIN_HALFSYM.ext .ext = .inp, .err, .mntr, .out, .db, .rst unmerge.mac, unmerge2.mac	Elastic-plastic SL D analysis files.	06/19/2017 22:48:11

Notes:
[1] The date & time (EST) for the main runs are from the listing at the end of output file.

(2) ANSYS FE models are taken from Section 8.0 of Ref. [5.3].

Table 1 – Internal Pressure in the 61BTH Type 1 DSC (Ref. [5.3])

Design Condition	Maximum Calculated Pressure [psi]	Design Pressure used in this Calculation [psi]
Normal	7.3	10
Off-Normal	10.9	20
Accident	56.1	65

Table 2 – Maximum Temperatures in the 61BTH Type 1 DSC Shell (Ref. [5.3])

Design Condition		Maximum Calculated Temperature [ºF]	Design Temperature used in This Calculation [ºF]
Normal	Storage	374	500
	Transfer	439	500
Off-Normal	Storage	399	500
	Transfer	416	500
Accident	Storage	611	625
	Transfer	467	500

Table 3 – Properties of SA-240 Type 304. Ref. [5.3]

Temp [°F]	E Modulus of Elasticity [ksi]	S_m Allowable Stress Intensity [ksi]	S_y Yield Stress [ksi]	S_u Ultimate Tensile Strength [ksi]	Yield Stress for SL A/B Limit Load Analysis [ksi]	Yield Stress for SL D Limit Load Analysis [ksi]
70	28,300	20.0	30.0	75.0	30.0	46.0
100	28,138	20.0	30.0	75.0	30.0	46.0
200	27,600	20.0	25.0	71.0	30.0	46.0
300	27,000	20.0	22.4	66.2	30.0	46.0
400	26,500	18.7	20.7	64.0	28.1	43.0
500	25,800	17.5	19.4	63.4	26.3	40.3
600	25,300	16.4	18.4	63.4	24.6	37.7
625	25,175	16.3	18.2	63.4	24.5	37.5
700	24,800	16.0	17.6	63.4	24.0	36.8

Table 4 – Properties of SA-36. Ref. [5.3]

Temp [°F]	E Modulus of Elasticity [ksi]	S_m Allowable Stress Intensity [ksi]	S_y Yield Stress [ksi]	S_u Ultimate Tensile Strength [ksi]	Yield Stress for SL A/B Limit Load Analysis [ksi]	Yield Stress for SL D Limit Load Analysis [ksi]
70	29,500	19.3	36.0	58.0	29.0	40.6
100	29,338	19.3	36.0	58.0	29.0	40.6
200	28,800	19.3	33.0	58.0	29.0	40.6
300	28,300	19.3	31.8	58.0	29.0	40.6
400	27,700	19.3	30.8	58.0	29.0	40.6
500	27,300	19.3	29.3	58.0	29.0	40.6
600	26,700	17.7	27.6	58.0	26.6	40.6
625(1)	26,400	17.6	27.2	58.0	26.4	40.4
700	25,500	17.3	25.8	58.0	26.0	39.8

Note:

(1) All values are interpolated from the 600 °F and 700 °F values.

Table 5 – Summary of Limit Load Analysis for the maximum weld flaws

Sl. No.	Name	Loading	Temp. [F]	Analysis Criteria	Design Pressure (psi)	Requirement of pressure to Safety Limit load Criteria (psi)	Limit Load Collapse Pressure (psi)
1	2D-Axisymmetric	Internal pressure	500	SL A/B	32	60	86.3
2	2D-Axisymmetric	Internal pressure	625	SL D	65	90.2	122.2
Sl. No.	Name	Loading	Temp. [F]	Analysis Criteria	Design G-load (g)	Required G-load to Satisfy Limit load Criteria (g)	Limit Load Collapse G-Load (g)
3	3D-Half-symmetric	Side drop with 20 psi off-normal IP	500	SL D	75	104	179.5(1)

Note:

(1) To be compared with 188.5g with the original Case #1 weld flaws of Ref. [5.3], see APPENDIX A

Table 6 – Summary of Peak Strain Values for Elastic-Plastic Analyses for the maximum weld flaws

Load Case	Specific loading Internal Pressure (psi)	Peak Equivalent Plastic Strain		Material Strain Limit(1)
		at 65 psi internal Pressure	at 100 psi internal Pressure	
2D-Axisymmetric Internal Pressure Service Level D	65	7.4%	13.6%	28%
Load Case	Specific loading Side Drop G-Load (g)	Peak Equivalent Plastic Strain		Material Strain Limit(1)
		at 75g loading	at 112.5g loading	
3D-Half-symmetric Side Drop Service Level D	75	11.1%	23.0%	28%

Note:

(1) The weld uncertainty factor of 0.8 (See Section 3.4 of Ref. [5.3]) is applied to the minimum of the ASME specified minimum elongation of SA-240 304 (40%) and E308-XX (35%). Therefore strain limit is taken as 0.8*35=28%- See Section 3.3.

Table 7 – Summary of Elastic-Plastic Analysis Results for the maximum weld flaws

Analysis Case	Result	Plastic Strain
Internal Pressure Service Level A 2D-Axisymmetric[(1)]	Equivalent Plastic Strain at 32 psi Internal Pressure[(1)]	3.1%
Internal Pressure Service Level D 2D-Axisymmetric	Equivalent Plastic Strain at 65 psi Internal Pressure	7.4%
Side Drop Service Level D 3D-Half-Symmetry	Equivalent Plastic Strain at 75g Acceleration	11.1%

Note:

[(1)] The 32 psi internal pressure is bounding for Service Levels A and B and includes design internal pressure of 10 psi plus an additional 22 psi to account for inertial loading of the DSC contents onto the lid.

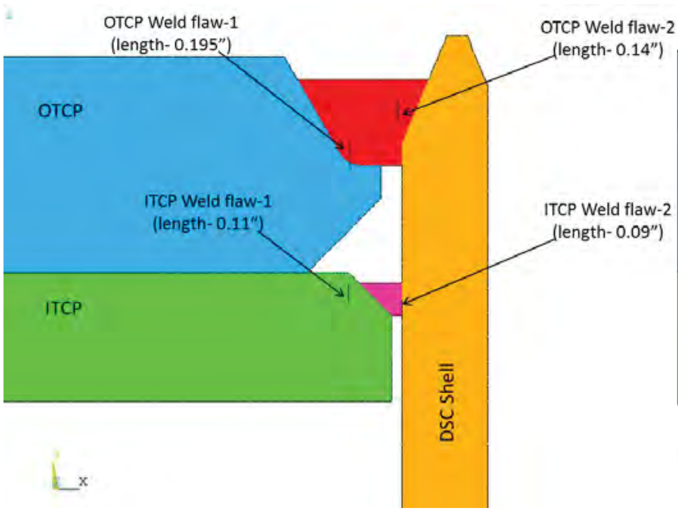

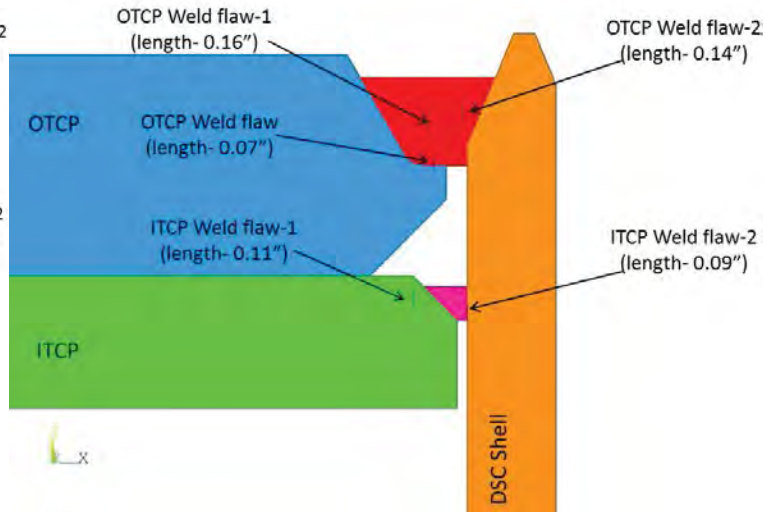

Flaw Case #1 Flaw Case #2

Figure 1 – Weld Flaws in Original Model (Ref. [5.3])

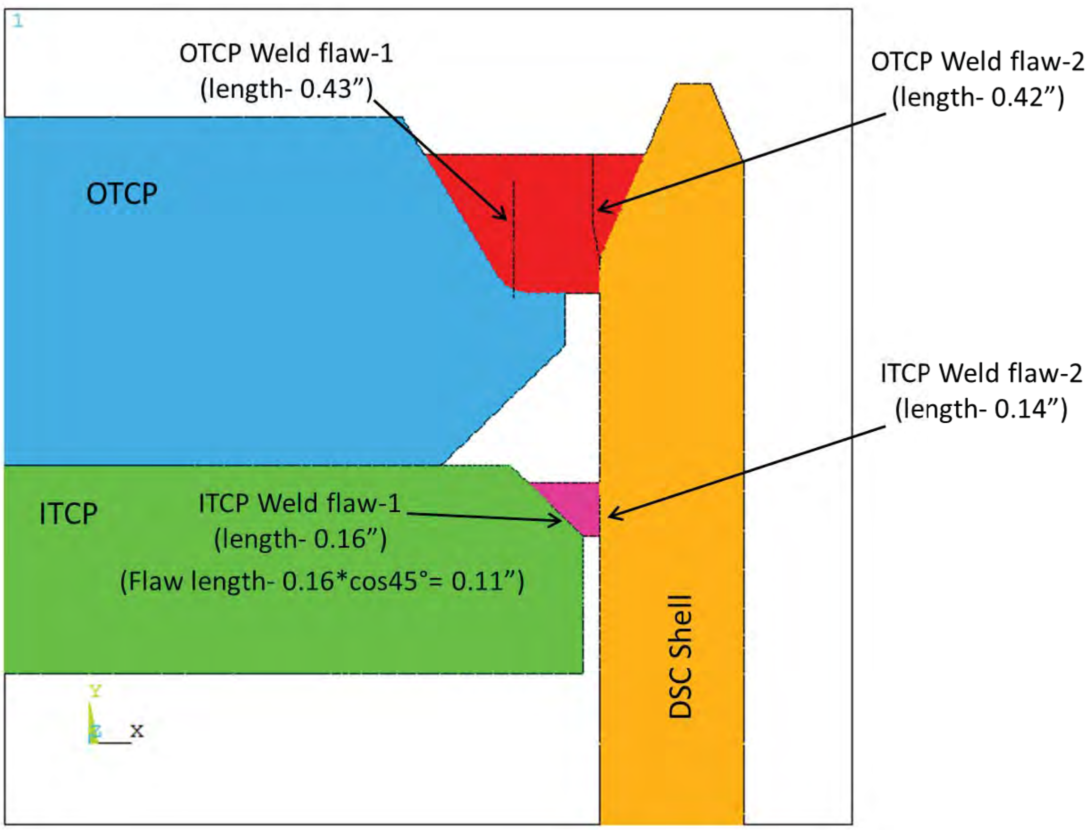

Figure 2 – Maximum Weld Flaws based on the allowed design limits

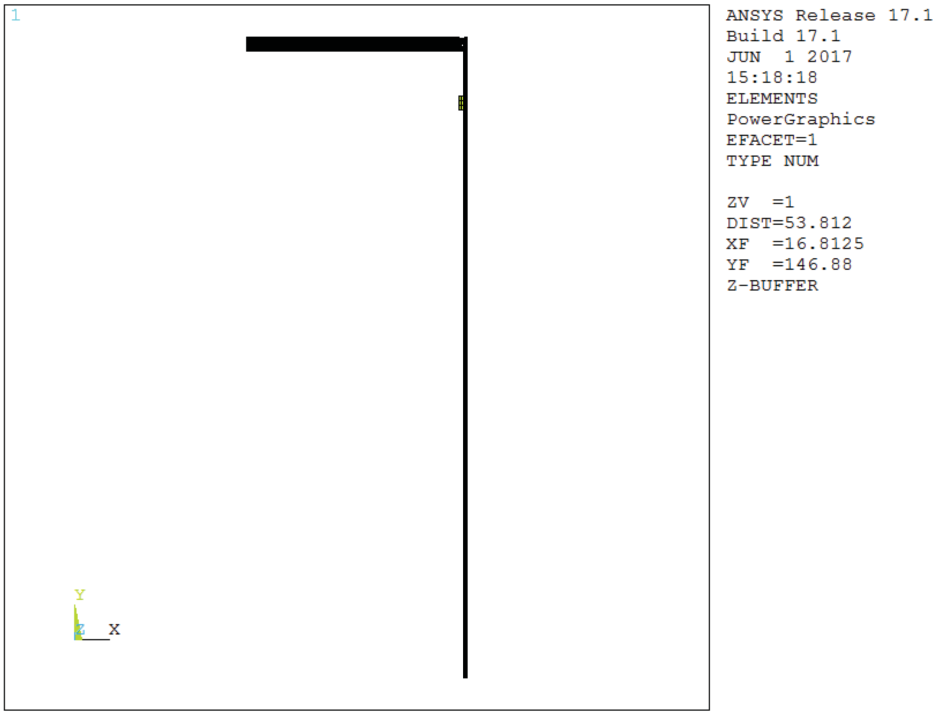

Figure 3 – Overview of the 2D-Axisymmetric Model

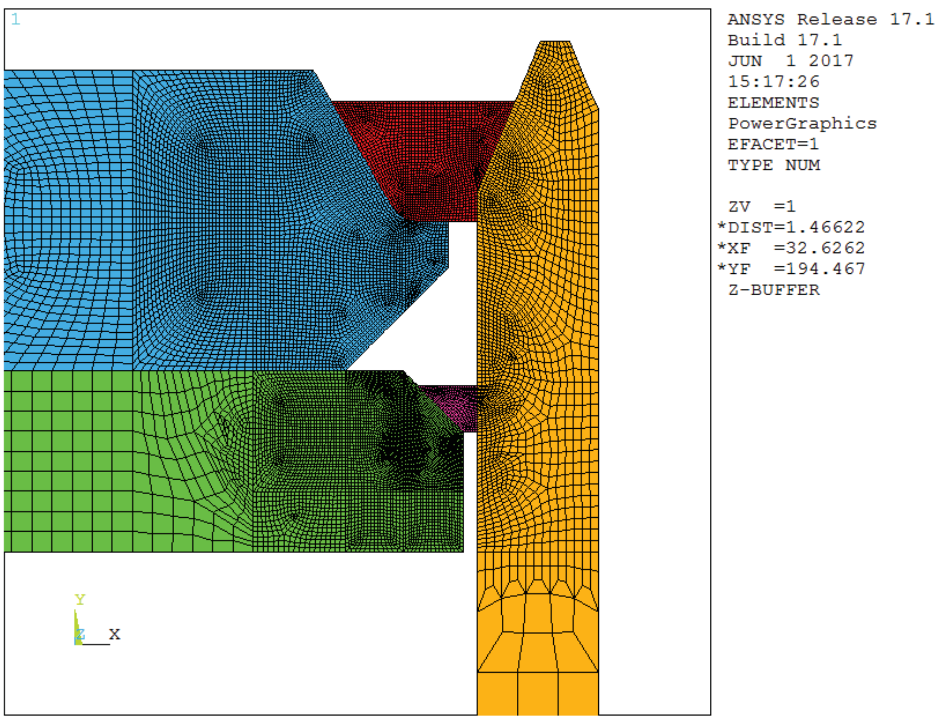

Figure 4 – Mesh Details at the Welds for 2D-Axisymmetric Model

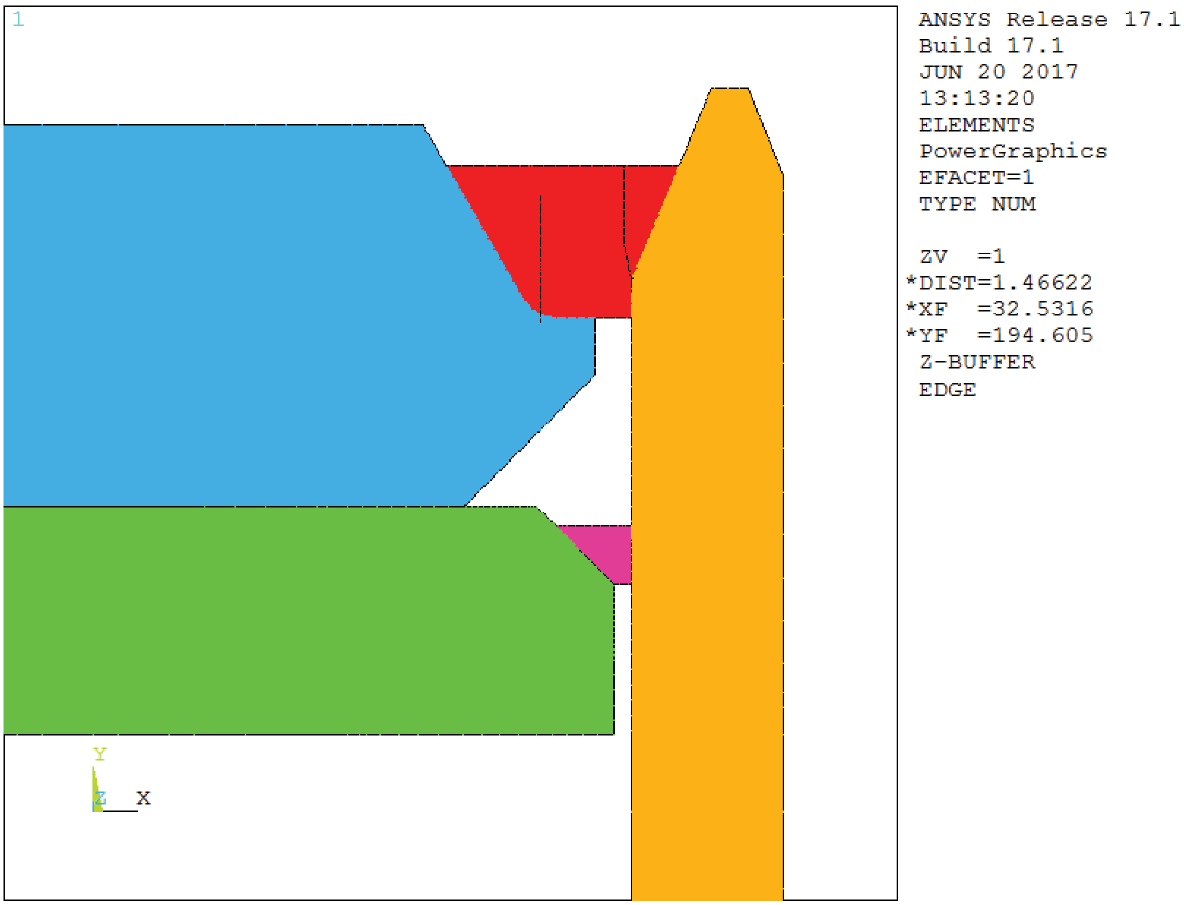

Figure 5 – Flaw Locations for 2D-Axisymmetric Model

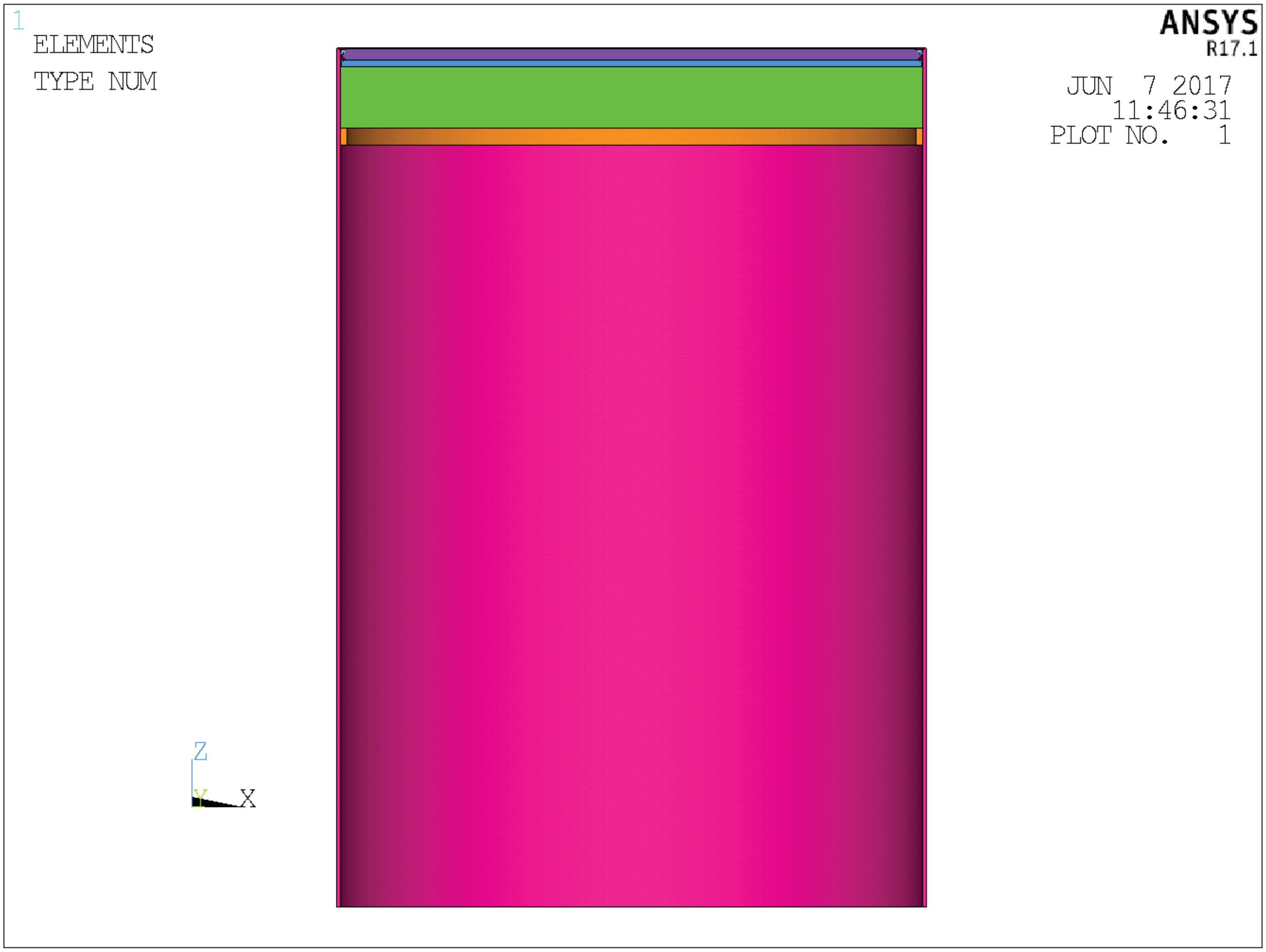

Figure 6 – Overview of the 3D-Half-Symmetric Model

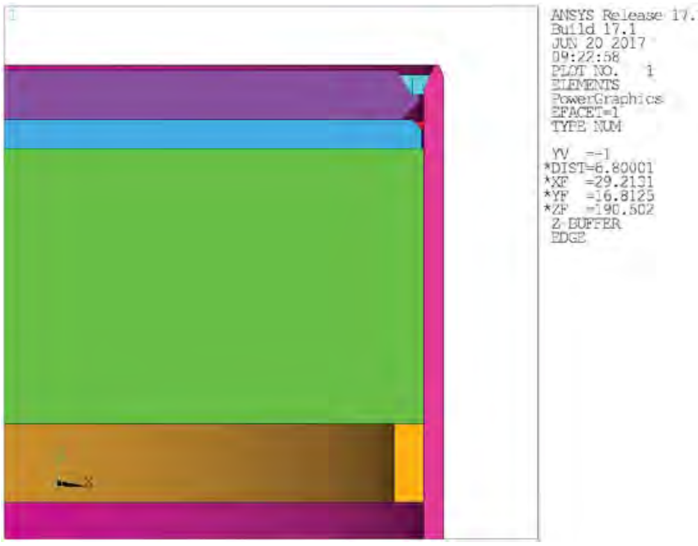

(a) Lid Region Solid View

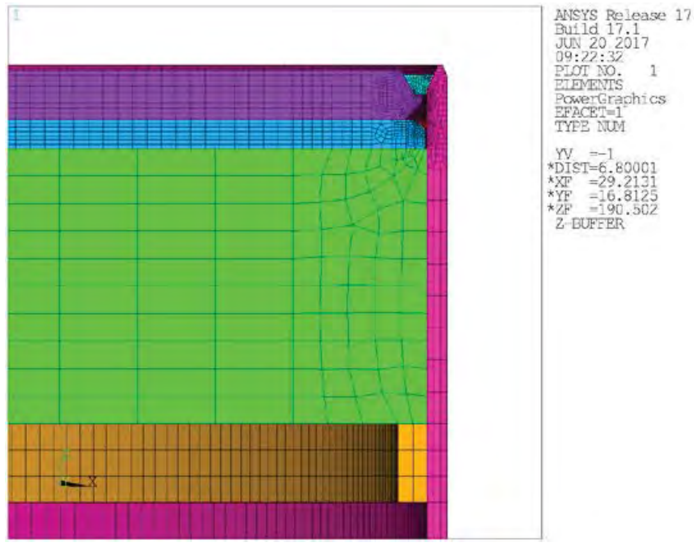

(b) Lid Region Mesh

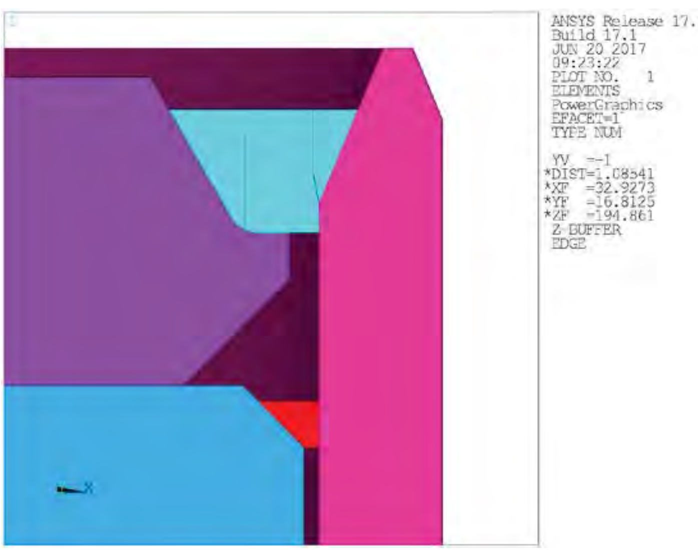

(c) Weld Region Solid View with Flaws Visible

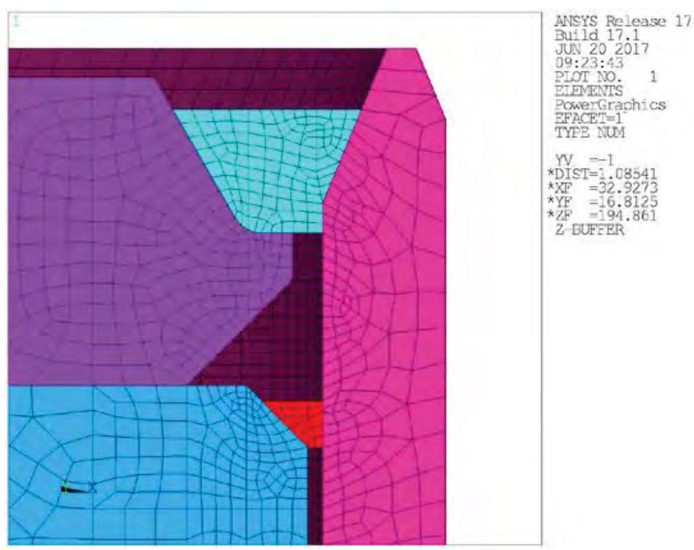

(d) Weld Region Mesh

Figure 7 – Detail Views and Mesh Plots of the 3D-Half Symmetric Model

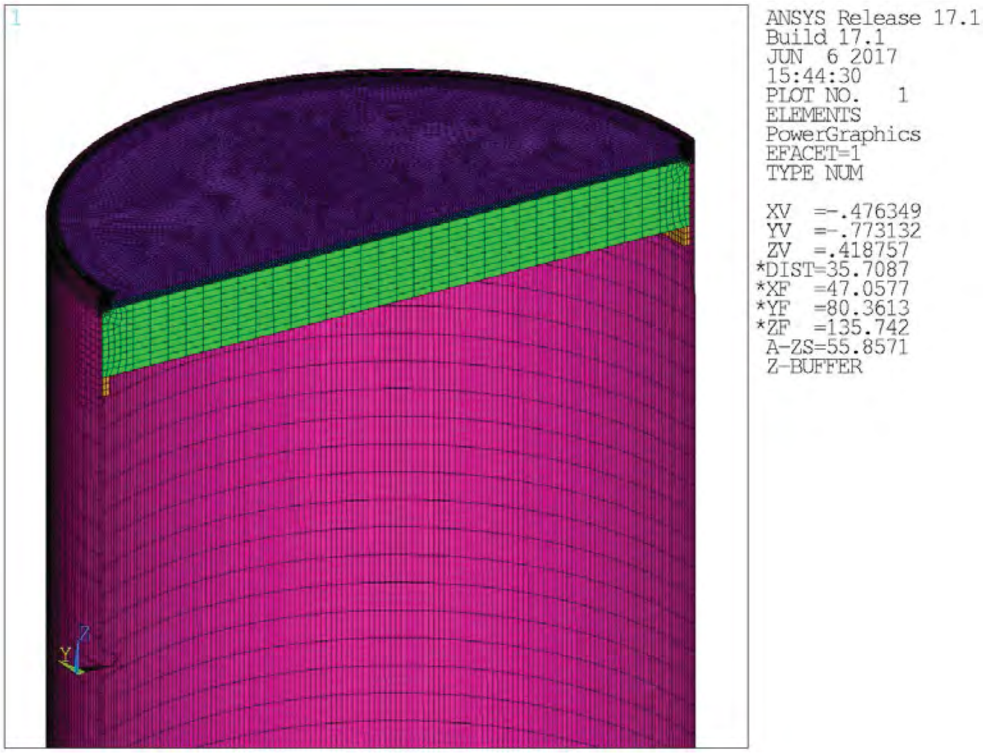

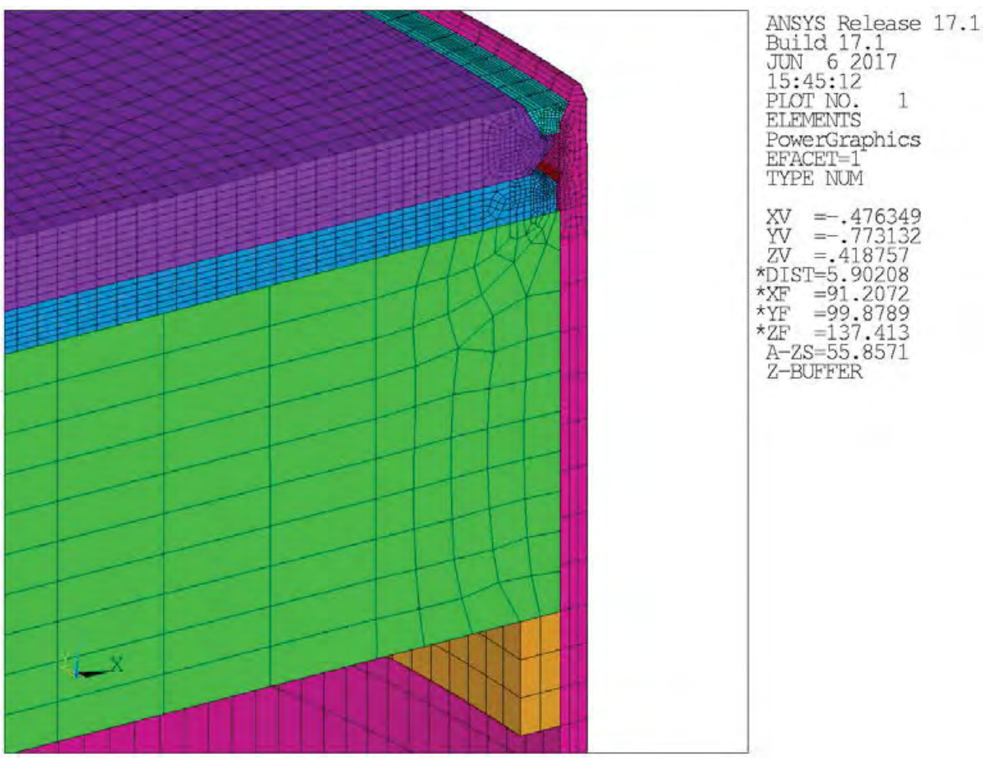

Figure 8 – Isometric Views of 3D-Half-Symmetric Model

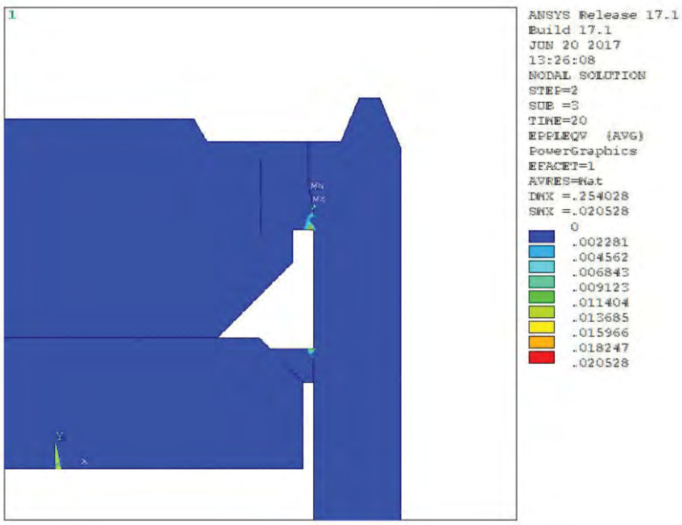

(a) Equivalent Plastic Strain in Weld Region [in/in] at 20 psi Internal Pressure

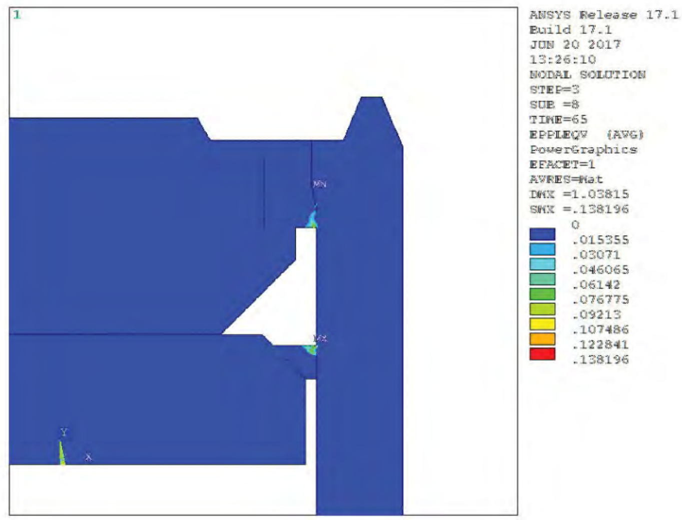

(b) Equivalent Plastic Strain in Weld Region [in/in] at 65 psi Internal Pressure

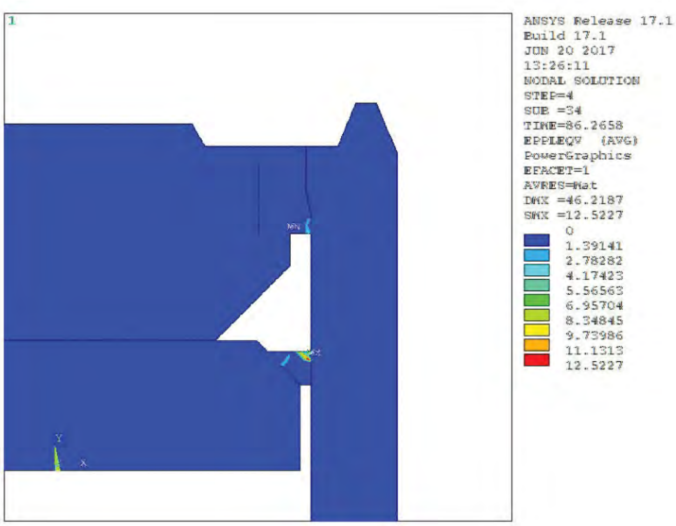

(c) Equivalent Plastic Strain in Weld Region [in/in] at 86.3 psi Internal Pressure

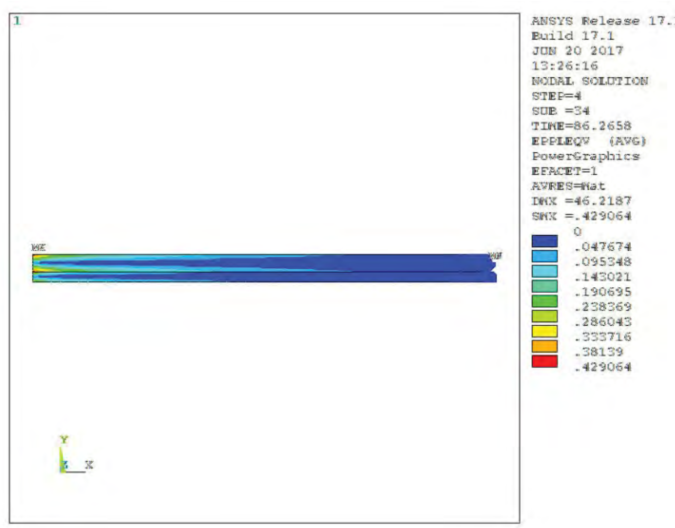

(d) EQV Plastic Strain in the Cover Plates at 86.3 psi

Figure 9 – Results of Limit Load for 2D-Axisymmetric Model – Service Level A/B

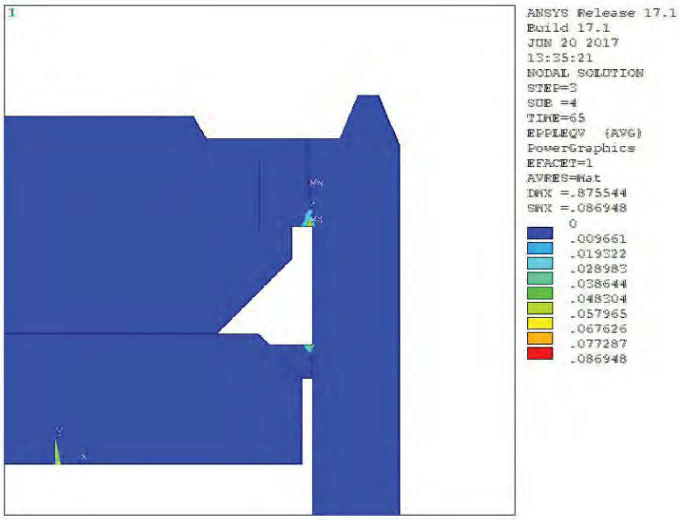

(a) Equivalent Plastic Strain in Weld Region [in/in] at 65 psi Internal Pressure

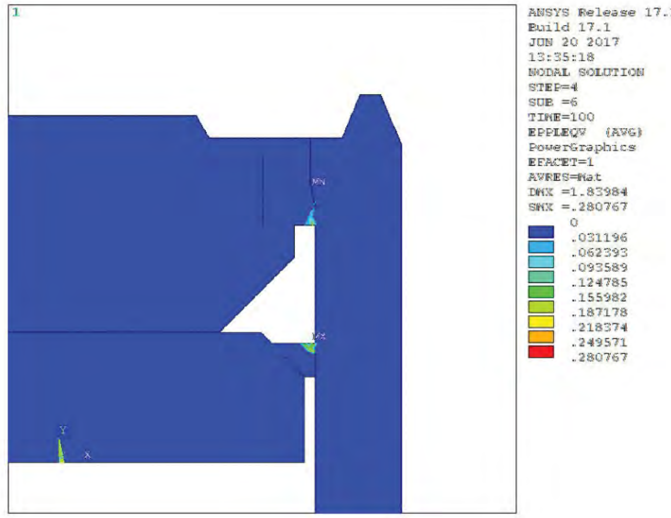

(b) Equivalent Plastic Strain in Weld Region [in/in] at 100 psi Internal Pressure

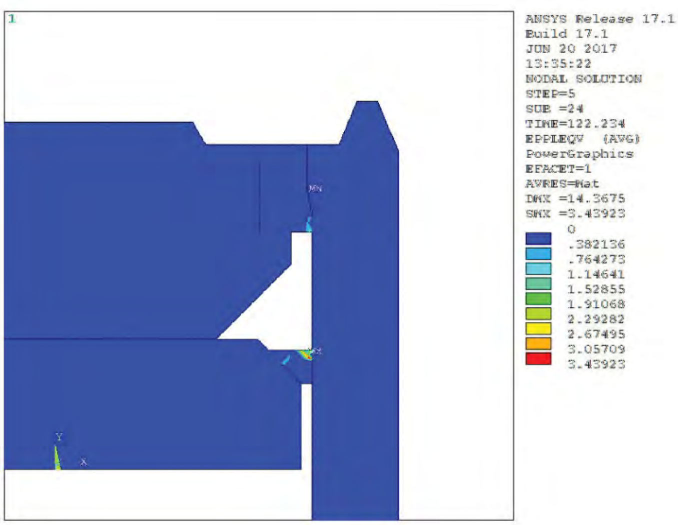

(c) Equivalent Plastic Strain in Weld Region [in/in] at 122.2 psi Internal Pressure

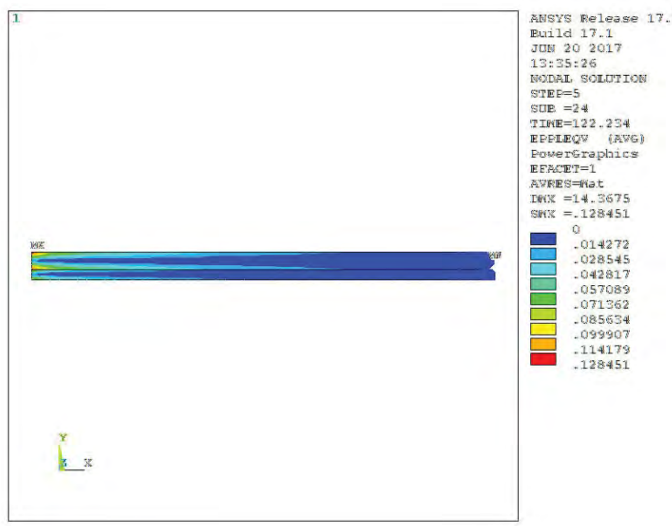

(d) EQV Plastic Strain in the Cover Plates at 122.2 psi

Figure 10 – Results of Limit Load for 2D-Axisymmetric Model – Service Level D

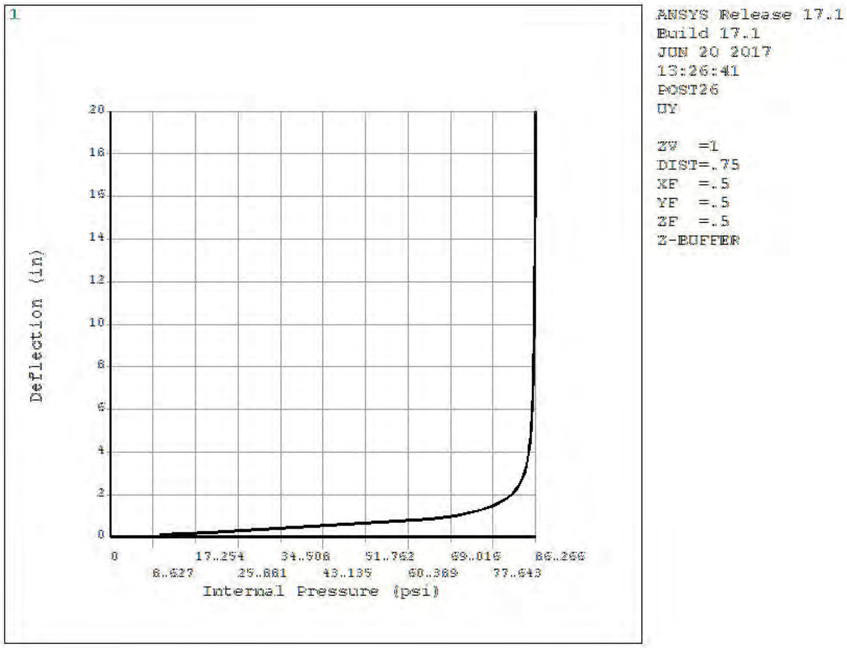

(a) Service Level A/B

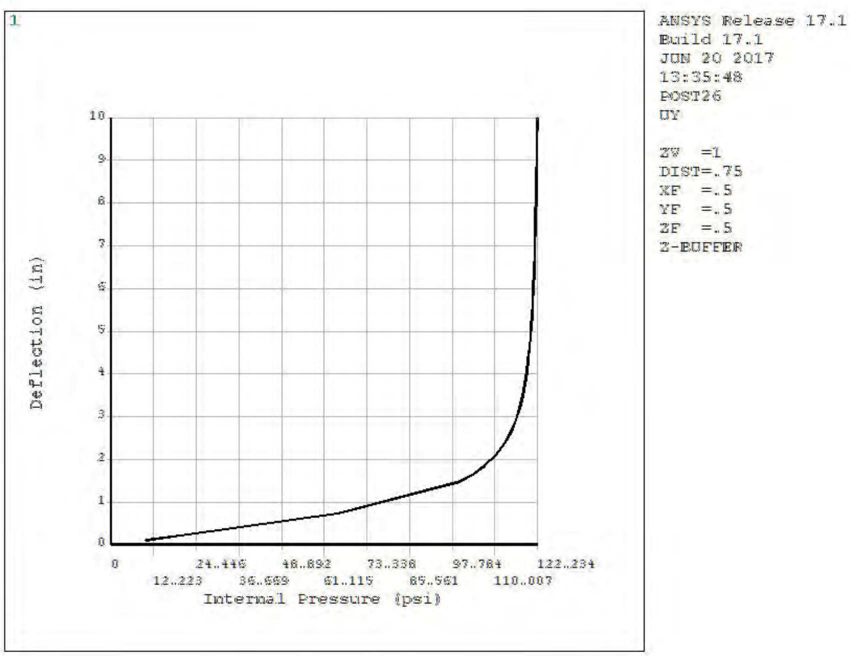

(b) Service Level D

Figure 11 – Deflection at the Center of the OTCP for the 2D-Axisymmetric Model for Limit Load (Maximum deflection occurs at the center point of the lids, in the outward axial direction)

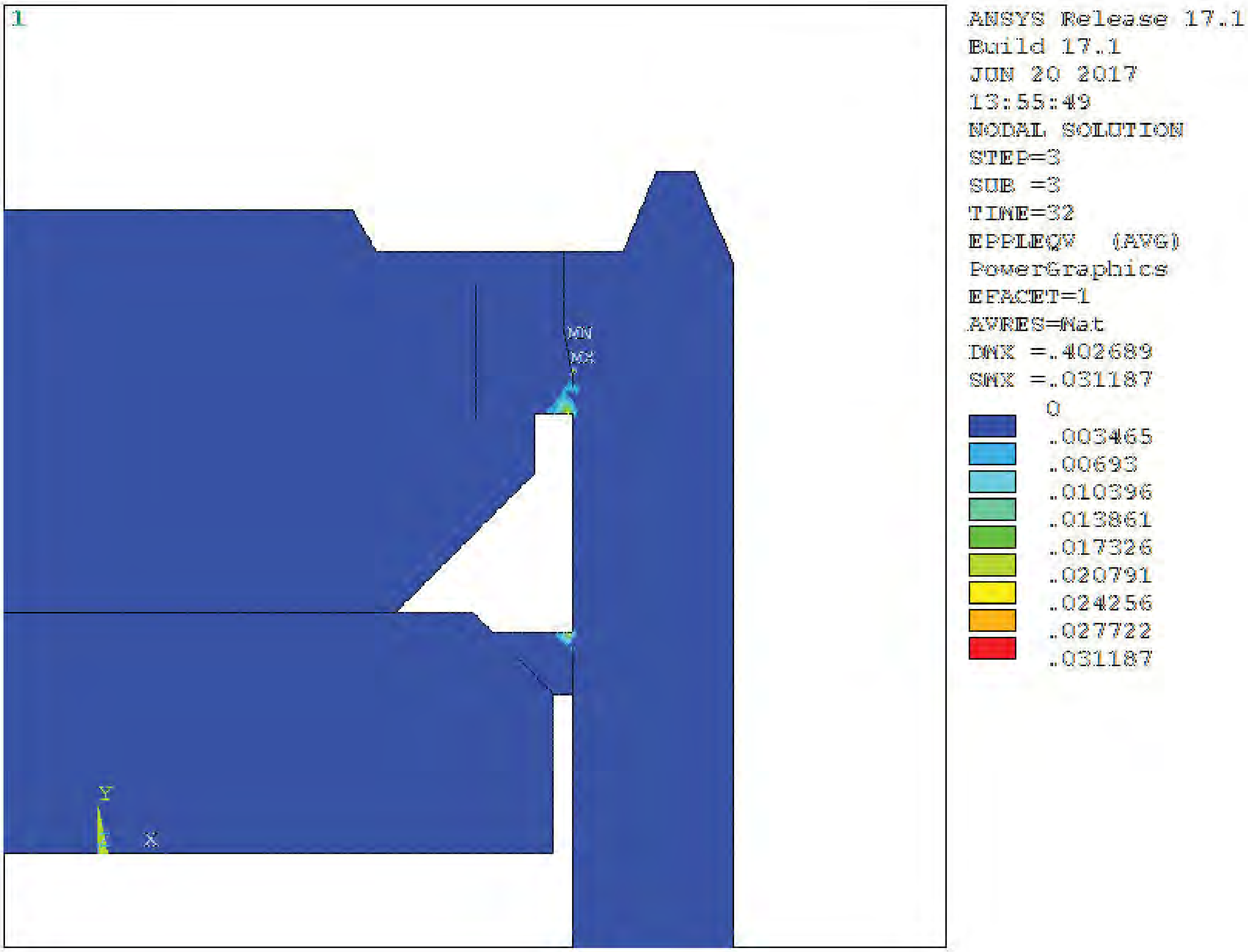

Figure 12 – Equivalent Plastic Strain at 32 psi for 2D-Axisymmetric Elastic Plastic Analysis - SL A/B Internal Pressure

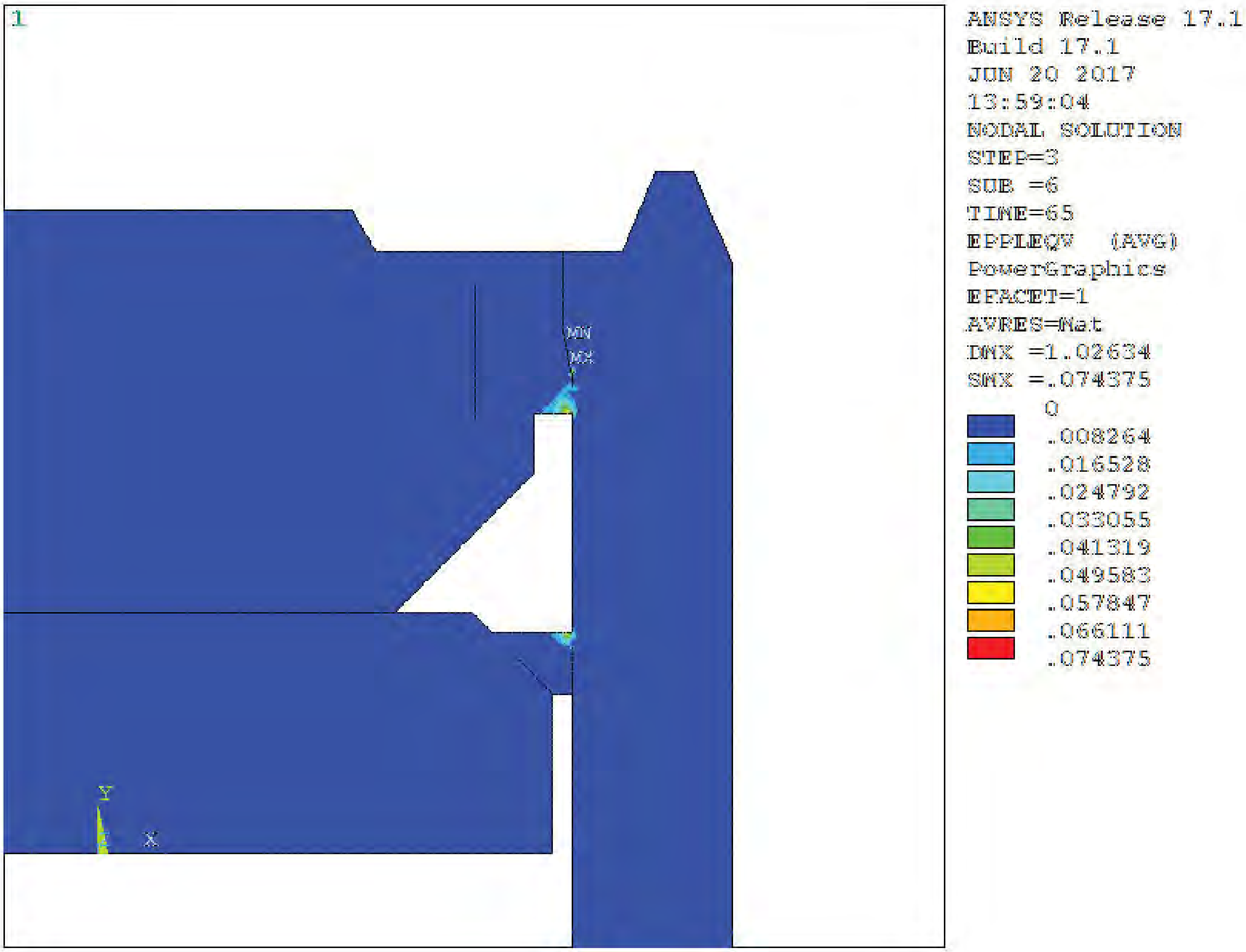

Figure 13 – Equivalent Plastic Strain at 65 psi for 2D-Axisymmetric Elastic Plastic Analysis - SL D Internal Pressure

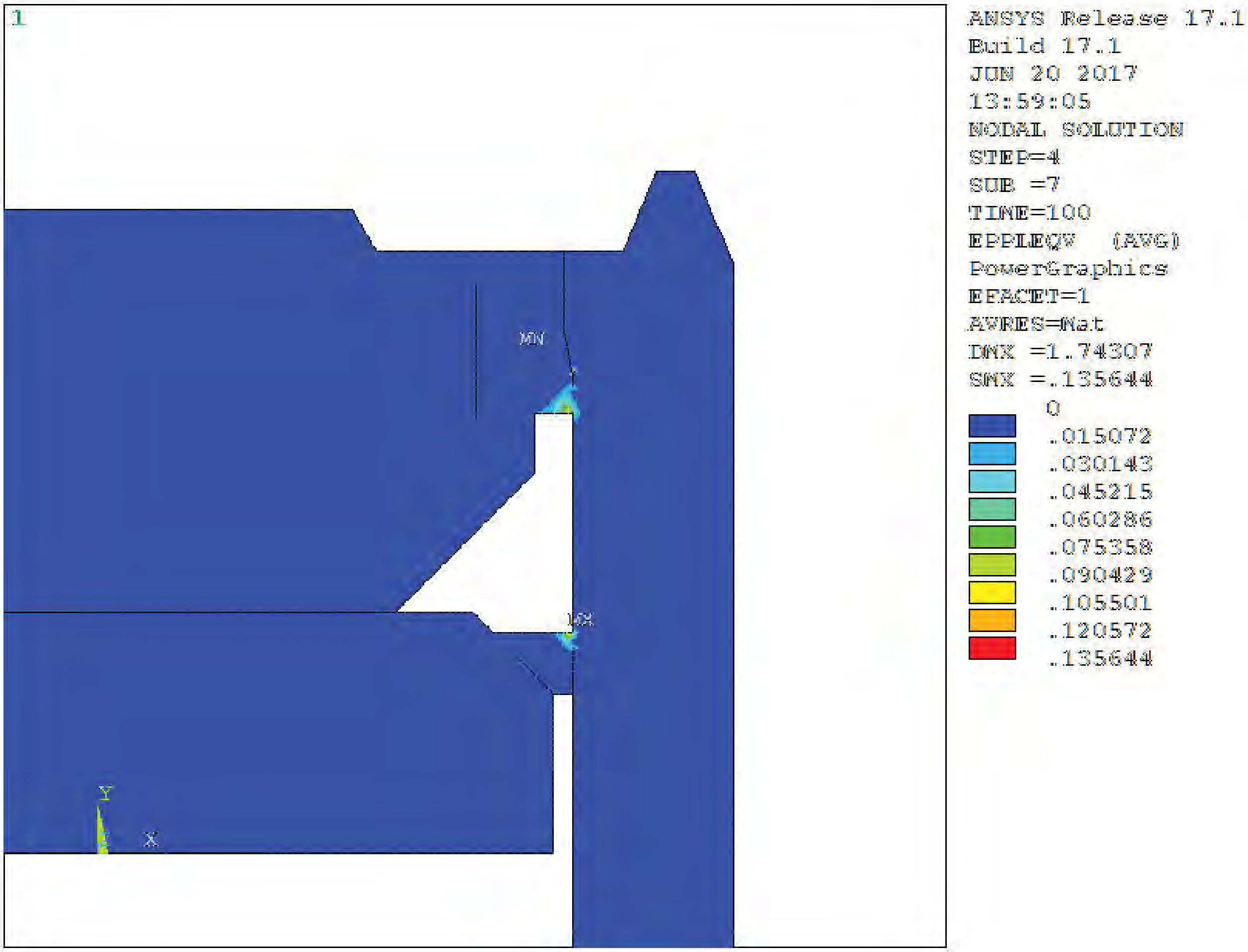

Figure 14 – Equivalent Plastic Strain at 100 psi for 2D-Axisymmetric Elastic Plastic Analysis - SL D Internal Pressure

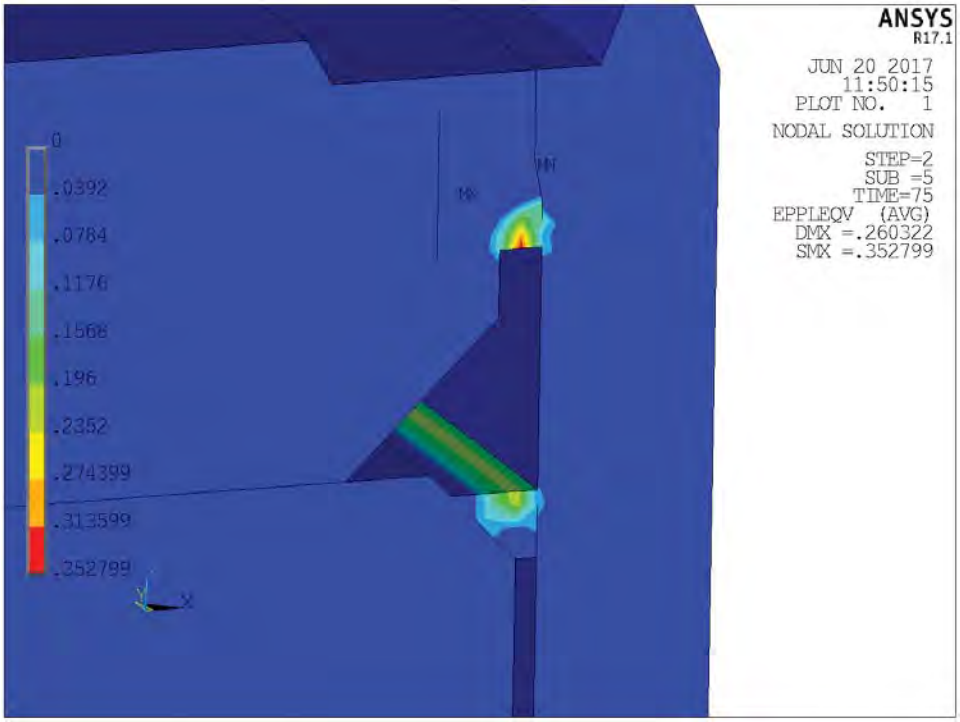

(a) Equivalent Plastic Strain in Weld Region [in/in] at 75g.

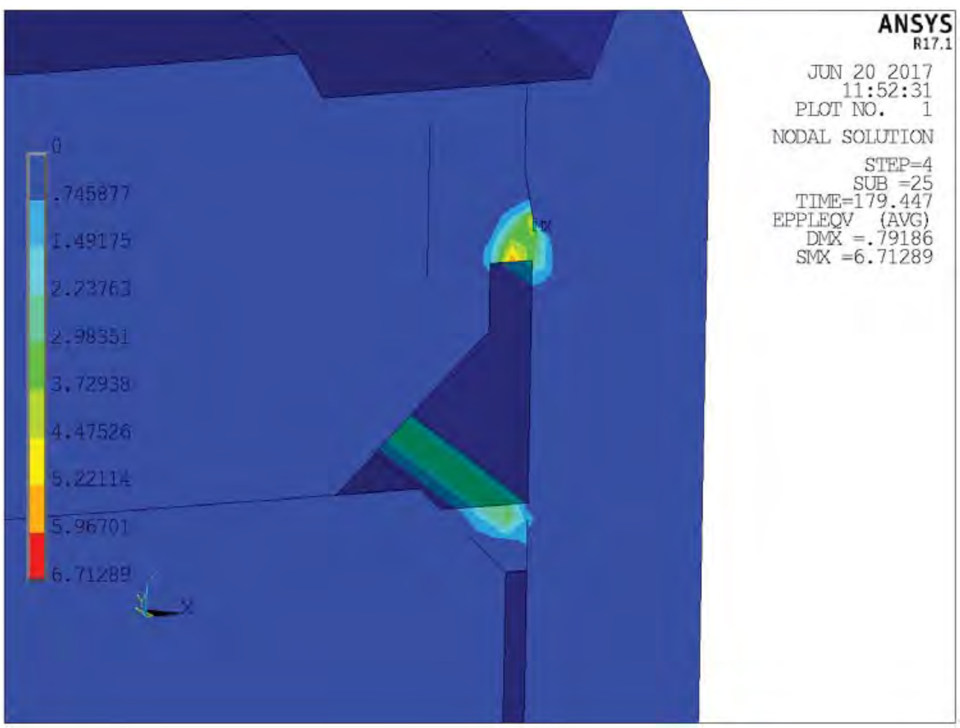

(b) Equivalent Plastic Strain in Weld Region [in/in] at 179.5g.

Figure 15 – Equivalent Plastic Strain Plots for 3D-Half-Symmetric Limit Load Analysis – SL D Side Drop with Off-Normal Internal Pressure

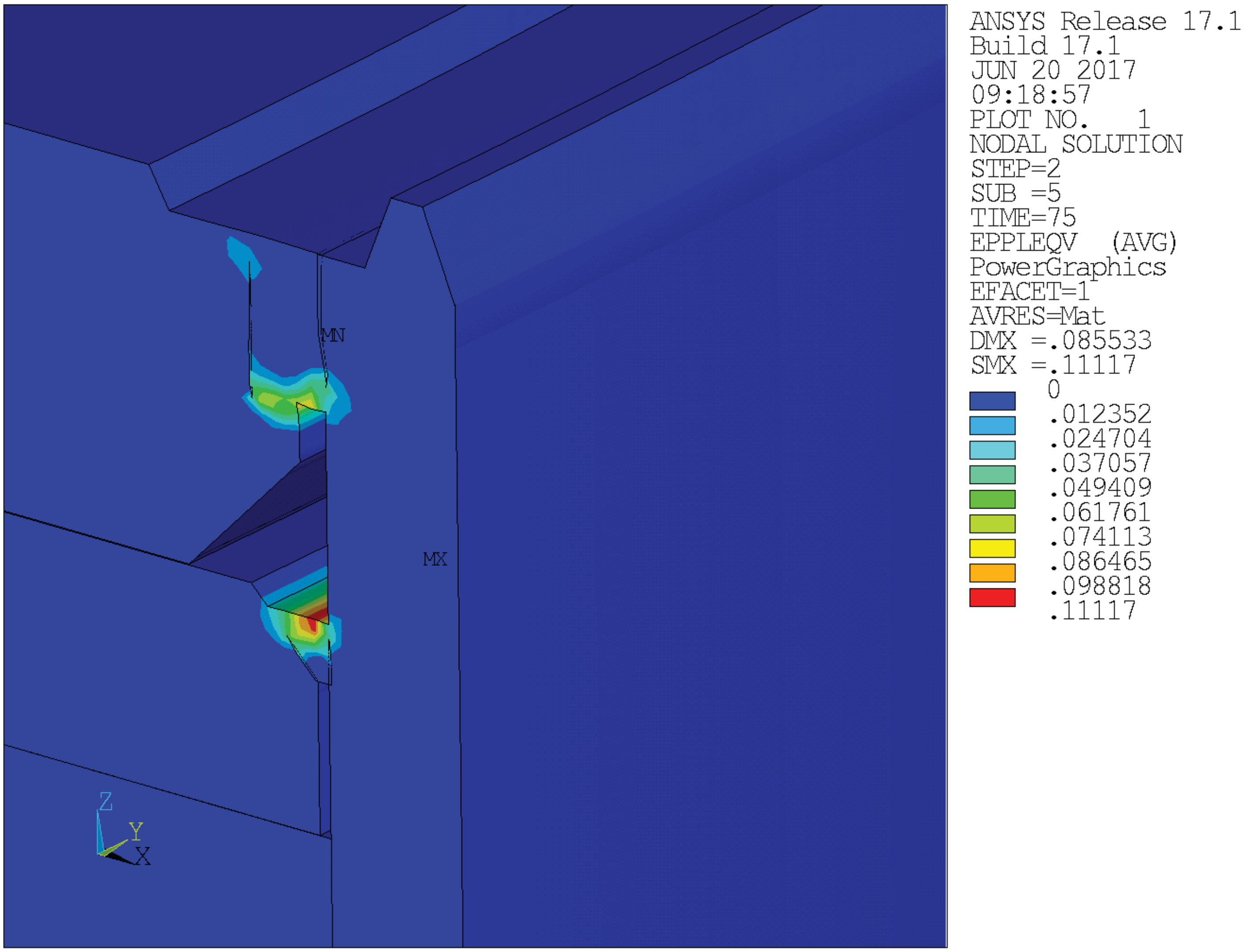

Figure 16 – Equivalent Plastic Strain at 75g for 3D-Half-Symmetric Elastic-Plastic Analysis - SL D Side Drop

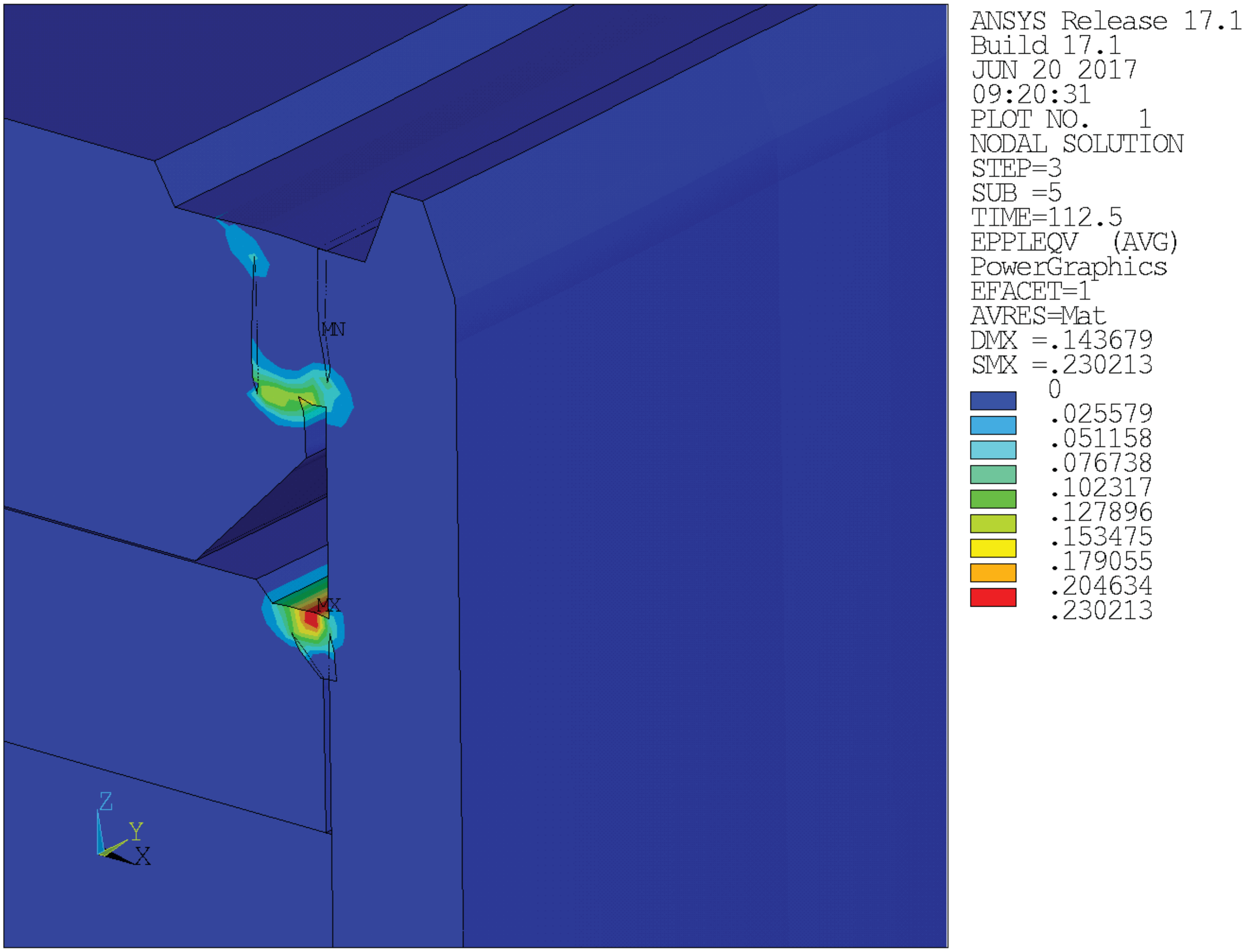

Figure 17 – Equivalent Plastic Strain at 112.5g for 3D-Half-Symmetric Elastic-Plastic Analysis - SL D Side Drop

APPENDIX A

Sensitivity Study of ANSYS Release 14.0 and 17.1

ANSYS computer program Release 14.0 has been used in stress calculation in Ref. [5.3]. ANSYS Release 17.1 is used in this calculation. Release 17.1 Ref. [5.1] was installed in accordance with QAP and TIP 3.3 requirements and is verified against empirical Data. The purpose of Appendix A is to determine the effect of using different releases of ANSYS on the same FE model. The following bounding 3D-half-symmetric load cases from the main part of this document are considered for the sensitivity analysis:

1) Elastic-Plastic analysis: Side drop 75g and 112.5g

2) Limit Load analysis: Side drop with off-normal internal pressure

A.1 Elastic-Plastic sensitivity analysis

Ref. [5.3] Elastic-Plastic analysis on the 3D-half-symmetric FE model uses ANSYS 14.0 and provides a peak equivalent plastic strain of 6.09% for 75g and 12.6% for 112.5g (Line 1 of Table A-1). The same ANSYS FE model was resumed in ANSYS 17.1 Ref. [5.1] and analyzed without any modification. The results for ANSYS 17.1 peak equivalent plastic strain are found to be 5.60% and 11.76% for 75g and 112.5g respectively (Line 2 of Table A-1). The default surface-to-surface contact stiffness's between the two releases are different and are found to be higher in ANSYS 17.1 resulting in lower equivalent plastic strains. Therefore the contact stiffness's were reduced by a 4.2873 factor to match the default surface-to-surface contact stiffness's of ANSYS 14.0. As the contact stiffness coefficient FKN used in ANSYS 14.0 is 0.1, the new contact stiffness coefficient in ANSYS 17.1 is 0.1 / 4.2873=0.02332. Once this modification implemented, ANSYS 17.1 provides exactly the same results (Line 3 of Table A-1) as ANSYS 14.0.

Table A-1: Comparison ANSYS 14.0 vs 17.1 – 3D-half-symmetric Model - Elastic Plastic analysis

		Peak Equivalent Plastic Strain	
Sl. No.	Side Drop	at 75g	at 112.5g
1	ANSYS 14.0	6.09% Table 7 of [5.3]	12.6% Table 7 of [5.3]
2	ANSYS 17.1	5.60%	11.76%
3	ANSYS 17.1 modified	6.09%	12.59%

A.2 Limit Load sensitivity analysis

Ref. [5.3] Limit Load analysis on the 3D-half-symmetric FE model uses ANSYS 14.0 and provides a limit load of 180.6g (Line 1 of Table A-2). The same ANSYS FE model was resumed in ANSYS 17.1 Ref. [5.1] and analyzed without any modification. The result for ANSYS 17.1 limit load is found to be 188.52g (Line 2 of Table A-2). The same contact stiffness's modification described in Section A.1 was implemented for the Limit Load case. However, the limit load stayed identical (188.56g, Line 3 of Table A-2) to the unmodified ANSYS 17.1 result.

Table A-2: Comparison ANSYS 14.0 vs 17.1 – 3D-half-symmetric Model - Limit Load analysis

Sl. No.	Side Drop	Limit Load Collapse G-Load (g)	Loading	Temp [°F]	Design G-load (g)	Required G-load to Satisfy Limit load Criteria (g)
1	ANSYS 14.0	180.6 Table 6 of [5.3]	Side drop with off-normal IP	500	75	104
2	ANSYS 17.1	188.52				
3	ANSYS 17.1 modified	188.56				

Although the ANSYS 17.1 runs converge up to 188.5g instead of 180.6g for ANSYS 14.0, Figure A-1 clearly shows that the results (here the maximum displacement in the model) are identical up to the point where ANSYS 14.0 stop converging.

The limit load for the Case #1 weld flaws is thus considered to be 188.5g in this calculation and is the reference for comparison with the increased flaws calculation results presented in Table 5.

A.3 Conclusion

Based on the sensitivity evaluations performed in Appendix A, it is concluded that the results are independent of the ANSYS release for the 3D-Half-Symmetric model.

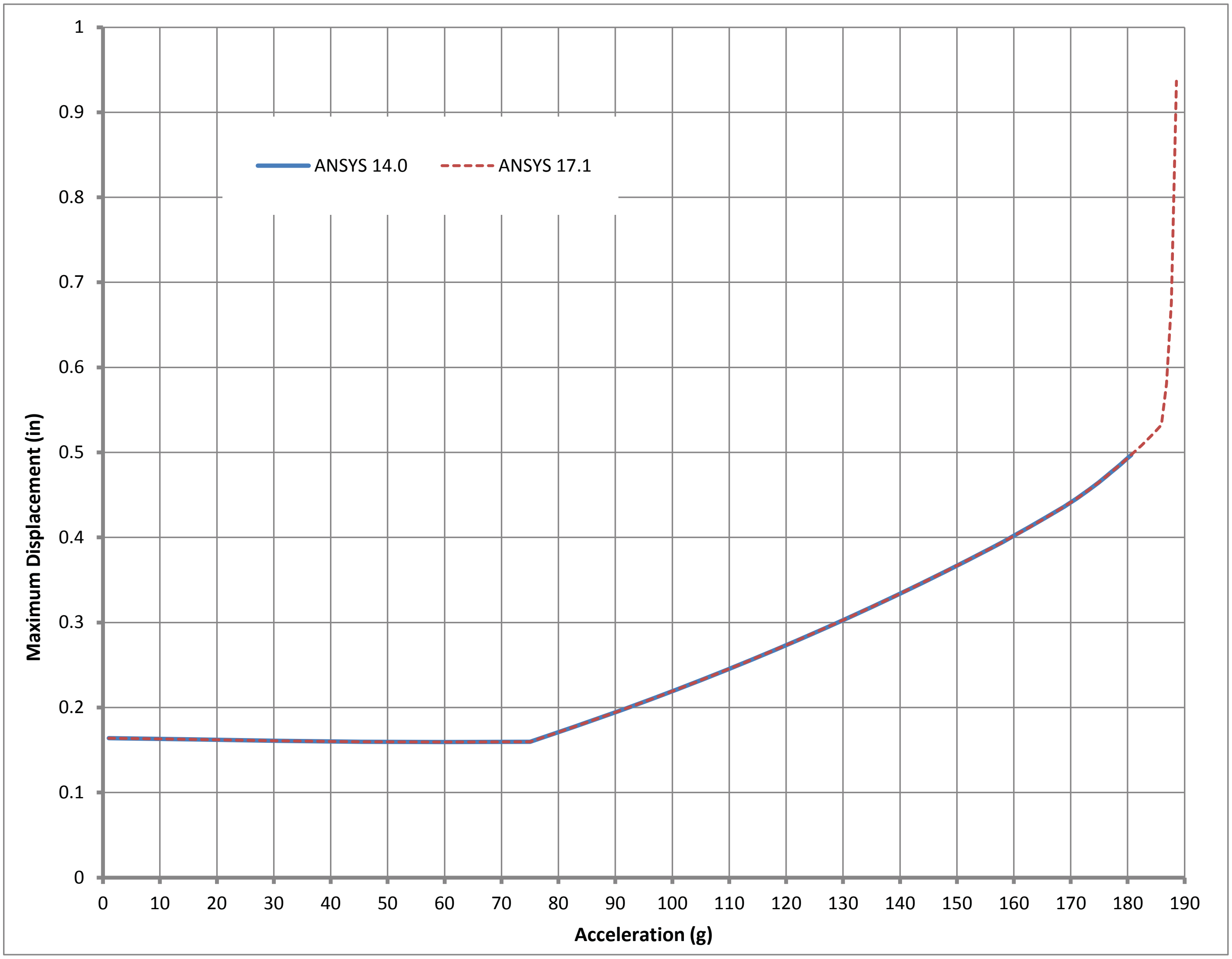

Figure A-1: Comparison ANSYS 14.0 vs 17.1 – Limit Load analysis

A.4 Listing of computer files

Finite Element Analyses were performed using ANSYS Version 17.1 Ref. [5.1]. All analyses were performed on HPC v2 Linux platform.

Load Case	Analysis Type	File Name	Description	Date / Time[(1)]
Side Drop Half-Symmetric model **Input Identical to Ref [5.3]**	Limit load analysis SL- D	61BTH_WeldFlaw_1GC.db	Reference .db file for half-symmetric limit load analysis	Note [(2)]
		SOLUTION_HALFSYM_SD.INP SOLUTION_HALFSYM_SD.out 3D_WeldFlaw.ext .ext = .mntr, .db, .rst	Limit load analysis files	05/25/2017 21:46:23
	Elastic-plastic analysis SL- D	61BTH_WeldFlaw_1GC.db	Reference .db file for half-symmetric elastic-plastic analysis	Note [(2)]
		STRAIN_HALFSYM.ext .ext = .inp, .err, .mntr, .out, .db, .rst	Elastic-plastic analysis files	06/07/2017 16:18:02
		61BTH_WELDFLAW_MATERIALS _ElasticPlastic_RamOsTrue.INP		
Side Drop Half-Symmetric model **Input Modified (See Section A-1)**	Limit load analysis SL- D	61BTH_WeldFlaw_1GC.db	Reference .db file for half-symmetric limit load analysis	Note [(2)]
		SOLUTION_HALFSYM_SD.ext .ext=.INP, .out, .err 3D_WeldFlaw.ext .ext = .mntr, .db, .rst	Limit load analysis files	05/28/2017 05:12:40
	Elastic-plastic analysis SL- D	61BTH_WeldFlaw_1GC.db	Reference .db file for half-symmetric elastic-plastic analysis	Note [(2)]
		SOLUTION_HALFSYM_SD.ext .ext=.INP, .out, .err 3D_WeldFlaw.ext .ext = .mntr, .db, .rst	Elastic-plastic analysis files	05/27/2017 16:39:11
		61BTH_WELDFLAW_MATERIALS _ElasticPlastic_RamOsTrue.INP		

Notes:
(1) The date & time (EST) for the main runs are from the listing at the end of output file.
(2) ANSYS FE models are taken from Section 8.0 of Ref. [5.3].

ENCLOSURE 7

AREVA CALCULATION 11042-0208, REVISION 0

SITE SPECIFIC NUHOMS® 61BTH TYPE 1 DSC ITCP AND OTCP MARGIN EVALUATION FOR MAXIMUM WELD FLAW

23 pages follow

AREVA	Form 3.2-1 Calculation Cover Sheet Revision 12	**Calculation No.:**	11042-0208
		Revision No.:	0
		Page: 1 of 23	

DCR NO (if applicable): N/A	**PROJECT NAME:** NUHOMS® 61BTH Type 1 DSCs for Monticello Nuclear Generating Plant
PROJECT NO: 11042	**CLIENT:** Xcel Energy

CALCULATION TITLE:
Site Specific NUHOMS® 61BTH Type 1 DSC ITCP and OTCP margin evaluation for Maximum Weld Flaw.

SUMMARY DESCRIPTION:

1) Calculation Summary

This calculation evaluates the margins for Site-Specific Monticello NUHOMS® 61BTH Type 1 DSCs with the maximum flaws in the Inner Top Cover Plate (ITCP) and Outer Top Cover Plate (OTCP) closure welds based on as loaded temperature and pressure conditions.

2) Storage Media Description

- Coldstor - /areva_tn/11042/11042-0208-000

If original issue, is licensing review per TIP 3.5 required?

Yes ☐ **No** ☒ **(explain below)** **Licensing Review No.:**

This calculation is prepared in support of license exemption request which will be subjected to NRC review and approval. Therefore, a licensing review per TIP 3.5 is not required.

Software utilized (subject to test requirements of TIP 3.3):	**Software Version:**	**Software Log Revision:**
ANSYS	17.1	35

Calculation is complete Originator Name and Signature: Naveen Naveen SINGH	**Date:** 08/09/17
Calculation has been checked for consistency, completeness, and correctness Checker Name and Signature: Samuel TISSOT	**Date:** 08/09/2017
Calculation is approved for use Project Engineer Name and Signature: Raheel Haroon	**Date:** 8/9/2017

REVISION SUMMARY

Rev.	Description	Affected Pages	Affected Files
0	Initial issue	All	All

TABLE OF CONTENTS

Page

LIST OF TABLES

Page

LIST OF FIGURES

Page

1.0 PURPOSE

The purpose of this calculation is to evaluate the margins for the NUHOMS® 61BTH Type 1 DSCs at the Monticello Nuclear Generating Plant (MNGP) per ASME Section III criteria with the maximum postulated flaws in the Inner and Outer Top Cover Plates (ITCP and OTCP) closure welds based on the evaluation performed in the reference calculation [5.4]. The as-loaded site specific bounding temperatures and pressures used in this calculation are provided in Ref. [5.5].

2.0 ASSUMPTIONS

1. Assumptions 1 through 6 of Ref. [5.3] are applicable to this calculation.

3.0 DESIGN INPUT/DATA

3.1 Flaws Details and Geometry

The flaws details are identical to the maximum weld flaws evaluated in Ref. [5.4]. The geometry of the DSC structure is identical to the geometry used in References [5.3] and [5.4].

3.2 Material Properties

The material properties for the DSC structure are identical to the material properties of References [5.3] and [5.4]. They are duplicated here in Table 3 and Table 4 for convenience.

3.3 Design Criteria

All of the applicable design bases loading conditions are considered in accordance with the requirements of ASME Section III Subsection NB Ref. [5.2]. Section 4.1 details the methods used to perform the code Ref. [5.2] qualifications.

4.0 METHODOLOGY

4.1 Analysis Method and Acceptance Criteria

The analysis methods, finite element model details and acceptance criteria are the same as discussed in Ref. [5.3]. The ITCP and OTCP maximum weld flaws as evaluated in Ref. [5.4] are analyzed and margins are evaluated for Limit load and Elastic Plastic analyses. The as-loaded site specific bounding temperatures and pressures used in this calculation are provided in Ref. [5.5].

4.2 FEA Model Details

Finite element model details of the DSC structure are identical to the ones described in Ref. [5.4].

Axisymmetric Model (2D)

A 2D-axisymmetric model is used as described in Section 4.2 of Ref. [5.4].

Half-Symmetric Model (3D)

A 3D-half-symmetric model is used as described in Section 4.2 of Ref. [5.4].

4.3 Limit Load Solution Details

Limit load solution details are the same as detailed in Section 4.4 of Ref. [5.3].

4.4 Elastic Plastic Solution Details

Elastic Plastic solution details are the same as detailed in Appendix-A of Ref. [5.3].

4.5 Load Cases

The analyses performed in this calculation are using values of peak accident internal pressure calculated using the bounding value for actual canister heat load. Table 1 summarizes the actual values which are taken from Table 2 of Ref. [5.3]. Peak Accident internal pressure is taken as 45.91 psi from Table 7-5 of Ref. [5.5].

Temperatures used for the material properties for each Service Level condition are listed in Table 2. The Maximum Service Level (SL) D temperature of the DSC shell is taken as 370 °F as per Table 7-2 of Ref. [5.5] for a blocked vent accident. The same table also gives the maximum DSC shell SL-B temperature as 237 °F, before the blocked vent accident.

Four 2D-Axisymmetric analyses for bounding Service Level (SL) A/B and D, and two 3D-Half-Symmetric analyses for bounding SL D are performed in this calculation.

5.0 REFERENCES

5.1. ANSYS Version 17.1. ANSYS Inc. (Including the ANSYS Mechanical APDL Documentation).

5.2. ASME Boiler and Pressure Vessel Code, Section III Subsection NB. 1998 Edition with Addenda through 2000.

5.3. AREVA Document No. 11042-0205 Revision 3. "61BTH ITCP and OTCP Closure Weld Flaw Evaluation"

5.4. AREVA Document No. 11042-0207 Revision 0. "NUHOMS® 61BTH Type 1 DSC ITCP and OTCP Maximum Weld Flaw Evaluation"

5.5. AREVA Document No. 11042-0400 Revision 0. "Site-Specific Thermal Evaluation of 61BTH Type 1 DSCs stored in HSM-H at Monticello Nuclear Generating Plant"

5.6. ASME Section II Part A. Ferrous Material Specifications. 1998 Edition with Addenda through 2000.

5.7. ASME Section II Part C. Specifications for Welding Rods, Electrodes, and Filler Metals 1998 Edition with Addenda through 2000

6.0 ANALYSIS AND RESULTS

6.1 LIMIT LOAD ANALYSIS

6.1.1 2D-Axisymmetric Analyses for Internal Pressure

Two analyses are performed with the 2D-Axisymmetric model: one case for Service Level A/B and the other case for Service Level D. The collapse pressures were determined to be 98.4 psi for Service Level A/B and 144.1 psi for Service Level D. Figure 1 shows various plots of the plastic strain for Service Level A/B at various locations and levels of loading. Figure 2 shows various plots of the plastic strain for Service Level D. These strain plots are also representative of the behavior of the Service Level D analysis. Figure 3 shows the deflection history at the center of the lid, and indicates the expected plastic instability that occurs as the limit load is approached. Note that both the strains and displacements presented in these figures show only the load (pressure) at which the solution fails to converge.

6.1.2 3D-Half Symmetric Analyses for Side Drop Loading

The 3D-half-symmetric model described in Section 4.2 is used to perform the side-drop limit load analysis. The case includes the side-drop acceleration loading of 75g as well as the off-normal internal pressure of 10.9 psi. The collapse g-load for side-drop loading was found to be approximately 204g. Plots of the plastic strains in the side drop analyses are shown in Figure 7.

The results for Limit load analysis are summarized in Table 5.

6.2 ELASTIC-PLASTIC ANALYSIS

6.2.1 2D-Axisymmetric Analyses for Internal Pressure

Two analyses are performed with the 2D-Axisymmetric model: one case for Service Level A/B and the other case for Service Level D. The Equivalent Plastic Strain was determined to be 2.7% for Service Level A/B pressure and 4.4% for Service Level D pressure. Figure 4 shows a plot of the plastic strain for Service Level A/B. Figure 5 shows a plot of the plastic strain for Service Level D. The results for elastic-plastic analyses are summarized in Table 7. As shown by the results, the strain levels remain well below the minimum specified elongation limits (28%) of Type 304 steel and Type 308 weld electrodes Ref. [5.6] and Ref. [5.7]. Therefore, material rupture will not occur at the as loaded conditions.

The maximum strains at loads up to 1.5x the specified loading are also extracted. These results are shown in Table 6, which also includes a comparison of the peak strain values to the ductility limit of the material reduced by the uncertainty factor of 0.8 due to PAUT examination discussed in Section 3.4 of Ref. [5.3].

6.2.2 3D-Half Symmetric Analyses for Side Drop Loading

The 3D-half-symmetric model described in Section 4.2 is used to perform the SL D side-drop limit load analysis. The case includes the 75g side-drop acceleration loading only. The maximum strains at loads up to 1.5x the specified loading (112.5g) are also extracted and compared with the material strain limit.

The equivalent plastic strain was determined to be 9.8% for 75g and 19.0% for 112.5g. Figure 8 and Figure 9 show the corresponding plastic strain plots. The results for elastic-plastic analyses are summarized in Table 7.

7.0 DISCUSSION AND CONCLUSIONS

Limit Load Analyses:

The lower bound collapse pressure for Service Level A/B criteria was found to be 98.4 psi which is greater than the limiting pressure of 60 psi (Table 5). Therefore the Service Level A/B criterion is satisfied.

The lower bound collapse pressure for Service Level D criteria was found to be 144.1 psi which is greater than the limiting pressure of 90.2 psi (Table 5). The lower bound collapse G-Load for Service Level D side drop criteria was found to be 204 g which is greater than the limiting G-Load of 104 g (Table 5). Therefore the Service Level D criterion is satisfied.

Elastic-Plastic Analyses:

Table 6 lists the peak strains predicted by the elastic-plastic analyses for the bounding Service Level D event. As shown in the table, the peak strain values remain below the material ductility limits (28%) at the specified loading conditions, and also at 1.5x the specified loads, with a minimum margin of safety of 1.86. Therefore the elastic plastic analyses criteria are satisfied.

8.0 LISTING OF COMPUTER FILES

Finite Element Analyses were performed using ANSYS Version 17.1 Ref. [5.1]. All analyses were performed on HPC v2 Linux platform.

Load Case	Analysis Type	File Name	Description	Date / Time(1)
Internal Pressure 2D-Axisymmetric model	Limit load analysis SL-A/B	AXISYMM_IP_LimitLoad.db	Reference .db file for Axisymmetric SL-A/B Limit load analysis	Note (2)
		AXISYMM_IP_LimitLoad-237.ext .ext = .inp, .err, .mntr, .out, .db, .rst	Limit load analysis files for SL- A/B	06/27/2017 16:12:31
	Limit load analysis SL-D	AXISYMM_IP_LimitLoad_SLD.db	Reference .db file for Axisymmetric SL- D Limit load analysis	Note (2)
		AXISYMM_IP_LimitLoad_SLD-370.ext .ext = .inp, .err, .mntr, .out, .db, .rst	Limit load analysis files for SL- D	06/27/2017 13:00:25
	Elastic-plastic analysis SL-A/B	AXISYMM_IP_500F.db	Reference .db file for Axisymmetric SL-A/B Elastic-plastic analysis	Note (2)
		AXISYMM_IP-237F.ext .ext = .inp, .err, .mntr, .out, .db, .rst 11042-0208_Material_Properties_Macro.INP	Elastic-plastic analysis files for SL-A/B	06/27/2017 16:03:51
	Elastic-plastic analysis SL-D	AXISYMM_IP_625F.db	Reference .db file for Axisymmetric SL-D Elastic-plastic analysis	Note (2)
		AXISYMM_IP-370F_SLD.ext .ext = .inp, .err, .mntr, .out, .db, .rst 11042-0208_Material_Properties_Macro.INP	Elastic-plastic analysis files for SL-D	06/27/2017 16:05:25
Side Drop 3D-Half-Symmetric model	Limit load analysis SL-D	LIMIT_HALFSYM.db	Reference .db file for half-symmetric limit load analysis	Note (2)
		LIMIT_HALFSYM-237.ext .ext = .inp, .err, .mntr, .out, .db, .rst	Limit load SL-D analysis files.	06/29/2017 03:44:12
	Elastic-plastic analysis SL-D	STRAIN_HALFSYM.db	Reference .db file for half-symmetric elastic-plastic analysis	Note (2)
		STRAIN_HALFSYM-237.ext .ext = .inp, .err, .mntr, .out, .db, .rst 11042-0208_Material_Properties_Macro.INP	Elastic-plastic SL-D analysis files.	06/28/2017 10:47:28
Excel File		11042_0208_Elastic-Plastic_Stress-Strain.xls	SS 304 true strain / stress temperature dependent curves evaluation	6/29/2017 13:15:19

Notes:

(1) The date & time (EST) for the main runs are from the listing at the end of output file.

(2) ANSYS FE models are taken from Section 8.0 of Ref. [5.4].

Table 1 – Internal Pressure in the 61BTH Type 1 DSC

Design Condition	Maximum Calculated Pressures used in this Calculation [psi]	Design Pressures [psi]
Normal	7.3 [5.3]	10
Off-Normal	10.9 [5.3]	20
Accident	45.9 [5.5]	65

Table 2 – Maximum Temperatures in the 61BTH Type 1 DSC Shell [5.5]

Design Condition		Maximum as loaded calculated Temperatures used in This Calculation [ºF]	Design Temperature [°F]
Normal	Storage	237	500
	Transfer	237	500
Off-Normal	Storage	237	500
	Transfer	237	500
Accident	Storage	370	625
	Transfer	237	500

Table 3 – Properties of SA-240 Type 304. Ref. [5.4]

Temp [°F]	E Modulus of Elasticity [ksi]	S_m Allowable Stress Intensity [ksi]	S_y Yield Stress [ksi]	S_u Ultimate Tensile Strength [ksi]	Yield Stress for SL A/B Limit Load Analysis [ksi]	Yield Stress for SL D Limit Load Analysis [ksi]
70	28,300	20.0	30.0	75.0	30.0	46.0
100	28,138	20.0	30.0	75.0	30.0	46.0
200	27,600	20.0	25.0	71.0	30.0	46.0
300	27,000	20.0	22.4	66.2	30.0	46.0
400	26,500	18.7	20.7	64.0	28.1	43.0
500	25,800	17.5	19.4	63.4	26.3	40.3
600	25,300	16.4	18.4	63.4	24.6	37.7
700	24,800	16.0	17.6	63.4	24.0	36.8

Table 4 – Properties of SA-36. Ref. [5.4]

Temp [°F]	E Modulus of Elasticity [ksi]	S_m Allowable Stress Intensity [ksi]	S_y Yield Stress [ksi]	S_u Ultimate Tensile Strength [ksi]	Yield Stress for SL A/B Limit Load Analysis [ksi]	Yield Stress for SL D Limit Load Analysis [ksi]
70	29,500	19.3	36.0	58.0	29.0	40.6
100	29,338	19.3	36.0	58.0	29.0	40.6
200	28,800	19.3	33.0	58.0	29.0	40.6
300	28,300	19.3	31.8	58.0	29.0	40.6
400	27,700	19.3	30.8	58.0	29.0	40.6
500	27,300	19.3	29.3	58.0	29.0	40.6
600	26,700	17.7	27.6	58.0	26.6	40.6
700	25,500	17.3	25.8	58.0	26.0	39.8

Table 5 – Summary of Limit Load Analysis for the maximum weld flaws

Sl. No.	Name	Loading	Temp. [F]	Analysis Criteria	Applied Pressure (psi)	Requirement of pressure to Safety Limit load Criteria[1] (psi)	Limit Load Collapse Pressure (psi)	Code Limit Load Criteria Satisfied?
1	2D-Axisymmetric	Internal pressure	237	SL A/B	29.3	60	98.4	Yes
2	2D-Axisymmetric	Internal pressure	370	SL D	45.9	90.2	144.1	Yes
Sl. No.	Name	Loading	Temp. [F]	Analysis Criteria	Design G-load (g)	Required G-load to Satisfy Limit load Criteria[1] (g)	Limit Load Collapse G-Load (g)	Code Limit Load Criteria Satisfied?
3	3D-Half-symmetric	Side drop with 10.9 psi off-normal IP	237	SL D	75	104	204.0	Yes

Note:

[1] See paragraph Limit Load Analyses, Section 7.0, Ref. [5.3]

Table 6 – Summary of Peak Strain Values for Elastic-Plastic Analyses for the maximum weld flaws

Load Case	Specific loading Internal Pressure (psi)	Peak Equivalent Plastic Strain		Material Strain Limit	Margin of Safety at Specified Loading[2]
		at 45.9 psi internal Pressure	at 69 psi internal Pressure[1]		
2D-Axisymmetric Internal Pressure Service Level D	45.9	4.4%	7.1%	28%	5.36
Load Case	Specific loading Side Drop G-Load (g)	Peak Equivalent Plastic Strain		Material Strain Limit	Margin of Safety at Specified Loading[2]
		at 75g loading	at 112.5g loading[1]		
3D-Half-symmetric Side Drop Service Level D	75	9.8%	19.0%	28%	1.86

Note:

[1] 1.5x Specified Loads

[2] Margin of Safety is calculated as (Strain Limit/Actual Strain)-1

Table 7 – Summary of Elastic-Plastic Analysis Results for the maximum weld flaws

Analysis Case	Result	Plastic Strain
Internal Pressure Service Level A/B 2D-Axisymmetric[(1)]	Equivalent Plastic Strain at 29.3 psi Internal Pressure[(1)]	2.7%
Internal Pressure Service Level D 2D-Axisymmetric	Equivalent Plastic Strain at 45.9 psi Internal Pressure	4.4%
Side Drop Service Level D 3D-Half-Symmetry	Equivalent Plastic Strain at 75g Acceleration	9.8%

Note:

[(1)] The 29.3 psi internal pressure is bounding for Service Levels A and B and includes calculated internal pressure of 7.3 psi plus an additional 22 psi to account for inertial loading of the DSC contents onto the lid.

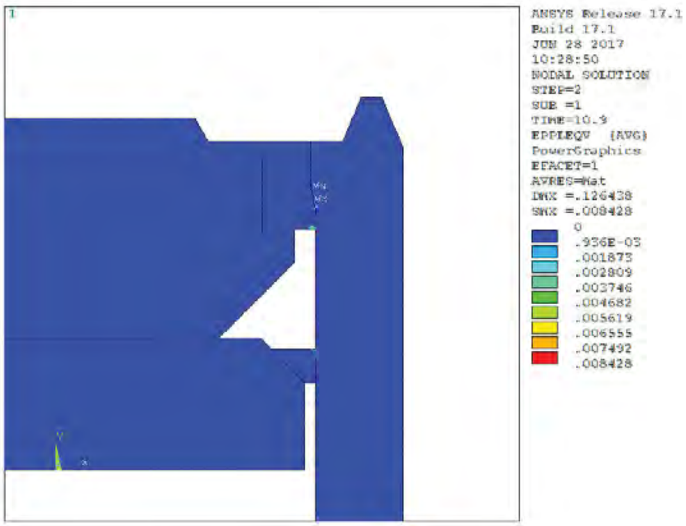

(a) Equivalent Plastic Strain in Weld Region [in/in] at 10.9 psi Internal Pressure

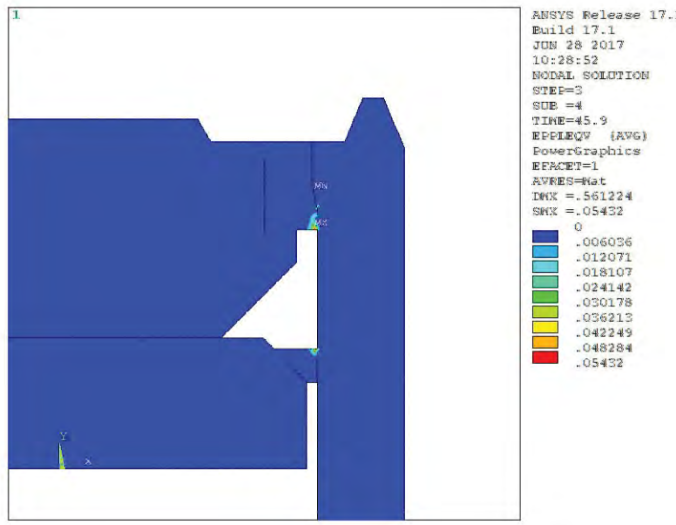

(b) Equivalent Plastic Strain in Weld Region [in/in] at 45.9 psi Internal Pressure

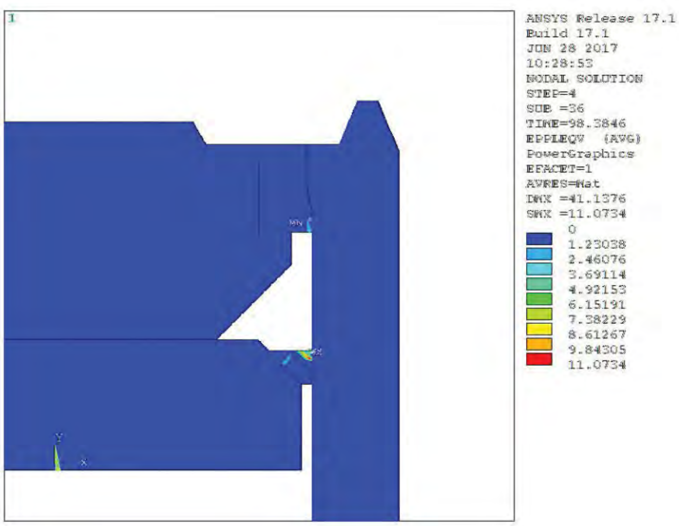

(c) Equivalent Plastic Strain in Weld Region [in/in] at 98.4 psi Internal Pressure

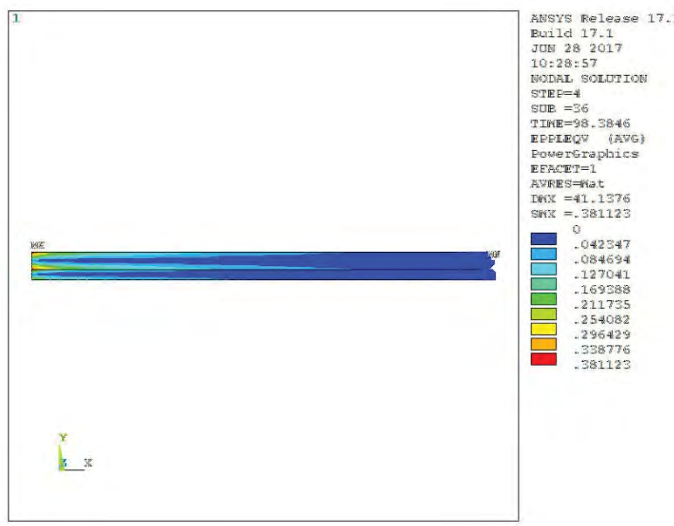

(d) EQV Plastic Strain in the Cover Plates at 98.4 psi

Figure 1 – Results of Limit Load for 2D-Axisymmetric Model – Service Level A/B

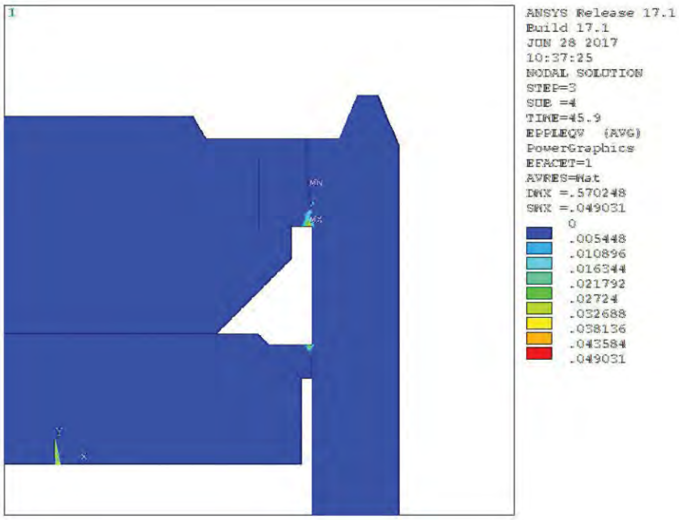

(a) Equivalent Plastic Strain in Weld Region [in/in] at 45.9 psi Internal Pressure

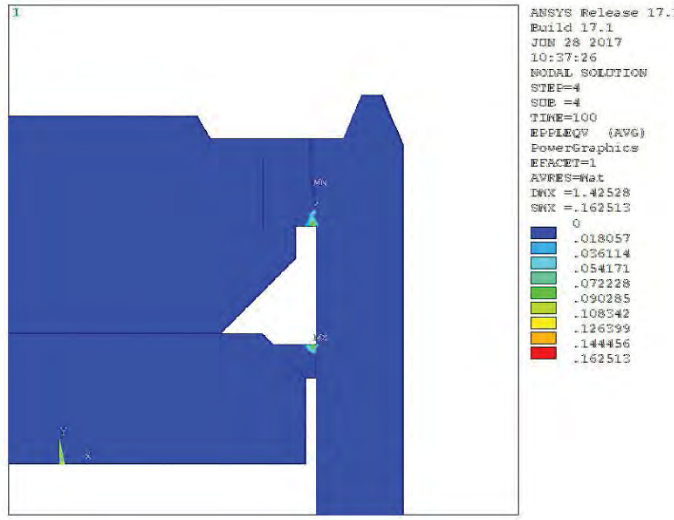

(b) Equivalent Plastic Strain in Weld Region [in/in] at 100 psi Internal Pressure

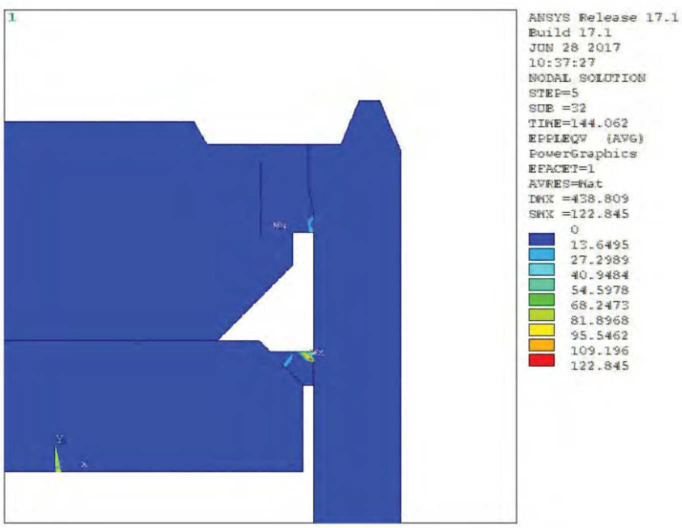

(c) Equivalent Plastic Strain in Weld Region [in/in] at 144.1 psi Internal Pressure

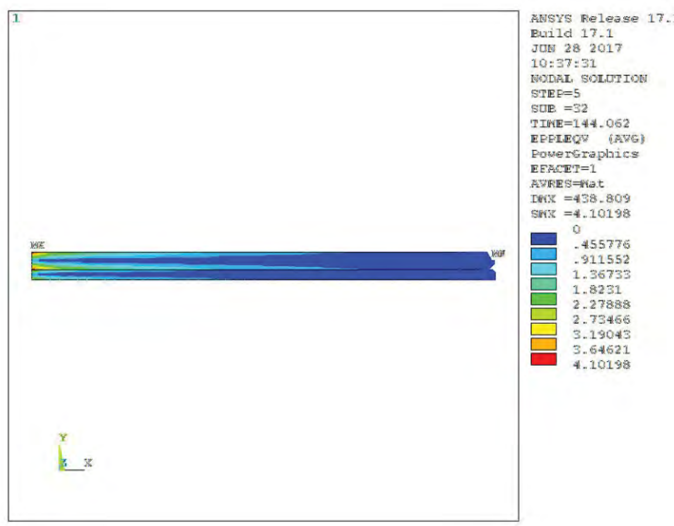

(d) EQV Plastic Strain in the Cover Plates at 144.1 psi

Figure 2 – Results of Limit Load for 2D-Axisymmetric Model – Service Level D

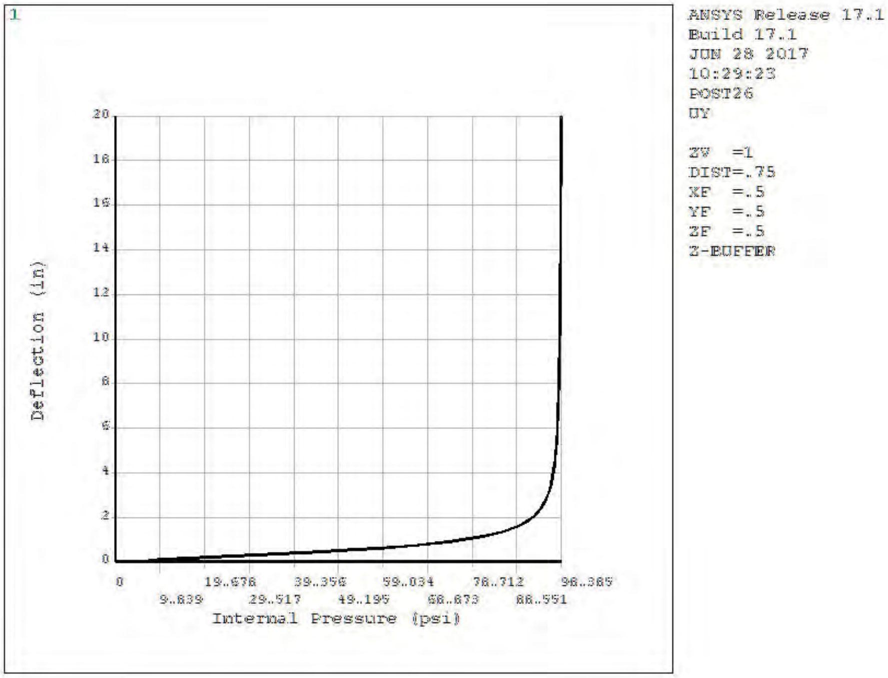

(a) Service Level A/B

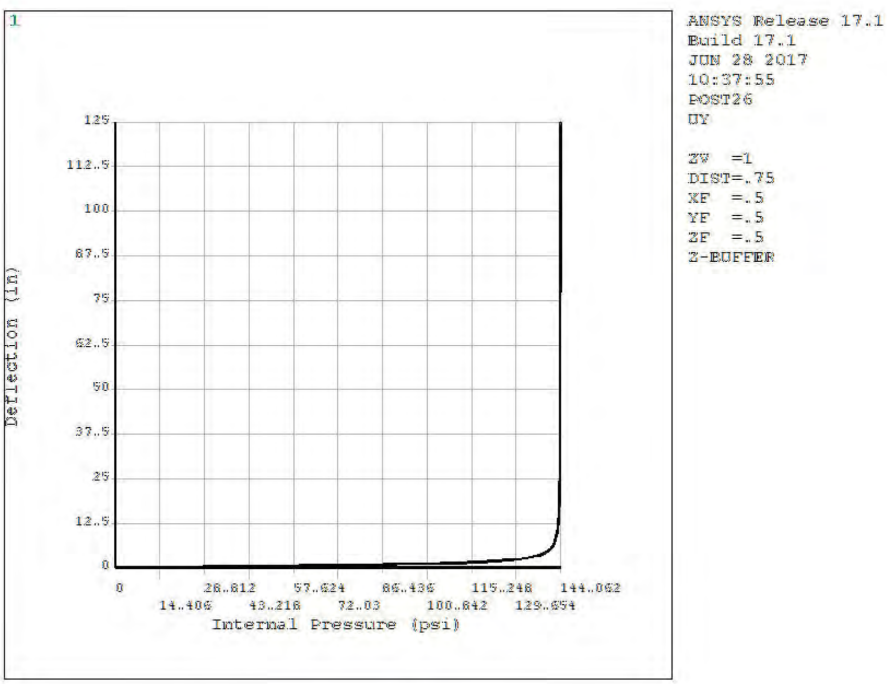

(b) Service Level D

Figure 3 – Deflection at the Center of the OTCP for the 2D-Axisymmetric Model for Limit Load (Maximum deflection occurs at the center point of the lids, in the outward axial direction)

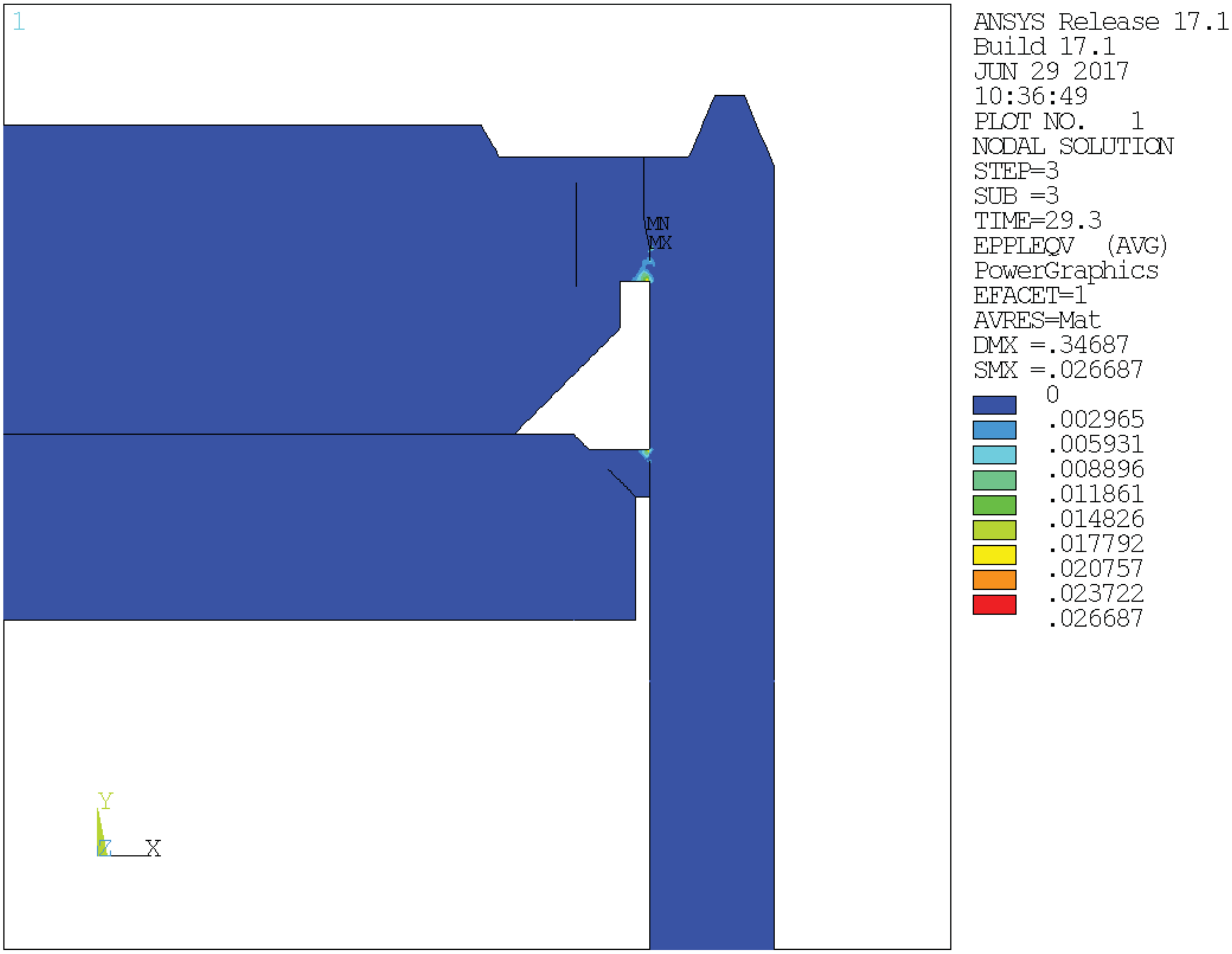

Figure 4 – Equivalent Plastic Strain at 29.3 psi for 2D-Axisymmetric Elastic Plastic Analysis - SL A/B Internal Pressure

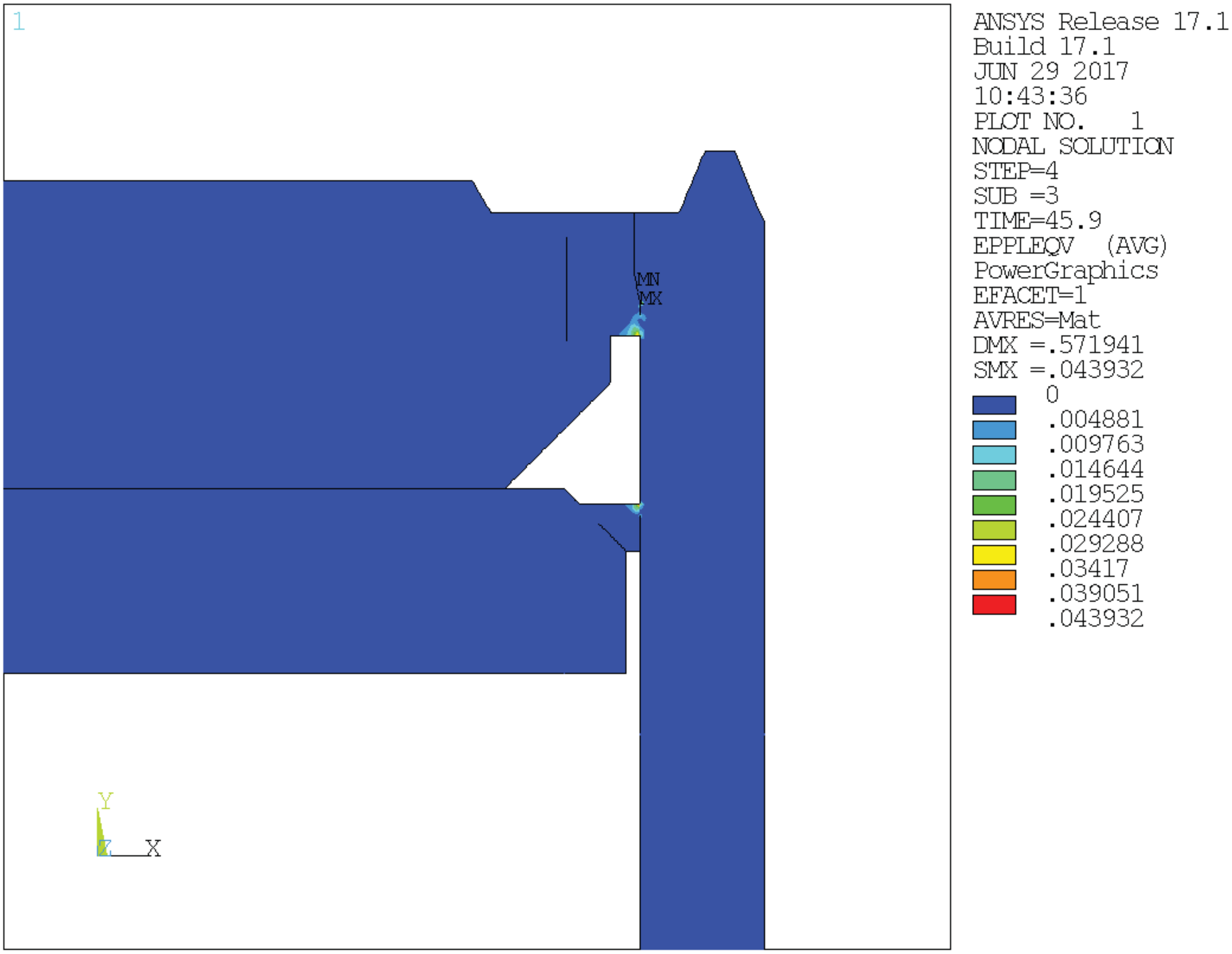

Figure 5 – Equivalent Plastic Strain at 45.9 psi for 2D-Axisymmetric Elastic Plastic Analysis - SL D Internal Pressure

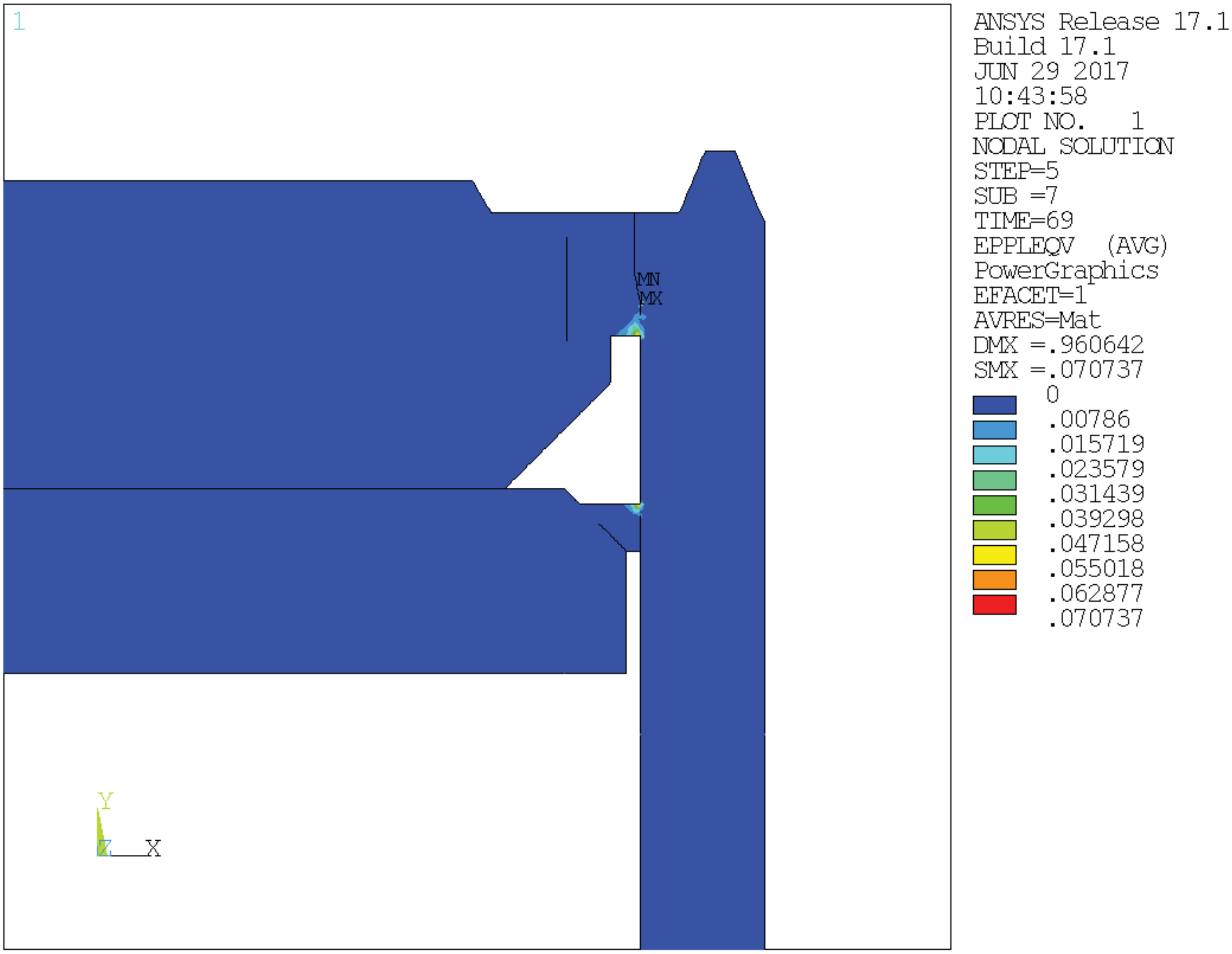

Figure 6 – Equivalent Plastic Strain at 69 psi for 2D-Axisymmetric Elastic Plastic Analysis - SL D Internal Pressure

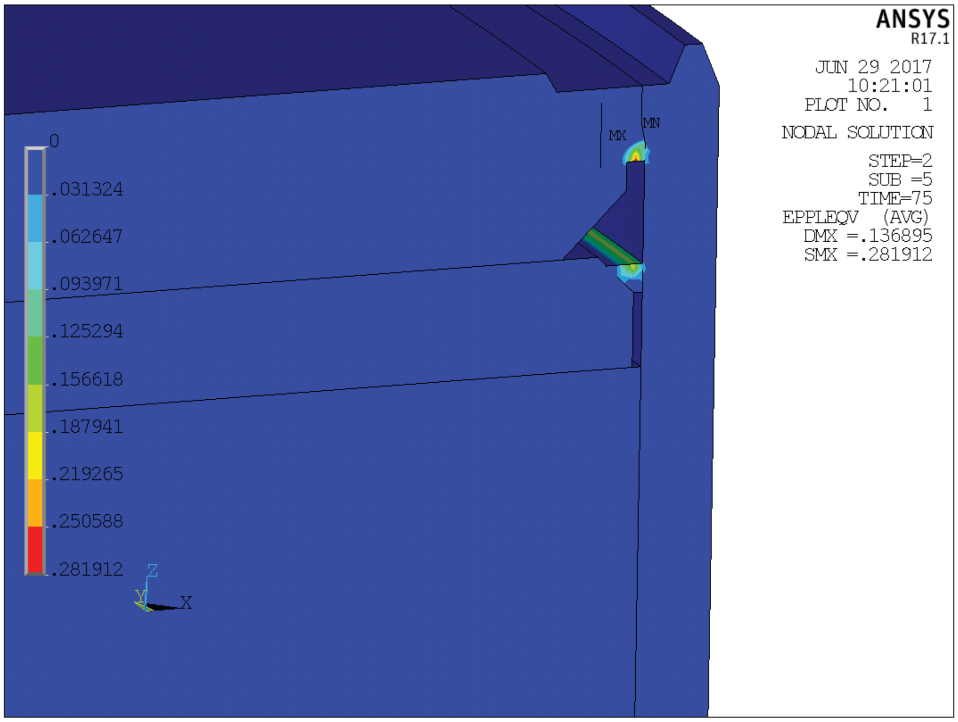

(a) Equivalent Plastic Strain in Weld Region [in/in] at 75g.

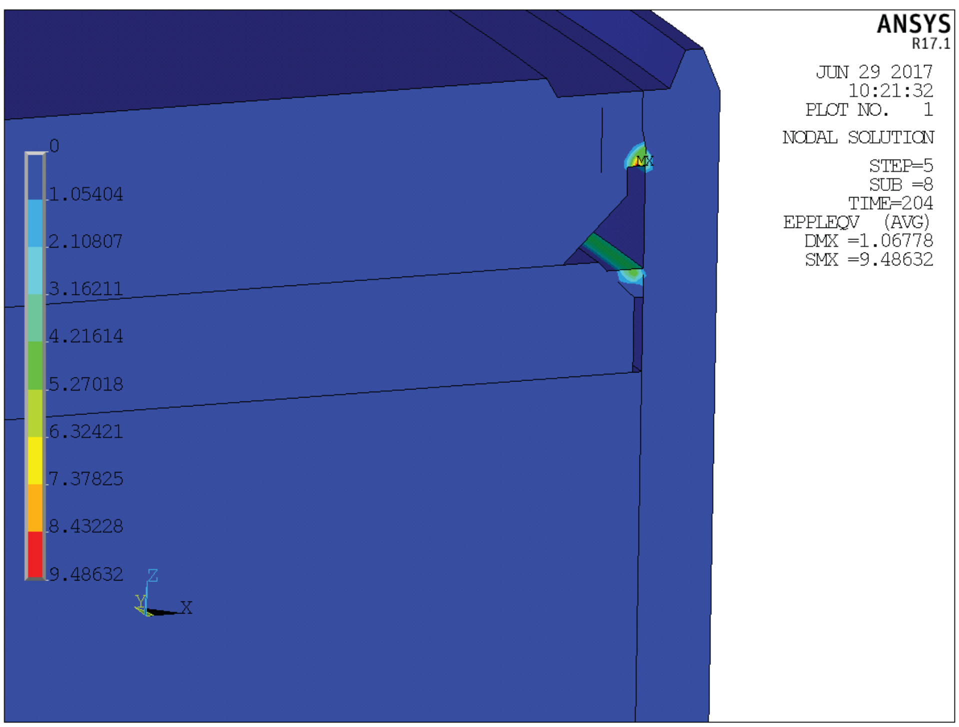

(b) Equivalent Plastic Strain in Weld Region [in/in] at 204g.

Figure 7 – Equivalent Plastic Strain Plots for 3D-Half-Symmetric Limit Load Analysis – SL D Side Drop with Off-Normal Internal Pressure

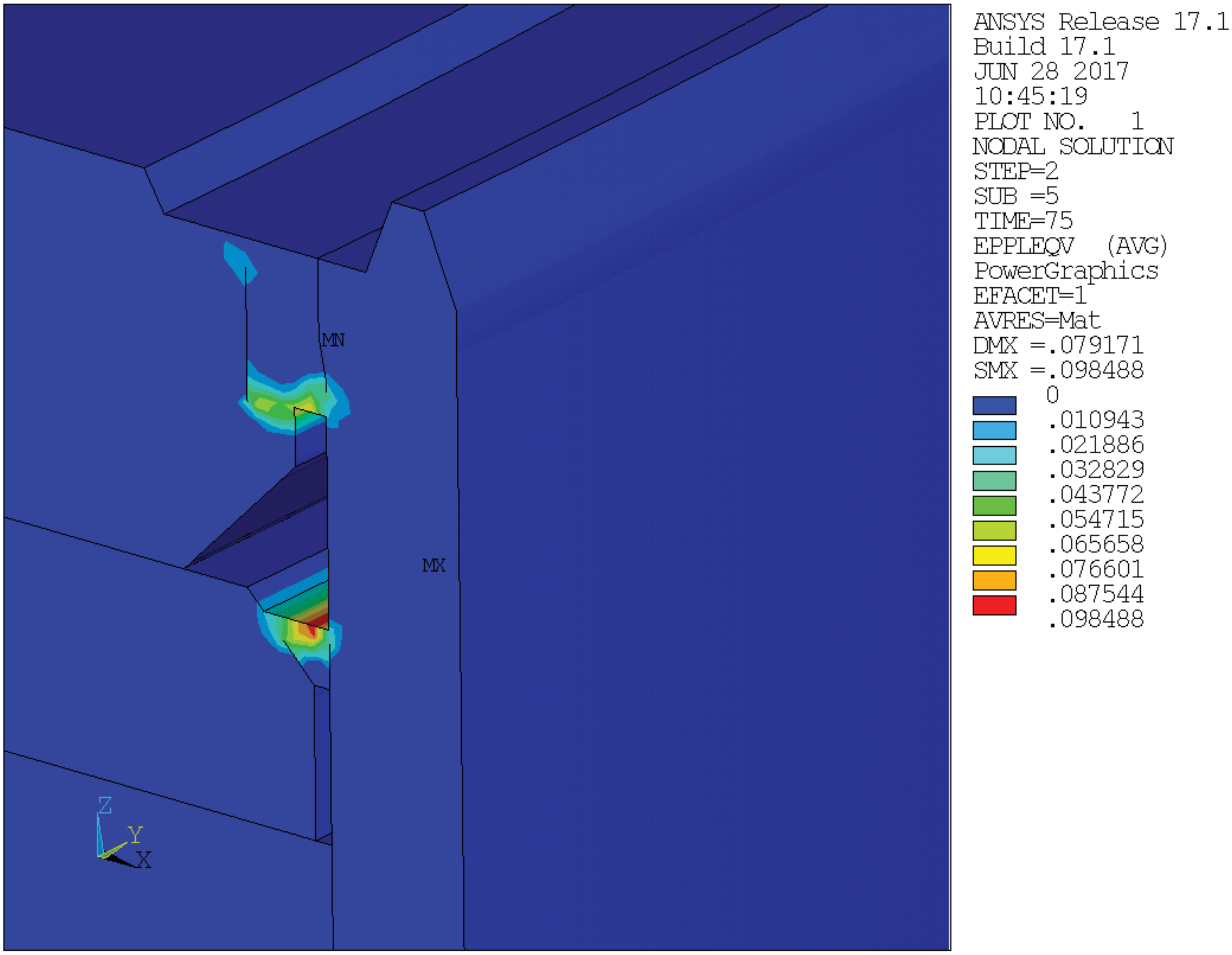

Figure 8 – Equivalent Plastic Strain at 75g for 3D-Half-Symmetric Elastic-Plastic Analysis - SL D Side Drop

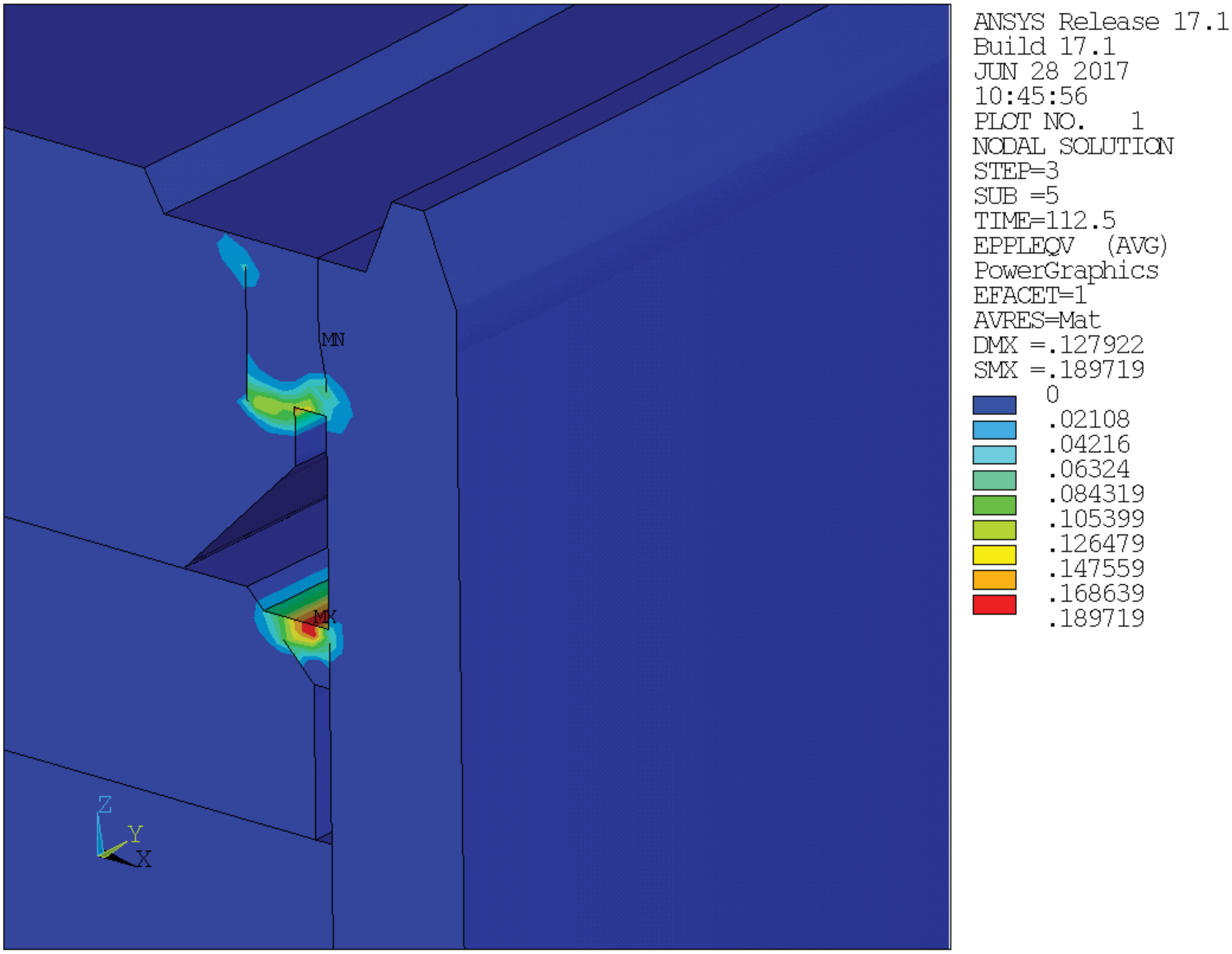

Figure 9 – Equivalent Plastic Strain at 112.5g for 3D-Half-Symmetric Elastic-Plastic Analysis - SL D Side Drop

ENCLOSURE 8

AREVA CALCULATION 11042-0209, REVISION 0

SITE SPECIFIC NUHOMS® 61BTH TYPE 1 DSC ITCP AND OTCP MARGIN EVALUATION FOR MAXIMUM WELD FLAW WITH SIDE DROP LOADS

20 pages follow

AREVA	Form 3.2-1 Calculation Cover Sheet Revision 12	**Calculation No.:** 11042-0209 **Revision No.:** 0 Page: 1 of 20

DCR NO (if applicable): N/A	**PROJECT NAME:** NUHOMS® 61BTH Type 1 DSCs for Monticello Nuclear Generating Plant
PROJECT NO: 11042	**CLIENT:** Xcel Energy

CALCULATION TITLE:
Site Specific NUHOMS® 61BTH Type 1 DSC ITCP and OTCP margin evaluation for Maximum Weld Flaw with side drop loads

SUMMARY DESCRIPTION:
1) Calculation Summary

This calculation evaluates the margins for Site-Specific Monticello NUHOMS® 61BTH Type 1 DSCs with the maximum flaws in the Inner Top Cover Plate (ITCP) and Outer Top Cover Plate (OTCP) closure welds based on as loaded temperature and pressure conditions, and site specific side drop loads.

2) Storage Media Description

- Coldstor - /areva_tn/11042/11042-0209-000

If original issue, is licensing review per TIP 3.5 required?
Yes ☐ **No** ☒ **(explain below)** **Licensing Review No.:**

This calculation is prepared in support of license exemption request which will be subjected to NRC review and approval. Therefore, a licensing review per TIP 3.5 is not required.

Software utilized (subject to test requirements of TIP 3.3):	**Software Version:**	**Software Log Revision:**
ANSYS	17.1	35

Calculation is complete Originator Name and Signature: Naveen SINGH Naveen	**Date:** 08/09/17
Calculation has been checked for consistency, completeness, and correctness Checker Name and Signature: Samuel TISSOT	**Date:** 08/09/2017
Calculation is approved for use Project Engineer Name and Signature: Raheel Haroon	**Date:** 8/9/2017

REVISION SUMMARY

Rev.	Description	Affected Pages	Affected Files
0	Initial issue	All	All

TABLE OF CONTENTS

Page

LIST OF TABLES

Page

LIST OF FIGURES

1.0 PURPOSE

The purpose of this calculation is to evaluate the margins for the NUHOMS® 61BTH Type 1 DSCs at the Monticello Nuclear Generating Plant (MNGP) per ASME Section III criteria with the maximum postulated flaws in the Inner and Outer Top Cover Plates (ITCP and OTCP) closure welds for Limit load and Elastic-Plastic analyses based on the side drop load cases performed in the reference calculation [5.5]. The as-loaded site specific bounding temperatures and pressures used in this calculation are provided in Ref. [5.6].

The site specific side drop load is used to better represent the actual Independent Spent Fuel Storage Installation's (ISFSI) approach slab at MNGP, instead of using the bounding 75g design side drop load.

2.0 ASSUMPTIONS

1. Assumptions 1 through 6 of Ref. [5.3] are applicable to this calculation.

3.0 DESIGN INPUT/DATA

3.1 Flaws Details and Geometry

The flaws details are identical to the maximum weld flaws evaluated in Ref. [5.4] and [5.5]. The geometry of the DSC structure is identical to the geometry used in Ref. [5.3], [5.4] and [5.5].

3.2 Material Properties

The material properties for the DSC structure are identical to the material properties of Ref. [5.3], [5.4] and [5.5]. They are duplicated here in Table 4 and Table 5 for convenience.

3.3 Design Criteria

All of the applicable design bases loading conditions are considered in accordance with the requirements of ASME Section III Subsection NB Ref. [5.2]. Section 4.1 details the methods used to perform the code Ref. [5.2] qualifications.

4.0 METHODOLOGY

4.1 Analysis Method and Acceptance Criteria

The analysis methods, finite element model details and acceptance criteria are the same as discussed in Ref. [5.3]. The ITCP and OTCP maximum weld flaws as evaluated in Ref. [5.4] are analyzed and margins are evaluated for Limit load and Elastic Plastic analyses. The as loaded site specific bounding temperatures and pressures used in this calculation are provided in Ref. [5.6].

The side drop and end drop design loads are set to 75g. These g-loads represent the ultimate capacity of the concrete slab, independently of the drop height (usually assumed at 80"), calculated with the Target hardness model used in Ref. [5.7] and validated in Ref. [5.8]. This ultimate capacity includes a 1.5 Dynamic Load Factor (DLF) and is assessed for the main ISFSI pad which is usually only present under the HSM's location. Therefore, several modifications of the drop g-load can be done by taking into account:

1. A low drop height. For MNGP, the drop height could be reduced to 64.5", but this method requires a full dynamic finite element analysis of the Transfer Cask (TC) drop on the pad.

2. The actual MNGP ISFSI pad design instead of the generic 36" thick pad design leading to the 75g load

3. The actual Approach slab parameters, instead of the ISFSI pad.

In this calculation, only modification 3 is done, using the slabs Target hardness model to derive a g-load reduction factor between the 30" MNGP ISFSI pad and the 15" Approach slab, for both side and end drop loads. Conservatively the 75g drop load derived for the generic 36" thick pad is considered also for the MNGP ISFSI 30" thick pad. The evaluation is done using the characteristic of the NUHOMS® TC OS197.

4.2 g-load Evaluation

The Target hardness model methodology of g-load evaluation is presented and validated in Ref. [5.8]. It was previously used for the NUHOMS® OS197 transfer cask in Ref. [5.7]. Although the NRC questioned the validity of the Target hardness model methodology (Page 3-19 of Ref. [5.11]), the 75g bounding drop load is accepted by the NRC. The methodology is not used here to evaluate a specific g-load value, but rather to find a ratio to evaluate the site specific g-load compared to the generic design 75g drop load.

Table 1 – Parameters for g-load Evaluation from Ref. [5.9]

Sl. No.	Parameters	30" ISFSI Pad	15" Approach Slab
1	28 day compressive strength of concrete, f'c (1)	4000 psi	4690 psi
2	Yield strength of reinforcement, fy (1)	60 ksi	72.3 ksi
3	Soil subgrade stiffness, k	50 pci	100 pci
4	Elastic modulus of concrete, Ec	$3.834E^6$ psi	$4.152E^6$ psi
5	Poisson ratio of soil, ν_S	0.33	0.33
6	Poisson ratio of concrete, ν_C	0.17	0.17
7	Impulse duration	0.016 sec	0.016 sec
8	Width of TC contact area (side drop), b	20 in.	20 in.
9	Concrete Pad thickness, h	30 in.	15 in.

Note:
(1) Parameters conservatively taken as designed for 30" ISFSI pad and maximum measured for 15" Approach slab

The correlation has been established between "limiting static deceleration" of the cask and "Target Hardness" (Page 2-1 of Ref. [5.8])

$$G = -345 + 33.5\ln(S) \qquad \text{for } 120{,}000 \le S \le 14.7 \times 10^6$$

$$G = -\,88 + 11.5\ \ln(S) \qquad \text{for } 13{,}300 \le S < 120{,}000$$
$$G = -\,15.35 + 3.85\ \ln(S) \qquad \text{for } S < 13{,}300$$

where:

G = limiting equivalent static deceleration as a multiplier on gravity

S = target hardness number (non-dimensional)

4.2.1 Bounding Static Deceleration for End Drop:

The bounding static deceleration values, based on the Ref. [5.8], are function of a "target hardness" parameter, S, given empirically as:

$$S = \frac{2rAK\ M_u\ f_c^{'}}{W^3\ (1 - e^{-\beta r}\ \cos\beta\ r)}$$

where:

M_u = ultimate moment capacity of the slab (lb-in),

W = weight of Transfer Cask (lb), 186175 lb for TC OS197 [5.7]

$f_c^{'}$ = ultimate strength of concrete (psi),

A = cask footprint area = $\pi \times r^2$ (in^2),

ν_S = Poisson's ratio of soil

ν_C = Poisson's ratio of concrete

k = soil subgrade stiffness,

r = cask radius (in), 39.56" for TC OS197 [5.7]

h = concrete pad thickness (in),

α = 1.15 (for a circle per Page 2-3 of Ref. [5.8])

$$\beta = \left(\frac{E_S}{4D_C}\right)^{1/4},$$

$$D_C = \frac{E_C h^3}{12\left(1-\nu_C^2\right)}$$ concrete slab rigidity (lb-in^2),

$$K = \frac{\pi E_s}{\left(1-\nu_s^2\right)}$$ foundation modulus,

$E_s = \dfrac{1-\nu_s^2}{\alpha} k\sqrt{A_s}$, soil's elastic modulus,

$A_s = \pi(2r+2h)^2/4$, effective bearing area of the concrete slab/soil interface,

$M_u = A_{st} f_y (h - 2c_{eff})$, ultimate moment capacity of the slab (lb-in) with

A_{st} = area of steel reinforcement

c_{eff} = effective concrete cover of the reinforcement

4.2.2 Bounding Static Deceleration for Side Drop:

The bounding static deceleration values, based on the Ref. [5.8], are function of a "target hardness" parameter, S, given empirically as:

$$S = \frac{2\,b\,L\,E_S\,M_u\,f_c'}{W^3 \beta}$$

where:

L = Length of cask (in), 207 in for TC OS197 Ref. [5.10]

α = 1.41 (for a rectangle per Page 2-3 of Ref. [5.8])

$$\beta = \left(\frac{E_S}{4E_C I_C}\right)^{1/4}$$

$$I_C = \left(\frac{1}{12}\right) L\, h^3$$

$$A_s = ((L+2h)(b+2h)$$

All other parameters are identical to the End drop parameters.

4.2.3 g-load Evaluation results

The above expressions of S depict the relationship between the g-load for end and side drops and the above input parameters. The parameter S is directly proportional to the concrete strength, soil modulus of elasticity, concrete pad thickness & inversely proportional to the weight of cask. Effects of concrete strength, concrete pad thickness and soil subgrade stiffness are higher as compared to the other parameters.

Table 1 shows that compressive strength of concrete is increased and concrete pad thickness is decreased. The dynamic amplification factor is the same, so it does not affect the evaluation here. The ratio new G to old G for side drop is conservatively taken as 0.7 as per parameters calculated in Section 9.0. 75g load is taken for the Side drop in Ref. [5.5]. The new site specific g-load is = 0.7 X 75 = 52.5g.

4.3 FEA Model Details

Finite element models detail of the DSC structure are identical to the ones described in Ref. [5.4].

4.4 Limit Load Solution Details

Limit load solution details are the same as detailed in Section 4.4 of Ref. [5.3].

4.5 Elastic Plastic Solution Details

Elastic Plastic solution details are the same as detailed in Appendix-A of Ref. [5.3].

4.6 Load Cases

Table 2 summarizes the actual internal pressure values which are taken from Table 2 of Ref. [5.3].

Temperatures used for the material properties for each Service Level condition are listed in Table 3. The Maximum Service Level (SL) D temperature of the DSC shell is taken as 370 °F as per Table 7-2 of Ref. [5.6] for a blocked vent accident. The same table also gives the maximum DSC shell SL-B temperature as 237 °F, before the blocked vent accident.

Two 3D-Half-Symmetric analyses for bounding SL D are performed.

5.0 REFERENCES

5.1. ANSYS Version 17.1. ANSYS Inc. (Including the ANSYS Mechanical APDL Documentation).

5.2. ASME Boiler and Pressure Vessel Code, Section III Subsection NB. 1998 Edition with Addenda through 2000.

5.3. AREVA Document No. 11042-0205 Revision 3. "61BTH ITCP and OTCP Closure Weld Flaw Evaluation"

5.4. AREVA Document No. 11042-0207 Revision 0. "NUHOMS® 61BTH Type 1 DSC ITCP and OTCP Maximum Weld Flaw Evaluation"

5.5. AREVA Document No. 11042-0208 Revision 0. "Site Specific NUHOMS® 61BTH Type 1 DSC ITCP and OTCP margin evaluation for Maximum Weld Flaw"

5.6. AREVA Document No. 11042-0400 Revision 0. "Site-Specific Thermal Evaluation of 61BTH Type 1 DSCs stored in HSM-H at Monticello Nuclear Generating Plant"

5.7. AREVA Document No. NUH-04.0110 Revision 0. "NUHOMS® ISFSI Cask Drop Acceleration"

5.8. Anatech Report TR-108760 prepared for EPRI, "Validation of EPRI Methodology of Analysis of Spent-Fuel Cask Drop and Tipover Events", August 1997.

5.9. AREVA Document DI-11042-04 Revision 0, Xcel Energy "DIT No. 60115-002 – Transmittal of MNGP Design Documents", 07/06/2017

5.10. AREVA Drawing DWG-NUH-06-8003, Revision 11. "NUHOMS® - OS197-1 Outer Transfer Cask Main Assembly"

5.11. US NRC, SER 1004, December 1994, "SER of SAR for the Standardized NUHOMS Horizontal Modular Storage System for Irradiated Nuclear Fuel"

6.0 ANALYSIS AND RESULTS

6.1 LIMIT LOAD ANALYSIS

3D-Half Symmetric Analyses for Side Drop Loading

Limit load analysis result for 3D half Symmetric model is presented in Section 6.1.2 of Ref. [5.5]. The collapse g-load for side-drop loading was found to be approximately 204g. Plots of the plastic strains in the side drop analyses are shown in Figure 1. The results for Limit load analysis are summarized in Table 6.

6.2 ELASTIC-PLASTIC ANALYSIS

3D-Half Symmetric Analyses for Side Drop Loading

The 3D-half-symmetric model described in Section 4.3 is used to perform the SL D side-drop limit load analysis. The case includes the 52.5g side-drop acceleration loading only. The maximum strains at loads up to 1.5x the specified loading (79g) are also extracted and compared with the material strain limit. The equivalent plastic strain was determined to be 5.8% for 52.5g and 10.6% for 79g. Figure 2 and Figure 3 show the corresponding plastic strain plots. The results for elastic-plastic analyses are summarized in Table 7.

7.0 DISCUSSION AND CONCLUSIONS

The analyses are done for site specific side drop g-load based on the Target hardness model which is used to derive the ultimate reinforced concrete slab capacity on which the TC could drop. This bounding g-load is found to be 52.5g for the MNGP site as compared to the 75g design load.

Limit Load Analyses:

The lower bound collapse G-Load for Service Level D side drop criteria was found to be 204 g which is greater than the limiting G-Load of 104 g (Table 6). Therefore the Service Level D criterion is satisfied.

Elastic-Plastic Analyses:

Table 7 lists the peak strains predicted by the elastic-plastic analyses for the bounding Service Level D. As shown in the table, the peak strain values remain below the material ductility limits at the specified loading conditions with a minimum margin of safety of 3.83. Therefore the elastic plastic analyses criteria are satisfied.

8.0 LISTING OF COMPUTER FILES

Finite Element Analyses were performed using ANSYS Version 17.1 Ref. [5.1]. All analyses were performed on HPC v2 Linux platform.

Load Case	Analysis Type	File Name	Description	Date / Time (1)
Side Drop 3D-Half-Symmetric model	Limit load analysis SL- D	LIMIT_HALFSYM.db	Reference .db file for half-symmetric limit load analysis	Ref.[5.5]
		LIMIT_HALFSYM-237.ext .ext = .inp, .err, .mntr, .out, .db, .rst	Limit load SL-D analysis files.	
	Elastic-plastic analysis SL- D	STRAIN_HALFSYM-237.db	Reference .db file for half-symmetric elastic-plastic analysis	Note (2)
		STRAIN_HALFSYM-52.5g.ext .ext = .inp, .err, .mntr, .out, .db, .rst	Elastic-plastic SL-D analysis files.	07/14/2017 20:13:57
		G-Factor_calculation.xlsx	Excel file to calculate G-Factor	07/17/2017 12:10

Notes:

(1) The date & time (EST) for the main runs are from the listing at the end of output file.

(2) ANSYS FE models are taken from Section 8.0 of Ref. [5.5].

Table 2 – Internal Pressure in the 61BTH Type 1 DSC [5.5]

Design Condition	Maximum Calculated Pressures used in this Calculation [psi]	Design Pressures [psi]
Normal	7.3	10
Off-Normal	10.9	20
Accident	45.9	65

Table 3 – Maximum Temperatures in the 61BTH Type 1 DSC Shell [5.6]

Design Condition		Maximum as loaded calculated Temperatures used in This Calculation [ºF]	Design Temperature [°F]
Normal	Storage	237	500
	Transfer	237	500
Off-Normal	Storage	237	500
	Transfer	237	500
Accident	Storage	370	625
	Transfer	237	500

Table 4 – Properties of SA-240 Type 304. Ref. [5.4]

Temp [^{o}F]	E Modulus of Elasticity [ksi]	S_m Allowable Stress Intensity [ksi]	S_y Yield Stress [ksi]	S_u Ultimate Tensile Strength [ksi]	Yield Stress for SL A/B Limit Load Analysis [ksi]	Yield Stress for SL D Limit Load Analysis [ksi]
70	28,300	20.0	30.0	75.0	30.0	46.0
100	28,138	20.0	30.0	75.0	30.0	46.0
200	27,600	20.0	25.0	71.0	30.0	46.0
300	27,000	20.0	22.4	66.2	30.0	46.0
400	26,500	18.7	20.7	64.0	28.1	43.0
500	25,800	17.5	19.4	63.4	26.3	40.3
600	25,300	16.4	18.4	63.4	24.6	37.7
700	24,800	16.0	17.6	63.4	24.0	36.8

Table 5 – Properties of SA-36. Ref. [5.4]

Temp [°F]	E Modulus of Elasticity [ksi]	S_m Allowable Stress Intensity [ksi]	S_y Yield Stress [ksi]	S_u Ultimate Tensile Strength [ksi]	Yield Stress for SL A/B Limit Load Analysis [ksi]	Yield Stress for SL D Limit Load Analysis [ksi]
70	29,500	19.3	36.0	58.0	29.0	40.6
100	29,338	19.3	36.0	58.0	29.0	40.6
200	28,800	19.3	33.0	58.0	29.0	40.6
300	28,300	19.3	31.8	58.0	29.0	40.6
400	27,700	19.3	30.8	58.0	29.0	40.6
500	27,300	19.3	29.3	58.0	29.0	40.6
600	26,700	17.7	27.6	58.0	26.6	40.6
700	25,500	17.3	25.8	58.0	26.0	39.8

Table 6 – Summary of Limit Load Analysis for the maximum weld flaws [5.5]

Sl. No.	Name	Loading	Temp. [F]	Analysis Criteria	Site Specific G-load (g)	Required G-load to Satisfy Limit load Criteria[1] (g)	Limit Load Collapse G-Load (g)	Code Limit Load Criteria Satisfied?
1	3D-Half-symmetric	Side drop with 10.9 psi off-normal IP	237	SL D	52.5	104.0	204.0	Yes

Note:

[1] See paragraph Limit Load Analyses, Section 7.0, Ref. [5.3]

Table 7 – Summary of Peak Strain Values for Elastic-Plastic Analyses for the maximum weld flaws

Load Case	Specific loading Side Drop G-Load (g)	Peak Equivalent Plastic Strain		Material Strain Limit	Margin of Safety at Specified Loading[2]
		at 52.5g loading	at 79g loading[1]		
3D-Half-symmetric Side Drop Service Level D	52.5	5.77%	10.6%	28%	3.83

Note:

[1] 1.5x Specified Loads
[2] Margin of Safety is calculated as (Strain Limit/Actual Strain)-1

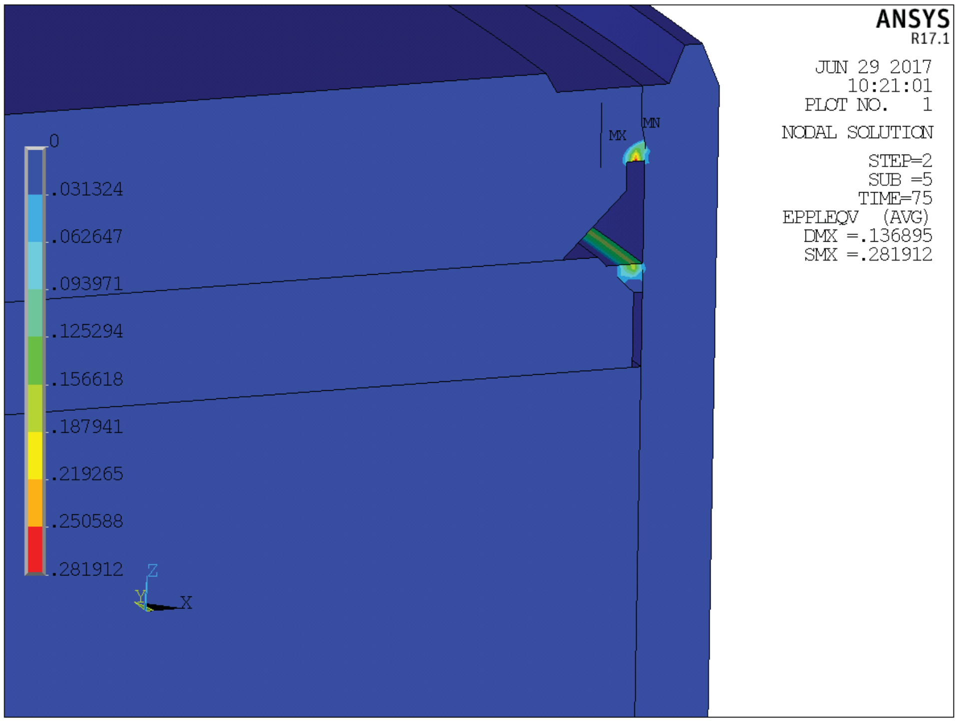

(a) Equivalent Plastic Strain in Weld Region [in/in] at 75g.

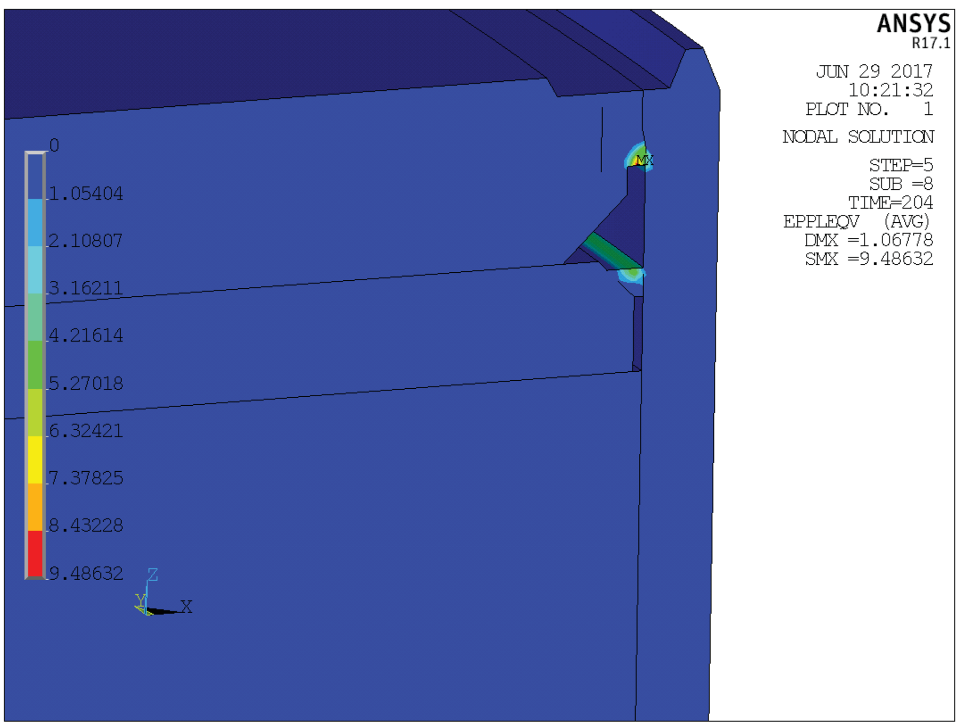

(b) Equivalent Plastic Strain in Weld Region [in/in] at 204g.

Figure 1 – Equivalent Plastic Strain Plots for 3D-Half-Symmetric Limit Load Analysis – SL D Side Drop with Off-Normal Internal Pressure (Ref. [5.5])

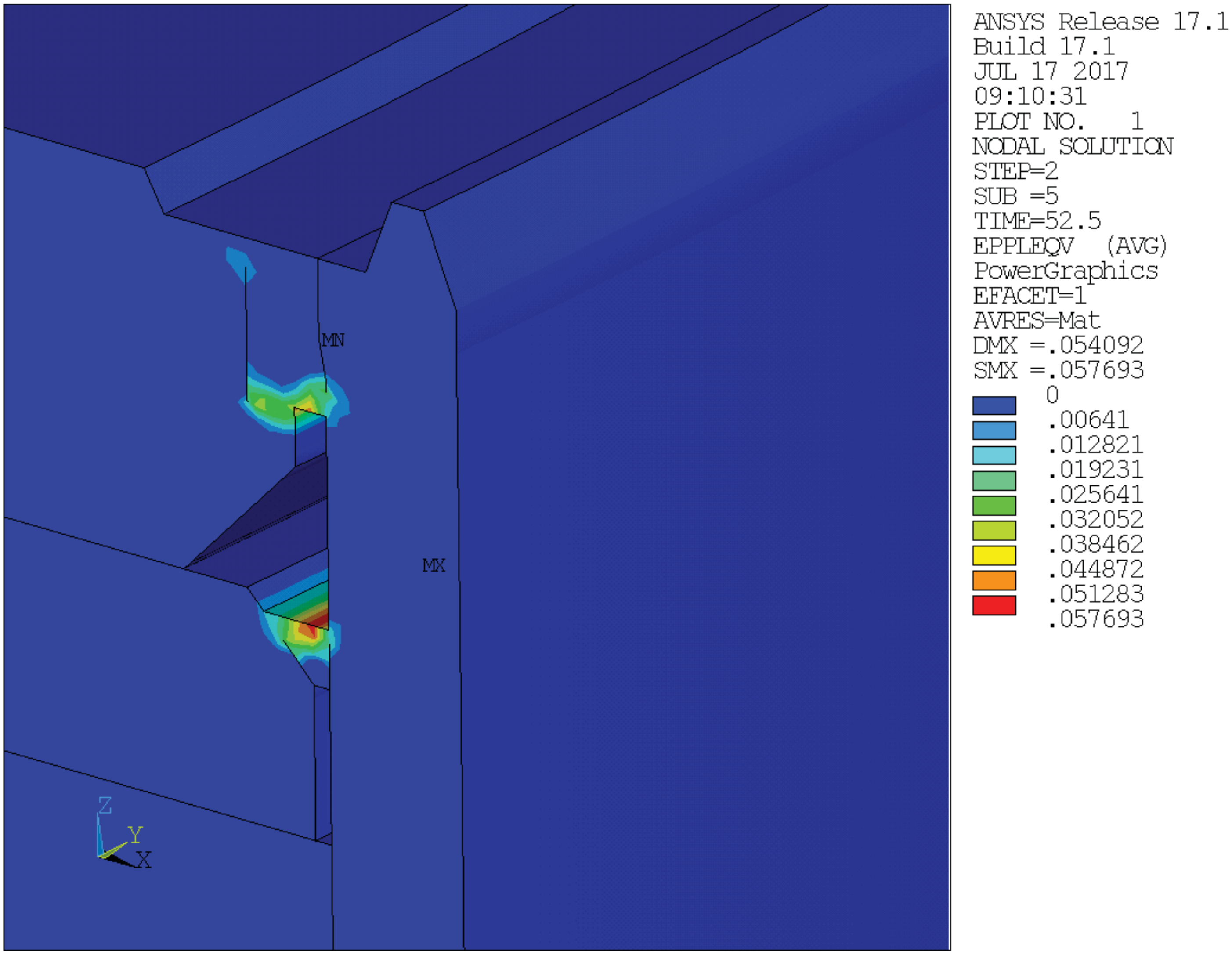

Figure 2 – Equivalent Plastic Strain at 52.5g for 3D-Half-Symmetric Elastic-Plastic Analysis - SL D Side Drop

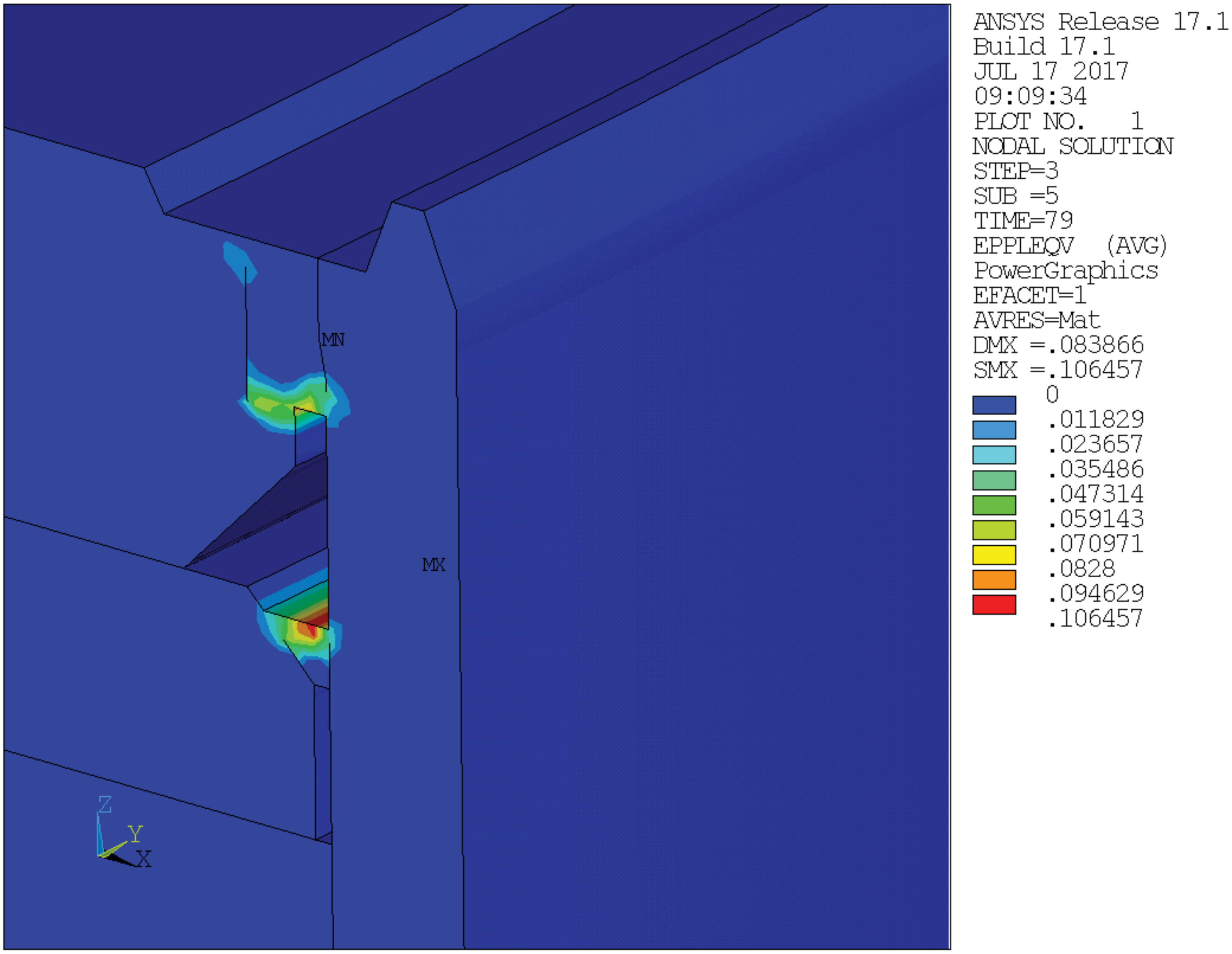

Figure 3 – Equivalent Plastic Strain at 79g for 3D-Half-Symmetric Elastic-Plastic Analysis - SL D Side Drop

9.0 APPENDIX A – CALCULATION FOR FACTOR G

30" ISFSI Pad		
	End drop	**Side drop**
r	39.56	
L		207
W	186175	186175
b		20
A	4916.57	
α	1.15	1.41
h	30.00	30.0
A_s	1.27	1.27
c_{eff}	3.0	3.0
k	50	50
fc'	4000	4000
fy	60000	60000
ν_S	0.33	0.33
ν_C	0.17	0.17
A_s	1.520E+04	2.136E+04
Ic		4.658E+05
Ec	3.83E+06	3.83E+06
Mu	1.824E+06	1.824E+06
Es	4777	4.618E+03
K	1.684E+04	
β	1.915E-02	5.043E-03
Dc	8.884E+09	8.884E+09
S	1.123E+04	8.575E+03
G_{old}	**20.6**	**19.5**
DLF	1.5	1.5

15" Approach Slab		
	End drop	**Side drop**
r	39.56	
L		207
W	186175	186175
b		20
A	4916.57	
α	1.15	1.41
h	15.00	15.0
A_{st}	0.44	0.44
c_{eff}	3.0	3.0
k	100	100
fc'	4690	4690
fy	72300	72300
ν_S	0.33	0.33
ν_C	0.17	0.17
A_s	9.352E+03	1.185E+04
Ic		5.822E+04
Ec	4.152E+06	4.152E+06
Mu	2.875E+05	2.875E+05
Es	7.493E+03	6.880E+03
K	2.642E+04	
β	3.533E-02	9.184E-03
Dc	1.202E+09	1.202E+09
S	2.243E+03	1.296E+03
G_{new}	**14.4**	**12.2**
DLF	1.5	1.5

For End drop: G_{new}/G_{old} = 14.4/20.6 = 0.70

For Side drop: G_{new}/G_{old} = 12.2/19.5 = 0.63

The designed g-load is 75g, the maximum ratio of G_{new}/G_{old} is 0.70. So the new g-load is =0.7X75 = 52.5g.

ENCLOSURE 10

APPLIED ANALYSIS CORPORATION CALCULATION MNGP-018, REVISION 0

ACCIDENT DOSE ASSESSMENT FOR MNGP DSCS 11-15

38 pages follow

APPLIED ANALYSIS CORP.

Calculation for:

XCEL ENERGY INC

MONTICELLO NUCLEAR GENERATING PLANT

MNGP-018

Accident Dose Assessment for MNGP DSCs 11 - 15

Assumptions Requiring Later Verification: ☐ No ☒ Yes Assumption 3.7

Nuclear Quality Status: Nuclear Quality

Method of Verification: ☑ Design Review ☐ Alternate Calculation

APPROVAL

Revision: 0

Prepared By: R. E. Anderson Date: 08/16/2017

Reviewed By: J. M. Cajigas Date: 08/16/2017

Approval By: J. M. Cajigas Date: 08/16/2017

For signatures see electronic file: MNGP-018 R0.pdf

LIST OF EFFECTIVE PAGES & ATTACHMENTS

PAGE	REV.	ATT. NO.	REV.	ATT. NO.	REV.
1-38	0	Att. 1	0		
		Att. 2	0		
		Att. 3	0		
		Att. 4	0		
		Att. 5	0		
		Att. 6	0		
		Att. 7	0		
		Att. 8	0		
		Att. 9	0		
		Att. 10	0		
		Att. 11	0		
		Att. 12	0		
		Att. 13	0		
		Att. 14	0		
		Att. 15	0		
		Att. 16	0		
		Att. 17	0		

TABLE OF CONTENTS

DESCRIPTION PAGE

LIST OF FIGURES

FIGURE # TITLE PAGE

None

LIST OF TABLES

LIST OF ATTACHMENTS

13. ORIGEN-ARP Input/Output, Electronic Files:
    MNGP DSC Decay – 0 Cutoff – 41 GWD.inp/arp/out/f71

Attachments 14-16 are electronic files:

14. RADTRAD Input/Output Files – DSC Source Term – EPRI Area 1.psf/o0
15. RADTRAD Input/Output Files – DSC Source Term – EPRI Area 2.psf/o0
16. RADTRAD Input/Output Files – DSC Source Term – EPRI Area 3.psf/o0

17. Design Verification Comment Sheet, Electronic File: DVCS - MNGP-018 R0

Revision History

Rev. #	Date	Purpose of Revision
0	08/16/17	Initial Issue

DEFINITIONS

AAC	Applied Analysis Corp.
AST	Alternative Source Term
BWR	Boiling Water Reactor
CFR	Code of Federal Regulations
Ci/MTU	Curies per Metric Ton Uranium
Ci/MWth	Curies per Megawatt Thermal
DCF	Dose Conversion Factor
DI	Design Input
DSC	Dry Shielded Canister
EAB	Exclusion Area Boundary (also referred to as Owner Controlled Area (OCA) Boundary)
EPU	Extended Power Uprate
GUI	Graphical User Interface
GWD	Gigawatt Days
ISFSI	Independent Spent Fuel Storage Installation
MNGP	Monticello Nuclear Generating Plant
MTU	Metric Tons Uranium
MWD	Megawatt Days
MWth	Megawatts Thermal
PU	Power Uprate Thermal Power
RG	Regulatory Guide
SQAP	Software Quality Assurance Program
SVVR	Software Validation and Verification Report
USNRC	United States Nuclear Regulatory Commission

COMPUTER DATA

The ORIGEN-ARP Version 5.1.01 computer program included with the SCALE Version 6.0 package (Reference 2.1) was used in accordance with the AAC SQAP Revision 0 (Reference 2.2). The originator has executed the sample problems per SVVR Section 6.4.1 and verified proper installation and execution (see Attachment 1).

The RADTRAD Version 3.03 program (Reference 2.3) was used in accordance with the AAC SQAP Revision 0 for RADTRAD Version 3.03 (Reference 2.4). The originator has executed the sample problems per SQAP Section 6.1.1 and verified proper installation and execution (see Attachment 2).

1.0 PURPOSE

MNGP is planning an Exemption Request for five (5) NUHOMS Dry Shielded Canisters (DSCs) that were placed in service at the MNGP Independent Spent Fuel Storage Installation (ISFSI) with noncompliant dye penetrant examinations (PTs). In support of this exemption request, an offsite radiological dose consequence analysis from an accidental release from an affected DSC is provided.

In accordance with Reference 2.5, the MNGP DSCs will not release radioactive effluents under any accidental circumstances. However, in order to support a justification of the above described Exemption Request, a radiation dose consequence analysis will be performed to determine the radiological dose consequences from a postulated accidental release from a single DSC at the MNGP ISFSI pad location to the site boundary (EAB).

As noted in calculation Section 7, the computed accident dose results are considered to be conservative for several reasons. Conservatisms that are directly scalable include the RG 1.109 calculated X/Q dispersion value and the use of a 100% occupancy factor by the public at the nearest plant EAB. Conservatisms that are not directly scalable include the impact from the failed fuel percentage, the calculated natural deposition coefficient and the consideration of DSC leakage at the maximum critical flux rate for the entire 30 day postulated accident duration.

Accident dose acceptance criteria per 10CFR72.106 (Reference 2.31) and NUREG-1567 (Reference 2.12) is shown in Tables 7.1 and 7.2.

2.0 LIST OF REFERENCES

2.1 ORNL/TM-2005/39, Version 6, Vol. I, Section D1, “ORIGEN-ARP: Automatic Rapid Processing For Spent Fuel Depletion, Decay, and Source Term Analysis”.

2.2 AAC Software Quality Assurance Plan SQAP–ORIGEN-ARP-R0, “Software Quality Assurance Plan, ORIGEN-ARP”, Revision 0.

2.3 NUREG/CR-6604, “RADTRAD: A Simplified Model for RADionuclide Transport and Removal and Dose Estimation”, December 1997, NUREG/CR-6604 (SAND98-0272/1), Supplement 1, “RADTRAD: A Simplified Model for RADionuclide Transport and Removal and Dose Determination”, June 8, 1999, and NUREG/CR-6604, Supplement 2, “RADTRAD: A Simplified Model for RADionuclide Transport and Removal and Dose Determination”, October 2002.

2.4 Applied Analysis Corp. Software Quality Assurance Plan, Revision 0, “SQAP – RADTRAD – R0”.

2.5 Monticello Nuclear Generating Plant, Independent Spent Fuel Storage Installation (ISFSI), 10CFR72.212(b)(5)(iii) Radiological Evaluation.

2.6 MNGP Calculation 16-090, “MNGP EPU – Core Inventory With GE14 Fuel With 37 GWD/MTU Exposure”, Revision 0.

2.7 EPU Correspondence Number: MNGP-375-GE, dated 11/15/07, “MNGP EPU Radiological Design Basis Update – AST DIR R2”, Attachment EPU-DIT-0198.

2.8 MNGP Calculation 11-245, “Task Report T0802 Core Source Term (GE -NE-0000-0064-6767-TR-RO)”, Revision 0.

2.9 DIT-AAC-001 (EC-18508), “CORE RELOAD MOD FOR CYCLE 29 OPERATION”, 12/14/2016.

2.10 Design Information Transmittal (DIT) No. 48 (EC-18508), 6/06/2013, “Subject: Design Inputs for MNGP AST Calculations (CRDA and LOCA)”.

2.11 Design Information Transmittal (DIT) 67492-001 (Mod/Tracking No. 18624), “Spent Fuel Loading of Dry Shielded Canisters 6A-10B”, 5/19/2017.

2.12 USNRC NUREG-1567, "Standard Review Plan for Spent Fuel Dry Storage Facilities," U.S. Nuclear Regulatory Commission, February 2000.

2.13 USNRC NUREG-1864, “A Pilot Probabilistic Risk Assessment Of a Dry Cask Storage System At a Nuclear Power Plant”, Published March 2007.

2.14 USNRC NUREG-1536, "Standard Review Plan for Spent Fuel Dry Storage Systems at a General License Facility," Revision 1, U.S. Nuclear Regulatory Commission, July 2010.

2.15 “Table of Isotopes”, Eighth Edition, Richard B. Firestone, V. S. Shirley.

2.16 USNRC Regulatory Guide 1.109, Calculation of Annual Doses to Man from Routine Releases of Reactor Effluents for the Purpose of Evaluating Compliance With 10CFR50 Appendix I," Revision 1, October 1977.

2.17 USNRC Regulatory Guide 1.145, Atmospheric Dispersion Models For Potential Accident Consequence Assessments At Nuclear Power Plants," Revision 1, November 1982.

2.18 Federal Guidance Report (FGR) 11, "Limiting Values of Radionuclide Intake and Air Concentration and Dose Conversion Factors," 1989.

2.19 Federal Guidance Report (FGR) 12, "External Exposure to Radionuclides in Air, Water, and Soil," 1993.

2.20 Monticello Nuclear Generating Plant, Unit No. 1 Facility Operating License, Amendment No. 147 dated July 5, 2006.

2.21 USNRC Document SMSAB-00-03, "Best-Estimate Offsite Dose from Dry Storage Cask Leakage," Prepared by Jason H. Shaperow, June 2000.

2.22 USNRC Regulatory Guide 1.183, Alternative Radiological Source Terms For Evaluating Design Basis Accidents At Nuclear Power Reactors," July 2000.

2.23 Transnuclear, "Final Safety Analysis Report, Standardized NUHOMS Horizontal Modular Storage System for Irradiated Nuclear Fuel", NUH-003, Revision 8, Appendices K & L.

2.24 PNL 10286, "Atmospheric Dispersion Estimates In The Vicinity Of Buildings", By J. V Ramsdell, Jr and C. J Fosmire, dated January 1995.

2.25 American National Standards – ANSI N14.5-1997, "For Radioactive Materials – Leakage Tests on Packages for Shipment".

2.26 USNRC 10 CFR Part 71, "Packaging And Transportation Of Radioactive Material".

2.27 "Introduction to Unsteady Thermofluid Mechanics", F. J. Moody, 1990.

2.28 "Basic Principles and Calculations in Chemical Engineering", 2nd Edition, D. M. Himmelblau.

2.29 Design Information Transmittal (DIT) 67492-002 (Mod/Tracking No. 18624), "Spent Fuel Loading of Dry Shielded Canisters 6A-10B", 6/9/2017.

2.30 Transnuclear, "Final Safety Analysis Report, Standardized NUHOMS Horizontal Modular Storage System for Irradiated Nuclear Fuel", NUH-003 Revision 11, Appendix T.

2.31 USNRC 10 CFR Part 72, "Licensing Requirements For The Independent Storage Of Spent Nuclear Fuel, High-Level Radioactive Waste, And Reactor-Related Greater Than Class C Waste".

2.32 Holtec International .Topical Safety Analysis Report for the Holtec International Storage, Transport, and Repository Cask System (HI-Star 100 Cask System). NRC Docket No. 721008, Holtec Report HI-941184, Rev. 8. August 1998.

2.33 Design Information Transmittal (DIT) 67492-004 (Mod/Tracking No. 18624), "Spent Fuel Loading of Dry Shielded Canisters 6A-10B", 7/13/2017.

2.34 AREVA Calculation 11042-0400 R0, "NUHOMS®° 61BTH Type 1 DSCs for Monticello Nuclear Generating Plant".

3.0 ASSUMPTIONS

3.1 ORIGEN-ARP calculations are performed on a 1 MTU reference basis.

3.2 For DSC accident, fraction of fuel rods assumed to fail is 1.0 (100% of available fuel rods), Reference 2.11, Item A.9.

3.3 For DSC accident, fraction of gases in fuel rods assumed available for release is 1.0 (100%).

3.4 For the DSC accident, a public individual is assumed present at the nearest EAB boundary for the accident duration, i.e., 100% Occupancy Factor.

3.5 For calculation of the natural deposition removal coefficient, λ Hr^{-1}, use of the Reference 2.21 “best estimate” (50^{th} percentile) settling velocity of 0.00082 m/sec is used. Use of the 50^{th} percentile or “best estimate” is deemed as the most appropriate methodology for the evaluation of a “realistic” accident dose.

3.6 Calculations to be performed at 102% of the re-rated power level (1775 MWth) (Also referred to as Power Uprate, PU) which was the highest power limit when the subject fuel assemblies in DSCs 11 – 15 were irradiated., see Section 4.9.

3.7 MNGP site specific preliminary AREVA Calculation 11042-0400 R0 (Reference 2.34) based on actual DSC 11-15 heat loads predicts a peak accident DSC pressure of 45.91 psig (use 46 psig) and a peak accident temperature of 404.75 °F (use 405 °F). ***This assumption requires later verification.***

3.8 No additional assumptions used.

4.0 DESIGN INPUT

ORIGEN-ARP DSC Source Term:
Design Input items 4.1 – 4.4 are initially pulled from calculation 16-090 R0, Reference 2.6 (with the exception of the reference numbers and wording) and modified as described below. This information is provided herein for completeness as the ORIGEN-ARP model used to determine the source term within the MNGP DSC is the exact same model as developed in 16-090 R0 (See Reference 2.11, Item A.1) with the exception of post-operation decay time and average fuel exposure (See Sections 4.3, 4.5 and Section 6.1 discussions).

4.1 The baseline DSC ORIGEN-ARP source term analysis is performed at 102% of the EPU power level (2044 MWth, Reference 2.7 Item B.1). Final ORIGEN-ARP results are scaled in Attachment 5 to PU (re-rated) power, see Section 4.9. Note that this is an appropriate conservative analytical approach for this evaluation because the actual fuel loaded in DSCs 11 – 15 pre-date MNGP EPU. The fuel stored in DSCs 11 -15 have an exposure based on plant operation at PU (1775 MWth) and 41 GWD/MTU or less.

4.2 The MNGP EPU core is based on GE14 fuel. The design parameters of that fuel are identified per Table 3.2.1 of Reference 2.8 which is repeated below (Also see Reference 2.6).

Table 4-1 - Reference 2.8 Table 3.2.1 – Key Inputs

Item	Parameter	Value	Units
1	Fuel type	GE14	N/A
2	Fuel bundle mass (Uranium)	182	Kg
3	Fuel bundle average enrichment	4.6	%
4	MNGP specific fuel bundle thermal power density based on the 2044 MWth and 484 fuel bundles per core data from above (2044 MWth / 484 fuel bundles)	4.223	MWth
5	Core average end of cycle exposure	***41 (See 4.3)***	GWD/MTU
6	Maximum discharge bundle exposure	58	GWD/MTU

4.3 In the Reference 2.9 and Reference 2.6 ORIGEN-ARP model, the core average end of cycle exposure considered was 37 GWD/MTU. As noted in Item 4.1 and Reference 2.33 Item A.1, the DSCs 11-15 canister average fuel assembly exposure is based on PU plant operation (1775 MWth) at a maximum of 41 GWD/MTU. See the Attachment 12 spreadsheet which calculates the average exposure of the 61 fuel assemblies within each of DSCs 11-15 based on the Cask Loading Reports supplied via Reference 2.11, Item A.1.

4.4 Number of fuel assemblies (bundles) in MNGP GE14 core = 484 (Reference 2.10, Attachment 1, Item 3.c)

4.5 Decay time of fuel within DSC is 15.53 years (Reference 2.11, Item A.2). From inspection of Cask Loading Reports (CLRs) the lowest value of Cooling Years is 10.06, but that is just one assembly (an outlier). Since the source term is a summation of all assemblies in a DSC, it is mathematically appropriate to use an average across the entire canister (CLRs report Cooling Years ranging up to 20.30 years). However, to keep the calculation simple, it is appropriate and conservative to use the second-lowest cooling-time increment (11.53 years associated with a discharged batch of fuel) and add the 4 years that have transpired from the data date on the CLRs (5/16/2017 minus 5/16/2013).

4.6 MNGP DSC is a NUHOMS 61BTH Type 1 Model containing 61 fuel assemblies (Reference 2.11, Item A.3)

4.7 Source term isotopes of concern determined using ORIGEN-ARP to be consistent with the guidance of NUREG-1567 (Reference 2.12) Section 9 and Table 9.2 and Reference 2.14 Table 5.2 specifications (See Reference 2.11, Items A.4 and A.5).

1. Crud as Co-60 determined as per DI Item 4.8 (See Reference 2.12, Table 9.2 footnote "#", Co-60 activity specified as 1254 $\mu Ci/cm^2$ and Reference 2.14, Table 5.2).
2. Iodines
3. Fission products which are greater than 0.1% of total design basis activity
4. Actinides which are greater than 0.01% of total design basis activity

4.8 DSC Co-60 activity per fuel assembly calculated as follows.

Fuel Rod Activity = 1254 $\mu Ci/cm^2$ per DI Item 4.7
Maximum Crud Reduction Factor = 2 per NUREG 1864 Table D.1, axial distribution (Reference 2.13)
Fuel Rods per Assembly = 92 (Reference 2.11, Item A.6)
Fuel Rod Length = 150 inches (Reference 2.11, Item A.7)
Fuel Rod Outside Diameter = 0.483 inch (Reference 2.11, Item A.8)

Fuel Assembly Surface (cm^2) = 92 * (150 * 2.54) * π * (0.483 * 2.54) = 135,096

Co-60 half-life = 5.2714 years (Reference 2.15, Table 1, page 277)

Co-60 Activity (Ci) = ((1254 / 2) *135096) / 1E+06 * (exp (-ln(2)*15.53/5.2714)) = 10.99

4.9 The Power Uprate (PU) power level is 102% if 1775 MWth = 1810.5 MWth (References 2.20 and 2.33, Item A.1). The ORIGEN-ARP source term (Attachment 13) will be <u>scaled</u> to this power level in Attachment 5.

RADTRAD DSC Dose Calculation:

4.10 Isotopic fuel rod activity released from fuel rods to DSC volume (See Reference 2.11, Item A.10).

NUREG-1567 Table 9.2:
Gases Fraction = 0.3
Volatiles Fraction = 2.0E-04 Per (per footnote, Cs-134, 135 & 137; Ru-103 & 106, Sr-89 & 90)
Fuel fines Fraction = 3.0E-05
Crud (Co-60) fraction = 1.0

Co-60 activity release fraction is reduced to 0.015 based on further justification per Reference 2.13, Section D.2.4.2 and Table D.7.

4.11 Adult Breathing Rate = 2.50E-04 m^3/sec per Reference 2.11, Item A15 and Reference 2.16.

4.12 Distance to nearest EAB location from SW corner of HSM-6A = 245 m (Reference 2.29). Also given distance to nearest EAB location from SW corner of 30 HSM Array = 235 m (Reference 2.11, Item A.13).

4.13 χ/Q value calculated per RG 1.145 (Reference 2.11, Item A.14 & Reference 2.12, page 9-15 based on wind stability Class F and a wind speed of 1 m/sec)

Nearest EAB Distance = 235 m minimum (See DI Item 4.12 above)
Wind Stability Class = F
Wind Speed = 1 m/sec

Per Reference 2.17 Section 1.3.1.a:
Min Vertical Plane X-Sectional Area = 0 m (conservative value)
Note that the scale of Figures 1, 2 & 3 (log-log scale) are too large to distinguish between 235 and 245 m.
σ_y, m = 10 (Interpolated per Reference 2.17, Figure 1)
σ_z, m = 5 (Interpolated per Reference 2.17, Figure 2)
M = 4 (Per Reference 2.17, Figure 3)
$\sum_y = M * \sigma_y = 4 * 10 = 40$

Equation 1 = $1 / (1 * (\pi * \sigma_y * \sigma_z + 0/2)) = 6.37E-03$ sec/m^3
Equation 2 = $1 / (1 * (3 * \pi * \sigma_y * \sigma_z)) = 2.12E-03$ sec/m^3
Equation 3 = $1 / (1 * (\pi * \sum_y * \sigma_z)) = 1.59E-03$ sec/m^3

Select largest χ/Q value from Eqn. 1 &2 = 6.37E-03 sec/m^3
Select smallest χ/Q value from above and Eqn. 3 = 1.59E-03 sec/m^3

See Section 6.3 for discussion of χ/Q value modification

4.14 Inhalation Dose Conversion Factors per Reference 2.18 and Reference 2.11, Item A.16 with additional guidance per Reference 2.3.

4.15 Submersion Dose Conversion Factors per Reference 2.19 and Reference 2.11, Item A.17 with additional guidance per Reference 2.3.

4.16 DSC free volume = 365000 in^3 = 211.2 ft^3, Reference 2.11, Item A.21.

4.17 DSC channel opening dimension are 5.8 inch by 5.8 inch, Reference 2.29.

4.18 DSC channel length = 164 inches per Reference 2.29.

4.19 DSC cavity free volumes – Table T.4-29 per Reference 2.11, Item A.21 & Reference 2.30.
Cavity volume = 618,766 in^3
Basket volume = 108,888 in^3
Fuel volume = 141,947 in^3
Bounding free volume = 365,000 in^3

4.20 DSC accident pressure – 46 psig per Reference 2.33, Item A.22 and Assumption 3.7 (requiring later verification)

4.21 DSC accident temperature – 405 °F per Reference 2.33, Item A.23 and Assumption 3.7 (requiring later verification)

4.22 DSC gas mass from Table T.4-24 of Reference 2.30:
DSC Cavity He Fill Gas = 192.9 g-mole
Fuel Rod He Gas = 83 g-mole
Fission Product Gases = 369.7 g-mole

5.0 METHODOLOGY

5.1 ORIGEN-ARP DSC Source Term:

The first step in this assessment is to re-run the Reference 2.6 Attachment 3 ORIGEN-ARP model and confirm a match.

The second step in this assessment is to modify the existing ORIGEN-ARP model from Attachment 3 of Reference 2.6 to reflect the additional decay time consistent with the fuel assemblies within the subject MNGP DSC and to subsequently run ORIGEN-ARP with an average fuel exposure of 37 GWD/MTU. This step is also used as a confirmation, this time to confirm that the isotopic activity at a decay time of 180 days matches the existing ORIGEN-ARP model from Attachment 3.

The third step repeats step two with the additional modification of an average fuel exposure of 41 GWD/MTU.

The fourth step is to take the step 3 ORIGEN-ARP output and manipulate this data to:

1. Determine fission product isotopes that meet the 0.1% of total design basis activity criterion
2. Determine actinide isotopes that meet the 0.01% of total design basis activity criterion
3. Convert the step 3 & 4 isotopic data (units of Ci/MTU) to Ci activity in a single DSC

This fourth step is accomplished using an Excel spreadsheet (Attachment 5).

5.2 RADTRAD DSC Dose Calculation:

The organ dose calculations are performed using the RADTRAD computer code (Reference 2.3) and the Attachment 5 Excel spreadsheet. A simple two volume (DSC & Environment), one pathway (DSC to Environment) and one dose location (EAB) model is developed. Default RADTRAD input files are modified as outlined below:

1. Source Term File (*.NIF) – 14 of the Table 6-1 isotopes exist in the default BWR LOCA “NIF” file. For those 14 isotopes, the Table 6-1 source is input appropriately. An additional 7 isotopes (plus Sm-151) from Table 6.1 are added to the new “NIF” file by replacing default isotopes 21 – 28 which are not needed for this calculation. The source term for the remaining 39 isotopes (default 60 – 21) are zeroed.
2. Release Fraction & Timing File (*.RFT) – The default BWR “RFT” is modified to instantaneously (0.01 Hours) release the Table 6.1 source term to the RADTRAD DSC volume in accordance with the defined “Fuel to DSC” release fractions given in DI Item 4.10. Release fractions for nuclide groups not represented by the 21 isotopes in Table 6.1 are zeroed.
3. Dose Conversion Factors, DCF (*.INP) – Inhalation DCFs are given per DI Item 4.14. Submersion DCFs are given per DI Item 4.15.

6.0 RESULTS

6.1 ORIGEN-ARP DSC Source Term:

The ORIGEN-ARP input deck is generated by importing the Reference 2.6, Attachment 3 ORIGEN-ARP model as described below. Changes to the Reference 2.6, Attachment 3 model to reflect the DI Item 4.3 specific DSCs 11-15 fuel assembly burnup and DI Item 4.5 DSC fuel assembly decay time of 15.53 years are shown in bold italics below.

Title:	***MNGP DSC Decay – 0 Cutoff - 41 GWD Fuel***
Fuel Type:	ORIGEN-ARP fuel type GE10x10-8 which represents GE 10x10 fuel (GE14) as per calculation Item 4.2
Uranium Mass:	1.0E6 grams (Assume 1.0 MTU as reference basis, Assumption 3.1)
Fuel Enrichment:	4.6% per calculation Item 4.2
Fuel Burnup:	***41***000 MWD/MTU (***41*** GWD/MTU) per calculation Item 4.3
Irradiation Cycles:	3 (Using default number. The problem has 1 decay cycle following the third irradiation cycle and no intermediate decay cycles)
Cooling Time:	***5668*** days (Assumed decay duration with default intervals***, see change from 180 day to 15.53 years (5668 days) described below)***
Moderator Density:	0.7332 g/cc (Default value)
Power History:	100% continuous operation (No intermediate decay cycles)
Average Power:	Data from calculation Item 4.2 and 4.4

1000kg/MTU * 2044 MWth/ (484 bundles * 182 kg/bundle) = 23.2 MWth/MTU

Decay Cycle Options:	Access by selecting the “Apply” and “OK” tabs to exit the “Express” option. On leftmost column of ORIGEN-ARP screen select “Cases” tab. On the pop-up dialog box entitled “Case Data” under the “Select Existing Case” column select the “Decay – 3 Cycle Down” case and Click “OK” at bottom of dialog box. ***Modify input decay times per the Rule of 3’s (decay time step roughly no greater than a factor of 3) to be 10, 30, 100, 180, 500, 1000, 2500, 5668 days (5668 days = 15.53 years). The 180 day decay time value is chosen to facilitate comparison with the Reference 2.6, Attachment 3 results.*** On the lower horizontal tab bar select the “Options” tab. In the “Decay Output Options” dialog box, change “Table cutoff to 0.00%. Change “Results In” from grams to Curies. Check all selections under the “Tables” and “Edit By” tabs then click “OK” at dialog box bottom. Save and run case.

The input data was developed using the ORIGEN-ARP GUI. The problem was executed on a microcomputer operating under WindowsXP and the input/output files are saved as MNGP DSC Decay – 0 Cutoff – 41 GWD.* and may be found as Attachment 13 of this calculation.

In Attachment 5, Excel Spreadsheet entitled "MNGP – DSC Source Term to RADTRAD", worksheet entitled "MNGP EPU – GE14 Fuel – 37 GWD", the Reference 2.6, Attachment 3 ORIGEN-ARP selected isotopic output data is copied and pasted for comparison purposes.

In Attachment 5, Excel Spreadsheet entitled "MNGP – DSC Source Term to RADTRAD", worksheet entitled "DSC Decay – 0 Cutoff – 37 GWD", the Attachment 4 ORIGEN-ARP selected isotopic output data from this calculation is summarized in columns A-L. The Attachment 4 ORIGEN-ARP model is identical to the Attachment 13 model described above except that the fuel burnup value is 37000 MWD/MTU. The sole purpose of Attachment 4 is to demonstrate that with the modification of decay timing that the output isotopic activity at 180 days replicates the 180 day decay data from the Attachment 3 base case. There is no additional use for the Attachment 4 output. Column Q is used to tabulate the Reference 2.6, Attachment 3 isotopic activity with 180 days decay in Ci/MTU. Column R is used to tabulate the worksheet isotopic activity with 180 days decay in Ci/MTU. Column S is used to calculate the Columns Q/R isotopic activity ratio. A value of 1.0 represents a match.

In Attachment 5, Excel Spreadsheet entitled "MNGP – DSC Source Term to RADTRAD", worksheet entitled "DSC Decay – 0 Cutoff – 41 GWD", the Attachment 13 ORIGEN-ARP selected isotopic output data from this calculation is summarized in columns A-L. Columns U & V are used to determine which isotopes meet the specifications of DI Item 4.7. As an actinide example, Cell U8 calculates whether the Cell L8 5668 day decay value of 3.122E-13 Ci/MTU exceeds the 0.01% threshold of total actinide activity given in Cell L150 of 5.610E+04 Ci/MTU. As a fission product example, Cell U160 calculates whether the Cell L160 5668 day decay value of 2.864E+02 Ci/MTU exceeds the 0.1% threshold of total fission product activity given in Cell L1424 of 3.246E+05 Ci/MTU. Isotopes that meet the criteria are highlighted in Column V.

In Attachment 5, Excel Spreadsheet entitled "MNGP – DSC Source Term to RADTRAD", worksheet entitled "Accident Source Term", the isotopes that meet the DI Item 4.7 criteria are tabulated in Column A. In column B these isotopes are characterized according to DI Item 4.10 categories. In Column C the isotopic Ci/MTU from the Worksheet entitled "DSC Decay – 0 Cutoff – 41 GWD" are copied. In Column D, the baseline core average power in MWth/MTU is entered (See Section 6.1, ORIGEN-ARP input description). In column E, 102% of PU is entered as the fuel contained in the DSC has an exposure consistent with the PU (See References 2.20, 2.33, Item A.1 and DI Item 4.9). In Column F, the average core isotopic Ci are calculated as the product of Columns C, D & E (For example, Am-241 – Cell F7 (1.550E+05 Ci) is the product of Cell C7 / Cell D7 * Cell E7).

In Column G, the number of fuel assemblies per MNGP core is entered as 484 (See Design Input Item 4.4). In Column H, the isotopic activity in Ci per fuel assembly is calculated (For example, Am-241 – Cell H7 (3.202E+02 Ci) is the product of Cell F7 / Cell G7). In Column J, the number of fuel assemblies in the MNGP NUHOMS 61BTH Type 1 DSC is entered (See DI Item 4.6). In Column K, the isotopic activity per DSC is calculated (For example, Am-241 – Cell K7 (1.9533E+04 Ci) is the product of Cell H7 * Cell J7). The Column K results are subsequently used as input to the RADTRAD source term file given as Attachment 6. This work is provided below as Table 6.1.

Table 6.1 – DSC Activity

Isotope	Nuclide Group	EPU-41 GWD (Curies/MTU)	EPU-41 GWD Avg Power (MWth/MTU)	DSCs 11-15 Power Level (MWth)	DSCs 11-15 Avg Core (Curies)	Fuel Assembly Per Core	DSCs 11-15 Average Fuel Assembly (Curies)		DSC Total Fuel Assemblies	DSC Total Activity in All Fuel Rods (Curies)
Am-241	Fuel Fines	1.986E+03	2.320E+01	1.8105E+03	1.550E+05	4.84E+02	3.202E+02		61	1.9533E+04
Am-242m	Fuel Fines	8.342E+00	2.320E+01	1.8105E+03	6.510E+02	4.84E+02	1.345E+00		61	8.2047E+01
Am-242	Fuel Fines	8.304E+00	2.320E+01	1.8105E+03	6.480E+02	4.84E+02	1.339E+00		61	8.1674E+01
Am-243	Fuel Fines	1.737E+01	2.320E+01	1.8105E+03	1.356E+03	4.84E+02	2.801E+00		61	1.7084E+02
Ba-137m	Fuel Fines	8.543E+04	2.320E+01	1.8105E+03	6.667E+06	4.84E+02	1.377E+04		61	8.4024E+05
Cm-242	Fuel Fines	6.868E+00	2.320E+01	1.8105E+03	5.360E+02	4.84E+02	1.107E+00		61	6.7550E+01
Cm-243	Fuel Fines	1.003E+01	2.320E+01	1.8105E+03	7.827E+02	4.84E+02	1.617E+00		61	9.8650E+01
Cm-244	Fuel Fines	9.512E+02	2.320E+01	1.8105E+03	7.423E+04	4.84E+02	1.534E+02		61	9.3555E+03
Co-60	Crud						1.099E+01		61	6.7047E+02
Cs-134	Volatiles	7.550E+02	2.320E+01	1.8105E+03	5.892E+04	4.84E+02	1.217E+02		61	7.4258E+03
Cs-137	Volatiles	9.047E+04	2.320E+01	1.8105E+03	7.060E+06	4.84E+02	1.459E+04		61	8.8981E+05
Eu-154	Fuel Fines	1.690E+03	2.320E+01	1.8105E+03	1.319E+05	4.84E+02	2.725E+02		61	1.6622E+04
Kr-85	Gaseous	4.557E+03	2.320E+01	1.8105E+03	3.556E+05	4.84E+02	7.348E+02		61	4.4820E+04
Np-239	Fuel Fines	1.737E+01	2.320E+01	1.8105E+03	1.356E+03	4.84E+02	2.801E+00		61	1.7084E+02
Pm-147	Fuel Fines	3.136E+03	2.320E+01	1.8105E+03	2.447E+05	4.84E+02	5.056E+02		61	3.0844E+04
Pu-238	Fuel Fines	2.532E+03	2.320E+01	1.8105E+03	1.976E+05	4.84E+02	4.083E+02		61	2.4903E+04
Pu-239	Fuel Fines	2.746E+02	2.320E+01	1.8105E+03	2.143E+04	4.84E+02	4.428E+01		61	2.7008E+03
Pu-240	Fuel Fines	4.956E+02	2.320E+01	1.8105E+03	3.868E+04	4.84E+02	7.991E+01		61	4.8745E+03
Pu-241	Fuel Fines	4.979E+04	2.320E+01	1.8105E+03	3.886E+06	4.84E+02	8.028E+03		61	4.8971E+05
Sr-90	Volatiles	6.868E+04	2.320E+01	1.8105E+03	5.360E+06	4.84E+02	1.107E+04		61	6.7550E+05
Y-90	Fuel Fines	6.870E+04	2.320E+01	1.8105E+03	5.361E+06	4.84E+02	1.108E+04		61	6.7570E+05
		3.795E+05								3.7334E+06

6.2 RADTRAD DSC Dose Calculation:
RADTRAD "NIF" File:

The RADTRAD BWR default nuclide inventory as shown in Reference 2.3, Section 1.4.3.2 and Table 1.4.3.2-3 is modified for the purposes of this calculation as described below.

1. As noted in calculation Section 5.2, 14 of the isotopes from Table 6.1 are already part of the RADTRAD Table 1.4.3.2-3 nuclide inventory. The Ci value from Table 6.1 is input as line 6 for each of these isotopes.
2. The remaining 7 isotopes (plus Sm-151) are incorporated as nuclides 21 – 28 of the modified "NIF" file (replacing the RADTRAD default nuclides 21 – 28. For isotopes Ba-137m, Pm-147, Eu-154, Am-243 and Cm-243 nuclide parameters are as previously developed in Reference 2.21, Appendix A nuclides 31, 33, 34, 36 and 37 (except for decay times as noted). Sm-151 (previously developed for Attachment 4, but failed to satisfy the Design Input Item 4.7 criteria based on Attachment 13 results), Am-242m and Am-242 data is developed below.

Nuclide 021:
Ba-137m
6
1.5312000000E+02 Reference 2.15, Table 1, page 1242
0.1370E+03
8.4024E+05 Table 6.1
none 0.0000E+00
none 0.0000E+00
none 0.0000E+00
Nuclide 022:
Pm-147
9
8.2731542400E+07 Reference 2.15, Table 1, page 1431
0.1470E+03
3.0844E+04 Table 6.1
none 0.0000E+00
none 0.0000E+00
none 0.0000E+00
Nuclide 023:
Eu-154
9
2.7098884800E+08 Reference 2.15, Table 1, page 1630
0.1540E+03
1.6622E+04 Table 6.1
none 0.0000E+00
none 0.0000E+00
none 0.0000E+00
Nuclide 024:

Sm-151	
9	Lanthanides Series – Reference 2.22, Table 5
2.8382400000E+09	Reference 2.15, Table 1, page 1532
0.1510E+03	
0.0000E+00	Per Attachment 13, fails DI Item 4.7 criteria
none 0.0000E+00	Reference 2.15, Table 1, page 1532
none 0.0000E+00	
none 0.0000E+00	
Nuclide 025:	
Am-242m	
9	Lanthanides Series – Reference 2.22, Table 5
4.4465760000E+09	Reference 2.15, Table 1, page 2807
0.2420E+03	
8.2047E+01	Table 6.1
Am-242 1.0000E+00	Reference 2.15, Table 1, page 2807
none 0.0000E+00	
none 0.0000E+00	
Nuclide 026:	
Am-242	
9	Lanthanides Series – Reference 2.22, Table 5
5.7672000000E+04	Reference 2.15, Table 1, page 2807
0.2420E+03	
8.1674E+01	Table 6.1
Cm-242 0.8270E+00	Reference 2.15, Table 1, page 2807
none 0.0000E+00	
none 0.0000E+00	
Nuclide 027:	
Am-243	
9	
2.3242032000E+11	Reference 2.15, Table 1, page 2812
0.2430E+03	
1.7084E+02	Table 6.1
none 0.0000E+00	
none 0.0000E+00	
none 0.0000E+00	
Nuclide 028:	
Cm-243	
9	
9.1769760000E+08	Reference 2.15, Table 1, page 2812
0.2430E+03	
9.8650E+01	Table 6.1
none 0.0000E+00	
none 0.0000E+00	
none 0.0000E+00	

3. Nuclides other than the 21 identified in Table 6.1 have their activity zeroed (line 6).

   The RADTRAD "NIF" file for the MNGP DSC source term is given as Attachment 6.

RADTRAD "RFT" File:
The RADTRAD BWR default release and timing file as shown in Reference 2.3, Section 1.4.3.1 and Table 1.4.3.1-3 is modified for the purposes of this calculation as described below.

1. Gap release timing is set to 0.01 hours (instantaneous) consistent with Reference 2.21, Appendix A. All other times set to zero.
2. 6 RADTRAD nuclide groups are represented by the 21 isotopes in Table 6.1. The release fraction for these isotopes is defined per DI Item 4.10. All other RADTRAD nuclide groups release fractions are zeroed. Note that Co-60 is part of the Noble Metals Group (or Ruthenium Series).

```
Release Fraction and Timing Name:
 MNGP-018 R0 - DSC with 15.53 Year Decay
 Duration (h):   DSC Decay
  0.1000E-01  0.0000E+00  0.0000E+00  0.0000E+00
 Noble Gases:
  0.3000E+00  0.0000E+00  0.0000E+00  0.0000E+00
 Iodine:
  0.0000E+00  0.0000E+00  0.0000E+00  0.0000E+00
 Cesium:
  2.0000E-04  0.0000E+00  0.0000E+00  0.0000E+00
 Tellurium:
  0.0000E+00  0.0000E+00  0.0000E+00  0.0000E+00
 Strontium:
  2.0000E-04  0.0000E+00  0.0000E+00  0.0000E+00
 Barium:
  3.0000E-05  0.0000E+00  0.0000E+00  0.0000E+00
 Ruthenium:
  1.5000E-02  0.0000E+00  0.0000E+00  0.0000E+00
 Cerium:
  3.0000E-05  0.0000E+00  0.0000E+00  0.0000E+00
 Lanthanum:
  3.0000E-05  0.0000E+00  0.0000E+00  0.0000E+00
 Non-Radioactive Aerosols (kg):
  0.0000E+00  0.0000E+00  0.0000E+00  0.0000E+00
 End of Release File
```

The RADTRAD "RFT" file for the MNGP DSC source term is given as Attachment 7.

RADTRAD "INP" File:
The RADTRAD NUREG-1465 default conversion factors file as shown in Reference 2.3, Section 1.4.3.3 and Table 1.4.3.3-2 is modified for the purposes of this calculation as described below.

1. As noted in calculation Section 5.2, 14 of the isotopes from Table 6.1 are already part of the RADTRAD Table 1.4.3.3-2 nuclide inventory. Note that the values provided in RADTRAD Table 1.4.3.3-2 are consistent with Reference 2.18 and 2.19 (one exception is the Cs-137 Submersion DCF value where the Table 1.4.3.3-2 table list DCFs for the combined Cs-137 – Ba-137m parent daughter. However, since the FGR 12 DCF value for Ba-137m is higher than the RADTRAD default file DCF for Cs-137, the FGR 12 DCF values are input for Ba-137m.
2. The remaining 7 isotopes (plus Sm-151) are incorporated as nuclides 21 – 28 of the modified "INP" file (replacing the RADTRAD default nuclides 21 – 28. For isotopes Ba-137m, Pm-147, Eu-154, Sm-151 (DCFs zeroed), Am-242m, Am-242, Am-243 and Cm-243 DCFs are taken from References 2.18 (FGR 11, Table 2.1) and 2.19 (FGR 12, Table III-1).
3. All DCF values not used are zeroed. Thus DCF values remain only for the 9 organs listed for RADTRAD designated columns "Inhaled Chronic" (FGR 11 – Inhalation) and "Cloudshine" (FGR 12 – Submersion).
4. Inhalation DCFs are tabulated in Table 6.2 below. Submersion DCFs are tabulated in Table 6.3 below.

The base RADTRAD "INP" file for the MNGP DSC source term is given as Attachment 8.

Table 6.2 - Inhalation DCFs (Sv/Bq) - FGR-11 Table 2.1

				Red	Bone					
Isotope	**Gonad**	**Breast**	**Lungs**	**Marrow**	**Surface**	**Thyroid**	**Remainder**	**Effective**	**Skin**	
Am-241	3.250E-05	2.670E-09	1.840E-05	1.740E-04	2.170E-03	1.600E-09	7.820E-05	1.200E-04	0.000E+00	Class W
Am-242m	3.210E-05	1.380E-09	4.200E-06	1.690E-04	2.120E-03	5.640E-10	7.480E-05	1.150E-04	0.000E+00	Class W
Am-242	1.940E-09	2.940E-12	5.200E-08	1.320E-08	1.650E-07	2.520E-12	8.540E-09	1.580E-08	0.000E+00	Class W
Am-243	3.260E-05	1.520E-08	1.780E-05	1.730E-04	2.170E-03	8.290E-09	7.740E-05	1.190E-04	0.000E+00	Class W
Ba-137m	0.000E+00	0.000E+00	0.000E+00	0.000E+00	0.000E+00	0.000E+00	0.000E+00	0.000E+00	0.000E+00	
Cm-242	5.700E-07	9.440E-10	1.550E-05	3.900E-06	4.870E-05	9.410E-10	2.450E-06	4.670E-06	0.000E+00	Class W
Cm-243	2.070E-05	6.290E-09	1.940E-05	1.180E-04	1.470E-03	3.830E-09	5.760E-05	8.300E-05	0.000E+00	Class W
Cm-244	1.590E-05	1.040E-09	1.930E-05	9.380E-05	1.170E-03	1.010E-09	4.780E-05	6.700E-05	0.000E+00	Class W
Co-60	4.760E-09	1.840E-08	3.450E-07	1.720E-08	1.350E-08	1.620E-08	3.600E-08	5.910E-08	0.000E+00	Class Y
Cs-134	1.300E-08	1.080E-08	1.180E-08	1.180E-08	1.100E-08	1.110E-08	1.390E-08	1.250E-08	0.000E+00	Class D
Cs-137	8.760E-09	7.840E-09	8.820E-09	8.300E-09	7.940E-09	7.930E-09	9.120E-09	8.630E-09	0.000E+00	Class D
Eu-154	1.170E-08	1.550E-08	7.920E-08	1.060E-07	5.230E-07	7.140E-09	1.130E-07	7.730E-08	0.000E+00	Class W
Kr-85	0.000E+00	0.000E+00	0.000E+00	0.000E+00	0.000E+00	0.000E+00	0.000E+00	0.000E+00	0.000E+00	
Np-239	7.450E-11	1.630E-11	2.360E-09	2.080E-10	2.030E-09	7.620E-12	9.590E-10	6.780E-10	0.000E+00	Class W
Pm-147	8.250E-15	3.600E-14	7.740E-08	1.610E-09	2.010E-08	1.980E-14	1.560E-09	1.060E-08	0.000E+00	Class Y
Pu-238	1.040E-05	4.400E-10	3.200E-04	5.800E-05	7.250E-04	3.860E-10	2.740E-05	7.790E-05	0.000E+00	Class Y
Pu-239	1.200E-05	3.990E-10	3.230E-04	6.570E-05	8.210E-04	3.750E-10	3.020E-05	8.330E-05	0.000E+00	Class Y
Pu-240	1.200E-05	4.330E-10	3.230E-04	6.570E-05	8.210E-04	3.760E-10	3.020E-05	8.330E-05	0.000E+00	Class Y
Pu-241	2.760E-07	2.140E-11	3.180E-06	1.430E-06	1.780E-05	9.150E-12	6.020E-07	1.340E-06	0.000E+00	Class Y
Sm-151	0	0	0	0	0	0	0	0	0	Class W
Sr-90	2.690E-10	2.690E-10	2.860E-06	3.280E-08	7.090E-08	2.690E-10	5.730E-09	3.510E-07	0.000E+00	Class Y
Y-90	5.170E-13	5.170E-13	9.310E-09	1.520E-11	1.510E-11	5.170E-13	3.870E-09	2.280E-09	0.000E+00	Class Y

Table 6.3 - Submersion DCFs (Sv/sec per Bq/m3) - FGR-12 Table III.1

Isotope	Gonad	Breast	Lungs	Red Marrow	Bone Surface	Thyroid	Remainder	Effective	Skin
Am-241	8.580E-16	1.070E-15	6.740E-16	5.210E-16	2.870E-15	7.830E-16	6.340E-16	8.180E-16	1.280E-15
Am-242m	3.800E-17	6.010E-17	1.720E-17	1.720E-17	7.940E-17	2.950E-17	1.940E-17	3.170E-17	1.360E-16
Am-242	6.090E-16	7.300E-16	5.510E-16	4.770E-16	1.880E-15	5.940E-16	5.180E-16	6.150E-16	8.200E-15
Am-243	2.190E-15	2.610E-15	1.920E-15	1.550E-15	7.470E-15	2.090E-15	1.790E-15	2.180E-15	2.750E-15
Ba-137m	2.820E-14	3.220E-14	2.800E-14	2.730E-14	4.630E-14	2.880E-14	2.680E-14	2.880E-14	3.730E-14
Cm-242	7.830E-18	1.480E-17	1.130E-18	1.890E-18	1.060E-17	4.910E-18	2.270E-18	5.690E-18	4.290E-17
Cm-243	5.770E-15	6.680E-15	5.500E-15	5.000E-15	1.500E-14	5.760E-15	5.190E-15	5.880E-15	9.790E-15
Cm-244	6.900E-18	1.330E-17	7.080E-19	1.460E-18	8.820E-18	4.190E-18	1.810E-18	4.910E-18	3.910E-17
Co-60	1.230E-13	1.390E-13	1.240E-13	1.230E-13	1.780E-13	1.270E-13	1.200E-13	1.260E-13	1.450E-13
Cs-134	7.400E-14	8.430E-14	7.370E-14	7.190E-14	1.200E-13	7.570E-14	7.060E-14	7.570E-14	9.450E-14
Cs-137	2.669E-14	3.047E-14	2.649E-14	2.583E-14	4.382E-14	2.725E-14	2.536E-14	2.725E-14	4.392E-14
Eu-154	6.000E-14	6.810E-14	5.990E-14	5.870E-14	9.430E-14	6.150E-14	5.750E-14	6.140E-14	8.290E-14
Kr-85	1.170E-16	1.340E-16	1.140E-16	1.090E-16	2.200E-16	1.180E-16	1.090E-16	1.190E-16	1.320E-14
Np-239	7.530E-15	8.730E-15	7.180E-15	6.500E-15	2.000E-14	7.520E-15	6.760E-15	7.690E-15	1.600E-14
Pm-147	7.480E-19	9.560E-19	5.450E-19	4.460E-19	2.180E-18	6.750E-19	5.260E-19	6.930E-19	8.110E-16
Pu-238	6.560E-18	1.270E-17	1.060E-18	1.680E-18	9.300E-18	4.010E-18	1.990E-18	4.880E-18	4.090E-17
Pu-239	4.840E-18	7.550E-18	2.650E-18	2.670E-18	9.470E-18	3.880E-18	2.860E-18	4.240E-18	1.860E-17
Pu-240	6.360E-18	1.230E-17	1.090E-18	1.650E-18	9.260E-18	3.920E-18	1.960E-18	4.750E-18	3.920E-17
Pu-241	7.190E-20	8.670E-20	6.480E-20	5.630E-20	2.190E-19	6.980E-20	6.090E-20	7.250E-20	1.170E-19
Sm-151	0	0	0	0	0	0	0	0	0
Sr-90	7.780E-18	9.490E-18	6.440E-18	5.440E-18	2.280E-17	7.330E-18	6.110E-18	7.530E-18	9.200E-15
Y-90	1.890E-16	2.200E-16	1.770E-16	1.620E-16	4.440E-16	1.870E-16	1.680E-16	1.900E-16	6.240E-14

RADTRAD Model:
A simple 2 volume, one pathway and one dose location RADTRAD model is developed to analyze the postulated DSC accident dose to the site boundary (EAB). The RADTRAD input is developed below.

RADTRAD Volume 1 represents the MNGP DSC:

- DSC free volume is modeled as 211.2 ft^3 (DI Item 4.16)
- 100% of the Table 6.1 source term released to the DSC volume
- User defined natural deposition removal coefficient = 20 Hr^{-1} – See below
- No additional inputs

Natural Deposition:
The methodology utilized for the calculation of natural deposition of the aerosols released from the assumed damaged fuel rods to the DSC free volume is developed in Reference 2.21, page 7, paragraph underneath Table 8.

Per the above, the preferred method to determine the natural deposition removal coefficient is to divide the given settling velocity by the characteristic fall height within the DSC. For this analysis, the best-estimate or 50^{th} percentile settling velocity of 0.00082 m/sec is chosen for determination of the removal coefficient.

The fall height is calculated per the methodology described on page 10 of Reference 2.21 underneath Table 12. For a cask on its side, the fall height is modeled to be the free volume of the lodgment divided by the area of one side of the lodgment. For the NUHOMS 61BTH, each of the 61 horizontal channels houses 1 fuel assembly. Fall height calculation parameters are given below.

1. Per DI Item 4.17 the channel opening face dimensions are 5.8" x 5.8".
2. Per DI Item 4.18, the channel length is 164 inches.
3. Per DI Item 4.19, Reference 2.11, Item A.21 indicates that the channel free volume can be calculated using parameters in attached Table T.4-29.

   618,766 in^3 (DSC Cavity Volume) – 108,888 in^3 (Basket Volume) = 509,878 in^3
   509,878 in^3 - 141,947 in^3 (Fuel Volume) = 367,931 in^3 (free volume)
   141,947 in^3 (Fuel Volume) / 61 (Fuel Assemblies) = 2,327 in^3 per channel
   Channel volume = 5.8 in * 5.8 in * 164 in = 5,516.96 in^3
   Channel free volume = 5,516.96 in^3 – 2,327 in^3 = 3,189.96 in^3
   Channel lodgment side area = 5.8 in * 164 in = 951.2 in^2
   Channel characteristic height = fall height = 3,189.96 in^3 / 951.2 in^2 = 3.3536 in = 0.0852 m

   For conservatism, use wall height of 5.8 inch as fall height = 0.14732 m

Natural deposition removal coefficient, λ = 0.00082 m/sec / 0.14732 m * 3600 sec/hr = 20.038 Hr^{-1} , use λ = 20 Hr^{-1} for 30 day duration. Note that in Reference 2.21, Section entitled "Effect of Aerosol Concentration," an evaluation of the effect of DSC aerosol concentration on the deposition rate is presented. That effect is not considered in the RADTRAD model. However, the Reference 2.21 evaluation demonstrates that the concentration effect is negligible.

RADTRAD Volume 2 represents the Environment:

- No inputs

RADTRAD Pathway 1 represents the leakage from the DSC to the Environment:

- A filter pathway is modeled with filter removal efficiencies set to zero
- Pathway flow rate is 3.333E-03 CFM (see Section 6.4) conservatively modeled for the 30 day accident duration based on continuous critical flux flow (not terminated when the DSC pressure reduces to 14.7 psia).
- No additional inputs

RADTRAD Dose Location 1 – MNGP EAB:

- χ/Q value equals 1.59E-03 sec/m^3 for 30 days per DI Item 4.13
- Adult breathing rate value 2.50E-04 m^3/sec for 30 days per DI Item 4.11
- No additional inputs

RADTRAD Source Term:

- User Inventory File "DSC Decay Source.NIF" (Attachment 6). This file is developed utilizing the released activity as described in Section 6.1
- Modeled plant power set as 1 MWth, since the source is based on curies
- Model isotopic decay and daughter in-growth
- User Release Fraction and Timing File "DSC Decay Source.RFT" (Attachment 7)
- User Inventory Input File "DSC Decay Source.INP" (Attachment 8)
- No additional inputs

The resulting RADTRAD input/output files (psf/o0) are given as Attachment 9.

From Attachment 9, the following 30 day organ doses are calculated directly via RADTRAD.

1. Thyroid = 1.1366E-04 Rem
2. Effective = 2.1128E-02 Rem TEDE

Other organ doses are calculated in the Attachment 5 spreadsheet in Worksheet entitled "Accident Source Term" via the following steps.

1. Sum each organ submersion DCFs (Example: Gonad Submersion DCF sum in Cell V32 is the sum of Cells V7 – V27).
2. Sum each organ inhalation DCFs (Example: Gonad Inhalation DCF sum in Cell AI32 is the sum of Cells AI7 – AI27).

3. The total combined organ DCF sum is the sum of the total Submersion DCF plus the total Inhalation DCF (Example: the Gonad total combined DCF sum in Cell AI33 is the sum of Gonad Submersion DCF in Cell V32 plus the Gonad Inhalation DCF in Cell AI32).
4. The RADTRAD calculated Thyroid dose (1.1366E-04) and the Effective dose (2.1128E-02) are placed is Cells AN34 and AP34, respectively.
5. The remaining organ doses are calculated by multiplying the Effective dose by the ratio of the summed organ dose DCF divided by the summed Effective organ dose DCF (Example: Gonad dose (Cell AI35) equals Cell AP34 (2.1128E-02) times [(Cell AI33, 1.691E-04) / (Cell AP33, 7.550E-04)] = 4.73E-03.

6.3 χ/Q Value Modification:

This section justifies a reduction factor of 4.5 that can be applied to Regulatory Guide 1.145 χ/Qs as calculated in Section 4.13 to obtain more realistic dispersion factor estimates.

Report PNL-10286 (Reference 2.24), Figure 9 (Attachment 10), shows the biases in Regulatory Guide 1.145's methodology for calculating χ/Qs compared to data from site tracer tests. Figure 9 shows overestimates of 1 to 2 orders of magnitude for low wind speeds. The lower speeds typically occur with stable to neutral conditions and result in larger X/Q values. At greater wind speeds, the biases decrease. Under prediction may occur at the highest speeds; however, the X/Q values tend to be numerically much smaller than low speed χ/Qs due to increased wind speed and turbulence (unstable meteorology). Consequentially, the low speeds are more limiting with respect to assessing doses.

The data in PNL-10286, Figure 9, was analyzed to demonstrate the amount of bias in Regulatory Guide 1.145's methods and provide a basis for applying this conservatism to engineering evaluations. The analysis proceeded as follows:

1. Three data bins, each of width 0.5 m/s, were used to examine the biases (X/Q overestimates) for low speeds from 0.5 to 2.0 m/s. See Attachment 11.
2. The data were visually extracted and tabulated in an Excel spreadsheet as Bins #1 (0.5 to 1 m/s), #2 (1 to 1.5 m/s) and #3 (1.5 to 2 m/s). See Attachments 10 and 11.
3. The geometric mean was calculated for each bin. Also, the arithmetic mean and median were determined for perspective.
4. The geometric mean is reasonable for this type analysis and follows from Ramsdell in Reference 2.24. Additional justification is provided in the Notes to Attachment 11.
5. The geometric means of the biases for low speed Bins #1, #2 and #3 range from 14.7 to 100. The geometric mean for the range 0.5 to 2 m/s is 30. See Attachment 11.
6. The above procedure was repeated for higher speed ranges comprising Bins #4 to #9. Biases may be observed in Attachment 11 to decrease with increasing speed. Underestimates are more likely at the higher wind speeds.
7. The overall geometric mean of the bias across all speeds (0.5 to 12 m/s) is 4.76. See Attachment 11.

The overall geometric mean bias (4.76) for the entire ensemble of data appears to be a reasonable, yet conservative factor to apply to χ/Qs. This value is very conservative relative to the 0.5 to 2 m/s speeds where a much greater overestimate bias occurs (i.e., geometric mean of 30). Thus, use of a 4.5 χ/Q reduction factor is conservative and justifiable for dose values developed in Sections 6.1 and 6.2 and summarized in Section 7.

The bias factor is most applicable to the χ/Q at the EAB where, normally, conditions are assumed invariant for a two hour interval. It can be applied to longer time intervals as long as the downwind direction, wind speed, and stability are assumed to remain constant. The bias factor use would be valid for bounding type accident assessments where dispersion conditions are not postulated to change for the accident as assumed in this calculation.

6.4 DSC Leakage Rate:

Based on a licensing basis that postulates no confinement failure and a satisfactory “leak tight” helium leak test on each canister (DSC 11 – 15), References 2.23 and 2.30, there is no basis and no method for theorizing a potential leak flow rate based on leak testing requirements.

To arrive at a hypothetical accident release for the DSCs 11-15 with noncompliant dye penetrant examinations, the following methodology is utilized.

1. This hypothetical accident release is not triggered by a cask drop event, fire or any known material stress/corrosion failure process.
2. As such, a reasonable upper limit realistic leak diameter (hole size) is postulated to be no larger than the maximum allowable leak diameter associated with packaging and transport of radioactive materials.
3. Review of the Table 6.1 DSC activity and Attachment 5 identifies isotopes of interest and is used to determine the specific activity within the DSCs. 10 CFR 71 is then utilized to determine the maximum allowable “package” activity limit. As shown in the calculation below, Kr-85 is the limiting isotope remaining within the subject DSCs.
4. ANSI N14.5-1997 may then be used to calculate an allowable release rate (consistent with 10 CFR 71) and via Table B.2 to back-calculate an associated leak diameter (hole size).
5. The leak diameter calculated in step 4 above can then be used to calculate a hypothetical accident release based upon the critical mass flux release rate resulting from limiting pressure/temperature conditions within the DSCs from other postulated events. For this assessment, the limiting event is considered to be the Blocked Vent event with elevated internal pressure and temperature conditions within the subject DSCs.

Determination of Leakage Area (Hole Size) – ANSI N14.5-1997 Methodology:
The following procedure will be assumed to determine the postulated accident release hole size. This procedure is deemed reasonable in that the DSC is not subject to a cask drop or fire. The leak is thus based on the 10 CFR Part 71 maximum “package” activity limit (using Kr-85 as the representative isotope, R_A values bounds other Table 6.1 isotopes) as a guideline. In accordance with the NUHOMS FSAR, Reference 2.23, Section 1: *“The NUHOMS-61BT DSC is designed to store 61 intact BWR fuel assemblies and meets the storage and transportation requirements of 10CFR72 and 10CFR71, respectively.”*

1. Determine C_A , average activity in the DSC in Ci/cm^3 per the total activity released into the DSC divided by the DSC free volume.

   Determine C_A:
   From Attachment 5, Cell Q28, the activity released into the DSC is calculated to be 1.3834E+04 Ci.

   DSC free volume = 5.9813E+06 cm^3 (365,000 in^3) from DI Item 4.16.

   C_A = 1.3834E+04 / 5.9813E+06 = 2.3129E-03 Ci/cm^3

2. Determine R_A , allowable release rate under accident conditions in Ci/sec using the Kr-85 A_2 value per Appendix A of 10 CFR Part 71. This is assumed reasonable since the bulk of the activity released from the fuel is Kr-85 (1.3446E+04 Ci, Attachment 5, Cell Q19) in accordance with the ORIGEN-ARP analysis.

From ANSI N14.5-1997 (Reference 2.25)
$R_A = 1.65 \times 10^{-6} * A_2$ per second in accordance with Section 5.4.2 of ANSI N14.5-1997.
A_2 for Kr-85 = $10 * A_2$ in accordance with Section 6.1 of ANSI N14.5-1997

From 10CFR71
A_2 (Kr-85) = 270 Ci per Appendix A of 10 CFR Part 71 (Reference 2.26)

Thus Kr-85A_2 = 2700 Ci/sec
$R_A = 2700 * 1.65 \times 10^{-6} = 4.455 \times 10^{-3}$ Ci/sec

3. Determine L_A allowable leakage rate of the medium (cm^3/s) under hypothetical accident conditions per Section 6.1 of ANSI N14.5-1997:

$L_A = R_A / C_A$ = 4.455E-03 Ci/sec / 2.3129E-03 Ci/cm^3 = 1.926 cm^3/sec

Thus the ANSI N14.5-1997 accident allowable leakage rate is 1.926 cc/sec.

4. Table B2 of ANSI N14.5-1997 lists representative DSC leakage rates vs pressure drop conditions at given leak hole diameters. Interpolating in Table B2 (Column 2 for low dP) of ANSI N14.5-1997 with the step 3 allowable leak rate of 1.926 cm^3/sec yields a hole size of approximately 0.0106 cm in diameter, conservatively use 0.011 cm (Area = 9.5033E-05 cm^2 = 1.0229E-07 ft^2).

Note that the proposed hole size of 0.011 cm diameter is among that largest hole sizes considered in Table B2 of ANSI N14.5-1997. Thus this hole size, based on allowable leak rate, is deemed conservative for a postulated accident event not involving a cask drop or fire.

Determination of Critical Mass Flux (Leakage Rate) – Based on Blocked Vent Accident Conditions:
Per Reference 2.27, Equation 2.60, the critical mass flux for an ideal gas through an orifice with an upstream pressure P_0 is defined as:

$$\frac{G_c}{\sqrt{k g_0 P_0 \rho_0}} = \left(\frac{2}{k+1}\right)^{(k+1)/2(k-1)}$$

where:

k = specific heat ratio

g_0 = conversion constant or 32.174 ft-lbm/lbf-sec^2 (page 8 Reference 2.28)
P_0 = vessel pressure, psi
ρ_0 = gas density in lbm/ft^3

For this case, the gas is composed of DSC He fill gas, fuel gap He gas, and fuel gap fission gas. Per DI Item 4.22 (Reference 2.30, Table T.4-24), the gas mass for a single DSC @ accident conditions is listed as:

He in fuel: 83 gr-mole
He in DSC (fill gas) = 192.9 gr mole
Fission gases in fuel: 369.7 gr-mole
Total: 645.6 gr-mole

Thus the corresponding gas mass fractions are:

Fission gas mass fraction = 369.7/645.6 = 0.5726
He gas fraction = 1 - 0.5726 = 0.4274

Using ideal gas density calculations, the English units basis for an ideal gas is given on page 130 of Reference 2.28 as:

P= 14.7 psia
T= 492°R
Specific volume = 359 ft^3/lbm- mole

Per DI Item 4.20 (Reference 2.33, Item A.22), the DSC maximum accident pressure is 46 psig (60.7 psia). Per DI Item 4.21 (Reference 2.33, Item A.23), the DSC maximum accident temperature is 405 °F or 865 °R.

Thus, for 1 ft^3 Basis of He, at an Atomic Weight of 4.0026 (Appendix B, Reference 2.28):

$$1\ \text{ft}^3 * \frac{492°R}{865°R} * \frac{60.7\ psia}{14.7\ psia} * \frac{1\ lb-mole}{359\ ft^3} * \frac{4.0026\ lb}{lb\ mole} = 0.0262\ \text{lbm}$$

Thus, the density of He at these conditions is: ρ = 0.0262 lbm/ft^3

Similarly for the fission gases, assuming the high density Xe as representative, Atomic Weight of 131.30 (Appendix B, Reference 2.28):

$$1\ \text{ft}^3 * \frac{492°R}{865°R} * \frac{60.7\ psia}{14.7\ psia} * \frac{1\ lb-mole}{359\ ft^3} * \frac{131.30\ lb}{lb\ mole} = 0.8590\ \text{lbm}$$

Thus, the density of fission gases at these conditions is: ρ = 0.8590 lbm/ft^3

Using ideal gas law:

$C_P = C_V + R$
Dividing above by C_V, we get $C_P/C_V = 1 + R/C_V$

For a monoatomic gas, $C_v = 1.5$ R

Thus, $k = C_P/C_V = 1 + R/C_V = 1 + R/(1.5R) = 1 + 1/1.5 = 1.6667$

Thus k(He) = k(Xe) = 1.6667

Using the DSC gas mass fractions calculated above:

$\rho_{ave.} = 0.8590 * 0.5726 + 0.0262 * 0.4274 = 0.5031$ lbm/ft^3

Solving for G_C :

$$G_C = \sqrt{k g_0 P_0 \rho_0}\left(\frac{2}{k+1}\right)^{(k+1)/2(k-1)} = 0.5625\sqrt{k g_0 P_0 \rho_0}$$

$G_C = 0.5625 * (1.6667 * 32.174 * 60.7 * 0.5031 * 144)^{0.5}$
G_C = 273.2 lbm/ft^2 –sec

Calculating volumetric flow rate:
V_C = 273.2 lbm/ft^2 –sec * 1.0229E-07 ft^2 * (1 / 0.5031 lbm/ft^3) * 60 sec/min = 3.333E-03 CFM

Converting to cc/sec:

3.333E-03 ft^3/min * 1 min/60 sec * 28316.85 cc/ft^3 = 1.573 cc/sec.

Note that this leakage rate, which will be used in the dose analysis, is less than the ANSI N14.5-1997 accident allowable leakage rate of 1.926 cc/sec calculated above but is representative of the conservative accident conditions assumed.

This assumed leakage rate is very conservative as compared to DSC Leak Accident leak rates postulated in Reference 2.21, 1.3E-05 cc/sec and Reference 2.32, 1.58E-05 cc/sec.

In addition to the DSC leak rate calculated above, three additional leak rates are assumed based on hole sizes of 4.0E-03 cm^2, 2.5E-2 cm^2, and 1.0E-01 cm^2. Dose calculation results are documented in Section 7.

7.0 CONCLUSIONS

The activity contained within the fuel rods of the subject DSC following 15.53 years of decay is tabulated in Table 6.1.

For a postulated accidental release from an affected DSC having noncompliant dye penetrant examinations (PTs), offsite radiological dose consequence analyses were performed. The results of these dose consequence analyses are tabulated below for each organ. Table 7.1 is based on RG 1.145 calculated X/Q values.

Table 7.1 – Organ Dose with RG 1.145 χ/Q Data

	Gonad	Breast	Lung	Red Marrow	Bone Surface	Thyroid	Remainder	Effective	Skin
Dose (Rem)	4.73E-03	2.28E-06	2.99E-02	2.58E-02	3.23E-01	1.14E-04	1.19E-02	2.11E-02	1.48E-11
Dose Limit* (Rem)	50	50	50	50	50	50	50	5	50

* 10CFR72.106

Per NUREG-1567 page 9-14 (Reference 2.12), the Lens Dose equals the sum of the Skin and Effective dose not to exceed 15 Rem. From Table 7.1 above the calculated Lens Dose = 2.11E-02.

As noted in Section 6.4 additional hole sizes were considered. The thyroid and effective dose for these cases is summarized below along with the base hole size for comparison, Table 7.1a.

Table 7.1a – Organ Dose with RG 1.145 χ/Q Data – Additional Hole Sizes

RG 1.145 X/Q Values					
			Leakage	Thyroid	Effective
Diameter	Area	Area	Rate	Dose	Dose
(cm)	(cm2)	(ft2)	(CFM)	(Rem)	(Rem TEDE)
1.10E-02	9.5033E-05	1.0229E-07	3.333E-03	1.1366E-04	2.1128E-02
	4.0000E-03	4.3056E-06	1.403E-01	4.7750E-03	7.0204E-01
	2.5000E-02	2.6910E-05	8.768E-01	2.9533E-02	4.2875E+00
	1.0000E-01	1.0764E-04	3.507E+00	1.1392E-01	1.6534E+01

Calculation and Conclusion Conservatisms:

1. RG 1.145 X/Q values are quite conservative (as demonstrated in calculation Section 6.3). Table 7.2 is based on RG 1.145 X/Q values reduced by the 4.5 factor calculated in Section 6.3. The Table 7.2 data is more realistic for the proposed comparison.

Table 7.2 – Organ Dose with Realistic Dispersion Factor Data

	Gonad	Breast	Lung	Red Marrow	Bone Surface	Thyroid	Remainder	Effective	Skin
Dose (Rem)	1.05E-03	5.08E-07	6.64E-03	5.74E-03	7.17E-02	2.53E-05	2.65E-03	4.70E-03	3.28E-12
Dose Limit* (Rem)	50	50	50	50	50	50	50	5	50

* 10CFR72.106

Per NUREG-1567 page 9-14 (Reference 2.12), the Lens Dose equals the sum of the Skin and Effective dose not to exceed 15 Rem. From Table 7.2 above the calculated Lens Dose = 4.70E-03.

As noted in Section 6.4 addition hole sizes were considered. The thyroid and effective dose for these cases is summarized below along with the base hole size for comparison, Table 7.2a.

Table 7.2a – Organ Dose with Realistic Dispersion Factor Data – Additional Hole Sizes

RG 1.145 X/Q Values / 4.5					
			Leakage	Thyroid	Effective
Diameter	Area	Area	Rate	Dose	Dose
(cm)	(cm2)	(ft2)	(CFM)	(Rem)	(Rem TEDE)
1.10E-02	9.5033E-05	1.0229E-07	3.333E-03	2.5258E-05	4.6951E-03
	4.0000E-03	4.3056E-06	1.403E-01	1.0611E-03	1.5601E-01
	2.5000E-02	2.6910E-05	8.768E-01	6.5629E-03	9.5278E-01
	1.0000E-01	1.0764E-04	3.507E+00	2.5316E-02	3.6742E+00

2. This postulated accident assumes an Occupancy Factor of 1.0 (individual always present at EAB). Tables 7.1 and 7.2 dose values would reduce linearly with any change in assumed occupancy factor.

3. This postulated accident is a static event (i.e., not the result of a dynamic event such as a DSC drop or a fire) although 100% of the fuel rods are assumed damaged. Crediting less fuel damage would be a reasonable basis for analysis. Caution would need to be observed as any reduction in failed fuel would reduce the Tables 7.1 and 7.2 dose results but the reduction amount would not be linear. Based on the methodology developed in Section 6.4, the ρ_o term would be altered by a less than 100% failed fuel assumption, but not linearly. Thus the G_C and V_C terms also would not reduce linearly with the failed fuel percentage.

4. The natural deposition removal coefficient, λ (20.0 Hr^{-1}), was conservatively calculated based on a fall height of 5.8 inch (fuel channel height). Based on the methodology of Reference 2.21, the characteristic height (3.3536 inch) of the fuel channel is appropriate for determination of λ which would result in a less conservative natural deposition removal coefficient value of 34.65 Hr^{-1}.

5. This postulated accident assumes a volumetric critical flux release for the entire 30 day duration of the postulated accident. This analysis approach is surely conservative since at some point in the 30 day accident time frame the DSC pressure may be reduced below the critical pressure and maximum critical flux flow would no longer occur. The degree of conservatism of assuming constant leakage at the critical flow rate may be assessed by determining the time at which the DSC would reach 14.7 psia and review of the RADTRAD results to determine incremental dose accrual after the calculated time for the DSC to reach 14.7 psia (see Reference 2.27, Eqn 2.78). See AAC DVCS, Attachment 14, Comment No. 3.

6. In the Reference 2.3 default “INP” file the Cs-137 submersion DCFs are noted as including the impact of the Ba-137m daughter. Review of FGR 12 for Ba-137m submersion DCFs shows greater DCF values for Ba-137m than the combined value given in Reference 2.3 under the Cs-137 isotope. Conservatively, the Reference 2.3 DCFs for Cs-137 and the FGR 12 DCFs for Ba-137m are used.

ENCLOSURE 11

JENSEN HUGHES REPORT 016045-RPT-01, REVISION 0

RISK ASSESSMENT OF MNGP DSC 11-15 WELDS USING NUREG-1864 METHODOLOGY RESULTS TO DSC 11-15

53 pages follow

JENSEN HUGHES

158158 West Gay Street | Suite 400
West Chester, PA 19380 USA
jensenhughes.com
O: +1 610-431-82608260

RISK ASSESSMENT OF MNGP DSC 11-15 WELDS USING NUREG-1864 METHODOLOGY RESULTS TO DSC 11-15

Prepared For

Xcel Energy
414 Nicollet Mall, 414-7
Minneapolis, MN 55401

Revision: 0

Project #: 1RCA16045.000
Project Name: Risk Assessment of MNGP DSC 11-15 Welds Using NUREG-1864 Methodology
Report #: 016045-RPT-01

Risk Assessment of MNGP DSC 11-15 Welds Using NUREG-1864 Methodology

Project No. 1RCA16045.000

Report #: 1RCA16045.000-001

Revision No. 0

Preparer:	Richard Anoba Digitally signed by Richard Anoba DN: C=US, E=ranoba@jensenhughes.com, O=Jensen Hughes, OU=Risk Informed Engineering, CN=Richard Anoba Location: Raleigh, NC Reason: I am the author of this document Contact Info: 650-678-6784 Date: 2017.08.29 14:21:12-04'00' Richard Anoba	Date:	8-29-2017
Preparer:	Digitally signed by Matt Johnson Date: 2017.08.29 10:08:24-05'00' Matt Johnson	Date:	8-29-2017
Reviewer:	Grant Teagarden Digitally signed by Grant Teagarden Date: 2017.08.29 11:39:17 -07'00' Grant Teagarden	Date:	8-29-2017
Reviewer:	Vincent Andersen	Date:	8-29-2017
Approver:	Richard Anoba Digitally signed by Richard Anoba DN: C=US, E=ranoba@jensenhughes.com, O=Jensen Hughes, OU=Risk Informed Engineering, CN=Richard Anoba Location: Raleigh, NC Reason: I am approving this document Contact Info: 650-678-6784 Date: 2017.08.29 14:21:45-04'00' Richard Anoba	Date:	8-29-2017

REVISION RECORD SUMMARY

Revision	Revision Summary
0	Initial Issue

TABLE OF CONTENTS

1.0 INTRODUCTION

1.1 Purpose

This report documents the risk assessment of non-compliant weld inspections of five (5) spent fuel dry storage casks (DSCs 11 thru 15) at the Monticello Nuclear Generating Plant (MNGP) plant. This risk assessment employs the approaches used by the NRC in NUREG-1864 [1]. The purpose of this analysis is to compare the calculated risk of the alternative of leaving these casks as-is in their current stored location versus the alternative of transferring these casks back into the reactor building for inspection and then returning them to their storage location.

1.2 Background

Xcel Energy is planning to submit an Exemption Request for five (5) NUHOMS Dry Shielded Canisters (DSCs) that were placed in service at the MNGP Independent Spent Fuel Storage Installation (ISFSI) with non-compliant dye penetrant examinations (PTs). Xcel Energy requested JENSEN HUGHES to develop a methodology to apply/extrapolate NUREG-1864 [1] results to MNGP DSC 11-15 and to apply the methodology to arrive at a comparative evaluation of the risks. The desired outcome is a report that provides an evaluation of the risks similar to Table 19 of NUREG-1864 [1] for the applicable initiating events and conditions facilitate decision-making regarding the following two proposed plan alternatives:

- Alternative 1: DSC 11-15 continued storage as-is
- Alternative 2: DSC 11-15 transfer, exam, return, and continued storage.

1.3 Scope

The objective of this analysis is to develop and apply a methodology to compare the risk of moving the subject DSCs with non-compliant PT examinations (for the purpose of conducting further non-destructive examination) to the risk of leaving the subject DSCs in service for twenty years with non-compliant PT examinations. The scope of this work does not include any structural or radiological analyses, nor development of a PRA model.

This report documents the analysis according to the following two major tasks:

- Task 1 - Develop a methodology to apply/extrapolate NUREG-1864 [1] results (Section 2 of Report)
- Task 2 - Apply methodology to apply/extrapolate NUREG-1864 [1] results (Section 3 of Report)

Cask DSC 16 has a similar non-conforming weld inspection; DSC 16 has been previously exempted from certain 10 CFR 72 regulations [24] and is not part of this risk analysis.

2.0 DEVELOPMENT OF METHODOLOGY TO APPLY/EXTRAPOLATE NUREG-1864 RESULTS TO DSC 11-15 PROCESS

2.1 Overview of Methodology

The approach and methodologies in NUREG-1864 [1] are used as the basis for this risk assessment. NUREG-1864 [1] documents the NRC risk assessment of a spent fuel dry cask storage system at a U.S. boiling water reactor (BWR) site. The NUREG-1864 [1] study is for the Holtec International HI-STORM 100 cask system and covers the onsite handling, transfer, and storage phases of the cask life cycle. The analysis covers a broad spectrum of postulated initiating events and hazards (e.g., drop scenarios, external hazards) and calculates the risk associated with the postulated initiating events

JENSEN HUGHES has developed a methodology to apply/extrapolate NUREG-1864 [1] methodologies and results by leveraging the configuration similarities between the MNGP model and the NUREG-1864 [1] model AND applying MNGP site specific (fuel loaded, flood hazard, seismic risk, etc.) and technology specific configuration (horizontal storage versus vertical) inputs where applicable. The overall goal is to compare the risks of the two alternatives using the plant-specific adaptation the NUREG-1864 methodology. The methodologies of this risk assessment are discussed in this section and Section 3 discusses the analysis.

The NUREG-1864 [1] analysis is presented according to the following main analysis areas:

- Initiating event identification and frequencies
- Release from MPC
- Release from secondary containment
- Consequence assessment

As such, the methodology used in this risk assessment is presented below according to the above analysis areas. In addition, the following analysis topics are discussed in this section:

- Risk quantification and results
- Risk acceptance criteria

2.2 Initiating Events

Section 3 of NUREG-1864 [1] documents the initiating events analysis for the pilot PRA study. The analysis includes initiating event identification, screening, and quantification. Table 1 provides a summary of initiating events addressed in NUREG-1864 [1]. Table 1 also identifies MNGP data sources that contain plant-specific information of interest.

Table 1: Summary of Initiating Events Addressed in NUREG-1864

Initiating Events	Screened in NUREG-1864	Section of NUREG-1864 Addressed	Monticello Data Sources
Floods	x	3.2.1	IPEEE, ISAR, and JENSEN HUGHES Report 1SML16012.000-1, Table 4-1.
Tsunamis	x	3.2.2	IPEEE, ISAR and any subsequent analysis
Volcanic Activity	x	3.2.4	IPEEE, ISAR and any subsequent analysis
Intense Precipitation	x	3.2.5	IPEEE, ISAR
Storage Tanks, Transformers, Barges, Trucks, Railcars, and Nearby Industrial Facilities	x	3.2.6	IPEEE, ISAR and any subsequent analysis
Dropped Fuel Assembly		3.3.1	ISAR and Monticello-specific information
Dropped Transfer Cask		3.3.2	ISAR and Monticello-specific information
Seismic Events		3.3.3	ISAR ML14136A289, S&A Report 14C4229-RPT-001 Rev. 3
High Winds		3.3.4	ISAR NUREG/CR-4461, Rev 2, Table 6-1 NEI 17-02, Section 6
Meteorites		3.3.5	IPEEE, ISAR and any subsequent analysis
Lightning Strikes		3.3.6	IPEEE, ISAR and any subsequent analysis
Aircraft		3.3.7	IPEEE, ISAR and any subsequent analysis

This risk assessment re-assesses the NUREG-1864 [1] initiating event screening process and frequency estimation to consider MNGP specific attributes.

2.2.1 Flood

Section C.2.3.1 of the MNGP IPEEE [5], the MNGP ISAR [7] are used to re-assess whether to confirm that external floods can be screened out from further consideration due to non-significant or no impact on the MNGP ISFSI and associated DCS/HSM modules. If this hazard initiator cannot be screened out, then report 1SML16012.000-1 or other current analyses will be used as the primary source of the external flooding hazard and the initiator carried forward into the analysis to consider the impact of the hazard on the potential for radionuclide release from the casks.

2.2.2 Tsunamis

Section 3.2.2 of NUREG-1864 [1] addresses the impact of tsunamis on the ISFSI of the reference site. Tsunamis were screened out on the basis that the reference site is far enough inland that it will not be affected by a tsunamis.

Section C.2.4 of the MNGP IPEEE [5] and the ISAR [7] are used to confirm that tsunamis can be screened out from further consideration due to no impact on the MNGP ISFSI and associated DCS/HSM modules, as well as the TC/DSC while in transfer or RX Building. If the MNGP documents do not address tsunamis, then perform a qualitative assessment similar to NUREG-1864 [1].

2.2.3 Volcanic Activity

Section 3.2.3 of NUREG-1864 [1] addresses the impact of volcanic activity on the ISFSI of the reference site. Volcanic activity was screened out on the basis that the reference site is far from volcanic regions and well out of the influence of volcanic activity. Section C.2.4 of the MNGP IPEEE [5] and the ISAR [7] are used to confirm that volcanic activity can be screened out from further consideration due to non-significant or no impact on the MNGP ISFSI and associated DCS/HSM modules.

2.2.4 Intense Precipitation

Section 3.2.4 of NUREG-1864 [1] addresses the impact of intense precipitation on the ISFSI of the reference site. intense precipitation was screened out on the basis that the ISFSI of reference site is designed so that graded land and drains conduct water away from the storage pads. Section C.2.3.2 of the MNGP IPEEE [5] and the ISAR [7] are used to confirm that intense precipitation can be screened out from further consideration due to non-significant or no impact on the MNGP ISFSI and associated DCS/HSM modules.

2.2.5 Storage Tanks, Transformers, Barges, Trucks, Railcars, and Nearby Industrial Facilities

Section 3.2.5 of NUREG-1864 [1] addresses the impact of storage tanks, transformers, barges, trucks, railcars, and nearby industrial facilities on the ISFSI of the reference site. Storage tanks, transformers, barges, trucks, railcars, and nearby industrial facilities were screened out based on proximity of these hazard sources to the ISFSI of the reference site. Section C.2.4 of the MNGP IPEEE [5], the ISAR [7], and the 72.212-A [26] are used to re-assess whether to confirm that storage tanks, transformers, barges, trucks, railcars, and nearby industrial facilities can be screened out from further consideration due to non-significant or no impact on the MNGP ISFSI and associated DCS/HSM modules. If one or more of these hazard initiators cannot be screened out, then a reasonable estimate of the hazard frequencies will be determined from the MNGP IPEEE and/or from industry studies and the initiator(s) carried forward into the analysis to consider the impact of the hazard on the potential for radionuclide release from the casks.

2.2.6 Dropped Fuel Assembly

Section 3.3.1 of NUREG-1864 [1] provides the basis for calculating frequency of a dropped fuel assembly during transfer operations to the ISFSI of the reference site. The MNGP alternatives considered in this report do not involve individual fuel assembly handling and dropped fuel assembly events can be screened out.

2.2.7 Dropped Transfer Cask

Section 3.3.2 of NUREG-1864 [1] provides the basis for calculating frequency of a dropped transfer cask during transfer operations to the ISFSI of the reference site. The drop rate used in NUREG-1864 [1] is taken from NUREG-1774 [20] and known to be potentially conservative and based on events that do not necessarily apply to the reference plant or to the MNGP plant configuration and procedures. The ISAR [7] and other plant-specific documents are used to assess Monticello specific aspects and to adjust the cask drop failure rate (NUREG-1774 [20] data is used in this re-assessment), haul path, and to confirm that the NUREG-1864 [1] frequency estimate can be applied to MNGP.

2.2.8 Seismic

Section 3.3.3 of NUREG-1864 [1] addresses the impact of seismic events on the ISFSI of the reference site. The seismic hazard curve used in NUREG-1864 [1] is provided in Figure 8 of the report and obtained from NUREG-1488 [21]. The seismic frequency used for risk quantification was based on the minimum ground acceleration of 1.35g Peak Ground Acceleration (PGA) necessary to cause storage cask tipping of a HI-STORM 100 cask on the ISFSI. Minimum required ground acceleration to result in cask tipping was calculated as 9 times the design basis earthquake ground acceleration of 0.15g PGA.

The seismic initiating event is retained in the risk assessment; however, NUREG-1488 based seismic hazard curves for U.S. nuclear power plant sites have been deemed obsolete for risk-informed interactions with the NRC following Generic Issue 199 [22]. As such, this risk assessment should use the latest available MNGP seismic hazard curve produced using methodologies accepted by the NRC. The seismic hazard curves for MNGP are provided in Figure 2.3.7-1 of the S&A Seismic hazard screening report [3]. The PGA hazard curve could be used in this assessment. Due to the differences in design, the NUHOMs canisters stored at MNGP in the horizontal position are not subject to tip over. Consequently, a plant-specific seismic-induced damage mechanism (if plausible) will have to be applied to determine the seismic hazard frequency.

2.2.9 High Winds

Section 3.3.4 of NUREG-1864 [1] addresses the impact of high wind events on the ISFSI of the reference site. The tornado hazard curve used in NUREG-1864 [1] is based on data provided in Table 8 and Figure 9 of the report. The tornado hazard was screened out based on extremely low frequencies associated with wind speed required to cause a storage cask to slide on the storage pad (400 mph), to cause storage cask to tip over on storage pad (600 mph), and to propel a heavy object onto a storage cask to cause damage (900 mph).

The high wind assessed in NUREG-1864 [1] is a tornado wind. This wind hazard remains the applicable significant wind for the MNGP site (e.g., hurricanes do not apply to the MNGP site). The tornado hazard curves for MNGP can be generated using plant-specific data from Table 6-1 of NUREG/CR-4461 [2]. The Fujita Scale data (annual exceedance frequency versus wind speed) is entered into MS Excel and used as the input to develop the tornado hazard curve. The trending function in MS Excel is used to generate the tornado hazard curve for MNGP. Section 6.29 of the ISAR [7] indicates that the design basis tornado is 360 mph. A preliminary review of the ISAR [7] indicates that cask tipping can be screened out for the MNGP configuration. If this is confirmed, then review the plant-specific documentation to identify other tornado induced failure mechanisms that can be used to estimate the tornado initiating event frequency. Review the ISAR [7] and other plant-specific documents to determine the wind speed required to cause a storage cask to slide on storage pad, to cause storage cask damage on storage pad, and to propel a heavy object onto a storage cask to cause damage. Use the tornado hazard curve for MNGP to determine the tornado frequency that would be used for quantification. Compare the NUREG-1864 [1] value against the MNGP value to determine if the NUREG-1864 [1] value is bounding. If NUREG-1864 [1] is not bounding, then use plant-specific information to estimate the impact. Due to the differences in design, the NUHOMs canisters stored at MNGP in the horizontal position are not subject to tip over. Consequently, a plant-specific tornado-induced damage mechanism (if plausible) will have to be applied to determine the tornado hazard frequency.

2.2.10 Meteorites

Section 3.3.4 of NUREG-1864 [1] addresses the impact of meteorites on the ISFSI of the reference site. This initiating event is retained in this risk assessment and the NUREG-1864 [1] frequency estimate for meteorite strike per area is used for MNGP.

2.2.11 Lightning Strikes

Section 3.3.6 of NUREG-1864 [1] addresses the impact of lightning strikes on the ISFSI of the reference site. Lightning strike induced radionuclide release accidents are determined in NUREG-1864 [1] to be non-credible. NUREG-1864 [1] information, the MNGP IPEEE [5], ISAR [7] and other plant-specific documents are used in this risk assessment to document that lightning strike induced accidents are non-credible radionuclide release accidents for the MNGP NUHOMS dry cask storage system.

2.2.12 Aircraft

Section 3.3.7 of NUREG-1864 [1] addresses the impact of aircraft impact on the ISFSI of the reference site. This hazard is maintained in this risk assessment. The MNGP IPEEE [5], ISAR [7] and other plant-specific documents are used to re-assess the aircraft impact frequency estimate for MNGP.

2.2.13 Blocked Vent

Blocked vents are evaluated for the MPC failure model due to thermal events. The DSC failure model thermal event discussion is contained in Section 3.3.2.

2.3 Multipurpose Canister (MPC) Failure Model

Section 4.3.2 of NUREG-1864 [1] addresses the probabilities of MPC failures for the reference site. Table 12 of NUREG-1864 [1] provides a summary of MPC probabilities for the reference site. The MPC failure probabilities are a function of mechanical impact load due to various event scenarios. Many of the event scenarios involve load drops at various heights. The drop heights on Table 12 of NUREG-1864 [1] were derived from Table 1 of NUREG-1864 [1], which defines the stages of dry cask operations for the reference site. Table 1 of NUREG-1864 [1], seems to indicate that the MPC failure probability is a strong function of drop height. Table 2 of the report provides a comparison of the reference site dry cask operations on Table 1 of NUREG-1864 [1] against the MNGP dry cask operations.

Information in Table 2 [34] of this report and other MNGP documentation are used to assess plant-specific DSC failure probabilities given an initiating event challenge. The DSC provides the equivalent function of the MPC evaluated in NUREG-1864 [1].

Certain accident scenarios (e.g., meteorite strike) in NUREG-1864 [1] use a conditional failure probability of 1.0 for the MPC; this same approach is used in this risk assessment for these scenarios.

Table 2: Stages of Dry Cask Storage Operation – NUREG-1864 Compared to MNGP Alternatives

NUREG 1864: Table 1. Stages of the Dry Cask Storage Operation				Monticello Operations to Consider for DSC 11-15		
Stages		**Height (A) m**	**Height (A) ft**	**MNGP Step (Reference Lesson Plan M-9014L-058 for Steps)** MNGP 9500-Series Procedure & Part(s) Listed with Description		**Height**
1	Loading fuel assemblies into the MPC (B)	4.8	16	6	N/A, DSC 11-15 already loaded, sealed and placed in HSM. 9505 Rev 12, Part I	16.75' Ref. 36
2	Placing the MPC lid onto the MPC and engaging the lift yoke on the transfer cask (C)	0	0	7	N/A, DSC 11-15 already loaded, sealed and placed in HSM. 9506 Rev 17, Parts B & C	0
3	Lifting the transfer cask out of the cask pit	13	42.5	8	N/A, DSC 11-15 already loaded, sealed and placed in HSM. 9506 Rev 17, Part D	39.5' Ref. 37
4	Moving the transfer cask over a railing of the spent fuel pool	0.9	3	8	N/A, DSC 11-15 already loaded, sealed and placed in HSM. 9506 Rev 17, Part D	
5	Moving the transfer cask to the preparation area (1st segment)	0.3	1	8	N/A, DSC 11-15 already loaded, sealed and placed in HSM. 9506 Rev 17, Part D	6.5"-8.5" Ref. 38
6	Moving the transfer cask to the preparation area (2nd segment)	0.3	1	8	N/A, DSC 11-15 already loaded, sealed and placed in HSM. 9506 Rev 17, Part D	6.5"-8.5" Ref. 38
7	Moving the transfer cask to the preparation area (3rd segment)	0.3	1	8	N/A, DSC 11-15 already loaded, sealed and placed in HSM. 9506 Rev 17, Part D	6.5"-8.5" Ref. 38
8	Lowering the transfer cask onto the preparation area (D)	0.3	1	8	N/A, DSC 11-15 already loaded, sealed and placed in HSM. 9506 Rev 17, Part D	6.5"-8.5" Ref. 38
9	Preparing (draining, drying, inerting, and sealing) the MPC for storage	0	0	9-19	N/A, DSC 11-15 already loaded, sealed and placed in HSM. 9506 Rev 17, Parts F through Q	0
				The following sequences represent PAUT of a DSC, followed by moving the DSC and placing in the HSM storage module		
					Perform PAUT (Phased Array Ultrasonic Test) of DSC while in the TC on the refueling floor.	0

Table 2: Stages of Dry Cask Storage Operation – NUREG-1864 Compared to MNGP Alternatives						
NUREG 1864: Table 1. Stages of the Dry Cask Storage Operation				**Monticello Operations to Consider for DSC 11-15**		
Stages		**Height (A)**		**MNGP Step (Reference Lesson Plan M-9014L-058 for Steps)** MNGP 9500-Series Procedure & Part(s) Listed with Description		**Height**
		m	**ft**			
				20	Install the TC lid 9507 Rev 19, Part B	
10	Installing the short stays and attaching the lift yoke (D)	0	0	21	Similar: Attaching the lift yoke (D) 9507 Rev 19, Part C	0
11	Lifting the transfer cask	0.6	2	21	Same 9507 Rev 19, Part C	6.5" – 8.5" Ref. 38
12	Moving the transfer cask to exchange bottom lids of the transfer cask (1st segment)	0.6	2		N/A for NUHOMS system	
13	Moving the transfer cask to exchange bottom lids of the transfer cask (2nd segment)	0.6	2		N/A for NUHOMS system	
14	Replacing the pool lid with the transfer lid	0.1	0.25		N/A for NUHOMS system	0
15	Moving the transfer cask near the equipment hatch	0.6	2	21	Same 9507 Rev 19, Part C	6.5" – 8.5" Ref. 38
16	Holding the transfer cask	0.6	2	21	Same 9507 Rev 19, Part C	6.5" – 8.5" Ref. 38
17	Moving the transfer cask to the equipment hatch	0.6	2	21	Same 9507 Rev 19, Part C	6.5" – 8.5" Ref. 38
18	Lowering the transfer cask to the over-pack through the equipment hatch	24.4	80	22-23	Similar: Lowering the transfer cask to the transfer trailer (TT) through the equipment hatch. Based on 1027.67 + 0.71 carry height minus 935 (assuming TT is missing). Height to the TT trunnion is about 8 fewer feet – 85.4' 9507 Rev 19, Part C	93.4' Ref. 39
19	Preparing (remove short stays, disengage lift yoke, attach long stays) to lower the MPC	0	0		N/A for NUHOMS system	
20	Lifting the MPC and opening doors of transfer lid	5.8	19		N/A for NUHOMS system	
21	Lowering the MPC through the transfer cask into the storage cask	5.8	19		N/A for NUHOMS system	

Table 2: Stages of Dry Cask Storage Operation – NUREG-1864 Compared to MNGP Alternatives						
NUREG 1864: Table 1. Stages of the Dry Cask Storage Operation				**Monticello Operations to Consider for DSC 11-15**		
Stages		**Height (A)**		**MNGP Step (Reference Lesson Plan M-9014L-058 for Steps)** MNGP 9500-Series Procedure & Part(s) Listed with Description		**Height**
		m	**ft**			
				22-23	Down-end onto the TT and disengage the lift yoke [Once the bottom trunnion is seated a long TC would rotate and drop 148.5 inches until the top trunnion is seated. 138.5" for the short TC.] 9507 Rev 19, Part C	148.5" Ref. 40
22	Moving the storage cask into the airlock on Helman rollers	0	0	25	Similar: Moving the storage cask into the airlock on TT (Based on max 43" trailer deck height per NUH-07-0218) 9510 Rev 13, Part A	64.5" Ref. 41
23	Moving the storage cask out of the airlock on Helman rollers	0	0	25	Similar: Moving the storage cask out of the airlock on TT 9507 Rev 19, Part D	64.5" Ref. 41
24	Moving the storage cask away from the secondary containment on Heiman rollers	0	0	25	Similar: Moving the storage cask away from the secondary containment on TT 9507 Rev 19, Part D	64.5" Ref. 41
25	Preparing (installing lid, vent shield cross-plates, vent screens) the storage cask for storage	0	0		N/A for NUHOMS system	
26	Lifting the storage cask above the Heiman rollers with the over-pack transporter	0.1	0.25		N/A for NUHOMS system	
27	Moving the storage cask above a cushion on the preparation area	<0.1	<0.25		N/A for NUHOMS system	
28	Holding the storage cask above the cushion while attaching a Kevlar belt	<0.1	<0.25		N/A for NUHOMS system	
29	Moving the storage cask above the concrete surface of the preparation area	0.3	1	25	Same (Based on max 43" trailer deck height per NUH-07-0218) 9508 Rev 17, Part D	64.5" Ref. 41
30	Moving the storage cask above the asphalt road	0.3	1	25	Same 9507 Rev 19, Part D	64.5" Ref. 41
31	Moving the storage cask above the gravel surface around the storage pads	0.3	1	25	Same 9507 Rev 19, Part D	64.5" Ref. 41

Table 2: Stages of Dry Cask Storage Operation – NUREG-1864 Compared to MNGP Alternatives						
NUREG 1864: Table 1. Stages of the Dry Cask Storage Operation				**Monticello Operations to Consider for DSC 11-15**		
Stages		**Height (A)**		**MNGP Step (Reference Lesson Plan M-9014L-058 for Steps)** MNGP 9500-Series Procedure & Part(s) Listed with Description		**Height**
		m	**ft**			
32	Moving the storage cask above the concrete storage pad	0.3	1	25	Same 9508 Rev 17, Part D	64.5” Ref. 41
33	Lowering the storage cask onto the storage pad	0.3	1		N/A for NUHOMS system	70.4” Ref. 42
				26-34	Remove TC lid, align to HSM, grapple DSC and insert into HSM and install the door 9508 Rev 17, Parts D through K	70.4” Ref. 42
				The sequence above would be performed in reverse to remove DSC 11-15 from the HSM and return to the refueling floor for PAUT.		
34	Storing the storage cask on the storage pad for 20 years	0	0		Same	0
(A) Height is the distance the cask would fall if the support system failed. (B) Prior to Stage 1, the MPC is inserted into the transfer cask, and after other preparations, lowered into the cask pit. The storage over-pack is placed on Heiman rollers and moved under the equipment hatch. (C) The lift yoke attaches to the trunnions of the transfer cask. (D) Stays attach to the lift yoke on one end and cleats of the MPC on the other end.				(A) Height is the distance the cask would fall if the support system failed (B) Prior to Stage 1, the DSC is inserted into the transfer cask, and after other preparations, lowered into the cask pit. The transfer trailer is moved under the equipment hatch. (C) The lift yoke attaches to the trunnions of the transfer cask. (D) Lift yoke is disconnected during preparation and re-attached prior to next movement.		

2.4 Fuel Assembly Failure Model

Section 4.4 of NUREG-1864 [1] addresses the probabilities of fuel and cladding failures due to dynamic loadings (i.e., drop scenarios) for the reference site. As discussed in sections 2.2.6 and 3.2.6 of this report, fuel assembly drops have been screened out based on the defined scope of this PRA. The fuel can fail given a drop of the DSC. In NUREG-1864 [1] fuel failure is included in the overall failure of the MPC given a drop, and this is applied to this evaluation as well. Table 3 shows the probability of release given failure of the fuel and MPC based on the NUREG-1864 [1] template, and for MNGP, Tables 14 and 15 contain the probability of release from the fuel and DSC.

2.5 Secondary Containment Isolation Model

Section 5.0 of NUREG-1864 [1] describes the secondary isolation model for the reference site that is applied for accident scenarios initiating within the reactor building. A logic model was developed to quantify the failure probability of the Secondary Isolation System. Figure 17 of NUREG-1864 [1] provides a flow diagram for the Secondary Isolation System for the reference plant.

This aspect of the analysis applies to MNGP, as well. This aspect of the analysis is an assessment of the secondary containment isolation system and the configuration of the secondary containment boundary at the time of postulated accidents. MNGP documents and drawings are used to determine the plant-specific differences for the Secondary Containment Isolation System. Section 5.3 of the Monticello USAR [12] provides a description of the Secondary Containment Isolation System. The flow diagrams, provided in References [13] through [17], provide the details of the Monticello Secondary Isolation System. Simplified flow diagrams for Monticello Secondary Isolation System is provided in Figures 1 through 3. Compare the NUREG-1864 [1] system against the MNGP system to determine if the NUREG-1864 [1] system failure probabilities are bounding based on system considerations.

Security-Related Information Figure Withheld Under 10 CFR 2.390.

Figure 1 – MNGP Secondary Containment Isolation Sheet 1

Security-Related Information
Figure Withheld Under 10 CFR 2.390.

Figure 2 – MNGP Secondary Containment Isolation Sheet 2

Security-Related Information
Figure Withheld Under 10 CFR 2.390.

Figure 3 – MNGP Secondary Containment Isolation Sheet 3

2.6 Consequence

Section 6.0 of NUREG-1864 [1] describes the consequence analysis for the reference site. Important consequence related parameters and inputs noted in NUREG-1864 [1] include the following:

- Fuel type and exposure
- Radionuclide inventory
- Source term (e.g., release fraction)
- Initial plume dimensions
- Plume heat content
- Population density/distribution
- Site weather

Review the MNGP documents to determine the parameters and inputs to support comparison to NUREG-1864 [1] and to account for plant-specific differences. Table E-1 of NUREG-1864 [1] provides the DSC radionuclide inventory used in the consequence analysis for the reference plant. Table 6-1 of Reference [8] provides DSC radionuclide inventory for the Monticello. Reference [11] provides the population estimate for Monticello. The population estimate for the Hatch Nuclear Plant is assumed to be applicable for the reference plant.

NUREG-1864 [1] presents MACCS2 conditional consequence results in Table E.3 for six (6) cases. The six cases reflect the consequence associated with a 100 ft. inadvertent cask drop, but with differing attributes of fuel damage, release height, and filter system. Only one of these six cases (i.e., the bounding case) was used in the final NUREG-1864 [1] risk assessment as reflected in Table 18 of that document. However, the other cases may be applicable to represent the lower expected release associated with releases from a DSC on the pad.

Review, select, or if required adjust, the consequence result from Table E.3 of NUREG-1864 [1] that best reflects or bounds the applicable MNGP configurations (e.g., based on stage).

2.7 Risk Quantification and Results

This risk assessment does not require building or quantification of PRA event tree and fault tree models. The initiating event frequencies and associated conditional probabilities of releases and consequences are easily multiplied in a spreadsheet to determine the risk results. Structural failure probabilities given a drop from NUREG-1864 [1] are assessed as reasonable for MNGP with scaling factor used for the presence of weld flaws. Offsite consequence results from NUREG-1864 [1] are evaluated as reasonable to represent MNGP specifics; building and quantification of detailed offsite consequence models is not performed as part of this risk assessment.

Section 6.0 of NUREG-1864 [1] describes the results of the risk calculations for the reference site. Table 19 of NUREG-1864 [1] provides the summary of risk results for the reference site. The tabular results presentation approach of NUREG-1864 [1] Table 19 is used in this risk assessment for MNGP. Table 3 below provides the template used in this assessment for tabulating the MNGP risk results similar to the NUREG-1864 [1] results. The shaded rows are not applicable to MNGP, based on the comparison on Table 2. The MNGP specific process steps in Table 2 are related to the NUREG-1864 [1] stages.

The results information is presented as follows in each of the columns:

- Stage: This column lists individual stages of cask onsite loading, transportation and storage. This allows traceability to the NUREG-1864 analysis approach as well allows identification of different challenges (i.e., initiating events) at different stages.
- Initiating Event: This column lists the challenges (i.e., initiating event) by stage that are considered further in this risk assessment.
- Initiating Event Frequency: This column lists the frequency of occurrence per calendar year of the initiating events.
- Probability of Release from Fuel Rod and MPC: This column provides the probability of release from the fuel rod and MPC given the initiating event. The values in this column are conditional probabilities given the associated initiating event frequency.
- Consequences: This column provides the probability of public consequences in terms of latent individual cancer fatalities within 10 miles. The values in this column are conditional probabilities given radionuclide release from the MPC in NUREG-1864 (and for the MNGP DSC for this evaluation)
- Risk: This column provides the occurrence frequency, in terms of latent individual cancer fatalities within 10 miles, for each of the analyzed initiating event induced radionuclide release scenarios. The values in this column are calculated by multiplying the initiating event frequency, release probability and consequence probability. The results are presented in units of per calendar year.

Table 3: Template for MNGP Risk Results Tabulation

Stages			Initiating Event	Initiating Event Frequency (Sections 2.2 and 3.2)	Probability of Release from fuel rod and MPC (Sections 2.3 and 3.3)	Probability of Release from Containment (Sections 2.5 and 3.5)	Consequences (Sections 2.6 and 3.6)	Risk
NUREG -1864	MNGP	Description						
1	6	Loading fuel assemblies into the MPC (B)	Fuel assembly dropped					
2	7	Placing the MPC lid onto the MPC and engaging the lift yoke on the transfer cask (C)						
3	8	Lifting the transfer cask out of the cask pit	Transfer cask dropped					
4	8	Moving the transfer cask over a railing of the spent fuel pool	Transfer cask dropped					
5	8	Moving the transfer cask to the preparation area (1st segment)	Transfer cask dropped					
6	8	Moving the transfer cask to the preparation area (2nd segment)	Transfer cask dropped					
7	8	Moving the transfer cask to the preparation area (3rd segment)	Transfer cask dropped					
8	8	Lowering the transfer cask onto the preparation area (D)	Transfer cask dropped					
9	9-19	Preparing (draining, drying, inerting, and sealing) the MPC for						

Table 3: Template for MNGP Risk Results Tabulation

Stages			Initiating Event	Initiating Event Frequency (Sections 2.2 and 3.2)	Probability of Release from fuel rod and MPC (Sections 2.3 and 3.3)	Probability of Release from Containment (Sections 2.5 and 3.5)	Consequences (Sections 2.6 and 3.6)	Risk
NUREG -1864	MNGP	Description						
		storage						
		Perform PAUT of DSC while in the TC on the refueling floor.						
	20	Install the TC Lid						
10	21	Installing the short stays and attaching the lift yoke (D)						
11	21	Lifting the transfer cask	Transfer case dropped					
12		Moving the transfer cask to exchange bottom lids of the transfer cask (1st segment)	Transfer cask dropped					
13		Moving the transfer cask to exchange bottom lids of the transfer cask (2nd segment)	Transfer cask dropped					
14		Replacing the pool lid with the transfer lid	Transfer cask dropped					
15	21	Moving the transfer cask near the equipment hatch	Transfer cask dropped					
16	21	Holding the transfer cask	Transfer cask dropped					

Table 3: Template for MNGP Risk Results Tabulation

Stages			Initiating Event	Initiating Event Frequency (Sections 2.2 and 3.2)	Probability of Release from fuel rod and MPC (Sections 2.3 and 3.3)	Probability of Release from Containment (Sections 2.5 and 3.5)	Consequences (Sections 2.6 and 3.6)	Risk
NUREG -1864	MNGP	Description						
17	21	Moving the transfer cask to the equipment hatch	Transfer cask dropped					
18	22-23	Lowering the transfer cask to the over-pack through the equipment hatch	Transfer cask dropped					
19		Preparing (remove short stays, disengage lift yoke, attach long stays) to lower the MPC	MPC drop					
20		Lifting the MPC and opening doors of transfer lid	MPC drop					
21		Lowering the MPC through the transfer cask into the storage cask	MPC drop					
	22-23	Down-end onto the TT and disengage the lift yoke [Once the bottom trunnion is seated a long TC would rotate and drop 148.5 inches until the top trunnion is seated. 138.5" for the short TC.]	Transfer cask dropped					
22	25	Moving the storage cask into the airlock on Helman rollers (TT for MNGP)						
23	25	Moving the storage cask out of the						

Table 3: Template for MNGP Risk Results Tabulation

Stages			Initiating Event	Initiating Event Frequency (Sections 2.2 and 3.2)	Probability of Release from fuel rod and MPC (Sections 2.3 and 3.3)	Probability of Release from Containment (Sections 2.5 and 3.5)	Consequences (Sections 2.6 and 3.6)	Risk
NUREG -1864	MNGP	Description						
		airlock on Helman rollers (TT for MNGP)						
24	25	Moving the storage cask away from the secondary containment on Heiman rollers (TT for MNGP)						
25		Preparing (installing lid, vent shield cross-plates, vent screens) the storage cask for storage						
26		Lifting the storage cask above the Heiman rollers with the over-pack transporter	Storage cask dropped					
27		Moving the storage cask above a cushion on the preparation area	Storage cask dropped					
28		Holding the storage cask above the cushion while attaching a Kevlar belt	Storage cask dropped					
29	25	Moving the storage cask above the concrete surface of the preparation area	Storage cask dropped					
30	25	Moving the storage cask above the asphalt road	Storage cask dropped					

Table 3: Template for MNGP Risk Results Tabulation

Stages			Initiating Event	Initiating Event Frequency (Sections 2.2 and 3.2)	Probability of Release from fuel rod and MPC (Sections 2.3 and 3.3)	Probability of Release from Containment (Sections 2.5 and 3.5)	Consequences (Sections 2.6 and 3.6)	Risk
NUREG -1864	MNGP	Description						
31	25	Moving the storage cask above the gravel surface around the storage pads	Storage cask dropped					
32	25	Moving the storage cask above the concrete storage pad	Storage cask dropped					
33		Lowering the storage cask onto the storage pad	Storage cask dropped					
	26-34	Remove TC lid, align to HSM, grapple DSC and insert into HSM and install the door						
34A		Storing the storage cask on the storage pad for 20 years	Tipped be Seismic Event					
34B		Storing the storage cask on the storage pad for 20 years	Struck by aircraft					
34C		Storing the storage cask on the storage pad for 20 years	Struck by meteorite					
34D		Storing the storage cask on the storage pad for 20 years	Heated by aircraft fuel					

The risk analysis is performed to model the following two proposed alternatives:

- Alternative 1: DSCs 11-15 Remain As-Is in the HSM
- Alternative 2: DSCs 11-15 Transferred to RB for Inspection and then back to the HSM

Table 4 provides a summary of the risk analysis quantification approach used to apply the NUREG-1864 [1] results to model the MNGP DSCs 11-15 non-compliant weld inspection issues.

Table 4: MNGP Dry Cask Risk Assessment Approach

Topic	MNGP Alternative 1 Leave DSCs 11-15 As-Is in the HSM	MNGP Alternative 2 Transfer DSCs 11-15 to RB for Inspection and then Transfer Back to the HSM
PRA Case	Adjustments to base case risk scenarios are made to reflect that 5 casks on the pad have weld inspection issues	Adjustments to base case risk scenarios are made to reflect that the 5 casks on the pad with weld inspection issues are transported back into RB for inspection, inspected and then transported back out to pad
Delta and Absolute Risk	From the above two cases, the absolute risk of the two alternatives as well as the delta risk between the alternatives is determined.	

The case for each alternative incorporates the non-compliant weld inspections for DSCs 11-15, as well as the additional postulated accident scenarios (i.e., additional drop scenarios) for Alternative 2 given the transfer of the casks back into the reactor building for inspection). The modeling adjustments for the non-compliant weld inspections are treated by assuming the presence of weld flaws degrades the capacity of the lid welds to resist failure. Postulated thermal cycling induced through-wall cracks in the cask welds and resulting release accidents are non-credible scenarios over the life of the cask on the ISFSI for both alternatives.

These cases for the two alternatives allow calculation of the absolute risk for each alternative, as well as the delta risk for each alternative. The primary risk metric used in this risk assessment is latent cancer fatality to the public (/yr). NUREG-1864 [1] analysis determined that acute fatalities to the public are not applicable to dry cask storage accident scenarios; that determination is applicable to MNGP, as well.

Risk Acceptance Criteria

Reference [9] provides proposed guidance for “Risk-Informed Decision-Making for Nuclear Material and Waste Applications.” Reference [9] indicates that for exemptions and changes to the licensing basis of a facility that would tend to increase risk, very general guidance can be adapted from the RG 1.174 [10]. Specific requirements may be relaxed if the initial risk is already low and the incremental increases from a change are also small. Table 5 provides the Quantitative Health Guidelines (QHGs) proposed for determining negligible risk.

Table 5: Proposed Criteria for Acceptable Risk Change

Quantitative Health Guidelines	Risk Metric	Criteria for Risk Change
QHG-1	Public individual risk of acute fatality	Negligible if ≤ 5x10-7 /yr
QHG-2	Public individual risk of latent cancer fatality	Negligible if ≤ 2x10-6 /yr
QHG-3	Public individual risk of serious injury	Negligible if ≤ 1x10-6 /yr
QHG-4	Worker individual risk of acute fatality	Negligible if ≤ 1x10-6 /yr
QHG-5	Worker individual risk of latent cancer fatality	Negligible if ≤ 1x10-5 /yr
QHG-6	Worker individual risk of serious injury	Negligible if ≤ 5x10-6 /yr

Table 4.2 of Reference [9] suggests that a 10% change in QHG would be acceptable. This is consistent with the criteria provided in Figures 4 and 5 for RG 1.174 [10]. Figure 4 of this report provides an adaptation of the RG. 1.174 [10] for QHG-2. Table 18 of NUREG-1864 [1] indicates that the risk metrics associated with QHG-1 and QHG-2 were quantified for the reference site. Table 18 also indicates that the contribution for QHG-1 was negligible for the reference site. It is reasonable to assume that the MNGP results for QHG-1 would be similar. Consequently, the primary focus of this risk analysis is with respect to QHG-2. As such, the risk criteria shown in Figure 4 are used in this analysis to assess the acceptability of the proposed alternatives. Acceptability is shown as a measure of the calculated delta risk with respect to the absolute risk.

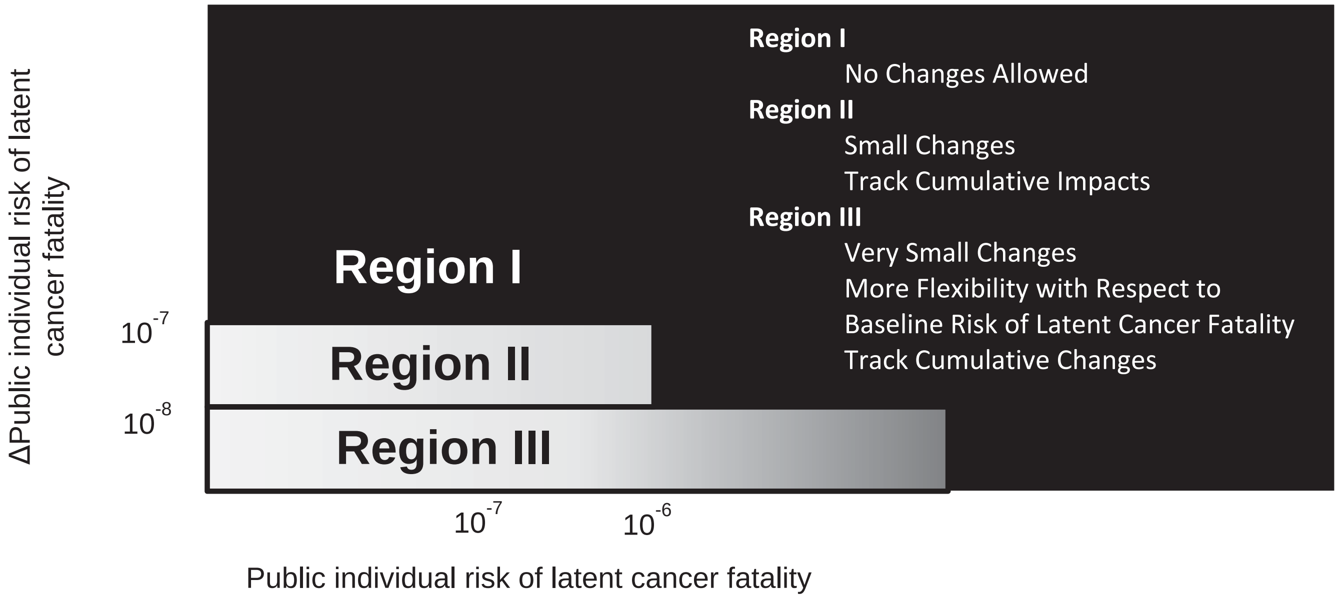

Figure 4 – Proposed Risk Criteria for NUREG-1864 Comparison

3.0 APPLICATION OF METHODOLOGY TO APPLY/EXTRAPOLATE NUREG-1864 RESULTS TO DSC 11-15

In this section of the report, JENSEN HUGHES documents the application of the methodology developed in Section 2 to arrive at a comparative evaluation of the risks for (1) transfer, examination, and return of the canisters for continued storage versus (2) continued storage of the non-compliant canisters in horizontal storage modules (HSMs). This task includes a review of all relevant and available documents and the collection of appropriate data to support the evaluation.

3.1 Overview of Application

In Section 2.0 of this report, JENSEN HUGHES documents the application of the methodology developed in Section 3.

3.2 Initiating Events

Section 2.2 of this report provides the methodology to address in the MNGP adaptation of NUREG-1864 [1].

3.2.1 Flood

Section 2.2.1 of NUREG-1864 [1] addresses the external flood impact on the ISFSI of the reference site. External floods are screened out from further on the basis that the flood waters for the combined maximum storm, sustained winds, and dam failures would be insufficient to reach the storage cask on the storage pad.

As discussed in the MNGP IPEEE [4], the probable maximum flood for MNGP corresponds to a peak elevation of 939.2, which is 9 feet above plant grade. A recent flood re-evaluation report [25] concluded that this flood elevation bounds the actual hazard at MNGP.

The MNGP ISFSI is located at 943 feet above MSL [6], thus the probable maximum flood will not reach the bottom of the casks, thus, floods events are screened out of this evaluation.

3.2.2 Tsunamis

Section 3.2.2 of NUREG-1864 [1] addresses the impact of tsunamis on the ISFSI of the reference site. Tsunamis are screened out on the basis that the reference site is far enough inland that it will not be affected by a tsunami.

Tsunamis are not explicitly addressed in the MNGP IPEEE [4]. Consistent with NUREG-1864 [1], tsunamis can be screened out because the site is far enough inland that it will not be affected by tsunamis.

3.2.3 Volcanic Activity

Section 3.2.3 of NUREG-1864 [1] addresses the impact of volcanic activity on the ISFSI of the reference site. Volcanic activity was screened out on the basis that the reference site is far from volcanic regions and well out of the influence of volcanic activity.

The MNGP IPEEE [4] screened out volcanic activity generically with the statement that such events do not apply to Monticello. There are no volcanoes nearby. Volcanic activity hazards are screened out from further consideration in this evaluation.

3.2.4 Intense Precipitation

Section 3.2.4 of NUREG-1864 [1] addresses the impact of intense precipitation on the ISFSI of the reference site. Intense Precipitation was screened out on the basis that the ISFSI of reference site is designed so that graded land and drains conduct water away from the storage pads. Intense precipitation is included in flood analysis discussed in Section 3.2.1 of this report, which concluded that a flood event could not impact the MNGP ISFSI. Consequently, intense precipitation is screened out from further consideration in this evaluation.

3.2.5 Storage Tanks, Transformers, Barges, Trucks, Railcars, and Nearby Industrial Facilities

Section 3.2.5 of NUREG-1864 [1] addresses the impact of storage tanks, transformers, barges, trucks, railcars, and nearby industrial facilities on the ISFSI of the reference site. Storage tanks, transformers, barges, trucks, railcars, and nearby industrial facilities were screened out based on proximity of these hazard sources to the ISFSI of the reference site.

Storage tanks, transformers, barges, trucks, railcars, and nearby industrial facilities potentially pose fire and/or explosive hazards to the MNGP ISFSI and to the storage cask when being transported from the reactor building to the ISFSI. The ISFSI Fire Hazards Analysis (72.212-A) [26] evaluated the heat flux from potential fire sources and compared the heat flux to the design capacity of the storage cask and the HSM. A similar evaluation was performed to evaluate the potential for explosive shockwaves to damage the storage cask or the HSM. Appendix A.1 [26] contains the list of potential fire/explosion sources that were evaluated. The following summarizes the results of the fire hazards analysis:

- Fires: No fire source can produce sufficient heat flux to damage the storage cask, whether on the haul path or at the MNGP ISFSI, with the exception of diesel and gasoline delivery trucks which present a hazard to the storage cask on the haul route (if allowed on the haul route). Due to the potential of a damaging fire from diesel or gasoline delivery trucks, administrative controls are in place to keep delivery trucks sufficient distance from the haul path. During construction operations (i.e., when additional HSMs are added to the MNGP ISFSI over time), multiple vehicles burning simultaneously could damage the HSM. Administrative controls limit the number of construction vehicles allowed near the HSM during construction operations, and provide for fire watches when a single vehicle is allowed near the HSM. A fire involving the fuel load at the transfer trailer was evaluated, and the conclusion was that the fire would not result in fuel cladding temperature near the short or long-term limits.
- Explosions: No explosive source can produce a sufficient blast shockwave that would damage the storage cask or HSM with the exception of the diesel and gasoline delivery trucks, as discussed for fires. The same administrative controls are used to ensure such vehicles are sufficient distance from the storage cask when on the haul route and sufficient distance from the MNGP ISFSI.

The administrative controls preclude a sufficient fire or blast from damaging the storage cask, whether on the haul route or at the MNGP ISFSI, and preclude damage to the HSM. Although administrative controls are considered effective enough to screen the hazard deterministically, plant staff could fail to implement the controls and a delivery truck could approach the storage cask on the haul path or approach the MNGP ISFSI. Should this occur, an accident or event that triggers an explosion would need to occur, and the truck would need to be close to the storage cask or ISFSI for any damage to result. Such an event could be an accident involving the transfer trailer and delivery vehicle, which, if the vehicles approached each other on the haul path, would presumably be avoided by each driver to the maximum extent possible. At the ISFSI, the HSM would provide shielding for the DSC. The likelihood of the additional event or accident, combined with the likelihood of failure to follow the administrative controls, is considered low enough that failure to follow the administrative controls with subsequent accident causing a fire/explosion is assumed low and can be screened out from this evaluation.

3.2.6 Dropped Fuel Assembly

The scope of this assessment does not include a dropped fuel assembly. The fuel assemblies do not have to be removed from the DSC in either Alternative 1 or Alternative 2.

3.2.7 Dropped Transfer Cask

This hazard does not apply to Alternative 1 but does apply to Alternative 2.

This hazard involves consideration of two attributes: 1) number of lifts; and 2) postulated inadvertent drop rate.

Alternative 2 includes two separate lifts per cask. One lift transports the Storage Cask up the equipment hatch and across the refueling floor to an area where inspections/welding is normally performed. The other lift is the reverse of this first lift to lower the cask back down the equipment shaft so it can be transported back to the ISFSI. No lifts occur on the ISFSI or transport from the RB to the ISFSI.

The drop rate frequency in NUREG-1864 [1] is developed using data in NUREG-1774, Survey of Crane Operating Experience at U.S. Nuclear Power Plants from 1968 through 2002 [20]. The data used in the NUREG-1864 analysis is the NUREG-1774 drop rate frequency for “very heavy” loads. NUREG-1774 defines “very heavy” loads as those greater than 30 tons. NUREG-1774 review of very heavy load lifts at nuclear plants showed no records of crane equipment related failures; the three very heavy load drops identified in NUREG-1774 were assessed as due to human error and not due to crane equipment failure. The NUREG-1774 “very heavy” loads inadvertent drop frequency is calculated as 3 very heavy load drops in 54,000 lifts, which is a drop rate of 5.56E-05/lift.

NUREG-1864 recognizes that this frequency may be conservative because, among other reasons, the NUREG-1774 very heavy load drop incidents involved mobile cranes whereas the reference plant uses a fixed single failure proof crane. However, discussion in NUREG-1774 indicates that although a fixed single failure proof crane contributes to a lower drop frequency it does not preclude the potential of a load drop. The three very heavy load drop events identified in NUREG-1774 were all due to operator error that caused the nylon (in one case) and Kevlar (in two cases) slings to fail. Although MNGP does not use Kevlar or other fabric slings for DSC movements, rigging errors (although very remote given the controls and apparatus) can still be postulated. As such, the NUREG-1774 “very heavy” load drop frequency of 5.56E-5/lift, although likely conservative, is considered reasonable for the purposes of this risk assessment.

3.2.8 Seismic

As discussed in Section 2.2.8 of this report, due to the differences in design, the NUHOMs canisters stored at MNGP in the horizontal position and are not subject to tip over. For transfer operations, consistent with NUREG-1864 [1], time based initiating events are considered unlikely during the short amount of time of transfer and tipping of the transfer trailer or seismic induced drop of the DSC inside the reactor building is screened out based on low likelihood.

During storage, a seismic event could induce an acceleration load on the DSCs. The ISAR [7] evaluated large magnitude accelerations on the DSC for drop scenarios, and concluded the DSC has margin to withstand high acceleration events of 25g for a corner drop and 75g for a vertical or side drop. The frequency of seismic events that would induced an equivalent acceleration on the DSC would be very low, based on the hazard curve in Reference 3, and thus seismically induced failure for reasons other than tipping during storage is not considered a plausible failure mode for the DSC.

3.2.9 High Winds

As discussed in section 2.2.8 of this report, due to the differences in design, the NUHOMs canisters stored at MNGP are in the horizontal position are not subject to tip over. A tornado wind induced missile could impact the storage cask or the HSM. For transfer operations, consistent with NUREG-1864 [1], time based initiating events are screened out from further consideration due to very low likelihood of occurrence during the comparatively short amount of DSC cask transfer time of transfer (e.g., the conditional probability of a sufficiently extreme tornado occurring onsite during the short time period of a DSC transfer outdoors is on the order of E-10). As such, high-wind induced tipping of the transfer trailer or impact due to tornado missile during transfer operations is screened out from further consideration as a non-significant risk contributor.

During storage, a wind-induced missile could impact the HSM. The minimum wall thickness for the HSM exterior walls is at least 30 inches. The end module shield walls are 24 inches. The evaluation in the ISAR concludes that missiles (including a “massive” vehicle missile) cannot affect the DSC. Based on the evaluation in the ISAR [7], high winds and high wind induced missile impacts are screened out from further consideration in this assessment.

3.2.10 Meteorites

Section 3.3.5 of NUREG-1864 [1] addresses the impact of meteorites on the ISFSI of the reference site. This initiating event is retained in this risk assessment and the NUREG-1864 [1] frequency estimate for meteorite strike per area is used for MNGP.

The frequency of a meteorite strike per area from NUREG-1864 [1] was applied to the MNGP specific area of the five DSCs considered in this evaluation. Meteorites that strike the transfer cask while on the haul path were not considered, based on the small fraction of time spent on the haul path relative to the amount of time spent in storage at the MNGP ISFSI. The five DSCs are enclosed in five HSMs. Consistent with NUREG-1864 [1], the roof dimensions are used to define the strike area. The roof dimension of an HSM is 9’-8” by 20’-8” (.0029464 km by .0062992 km) which yields a surface area for a single HSM of 1.85599E-05 sq km. The frequency is 4E-09/ km2, which yields of a strike frequency on a single HSM of 7.42E-14/yr. Multiplying by 5 yields a strike frequency on the area of the 5 HSMs of 3.71E-13/yr.

3.2.11 Lightning Strikes

Lightning strike induced radionuclide release accidents are determined in NUREG-1864 [1] to be non-credible. The ISAR [7] evaluated potential lightning strikes and states that the HSM will not be damaged by current flow through the concrete and will not affect the normal operation of the HSM. Lightning strikes are screened out from further consideration this assessment.

3.2.12 Aircraft Accidents

Section 3.3.7 of NUREG-1864 [1] addresses the impact of aircraft impact on the ISFSI of the reference site. This hazard is maintained for MNGP in this risk assessment.

Consistent with NUREG-1864 [1], airport sites within approximately 29 miles of MNGP were evaluated for the potential for an accident impacting the five HSMs. The five airport sites and the number of flights are shown in the Table 6. The source of the data are the FAA master records for each airfield, which can be accessed using the following website: http://www.gcr1.com/5010web/

The distance from MNGP (45.34° N/98.34°W) to each airport in Table 6 was approximated using google maps distance measurement feature at the following website: https://www.google.com/maps

Table 6: Airfields near MNGP

Airfield	Appx. Distance from MNGP (mi)	Annual Number of Flights
Maple Lake Municipal airport (MGG)	9	20,800
Buffalo Municipal Airport (CFE)	13	22,350
St. Cloud Regional Airport (STC)	18	28,316
Princeton Municipal Airport (PNM)	20	13,300
Crystal Airport (MIC)	30	42,351

NUREG-1864 [1] utilized NUREG-0800, Rev 2, to provide the methodology for computing the aircraft impact frequency. The current revision of NUREG-0800 is Revision 4 [28]. Revision 4 documents the same approach as Revision 2. Using equation 4 from Reference 1, the values of the following are needed to complete the estimate:

- Effective target area for a plane to strike the target on takeoff or landing (based on the effective area of 5 HSMs and a shadow and skid length).
- Probability per square kilometer (this evaluation uses miles) of crash of aircraft at each airfield. This value is provided in NUREG-0800 [28] for distances of up to 10 miles. For airfields greater than 10 miles away, the probability was extrapolated from the values in Reference 28.
- Number of movements at each airfield. The number of movements is taken from the FAA master record for each of the airfields in Table 6.

The product of the probability per mile of crash of an aircraft from a given field is multiplied by the number of movements from that field. The resulting probabilities for all movements of aircraft from each airfield are summed, and the sum is multiplied by the effective target area for the HSMs.

Reference 28 provides the ability to estimate the frequency based on the type of aircraft operation. The FAA master records for each facility provide the aircraft type. The aircraft types for each airfield are shown in Table 7:

Table 7: Aircraft Types per Airfields near MNGP

Airfield	Air Carrier	Air Taxi	GA Local	GA In Transit	Military
Maple Lake Municipal airport (MGG)	0	1000	15000	4000	800
Buffalo Municipal Airport (CFE)	0	130	11000	11000	220
St. Cloud Regional Airport (STC)	241	508	11558	12911	3098
Princeton Municipal Airport (PNM)	0	0	6500	6500	300
Crystal Airport (MIC)	0	549	19250	22458	94

The probability of crash per aircraft movement in Reference 28 is provided for Air Carrier, General Aviation, U.S. Navy/U.S. Marine, and U.S.A.F. For the purposes of this evaluation, the number of operations in Table 6 are assigned to these four categories. The Air Carrier crash probability in Reference 28 is considered applicable to Air Carrier and Air Taxi flights. The General Aviation crash probability is considered applicable to GA local and GA Intransit flights. There are two military categories (U.S. Navy/U.S. Marine, and U.S.A.F). The U.S.A.F crash probability is higher than the U.S. Navy/U.S. Marine crash probability in Reference 28, so all Military flights were considered applicable to the U.S.A.F crash probability.

The effective target area of the plane is not known and would change for each type of plane that could impact the five HSMs. Considering the uncertainty regarding the dimensions of the aircraft operating from each airfield, the same aircraft dimensions used in NUREG-1864 are assumed here. Similarly, the shadow and skid length is assumed the same as used in NUREG-1864. These dimensions are:

- Diameter of Engine: 5.2 ft.
- Centerline Spacing Between Engine: 13.8 ft.
- Width of 5 HSMs: (5 times 9’-8”): 48.3 ft.
- Shadow and Skid Length (from NUREG-1864): 200 ft.

The sum of the plane and HSM dimensions listed above is 67.3 ft. (.01275 miles). The shadow and skid length is 200 ft. (.03788 miles). The area in square miles is 4.83E-04.

Using the data in Table 7 and the probabilities in Reference 28, the aircraft type frequencies from each site are summed and multiplied by the target area. The resulting frequency is 7.43E-08.

Overflight crash hazards can be calculated using the same method in NUREG-1864 [1]. Consistent with NUREG-1864 [1], overflights are assumed to be a large aircraft. The frequency of an overflight crash is 4E-07 crashes per square mile per year. The target area is the same as described for accidents originating at nearby airfields. Multiplying the two gives an overflight crash frequency of 1.93E-10.

The assumption made in NUREG-1864 [1] is that only large aircraft travelling at high velocity can fail the MPC, which requires an overflying airplane larger than a Gulfstream IV jet. The vast majority of air traffic landing or departing airports near MNGP is general aviation traffic, which are typically smaller airplanes travelling at slow velocities relative to large aircraft on overflight routes. St. Cloud Regional Airport (STC) does have some air carrier flights; however, even if the airplanes are larger than a Gulfstream IV, the airplanes would be travelling at slow velocity because they would be approaching to land or departing on takeoff. Based on this, the probability of DSC failure given aircraft strike is set equal to the probability of an overflight aircraft impact, which does not depend on the airports nearby, which is consistent with the evaluation of aircraft impacts in NUREG-1864 [1].

Therefore, the total initiating event frequency for aircraft impact on the subject DSCs is 7.45E-08/yr (i.e., 7.43E-08 + 1.93E-10). Dividing the overflight impact frequency by the total aircraft impact frequency gives the conditional probability the aircraft accident is a large aircraft on overflight, which is 2.59E-03.

3.3 Dry Storage Canister (DSC) Failure Model

For each of the two modeled alternatives, the DSC failure model for this evaluation considers the following failure mechanisms:

- Mechanical failure of the DSC given a drop, including
  - Failure of the DSC shell (NUREG-1864 [1] MPC failure probabilities assumed applicable to the DSC)
  - Failure of the DSC lid welds (for a DSC with and without postulated weld flaws)
- Mechanical failure of the DSC, given a meteorite strike, or overflight aircraft accident
- Thermal failure scenarios, caused by
  - Blocked air inlet and outlet vents
  - Aircraft fuel fires

3.3.1 Mechanical Failures

The DSC can fail given a drop or upon a meteorite or large aircraft strike. Alternative 1 includes the risk of meteorite and large aircraft strike, while Alternative 2 includes the additional drop failure mode. For meteorite strikes and large aircraft strikes, the failure probability is assumed to be 1.0. This is consistent with the assumption in NUREG-1864 [1] for these events. For drops, Alternative 2 postulates four different drops with two unique drop heights. NUREG-1864 [1] evaluated the MPC and concluded that the MPC lid welds were rugged based on the weld type and the redundancy in the welds, and only evaluated the MPC shell for mechanical failure given a drop. For the DSC, considering the potential for weld flaws, both the DSC shell and lid welds need evaluation to estimate the probability of failure given a drop.

For mechanical failures of the DSC, consistent with the evaluation of MPC lid welds as robust in NUREG-1864 [1], it is assumed that the DSC lid welds would be robust if they were at nominal conditions with all requisite inspections completed satisfactorily, with higher capacity to resist failure given a drop than the DSC shell welds. To account for the presence of weld flaws, the DSC lid welds with potential weld flaws are assumed to have the same capacity as the shell (rather than be robust if the weld were at nominal conditions). The DSC shell is assumed to be similar to the MPC shell such that the probabilities of failure from NUREG-1864 [1] for the MPC shell given a drop can be directly applied to the DSC shell and, with the assumption that the presence of weld flaws decreases the lid weld capacity to resist failure to be equal to the capacity of the shell, the probabilities can also be applied to the lid welds. This is reasonable, considering the following:

- The MPC and DSC are comprised of the same type of stainless steel (SA240 304).
- The MPC and DSC are of similar dimensions and the steel is of similar thickness.

- The MPC and DSC are designed to the requirements of the same ASME class.
- The drop heights for the transfer operations in NUREG-1864 [1] and for the applicable MNGP Alternative 2 heights are similar.
- The drop surfaces are similar (refueling floor, concrete or transfer trailer/storage overpack, with concrete drop being limiting and used in this evaluation).
- The MPC lid welds were evaluated to be robust and not analyzed for failure in NUREG-1864 [1], meaning they have higher nominal capacity to resist failure relative to the capacity of the shell.

The combined failure probability for the DSC shell and lid welds is the sum of the probability of failure of the shell and failure of the lid welds. This sum equates to twice the failure probability of the MPC evaluated in NUREG-1864 [1] for a given drop height equivalent to the applicable drop height in MNGP Alternative 2. The stages applicable to the MNGP Alternative have probabilities for release from the fuel rod and MPC of 1E-06 and 1.96E-02, thus, for the MNGP DCSs with potential weld flaws, the probabilities are 2E-06 and 3.92E-02, respectively.

3.3.2 Thermal Failures

Thermal failures can result from heating of the DSC via blocked air inlet and outlet vents or a fire affecting the HSM. Each of these thermal scenarios is evaluated for potential impact to the DSC, given the potential condition of weld flaws for DSC lid welds.

For a DSC at design capacity, the ISAR [7] evaluated the blocked inlet and outlet air vent scenario using a set of conservative assumptions. The evaluation concluded that neither the fuel cladding nor the DSC would exceed temperature limits with vents blocked for up to five days. The evaluation concluded that the decay heat from the fuel would be transferred to the HSM and because the HSM has a very slow heat-up time, the heat transfer can be considered steady state. Although the fuel and DSC temperature limits would not be exceeded, the HSM temperature limit may be exceeded, and a daily surveillance is conducted to ensure that inlet and outlet vents are clear of debris or thermal performance is monitored which would limit the heat-up time.

NUREG-1864 [1] evaluated a blocked vent scenario for the 20-year duration of the storage phase. The conclusion was that although some fuel damage would occur, the MPC would not fail. NUREG-1864 [1] evaluated a jet fuel fire from an aircraft crash and concluded that the MPC would not fail given a three-hour duration fire that occurs after 20 years of blocked vents. The statement is made that a 30-minute fire scenario is more realistic, which means the three-hour jet fuel fire scenario is very conservative.

The NUREG-1864 [1] model did not explicitly evaluate MPC lid welds. The model evaluated the MPC shell including the axial and circumferential shell welds for limit load and creep rupture. The load limit model never contributed to failure for any of the heat-up scenarios. Creep rupture was evaluated with the presence of weld flaws. The creep rupture model calculated the time to rupture given a time at temperature and the stress at that temperature. The presence of weld flaws was modeled as a stress magnification factor which increases the stress for a given temperature and reduced the time to creep rupture failure.

Even with flaws assumed in the axial and circumferential welds on the MPC shell, 20 years of blocked vents or a 3-hour aircraft fuel fire did not result in the failure MPC. This evaluation shows that the MPC, including shell welds, which are considered by NUREG-1864 to be less robust than lid welds, is very robust against failure due to thermal scenarios. For the MNGP DSC, the capacity of the DSC to resist failure given a blocked vent and/or fire scenario, and the presence of potential weld flaws in the lid welds, is considered to be similar to the capacity of the MPC shell with presence of shell weld flaws evaluated for the MPC shell weld creep rupture model. Thus, the MNGP DSC is assumed to be relatively robust to thermal failures. Considering the daily surveillance requirement to ensure the air inlet and outlet vents are clear of debris or thermal performance monitoring, DSC failure from a blocked vent is deemed incredible and is screened out from this evaluation. For potential aircraft accidents involving a jet fuel fire a realistic fire scenario will be less than 3 hours and suppression of the fire will preclude sufficient heat-up that leads to creep rupture, and this event is deemed incredible and screened out from this evaluation. No thermal scenarios are included in the risk of Alternative 1 and Alternative 2.

3.4 Fuel Assembly Failure Model

Fuel assemblies can fail given a drop of the DSC. In NUREG-1864 [1], fuel failure is included in the overall failure of the MPC given a drop, and this is applied to this evaluation as well. The probability of fuel failure given a drop scenario from NUREG-1864 [1] is assumed applicable because the drop scenarios are similar. For shorter drops, fuel failure is not expected and is bound by the low probability of failure of the DSC. For long drops, the probability of fuel failure is likely, but the DSC has to fail to generate a release.

3.5 Secondary Containment Isolation Model

The MNGP Secondary Containment Isolation system functions to isolate the containment from the environment and activate the SGTS (Standby Gas Treatment System), which is the same function modeled in NUREG-1864 [1] for the reference site. For the purposes of this evaluation, the Secondary Containment Isolation model in NUREG-1864 [1] is considered applicable to the MNGP Secondary Containment Isolation system based on the following similarities to the model in NUREG-1864 [1]:

- MNGP and the NUREG-1864 reference plant are similar reactor containment designs (i.e., GE BWR Mark I).
- The MNGP reactor building is maintained at a slightly negative pressure relative to the environment, which minimizes the amount of exfiltration [12].
- The MNGP secondary containment isolation system is highly redundant, and consists of multiple detector trains, redundant isolation dampers at the secondary containment boundary, and trip signals to isolate fans on initiation of SGTS [12].
- Redundant isolation dampers close on detection of radiation in the reactor building exhaust plenum or in the area of the spent fuel pool and provide for SGTS initiation [12].

The NUREG-1864 [1] model is for a two-unit site. The model in Figure 18 [1] shows that the reference site has more isolations to complete to isolate the secondary containment (due to the shared nature of the reactor building shown in Figure 17 [1]), which would tend to increase the probability of failing to isolate relative to MNGP. The NUREG-1864 [1] model includes credit for both SGTSs, whereas MNGP only has one SGTS with two trains, which would tend to decrease the probability of failure relative to MNGP. Without a detailed fault tree of the secondary containment isolation model in NUREG-1864 [1] and without a detailed fault tree model for the MNGP secondary containment isolation and SGTS, an exact comparison is not feasible. However, given the similarities discussed above, the NUREG-1864 [1] probability for failure to isolate the secondary containment is assumed applicable to the MNGP configuration in this evaluation.

There are different probabilities of failing to isolate the secondary containment in the results of this assessment. The two probabilities of failing to isolate the secondary containment are 1.0 for noble gas releases, and 1.57E-04 for all other releases. Noble gases are not captured by the exhaust filters and thus the probability of failing to isolate the secondary containment is 1.0 for noble gas releases.

3.6 Consequence Model

This section applies the methodology outlined in Section 2.6.

Section 6.0 of NUREG-1864 [1] describes the consequence analysis for the reference site. Important consequence related parameters and inputs noted in NUREG-1864 [1] include the following:

- Fuel type and exposure
- Radionuclide inventory
- Source term (e.g., release fraction)
- Initial plume dimensions
- Plume heat content
- Population density/distribution
- Site weather

Each of these inputs is reviewed for applicability and comparison to the MNGP configurations.

3.6.1 Fuel Type and Exposure

The NUREG-1864 [1] consequence results are based on a single core containing 68 BWR fuel assemblies that were high burnup (i.e., 50 GWd/MTU) with 10 years of cooling.

The MNGP cask contains 61 BWR fuel assemblies with a core average exposure of 41 GWd/MTU (i.e., not high burnup fuel, where high burnup fuel is defined in NUREG-1864 [1] as greater than 45 GWd/MTU), with 15.5 years of cooling [35]. Thus, the MNGP fuel type and exposure parameters are all bounded by the NUREG-1864 [1] parameters.

3.6.2 Radionuclide Inventory

The NUREG-1864 [1] nuclide inventory for a single cask is provided in Table E-1 of that document. It is reproduced in Table 8 below, with the MNGP values taken from Table 6-1 of Reference [8] included for comparison. On average, the cask radionuclide inventory activity for the NUREG-1864 [1] cask is 7.0 times that of MNGP cask. Therefore, the NUREG-1864 [1] inventory is found to bound that of the subject MNGP casks with significant margin.

Table 8: Cask Radionuclide Inventory Comparison

RADIONUCLIDE	NUREG-1864 (CI)	MNGP DSC (CI)	RATIO (1864 / MNGP)	CONCLUSION
Am-241	3.2504E+04	1.6758E+04	1.94	Bounded
Am-242m	5.32E+02	6.7903E+01	7.83	Bounded
Am-242	N/A	6.7598E+01	--	Indeterminate
Am-243	8.30E+02	1.1141E+02	7.45	Bounded
Ba-137m	N/A	7.1753E+05	--	Indeterminate
Ce-144	1.374E+03	N/A	--	Indeterminate
Cm-242	N/A	5.5901E+01	--	Indeterminate
Cm-243	8.16E+02	6.5201E+01	12.52	Bounded
Cm-244	1.53000E+05	5.3060E+03	28.84	Bounded
Co-60	3.133E+03	6.7047E+02	4.67	Bounded
Cs-134	1.38720E+05	5.8502E+03	23.71	Bounded
Cs-137	1.496000E+06	7.5991E+05	1.97	Bounded
Eu-154	1.12200E+5	1.3159E+04	8.53	Bounded
Kr-85	7.4800E+04	3.9393E+04	1.90	Bounded
Np-239	N/A	1.1141E+02	--	Indeterminate
Pm-147	9.1120E+04	2.9001E+04	3.14	Bounded
Pu-238	1.07440E+05	1.8304E+04	5.87	Bounded

Table 8: Cask Radionuclide Inventory Comparison

RADIONUCLIDE	NUREG-1864 (CI)	MNGP DSC (CI)	RATIO (1864 / MNGP)	CONCLUSION
Pu-239	5.060E+03	2.5568E+03	1.98	Bounded
Pu-240	9.384E+03	4.1678E+03	2.25	Bounded
Pu-241	1.414400E+06	4.2150E+05	3.36	Bounded
Ru-106	7.888E+03	N/A	--	Indeterminate
Sm-151	N/A	2.7539E+03	--	Indeterminate
Sr-90	9.18000E+05	5.8899E+05	1.56	Bounded
Y-90	918000E+05	5.8909E+05	1.56	Bounded

(1) The MNGP DSC radionuclide inventory reflects the activity at end of core and does not include the 15.5 years of decay time. Inclusion of the decay time would be expected to increase the calculated 1864 / MNGP ratio for most radionuclides, adding additional margin.

3.6.3 Source Term

NUREG-1864 [1] presents MACCS2 conditional consequence results in Table E.3 for six (6) cases. The six cases reflect the consequences associated with a 100 ft. cask drop, but with differing attributes of fuel damage, release height, and release filtering. Section 6.2.2 of NUREG-1864 identifies one other consequence result for a release of only noble gases. Table 9 below summarizes these seven consequence results (latent individual cancer fatalities within 10 miles). The final NUREG-1864 [1] risk assessment as reflected in Table 18 of that document primarily relies upon the bounding consequence result of 3.6E-04/yr (see Case 1 in Table 9 below). However, the other cases may be applicable to certain configurations (e.g., to represent the lower expected release associated with releases from a DSC on the pad). For example, Case 6 would be judged to best represent a DSC located on the pad which was not subject to a cask impact failure (e.g., drop), where the release pathway would be through a weld flaw. Absent a cask impact, the fuel pellet rim fracture factor of 1.24E-04 (the value representative of the fuel pellet as a whole) is judged most representative. It is noted that, per NUREG-1864, the formation of a rim on the fuel pellet is primarily a phenomenon associated with only high burnup fuel and would be conservative for MNGP fuel. Without an impact, a release of noble gases, fuel particles, and CRUD (i.e., Chalk River unidentified deposits) would be conservative given that the release would generally be limited to only CRUD. The torturous release pathway of the weld flaw would also be expected to reduce the release in a manner akin to a filtered release.

In summary, review of the NUREG-1864 source term attributes indicate that they would adequately represent or bound those of the MNGP configuration, depending upon the case selected.

Table 9: NUREG-1864 Consequence Result Cases

CASE	FUEL PELLET RIM FRACTURE FACTOR	RELEASE FRACTION CONTRIBUTORS	RELEASE HEIGHT (M)	RELEASE FILTERING	INDIVIDUAL CANCER FATALITY RISK (/YR)
1	1.0	Noble Gas, Fuel Particles, CRUD	50	Not Filtered	3.6E-04
2	1.0	Noble Gas, Fuel Particles, CRUD	120	Not Filtered	2.1E-04
3	1.0	Noble Gas, Fuel Particles, CRUD	50	Filtered	5.2E-05
4	1.24E-4	Noble Gas, Fuel Particles, CRUD	50	Not Filtered	4.3E-06
5	1.24E-4	Noble Gas, Fuel Particles, CRUD	120	Not Filtered	2.6E-06
6	1.24E-4	Noble Gas, Fuel Particles, CRUD	50	Filtered	4.3E-07

Table 9: NUREG-1864 Consequence Result Cases

CASE	FUEL PELLET RIM FRACTURE FACTOR	RELEASE FRACTION CONTRIBUTORS	RELEASE HEIGHT (M)	RELEASE FILTERING	INDIVIDUAL CANCER FATALITY RISK (/YR)
7	1.0	Noble Gas only	50	Not Filtered	1.0E-10

3.6.4 Initial Plume Dimensions

The initial plume dimensions used in the MACCS2 code are dependent upon the building wake effects, as calculated based on the building width and height (typically 40m to 50m). For the NUREG-1864 [1] consequence analysis, a structure size of 4m wide by 4m high was used, approximating the dimensions of a cask. It should be noted that this value was used even for drops postulated to occur inside the site reactor building where plume effects would actually be based on the reactor building structure. The MNGP NUHOMs storage system is comprised of individual HSMs (10' wide, 20' long, 15' tall) situated back-to-back and side-to-side to comprise a 2x15 array that is 150' wide across HSM fronts, 40' wide (two HSMs back-to-back) and 15' tall [27, 32, 33]. For the purposes of the consequence assessment, the NUHOMs storage system configuration is judged to be adequately represented by the initial plume dimension parameters used in the NUREG-1864 [1] consequence calculation. Likewise, a release from the DSC during transfer (along with haul path) and from the reactor building would also be represented by the NUREG model.

3.6.5 Plume Heat Content

The NUREG-1864 [1] notes that the plume heat content for a cask release is estimated to be that of the spent fuel. For ten-year old spent fuel, NUREG-1864 [1] estimates the maximum decay heat load to be 264 watts per assembly. For the Monticello DSCs, the fuel is over 15 years old and the maximum decay heat load (i.e., approximately 220 watts per assembly per Reference [35]) is bounded by the NUREG-1864 [1] estimate. NUREG-1864 [1] notes that the plume resulting from the release will not be thermally hot enough to produce significant plume rise.

3.6.6 Population

The NUREG-1864 [1] consequence results of interest in the risk assessment are presented in the form of Individual Risk of Cancer Fatality. These results are developed by taking the population-weighted health effect risk and dividing by the total population in the region to develop the metric for <u>individual</u> risk. Since the consequence metric is based on individual risk, the metric should be relatively insensitive to absolute population differences between the NUREG-1864 [1] site and the MNGP site.

The NUREG-1864 [1] population is based on year 2000 population data using the SECPOP code, and is assumed to be the Hatch site. For this current assessment, the same SECPOP code (ver. 4.2) [31] was used to develop the 10-mile radius population distribution for the Hatch site for year 2000 and the MNGP site for year 2010 for comparison purposes. Tables 10 and 11 present the results for Hatch and Monticello, respectively.

The 10-mile population for Hatch is 8,539, while that of Monticello is 58,869. The larger population of Monticello however, does not automatically translate into a linear increase in individual risk consequence results. The following insights are noted from comparing the population distribution for the two sites:

- Both Hatch and Monticello have some population variation as a function of direction from the site. Prevailing wind directions could thus have impacts or radiological dispersion. This is evaluated in the comparison of weather.

- The Hatch and Monticello population distribution has some variation as a function of distance from the site. For releases at ground level, a closer population would tend to increase radiological impacts. A release from the pad would be expected to have deposition closer to the site rather than further from the site. For elevated releases, a closer population would tend to decrease radiological impacts given that the radiological plume would tend to travel over areas near the site with deposition occurring more once the plume expands in the vertical direction down to the grade elevation. Review of Tables 10 & 11 show that the percent of total population within 3 miles of the site is higher for Hatch than for Monticello (i.e., 10% as compare to 8%, respectively). Therefore, with respect to releases from the pad, the Hatch attributes for population distance distribution are judged to bound those for MNGP. With respect to releases from the reactor building, the population distribution for Hatch is judged to adequately represent those for MNGP, considering the many potential areas of variability associated with atmospheric dispersion and deposition.

Table 10: Hatch Population Distribution (Year 2000)

Sector	0-0.3 miles	0.3-1 miles	1-2 miles	2-3 miles	3-4 miles	4-5 miles	5-7 miles	7-10 miles	0-10 miles	% of Total
N	0	0	20	4	19	103	65	251	462	5%
NNE	0	0	0	0	0	18	48	282	348	4%
NE	0	0	0	0	21	30	57	276	384	4%
ENE	0	0	0	0	0	2	19	101	122	1%
E	0	0	0	0	0	23	0	21	44	1%
ESE	0	0	0	27	0	14	72	199	312	4%
SE	0	0	0	64	13	63	136	104	380	4%
SSE	0	0	0	30	71	110	217	321	749	9%
S	0	0	43	127	53	40	374	1855	2492	29%
SSW	0	0	54	78	72	72	87	201	564	7%
SW	0	0	89	0	38	35	89	126	377	4%
WSW	0	0	0	144	0	55	77	317	593	7%
W	0	0	91	0	0	0	20	88	199	2%
WNW	0	0	37	5	223	0	42	155	462	5%
NW	0	0	0	0	4	0	155	177	336	4%
NNW	0	0	1	20	54	47	168	425	715	8%
Total	0	0	335	499	568	612	1626	4899	**8539**	100%
% of Total	0	0	4%	6%	7%	7%	19%	57%	100%	
% Cum	0	0%	4%	10%	16%	24%	43%	100%		

Table 11: Monticello Population Distribution (Year 2010)

Sector	0-0.3 miles	0.3-1 miles	1-2 miles	2-3 miles	3-4 miles	4-5 miles	5-7 miles	7-10 miles	0-10 miles	% of Total
N	0	0	4	0	668	719	334	445	2170	4%
NNE	0	0	0	2	155	190	397	1241	1985	3%
NE	0	0	0	11	262	621	675	1229	2798	5%
ENE	0	0	57	32	1356	2506	1665	2010	7626	13%
E	0	0	205	110	276	1876	3293	2191	7951	14%
ESE	0	0	63	586	214	827	1314	1662	4666	8%
SE	0	0	886	1278	2271	2369	3428	480	10712	19%
SSE	0	0	349	46	1277	639	152	116	2579	5%
S	0	22	3	58	130	263	226	4508	5210	9%
SSW	0	0	143	220	0	124	174	703	1364	2%
SW	0	0	0	0	322	92	323	643	1380	2%
WSW	0	0	0	94	84	29	108	656	971	2%
W	0	0	183	22	164	11	358	624	1362	2%
WNW	0	0	98	1	32	232	274	524	1161	2%
NW	0	0	0	0	29	39	36	470	574	1%
NNW	0	0	0	0	44	1044	2311	961	4360	8%
Total	0	22	1991	2460	7284	11581	15068	18463	**56869**	100%
% of Total	0	0.04%	4%	4%	13%	20%	26%	32%	100%	
% Cum	0	0%	4%	8%	21%	41%	68%	100%		

3.6.7 Site Weather

The NUREG-1864 [1] consequence results are based MACCS2 code sampling of an annual weather file, including data for wind speed, wind direction, atmospheric stability, and rainfall. The consequence results are based on the mean values generated from the weather sampling. It is not possible to compare all weather variables fully without a MACCS2 code calculation. However, some comparison can be made using the Exposure Index approached documented in NUREG-1437 [29].

NUREG-1437 (p. 5 - 25) notes the following:

> *While particular aspects of meteorology, such as rainfall, can have a significant impact on peak risk values, mean health effect values are relatively insensitive to meteorology. When the basic reasons for the risk influence of each factor are examined, these factors can generally be reduced to three issues: (1) the number of people exposed to the severe accident release, (2) the likelihood that any given individual receives an exposures, and (3) the amount of radiation the individual receives.*

NUREG-1437 [29] proceeds to develop the Exposure Index (EI) approach to estimate consequence results based on population and wind direction frequency (i.e., fraction of time per year that wind blows in each compass sector direction). An EI value is developed by multiplying the wind direction frequency by the downwind population out to a certain distance. Wind direction frequency for each site is available in Table A.4-1 of NUREG/CR-2239 [30].

Table 12 and 13 present the EI results for the Hatch and Monticello sites, respectively. The following insights are noted from comparing the population distribution for the two sites:

- For Hatch, the wind frequency in the most populated direction (south) is below average. Overall, the EI value is below average by approximately 14% indicating that the wind tends to blow towards lower populated sectors.
- For Monticello, the wind frequency in the most populated direction (southeast) is above average. Overall, the EI value is above average by approximately 7% indicating the wind tends to blow towards higher populated sectors.
- The differences between the two sites as explored with the exposure index are not considered substantial. Experience with the MACCS2 code has shown that using different annual weather data files (e.g., 2008 vs. 2009) for a given site will often result in differences of +/- 5% on calculated mean dose impacts. Such differences derive from the inherent variability of weather parameters from year to year. The variation exhibited between the two sites is not significantly greater. Therefore, with respect to site weather, the NUREG-1864 consequence results are judged to adequately represent those of MNGP.

Table 12: Hatch 10-Mile Exposure Index

Sector	NUREG/CR-2239 Wind Rose	0-10 Mile Pop	Exp Index	% of Total
N	0.055	462	25	6%
NNE	0.069	348	24	5%
NE	0.082	384	31	7%
ENE	0.073	122	9	2%
E	0.075	44	3	1%
ESE	0.077	312	24	5%
SE	0.072	380	27	6%
SSE	0.049	749	37	8%
S	0.04	2492	100	22%
SSW	0.038	564	21	5%
SW	0.051	377	19	4%
WSW	0.067	593	40	9%
W	0.081	199	16	4%
WNW	0.068	462	31	7%
NW	0.057	336	19	4%
NNW	0.044	715	31	7%
Total	0.998	8539	459	100%
		EI if ave	534	
		% off ave	-13.9%	

Table 13: Monticello 10-Mile Exposure Index

Sector	NUREG/CR-2239 Wind Rose	0-10 Mile Pop	Exp Index	% of Total
N	0.089	2170	193	5%
NNE	0.091	1985	181	5%
NE	0.063	2798	176	5%
ENE	0.055	7626	419	11%
E	0.03	7951	239	6%
ESE	0.089	4666	415	11%
SE	0.104	10712	1114	29%
SSE	0.119	2579	307	8%
S	0.036	5210	188	5%
SSW	0.041	1364	56	1%
SW	0.029	1380	40	1%
WSW	0.051	971	50	1%
W	0.031	1362	42	1%
WNW	0.055	1161	64	2%
NW	0.052	574	30	1%
NNW	0.065	4360	283	7%
Total	1	56869	3797	100%
		EI if ave	3554	
		% off ave	6.8%	

The consequence probabilities in NUREG-1864 [1] apply to failure of a single MPC. The consequence probabilities are judged to be reasonable to represent failure of the MNGP DSCs in this evaluation. Alternative 1 and 2 include hazards that can affect up to five (5) DSCs (aircraft strikes, meteorite strike) during years of storage. The consequences applied represent failure of a single DSC but the frequency of aircraft strike and meteorite strike assumes that any one of the five DSCs can be impacted by the hazard.

3.7 Results

The risk of Alternative 1 and Alternative 2 has been evaluated to determine the absolute value of latent cancer fatality risk for DSCs 11-15 and the relative risk of the alternatives considering the potential presence of flaws in the DSC lid welds.

The major assumptions used in this quantitative evaluation are:

1. Consistent with NUREG-1864 [1], time based initiating events (seismic events, high winds, floods) are assumed not to occur during transfer of the DSC to and from the Fuel Building and during inspection of the welds, based on the short amount of time that occurs during transport and inspection.
2. Tipping of the HSM due to a seismic or high wind event is assumed incredible, based on the horizontal configuration of the HSMs.
3. Sliding of the HSM is assumed to have no impact on the DSC. The likelihood of sliding is low based on the size and weight of the HSMs and the low likelihood that a wind or seismic

event occurs. If sliding occurred, no damage would occur to the DSC unless the HSM was slid into another object or off of the ISFSI pad.

4. The failure probabilities for the DSC shell given a drop are based on similarity to the MPC shell evaluated in NUREG-1864 [1]. DSC lid welds with flaws, are assumed to be the same capacity of the shell, which gives an overall DSC failure probability of twice the MPC shell failure probability from NUREG-1864 [1] for applicable drops. This is based on the evaluation in NUREG-1864 [1] that lid welds are robust compared to the MPC shell, based on weld type and weld redundancy, so the presence of weld flaws degrades the capacity from robust to be equal to the shell capacity.
5. Thermal scenarios were considered incredible based on the evaluation of the MPC in NUREG-1864 [1], which included weld flaws for shell welds, which indicate robust design capacity against thermal events, and assumed equivalence of the DSC shell and lid welds to the MPC, and the short time duration of blocked vent and aircraft fire events.
6. Consistent with NUREG-1864 [1], the conditional probability of failure of the fuel cladding and the DSC is assumed to be 1.0 for large aircraft overflight strikes, and meteor strikes. The presence of potential weld flaws does not impact the resulting risk calculations. If detailed evaluations showed the potential for DSC survival given a large aircraft or meteorite strike, the potential for weld flaws may impact the resulting probability of release, but given the uncertainty and the potential magnitude of these two events, it is assumed that the DSC will fail regardless of the presence of potential weld flaws.

A summary of each of the contributors to each Alternative is shown in Tables 14 and 15. A summary of the results in the risk tables is as follows:

- Storage stage risk is shown for one year of storage of all five DSCs in the individual rows in Tables 14 and 15 for Alternative 1 and 2. When included in the totals in Table 14 and 15, storage risk is multiplied by twenty years.
- Transport stage risk is shown for a single DSC in Table 15 for Alternative 2. When included in the total in Table 15, transport risk is multiplied by 5 DSCs and added to the risk of storage of all five DSCs for twenty years.
- For the storage risk of both alternatives, the frequency of aircraft strike and meteorite strike is adjusted to use the target area of all DSCs, so risk reflects a release from any of the five (5) DSCs, but not simultaneous release of multiple DSCs.
- For the unique transport stages of Alternative 2, although there are only two lifts, the probability of failure of the fuel rod and DSC with subsequent release depends on the distance the DSC would fall, thus, the two lifts are separated into four rows in the results in Table 15 in order to capture the different release probabilities. The results are slightly conservative, because a split fraction of the lift distance could be applied to the two rows as opposed to 100% of the lift frequency being applied to each, but the impact of the fraction on the results would be small because the higher probability of release given a drop down the equipment hatch is much more significant to the results compared to the probability of release given the very small drop distance when the DSC is moved over the refueling floor.
- Tables 14 and 15 include stages for each alternative. These stages are named for convenience and are in chronological order for Alternative 2. Also for Alternative 2, where applicable, the MNGP specific process steps from Table 2 are included.

Table 14: Alternative 1 Risk

	Stages	Initiating Event	Initiating Event Frequency per Year (Sections 2.2 and 3.2)	Probability of Release from fuel rod and MPC (Sections 2.3 and 3.3)	Probability of Release from Containment (Sections 2.5 and 3.5)	Consequences (Sections 2.6 and 3.6)	Risk Per Year
1-1	Storing the DSCs (for 1 year)	Struck by Aircraft (overflight)	7.45E-08	2.59E-03 (conditional probability of aircraft being large plane on overflight)	1.00 (no secondary containment at the HSM)	3.60E-04	6.95E-14
1-2	Storing the DSCs (for 1 year)	Struck by Meteorite	3.71E-13	1.00	1.00 (no secondary containment at the HSM)	3.60E-04	1.34E-16
						Total Risk of Alternative 1 for all 5 DSCs Sum of stages 1-1 and 1-2 multiplied by 20 years	**1.39E-12**

Table 15: Alternative 2 Risk

Stages (and MNGP Table 2 Steps)		Initiating Event	Initiating Event Frequency Per Year (Sections 2.2 and 3.2)	Probability of Release from fuel rod and MPC (Sections 2.3 and 3.3)	Probability of Release from Containment (Sections 2.5 and 3.5)	Consequences (Sections 2.6 and 3.6)	Risk Per Year
2-1 (25-34)	Removing the DSC from the HSM and transporting to the Equipment Hatch	None					
2-2 (22-23)	Lifting the DSC from the TT and raising through the Equipment Hatch (weld flaws assumed)	Dropped DSC	5.65E-05	3.92E-02	1.57E-04 1.0 (Noble Gases)	3.60E-04 1.0E-10	1.23E-13 2.18E-16
2-3 (21)	Lifting/moving the DSC over the Refuel Floor to the Inspection Area (weld flaws assumed)	Dropped DSC	5.65E-05	2E-06	1.57E-04	3.60E-04	6.29E-18
2-4	Inspecting and Repairing Welds, if necessary	None					
2-5 (20-21)	Lifting/moving the DSC over the Refuel Floor from the Inspection Area to the Equipment Hatch (weld flaws repaired)	Dropped DSC	5.65E-05	1E-06	1.57E-04	3.60E-04	3.15E-18
2-6 (22-23)	Lifting the DSC and lowering down the Equipment Hatch to the TT (weld flaws repaired)	Dropped DSC	5.65E-05	1.96E-02	1.57E-04 1.0 (Noble Gases)	3.60E-04 1.0E-10	6.17E-14 1.09E-16
2-7 (25-34)	Transporting the DSC to the HSM and re-inserting into the HSM	None					
2-8	Storing the DSCs (for 1 year)	Struck by Aircraft (overflight)	7.45E-08	2.59E-03 (conditional probability of aircraft being large plane on overflight)	1.00 (no secondary containment at the HSM)	3.60E-04	6.95E-14
2-9	Storing the DSCs (for 1 year)	Struck by Meteorite	3.71E-13	1.00	1.00 (no secondary containment at the HSM)	3.60E-04	1.34E-16
Total Risk of Alternative 2 for all 5 DSCs **Sum of stages 2-1 to 2-7 multiplied by 5 DSCs plus sum of stages 2-8 and 2-9 multiplied by 20 years**							**2.32E-12**

The total risk of each alternative is very low and is several orders of magnitude lower than the acceptance criteria in Table 5. These results are on the same order of magnitude as the results in NUREG-1864 [1], which is reasonable considering the similarity in cask designs and the overall low risk of release given an initiating event. The difference in risk between the two alternatives is 9.26E-13. Alternative 2 is higher in risk by a factor of 1.66.

The summary of results in shown in Table 16:

Table 16: Summary of Results

Alternative 2	Alternative 1	ΔRisk	Acceptance criteria	Result
2.32E-12	1.39E-12	9.26E-13	<1E-08	“Very Small” change in risk

4.0 SUMMARY

4.1 Summary of Methodology Development

The methodology in NUREG-1864 [1] has been adapted to develop a simplified Probabilistic Risk Assessment for the MNGP dry cask storage system. The methodology was to:

- Determine the stages of operation for two proposed alternatives to evaluate the latent cancer fatality risk of five MNGP DSCs (11-15) with non-compliant weld dye penetrant examinations,
- Screen the initiating events that could affect the integrity of the DSCs,
- Estimate initiating event frequencies based on MNGP specifics,
- Assess the failure probability of the DSC given an initiating event, and
- Quantify the latent cancer fatality risk given a failed DSC for each alternative.

4.2 Summary of Methodology Application

The evaluation in NUREG-1864 [1] has been applied/extrapolated to determine the risk of Alternatives 1 and 2 for MNGP DSCs 11-15. The stage evaluated for Alternative 1 is storage for 20 years; the potential initiating events applicable to these stages are aircraft impacts and meteorite strikes on any 1 of the 5 DSCs. All other initiating events are screened out as not applicable or non-risk significant.

The stages applicable to Alternative 2 are to:

- Remove the DSC from the HSM and transport to the Fuel Building,
- Lift the DSC up the Equipment Hatch to the Refuel Floor,
- Perform weld inspections,
- Lift the DSC and lower it down the Equipment Hatch to the transfer trailer,
- Transport it back the HSM and re-insert the DSC into the HSM, and
- Store the DSC for 20 years.

Like Alternative 1, Alternative 2 also includes aircraft impact and meteorite strike hazards during the storage stage with the DSCs in the HSMs. The initiating event unique to Alternative 2 is a potential drop while lifting the DSC during the movements in the reactor building. These stages apply to all 5 DSCs that need inspection, thus, the risk of Alternative 2 assumes all 5 are moved for inspection.

Latent cancer fatality risk has been quantified for both alternatives and shown to be well below potential risk acceptance guidelines for latent cancer risk, and shown to be not significantly different between alternatives. Risk is presented for all 5 DSCs for a period of 20 years.

4.3 Conclusions

In conclusion, the risk of Alternative 1 and Alternative 2 are both very small relative to the criteria in Table 5. The difference in risk between the alternatives is not significant. With regards to the welds with non-compliant PT examinations, the risk of Alternative 2 includes higher failure probabilities given a cask drop for the drops that occur prior to inspection. Alternative 1 risk, as estimated in this evaluation, is not affected by the potential presence of weld flaws because the included initiating events that can fail the DSC are assumed to fail the DSC with probability of 1.0, consistent with NUREG-1864 [1], for aircraft strikes and meteorite strikes, based on the uncertainty of and potential magnitude of such events.

The magnitude of risk of either alternative is similar to the magnitude of risk of the reference site in NUREG-1864 [1], with differences attributable to the number of stages applied to the risk model for MNGP and the different frequency of the initiating events at each site. Overall, the differences are small, in the context of the total quantified risk and the risk acceptance criteria.

5.0 REFERENCES

1. U.S. Nuclear Regulatory Commission. *A Probabilistic Risk Assessment of a Dry Cask Storage System at a Nuclear Plant*, NUREG-1864, March 2007.
2. U.S Nuclear Regulatory Commission. *Tornado Climatology of the Contiguous United States*. NUREG/CR-4461, Revision 2, February 2007.
3. Stevenson and Associates. *Monticello Nuclear Generating Plant Seismic Hazard and Screening Report,* NEI 05-04, Rev. 3, May 2014.
4. Northern States Power Company. *Monticello Individual Plant Evaluation of External Events (IPEEE),* NSPLMI 95-001, July 2010.
5. Hughes Associates. *External Flooding Evaluation for Monticello Nuclear Generating Plant,* 1SML16012.000-1, June 2013.
6. Monticello Nuclear Generating Plant, *Monticello Nuclear Generating Plan Independent Spent Fuel Storage Installation (ISFSI) 10 CFR 72.212 Evaluations Report,* 72.212, Revision 7, June 2013.
7. Transnuclear Incorporated, Updated Final Safety Analysis Report for the Standardized NUHOMS® Horizontal Modular Storage System *for Irradiated Nuclear Fuel*, NUH-003, Revision 12, January 2012.
8. Applied Analysis Corporation, Accident Dose Assessment for MNGP DSCs 11-15, MNGP-018, Revision 0, June 2017. (Approval pending)
9. Office of Nuclear Regulatory Research, Office of Nuclear Material Safety and Safeguards, Office of Federal and State Materials and Environmental Management Programs, and U.S. Nuclear Regulatory Commission, *Risk-Informed Decision-Making for Nuclear Material and Waste Applications,* Revision 1, February 2008.
10. U.S. Nuclear Regulatory Commission, *An Approach for Using Probabilistic Risk Assessment in Risk-Informed Decision on Plant-Specific Changes to the Licensing Basis*, RG 1.174, Revision 2, May 2011.
11. Monticello Nuclear Generating Plant, Application for Renewed Operating License, Appendix E –Environmental Report, 2005.
12. Monticello Nuclear Generating Plant, *Monticello Updated Final Safety Analysis Report*, USAR-05.03, Revision 34P.
13. MNGP Drawing NH-36267, Sheet 1 of 4, *Plant Air Flow*
14. MNGP Drawing NH-36267-3, Sheet 4 of 4, *Main Exhaust Plenum Room*
15. MNGP Drawing NH-36807, *Air Flow Diagram Reactor Building Lower Part*
16. MNGP Drawing NH-36808, *Air Flow Diagram Reactor Building Upper Part*
17. MNGP Drawing NH-36881, *Standby Gas Treatment Flow Diagram*
18. Not Used.
19. Not Used.
20. U.S. Nuclear Regulatory Commission. *A Survey of Crane Operating Experience at U.S. Nuclear Power Plants from 1968 through 2002*, NUREG-1774, July 2003.

21. Nuclear Regulatory Commission. *Revised Livermore Seismic Hazard Estimated for Sixty-Nine Nuclear Power Plant Sites East of the Rocky Mountains*, NUREG-1488, April 1994.
22. Nuclear Regulatory Commission. *Generic Issue 199: Implications of Updated Probabilistic Seismic Hazard Estimates in Central and Eastern United States on Existing Plants*, Information Notice 2010-18, September 2, 2010.
23. Not Used.
24. U.S. Nuclear Regulatory Commission letter to Peter Gardner (Site Vice President, Monticello Nuclear Generating Plant), Exemption from Certain Provisions of Standardized NUHOMS® Dry Shielded Canister 16 at Monticello Nuclear Generating Plant Independent Spent Fuel Storage Installation (CAC No. L25058), dated June 15, 2016 (Adams Accession No. ML16167A036).
25. Flood Hazard Reevaluation Report for the Monticello Nuclear Generating Plant, dated 4/25/2016 (ADAMS Accession No. ML16145A180).
26. Independent Spent Fuel Storage Installation Fire Hazards Analysis, 72.212-A, Revision 5.
27. NUH-03-7104 Sheet 2 of 3, Roof, Revision 3.
28. Nuclear Regulatory Commission. *Standard Review Plan*, NUREG-0800, U.S. Nuclear Regulatory Commission, Revision 4 (ADAMS accession no. ML100331298).
29. Nuclear Regulatory Commission. *Generic Environmental Impact Statement for License Renewal of Nuclear Power Plants,* NUREG-1437, U.S. Nuclear Regulatory Commission, Revision 1.
30. Nuclear Regulatory Commission. *Technical Guidance for Siting Criteria Development*, NUREG-2239 (ADAMS Accession ML072320420).
31. Nuclear Regulatory Commission. *SECPOP2000: Sector Population, Land Fraction, and Economic Estimation Program*, NUREG/CR-6525, Rev. 1. Code version 4.2.
32. NUH-03-7101 Sheet 1 of 6, General Arrangement, Revision 2
33. NUH-03-7104 Sheet 2 of 5, Base, Revision 3
34. SNFP-MT-2943-TN-0206, QF0939 – PIT #2 – Monticello Risk Informed Weld Issue – Table 1
35. SNFP-MT-2943-TN-0206, QF0939 – PIT #3 – Monticello Risk Informed Weld Issue – Cask Loading Reports
36. EC 783 Design Description, Drawing NUH61BTH-3000 Rev. 9, Drawing NUH-06-8003 Rev. 6
37. Drawing NF-36309 Rev. B, Procedure 9506 Rev. 17, Drawing NF-36393 Rev. B
38. Procedure 9506 Rev. 17
39. Drawing NF-36309 Rev. B, Procedure 9506 Rev. 17, Drawing NF-36306 Rev. 76
40. Drawing NUH-07-2101 Rev. 4 or NUH-06-8003 Rev. 6
41. Drawing NUH-07-2108 and DIT No. ISFSI-070
42. Drawing NUH-03-7103 Rev. 5, Drawing NUH61BTH-3000 Rev. 9, Drawing NF-201626 Rev. 0

ENCLOSURE 12

AREVA AFFIDAVIT

Affidavit #	Enclosure # - Document Number & Name
E-49704	Enclosure 9 – AREVA Calculation 11042-0400, Revision 0, “Site-Specific Thermal Evaluation of 61BTH Type 1 DSCs Stored in HSM-H at Monticello Nuclear Generating Plant”

1 page follows

AFFIDAVIT PURSUANT
TO 10 CFR 2.390

TN Americas LLC)
State of Maryland) SS.
County of Howard)

I, Jayant Bondre, depose and say that I am Chief Technology Officer of TN Americas LLC, duly authorized to execute this affidavit, and have reviewed or caused to have reviewed the information which is identified as proprietary and referenced in the paragraph immediately below. I am submitting this affidavit in conformance with the provisions of 10 CFR 2.390 of the Commission's regulations for withholding this information.

The information for which proprietary treatment is sought is listed below:

- Calculation 11042-0400, Rev. 0, "Site-Specific Thermal Evaluation of 61BTH Type 1 DSCs Stored in HSM-H at Monticello Nuclear Generating Plant"

This information has been appropriately designated as proprietary.

I have personal knowledge of the criteria and procedures utilized by TN Americas LLC in designating information as a trade secret, privileged, or as confidential commercial or financial information.

Pursuant to the provisions of paragraph (b) (4) of Section 2.390 of the Commission's regulations, the following is furnished for consideration by the Commission in determining whether the information sought to be withheld from public disclosure, included in the above referenced documents, should be withheld.

1) The information sought to be withheld from public disclosure involves the determination of bounding DSC shell temperatures and internal pressures during storage operations, an analysis which is owned and has been held in confidence by TN Americas LLC.

2) The information is of a type customarily held in confidence by TN Americas LLC and not customarily disclosed to the public. TN Americas LLC has a rational basis for determining the types of information customarily held in confidence by it.

3) Public disclosure of the information is likely to cause substantial harm to the competitive position of TN Americas LLC because the information consists of thermal analyses associated with the NUHOMS® 61BTH Type 1 DSCs, the application of which provide a competitive economic advantage. The availability of such information to competitors would enable them to modify their product to better compete with TN Americas LLC, take marketing or other actions to improve their product's position or impair the position of TN Americas LLC's product, and avoid developing similar data and analyses in support of their processes, methods or apparatus.

Further the deponent sayeth not.

Jayant Bondre
Chief Technology Officer, TN Americas LLC

Subscribed and sworn before me this 14th day of September, 2017.

Notary Public
My Commission Expires 10/16/19

RONDA JONES
NOTARY PUBLIC STATE OF MARYLAND
My Commission Expires October 16, 2019